Review

Metal Complexes of Organophosphate Esters and Open-Framework Metal Phosphates: Synthesis, Structure, Transformations, and Applications

R. Murugavel, Amitava Choudhury, M. G. Walawalkar, R. Pothiraja, and C. N. R. Rao

Chem. Rev., **2008**, 108 (9), 3549-3655 • DOI: 10.1021/cr000119q • Publication Date (Web): 28 June 2008

Metal Complexes of Organophosphate Esters and Open-Framework Metal Phosphates: Synthesis, Structure, Transformations, and Applications

R. Murugavel,*,† Amitava Choudhury,‡ M. G. Walawalkar,† R. Pothiraja,† and C. N. R. Rao*,‡

Department of Chemistry, IIT-Bombay, Powai, Mumbai-400076, India, and Chemistry and Physics of Materials Unit, Jawaharlal Nehru Center of Advanced Scientific Research, Jakkur P.O., Bangalore-560 064, India

Received July 5, 2005

Contents

* Corresponding authors. R.M.: fax +91-22-25723480, e-mail rmv@chem.iitb.ac.in. C.N.R.R.: fax +91-80-23622760, e-mail cnrrao@jncasr.ac.in.
† IIT-Bombay.
‡ Jawaharlal Nehru Center of Advanced Scientific Research.

10.1021/cr000119q CCC: $71.00
Published on Web 06/28/2008

1. Introduction

1.1. Scope

Phosphorus is a vital element both in living matter and in the Earth's crust. The human body contains about 1% by weight of the element phosphorus, about $^4/_5$ of this being present as hydroxyapatite in bones and teeth and the remaining phosphorus present as organic phosphates, which are in various forms such as their mono- and diesters.[1] On the other hand, a large number of metal phosphates are also found in Nature as minerals. The diversity in metal phosphates results from variations in their assemblies, the large number of cations to which they can coordinate, and the presence of additional anions or molecules.[2,3] As a result, there has been great interest in preparation of phosphate materials. Such materials have been used as ion exchangers,[4] fast-ion conductors,[5] and catalysts.[6] Further, because phosphate anions do not absorb in the UV−visible region, metal phosphates also find use as optical materials, for example, glasses, phosphors,[7] nonlinear optical materials,[8] and laser materials.[9] Amorphous phosphorite deposits are important as phosphate fertilizers.[10] The term "phosphate" refers oxyanions of pentavalent phosphorus, which range from the simple PO_4^{3-} through ring and chain anions to infinite networks.[11] Phosphodiesters find numerous applications, for example, plasticizers,[12] flame retardants,[13] reagents in the preparation of organophosphorus polymers,[14] reagents in solvent extraction of heavy metal ions, [15] and insecticides.[16] All phosphate esters are susceptible to hydrolysis, and this fact is of great importance in biological systems.[17]

Inorganic phosphate chemistry was dominated by the study of minerals for a long time. With the recent discovery of phosphate analogues of aluminosilicate zeolites with open framework structures, research on extended metal phosphate structures gained momentum. Similarly, recent realization that larger solids can be built rationally from preformed molecular precursors has led to an outburst of activity in the synthesis of smaller metal phosphate molecules. Although there have been a few review articles in the literature in recent years on developments in metal phosphate chemistry covering narrow themes, for example, phosphate ester hydrolysis (by a given metal system),[18] organophosphonates,[19] and focus on one type of framework solids (see section 3.1), no single review has appeared in the literature covering all aspects of interactions between metal ions and phosphates.

R. Murugavel received his B.Sc. and M.Sc. from University of Madras and Ph.D. from IISc, Bangalore. He was an Alexander-von-Humboldt Fellow in Goettingen before joining IIT-Bombay, where he is presently a Professor. His research focus is in the area of synthetic inorganic chemistry and main group chemistry applied to materials science and catalysis. He has published over 100 papers including two earlier *Chemical Reviews* papers. He is a recipient of J. C. Ghosh Medal, DAE Young Scientist Award, Swarnajayanti Fellowship, and Chemical Research Society of India Bronze Medal.

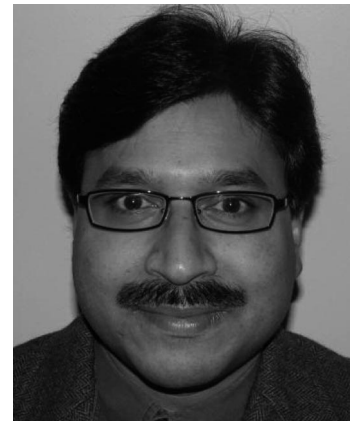

Amitava Choudhury received his M.Sc. in chemistry from the University of North Bengal. Afterwards, he received a Ph.D. degree from IISc, Bangalore, for his work on open-framework materials. His dissertation was recognized as the best thesis in materials science and was awarded the K. P. Abraham medal of IISc Bangalore in 2003. Currently he is a postdoctoral fellow at Colorado State University.

1.2. Coverage

Although it may seem that the areas of metal phosphate complexes and open framework phosphates are unconnected, recent results show that there is a strong interdependency between these themes. In a recent personal account,[20] we have shown how an exposure to both these areas can help to build new materials. During the writing of the *Accounts of Chemical Research* article,[20] we felt the need for a comprehensive review covering both smaller and open framework phosphates side by side. The result is this review article, which is presented in two major parts for the purposes of flow and ease of presentation (sections 2 and 3). In section 2, the chemistry of organophosphate ester complexes has been reviewed. All complexes that have been sufficiently well characterized, often through a single X-ray diffraction study, are included in this part of the review. The coverage

Mrinalini Walawalkar has studied chemistry at the University of Bombay, IIT-Bombay, IISc-Bangalore, and University of Goettingen. She has been an Alexander-von-Humboldt Fellow (Bochum and Goettingen), Scientific Officer, and DST Young Scientist (IIT-Bombay), and Reader (UICT) before she has taken a brief break from chemistry to be a homemaker and raise her little daughter Disha. Her research interests are in the area of inorganic materials and molecular assemblies. She has published over 50 papers including an earlier *Chemical Reviews* paper.

After completing a M.Sc. from Madurai Kamaraj University, R. Pothiraja obtained his Ph.D. degree in 2005 from IIT-Bombay working on the synthesis of organic soluble metal phosphates. Later he was a postdoctoral associate at the University of Florida, Gainesville. Presently he is an Alexander-von-Humboldt Fellow at the University of Bochum.

of the material in section 2 starts from the first structurally characterized phosphate ester metal complex and is up to date as of the beginning of 2007. There are number of studies on interaction of metal ions with phosphate groups of ATP, DNA, RNA, and other sugar molecules. While in some of these complexes the phosphate group coordinates to the metal, in most other complexes phosphate shows no direct bonding to the metal. Studies on such complexes have been excluded from this review other than one or two cases where the complexes of some sugar phosphate complexes resemble simple organophosphate metal complexes.

Section 3 of this review is restricted to phosphate-based materials and is based on a comprehensive survey of the available literature. (see section 3.1).

2. Metal Complexes of Organophosphate Esters

2.1. Phosphate Esters as Ligands

While phosphoric acid forms extended complexes because of the presence of three acidic protons, derivitazation of one or two hydroxyl groups of the phosphoric acid by ester formation $(OR)P(O)(OH)_2$ and $(OR)_2P(O)(OH)$ normally

C. N. R. Rao obtained his Ph.D. degree from Purdue University and D.Sc. degree from the University of Mysore. He is the Linus Pauling Research Professor at the Jawaharlal Nehru Centre for Advanced Scientific Research and Honorary Professor at the Indian Institute of Science (both at Bangalore). His research interests are in the chemistry of materials. He has authored over 1400 research papers and edited or written 40 books in materials chemistry. A member of several academies including the Royal Society and the U.S. National Academy of Sciences, he is the recipient of the Einstein Gold Medal of UNESCO, the Hughes Medal of the Royal Society, and the Somiya Award of the International Union of Materials Research Societies (IUMRS). In 2005, he received the Dan David Prize for materials research from Israel and the first India Science Prize.

results in the formation of metal complexes that are discrete molecules or clusters. A small number of examples of one-dimensional polymers formed by the organoesters are also covered in the first part of the review. Attempts have been made to cover every metal phosphate complex known in the literature with a single-crystal diffraction study,

The sections to follow will establish that the diesters of phosphoric acid, $(RO)_2P(O)(OH)$, are very similar to carboxylic acids in some ways (but different in many other ways) and hence form either mononuclear or dinuclear metal phosphates more readily than larger clusters. However, phosphate diesters do not exhibit a chelating mode of coordination, which is very common among metal carboxylates. While bridging two adjacent metal ions is the most preferred mode of coordination for the phosphate diesters, there are a number of complexes where these molecules are monodentate through the $P-O^-$ group with dangling $P=O$ groups. The presence of uncoordinated $P=O$ groups in many of the complexes leads to some interesting secondary interactions, normally through the formation of hydrogen bonds.

Phosphate monoesters, on the other hand, due to the presence of two acidic protons and one phosphoryl oxygen, tend to embrace more metal ions around them and form larger aggregates. Building units of several zeolitic structures can be modeled using these monophosphate esters, as in the case of phosphonic acids.

It should also be noted that phosphinic acids and phosphonic acids are essentially similar in their constitution to the phosphate diesters and monoesters, respectively, other than the presence of an extra oxygen between phosphorus and the alkyl or aryl group in the latter class of compounds (Figure 1). Parallel to the development of metal phosphate chemistry, there have been some exciting developments in the metal phosphinate and phosphonate chemistries. A full discussion on these developments is out of scope of this review both in terms of the nature of the products obtained and the volume of the work that has been carried out (see section 2.16).

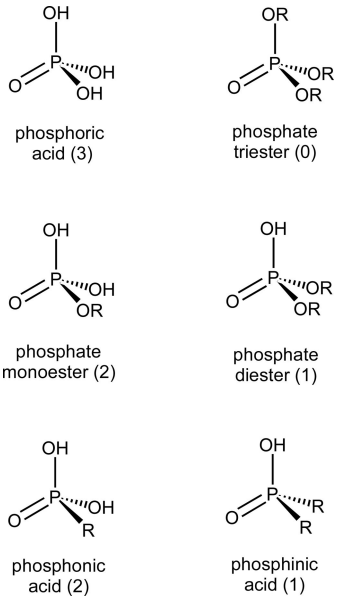

Figure 1. Phosphoric acid, phosphate esters, and phosphinic and phosphonic acids. The maximum number of acidic protons available for metalation reaction in each case is shown inside parentheses.

2.2. Group 1 and 2 Metal Phosphates

2.2.1. Group 1

Sodium and potassium salts of mono- and dialkyl/aryl phosphates have been extensively used for a long time as starting materials in the preparation of other metal phosphates through metathetical reactions. However, they are often generated *in situ* and hence no detailed studies have been carried out to establish their molecular structure in the solid state, although their spectral behavior in solution has been investigated.[21] The structurally characterized group 1 metal phosphates include $[(MeO)P(O)(ONa)_2]\cdot 6H_2O$ (**1**),[22a] $[(KO)(O)P(O^tBu)_2\cdot HO^iPr]_4\cdot 8HO^iPr$ (**2**),[22b] and K(18-crown-6)$]^+[(OCH_2CMe_2CH_2O)PO_2]^-\cdot H_2O$ (**3**) (Figure 2).[22c] In a recent study, four different potassium complexes of 4-nitrophenylphosphate (H_2NPP), namely, $[K(H_2NPP)(HNPP)]$ (**4a**), [K(HNPP)(MeOH)] (**4b**), $[K(H_2NPP)(OH_2)_2]$ (**4c**), and $[K_2(NPP)(OH_2)_4]$ (**4d**) along with the parent acid itself have been characterized by single-crystal X-ray diffraction studies by Kuczek et al.[22d]

Cubic and columnar thermotropic mesophases of potassium dialkylphosphate salts $[(CH_3(CH_2)_nO)_2P(O)(OK)]$ (n = 8−18) have recently been studied by differential scanning calorimetry (DSC), polarizing optical microscopy, and X-ray diffraction,[23a] while an early work reports on the synthesis of sodium salts of mono- and dialkylphosphates with long alkyl chains and the determination of d spacing in these systems by diffraction studies.[23b]

Ueyama and co-workers have recently studied the reaction of sterically hindered phosphate ester $[2,6\text{-}(Ph_3C\text{-}CONH)_2\text{-}C_6H_3OPO_3H_2]$ (LH_2) with sodium ion and isolated the hexameric sodium complex $[NEt_3H]_2[Na_3(\mu_3\text{-}L)(\mu_2\text{-}L)(\mu_2\text{-}MeOH)_2(OH_2)(MeOH)_5]_2$ (**5**) (Figure 2). In the centerosymmetric anionic part of the complex, the three sodium ions exhibit three different coordination geometries with coordination numbers 4, 5, and 6.[24]

There are no well-characterized phosphate complexes of other higher alkali metal ions. Other alkali metal ion phosphates, which also incorporate metal ions from other groups, have been discussed under the groups of the second metal ion.

2.2.2. Magnesium

Magnesium is one of the essential cofactors in biology. Magnesium ions participate in many important biochemical transformations including the hydrolysis of phosphate esters. The magnesium phosphate $[Mg(O_2P(OEt)_2)_2]$ (**6**), whose unit cell parameters were described as early in 1954,[25a] was later structurally characterized in 1973 by Ezra and Collin.[25b] The structure of **6** reveals that the Mg center is coordinated to four phosphoryl oxygens in a nearly tetrahedral arrangement. Magnesium diphenylphosphate,[26] $[Mg(dpp)_2]$ (**7a**) (dpp = diphenylphosphate) was synthesized from tris(tetrahydrofuran)magnesiumbromide and $(PhO)_2P(O)(OCH_3)$. The hydrated magnesium diphenylphosphate, $[Mg_3(dpp)_6(H_2O)_5]$ (**7b**) (Figure 3), has been synthesized by Ramirez et al.[26b] using magnesium diphenylphosphate as a precursor in wet diethyl ether. Compound **7a** consists of infinite chains of phosphodiester molecules linked through Mg^{2+} ions, and there are two types of magnesium ions with coordination numbers 5 and 6. Recently, a dimethyl formamide (DMF) adduct of magnesium diphenylphosphate, $[\{Mg(dpp)(DMF)\}(CF_3SO_3)]_n$ (**8**) has been structurally characterized by Adams et al.[27] The structure of **8** is a 1D polymer with octahedral magnesium ions that are bridged by dpp ligands in trans fashion. The other four coordination sites are occupied by neutral DMF ligands. A noncoordinated trifluoromethanesulfonate counterion provides charge balance.[27]

The carboxylate-bridged dinuclear magnesium unit, $[Mg_2(O_2CR)]^{3+}$, is emerging as a ubiquitous structural motif in many phosphate ester processing enzymes.[28] These magnesium-dependent enzymes, for example, phosphatase[29] and rat DNA polymerase,[30] reveal a carboxylate-bridged bimetallic active center. Synthesis and characterization of small inorganic complexes that contain a carboxylate-bridged dimagnesium(II) core are important to mimic the biologically active sites. In 1995, Lippard et al. have reported a magnesium phosphate, $[Mg_2(XDK)(dpp)(CH_3OH)_3(H_2O)(NO_3)]\cdot 3CH_3OH$ (**9**), in which magnesium centers are bridged by the carboxylate groups of XDK (H_2-XDK = *m*-xylylenediamine-bis(Kemp's triacid imide)) and by the bidentate diphenylphosphate ligand (Figure 3).[31] The structure of the related $[Mg_2(XDK)(dpp)_2(CH_3OH)_3(H_2O)]\cdot CH_3OH$ (**10**) contains both bridging and terminal diphenylphosphate groups (Figure 3). The corresponding calcium complex, $[Ca_2(XDK)(dpp)_2(CH_3OH)_3(H_2O)]\cdot CH_3OH$ (**11**), has also been reported.[31,32]

The presence of an additional functional group on the phosphate ligand has been investigated through the synthesis of $[MgL_2(H_2O)]\cdot 2H_2O$ (**12**), where L = $[HO_3POCH_2\text{-}CH_2NH_2]^-$, which exists in the form of zwitterionic $[^-O_3POCH_2CH_2NH_3^+]^-$.[33] The magnesium ion in **12** is surrounded by four water molecules in the equatorial plane and two phosphate groups on the axial sites (Figure 3). Two additional magnesium phosphates that fall in this category are the magnesium phenylphosphatosulfate, $\{[Mg(PhOPO_3\text{-}SO_3)(dmf)_3]\cdot dmf\}_2$ (**13**),[34] and magnesium bis(phosphoenolpyruvate)dihydrate, **14** (Figure 3).[35] Single-crystal X-ray diffraction studies reveal that the former complex **13** is a centrosymmetric dimer where each octahedral magnesium ion is surrounded by bridging phosphatosulfate and dmf ligands.[34] The magnesium ion in the latter complex **14** is surrounded by four phosphate oxygen atoms and two water molecules.[35]

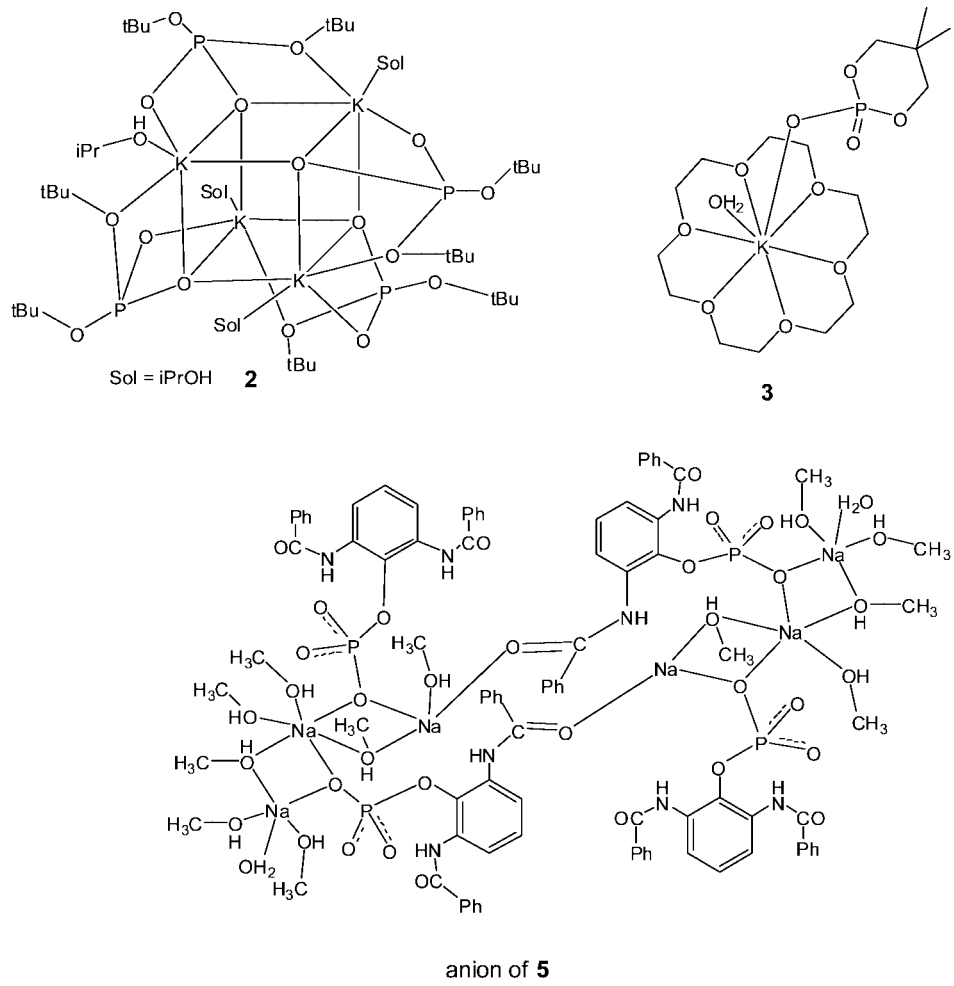

Figure 2. Alkali metal phosphates.

2.2.3. Calcium

Phosphate complexes of calcium ions are of great interest to chemists and biologists in view of the interaction of Ca^{2+} ion with phosphate sugars in biological systems and the importance of these ions in calcification inhibitors in vitro. Several complexes of calcium with a variety of phosphate ligands have been synthesized and isolated in the solid state, and the molecular structures have been determined by single-crystal X-ray diffraction studies. Significant among these complexes are the isolation of mononuclear, octanuclear, and 1D polymeric calcium phosphates derived from a monoaryl dihydrogen phosphate with strategically oriented bulky amide groups.[24,36] In $(NMe)_4[Ca(O_2P(OH)OAr)_3(MeCN)_3]$ (Ar = 2,6-$(Ph_3C\text{-}CONH)_2C_6H_3$) (**15**) (Figure 4), the arylphosphate ligand is only mono-deprotonated while $[(Ca(O_3POAr)_2\}\text{-}(OH_2)_3(MeOH)_2]$ (**16**) has the arylphosphate in the dianionic state. The calcium−oxygen (phosphate) linkages in these complexes have been proposed to contain a partial degree of covalency. A dynamic transformation of the calcium zigzag chain structure $[Ca(O_3POAr)_2(OH_2)_4(EtOH)]_n$ (Ar = 2,6-$(PhCONH)_2C_6H_3$) (**17**) (Figure 4) to the cyclic octanuclear form $[Ca_8(O_3POAr)_8(dmf)_8(OH_2)_{12}]$ (**18**) (Figure 4) is induced by changing the coordination of dimethylformamide ligands, resulting in a reorganization of the inter- and intramolecular hydrogen bond network.

Demadis et al. have reported on calcium complexes of naturally occurring phosphocitrate (PC) in order to understand the calcification inhibitor role in vivo.[37] A polymeric mixed salt of PC, $[CaNa(PC)_2(OH_2)]_n$ (**19**) (Figure 5), containing a nine-coordinated calcium center along with a Ca−O−P linkage, acts as a potent inhibitor of plaque formation in vivo as documented by calcification inhibition studies on rats.[37] The crystal structures of calcium aminoethyl hydrogen phosphate[33] and calcium bis(phosphoenolpyruvate)dehydrate,[38] have also been determined.

2.2.4. Strontium

The only structurally characterized phosphate complex of strontium ion,[39] $[Sr(O_2P(O\mathit{n}Bu)_2)_2(H_2O)(18\text{-crown-}6)]$ (**20**), was obtained by Burns et al. starting from strontium hydroxide, 18-crown-6 and di-*n*-butylphosphate. The molecular structure of **15** shows that the strontium ion is buried inside the 18-crown-6 cavity and is coordinated on either side by the oxygen atom of a di-*n*-butylphosphate. A water molecule additionally coordinates to the Sr^{2+} ion from one of the sides of the macrocyclic ring. The corresponding di-*tert*-butylphosphate complex also has a similar structure.

2.2.5. Barium

The first barium phosphate ester, $[Ba(O_2P(OEt)_2)_2]_n$ (**21**), which has been reported by Kyogoku et al.,[40] was synthesized by starting from triethylphosphate and barium hydroxide in the presence of hydrochloric acid. This molecule is polymeric in nature, and the central barium ion is coordinated to eight oxygen atoms from six diethylphosphate

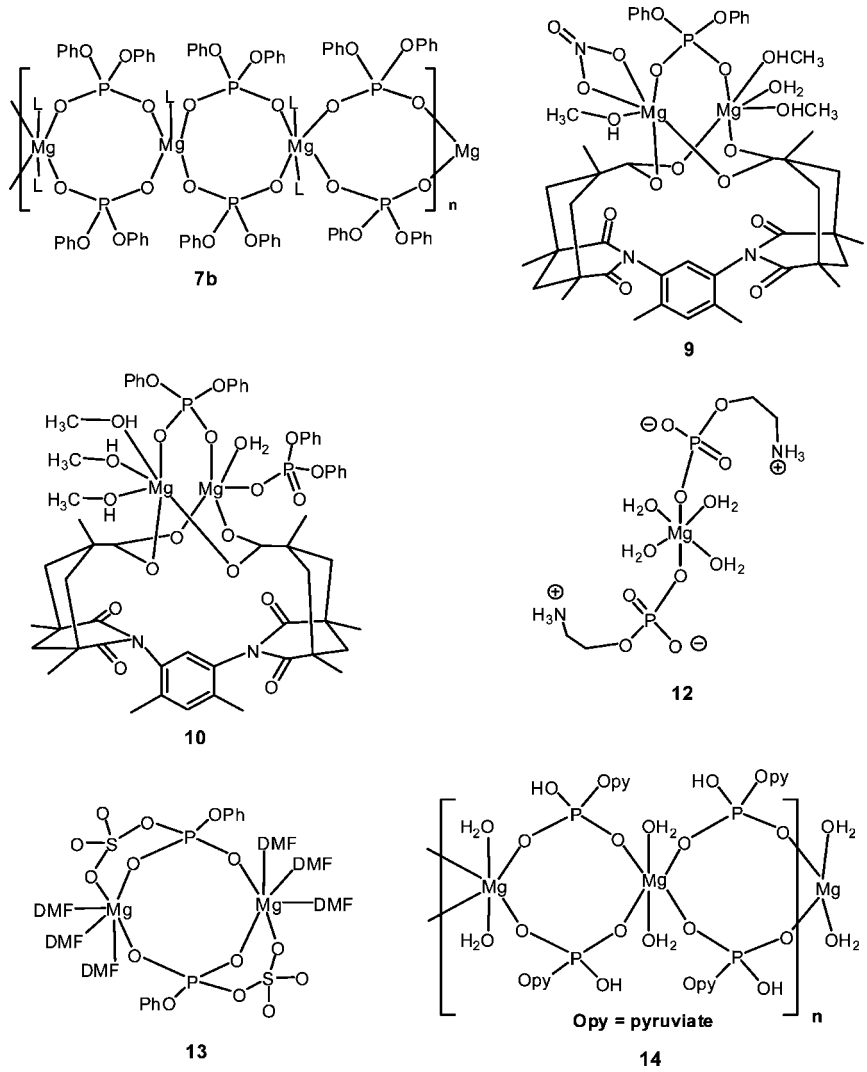

Figure 3. Monomeric, oligomeric, and polymeric magnesium phosphates.

ligands. Each diethylphosphate anion is bound to three barium ions through its oxygen atoms. Burns has also reported on bis(di-*n*-butylphosphate)aquabarium-18-crown-6, $[Ba(O_2P(OnBu)_2)_2(H_2O)(18\text{-crown-}6)]$ (**22**) (Figure 5) whose structure resembles that of the strontium complex **20**.[41]

2.3. Group 3 and 4 Metal Phosphates

2.3.1. Group 3

There are no fully characterized organophosphate complexes of group 3 metals in the literature. There are a few reports on the Sc and Y complexes of trialkylphosphates where the metal ion is coordinated by a phosphoryl P═O group rather than a $P-O^-$ moiety, and hence, these complexes do not warrant a discussion here.

2.3.2. Titanium

Titanium phosphate materials have been studied for a variety of applications such as ion-exchange materials,[42] nonlinear optical materials,[43] and fast ion conductors.[44] Thorn et al. have reported three families of titanium phosphate compounds, namely, chlorotitanium, imidotitanium, and oxotitanium phosphates.[45] The chlorotitanium phosphate derivative, $[Ti_2Cl_7(O_2P(OSiMe_3)_2)(OP(OSiMe_3)_3)]$ (**23**) (Figure 6), has been synthesized from the reaction between $TiCl_4$ and tris(trimethylsilyl)phosphate. The first example of a dimeric titanium compound, $[^tBuN{=}Ti(O_2P(OSiMe_3)_2)_2]_2$ (**24**) (Figure 6), with a terminal imido group was obtained by the elimination of Me_2NSiMe_3 from the reaction between $(Me_3SiO)_3PO$ and $[(Me_2N)_2Ti(\mu\text{-}N^tBu)]_2$. Oxotitanium complex $[TiO(OSiMe_3)(O_2P(O^tBu)_2)]_4$ (**25**) (Figure 6) has been obtained from the reaction of $Ti(OSiMe_3)_4$ with $(^tBuO)_2PO_2H$. This compound is structurally similar to the well-known cubane $M_4(\mu\text{-}X)_4$ cluster compounds.[46] The cubane structure can be considered as a model for the role of phosphate in the transformation of anatase to rutile because **25** has a core resembling that of the anatase form of TiO_2.

The titanium phosphates, $[Ti(OR)_3(O_2P(O^tBu)_2)]_n$ (R = Et, **26**; ^{i}Pr, **27**) (Figure 6), have been prepared starting from di-*tert*-butylphosphate and the corresponding titanium alkoxide precursor.[22b] Addition of KOEt to a solution of **26** leads the formation of potassium containing titanium phosphate, $[Ti_2K(OEt)_8(O_2P(O^tBu)_2)]_2$ (**28**) (Figure 6). This complex exists as a dimer containing two Ti-centered, face-sharing pseudooctahedra in the unique half of the dimer.

The five-coordinate titanium(IV) *tert*-butoxide $[LTi(O^tBu)]$ (LH_3 = tris(2-hydroxy-3,5-di-*tert*-butylbenzyl)amine) reacts readily with dibenzyl phosphate to form a complex of the empirical formula $[LTi\{O_2P(OCH_2Ph)_2\}]_2$ (**29**), where the metal is in octahedral geometry.[47] The dibenzyl phosphate groups do not chelate to the titanium; instead they

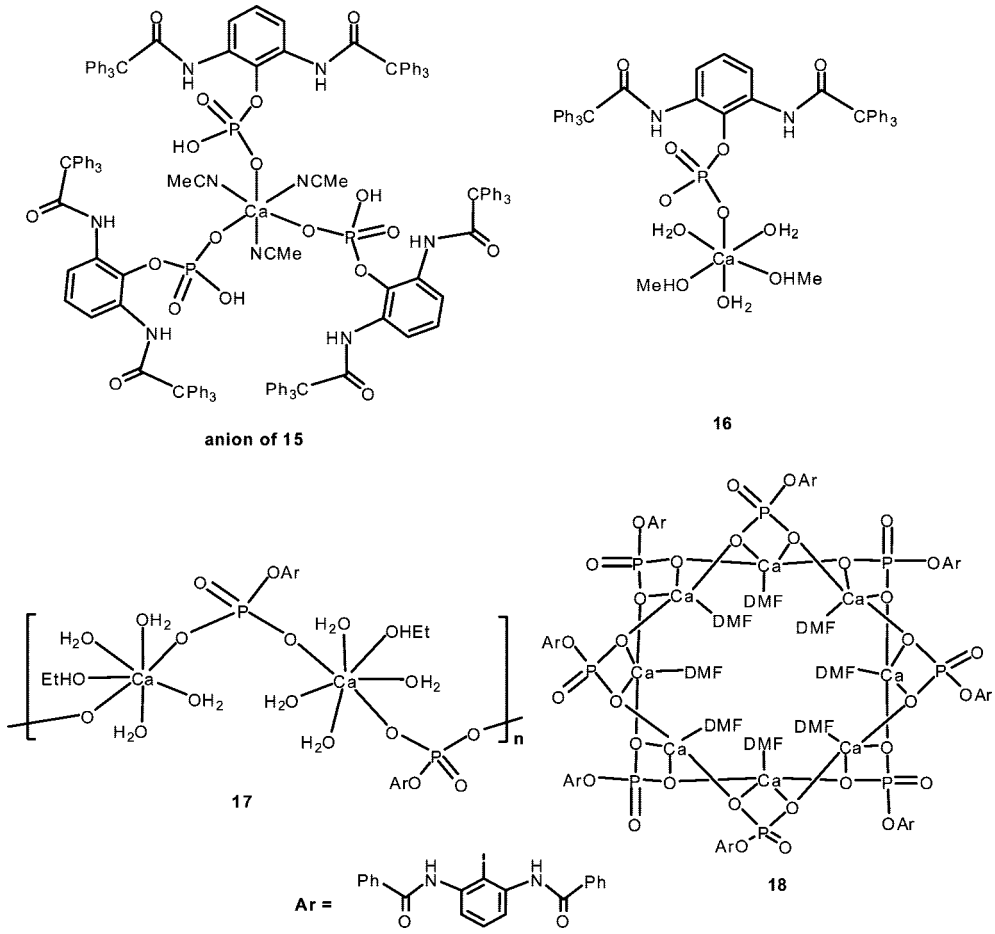

Figure 4. Calcium phosphates. In compound **18**, water molecules not shown.

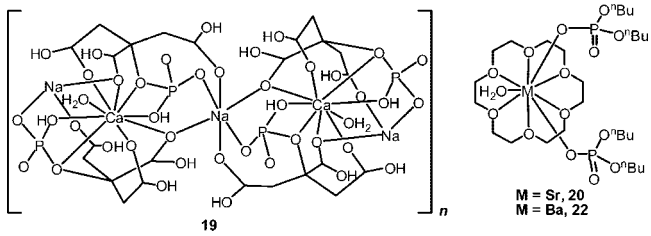

Figure 5. Molecular structure of calcium, strontium, and barium phosphates.

bridge two LTi centers forming a dimeric complex. The dimeric nature of the product is suggested by observation of a prominent peak at *m*/*z* 1986 in the FAB mass spectrum; the dimeric structure has further been established by single-crystal X-ray crystallography revealing a flat $Ti_2O_4P_2$ ring capped by the tetradentate L on each titanium.[47]

Dilithium salt of dimethyl(trimethylsilylmethyl)phosphonate in diethyl ether (with a trace of water) reacts with $[TiCl(O\textit{i}Pr)_3]$ to yield the lithium titanium phosphonate−phosphate **30** as green crystals.[48] Compound **30** incorporates two monolithiated titanium phosphonate units together with two LiCl, Li_2O, lithiated dimethylphosphonate, and lithiated dimethylphosphate as additional bridging ligands. It has been suggested that the formation of the bridging dimethylphosphate ligand in **30** is due to the decomposition product of a dilithiation−titanation sequence.[48]

2.3.3. Zirconium

The chemistry of zirconium phosphonates is very well developed and the synthesis and structural characterization of several layered mono- and diphosphonates have been reported. However, the molecular phosphate chemistry of zirconium is limited to a very few studies.

The treatment of $ZrO(NO_3)_2$ with the Klaui tripodal ligand $([CpCo\{P(O)(OEt)_2\}_3]^-$ (L^-) in dilute HNO_3 gives a water-soluble tetranuclear hydroxo-bridged Zr^{IV} compound, $[Zr_4L_4(\mu_3\text{-}O)_2(\mu\text{-}OH)_4(H_2O)_2](NO_3)_4$ (**31**), which reacts with a phosphodiester to give $[Zr_4L_4(\mu_3\text{-}PO_4)_4]$ (**32**) as a cubane cluster.[49] The reaction of $ZrO(NO_3)_2$ with NaL in the presence of Na_3PO_4 gave $[Zr_3L_3(\mu_3\text{-}O)(\mu\text{-}OH)_3(\mu_3\text{-}PO_4)]NO_3$ (**33**). The crystal structures of these complexes determined by X-ray diffraction studies reveal interesting structural features.[49]

Recently Kumara Swamy et al. have synthesized dimeric and trimeric zirconium phosphates $[Zr\{\mu,\mu'\text{-}O_2P(O^t\text{Bu})(OPh)\}(\mu\text{-}OPh)(O^t\text{Bu})_2]_2$ (**34**) and $Zr_3(\mu,\mu'\text{-}O_2P(O^t\text{Bu})_2)_5(O^t\text{Bu})_7\cdot 1/2C_6H_5CH_3$ (**35**) (Figure 6).[50] Compound **34** is a dimeric zirconium phosphate, in which each zirconium ion is octahedrally coordinated by two bridging phenoxide ions, two bridging phenyls, *tert*-butyl phosphate ions, and two terminal *tert*-butoxide ions. Trimeric zirconium compound **35** consists of three different zirconium atoms. One of the terminal zirconium ions is octahedrally coordinated by three bridging phosphate ions and three *tert*-butoxide ions, while the other terminal zirconium ion is pentacoordinated through two bridging phosphate ions and three *tert*-butoxide ions. The middle zirconium ion is hexacoordinated by five bridging phosphate ions and one *tert*-butoxide ion.

Leumann et al. have synthesized a Zr−porphyrinate−phosphate complex, $[(\mu\text{-}\eta_2\text{-mmp})(\mu\text{-dmp})_2ZrTPP]_2$ (**36**) (dmpH = dimethyl phosphate, $mmpH_2$ = monomethyl phosphate,

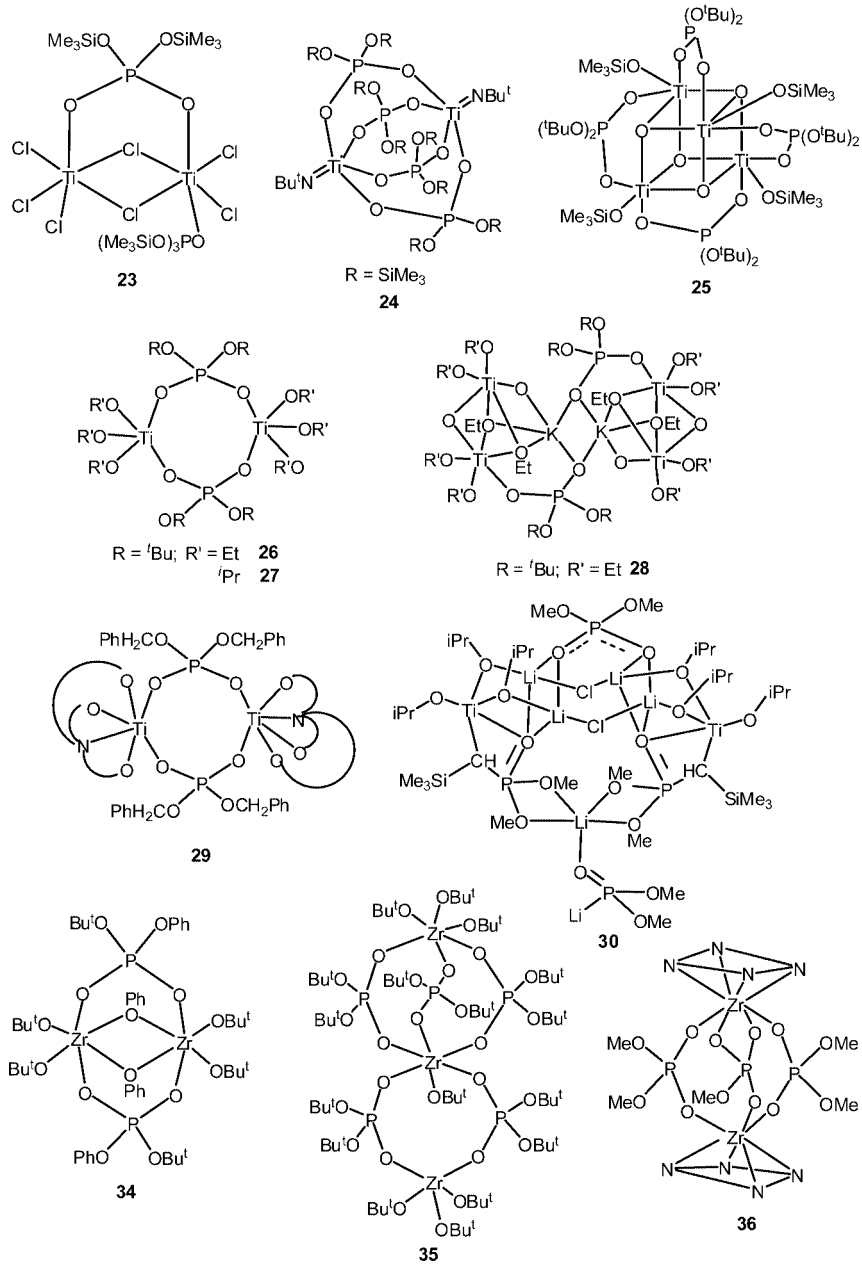

Figure 6. Group 4 metal phosphates.

and H_2TPP = tetraphenylporphyrine) (Figure 6) by the reaction of $Zr(TPP)Cl_2$ with dmpH.[51] The structure of the complex represents the first crystal structure of a Zr−porphyrinate−phosphate complex. In this compound two μ-dmp units and one μ-η_2-monomethylphosphate anion (mmp) bridge two zirconium ions and form a sandwich complex in which the Zr^{4+} ions are either seven- or eight-coordinate. All terminal oxygen atoms of phosphates are complexed to the metal. The occurrence of a monomethyl phosphate in the structure can be explained by the hydrolysis of dmp. The two porphyrinates are eclipsed.

2.3.4. Hafnium

All reports concering the hafnium phosphate complexes relate to either adduct formation with trialkylphosphates or solvent extraction of hafnium ions using phosphate extractants. No isolated and well-characterized organophosphate complex of hafnium exists in the literature.

2.4. Group 5 metal phosphates

2.4.1. Vanadium

Vanadium phosphates have been known as catalysts in various organic transformations (e.g., vanadyl pyrophosphate).[52] Molecular cluster precursors that are soluble and processable and can be readily decomposed by pyrolysis to yield pure phase metal phosphates provide structural insights into the catalyst active sites and clues to favorable structural motifs of the heterogeneous catalysts themselves. They also provide mechanistic clues to the surface chemistry responsible for the catalysis. The vanadyl phosphate, $[Cp_2V(OH_2)_2 \cdot 2(dpp)]$ (**37**), was reported by Marks et al.,[53] as a part of a more exhaustive study on the interaction of the organometallic antitumor agent Cp_2VCl_2 with nucleotides and phosphate esters in order to unravel mechanistic implications. The molecular structure of **37** consists of pseudotetrahedral $[V(\eta^5\text{-}C_5H_5)_2(OH_2)_2]^{2+}$ cations interacting via strong hydrogen bonds with the diphenylphosphate anions.

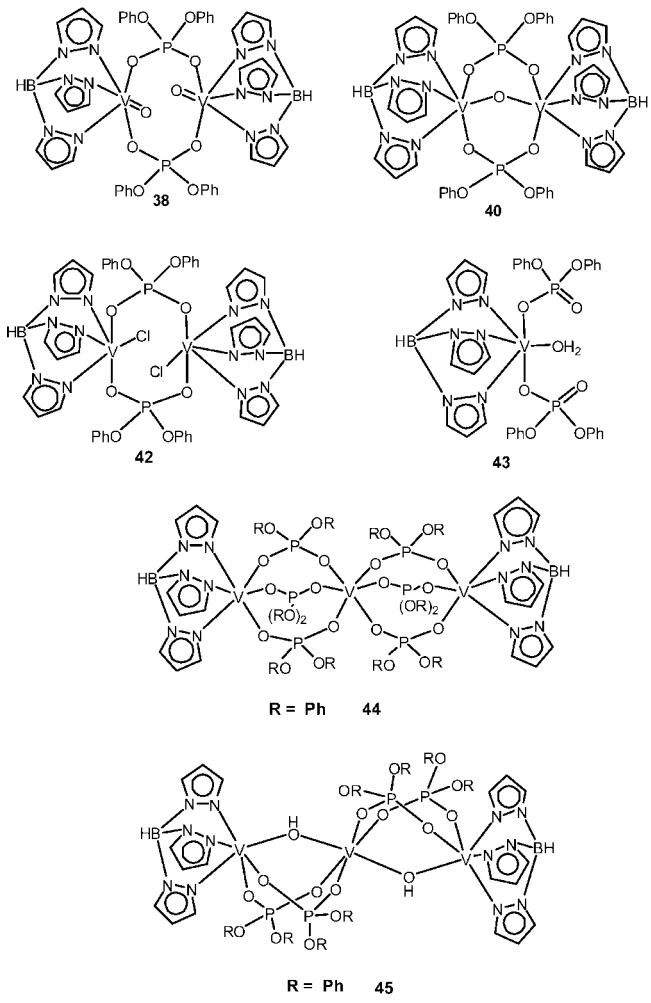

Figure 7. Structures of vanadyl phosphates. In the case of **44** and **45**, only the cationic part is shown.

A number of interesting vanadyl phosphates based on tridentate hydridotris(pyrazolyl)borate were recently reported by Carrano and co-workers. The diphenylphosphate complex, $[LVO(dpp)]_2$ (**38**) (L = hydridotris(pyrazolyl)borate) (Figure 7), reported in 1995,[54] contains the vanadium ions in a distorted octahedral coordination geometry. Three of the four terminal coordination sites at each vanadium center are occupied by the hydridotris(pyrazolyl)borate capping ligand. The vanadyl oxygen occupies the fourth terminal site. The remaining two coordination sites at each vanadium center are occupied by the oxygen atoms of the two bridging diphenylphosphate ligands resulting in the formation of a dinuclear cluster, **38**. The corresponding 3,5-dimethylpyrazolyl derivative, $[L'VO(dpp)]_2$ (**39**), (L′ = hydridotris(3,5-dimethyl-pyrazolyl)borate), has also been synthesized and structurally studied. The skeletal structure of this compound resembles that of **38**.[55]

An oxo-bridged vanadium phosphate, $[V_2O(dpp)_2(L)_2]$ (**40**) (Figure 7), and a hydroxo-bridged vanadium phosphate, $[V_2(OH)(dpp)_2)_2(L)_2](CF_3SO_3)$ (**41**) (L = hydridotris(pyrazolyl)borate), were prepared starting from $[V_2O(O_2CCH_3)_2(L)_2]$ and sodium diphenylphosphate. The structures of **40** and **41** are similar to those of **38** and **39**, where the terminal V=O groups are replaced by a V−O−V linkage.[55] Compounds $[LVCl(dpp)]_2$ (**42**) and $[LV(dpp)_2(H_2O)]$ (**43**) (L = hydridotris(pyrazolyl)borate; Figure 7) have been obtained from the reaction between $[LVCl_2(DMF)]$ and sodium diphenylphosphate.[56] In **42**, the V^{3+} ion is in a pseudo-octahedral geometry. Three of the coordination sites around the metal ion are occupied by the hydridotris(pyrazolyl)borate capping ligand, while a chloride ion and two phosphate oxygen atoms occupy the remaining sites. The oxygen atoms of the phosphate ligands bridge the vanadium centers. In **43**, the central V^{3+} ion is in a distorted octahedral environment with a facially coordinating hydridotris(pyrazolyl)borate, two unidentate diphenylphosphate moieties, and a coordinated water molecule.

Carrano et al.[57] have synthesized two homometallic trinuclear vanadium phosphates, $[(LV(dpp)_3)_2VL]PF_6$ (**44**) and $[(LV(dpp)_2(OH))_2V]ClO_4$ (**45**) (Figure 7). Complex **44** consists of two terminal V^{3+} ions capped by the hydridotris(pyrazolyl)borate group and linked to a central V^{3+} ion by three diphenylphosphate bridges. The later complex also has a similar structural type, where one bridging diphenylphosphate anion between the adjacent vavadium ions is replaced by a hydroxide ion. Magnetic measurements indicate that the replacement of one phosphate bridge by a hydroxide leads to a pronounced change in the nature of coupling between the V^{3+} ions (antiferromagnetic to ferromagnetic).[57]

Tetranuclear vanadium(III) phosphate, $[L_4V_4(PhOPO_3)_4]$ (**46**), its acetonitrile adduct, $[L_4V_4(PhOPO_3)_4]\cdot CH_3CN$ (**47**), and $[L_4V_4(O_2NC_6H_4OPO_3)_4]\cdot 4C_7H_8\cdot H_2O$ (**48**) (Figure 8),[58] synthesized from $LVCl_2$(dmf) and the corresponding $ArPO_3Na_2$, represent somewhat larger aggregates of the earlier described monomeric and dimeric phosphates **38**−**45**. The major difference that led to the isolation of larger aggregates, instead of monomeric or dimeric phosphates, is the use of monoaryl phosphate in place of the diarylphosphates. Tetrameric compounds **46**−**48** have a cubane type structure in which each phosphate coordinates three different V(III) centers and each V(III) center is, in turn, coordinated by three different phosphates. The cubane aspects of the structure are easily visualized in the polyhedral representation by placing four V(III) octahedra and four phosphate tetrahedra at alternate corners of a cube in a corner-sharing arrangement. The cubic core in these molecules is comparable to the tetrameric boron, aluminum, gallium, indium, and zinc phosphonate clusters reported in recent times.[58b]

Tetranuclear molecular phosphonate analogues, $[(^tBupz)_4V_4O_4(PhPO_3)]\cdot 2H_2O$ (**49**) and $[(^tBupz)_4V_4O_4(PhPO_3)]\cdot 4CH_3CN\cdot 0.6H_2O$ (**50**) (^{t}Bupz = 3-*t*-butylpyrazole), have also been synthesized using a similar synthetic strategy by reacting $[(^tBupz)_2VOCl_2]$ with disodium salt of phenylphosphonic acid.[58] Unlike the cubic core displayed by tetrameric phosphates **46**−**48**, the phosphonates **49** and **50** exist in the form of a trinuclear basket-shaped subcluster capped by a fourth vanadyl center. The bottom of the basket in this case is a phosphonate ligand that bridges all the three vanadyl centers of the subcluster.

Interestingly, the effective magnetic moment per V(III) ion in **46** is 2.60 μ_b at 278 K, which decreases gradually to 2.29 μ_b at 40 K and then decreases rapidly to 1.30 μ_b at 6 K. These values indicate a weak antiferromagnetic coupling leading to a ground spin state of $S = 0$ for the tetrameric cluster. In view of the large separation between V(III) ions in **46** (5.1 Å), any direct metal−metal coupling would be insignificant, and the probable exchange pathway should be through a superexchange mechanism involving the phosphate bridges. Preliminary magnetic studies have suggested that a

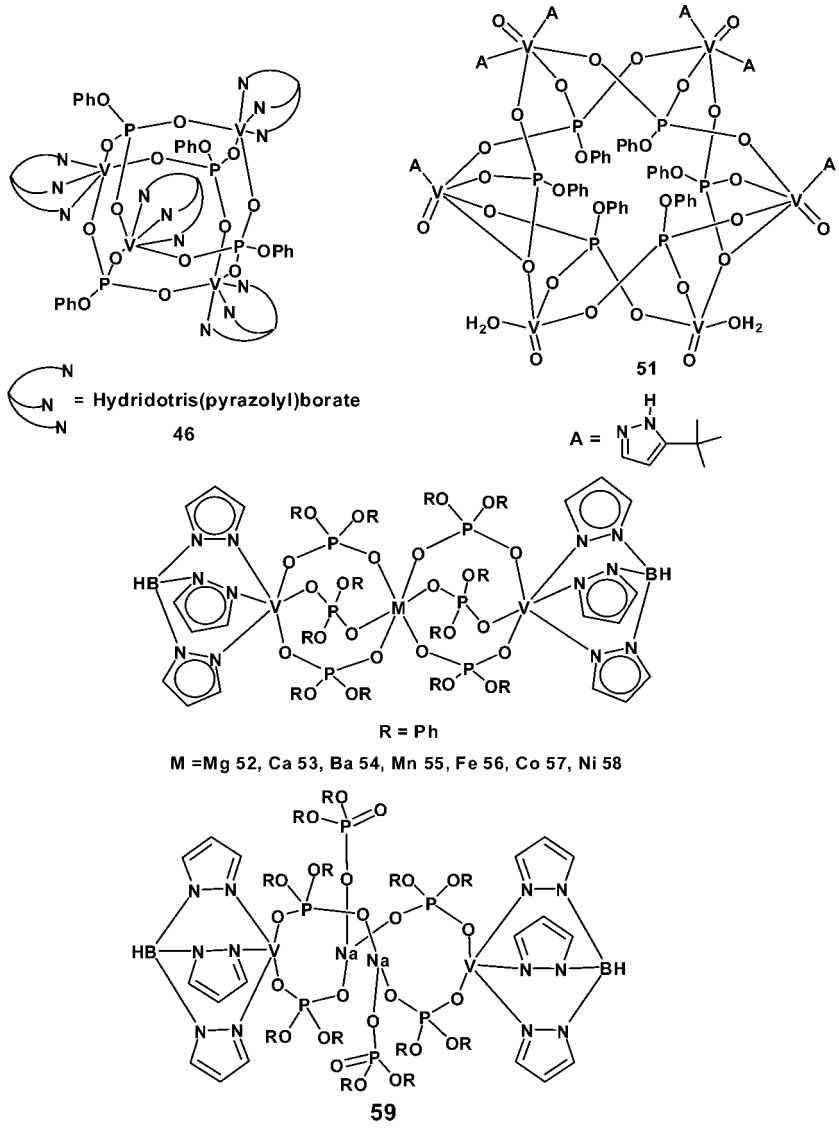

Figure 8. Cubane-like and other oligomeric vanadyl phosphates.

fairly strong antiferromagnetic coupling is observed in the basket-shaped phosphonate clusters **49** or **50**.[58]

A hexameric vanadium phosphate, $(PhOPO_3)_6(VO)_6(H_2O)_3 \cdot 2EtOH$ (**51**) (Figure 8),[59] was obtained by the reaction of aquatetrakis(3,5-*tert*-butylpyrazole)vanadyl chloride with monophenyl phosphate. This compound has three types of vanadium centers. The first type is tris(μ-phosphato)(aqua)-vanadyl with no coordinated pyrazoles. The second type is a tris(μ-phosphato)(pyrazolyl)vanadyl species, in which four phosphate oxygens bind to the metal phosphate. The third type is a tris(μ-phosphato)bis(pyrazolyl)vanadyl species.

Mixed metal complexes have attracted much attention recently because of their unusual magnetic properties and their ability to mimic biological systems. For example, enzyme phosphatase isolated from kidney beans contains a heterobincuclear ZnFe center.[60] Similarly a CoZn or MgZn core is found in bovine lens aminopeptidase,[61,62] while a MnCa unit is present in concanavalin.[63] In this context, nine vanadium-containing mixed metal complexes of the type $[LV(dpp)_3]_2M$ (M = Mg^{2+}, **52**; Ca^{2+}, **53**; Ba^{2+}, **54**; Mn^{2+}, **55**; Fe^{2+}, **56**; Co^{2+}, **57**; Ni^{2+}, **58**), $[L_2V_2(dpp)_6Na_2]$ (**59**), and $\{[LV(dpp)_3]_2M\}ClO_4$ (Al^{3+}, **60**; La^{3+}, **61**) (L = hydridotris(pyrazolyl)borate; Figure 8) have been reported by Carrano et al.[64] All these complexes are linear trinuclear species and show interesting magnetic behavior because they contain an integral spin on the central ion showing antiferromagnetic coupling.

Thorn et al.[65a] have synthesized vanadium diethylphosphate, $[(dipic)V(O)(O_2P(OEt)_2)]_2$ (**62a**; dipic-H_2 = pyridine-2,6-dicarboxylic acid; Figure 9) from diethylphosphate and [(dipic)V(O)(O^iPr)]. Compound **62a** exists as dimer with a $V_2O_4P_2$ central core surrounded by the dicarboxylate group and two bridging phosphate groups. Herron et al. have prepared the trinuclear cluster, $[(VO)_3(O_2P(OEt)_2)_6] \cdot CH_3CN$ (**62b**; Figure 9), from the reaction between diethylphosphate and vanadyl trisisopropoxide.[65b] Compound **62b** has been converted to $VO(PO_3)_2$ material at 500 °C by solid-state thermolysis. The material so formed shows catalytic activity towards oxidation of butane to maleic anhydride.

2.4.2. Niobium and Tanatalum

There is only one report in the literature on a well-characterized niobium phosphate complex. Tilley et al. have shown that the molecular precursor $[Nb(O^iPr)_4(O_2P(O^tBu)_2)]_2$ (**63**), prepared from niobium isopropoxide and di-*tert*-

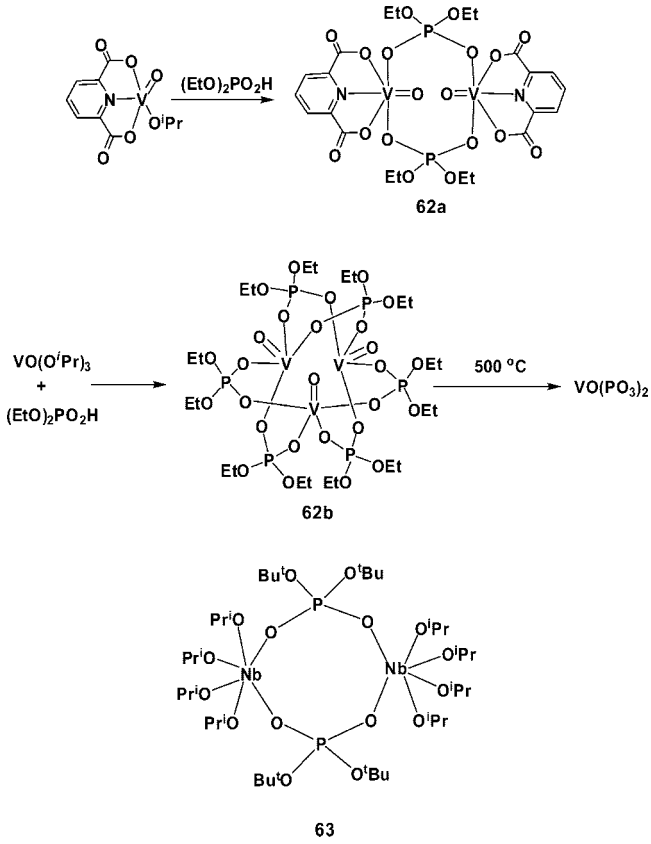

Figure 9. Synthesis of vanadium diethyl phosphates.

butylphosphate, undergoes facile thermal conversion to a low surface area niobium phosphate.[66]

Although reactions of tantalum halides with trialkyl and dialkyl phosphates have been sporadically investigated, in most cases the compounds isolated were simple adducts and hence are not described here in detail.

2.5. Group 6 Metal Phosphates

2.5.1. Chromium

Hexavalent chromium compounds are known to be potential carcinogens.[67] The uptake−reduction model suggests that chromate ion, which is isostructural to phosphate anion, enters the cell rapidly through anion channels. It is reduced intracellularly, producing intermediates such as Cr^{5+}, Cr^{4+}, free radicals, and Cr^{3+}, which react with DNA.[68] Analysis of cells of organisms that have been exposed to chromate reveal the existence of several types of stable Cr−DNA adducts containing complexes of Cr^{3+}.[69] Recent studies demonstrate that there is no base selectivity in binding of Cr to DNA and that the phosphate groups are the primary binding sites.[70]

In order to study the binding of Cr^{3+} ions to phosphodiesters as a model for DNA binding and to obtain structural, spectroscopic, and chemical information as a result of chromium phosphate complexation, Gibson et al. have reported the first model complex of the Cr^{3+}−DNA adducts, $[Cr(phen)_2(dpp)(H_2O)](NO_3)_2$ (**64**; Figure 10). [71] The synthesis of **64** is achieved from diphenylphosphate and $[Cr(H_2O)(phen)_2](NO_3)_3$. In this complex, Cr^{3+} ion is in an octahedral environment surrounded by two 1,10-phenanthroline (phen) ligands, one molecule of water, and one diphenylphosphate anion connected in a monodentate fashion. A oxo-bridged dinuclear chromium phenylphosphate complex, $[(tmpa)Cr(\mu\text{-}O)(\mu\text{-}(PhO)PO_3)Cr(tmpa)](ClO_4)_2\cdot NaClO_4\cdot 2H_2O$ (**65**; tmpa = tris(2-pyridylmethyl)-amine), has been synthesized by the reaction of $[Cr(tmpa)(OH)]_2(ClO_4)_2\cdot 4(H_2O)$ with the disodium salt of phenyl phosphate in acetonitrile.[72]

2.5.2. Molybdenum

Quadruply bonded metal−metal (M−M) systems offer opportunities to explore excited-state oxidation−reduction chemistry owing to the presence of low-energy excited states localized at a coordinatively unsaturated, redox-active bimetallic core.[73] In this connection, Trogler et al. have reported the synthesis of a tetrakis(diphenylphosphato)dimolybdenum complex, $[Mo_2(dpp)_4]$ (**66**) (Figure 10), starting from dpp-H and $Mo_2(CF_3SO_3)_4$.[74] The coordinating ligands around the Mo_2^{4+} core in this complex adopt an eclipsed conformation in which the diphenylphosphate moiety bridges the Mo−Mo quadruple bond, resulting in a D_{4h} symmetry for the Mo_2O_8 central unit. Cyclic voltametry suggests that one-electron oxidation of **66** occurs readily. The mixed valence complex $[Mo_2(dpp)_4]PF_6$ (**67**) was isolated by oxidizing **66** with $[Cp_2Fe]PF_6$. The electronic spectra of **66** and **67** exhibit $\delta\rightarrow\delta^*$ transitions (520 and 1530 nm, respectively) originating from Mo−Mo quadruple bonds.[74]

Nocera et al. have synthesized another mixed-valent Mo^{II}/Mo^{III} complex $[Mo_2(dpp)_4]BF_4$ (**68**) by reacting **66** with $NOBF_4$.[73,75] The structure of the cationic part of this complex is similar to the molecular structure of **66.** The Mo−Mo quadruple bond distance of 2.19 Å for the mixed-valent dimer **68** is 0.05 Å greater than that observed for the parent compound **66**. The mixed-valent dimer **68** shows a vibrational-structured $\delta\rightarrow\delta^*$ ($^2B_{1u}\leftarrow{}^2B_{2g}$) absorption band in the near-IR spectral region (λ_{max} = 1469 nm, ϵ = 142 M^{-1} cm^{-1}) with an energy spacing of 308 cm^{-1} that is consistent with a progression in the symmetric metal−metal stretching vibration. The mixed-valence complex **68** is reversibly reduced and oxidized by one electron. Quite interestingly, the photoreaction of $[Mo_2(dpp)_4]$ (**66**) with dichlorocarbons yields $[Mo_2(dpp)_4]^+$ and halogen-reduced organic photoproducts. For 1,2-dichloroalkanes, photoreaction is facile and affords the olefin with appreciable quantum yields, whereas photoreaction of 1,2-dichloroalkenes yields monohalogenated alkenes.[75]

Dimolybdenum(III) phosphates, $Mo_2(NMe_2)_2[\mu\text{-}O_2P(O^tBu)_2]_2[O_2P(O^tBu)_2]_2$ (**69**), $Mo_2(NMe_2)_2[OSi(O^tBu)_3]_2[\mu\text{-}O_2P(O^tBu)_2]_2$ (**70**), and $Mo_2(NMe_2)_2[\mu\text{-}O_2P(O^tBu)_2]_2\text{-}\{OB[OSi(O^tBu)_3]_2\}_2$ (**71**) (Figure 10), have been synthesized by Tilley and co-workers starting from thermally labile phosphate diester ligand dtbp-H and tri-*tert*-butoxy silanol.[76] The cis and trans isomers of **69** (**69a** and **69b**) and **70** (**70a** and **70b**) have also been isolated and structurally characterized. Owing to the presence of thermally labile *tert*-butoxy groups in these complexes, thermal decomposition of these compounds has been investigated through thermogravimetric analysis (TGA) and solution ^1H NMR spectroscopy. Xerogels with approximate compositions of $2MoO/1.5\cdot 2P_2O_5$ and $2MoO/1.5\cdot 2P_2O_5/2SiO_2$ were obtained from **69a** and **70**, respectively, via solution thermolysis in toluene. As-synthesized and dried xerogels, which contain 1 equiv of $HNMe_2$ per Mo center, have large surface areas (up to 270 m^2 g^{-1}). Upon calcination at 300 °C, the coordinated amines are lost and the surface areas are reduced to 40 and <5 m^2 g^{-1} for the materials derived from **69** and **70**, respectively. The ^{31}P-MAS NMR spectroscopy suggests that the as-

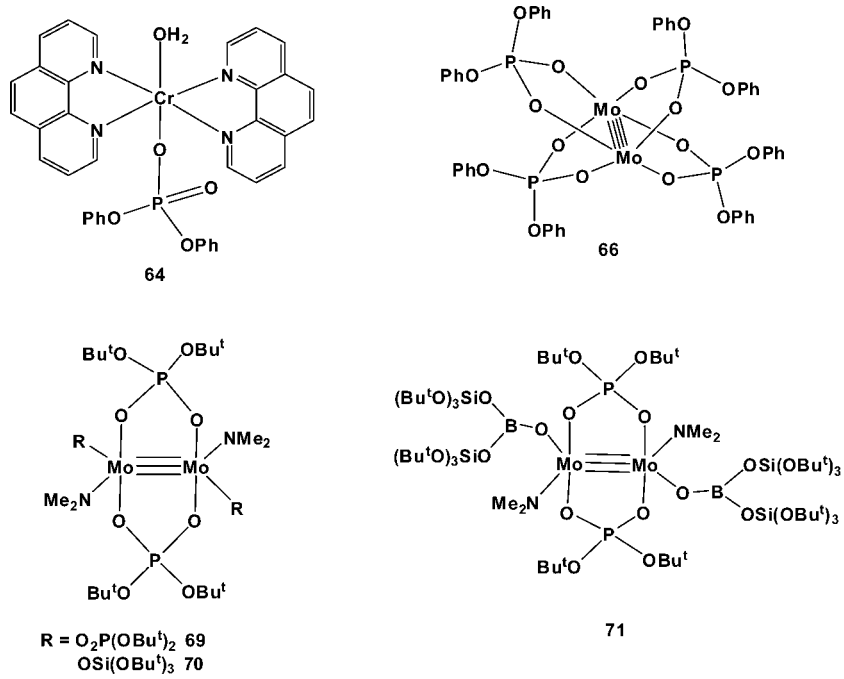

Figure 10. Group 6 metal phosphates. In the case of **64**, only the cationic part is shown.

synthesized xerogels retain structural features of the original starting molecular precursors, as indicated by the presence of resonances that correspond to both bridging and terminal $-O_2P(O^tBu)_2$ ligands. Upon calcination at 300 °C, the resonances for $-O_2P(O^tBu)_2$ groups are replaced by those for PO_4^{3-}. The material derived from **69** exhibits low activity and poor selectivity for the oxidative dehydrogenation (ODH) of propane to propylene. Cothermolysis of **68** and Bi[O-Si(O^{t}Bu)$_3$]$_3$ resulted in Bi/Mo/P/Si/O materials with improved performance for the ODH of propane.[76]

2.5.3. Tungsten

Structurally well-characterized examples of tungsten phosphate complexes have not been reported in the literature.

2.6. Group 7 Metal Phosphates

2.6.1. Manganese

There has been a great deal of interest in recent times in polynuclear complexes of manganese carboxylate complexes with a range of coligands as single-molecule magnets (SMMs).[77–81] The dodecanuclear manganese complex $[Mn_{12}O_{12}(O_2CPh)_{16}(H_2O)_4]$ is one of the most extensively studied SMMs with the largest energy barrier of 66 K ($U = S^2|D|$) for the reorientation of the magnetic moment due to its $S = 10$ ground state with a very large negative D parameter.[82] Although several chemical modifications of this cluster have been attempted,[83–86] one of the best modifications of this cluster to date is the synthesis of $[Mn_{12}O_{12}(O_2CPh)_{12}(dpp)_4(H_2O)_4]$ (**72**; Figure 11). Cluster **72** is obtained by Kuroda-Sowa at al. from the reaction of $[Mn_{12}O_{12}(O_2CPh)_{16}(H_2O)_4]$ with 4 equiv of $(PhO)_2PO_2H$.[87] The $Mn_{12}O_{12}$ core structure is very similar to that of $[Mn_{12}O_{12}(O_2CPh)_{16}(H_2O)_4]$. The central $[Mn_4O_4]^{8-}$ cubane and the outer ring of eight Mn^{III} ions are linked by eight μ^3-O^{2-} bridges. The peripheral bridging ligands are categorized into three groups. They are eight equatorial benzoates, four axial benzoates, and four axial phosphates. The axial benzoate groups are bridge Mn^{IV} and Mn^{III} ions whereas

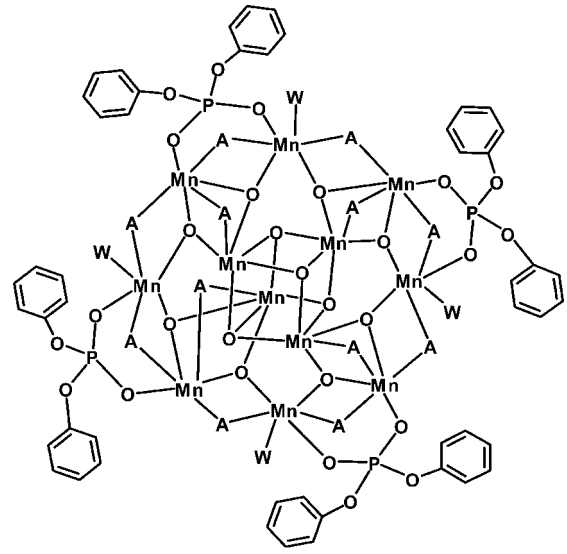

Figure 11. Molecular structures of $[Mn_{12}O_{12}(O_2CPh)_{12}((O_2P(OPh)_2)_4(H_2O)_4]$ (**72**) and $[Mn_{12}O_{12}(O_2CMe)_{12}((O_2P(OPh)_2)_4]$ (**73**).

the phosphates link two Mn^{III} ions. The arrangement of four coordinated water molecules is in a 1:1:1:1 fashion with alternating up and down positions. Four water oxygen atoms are involved in the elongated Mn−O bonds.

The same authors have synthesized the water-free acetate- and diphenyl phosphate-bridged manganese dodecamer $[Mn_{12}O_{12}(O_2CMe)_{12}(dpp)_4]$ (**73**; Figure 11) by the reaction of $[Mn_{12}O_{12}(O_2CMe)_{16}(H_2O)_4]$ with diphenyl phosphate in acetonitrile followed by vacuum distillation of the azeotrope of acetic acid and toluene.[88] The core structure of this compound is similar to **72**, except for the absence of coordinating water molecules. Compound **73** represents the only example of a Mn_{12} cluster without coordinated water molecules. The eight Mn^{III} ions in **73** can be divided into two groups: four Mn^{III} ions with six-coordination and four Mn^{III} ions with square pyramidal five-coordination, which

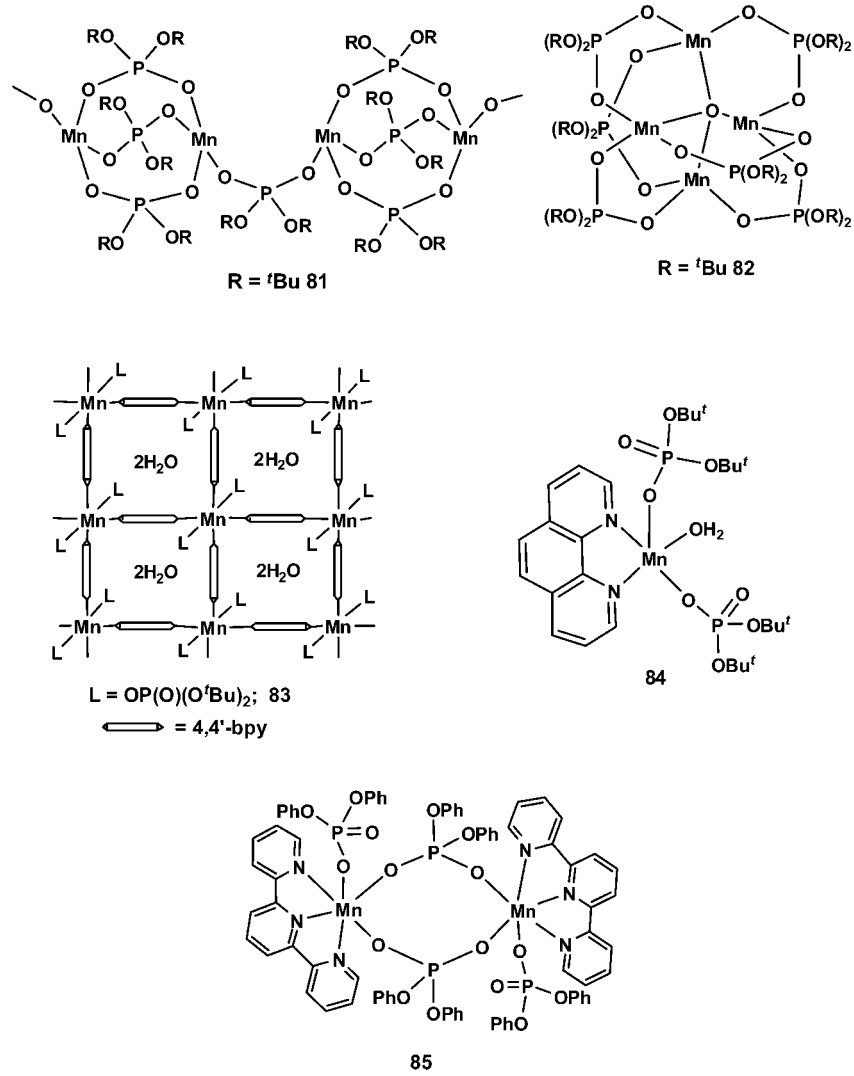

Figure 12. Molecular structures of manganese phosphates.

are arranged alternately in the cluster. The crystal structure determination further indicates that the four of the five-coordinate Mn^{III} ions have agostic interactions from one of the phenoxy hydrogen atoms of the phosphate ligand at the vacant coordination site. Detailed magnetic susceptibility measurements and magnetization hysteresis indicate that **73** is a SMM with quantum magnetization tunneling behavior. In a more recent study,[89] Kuroda-Sowa et al. have further expanded this chemistry and prepared an extended series of Mn_{12} single-molecule magnets having diphenylphosphate bridges, $[Mn_{12}O_{12}(O_2CR)_{16-x}(dpp)_x(H_2O)_y]$ (R = CH_3, x = 8, y = 2 (**74**); R = Ph, x = 8, y = 4 (**75**); and R = Et, x = 4, y = 4 (**76**)) and their tetraphenylphosphonium salts $[Ph_4P][Mn_{12}O_{12}(O_2CR)_{16-x}(dpp)_x(H_2O)_4]$ (R = CH_3, x = 4 (**77**); x = 8 (**78**); and R = Ph, x = 4 (**79**); x = 8 (**80**)).

As in the case of molybdenum, several di-*tert*-butylphosphate complexes of manganese have also been investigated with the objective of developing single source precursors to manganese phosphate materials. Reaction of $Mn(OAc)_2 \cdot xH_2O$ with di-*tert*-butylphosphate (dtbp-H) in a 1:2 molar ratio in MeOH followed by slow crystallization of the resultant solid in MeOH/THF medium gave three new polymeric metal phosphates $[Mn(dtbp)_2]_n$ (**81**; Figure 12).[90] The formation of $[Mn(dtbp)_2]_n$ proceeds via the tetrameric Mn phosphate $[Mn_4(O)(dtbp)_6]$ (**82**), which was also isolated in an analytically pure form. The molecular structure of **81** established by single-crystal X-ray diffraction studies reveal that the compound possesses a one-dimensional coordination polymeric structure with alternating triple and single dtbp bridges between the adjacent Mn^{2+} ions. Thermal analysis (TGA and DSC) indicates that **81** gets converted to the metaphosphate material $Mn(PO_3)_2$ at temperatures <500 °C. Similarly, the thermal decomposition of **82** resulted in the formation of both $Mn(PO_3)_2$ and $Mn_2P_2O_7$.[90]

The manganese one-dimensional polymer $[Mn(dtbp)_2]_n$ undergoes a facile room temperature transformation to $[Mn(dtbp)_2(4,4'\text{-bpy})_2 \cdot 2H_2O]_n$ (**83**; Figure 12) by the addition of 4,4-bipyridine.[91,92] Compound **83** forms a non-interpenetrating two-dimensional grid structure. Manganese ions in this extended solid have octahedral coordination geometry and are connected to four 4,4′-bipyridine moieties and two dtbp ligands in a trans arrangement. Each of the 4,4′-bipyridine ligand bridges two manganese atoms in an end-to-end fashion. The two unique manganese ions present in the system make two separate two-dimensional grids. These two unique grids lie one over the other in such a way that the metal ion on the second grid is in the middle of the cavity of the first grid in order to minimize the steric repulsion between the bulky phosphate ligands on the adjacent grids. The observed Mn···Mn distances offer an estimate of the size of voids or pores present in the grid structure. Interestingly, along the chain of propagation, the distances are

approximately 11.7−11.9 Å, while the distances across the grid window are 15.5 and 17.8 Å, indicating the grid windows are not exactly rectangular, but parallelepipeds. The sum of the angles within any given parallelepiped is 360°. The size of these voids, hence, allows incorporation of two water molecules per formula unit of the metal. These water molecules are hydrogen bonded to the phosphoryl oxygens of the phosphate group.[91,92]

The use of chelating diamines such as 1,10-phenanthroline in the reaction between manganese acetate and dtbp-H leads to the isolation of a monomeric phosphate $[Mn(dtbp)_2(phen)(OH_2)]$ (**84**; Figure 12).[93] Based on the molecular structure determination of the copper analogue (*vide infra*), it is assumed that in the structure of **84** the metal ion is five-coordinate with one chelating phen, two monodentate dtbp, and terminal water ligands.

Yashiro et al. have studied the reaction of a manganese−terpyridine (tpy) complex, $[MnCl_2(tpy)]$, with diphenyl phosphate and diribonucleoside monophosphate diester (NpN; N = adeninie, guanine, uracil, cytosine).[94] The hydrolysis of NpN by $[MnCl_2(tpy)]$ in aqueous solution proceeds smoothly to yield the expected hydrolysis products, monophosphate esters. The studies further revealed that the hydrolysis catalyzed by the terpyridine complex $[MnCl_2(tpy)]$ is 30 times faster than that by $MnCl_2$ at pH 7.0. On the other hand, the reaction of $[MnCl_2(tpy)]$ with diphenylphosphate does not lead to any ester hydrolysis but produces a stable dinuclear complex, $[(tpy)(dpp)Mn^{II}(\mu\text{-dpp})_2Mn^{II}(dpp)(tpy)]$ (**85**; Figure 12).[94] Each manganese ion in this complex is octahedrally coordinated by one terpyridine, two bridging diphenyl phosphate anions, and one terminal diphenyl phosphate anion.

2,6-Bis[*N*,*N*-di(2-pyridylmethyl)aminomethyl]-4-methylphenol (Hbpmp) reacts with manganese(II) ions in the presence of bis(*p*-nitrophenyl) phosphate to afford the dinuclear complex, $[Mn_2(bpmp)(bnp)_2]ClO_4$ (**86**), with two bnp^- ions.[95] The structure of **86**·2MeCN, determined by the single-crystal X-ray method, has a dinuclear core structure bridged by the phenolic oxygen atom of $bpmp^-$ and two bnp^- ions. Each metal center has a pseudo-octahedral geometry with an average Mn−donor distance of 2.207 Å. The $[M_2(bpmp)(bnp)_2]ClO_4$ (M = Ni or Zn) complexes are isostructural to **86**.[95]

2.6.2. Technetium and Rhenium

There are not many well-characterized organophosphate complexes of technetium and rhenium reported in the literature. Barring the examples of tri-*n*-butylphosphate based complexes (formed during the solvent extraction processes), technetium does not form any other stable phosphate complex. In the only example of a rhenium phosphate complex, the organophosphate, $[O_2P(OMe)_2]^-$, ligand is in fact synthesized *in situ* from the available PF_6^- anion and methanol in the reaction medium. Thus, the oxo group of $[ReO_2(1\text{-MeIm})_4]^+$ (1-MeIm = 1-methylimidazole) can be methylated with methyl trifluoromethanesulfonate in CH_2Cl_2 under mild conditions, leading to the isolation of $[ReO(OCH_3)(1\text{-MeIm})_4](CF_3SO_3)_2$, which is converted to the BPh_4^- and PF_6^- salts.[96] When the reaction is carried out in MeOH in the presence of excess PF_6^-, the phosphate ester complex $[ReO(O_2P(OMe)_2)(1\text{-MeIm})_4](PF_6)_2$ (**87**; Figure 13) is isolated. The IR spectrum shows ν(Re=O) vibrations near 960 cm^{-1} in all cases. The visible spectrum of the blue phosphate ester compound **87** resembles that of the oxo-aquo $[ReO(OH_2)(1\text{-MeIm})_4]^{3+}$ ion.[96]

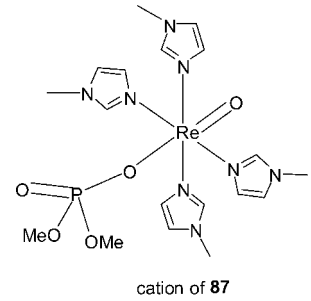

Figure 13. Structures of rhenium dimethylphosphate.

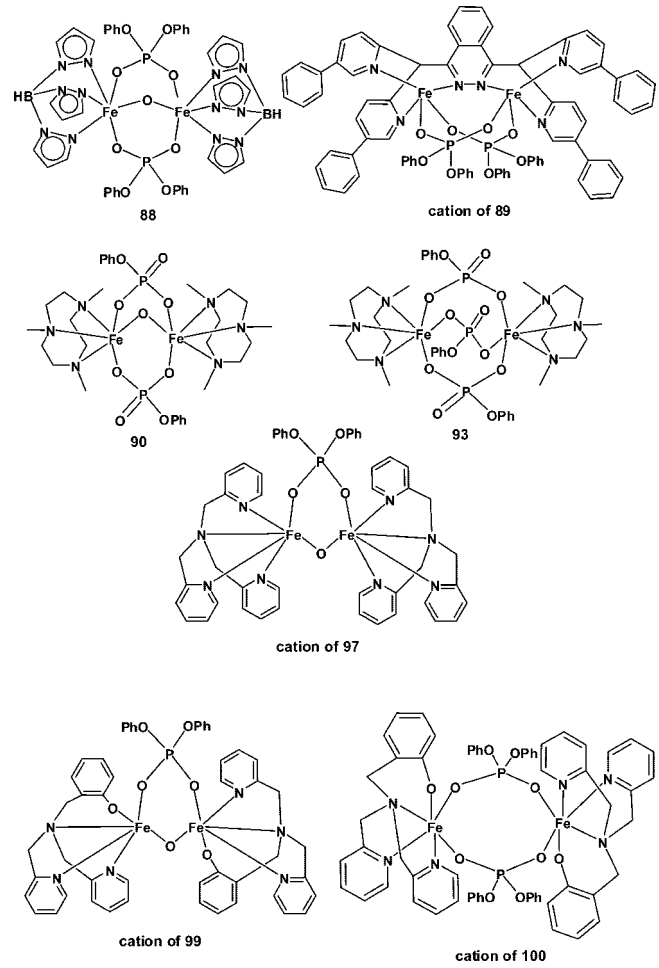

Figure 14. Iron phosphates containing polydentate nitrogen bases.

2.7. Group 8 Phosphates

2.7.1. Iron

Interactions of phosphate ligands with oxo-bridged diiron units are considered important in proteins such as purple acid phosphatases from bovine spleen,[97] ribonucleotide reductase from *Escherichia coli*,[98] the invertebrate respiratory protein hemerythrin,[99] and the mammalian iron storage protein ferritin.[100] The iron oxo/hydroxy core in ferritin contains an inorganic phosphate. The first structurally characterized iron organophosphate, $[Fe_2O(dpp)_2(L)_2]\cdot CHCl_3$ (**88**; L = hydridotris(pyrazolyl)borate; Figure 14), was reported by Lippard et al.[101,102] The structure of **78** reveals an oxo-bridged diiron core further bridged by two bidentate phosphate ligands

resulting in a $[Fe_2O(dpp)_2]^{2+}$ unit, which is capped by two pyrazolylborates. The Fe···Fe distance in **88** is 3.337(1) Å, while the Fe−O−Fe angle is 134.7(3)°. Compound **88** was characterized by magnetic ($J = -98$ cm^{-1}) and spectroscopic (IR, NMR, UV-visible) measurements.

Subsequently, Lippard et al. have reported on the synthesis and crystallographic characterization of a diiron(II) diphenylphosphate complex with a neutral sterically hindered bridging phthalazine ligand. $[Fe_2(\mu\text{-dpp})_2(Ph_4bdptz)](OTf)_2$ (**89**; Ph_4bdptz = 1,4-bis[bis(6-phenyl-2-pyridyl)methyl]phthalazine; Figure 14), synthesized from $Fe(OTf)_2 \cdot 2MeCN$, Ph_4bdptz, diphenylphosphate, and Et_3N in acetonitile, acts as a small molecular model for the catalytic sites in non-heme carboxylate-bridged diiron enzymes.[103] The aryl rings of Ph_4bdptz form a hydrophobic size-constrained pocket in which additional ligands can be accommodated, and they block the possible formation of a tetranuclear species. The Fe···Fe separation of 4.045 Å in **89** is the largest thus far observed for this type of diiron complex. The observed Mössbauer spectrum of **89** clearly reflects the symmetry of the Fe coordination environment.[103]

Model compounds for the oxidized uteroferrin−phosphate complex based on oxo-bridged μ-phosphato-binuclear iron(III) complexes have been reported as early in 1989 by Wieghardt et al.[104] Since the complexes containing (μ-oxo)bis(μ-oxoanion)diiron(III) core are possible structural models for the oxidized form of the uteroferrin-phosphato complexes, $[L_2Fe_2(\mu\text{-O})(\mu\text{-}O_3P(OPh))_2] \cdot NaClO_4 \cdot 2H_2O$ (**90**; L = 1,4,7-trimethyl-1,4,7-triazacyclononane; Figure 14) was prepared from $[L_2Fe_2(\mu\text{-O})(\mu\text{-OAc})_2](ClO_4)_2 \cdot H_2O$ (**91**) via substitution of the μ-acetato bridges by $O_3P(OPh)^{2-}$, whereas $[L_2Fe_2(\mu\text{-O})(\mu\text{-}HPO_4)_2] \cdot 3H_2O$ (**92**) was prepared, via hydrolysis of $LFeCl_3$ with Na_2HPO_4 in aqueous solution. $L_2Fe_2(\mu\text{-}XO_4)_3$ ($XO_4 = PO_3(OPh)^{2-}$, **93**; HPO_4^{2-}, **94**; Figure 14) formed in MeOH via spontaneous self-assembly from $LFeCl_3$ and the corresponding oxoanion. The diiron(III) centers in **90** and **92** show a strong intramolecular antiferromagnetic coupling, while only a very weak antiferromagnetic coupling was observed between the iron centers in **93** and **94**. These authors have further investigated the kinetics of the formation of **90** from **91** and $Na_2[O_3P(OPh)]$ in aqueous solution at pH = 8, and it has been found that the formation of **90** is zeroth-order with respect to $[O_3P(OPh)^{2-}]$.

Complexes containing a phosphate-bridged (μ-hydroxo)-diiron(III) core, such as may exist in the metalloproteins uteroferrin, beef spleen purple acid phosphatase, or the hydroxylase component of methane monooxygenase, have been prepared by Lippard et al.[105] $[Fe_2(OH)(dpp)_2(L)_2]BF_4 \cdot 2CH_3OH \cdot 0.5Et_2O \cdot H_2O$ (**95**) contains hydroxo-bridged diiron core that is additionaly bridged by two bidentate phosphate ligands. The resulting $[Fe_2(OH)(dpp)_2]^{2+}$ unit is capped by pyrazolylborate ligands and one BF_4^- anion.[105] A similar compound, $[Fe_2(dpp)_3(L)_2]BF_4 \cdot CH_2Cl_2$ (**96**), has three bidentate phosphate groups bridging two iron centers resulting in a $[Fe_2(dpp)_3]^{2+}$ unit capped with hydrotris(pyrazolyl)borate ligands.[105]

As a result of protonation of the bridging O atom, the dimetallic core in the hydroxo-bridged complex **95** is expanded relative to that in the corresponding μ-oxo complexes, with a concomitant decrease in the magnitude of the antiferromagnetic spin exchange coupling constants ($J \approx -10$ to -20 cm^{-1}) and correspondingly larger paramagnetic shifts in the ^{1}H NMR spectra. On the other hand, in complex **96**, where there is no μ-oxo or hydroxo ligand present, a very weak antiferromagnetic coupling ($J = -0.8$ cm^{-1}) and a large Fe···Fe separation (4.677(1) Å) are observed. For **95**, electronic transitions differ considerably from those of oxo-bridged complexes. Similarly, Mössbauer quadrupolar coupling parameters (0.25−0.40 mm/s) are considerably smaller in the hydroxo-bridged complex.[105]

A new family of (μ-oxo)(μ-phosphato)diiron(III) complexes, $[Fe_2O(dpp)(tpa)_2](ClO_4)_3 \cdot (Me_2CO)$ (**97**; tpa = tris(2-pyridylmethyl)-amine; Figure 14), has been synthesized by Que et al. starting from $tpa \cdot 3HClO_4$, Et_3N, $Fe(ClO_4)_3 \cdot 10H_2O$, and diphenylphosphate.[106] The crystal structure of **97** establishes the presence of a doubly bridged Fe_2 core. On the first iron, the amine nitrogen of tpa is trans to the oxo bridge, while one of the pyridine nitrogens is trans to the oxo bridge on the other Fe center. This complex exhibits electronic and Mössbauer spectral features and magnetic properties that are very similar to those of (μ-oxo)diiron(III) proteins as well as (μ-oxo)bis(μ-carboxylato)diiron(III) complexes, demonstrating that these properties are not significantly affected by the number of bridges and the inequivalence of the Fe sites. The Fe(III) sites remain distinct in solution as evidenced by ^{1}H NMR and resonance Raman spectroscopy. The inequivalence is manifested in the resonance Raman spectra as an enhancement of the ν_{as}(Fe−O−Fe) intensity, which is comparable to those found for (μ-oxo)diiron(III) proteins such as methemerythrin and ribonucleotide reductase.[106]

Three diiron(III) complexes of the tetradentate tripodal ligand *N*-(*o*-hydroxybenzyl)-*N*,*N*-bis(2-pyridylmethyl)amine (hdp), $[Fe_2(hdp)_2(O)(O_2CPh)]BPh_4$ (**98**), $[Fe_2(hdp)_2(O)(dpp)]BPh_4$ (**99**), and $[Fe_2(hdp)_2(dpp)_2](BPh_4)_2$ (**100**) (Figure 14), have been synthesized by Que et al. as models for the active site of the purple acid phosphatases.[107] Compound **98** has a (μ-oxo)(μ-benzoato)diiron(III) core, while complex **100** has a bis(μ-phosphato)diiron(III) core. The tetradentate HDP completes the coordination sphere about each Fe center in both complexes. Due to differences in their core structures, the Fe···Fe separations in **98** and **100** are 3.217(11) Å and 4.819(1) Å, respectively. Compound **99** is presumed to have a structure analogous to **98** with phosphate replacing the benzoate bridge. Both **98** and **99** exhibit strong antiferromagnetic coupling due to the presence of the oxo bridge ($J = -111$ and -96 cm^{-1}, respectively). The Fe(III) centers in **100** do not show any coupling. Compound **100** exhibits Curie behavior throughout the entire temperature range studied (6−300 K) with a magnetic moment commensurating with two high-spin Fe(III) centers. The three complexes exhibit visible absorption maxima at 522, 516, and 605 nm, respectively, arising from phenolate-to-Fe(III) charge transfer transitions. The shifts in the λ_{max} values have been rationalized from the Lewis acidities of the respective Fe(III) centers and compared with those of the purple acid phosphatases.[107]

There have been several attempts in the last decade to synthesize phosphatase model compounds that contain a phenoxy-bridged diiron core, either with or without mixed valency across the dinculear core. Notable among these are the mixed-valent iron phosphate $[Fe_2(dpp)_2(bpmp)](ClO_4)_2(CH_3OH)(H_2O)$ (**101**) and the mixed-metal phosphate $[ZnFe(dpp)_2(bpmp)](ClO_4)_2(CH_3OH)(H_2O)$ (**102**) (bpmp-H = 2,6-bis(bis(2-pyridylmethyl)aminomethyl)-4-methylphenol; Figure 15), which have been synthesized by Krebs et al.[108] These molecules contain a μ-phenoxo-bridged Fe^{2+}/Fe^{3+} or Zn^{2+}/Fe^{3+} unit, where the metal centers are additionally bridged by two diphenylphosphate moieties. It

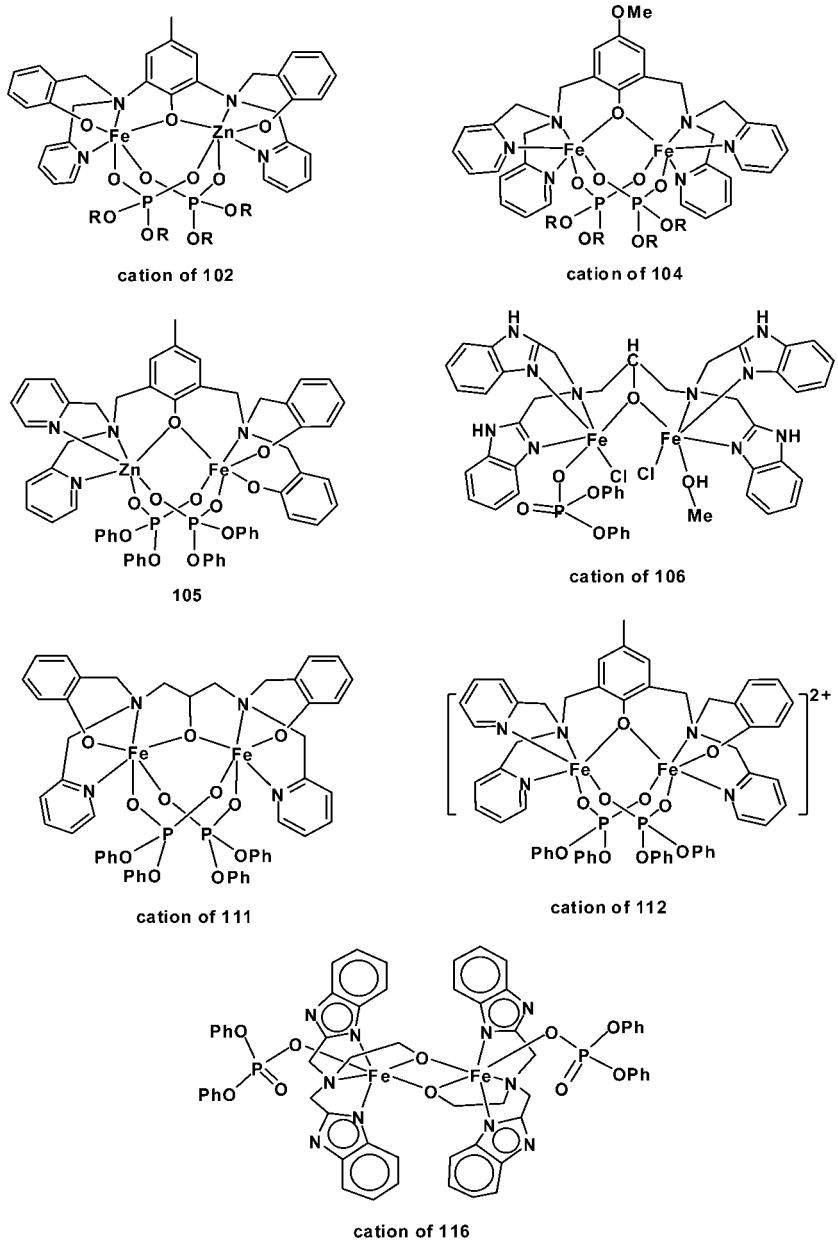

Figure 15. Iron diphenyl phosphates.

is of interest to note that the active site of uteroferrin (PP1) and of phosphatase from bovine spleen consists of a Fe^{2+}/Fe^{3+} moiety in its inactive form in which the two iron centers are strongly antiferomagnetically coupled, while the enzymatically active pink form of PP1 contains a mixed valent Fe^{2+}/Fe^{3+} center with a weaker antiferromagnetic coupling. In contrast, a phosphatase isolated from kidney beans (PP2) contains a Zn^{2+}/Fe^{3+} unit. Hence the synthesis of compounds **101** and **102** assumes importance in understanding the structure and properties of both active forms of purple phosphatases PP1 and PP2.[108] The nitrogen donors of the bpmp ligand offer an octahedral environment to the metal by facial coordination in **101** and **102**. Compound **102** has a room-temperature magnetic moment of 6.15 μ_B. The magnetic susceptibility of **101** shows an antiferromagnetic interaction with a coupling constant of $-6.2(5)$ cm^{-1}, which agrees with the value known for the reduced interoferrin phosphate complex. While **102** exhibits one reversible oxidation wave at +143 mV, **101** exhibits two reversible oxidation waves at +135 and +755 mV.

By introducing a methoxy group in place of the methyl group on the para-position of phenol ring of bpmp, Krebs et al. synthesized a new ligand, bpmop. Using this new ligand, they have investigated the preparation of complexes analogous to **101** and **102** described above.[109] The heterodinuclear $Zn^{II}Fe^{III}$ complex $[ZnFe(bpmop)(dpp)_2](ClO_4)_2 \cdot H_2O$ (**103**) and the isostructural $Fe^{II}Fe^{III}$ complex $[Fe_2(bpmop)(dpp)_2](ClO_4)_2 \cdot H_2O$ (**104**) (Figure 15) with the dinucleating ligand 2,6-bis[(bis(2-pyridylmethyl)amino)methyl]-4-methoxyphenol (Hbpmop) have thus been prepared and characterized by X-ray crystallography.[109] A pH-induced change in the coordination sphere of the metal centers has also been observed for these complexes. These complexes serve as models for the mixed-valence oxidation state in purple acid phosphatases.

The pH-dependent cleavage acceleration of the activated phosphodiester 2-hydroxypropyl *p*-nitrophenyl phosphate (hpnp) has also been studied in MeCN−water (1:1) in the presence of complexes formed by bpmop and its methyl analog. At the optimum pH value (8.5 ± 0.2), the $Zn^{II}Fe^{III}$

complex formed from bpmop (**103**) shows a two-fold higher rate acceleration compared with that of the complex containing bpmp (**104**). The diiron complex from bpmop is four-fold more reactive than the homologous complex from bpmp. The heterodinuclear $Zn^{II}Fe^{III}$ catalysts are at least 10-fold more reactive than the homonuclear $Fe^{II}Fe^{III}$ catalysts.[109]

Although the crystal structure of kidney bean purple acid phosphatase (KBPAP) shows the active site to be a heteronuclear $Zn^{II}Fe^{III}$ system with the metal ions in two chemically distinct environments, many complexes described as models for this enzyme contain the two different metal ions in very similar chemical environment. In a recent report, Krebs and co-workers have described a new heterodinuclear $Zn^{II}Fe^{III}$ μ-phenoxy complex, $[ZnFeL(dpp)_2]_2$ (**105**) (Figure 15), which was prepared from the unsymmetric ligand 2-{[bis(2-hydroxybenzyl)]amino}methyl-6-{[(2-pyridinylmethyl)amino]methyl}-4-methylphenol (H_3L).[110] This asymmetric ligand provides two distinct N- and O-rich donor sets. The regioselective complexation of this ligand to Zn and Fe ions is confirmed in solution ^1H NMR studies. The crystal structure of **105** interestingly reveals that the observed NO_5 coordination sphere around the Fe^{III} reproduces for the first time the O-rich coordination sphere around Fe^{III} in KBPAP.[110]

A binuclear iron(II) complex with a terminally coordinated phosphato ligand, $[Fe_2Cl_2(dpp)(tbpo)(MeOH)](ClO_4)_2 \cdot 3MeOH$ (**106**) (Figure 15), has been synthesized from the reaction of *N*,*N*,*N*′,*N*′-tetrakis(2-benzimidazolylmethyl)-2-hydroxy-1,3-diaminopropane di-HCl (Htbpo·2HCl) with $Fe(ClO_4)_3 \cdot 9H_2O$ and diphenylphosphate.[111] The X-ray structure showed the phosphate ligand to be terminally coordinated to one iron center, while a MeOH ligand is coordinated to the other iron center. This compound has been implicated as a model compound for the oxidized form of purple acid phosphatase from beef spleen.[111]

Que and co-workers further investigated the reduced forms of the dinuclear iron−bpmp complexes.[112] $[Fe_2(bpmp)(dpp)_2]X$ (X = Cl, **107**; BF_4, **108**, BPh_4, **109**) were prepared to provide insights into the integer-spin EPR signals found in the diferrous forms of diiron-oxo proteins. Compound **107** has a (μ-phenoxo)bis(μ-phosphato)diiron core. Compounds **107**−**109** exhibit EPR signals at $g = 15$, a resonance position that is incompatible with both strong and weak coupling models earlier proposed to explain the corresponding signals in similar carboxylate complexes. The EPR signals of **107**−**109** arise from an excited state; the coupling interaction between the Fe centers is antiferromagnetic. Further, the temperature dependence of the EPR signal indicates that the excited state is 12 cm^{-1} above the EPR silent ground state in these complexes. These observations are corroborated by magnetization data for polycrystalline **109**.[112]

Krebs et al., continuing their studies on model compounds for oxidized forms of uteroferrin phosphate complex, have reported on diiron(III) phosphates $[Fe_2(dpp)_2(bhpmp)]BPh_4 \cdot CHCl_3 \cdot CH_3OH$ (**110**), (bhpmp-H_3 = 2,6-bis[((2-hydroxybenzyl)(2-pyridyl methyl)amino)methyl]-4-methylphenol) and $[Fe_2(dpp)_2(bhpp)]ClO_4 \cdot H_2O$ (**111**) (Figure 15; bhpp-H_3 = 1,3-bis[(2-hydroxybenzyl)(2-pyridylmethyl)amino]-2-propanol).[113] The structure of **111** reveals that both ferric ions are coordinated by the trinegative heptadentate bhpp ligand. Each metal ion is also bonded to one pyridinic nitrogen, one tertiary nitrogen, the phenolate oxygen, and the bridging alkoxide oxygen. The distorted octahedral environment of each iron center in **111** is completed by coordination of two diphenylphosphate ligands. The structure of **110** is similar to that of **111**.[113]

Synthesis, structural, magnetic, and redox behaviors of asymmetric diiron $Fe^{II}Fe^{III}$ complexes with a single terminally bound phenolate ligand that have relevance to the PAP enzymes have been reported by Latour and co-workers.[114] Thus, new asymmetric ligands H_2L1 (2-[(bis(2-pyridylmethyl)amino)methyl]-6-[((2-pyridylmethyl)(2-phenol)amino)methyl]-4-methylphenol) and H_2L2 (2-[(bis(2-pyridylmethyl)amino)methyl]-6-[((2-pyridylmethyl)(6-methyl-2-phenol)amino)-methyl]-4-methylphenol) were synthesized by these authors to provide both a bridging and a terminal phenolate to a pair of iron ions in order to mimic the binding of a single terminal tyrosinate at the diiron center of the purple acid phosphatases. Mixed valence diiron complexes $[Fe^{II}Fe^{III}(L1)(dpp)_2]BPh_4$ (**112**) (Figure 15) and $[Fe^{II}Fe^{III}(L2)(dpp)_2]PF_6$ (**113**) and trivalent diiron complexes have been obtained starting from ferric nitrate, the corresponding asymmetric ligand, diphenylphosphate (dppH), and $NaBPh_4$ or $NaPF_6$. Diferric complexes $[Fe^{III}Fe^{III}(L1)(dpp)_2](I)_3BPh_4$ (**114**) and $[Fe^{III}Fe^{III}(L2)(dpp)_2](PF_6)_2$ (**115**) have been obtained also either by direct synthesis or by iodine oxidation of the mixed valence precursor. The electronic spectrum of the mixed-valence compounds are dominated by a charge transfer transition in the 400−600 nm domain, which moves to the 550−660 nm range upon oxidation to the diferric state. In addition, they exhibit a weak and broad intervalence transition close to 1100 nm. Electrochemical studies show that these systems exist in three redox states, $Fe^{II}Fe^{II}/Fe^{II}Fe^{III}/Fe^{III}Fe^{III}$. Moreover they show that the introduction of the terminal phenol group results in a thermodynamic destabilization of the diferrous state higher than the stabilization of the diferric state. An expanded stability domain of the mixed valence state is therefore observed that is attributed to the asymmetry of the products. Comparison of the carboxylate and phosphate derivatives leads to attributing it to the partial dissociation in solution of the carboxylate oxygen trans to the phenolate. The latter feature bears an intrinsic resemblance to the dissociation of iron that is observed when purple acid phosphatases are reduced by dithionite. These studies clearly show the importance of tyrosine binding on the redox properties of the PAP enzymes.[114]

Starting from an alkoxy bridging ligand with additional nitrogen donor sites, bis(benzimidazol-2-ylmethyl)(2-hydroxyethyl)amine (bhnH), Cheng et al. have synthesized a binuclear Fe^{3+} complex, $[Fe_2(dpp)_2(bhn)](ClO_4)_2$ (**116**) (Figure 15), which is a potential model for the oxidized form of purple acid phosphatase.[115] The Fe^{3+} ions in **116** are bridged by two oxygen atoms derived from the -OH group of bhn-H ligand. Each bhn ligand binds to one Fe atom through its three nitrogen atoms and the distorted octahedral environment around the Fe atom is reached by a terminal phosphate moiety.[115] Magnetic susceptibility measurements have been carried out for **116** in the range 4.2−300 K. The room-temperature magnetic moment of 6.22 μ_B drops to 0.64 μ_B at 8.7 K suggesting antiferromagnetic interactions between the two ferric ions at low temperatures. Further the calculations based on an isotropic Heisenberg model suggest antiferromagnetic coupling between the Fe(III) ions with $J = -17.5$ cm^{-1}.

The first iron(III)−nickel(II) heterodinuclear complex containing both terminal and bridged phosphato ligands relevant to structural core models for dimetalloenzymes has

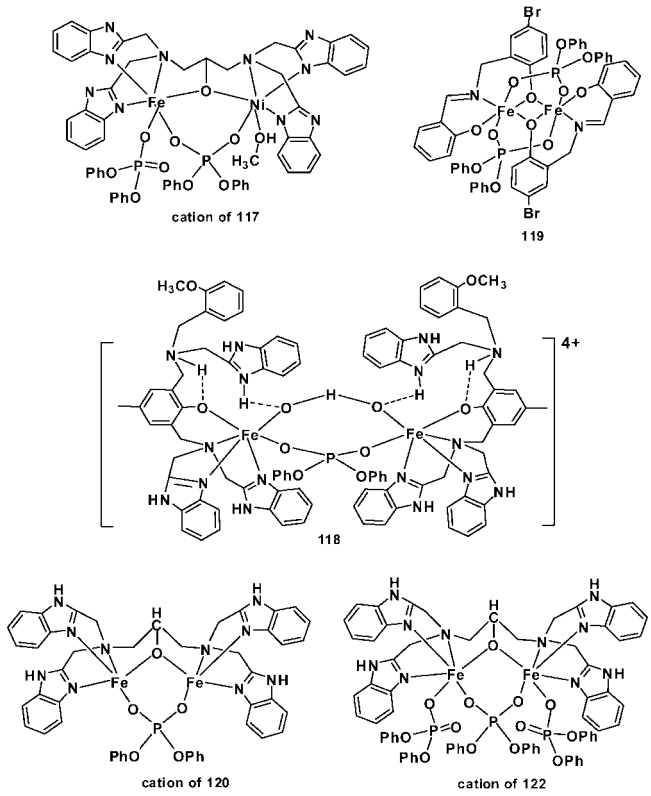

Figure 16. Iron phosphates with multidentate ligands.

been synthesized by Cheng and co-workers.[116] This heterodinuclear complex, $[FeNi(hptb)(dpp)_2(HOMe)](ClO_4)_2 \cdot 2H_2O$ (**117**) (hptb-H = *N*,*N*,*N*′,*N*′-tetrakis(2-benzimidazolylmethyl)-2-hydroxy-1,3-diamino-propane) (Figure 16), contains bidentate bridging and terminal monodentate coordinated diphenylphosphate ligands.[116]

The synthesis and characterization of a diiron(III) complex featuring a novel oxo-hydroxo bridge stabilized by hydrogen bonding to uncoordinated benzimidazole moieties of a polydentate unsymmetrical ligand has been reported by Rapta et al. In ethanol, the potentially dinucleating ligand 2-[bis(2-benzimidazolylmethyl)amino]methyl-4-methyl-6-[*N*-(2-benzimidazolylmethyl)-*N*-(2-methoxybenzyl)aminomethyl]phenol ($N_3O(H)N_2$-MeOB) binds to $Fe(ClO_4)_3$ in a 1:1 manner in the presence of diphenylphosphate and Et_3N to yield $[Fe_2(N_3O\text{-}N_2H_2^{2+}\text{-}MeOB)_2(\mu\text{-dpp})(\mu\text{-O}\cdots\text{H}\cdots\text{O})](ClO_4)_4 \cdot 6H_2O$ (**118**) (Figure 16).[117] Coordination at each iron is completed by a nitrogen(amine) trans to the oxo-hydroxo bridge, a phenolate oxygen trans to the phosphato bridge, and two trans-related nitrogen (imine) atoms. This complex represents the first example of a dinuclear iron complex with an oxo-hydroxo bridge, Fe−O···H ···O−Fe. This OHO^{3-} group, which is stabilized by hydrogen bonding to the N−H groups of the uncoordinated benzimadazole moieties, is suggestive of possible intermediates in the stepwise deprotonation of coordinated water molecule(s) because the OHO^{3-} group is the penultimate species in the hydrolysis of a bis(aquo)diiron(III) species to a (μ-oxo)diiron product. The Fe···Fe separation in this complex is remarkably long (5.164(2) Å), and hence a a very weak antiferromagnetic coupling is observed. ($J \approx -3$ cm^{-1}).[117]

A dinuclear phenoxo-bridged Fe(III) complex **119** (Figure 16) with *N*-salicylidene-2-hydroxy-5-bromobenzylamine (H_2L_a), has been synthesized and characterized by IR and electronic spectral studies as well as by magnetic susceptibility measurements.[118] Single-crystal X-ray analysis revealed that the dinuclear Fe(III) complex is bridged by two phenoxo-O atoms of the Schiff-base ligand. The dinuclear molecule is centrosymmetric with a crystallographic inversion center in the middle of the Fe_2O_2 core. The two iron atoms are further bridged by two diphenyl phosphates bridging in a syn−syn configuration. Each iron atom (Fe) is coordinated to two phenoxo oxygens and one imino nitrogen of the Schiff-base ligand L and one phenoxo oxygen atom of the other ligand L. The fifth and sixth coordination sites are occupied by the two diphenyl phosphate oxygen atoms. The iron centers are arranged in an approximate octahedral geometry. The magnetic susceptibility data shows a ferromagnetic interaction within a dinuclear core in **119**.[118]

The synthesis and crystal structure of a diferrous complex, $[Fe_2L(dpp)](ClO_4)_2 \cdot Et_2O$ (**120**; L = anion of *N*,*N*,*N*′,*N*′-tetrakis(*N*-ethyl-2-benzimidazolylmethyl)-2-hydroxy-1,3-diaminopropane) (Figure 16), and its reactivity with molecular dioxygen have been reported by Yan et al.[119a] The Fe(II) sites in this complex are bridged by an alkoxide of the dinucleating ligand and a phosphate, resulting in a diiron core with an Fe-μ-O−Fe angle of 131.20(3)° and an Fe−Fe distance of 3.649 Å. Both Fe(II) centers have trigonal bipyramidal geometry. Interestingly a dioxygen adduct of this complex is formed upon exposure to molecular oxygen at −60 °C. The adduct, **121**, which is stable only below −60 °C, decomposes upon warming. The complex exhibits visible absorption near 606 nm and resonance Raman features at 478 cm^{-1} (ν(Fe−O)) and 897 cm^{-1} (ν(O−O)). The latter is characteristic of a μ-1,2-peroxo species, indicating that dioxygen adducts can serve as a model for the putative oxygenated intermediate of some nonheme diiron-oxo proteins.

Yan et al. have reported on a dinuclear iron(III) complex with a bridging diphenylphosphate and two terminal diphenylphosphate ligands.[119b] This dinuclear Fe(III) complex, $[Fe_2(hptb)(\mu\text{-dpp})(dpp)_2](ClO_4)_2$ (**122**) (Figure 16), also acts as a model for the active site of purple acid phosphatase. Dinuclear Fe(III) centers are bridged by a μ-OR group from hptb, a bidentate bridging diphenylphosphate ligand. Two terminal diphenylphosphates also coordinate to the Fe(III) centers.

Nag and co-workers have very recently isolated a Fe−Zn heterobimetallic complex bearing a bnpp ligand, $[\{FeLZn(bnpp)\}_2(\mu\text{-O})](ClO_4)_2$ (**123**; L = tetraiminodiphenol macrocycle), starting from $[Fe(LH_2)(H_2O)Cl](ClO_4)_2 \cdot 2H_2O$, zinc perchlorate, and bis(nitrophenyl)phosphate. In complex **123**, the μ-O ligand bridges two heterobimetallic ZnFe.[120]

Apart from the well-defined iron complexes described above, where a phosphate binds to iron through the phosphate oxygen atoms, there have been a number of studies on the kinetics of phosphate mono- and diester hydrolysis by preformed and suitably designed iron mono- and dinuclear complexes.[121–125] Details of such studies are beyond the scope of this review since no stable phosphate complexes of iron have been isolated and characterized during these processes.

2.7.2. Ruthenium and Osmium

There are no structurally well-characterized complexes of these metals where a organophosphate ligand is directly linked to the metal.

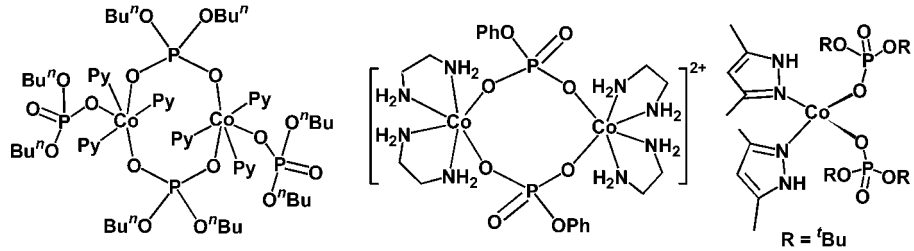

Figure 17. Cobalt phosphates derived from phenyl, *n*-butyl, and *t*-butyl phosphates.

2.8. Group 9 Metal Phosphates

2.8.1. Cobalt

Cobalt di-*n*-butylphosphate, $Co(O_2P(O^nBu)_2)_2$ (**124a**), was synthesized by Wongnawa et al.[126] in 1987 starting from cobalt chloride and excess tri-*n*-butylphosphate via a phosphate ester hydrolysis route. The predicted structure for **124a** is polymeric, and the geometry around cobalt is tetrahedral. The cyclic cobalt *n*-butylphosphate, $[Co(O_2P(O^nBu)_2)_2(py)_3]_2CHCl_3$ (**124b**) (Figure 17), reported in 1988, contains cobalt ions that are octahedrally surrounded by three pyridines, one monodentate *n*-butylphosphate, and two bridging di-*n*-butylphosphates.[127]

Glowiak et al. have synthesized a monomeric cobalt phosphate complex, $[Co(O_3POPh)(bpy)(OH_2)_3](H_2O)$ (**125**), by the reaction of cobalt phenyl phosphate with bpy.[128] The geometry about the six-coordinate cobalt ion involves a slightly distorted octahedron. The axial positions are occupied by the oxygen atom of the water molecules. The equatorial positions are occupied by two nitrogen atoms of the bpy ligand, one oxygen atom of the phosphate group, and the oxygen atom of the third water molecule.

The synthesis and structural characterization of the isomers of novel binuclear cobalt(III)−phenyl phosphate complexes incorporating the ethylenediamine ligand were reported by Jones et al.[129] The reaction between *cis*-$[Co(en)_2Cl_2]ClO_4$ and $[Ag_2(O_3POPh)]$ in anhydrous Me_2SO yielded the dimeric cation $\{[Co_2(en)_2(\mu\text{-}O_3POPh)]_2\}^{2+}$ (**126**; Figure 17) as the major product. An X-ray structure determination of the meso diastereomer as the triflate salt monohydrate showed that it consisted of two bis(ethylenediamine)cobalt(III) moieties bridged by two phosphate ester groups. The racemic diastereomer has been resolved, and the corresponding rotatory dispersion and CD spectral details have been probed.[129]

Recent studies on the exploitation of di-*tert*-butylphosphate complexes of transition metals for the preparation of fine particle phosphate materials have also been extended to cobalt complexes by Murugavel et al.[130] Reaction of $Co(OAc)_2 \cdot 4H_2O$ with di-*tert*-butylphosphate (dtbp-H) in a 4:6 molar ratio in MeOH or THF gave the tetranuclear metal phosphate cluster $Co_4(\mu_4\text{-}O)(dtbp)_6$ (**127**) in a nearly quantitative yield.[130] For the same reaction carried out in the presence of a donor auxiliary ligand such as imidazole (imz) or ethylenediamine (en), octahedral complexes $[Co(dtbp)_2(imz)_4]$ (**128**) and $[Co(dtbp)_2(en)_2]$ (**129**) were obtained.[130] The tetrameric cluster could be converted into mononuclear complexes **128** and **129**, respectively, by treating **127** with a large excess of imidazole or ethylenediamine. The use of slightly bulkier auxiliary ligand 3,5-dimethylpyrazole (3,5-dmp) in the reaction between cobalt acetate and dtbp gave the mononuclear tetrahedral complex $Co(dtbp)_2(3,5\text{-}dmp)_2$ (**130**; Figure 17) in nearly quantitative yields. The Co^{II} ion in **128** is octahedrally coordinated by four imidazole nitrogens, which occupy the equatorial positions, and oxygen atoms of two phosphate anions on the axial coordination sites. The crystal structure of **130** reveals that the central Co atom is tetrahedrally coordinated by two phosphate and two 3,5-dmp ligands. In **128** and **130**, the dtbp ligand acts as a monodentate, terminal ligand with free P═O phosphoryl groups. Thermal studies indicate that heating **127** at 171 °C leads to the loss of 12 equiv of isobutene gas yielding carbon-free $[Co_4(\mu_4\text{-}O)(O_2P(OH)_2)_6]$, which undergoes further condensation by H_2O elimination to yield $Co_4O_{19}P_6$ material. This sample of **127** when heated to >500 °C yields the crystalline metaphosphate $Co(PO_3)_2$ along with amorphous pyrophosphate $M_2P_2O_7$ in a 2:1 ratio. Similar heat treatment on mononuclear complexes **128**−**130** also results in the exclusive formation of the metaphosphate $Co(PO_3)_2$, albeit with nitrogen impurities.

In an attempt to isolate new structural forms of cobalt−dtbp complexes, cobalt acetate was reacted with dtbp-H in the presence of potentially tridentate 1,3-bis(3,5-dimethylpyrazol-1-yl)propan-2-ol. Quite surprisingly, the coligand does not coordinate to the metal, and the product isolated is the one-dimensional polymer $[Co(dtbp)_2]_n$ (**131**).[91,92] Compound **131**, which is a new structural form for cobalt−dtbp complexes, has been characterized with the aid of analytical and spectroscopic studies. A single-crystal X-ray diffraction study reveals that the molecular structure of **131** is similar to $[Mn(dtbp)_2]_n$ (**81**).[90] Alternating single and triple phosphate bridges are found between the adjacent Co ions in **131**, which are coordinated by four phosphate oxygen atoms in a tetrahedral geometry. The presence of *tert*-butoxy groups makes compound **131** an ideal candidate for the production of phosphate materials at low temperatures. The TGA of **131** reveals a weight loss of 47% in the range 114−152 °C corresponding to the loss of 4 equiv of isobutene to produce $Co(O_2P(OH)_2)_2$. Heating the sample to 350 °C results in a further weight loss that corresponds to the removal of two water molecules to result in $Co(PO_3)_2$.[91]

Cobalt polymer **131** transforms readily into a two-dimensional grid structure $[Co(dtbp)_2(4,4'\text{-}bpy)_2.(H_2O)_2]_n$ (**132**) by stirring **131** with 2 equiv of 4,4′-bpy in methanol for a few hours. Compound **132** crystallizes with two crystallographically unique metal ions in the asymmetric unit, which produce two separate two-dimensional grids in the crystal lattice. To minimize steric repulsion, these grids are offset from one another; the metal ion in one grid resides centered above the cavity in the adjacent grid. The distance between the metal−ligand planes of the two independent adjacent nets is half of the cell length along the *a* axis (∼7.9 Å). The molecular dimensions and the size of the void in cobalt grid **132** are comparable to those of the manganese grid phosphate **83**.

It is now well known that phosphate esters can be activated by direct coordination to metal ions. Numerous mono- and

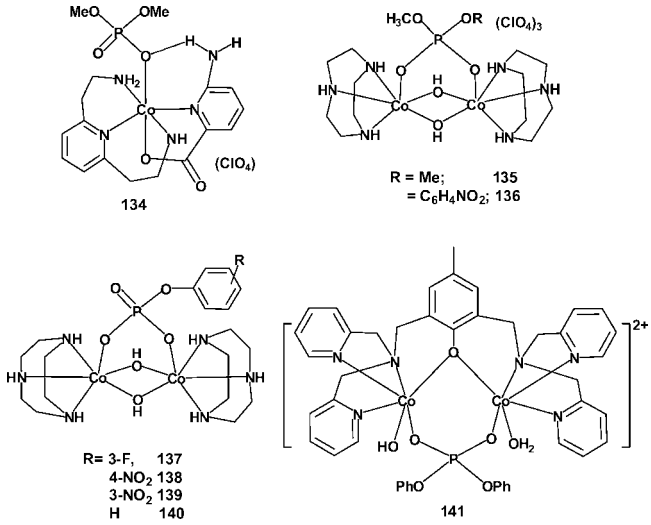

Figure 18. Mono- and dinuclear cobalt phosphates.

dinuclear metal complexes have been developed as models for nucleases, polymerases, and phosphatases. To sense phosphates efficiently, the receptor should bind tightly to the phosphates. However, it is generally difficult to achieve tight binding of phosphates in water. One way to overcome this difficulty may be to combine H-bonding and metal coordination. Using the synergistic effect between metal coordination and hydrogen bonding resulting in an enhanced phosphate recognition has been recently demonstrated in the case of a cobalt−dimethyl phosphate complex by Chin and coworkers.[131] Addition of NaOH and 2-aminopicolinate to $[Co(bamp)Cl_3]$ (bamp = bisaminomethyl pyridine) followed by the addition of $HClO_4$ produces the octahedral Co^{III} complex $[Co(bamp)(2\text{-aminopicolinate})(OH_2)](ClO_4)_2$ (**133**). The coordinated water molecule in this complex, due to the proximity of the amino group, forms a strong intramolecular N−H···O hydrogen bond. Treatment of **133** with sodium dimethyl phosphate at 80 °C produces the Co(III) phosphate complex $[Co(bmap)(2\text{-aminopicolinate})(O_2P(OMe)_2)](ClO_4)$ (**134**) (Figure 18). In **134**, the phosphate anion is bound trans to the carboxylate group and is H-bonded to the amino group (N−H···O, 2.77 Å). It has been further established that the equilibrium constant for binding of dimethyl phosphate to a Co(III) complex in water increases from 6.2 to 210 M^{-1} upon addition of a single hydrogen bond between the bound phosphate and the metal complex. This synergistic effect between metal coordination and hydrogen bonding has also been observed for fluoride binding but not for bromide.[131]

Using other cobalt complexes, Chin et al. have attempted to unravel the mechanism of hydrolysis of a phosphate diester that is doubly coordinated to the metal by synthesizing the dinuclear cobalt complexes $[Co_2(tacn)_2(OH)_2(O_2P(OCH_3)_2)](ClO_4)_3$ (**135**) and $[Co_2(tacn)_2(OH)_2(O_2P(OCH_3)(OC_6H_4\text{-}NO_2))](ClO_4)_3$ (**136**) (Figure 18) from the reaction of $[Co_2(tacn)_2(OH)_3](NO_3)_3$ (tacn = 1,4,7-triazacyclononane) and the sodium salt of the phosphate ester in aqueous $HClO_4$. In both complexes, the Co^{III} ions are bridged by one phosphate anion, two hydroxyl groups, and the tridentate amine.[132] Hydrolysis of the phosphate diester in complex **136** has been monitored by measuring the absorbance of the released *p*-nitrophenol by UV−vis spectroscopic methods. The half-life of the hydrolysis has been measured to be 6 s at pH 8, and the second-order rate constant for the hydroxide catalyzed hydrolysis of the diester in **136** was found to be 1.3×10^{-5} M^{-1} s^{-1} at 25 °C. Further mechanistic studies reveal that the diester unit in **136** is hydrolyzed by a mechanism involving double Lewis acid activation and the attack of a bridging, nucleophilic oxo ligand, which together lead to an unprecedented 10^{12}-fold rate enhancement for the hydrolysis. Recently, Hengge et al. have proposed altered mechanisms of reactions of phosphate ester in complexes of the type **136** using kinetic isotopic effects.[133]

Extending the chemistry of **135** and **136**, Chin et al. have studied the hydrolysis of phosphate monoesters coordinated to a dinuclear−tacn core. The hydrolysis of four substituted phenyl phosphate monoesters, $[Co_2(tacn)_2(OH)_2\{O_3P(OAr)\}]^{2+}$ (substituent on aryl group = *m*-F, **137**; *p*-NO_2, **138**; *m*-NO_2, **139**; unsubstituted, **140**; Figure 18), each coordinated to a dinuclear Co(III) complex, has been investigated.[134] Crystallographic data for the *p*-nitrophenyl derivative reveal that **138** is an excellent structural model of the active sites of several phosphatases such as protein phosphatase-1, kidney bean purple acid phosphatase, and calcineurin-α. All of these structures consist of two octahedral metal complexes connected by two oxygen bridges, forming a four-membered-ring diamond core. The pH−rate profile and the ^{18}O-labeling experiment for the hydrolysis of **138** indicate that the oxide bridging the two metal centers in the diamond core is acting as an intramolecular nucleophile for cleaving the coordinated phosphate monoester. The phosphate monoesters in this model system are hydrolyzed more rapidly than those in previously reported model systems. Hence, the dinuclear cobalt complexes **137**−**140** appear to be excellent structural and functional models of the above-mentioned phosphatases. The rate of hydrolysis of **137**−**140** is highly sensitive to the basicity of the leaving group.

The hydrolysis of phosphate monoester on a cobalt(III) dinculear complex without bridging hydroxyl groups has been investigated through the synthesis of $[Co_2(bpmp)(O_3P(OPh))(OH_2)(OH)](ClO_4)_2$ (**141**; bpmp-H = 2,6-bis(bis(2-pyridylmethyl)aminomethyl)-4-methylphenol; Figure 18).[135] The phosphate ester in complex **141** is hydrolyzed an unprecedented 10^{11}-fold more rapidly than the corresponding unbound phosphate. Clean cleavage of the bidentate monoester, together with the crystal structure of **141**, provides detailed mechanistic insight into the hydrolysis reaction in this case.[135]

A dinuclear metal(II) complex of 2,6-bis{*N*-[(2-dimethylamino)ethyl]-iminomethyl}-4-methylphenol (HL), $[Co_2L(OAc)_2]BPh_4$ (**142**), has been examined in the light of its hydrolytic activity toward tris(*p*-nitrophenyl) phosphate and bis(*p*-nitrophenyl) phosphate by both mass spectrometric and UV−visible spectroscopic studies.[136] The corresponding nickel and zinc complexes, $[Ni_2L(OAc)_2(MeOH)]BPh_4$ (**143**) and $[Zn_2L(OAc)_2]BPh_4$ (**144**), have also been synthesized starting from the same ligand. All the complexes hydrolyze the phosphate esters very efficiently.[136]

2.8.2. Rhodium

There are a few reports in the literature on the synthesis and catalytic studies of chiral rhodium phosphate complexes, although none of these complexes have been characterized by X-ray diffraction studies. For example, starting from a series of (*S*)-4,4′,6,6′-tetrasubstituted-1,1′-bi-2-naphthol phosphates, the synthesis of four new tetrakis[4,4′,6,6′-tetrasubstituted-1,1′-bi-2-naphtholphosphate]dirhodium(II) complexes **145**−**148** has been accomplished by Hodgson et al.[137] The use of these complexes as catalysts in the enantioselective tandem carbonyl ylide formation−intramolecular 1,3-dipolar

cycloaddition of an unsaturated 2-diazo-3,6-diketoester, generating cycloadduct (as high as 86% ee), has been demosntrated.[137] Similar chiral rhodium phosphates have been employed as catalysts in a number of organic transformations.[138–144]

2.8.3. Iridium

Phosphate complexes of iridium have been less studied. The phosphate diesters ethyl-4-nitrophenyl phosphate and bis(4-nitrophenyl) phosphate in the complexes *cis*-$[(en)_2Ir(OH)(O_2P(OR)_2)]^+$ (**149**, **150**) were found to react with the OH group of the complex at pH 8 and liberate nitrophenolate ion $\sim 10^6$-fold faster than for the free ligand under the same conditions.[145] The expected products of these reactions, the chelate phosphate esters, were not observed, but only the ring-opened monodentate monoester products were obtained as a result of P−O bond cleavage. It has been concluded that the *cis*-hydroxo ligand is a good nucleophile toward bound phosphate esters.

The same authors have examined the penta-ammine iridium phosphate complexes $[Ir(NH_3)_5(O_2P(OR)(OC_6H_4NO_2\text{-}4)](ClO_4)_2$ (R = Et, **151**; $C_6H_4NO_2$-4, **152**) for their reactivity under basic conditions.[146] It has been found that these complexes react predominantly via intramolecular attack of a deprotonated NH_3 ligand and liberate 4-nitrophenolate ion. It has been suggested that the four-membered phosphoramidato chelate ring opens via P−O and P−N rupture to yield N-bonded phosphoramidate monoester and O-bonded phosphate ester complexes. The rate constant for the intramolecular attack of the amido ion is enhanced considerably relative to the reactivity of the uncoordinated substrate under the same conditions.

Electron-poor 2-(3,5-bis(trifluoromethyl)phenyl)-4-trifluoromethylpyridine [HC^N] undergoes cyclometalation in the presence of trimethylphosphate at lower temperatures to yield the bis-cyclometalated derivative $[(C\text{^}N)_2Ir(\mu\text{-}O\text{-}P(OMe)_2\text{-}O)_2Ir(C\text{^}N)_2]$ (**153**). Interestingly, the light-emitting diodes (LEDs) constructed with **153** give blue-green emission with peak electroluminescent efficiency of 2 cd A^{-1}.[147]

2.9. Group 10 Metal Phosphates

2.9.1. Nickel

Dinuclear metal ions bridged by monodentate phosphodiester ligands are very important in the field of biology. Lippard et al.[148] reported a dimeric nickel compound, $[Ni_2(bpan)(dpp)_2(CH_3CN)_2](ClO_4)_2$ (**154**) (bpan = 2,7-bis[2-(2-pyridylethyl) aminomethyl]-1,8-naphthyridine; Figure 19), which was prepared by the reaction of $Ni(ClO_4)_2 \cdot 6H_2O$, bpan, and Na-dpp. The two phosphate diester ligands in **154** bridge the metal through only the O^- of the phosphate group. The phosphoryl oxygen atoms (P=O) are involved in hydrogen bond formation to one of the secondary amine groups of bpan and not in metal coordination. The bpan moiety connects two nickel centers in a tridentate fashion, while one acetonitrile molecule is bound to each metal ion in a terminal fashion.

Hydroxo- or carboxylate-bridged dinuclear Ni(II) complexes with *N*,*N*,*N*′,*N*′-tetrakis{(6-methyl-2-pyridyl)methyl}-1,3-diaminopropan-2-ol (Me_4tpdp-H) have been synthesized as models for Ni(II)-substituted phosphotriesterase by Yamaguchi et al.[149] These complexes have been transformed to $[Ni_2(Me_4tpdp)(dpp)(CH_3OH)_2](ClO_4)_2$ (**155**) (Figure 19), in which two octahedral Ni^{2+} ions are bridged by alkoxide and phosphate diester groups, by their reaction with diphenyl phosphate.

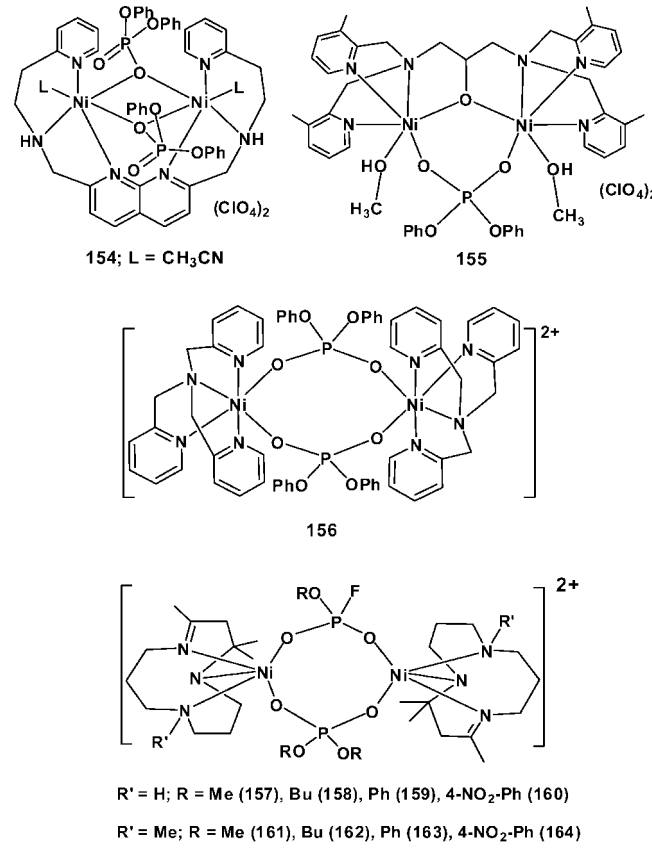

Figure 19. Dinuclear nickel phosphates.

Ito et al. have synthesized dimeric nickel phosphate complex $[(tpa)Ni(dpp)_2Ni(tpa)](ClO_4)_2$ (**156**) (Figure 19) by the reaction of $[(tpa)Ni(OH)_2Ni(tpa)](ClO_4)_2$ with triphenyl phosphate.[150] Each nickel(II) ion in the complex adopts a slightly distorted octahedral coordination environment with diphosphate anions bridging in syn−anti mode. The four coordination sites of each nickel ion are filled by the tpa ligand. The remaining two coordination sites are filled by the two bridging diphenyl phosphate anions. For charge neutrality, two perchlorate anions are present in the outer sphere.

Recently Santana et al. have synthesized the bis(phosphatediester)-bridged complexes $[\{Ni([12]aneN_3)(\mu\text{-}O_2P(OR)_2)\}_2](PF_6)_2$ (**157**−**164**) ([12]aneN$_3$ = 2,4,4-trimethyl-1,5,9-triazacyclododec-1-ene; R = Me (**157**), Bu (**158**), Ph (**159**), and Ph-4-NO_2 (**160**) and [12]aneN$_3$ = Me_4[12]aneN$_3$, 2,4,4,9-tetramethyl-1,5,9-triazacyclododec-1-ene; R = Me (**161**), Bu (**162**), Ph (**163**), and Ph-4-NO_2 (**164**)) (Figure 19) by hydrolysis of the phosphate triester with the hydroxo complex $[\{Ni([12]aneN_3)(\mu\text{-}OH)\}_2](PF_6)_2$ or by acid−base reaction of the dialkyl or diaryl phosphoric acid and the above hydroxo complex.[151] Complexes **158** and **159** have been characterized by single-crystal X -ray diffraction studies. The coordination geometry around the nickel atom is distorted trigonal bipyramidal for **158** and distorted square pyramidal for **159**. The magnetic-exchange pathways found in **158** and **159** were found to involve the phosphate bridges, because these favor antiferromagnetic interactions. The observation of a higher exchange parameter for compound **159** is a consequence of a favorable disposition of the O−P−O bridges. The kinetics for the hydrolysis of tris(4-

nitrophenyl)phosphate with the dinuclear Ni(II) hydroxo complex $[\{Ni(Me_3[12]aneN_3)(\mu\text{-}OH)\}_2](PF_6)_2$ has been studied by UV−visible spectroscopy and the proposed mechanism for hydrolysis can be described as a one-substrate, two-product mechanism and can be fitted to a Michaelis−Menten equation.

Reaction of $Ni(OAc)_2 \cdot 4H_2O$ with di-*tert*-butylphosphate (dtbp-H) in the presence of imidazole (imz) yields the octahedral complexe $[Ni(dtbp)_2(imz)_4]$ (**165**).[130] The nickel ion in **165** is surrounded by four imidazole ligands that are cis to each other and two phosphate ligands that are trans to each other. The phosphate ligands bind to the metal in a monodentate fashion.

2.9.2. Palladium and Platinum

There are not many reports on the synthesis and structural characterization of Pd or Pt organophosphate complexes,[152,153] although several nucleotide and sugar−phosphate complexes have been structurally characterized.

The first platinum phosphate complexes were reported in 1992 by Kemmit et al. They have shown that the treatment of *cis*-$[PtCl_2L_2]$ (L = a phosphine donor ligand) with phenylphosphate $(PhO)PO_3H_2$ in the presence of excess Ag_2O in refluxing CH_2Cl_2 yielded the platinum phosphates $[Pt\{O_2P(O)(OPh)\}L_2]$ (L = PPh_3 (**166**), $PPhMe_2$ (**167**), $AsPh_3$ (**168**); L_2 = dppe (**169**); dppp (**170**); dppb (**171**)). The X-ray crystal structure of the phenylphosphonate platinum complex $[Pt\{O_2P(O)(Ph)\}(PPhMe_2)_2]$ showed the presence of a slightly puckered metallacyclic ring with the phosphoryl O adopting an equatorial position.[152]

In 2002, using the same methodology, Battle et al. rerorted the synthesis of $[Pt(dpp)_2(en)]$ (**172**; dpp = diphenylphosphato, en = ethylenediamine) in the presence of Ag_2O. These authors have shown that the density functional studies (DFT) suggest square-planar coordination geometry around the central platinum ion in such complexes, with rather weak Pt−O bonds but very strong intramolecular N−H···O hydrogen bonds. They have further concluded that phosphates are weaker ligands to Pt(II) than nitrates and are therefore likely to be highly reactive.[153]

2.10. Group 11 Metal Phosphates

2.10.1. Copper

Copper−phosphate complexes have been investigated extensively over the last two decades. The chemistry of simple copper complexes of diphenyl phosphate is described in the beginning of this section, followed by a description of the chemistry of copper di-*tert*-butylphosphate complexes, which find applications as single source precursors for ceramic copper phosphates. At the end of this subsection, the use of copper−phosphate complexes as model compounds for phosphate diester hydrolysis reactions is highlighted.

Glowiak et al. have studied the interaction of copper ion with diphenyl phosphate in the presence and absence of other ligands and characterized the products obtained by X-ray diffraction studies. The synthesis of a monomeric copper diphenylphosphate $[Cu(dpp)_2(OH_2)_2]$ (**173**) (Figure 20) has been recently reported.[154] The copper ion is coordinated by the two phosphate ligands and two water molecules in a unidentate fashion to attain a square-planar geometry. A mixed aminocarboxylate−phosphate copper complex, $[Cu_2(O_2CCH_2CH_2NH_3)_4(dpp)_2][(dpp)_2] \cdot 2H_2O$ (**174**) (Figure

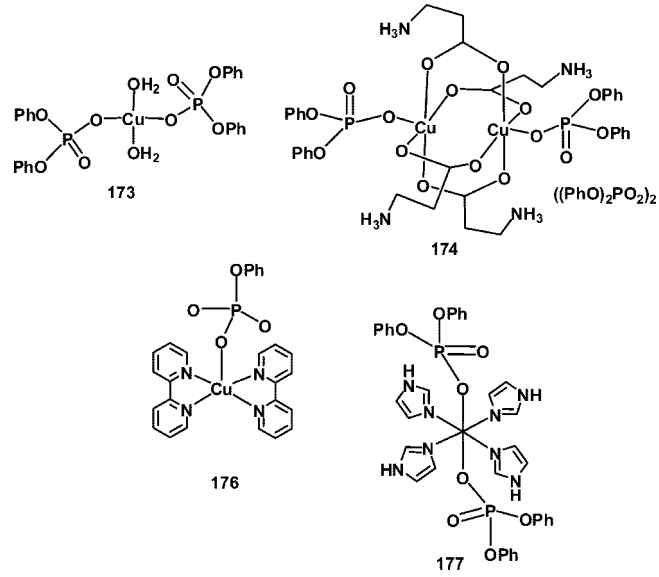

Figure 20. Copper mono- and diphenyl phosphates.

20), has been synthesized starting from barium diphenylphosphate, copper sulfate, and β-alanine.[154] The coordination polyhedron around each copper ion is square pyramidal and shows the copper acetate structure with four bidentate carboxylate groups of β-alanine zwitterionic molecules forming syn−syn bridges between two copper ions. The axial coordination site is occupied by a phosphate oxygen atom of the diphenylphosphate ligand.[154] The use of glycine instead of alanine leads to the isolation of a copper complex, $[Cu(H_2O)_6][(dpp)_2 \cdot (NH_3CH_2COO)_2]$ (**175**), in which the diphenylphosphate and glycine moieties are not coordinated to the copper but are hydrogen bonded via the coordinated water molecules.[155]

Addition of nitrogen donor ligands such as imidazole or 2,2′-bipyridine leads to the isolation of new mononuclear complexes **176**−**178**. In $[Cu(bpy)_2(PhOPO_3)](PhOPO_3H_2) \cdot H_2O$ (**176**), the $[Cu(bpy)_2(PhOPO_3)]$ unit involves a five-coordinate CuN_4O chromophore with a distorted trigonal-bipyramidal stereochemistry; the phosphate groups in the lattice are linked together by short H bonds of (P)−O−H···O−P type.[156] In tetrakis(imidazole)bis(diphenyl-phosphato)copper, $[Cu(imz)_4(dpp)]$ (**177**) (Figure 20), the central metal ion has a tetragonally distorted octahedral coordination geometry with four coplanar imidazole N atoms and the axial sites occupied by diphenyl phosphoato O atoms.[157] In pentakis(imidazole)copper monophenyl phosphate tetrahydrate, $[Cu(imz)_5((PhO)PO_3)] \cdot 4H_2O$ (**178**), the copper ion has distorted square-pyramidal coordination with equatorial Cu−N distances of 2.028−2.068 Å and an axial Cu−N distance of 2.230 Å.[158]

The use of di-*tert*-butyl phosphate as the phosphate ligand in copper chemistry has led to the isolation of structurally interesting molecules. Reaction of copper acetate with dtbp-H in a 1: 2 molar ratio in methanol followed by slow crystallization of the resultant solid in MeOH/THF medium results in the formation of a new polymeric metal phosphate $[Cu(dtbp)_2]_n$ (**179**) in good yields.[90] While alternating triple and single dtbp bridges are found between the adjacent Mn^{2+} ions in $Mn(dtbp)_2$ (**81**), uniform double dtbp bridges across the adjacent Cu^{2+} ions are present in **179**. The eight-membered $Cu_2O_4P_2$ rings, which are the repeating units of this polymer, exist in an almost planar conformation. The Cu···Cu separation along the polymeric chain (5.045 Å)

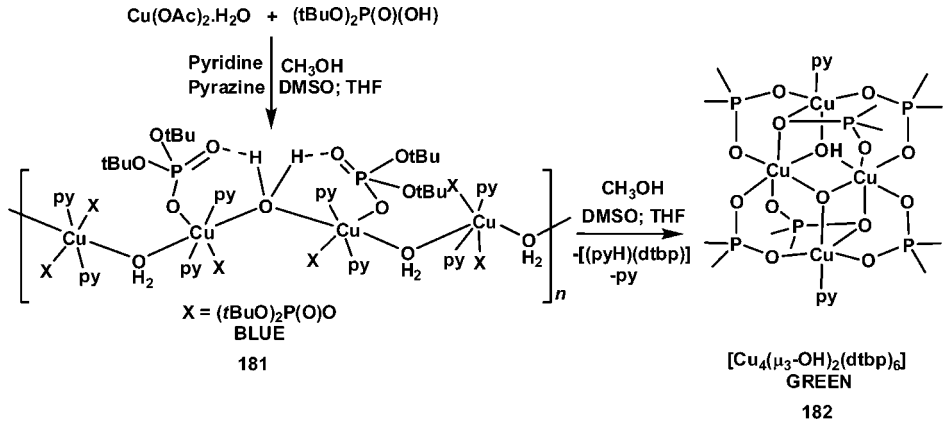

Figure 21. Synthesis of $[Cu(dtbp)_2(py)_2(H_2O)]_n$ (**181**) and $[Cu_4(\mu_3\text{-}OH)_2(dtbp)_6(py)_2]$ (**182**).

rules out any strong magnetic interactions between the copper ions, which exist in distorted square-planar geometry. Thermal analyses (TGA and DSC) indicate that compound **179** converts to the corresponding crystalline metaphosphate material $Cu(PO_3)_2$ at temperatures below 500 °C.

Either addition of 4 equiv of imidazole to **179** or the direct reaction between copper acetate, dtbp-H, and imidazole in a 1:2:4 ratio leads to the isolation of a monomeric copper complex $[Cu(dtbp)_2(imz)_4]$ (**180**) in nearly quantitative yields.[159] The molecular structure of **180** resembles the structure of the diphenylphosphate complex **177** described above. In **180**, the two phosphate ligands, which are trans to each other, lie 2.4475 Å away from the metal, while in the manganese analogue the Mn−O distance is only 2.188 Å.

The use of pyridine, instead of imidazole, in the reactions between copper acetate and dtbp leads to the isolation of a one-dimensional water-bridged polymer and a hydroxo-bridged tetramer. Thus, copper acetate reacts with dtbp-H in a reaction medium containing pyridine, DMSO, THF, and CH_3OH to yield a one-dimensional polymeric complex $[Cu(dtbp)_2(py)_2(\mu\text{-}OH_2)]_n$ (**181**) (Figure 21) as blue hollow crystalline tubes.[160] The copper atoms in **181** are octahedral and are surrounded by two terminal phosphate ligands, two pyridine molecules, and two bridging water molecules. The μ-OH_2 ligands that are present along the elongated Jahn−Teller axis are responsible for the formation of the one-dimensional polymeric structure. The molecular structure of **181** further shows some very strong hydrogen-bonding interactions involving the water hydrogen atoms and the uncoordinated phosphoryl group. Recrystallization of **181** in DMSO/THF/CH_3OH mixture results in the reorganization of the polymer and its conversion to a more stable tetranuclear copper cluster $[Cu_4(\mu_3\text{-}OH)_2(dtbp)_6(py)_2]$ (**182**) (Figure 21) in about 60% yield. The molecular structure of **182** is made up of a tetranuclear core $[Cu_4(\mu_3\text{-}OH)_2]$ that is surrounded by six bidentate bridging dtbp ligands. While two of the copper atoms are pentacoordinate with tbp geometry, the other two copper atoms exhibit a pseudo-octahedral geometry with five normal Cu−O bonds and an elongated Cu−O linkage. The pentacoordinate copper centers bear an axial pyridine ligand. The short Cu···Cu nonbonded distances found in the tetranuclear core of **182** lead to magnetic ordering at low temperature with an antiferromagnetic coupling at ~20 K. Although it has not been possible to clearly establish a mechanism or a reaction pathway for the observed conversion of **181** into **182**, it appears that in solution the polymer breaks into monomeric form from which the tetramer is assembled through formation of a $[Cu_2(\mu_3\text{-}OH)_2]$ central core.[160]

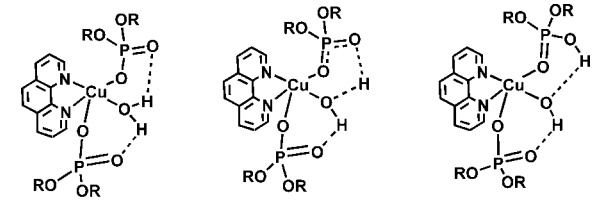

Figure 22. Suggested phosphoryl group assisted $OH_2 \rightarrow OH^-$ conversion in **184**.

When the reaction between di-*tert*-butylphosphate (dtbp-H) and copper acetate was carried out in the presence of collidine, large dark-blue crystals of monomeric copper complex $[Cu(dtbp)_2(collidine)_2]$ (**183**) formed as the only product. The molecular structure of **183**, on the other hand, clearly reveals that both the increased hydrophobicity and the steric crowding due to the presence of three methyl groups on collidine are the reasons for copper ions rejecting additional aqua ligands in **183**.[160] Hence, compound **183** stays as a monomeric square-planar complex, while the copper ions in **181** become octahedral due to the extra room available for μ-OH_2 ligands.

The reaction between copper acetate and dtbp-H has been extended beyond simple N-donors such as imidazole and pyridine. The use of a chelating N-donor such as 1,10-phenanthroline leads to the isolation of a five-coordinate monomeric copper complex $[Cu(phen)(dtbp)_2(OH_2)]$ (**184**) (Figure 22).[93] The molecular structure of compound **184** was initially solved using diffraction intensity data obtained at 293 K. Observation of some *unusual but interesting* O−H bond distances prompted the re-determination of the structure at 203 and 93 K. The molecule of **184** has two dtbp ligands, one chelating phen, and a water molecule bound to copper in a distorted tbp arrangement. The involvement of both the hydrogen atoms of the co-ordinated water molecule in intramolecular H-bonding with the P═O groups results in two six-membered Cu−O−P−O−H−O rings and several other interesting consequences. These H-bond interactions stabilize the bound phosphate ligands, clearly supporting the importance of synergism between metal coordination and H-bonding to achieve better phosphate recognition. The structural elucidation of **184** at three different temperatures reveals that this compound provides useful snap-shots of various steps in metal-catalyzed phosphate ester hydrolysis, namely, (a) strong phosphate recognition by the metal via strong intramolecular H-bonds, (b) generation of a hydroxide from the co-ordinated water through intramolecular activation

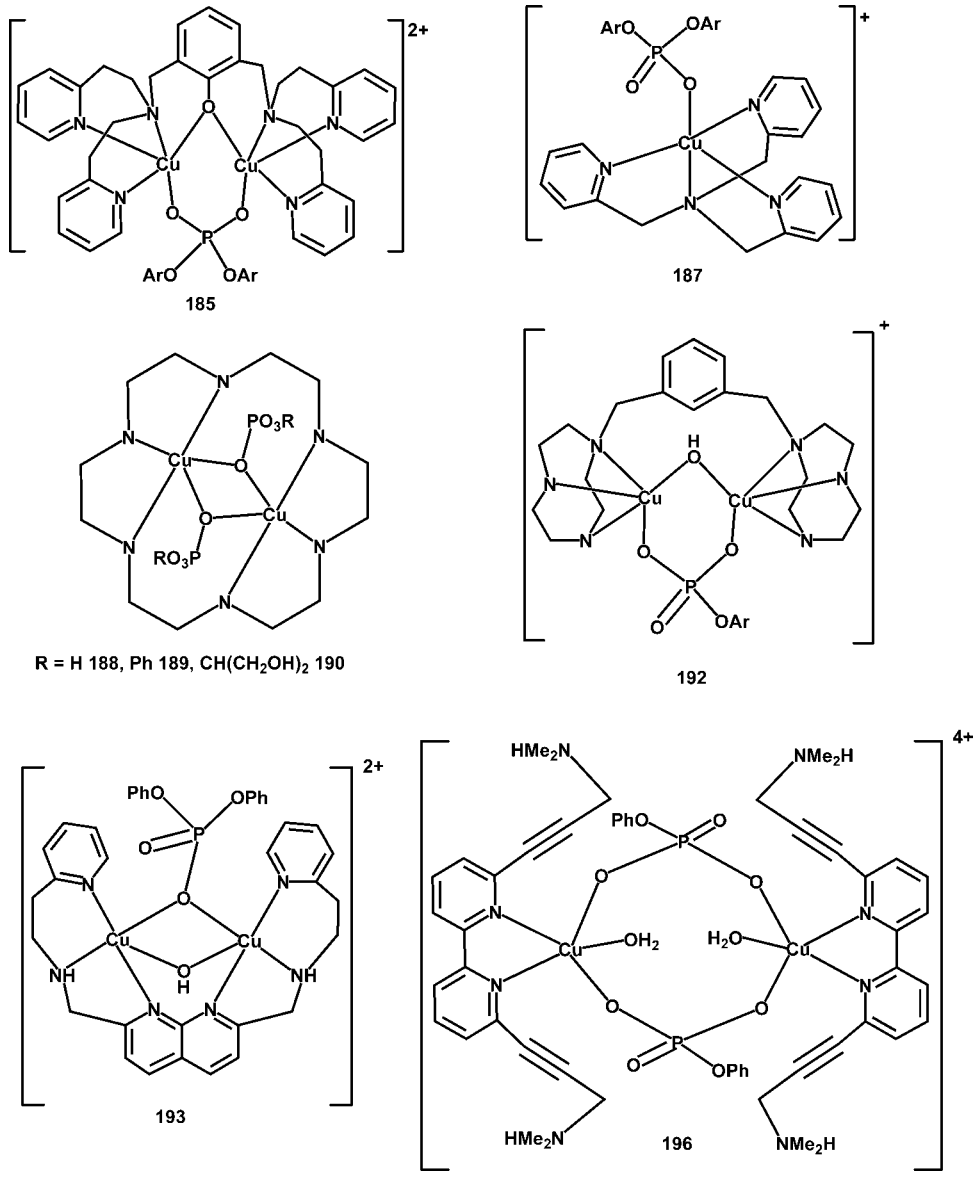

Figure 23. Mono- and dinuclear copper phosphates.

(Figure 22), and (c) presence of intermolecular C−H···O interactions to weaken the P−OR ester linkages.

A number of dicopper and monocopper complexes have been synthesized as catalysts for phosphate ester hydrolysis and DNA cleavage reactions because of the similar coordination chemistry of the copper(II) ion and superior Lewis acidity to that of Zn(II), which has been observed as a cofactor in many nucleases.[20] During the course of the phosphate ester hydrolysis studies catalyzed by these copper complexes, a model compound or an intermediate can be successfully isolated and structurally characterized. Such efforts have made it possible to isolate a number of copper complexes with a phosphate monoester or diester in their coordination sphere, with or without the activation of the ester linkage. Although several reports have dealt with various aspects of copper-catalyzed hydrolysis reactions, only those where a phosphate bound copper complex has been structurally well characterized are discussed below.

In 1993, Karlin et al. have shown that the reaction of $[Cu_2(UNO^-)(OH)](PF_6)_2$ with bnpp yields the dinuclear complex $[Cu_2(UNO^-)(bnpp)](PF_6)_2$ (**185**) (Figure 23). The related complex $[Cu_2(XYLO^-)(bnpp)](PF_6)_2 \cdot 1/2CH_2Cl_2 \cdot 1/2Et_2O$ (**186**) was synthesized from the corresponding hydroxy complex.[161] The molecular structure of **185** determined by X-ray diffraction shows that the copper ion is five-coordinated with ligation from two pyridyl nitrogens, one tertiary amine nitrogen, the phenolate oxygen, and one oxygen atom of the phosphate ester. The UNO and XYLO ligands in **185** and **186** are octadentate. The Cu···Cu separation in **185** has been found to be 3.773 Å.[161]

Two isomeric binuclear ligands, 1,4- and 1,3-bis[6-bis(2-pyridylmethyl)aminomethylpyridyl]benzene (pbtpa and mbtpa), and their Cu(II) complexes prepared by Zhu et al. were examined for the hydrolysis of a model phosphodiester substrate, bnpp.[162] A bell-shaped pH vs. rate profile, which is in agreement with one mechanism proposed for bimetallonucleases and phosphatases, was observed for the binuclear complex of Cu(II) and pbtpa. At pH 8.4, a maximum rate of 1.14×10^{-6} s^{-1}, more than 10^4-fold over uncatalyzed reactions, was achieved. This report also describes the single-crystal X-ray structure of a mononuclear copper complex, $[Cu(tpa)(bnpp)]ClO_4$ (**187**) (Figure 23). The copper atom adopts slightly distorted trigonal-bipyramidal coordination geometry. While tpa tetradentatively chelates the Cu^{2+},

bnpp$^-$ acts as a monodentate ligand occupying the fifth site of the coordination sphere around Cu(II) in the trans position with respect to the bridgehead nitrogen atom.

Ren et al. reported dicopper−1,4,7,10,13,16-hexaazacyclooctadecane ([18]ane-N6) complexes $[Cu_2(O_3P(OR))_2([18]ane\text{-}N_6)]$ (R = H (**188**), Ph (**189**), and $-CH(CH_2OH)_2$ (**190**)) (Figure 23),[163] synthesized from $[Cu_2(OAc)_2([18]ane\text{-}N_6)](PF_6)_2$ (**191**) and $(NH_4)_2HPO_4/(PhO)P(O)(ONa)_2/Na_2PO_6C_3H_7$. The bulk of the molecule **190** is a rugged rectangle consisting of the [18]ane-N_6 ring with two Cu(II) ions surrounded, and the latter are bridged by two phosphate ligands above and below the rectangle. The coordination sphere of the Cu center is best described as distorted square-pyramidal. It has been further revealed that the phosphate monoester binding to **191** is selective, as association constants for common anions are at least 2 orders of magnitude lower.

Spiccia et al. reported a binuclear copper(II) phosphate complex, $[Cu_2(L)(npp)(\mu\text{-}OH)](ClO_4)\cdot H_2O$ (**192**) (Figure 23; L = 1,3-bis(1,4,7-triazacyclonon-1-ylmethyl)benzene). Here the 4-nitrophenyl phosphate anion (npp) bridges two Cu(II) centers via two phosphate oxygen atoms.[164] A hydroxide bridge further connects the two metal centers.

Lippard et al. have reported the copper phosphate $[Cu_2(\mu\text{-}OH)(dpp)(bpan)](ClO_4)_2$ (**193**) (Figure 23) in which each copper ion has square-pyramidal geometry with a bridging −OH and a monodentate bridging diphenylphosphate ligand. This is the first example where one oxygen atom from a phosphate diester forms a single-atom bridge between two metal ions.[165]

The Cu(II) complexes $[(L1)Cu(NO_3)_4\cdot 2(H_2O)]$ (**194**) and $[(L2)Cu(NO_3)_4\cdot 2(H_2O)]$ (**195**) of the ammonium-functionalized ligands $[6,6'\text{-}(Me_2HNCH_2C{\equiv}C)_2bpy]^{2+}$ (L1) and $[6,6'\text{-}(Me_3NCH_2C{\equiv}C)_2bpy]^{2+}$ (L2) have been synthesized by Kraemer et al. for the hydrolysis of the activated phosphodiester bnpp. (L1)Cu accelerates hydrolysis of bnpp (4×10^7)-fold and is 1000 times more reactive than (L2)Cu. Probably the high reactivity of (L1)Cu is related to the interaction of the acidic $-NMe_2H^+$ group with the phosphodiester substrate. Bifunctional binding of a phosphate ester by metal coordination and H bonding with one NH_4^+ group is observed in the crystallographically characterized $[(L1)_2Cu_2(1,3\text{-}\mu\text{-}O_3P(OPh))_2(OH_2)_2](NO_3)_4$ (**196**) (Figure 23).[166]

The kinetics of cleavage of 2-hydroxypropyl-*p*-nitrophenylphosphate (hpnp) by [Cu(L1)Cl] (**197**) (HL1 = 2-[bis(2-benzimidazolylmethyl)aminomethyl]-4,6-dimethylphenol) and $[Cu_2(L2)Cl_2]Cl_2$ (**198**) (HL2 = 2,6-bis[bis(2-benzimidazolylmethyl)aminomethyl]-4-methylphenol) is pseudo-first-order, and the rate constants are 4.0×10^{-5} and 2.1×10^{-3} s^{-1}, respectively. The dinculear copper complex $[(L2)Cu_2(O_2P(OCH_2Ph)_2)](ClO_4)_2$ (**199**) (Figure 24) has been prepared and characterized by X-ray diffraction experiments to gain insight into the mechanistic role of enhanced hpnp cleavage by **198**. In **199**, the oxygen atoms of the phosphate diester bridge the two metal centers of the dinuclear complex with a Cu···Cu separation of 3.67 Å.[167] These authors have proposed that the key to the high reactivity of **198** for cleaving hpnp is double Lewis activation of the phosphate diester.

Crystal structures, solution properties, and RNase activity of Cu(II) complexes of a binucleating bis-pyridyl ligand (*N*,*N*′-bis(2-pyridylmethyl)-1,3-diaminopropan-2-ol, L) were studied by Gajda et al. The alkoxo-bridged dinuclear copper complex $[Cu_2(L)(dpp)(ClO_4)(CH_3OH)]ClO_4$ (**200**) (Figure 24)[168] is prepared from diphenyl phosphate, L·4HCl, NaOH, and $CuClO_4$ as deep blue crystals. There are two distinct copper ions in **200**, one in a distorted octahedral environment and the other in a square-pyramidal environment. The two copper ions are separated from each other by 3.499 Å, which is well within the range suggested for native dinuclear metallophosphoesterases.

Yamaguchi et al. have reported, $[Cu_2(Me_4tpdp)(bnpp)](ClO_4)_2$ (**201**) (Figure 24; Me_4tpdp-H = (*N*,*N*,*N*′,*N*′-tetrakis((6-methyl-2-pyridyl)-methyl)-1,3-diaminopropan-2-ol), in which the metal ions are bridged by alkoxide and phosphodiester moieties resulting in distorted square-pyramidal geometry around both the Cu centers.[149]

Dimeric copper complex $[Cu_2(bpy')_2(bnpp)_2(NO_3)_2]$ (**202**) (Figure 24) is formed between 4,4′-dimethyl-2,2′-bipyridine (bpy′), Cu(II), and bnpp. The molecule has a center of symmetry with the coordination geometry around copper being square-pyramidal. The phosphate oxygens occupy both in-plane and out-of-plane sites on the dinuclear complex. While the dimeric structure is similar to other five-coordinate Cu(II) complexes of bipyridine, the alternating in-plane and out-of-plane bridging of the Cu(II) centers by bnpp is unusual.[169]

The molecular recognition of two simple phosphate diesters by a terpyridine−copper complex was studied by X-ray crystallography and potentiometry. Molecular recognition of the substrate is the first step in a hydrolysis reaction. The two phosphate diesters, bis(*p*-nitrophenyl) phosphate (bnpp) and diphenyl phosphate (dpp), coordinate to form square-pyramidal Cu complexes [Cu(tpy)(bnpp)Cl] (**203**) and $[Cu(tpy)(dpp)Cl]\cdot H_2O$ (**204**) (Figure 24).[170] In the resulting square-pyramidal complexes, the phosphate ligand is axially coordinated, while the chloride and three terpyridine nitrogen atoms form the corners of the base. The molecular recognition constants for the formation of **203** and **204** were measured potentiometrically and have log values of 1.2 and 2.5, respectively. By a significant margin, the copper−tpy complex favors dpp over bnpp in solution. A pH vs. rate constant profile further shows that Cu(tpy)(OH) can hydrolyze bnpp but not dpp. Activated and unactivated phosphate diesters are typically hydrolyzed by similar mechanisms. The difference in reactivity lies outside the process of molecular recognition. Activating effects of the *p*-nitro groups on the nature of the leaving groups must play an important role in the susceptibility of phosphate diesters to hydrolysis.

In order to understand the reactivity and mechanistic aspects of hydrolysis of bis(2,4-dinitrophenyl)phosphate by $[Cu(bis(pyridylmethyl)amine)(OH_2)_2]Cl_2$ (**205**), $[Cu\{N\text{-}(2\text{-}hydroxyethyl)bis(pyridylmethyl)amine\}(OH_2)]Cl_2$ (**206**), and $[Cu\{N\text{-}(3\text{-}hydroxypropyl)bis(pyridylmethyl)amine\}(OH_2)]Cl_2$ (**207**), model complexes copper dimethyl phosphate $[(L1)Cu(OP(O)(OMe)_2)(HOMe)]Cl$ (L1 = bis(2-benzimidazolylmethyl)amine) (**208**) (Figure 24) and chloride complex [(L2)Cu(Cl)]Cl (L2 = N-(2-hydroxyethyl)bis(2-benzimidazolylmethyl)amine) (**209**) were studied as structural models.[171] Copper ions in both **208** and **209** are square-pyramidal with the phosphate or the −OH oxygen atom occupying the axial position. The four basal positions are occupied by nitrogen and chlorine atoms.

Spiccia et al. have reported the synthesis of a trimeric macrocyclic copper phosphate complex $[Cu_3(Me_3tacn)_3(PhOPO_3)_2](ClO_4)_2\cdot {}^1/_2H_2O$ (**210**) (Me_3tacn = 1,4,7-trimethyl-1,4,7-triazacyclononane; Figure 24), in which two phenyl phosphates (Ph-PO_3) bridge three Cu(II) centers.[172] It consists

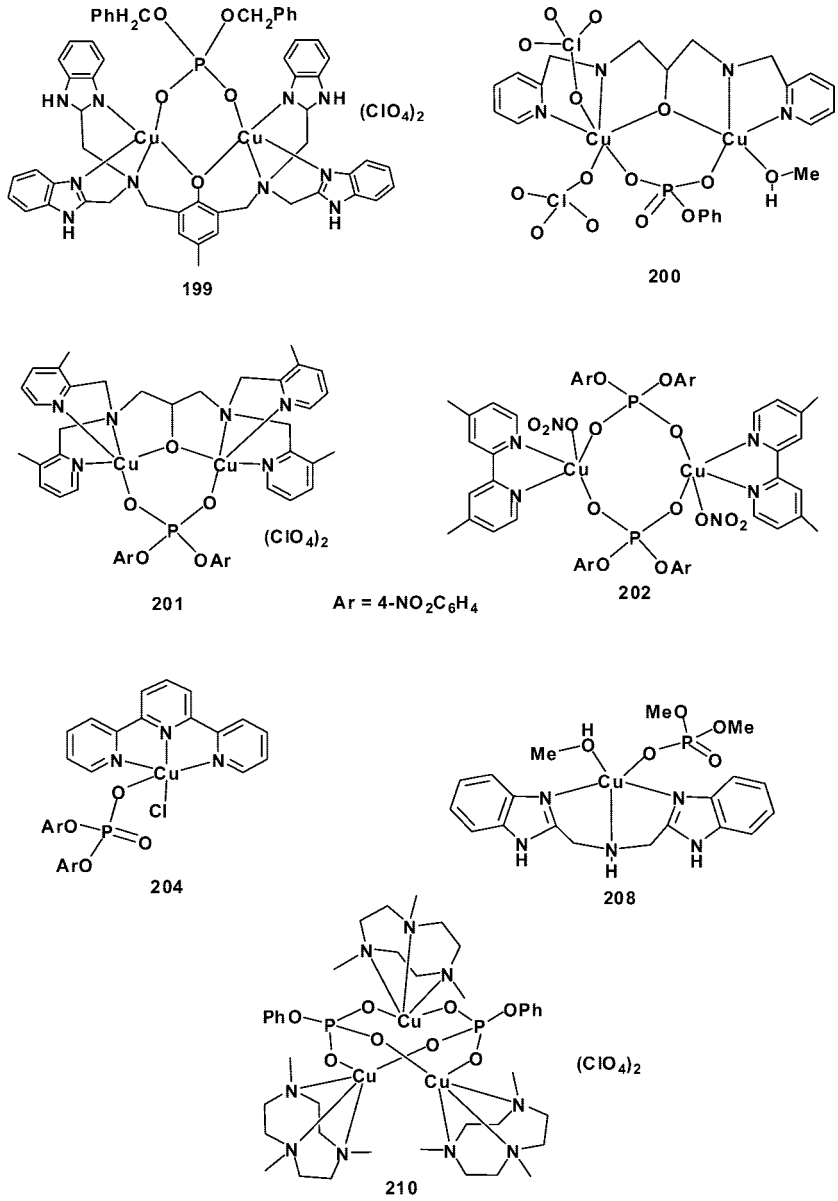

Figure 24. Schematic diagram of copper phosphates. The chloride anion in **208** is not shown.

of discrete $[Cu_3(Me_3tacn)_3(PhOPO_3)_2]^{2+}$ cations, perchlorate anions, and water of crystallization. The complex cation consists of three $[Cu(Me_3tacn)]^{2+}$ moieties linked together by the two phosphate esters via three oxygen atoms, and thus, all three Cu(II) centers are linked to each other by two Cu−O−P−O−Cu bridging units. The two phosphate esters lie above and below the plane defined by the $Cu(Me_3tacn)$ units, with the phenoxy groups located perpendicular to the triangular array of copper atoms. An interesting result of this binding of the two organophosphates is the generation of an empty 11-atom cage defined by the three Cu atoms and two $PhOPO_3^{2-}$ units. Each Cu(II) center is in a distorted square-pyramidal geometry with the Me_3tacn macrocycle occupying one face of a distorted square pyramid and phosphate oxygen atoms in the other two coordination sites. Complex **210** is unique in the sense that two organophosphates are bound to three Cu(II) centers. Most other Cu(II) complexes with coordinated phosphate moieties are usually binuclear and, often, have other groups bridging the two Cu(II) centers. The Cu···Cu distances in **210** are 4.14, 4.55, and 5.04 Å.

The compound $[Cu_2(bnpp)_2(bpa)_2](ClO_4)_2 \cdot 0.5CH_3CN$ (**211**) (bpa = bis(2-pyridylmethyl)amine; Figure 25) has been recently structurally characterized by Butcher et al.[173] This complex contains two Cu^{II} ions in a distorted square-pyramidal geometry. Two bnpp anions bridge Cu^{II} ions to form the dinuclear complex cation.

In a recent study, Rossi et al. have reported that $[Cu_2(Hbtppnol)(\mu\text{-}CH_3COO)](ClO_4)_2$ (**212**) (L = *N*-(2-hydroxybenzyl)-*N*,*N*′,*N*′-tris(2-pyridylmethyl)-1,3-diaminopropan-2-ol (H_2btppnol)) reacts with excess of the diester 2,4-BDNPP at pH 7.0 and results in the formation of the monoester phosphate coordinated copper dimer $[Cu_2(Hbtppnol)(\mu\text{-}((NO_2)_2\text{-}C_6H_3O)PO_3)]ClO_4$ (**213**) (Figure 25), which has been characterized by X-ray crystallography.[174] In addition, the stable μ-phosphate complex $[Cu_2(Hbtppnol)(\mu\text{-}(NO_2\text{-}C_6H_4O)PO_3)](ClO_4)$ (**214**) (Figure 25) was directly obtained from the reaction of 4-nitrophenyl phosphate with **212**. The kinetics for the promotion of bis(2,4-dinitrophenyl) phosphate (2,4-BDNPP) hydrolysis by complex **212** has been investigated as a function of pH, catalyst concentration, and substrate concentration. Complex **212** effectively promotes the cleavage of double-stranded genomic and plasmid DNA at physiological pH, probably through a hydrolytic mechanism in agreement with that proposed for the reaction of

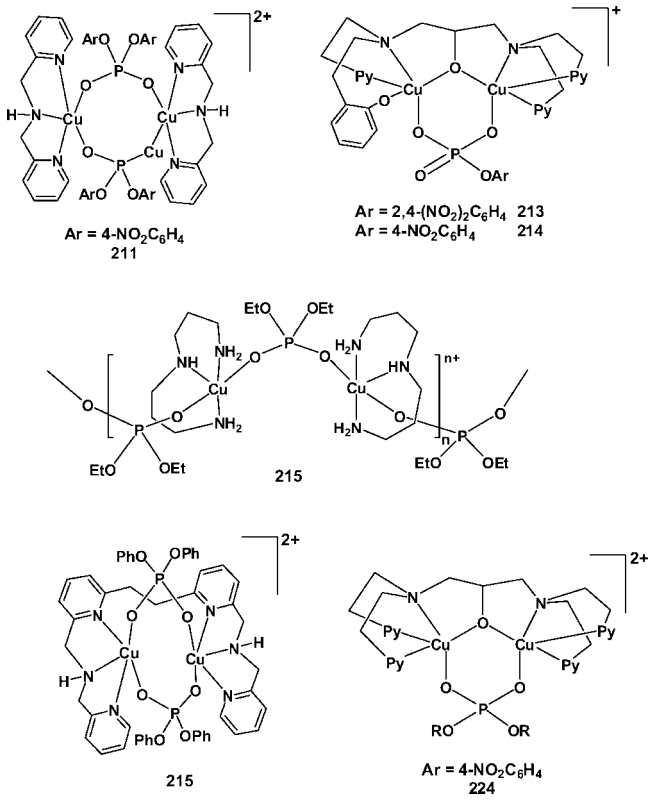

Figure 25. Copper phosphates.

212 with 2,4-BDNPP. Cytotoxic activity of **212** in a human small cell lung carcinoma cell line (GLC4) and its cisplatin-resistant subline (GLC4/CDDP) has been investigated, and the IC_{50} values were determined.

Fujii et al. have synthesized a polymeric copper phosphate, $[Cu(\mu\text{-}O_2P(OEt)_2)L]_n(PF_6)_n$ (**215**) (L = dipropylenetriamine; Figure 25) by the reaction of $CuSO_4 \cdot 7H_2O$ with diethyl phosphate in the presence of dipropylenetriamine and KPF_6 at pH 8.5. Each copper ion is coordinated by a dipropylenetriamine and two bridging diethyl phosphate anions, which leads to the formation of a polymeric chain.[175]

1,2-Bis(2-((methyl(pyridylmethyl)amino)methyl)-6-pyridyl)ethane (L) forms dinuclear $Cu_2(L)((PhO)_2PO_2)_2](ClO_4)_2$ (**216**) (Figure 25) or hexanuclear $[Cu_6(L)_3((PhO)PO_3)_4](ClO_4)_4$ (**217**) in the presence of $(PhO)_2PO_2^-$ or $(PhO)PO_3^{2-}$, respectively.[176] The structures in solution were studied by FAB and SCI MS spectrometers. L binds two Cu(II) ions with two pendant groups in tridentate chelate modes, and with the incorporation of phosphate esters, various dinuclear units are formed in **216** and **217**. In **217**, a dinuclear unit of $[Cu_2(L)]^{4+}$ links two dinuclear units of $[Cu_2(L_3)(PhOPO_3)_2]$ with four μ_3-1,3-$PhOPO_3^{2-}$ bridges.[176]

The copper acetate complex of the 1,4,7,10,13,16-hexaazacyclooctadecane macrocycle ([18]ane-N6) undergoes facile replacement of bridging OAc by phosphate monoester $[PO_3(OR)^{2-}]$ to yield a number of bis(phosphate monoester)-dicopper complexes where $ROPO_3^{2-}$ is hydrogen phosphate (**218**), phenyl phosphate (**219**), glycerol 2-phosphate (**220**), α-D-glucose phosphate (**221**), and DL-α-glycerol phosphate (**222**).[177] Structural studies of compounds **218**−**221** confirmed both the retention of the Cu_2{[18]ane-N6} core and a μ-O-PO_3(OR) coordination mode. Displacement of acetate by a phosphate monoester in water was accompanied by a significant change in the visible absorption, from which it has been established that the relative association constants

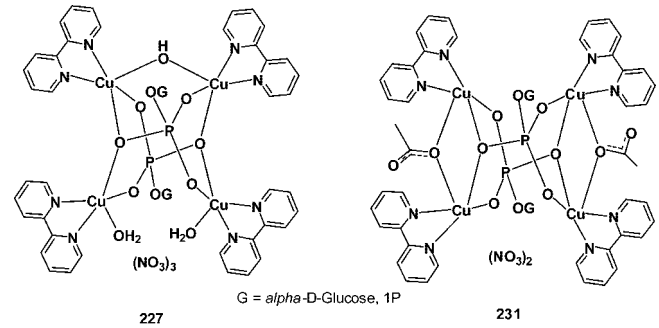

Figure 26. Schematic diagram for the molecular structures of $[Cu_4(\mu\text{-OH})(\alpha\text{-D-Glc-1P})_2(bpy)_4(H_2O)_2](NO_3)_3$ (**227**) and $[Cu_4(\alpha\text{-D-Glc-1P})_2(CH_3COO)_2(bpy)_4](NO_3)_2$ (**231**).

of $PO_3(OR)^{2-}$ are $\sim 10^4$ in the unbuffered solution and 10^3 in the buffered solution. The magnetic susceptibility data of compound **218** in the temperature range 5−300 K revealed a weak antiferromagnetic coupling the between two copper centers.[177]

Dinuclear copper(II) complex $[Cu_2(L2O)](CF_3SO_3)_3$ (**223**) (L2OH = bis[bis[2-(2-pyridyl)ethyl]amino]-2-hydroxypropane) reacts with BNPP to yield a hydrolytically inactive complex **224** in which a bis(*p*-nitrophenyl)phosphato ligand has displaced the trifluorosulfanato ligand.[178] The structure of complex **224** (Figure 25) has been determined using X-ray crystallography.

$Cu[O_2P(OMe)_2]_2$ (**225**) was synthesized by the reaction of CuCl with $OP(OMe)_3$. The poorly refined X-ray structure of this compound reveals that it forms an infinite one-dimensional polymer through O−P−O bridges of the phosphate ester with five-coordinate copper atoms.[179] On the other hand, treatment of $CuCl_2$ with dimethyl phosphate (DMP) with DMSO under N_2 afforded a light blue fluorescence powder. Slow evaporation of water−DMSO solution of this blue powder resulted in sky-blue crystals of a polymeric Cu(II) complex, $[Cu_2(DMP)_4(DMSO)]$ (**226**).[180] A square-pyramidal environment for the metal center was established by coordination of O atoms of four bridging DMP ligands in the basal positions and binding a tricentered O atom of DMSO in the apical disposition of Cu(II). The sixth position was also affected by a weak interaction with the S atom of another DMSO.

Kraemer et al. have reported a dinuclear copper dimethylphosphate complex incorporating a macrocyclic ligand as a part of their recent study on catalytic transesterification of dialkylphosphates by bioinspired dicopper(II) macrocyclic systems.[181]

Recently Tanase et al. reported on dicrete tetrameric and dimeric copper clusters containing sugar phosphates. The tetrameric complexes $[Cu_4(\mu\text{-OH})(\alpha\text{-D-Glc-1P})_2(bpy)_4(H_2O)_2]X_3$ (L = bpy, X = NO_3 (**227**), X = Cl (**228**), X = Br (**229**); L = phen, X = NO_3 (**230**); α-D-Glc-1P = α-D-glucose-1-phosphate) (Figure 26).[182,183] Each copper ion in **227**−**230** is ligated by two nitrogen atoms of phen and three oxygen atoms of phosphate, hydroxo, or water units and adopts $[N_2O_3]$ square-pyramidal coordination. The phosphate group of α-D-Glc-1P bridges three Cu atoms at equatorial sites and additionally binds the fourth Cu atom at its axial site, resulting in a trapezoidal tetracopper core with the upper side clipped by the hydroxo bridge.

Complex **227** readily reacted with carboxylic acids to afford the tetranuclear Cu(II) complexes $[Cu_4\{\mu\text{-}(\alpha\text{-D-Glc-1P})\}_2(\mu\text{-CA})_2(bpy)_4](NO_3)_2$ (CA = CH_3COO (**231**), *o*-C_6H_4(COO)(COOH) (**232**)).[182,183] Reactions with *m*-phe-

nylenediacetic acid [m-$C_6H_4(CH_2COOH)_2$] also gave a discrete tetrameric complex, [$Cu_4\{\mu$-(α-D-Glc-1P)$\}_2(\mu$-m-$C_6H_4(CH_2COO)(CH_2COOH))_2(bpy)_4](NO_3)_2$ (**233**), and a cluster polymer, $\{[Cu_4\{\mu$-(α-D-Glc-1P)$\}_2(\mu$-m-C_6H_4-$(CH_2COO)_2)(bpy)_4](NO_3)_2\}_n$ (**234**). A symmetric rectangular Cu_4 has been observed in the case of **231**, **232**, and **234**, where the original hydroxo bridge found in **227** is dissociated and, instead, two carboxylate anions bridge another pair of Cu(II) ions. Similar reactions were applied to incorporate sugar acids onto the tetranuclear Cu(II) centers. Thus, reactions of **227** with δ-D-gluconolactone, D-glucuronic acid, or D-glucaric acid in DMF gave discrete tetracopper complexes with sugar acids, [$Cu_4\{\mu$-(α-D-Glc-1P)$\}_2(\mu$-$SA)_2(bpy)_4](NO_3)_2$ (SA = D-gluconate (**235**), D-glucuronate (**236**), D-glucarateH (**237**)]. The structures of **235** and **236** are similar that of **231**. The reactions of **227** with with D-glucaric acid and D-lactobionic acid afforded chiral one-dimensional polymers, $\{[Cu_4\{\mu$-(α-D-Glc-1P)$\}_2(\mu$-D-glucarate)$(bpy)_4](NO_3)_2\}_n$ (**238**) and $\{[Cu_4\{\mu$-(α-D-Glc-1P)$\}2(\mu$-D-lactobionate)$(bpy)_4(H_2O)_2](NO_3)_3\}_n$ (**239**).

Dimeric copper complexes [$Cu_2(\mu$-OH)$(XDK)(L)_2$]X (H_2XDK = m-xylenediamine bis(Kemp's triacid imide), L = bpy, X = NO_3; L = phen, X = NO_3) readily react with diphenyl phosphate (HDPP) or bis(4-nitrophenyl) phosphate (HBNPP) to give [$Cu_2(\mu$-phosphate)$(XDK)(L)_2]NO_3$ (L = bpy, phosphate = DPP (**240**); L = phen, phosphate = DPP (**241a**), BNPP (**241b**)), where the phosphate diester bridges the two Cu ions (Cu···Cu = 4.268(3)−4.315(1) Å).[184] It is interesting to note that complexes such as [$Cu_2(\mu$-OH)$(XDK)(L)_2$]X could be reacted with a large number of sugar phosphate molecules and the corresponding dimeric or tetrameric copper complexes could be isolated.[184]

2.10.2. Silver

Silver diethylphosphate [$Ag(O_2P(OEt)_2]$ (**242**) reported in 1972 by Collin et al. is the only well-characterized silver organophosphate. Compound **242** was obtained starting from excess silver oxide and diethylchlorophosphate.[185] The silver ion in **227** is coordinated to four oxygen atoms of the two adjacent phosphate groups in a distorted tetrahedral arrangement.

2.10.3. Gold

The phosphate binding ability of Au(III), in the case of nucleosides and nucleotides, has been studied by examining the interaction of Au(III) with dimethyl phosphate,[186] which is a conformational analog of the phosphate backbone in the DNA chain.

2.11. Group 12 Metal Phosphates

2.11.1. Zinc

Zinc phosphates with different coordination geometries are important in the field of biology due to the occurrence of this element in several nucleases and phosphatases. There have been a number of reports on the synthesis of zinc-based model compounds and catalysts for the hydrolysis of model phosphate esters in the last two decades. Heteronuclear metal phosphates featuring zinc ions have already been dealt with in the preceding sections. The chemistry of other well-characterized zinc phosphates is described below. It should once again be emphasized that the role of zinc in hydrolases and nucleases is a very vast area and different aspects of this problem have been frequently reviewed. The treatment of zinc complexes as models for these enzymes in this review is confined to the structurally characterized zinc phosphate complexes.

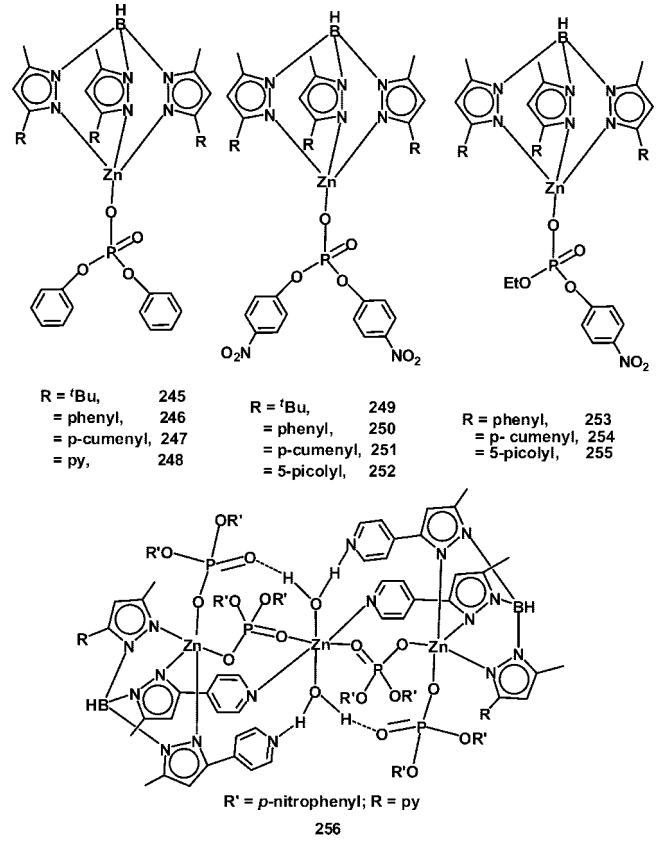

Figure 27. Zinc phosphates based on tris(pyrazolyl)borate ligands.

Notable among zinc phosphate complexes is the extensive series of complexes based on tris(pyrazolyl)borate and sterically crowded tripod ligands synthesized by Vahrenkamp et al. Making use of the steric protection provided by the tris(pyrazolyl)borate ligand on one side of the tetrahedron and an open −OH group on the other side, these workers have demonstrated how it is possible to exploit the hydrolytic activity of the zinc-bound hydroxyl group (or water, for that matter) to make new zinc phosphate complexes. Thus, Tp*ZnOH complex (Tp* is a substituted pyrazolylborate ligand) turns out to be one of the best nucleophiles to effect the hydrolysis of ester. In all, five different (pyrazolylborate)zinc hydroxide complexes Tp*ZnOH were used as hydrolytic reagents towards esters of various acids of phosphorus.

Pyrazolylborate-based Zn phosphate complexes **243**−**248** have been prepared by the reaction of substituted tris(pyrazolyl)-borate−zinc hydroxide and the corresponding phosphate triester via hydrolytic cleavage.[187] $(OMe)_3PO$ and $(MeO)_3P$ could not be cleaved by these complexes. $HP(OR)_2$ (R = Me, Ph) yielded $Tp^{tBu,Me}Zn[OPHO(OR)]$ (R = Me (**243**), R = Ph (**244**)). Phenylphosphate reacted slowly producing moderate yields of $[Tp^{R,Me}Zn(dpp)]$ (R = ^{t}Bu (**245**), Ph (**246**), Cum (**247**), Py (**248**)) (Figure 27). Tris(*p*-nitrophenyl)phosphate was cleaved rapidly, forming $Tp^{R,Me}Zn[bnpp]$ (R = ^{t}Bu (**249**), Ph (**250**), Cum (**251**), 5-picolyl (**252**)) and $Tp^*Zn[OC_6H_4NO_2]$ (Figure 27). Ethyl-bis(*p*-nitrophenyl) phosphates showed intermediate reactivity, losing *p*-nitrophenolate upon hydrolysis and producing $Tp^{R,Me}Zn$-$[OPO(OEt)(OC_6H_4NO_2)]$ (R = Ph (**253**), Cum (**254**), 5-pi-

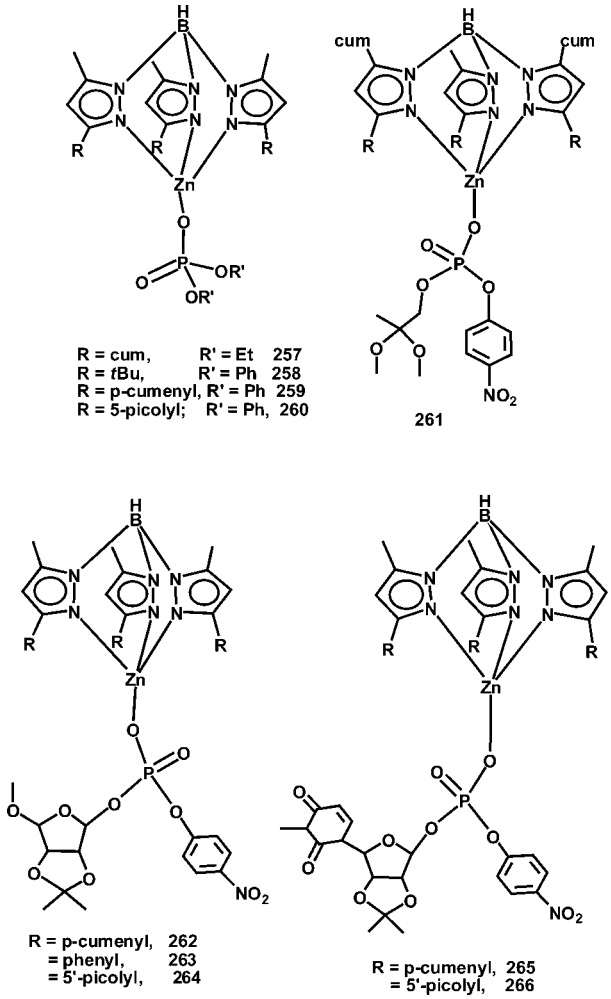

Figure 28. Tris(pyrazolyl)borate zinc phosphates.

colyl (**255**)) (Figure 27).[187] When phosphorus acid diesters were employed, condensation between the Zn-OH and P-OH functions occurred. Six structure determinations for the above complexes showed the structural variability of the resulting complexes. In $[(Tp^{Py,Me})_2Zn_3(bnpp)_4(H_2O)_2]$ (**256**) (Figure 27), the zinc ions are in a nearly octahedral ZnN_2O_4 environment and the double-bridged linkage between the peripheral and central zinc ions (via one phosphate and one pyrazole unit) represents a 10-membered heterocyclic ring.[187]

Extending these studies, these authors have shown how P−O−P linkages can be cleaved by Tp*ZnOH. For example, tetraethyl or tetraphenyl diphosphates are cleanly cleaved to yield products $Tp^{R,Me}$Zn-OP(O)(OR′)$_2$ (R = Cum, R′ = Et (**257**); R = ^{t}Bu, R = Ph (**258**), R = Cum, R′ = Ph (**259**), R = 5-picolyl, R′ = Ph (**260**)) (Figure 28).[188]

Instead of simple phosphate esters, phosphate derivatives that actually model intermediates of enzymatic glycoside transformations can also be reacted with Tp*ZnOH. Depending on the substrate or the reaction conditions, either phosphate ester cleavage or deprotonation of a nucleobase NH was observed. As a result, the Tp*Zn units were attached to the phosphate part or to the nucleobase part of the substrate. Nucleobase adducts were formed for uridine monophosphate derivatives. Phosphate adducts were obtained in the reactions with a hydroxyacetone monophosphate and a ribose phosphate and in reactions of uridine and *N*-methyluridine monophosphates. The products were identified by crystallographic and spectroscopic methods as tetrahedral Tp*Zn-X complexes **261**−**266** (Figure 28).[189]

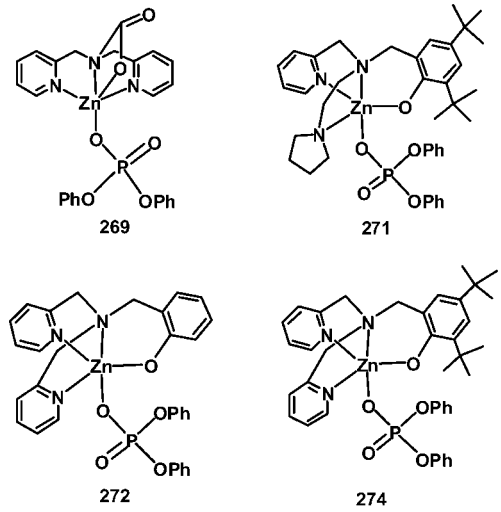

Figure 29. Zinc phosphates based on tripodal N_3O ligands.

The alkoxide derivatives, $Tp^{Ph,Me}$Zn-OMe and $Tp^{Cum,Me}$Zn-OMe, were tested for their reactivity toward substrates that are hydrolytically cleaved with Tp*Zn-OH complexes. They do not induce the cleavage of nonactivated esters, phosphoesters, lactones, or lactams. They however cleave the P−O−P linkage of tetraalkylpyrophosphates to produce products of the type **259**.[190]

Vahrenkamp and co-workers have recently studied newer pyrazolylborates as ligands in zinc complexes for the phosphate ester hydrolysis. These include $Tp^{Fu,Me}$Zn-X complexes ($Tp^{Fu,Me}$ = hydrotris(3-(2′-furyl)-5-methylpyrazolyl)borate, X = Cl, Br, I, NCS, CH_3COO, CF_3COO), $Zn(Tp^{Fu,Me})_2$, and $Tp^{Fu,Me}$Zn(OH). The latter complex models hydrolases by the hydrolytic cleavage of tris(*p*-nitrophenyl)phosphate and γ-thiobutyrolactone.[191] Similarly, they have shown that tris(thioimidazolyl)borate-Zn-thiolate complex (TtiXyl)Zn(SEt) reacts slowly with trimethyl phosphate in a nonpolar medium at room temperature, yielding (TtiXyl)Zn(OPO(OMe)$_2$) (**267**), which can be converted back to the thiolate complex with NaSEt.[192]

Vahrenkamp et al. have extended their zinc chemistry beyond tris(pyrazolyl)borate ligands, and introduced several tripodal ligands in the metal coordination sphere. For example, the *N*,*N*-bis(2-picolyl)glycine (L-H) complex [L·Zn]ClO_4·H_2O (**268**), a good starting material for the introduction of coligands forming complexes that mimic the coordination of Zn in enzymes with a N,N,O donor set, reacts with diphenyl phosphate (dpp) to yield the trigonal-bipyramidal complex [L·Zn(dpp)]·2H_2O (**269**) (Figure 29). In **269**, dpp acts as a monodentate ligand and occupies the axial position of the tbp geometry, which is trans to the bridgehead nitrogen atom of the ligand.[193]

Stepwise alkylation of 2-picolylamine has yielded the unsymmetrical tripodal ligand (2-picolyl)(*N*-pyrrolidinylethyl)(2-hydroxy-3,5-di-*tert*-butylbenzyl)amine (ppha). In the presence of diethylzinc, ppha is deprotonated at the phenolic OH function with formation of the unstable complex [(ppha)ZnEt] (**270**). Complex **270** reacts with diphenylphosphoric acid to yield [Zn(dpp)(ppha)] (**271**) (Figure 29).[194] Similarly, the tripodal N,O ligand bis(2-pyridylmethyl)(*o*-hydroxybenzyl)amine (bpha) on treatment with $ZnEt_2$ followed by addition of diphenylphosphate led to the isolation of [Zn(dpp)(bpha)] (**272**) (Figure 29).[195] In another variation of the same strategy, the sterically hindered N,N,O-tripodal ligand bis(2-picolyl)(2-hydroxy-3,5-di-*tert*-butylbenzyl)amine (bph-

ba) was treated with $ZnEt_2$ to yield [(bphba)ZnEt] (**273**). Organozinc derivative **273** reacts with diphenylphosphate to produce [Zn(dpp)(bphba)] (**274**) (Figure 29).[196] The molecular structures of **271**, **272**, and **274** resemble that observed for **269**.

Two types of new N,N,O ligands have been recently introduced recently by Vahrenkamp et al. in their zinc chemistry. The tridentate ligand *N*,*N*-(2-dimethylaminoethyl)-3,5-di-*tert*-butyl-salicylaldimine (LH) with $ZnEt_2$ and diphenylphosphate yields the phosphate complex [LZnOPO-$(OPh)_2$·MeOH] (**275**). The coordination geomertry of the metal, which is between trigonal bipyramidal and square pyramidal, and the character of the donors in the phosphate complex represent the transition state of a hydrolytic substrate cleavage in a Zn enzyme.[197]

In the second type, the N,N,O ligands that provide a hydrophobic cavity, such as (3,5-di-*tert*-butyl-2-hydroxybenzyl)(6-phenyl-2-pyridylmethyl)(2-pyridylmethyl)amine and (3,5-di-*tert*-butyl-2-hydroxybenzyl)bis(6-methyl-2-pyridylmethyl)amine, have been investigated as lignads in LZn(OH) complexes that effect the hydrolytic cleavage of tris(*p*-nitrophenyl) phosphate to bis(*p*-nitrophenyl) phosphate. The corresponding aqua complexes $LZn(OH_2)^+$ however do not cleave the phosphate esters.[198]

Vahrenkamp et al. have further shown that the N,N,S ligand (2-mercaptoisobutyl)(2-pyridin-2-yl-ethyl)methylamine forms a mononuclear zinc complex with ZnN_2S_2 coordination. This complex reacts with the alkylating agents CH_3I and $PO(OCH_3)_3$ in a two-step process. In the first step, the isobutylthiolate function is methylated and its position in the ligand sphere of Zn is taken by I^- or $OPO(OCH_3)^{2-}$, respectively. In the second step, the additional thiolate ligand is methylated and replaced by a second iodide or dimethyl phosphate anion.[199]

In an interesting variation of zinc phosphate chemistry, the reactions of condensed diphosphates were carried out with a zinc precursor in the presence of chelating, tridentate, and encapsulating tripod ligands. Zinc perchlorate, diorganodiphosphates (POP^{2-}), and chelating ligands L (L = 1,10-phenanthroline, neocuproine, 2,2′-bipyridine, oxinate) yield three types of ternary complexes. Type 1, (L_2Zn·POP) (**276**), contains octahedral zinc bound by the diphosphate as an OPOPO chelate ligand. Type 2, $[(LZn·POP)]_2$ (**277**) (Figure 30), consists of dimeric complexes containing five-coordinate zinc, with the diphosphates acting as OPOPO chelate ligands for one Zn ion and as OPO bridges between two Zn ions. Type 3, (L_2Zn_2·POP) (**278**), is observed only for oxinate, and contains two five-coordinate Zn ions bridged by the diphosphate as a tetradentate ligand.[200]

Diorganodiphosphates (POP^{2-}) and a triorganomethylenediphosphonate (PCP^-) have been combined with Zn salts and the tridentate ligands L (L = bis(benzimidazolylmethyl)amine, bis(2-pyridylmethyl)amine, triazacyclononane, trimethyltriazacyclononane, and (dimethylaminoethyl)(2-pyridylmethyl)amine). The resulting ternary complexes contain four-, five-, or six-coordinate Zn. Four-coordinate zinc was identified in the complex types $[L·Zn(PCP)]^+$ (**279**) and $[L·Zn(POP)Zn·L]^{2+}$ (**280**) (Figure 30). Five-coordinate Zn was found in [L·Zn(POP)] (**281**) with chelating diphosphate ligands. Six-coordinate Zn was found in the complex type [L·Zn(POP)·H_2O] (**282**) containing chelating diphosphates and in $[L·Zn(POP)]_2$ (**283**) in which the diphosphates act as tridentate bridging ligands (Figure 30). In a few cases, hydrolytic cleavage of the diphosphates resulted in trinuclear

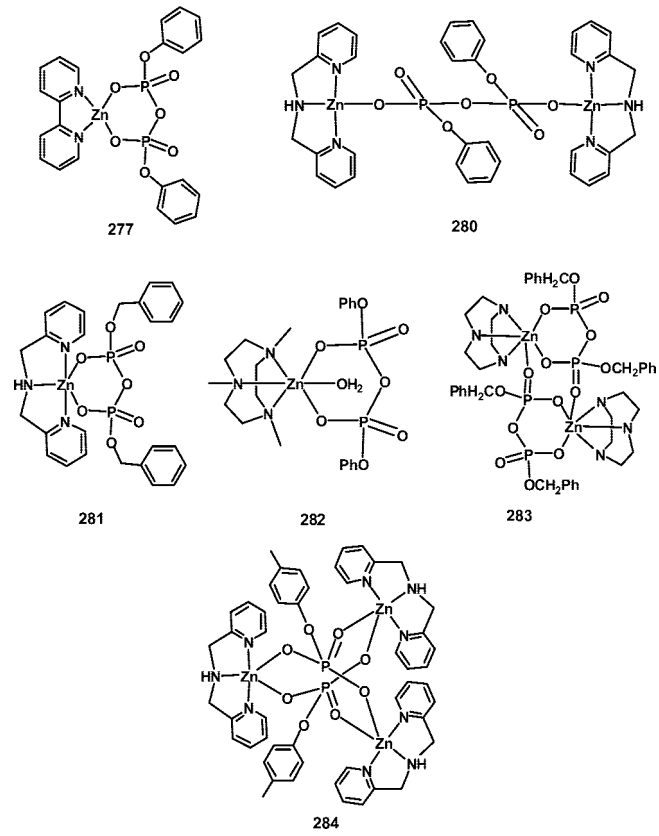

Figure 30. Diphosphates as ligands in zinc monomeric and oligomeric complexes. In the case of **280**, only the cationic part is shown.

$[(L·Zn)_3(ROPO_3)_2]HPO_4$ (**284**) with triply bridging monophosphates (Figure 30).[201]

Tris(benzimidazolylmethyl)amine (tba) and tris(pyrazolyl)borate (Tp) ligands were used to prepare ternary Zn complexes with triorganodiphosphates (R_3POP^-), triorganomethylenediphosphonates (R_3PCP^-), and diorganodiphosphates (R_2POP^{2-}) (Figure 31). The complexes $[(tba)Zn(R_3POP)]^+$ (**285**) and $[(tba)Zn(R_3PCP)]^+$ (**286**) contain trigonal-bipyramidal zinc with monodentate diphosphate ligands. By X-ray structure determination, complex [(tba)Zn(R_2POP)] (**287**) is found to contain the same ZnN_4O coordination pattern, which also was assigned to dinuclear $[(tba)Zn(R_2POP)Zn(tba)]^{2+}$ (**288**) incorporating the diphosphates as bis-monodentate bridging ligands. The same monodentate and bis-monodentate attachment of the diphosphates, but with tetrahedral Zn in a ZnN_3O environment, was identified in the pyrazolylborate complexes [TpZn(R_3POP)] (**289**) (Figure 31) and [TpZn(R_2POP)ZnTp] (**290**) (Figure 32).[202]

As early as 1992, phosphate ester cleavage with a zinc hydroxide complex containing a pyrazolyl borate ligand has been demonstrated. Hikichi et al. have shown that the P−O bond in a tris- or bis-phosphate ester is readily cleaved by [LZnOH] (L = hydrotris(3,5-diisopropyl-1-pyrazolyl)borate) to give [LZn(npp)ZnL] (**291**), [LZn(bnpp)] (**292**), and the phenoxide complex $[LZn(OC_6H_4NO_2\text{-}4)]$ (Figure 32).[203]

A carboxylate-bridged heterometallic phosphodiester complex $[ZnCo(XDK)(dpp)_2(CH_3OH)_2(H_2O)]·CH_3OH$ (**293**) (Figure 33; H_2-XDK = *m*-xylylenediamine-bis(Kemp's triacid imide)) has been synthesized by Lippard et al. from $[ZnCo(XDK)(acac)_2(CH_3OH)_2]$ and diphenylphosphate.[204] The structure contains a ZnCo core bridged by XDK through

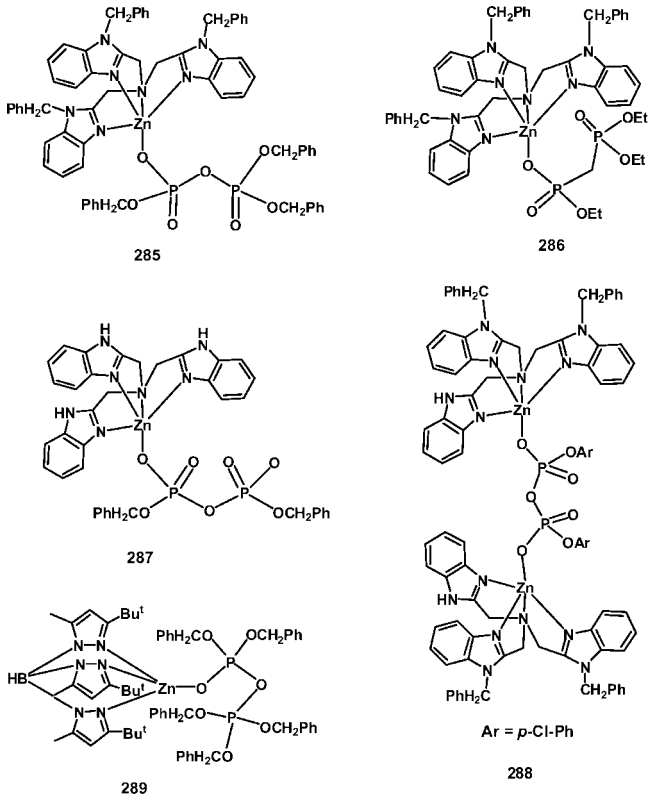

Figure 31. Zinc diphosphate complexes **285**−**289**. In the case of **285**, **286**, and **288**, only the cationic part is shown.

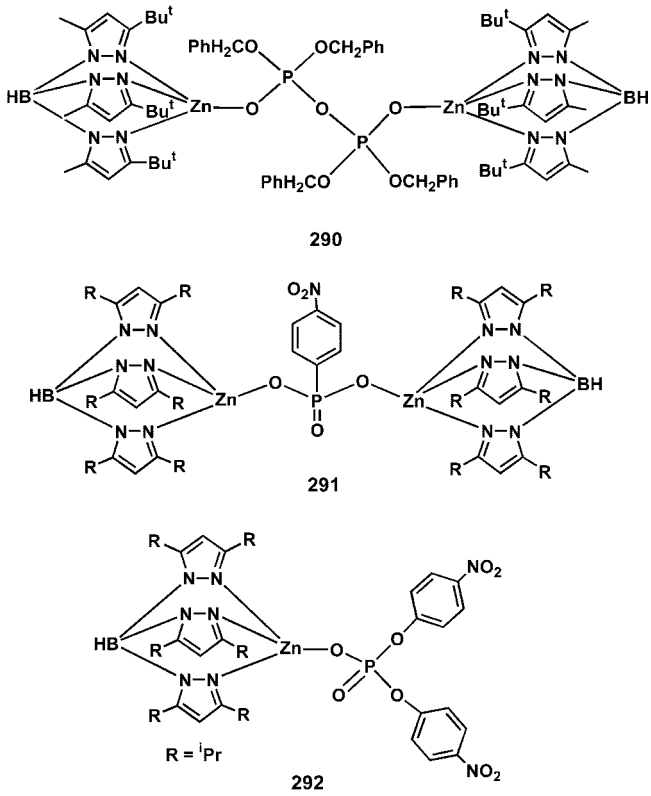

Figure 32. Zinc phosphate complexes **290**−**292** based on pyrazolyl borate ligands.

its two carboxylate groups and a diphenylphosphate ligand. The second diphenylphosphate ligand is terminally coordinated to the zinc atom in a monodentate fashion. Thus, the zinc ion is tetrahedrally coordinated by two carboxylate oxygen atoms of XDK, one bridging phosphate oxygen, and

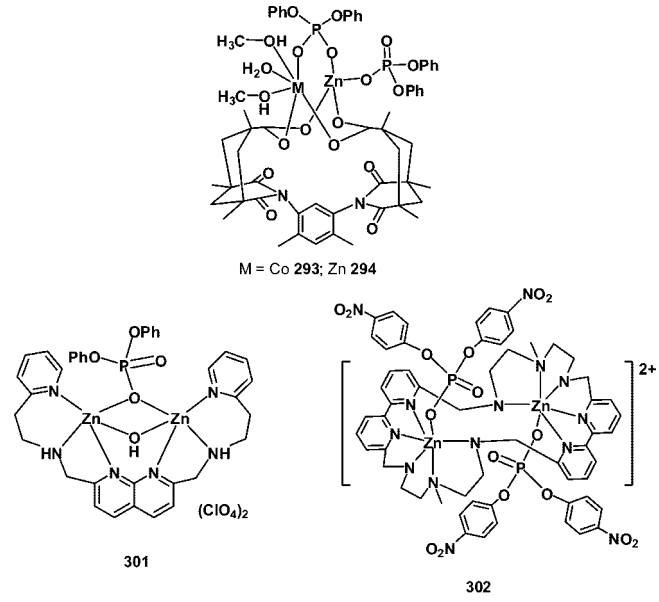

Figure 33. Carboxylate- and phosphate-bridged homo- and heterobinuclear zinc complexes.

one terminal phosphate oxygen, while the cobalt ion is octahedral with the help of additional ligation by two MeOH molecules and one water. An analogous bis(phosphate) homodinuclear complex, $[Zn_2(XDK)\{\mu\text{-}\eta^2\text{-dpp}\}\{\eta^1\text{-dpp}\}(MeOH)_2(H_2O)]$ (**294**) (Figure 33), was prepared by reacting $[Zn_2(XDK)(acac)_2(MeOH)_2]$ with diphenylphosphate in 64% yield. Compound **294**, which is isomorphous with **293**, has an asymmetric dizinc core bridged by XDK and a phosphate ligand (Zn···Zn = 3.869(2) Å). The monodentate diphenyl phosphate ligand dissociates from the dimetallic center of **294** in solution as revealed by molar conductivity and ^1H and ^{31}P NMR spectroscopic studies. The resulting free phosphate ligand exchanges with the bridging one in MeOH-d_4.

Lippard et al.[32] have also reported a binuclear zinc complex $[Zn_2(XDK)(dpp)_2(CH_3OH)_2(H_2O)]$ (**295**), where diphenylphosphate and the XDK anion bridge two metal centers. Further, one diphenylphosphate coordinates to one of the zinc ions in a monodentate fashion.[32]

The dinuclear XDK complex of zinc nitrate, $[Zn_2(XDK)(NO_3)_2(MeOH)(H_2O)_2]$ (**296**), reacts with phosphate ester salts $Na\{(RO)_2PO_2\}$ (R = Ph or *p*-$NO_2C_6H_4$) to yield the phosphate-bridged dinuclear zinc complexes $[Zn_2(XDK)\{\mu\text{-}(RO)_2PO_2\}(MeOH)_2](NO_3)$ (R = Ph (**297**); *p*-$NO_2C_6H_4$ (**298**)). Complexes **297** and **298** were further transformed into $[Zn_2(XDK)\{\mu\text{-}(RO)_2PO_2\}(py)_2](NO_3)$ (**299**, **300**) by treatment with pyridine. These phosphate ester-bridged dizinc compounds are structural models for postulated intermediates in the mechanism proposed for phosphate ester hydrolysis by *E. coli* alkaline phosphatase and DNA polymerase I, both of which contain a pair of zinc atoms in their active sites.[205]

In a somewhat different approach, Lippard et al. have synthesized another dinuclear zinc phosphate, $[Zn_2(OH)(dpp)(bpan)](ClO_4)_2$ (**301**), in which zinc ions are bridged by naphthyridine fragments of bpan, one hydroxide ion, and a diphenylphosphate group to result in a distorted tbp arrangement around the zinc ions. Unlike in **294**, the two zinc ions in **301** have identical coordination environments (Figure 33).[165]

Recently Bazzicalupi et al. have synthesized $[Zn_2L(bnpp)_2](bnpp)_2\cdot 4H_2O$ (**302**) (Figure 33).[206] The low-tem-

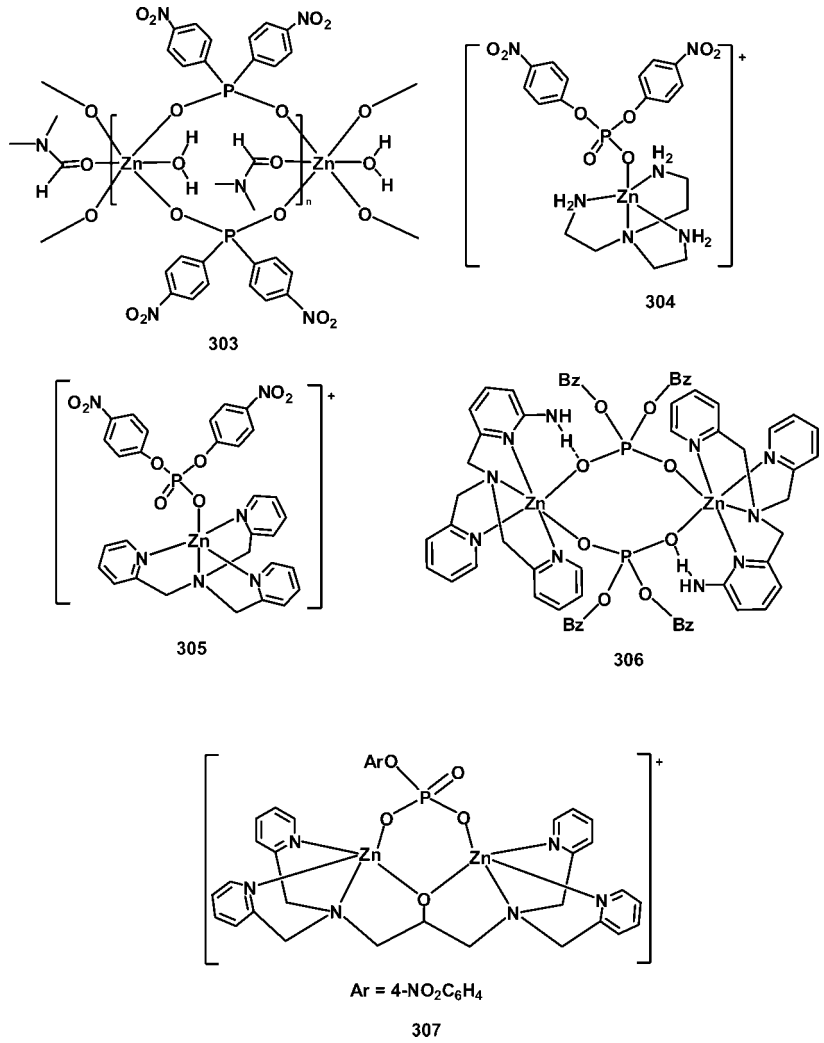

Figure 34. Zinc aryl and benzyl phosphates. In the case of **306**, only the dicationic part is shown.

perature crystal structure consists of $[Zn_2L(bnpp)_2]^{2+}$ cations, unbound bnpp anions, and water molecules. The $[Zn_2L(bnpp)_2]^{2+}$ cation displays two conformations, which differ only by a slightly different orientation of two nitrophenyl groups. The binuclear cation lies at an inversion center. The coordination geometry of each Zn(II) ion is a distorted octahedron. Each metal is coordinated to the dipyridine nitrogens and to the three amine groups of a single aliphatic side chain. The heteroaromatic nitrogen atoms and the benzylic ones define the equatorial plane, while the apical positions are occupied by the methylated nitrogen and the oxygen atom of one bnpp anion, which behaves as a monodentate ligand and actually replaces the iodide anion in the coordination sphere of Zn(II).

Angeloff et al. have synthesized a single-strand polymer of the hexacoordinated zinc(II) phosphodiester complex, *catena*-poly{aqua(dimethylformamide-*O*)bis{*m*-[bis(*p*-nitrophenyl)phosphato]}zinc(II) mono(dimethylformamide)} (**303**) (Figure 34); it consists of linear polymers in which adjacent Zn^{2+} cations are joined by the oxygen atoms of two bidentate bridging bis(*p*-nitrophenyl)phosphate diesters.[207] The metal shows an octahedral coordination geometry with the zinc ion connected to six oxygen atoms, four belonging to four different surrounding phosphate groups, one to a water molecule, and one to a DMF molecule. Each single strand is built-up from Zn octahedra having alternate configuration Δ or Λ.

Ichikawa et al. have synthesized $[Zn(tren)(bnpp)]ClO_4$ (**304**) (where tren = tris(2-aminoethyl)amine).[208] Ito et al. have synthesized $[Zn(tpa)(bnpp)]ClO_4$ (**305**) (Figure 34).[209] The essential part of these molecules consists of a Zn(II) ion, tren (or tpa), and a $bnpp^-$ anion. The zinc atom adopts a slightly distorted trigonal-bipyramidal coordination geometry. While tren (tpa) tetradentatively chelates the Zn^{2+}, $bnpp^-$ acts as a monodentate ligand occupying the fifth site of the coordination sphere around Zn(II) in the trans position with respect to the bridgehead nitrogen atom.

Rivas et al. have synthesized the dizinc complex $[(bpapa)Zn(\mu\text{-}\eta^2\text{-}DBP)_2Zn(bpapa)](PF_6)_2$ (**306**) (where, bpapa = *N*,*N*-bis-(2-pyridylmethyl)-*N*-(6-amino-2-pyridylmethyl)amine, DBP = dibenzyl phosphate) (Figure 34) with bridging η^2-phosphate diesters and internal N−H···O−P hydrogen bonding.[210]

A phosphate monoester dianion bridged dinuclear zinc(II) complex, $[Zn_2(L)(npp)](ClO_4)$ (**307**) (where L = alkoxide species of 1,3-bis[bis(pyridin-2-ylmethyl)amino]propan-2-ol) (Figure 34)[211] has been reported by Kinoshita et al. Both zinc(II) ions are in an equivalent distorted trigonal-bipyramidal environment, where they are coordinated by the two pyridyl amines and an alkoxide anion as equatorial donors and the ternary amine and one of the phosphate anionic oxygen atoms as apical donors.

Pyrazole-templated dinucleating ligands have been employed by Meyer and co-workers to synthesize the binu-

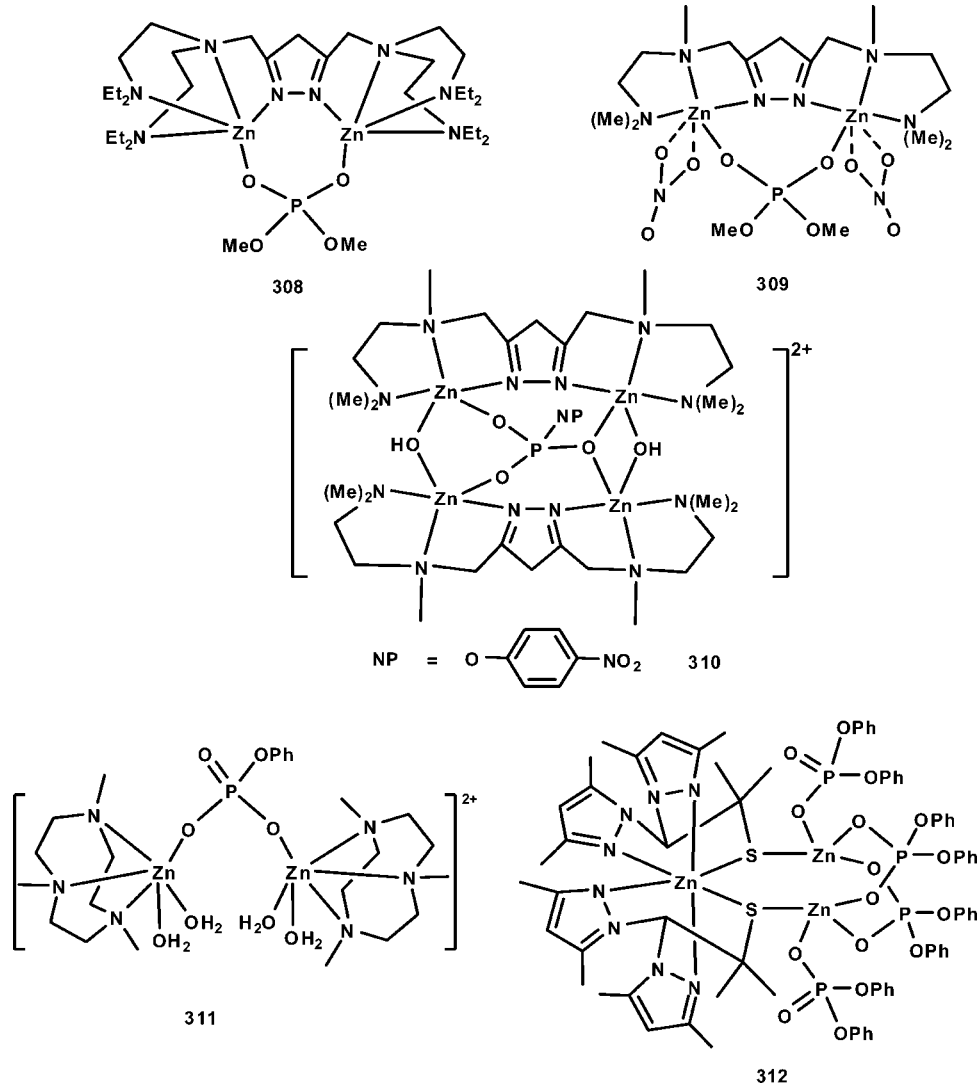

Figure 35. Zinc phosphates with polydentate ligands. In the case of **308**, only the dicationic part is shown.

clear zinc complexes $[Zn_2L((MeO)_2PO_2)](ClO_4)_2$ (**308**) and $[Zn_2L'((MeO)_2PO_2)(NO_3)_2]$ (**309**) and $[Zn_4(L')_2(OH)_2(npp)](ClO_4)_2$ (**310**) (where L-H, and L′-H are pyrazolate-based dinucleating ligands) (Figure 35).[212] In complex **308**, the $(MeO)_2PO_2$ substrate is coordinated in the expected fashion within the clamp of the two zinc ions. The structure resembles those of the dizinc cores, with bound phosphate diester substrate, proposed for many metallohydrolases. Interestingly, the zinc ions in **308** are severely displaced out of the plane of the pyrazolate heterocycle. In complex **309**, phosphate binds in the expected bidentate fashion to the dizinc unit. Due to fewer donor sites in L′ compared with L, the remaining coordination sites have to be occupied by additional ligands, such as the two nitrates. Each of these nitrates binds in a bidentate chelating mode to one of the zinc ions. The metals are thus found in a distorted octahedral environment. If weaker coordinating counter ions such as ClO_4^- are present instead of the nitrates, it is likely that solvent molecules would fill the exo coordination sites at the zinc ions. In complex **310**, each L′ bridges two Zn ions. Two such dimeric units are bridged by two hydroxyl groups, thus leading to the formation of a tetramer. All the zinc ions in the tetramer are further connected to each other by one npp. These authors have recenty extended their studies in these systems by investigating the effect of Zn···Zn separation on the hydrolytic activity of model dizinc phosphodiesterases.[213]

Spiccia et al. have reported a binuclear zinc(II) phosphate complex $[Zn_2(Me_3\text{-tacn})_2(H_2O)_4(PhOPO_3)](ClO_4)_2 \cdot H_2O$ (**311**) (Figure 35).[172] It consists of dinuclear $Zn_2(Me_3tacn)_2(H_2O)_4(PhOPO_3)]^{2+}$ cations in which one phosphate ester uses two oxygen atoms to bridge two Zn-Me_3tacn moieties. The distorted octahedral coordination sphere of each zinc(II) center is composed of the three macrocycle nitrogen atoms, two water ligands, and an oxygen atom from the bridging phosphate.

A trinuclear zinc phosphate, $[Zn_2\{(L3S)_2Zn\}\{dpp\}_4]$ (**312**) (Figure 35; L3SH = bis(3,5-dimethylpyrazolyl)(1-methyl-1-sulfanylethyl)methane) was synthesized by the reaction of $[Zn(L3S)(CH_3)]$ with diphenyl phosphate by Carrano et al.[214] This complex consists of one hexacoordinated and two tetracoordinated zinc ions. Two tetracoordinated zinc ions are bridged by two diphenyl phosphate anions. This dimeric unit is connected to the hexacoordinated zinc ion through two thiolate anions.

Yamami et al. have reported the heterometallic complex $[ZnPb(L)(bnpp)]ClO_4$ (**313**) (L = *N*,*N*′-bis(3-formyl-5-methylsalicylidene)ethylenediamine (Figure 36).[215] The molecule consists of macrocycle $(L)^{2-}$ and one $bnpp^-$ group; the perchlorate ion is free from coordination and captured

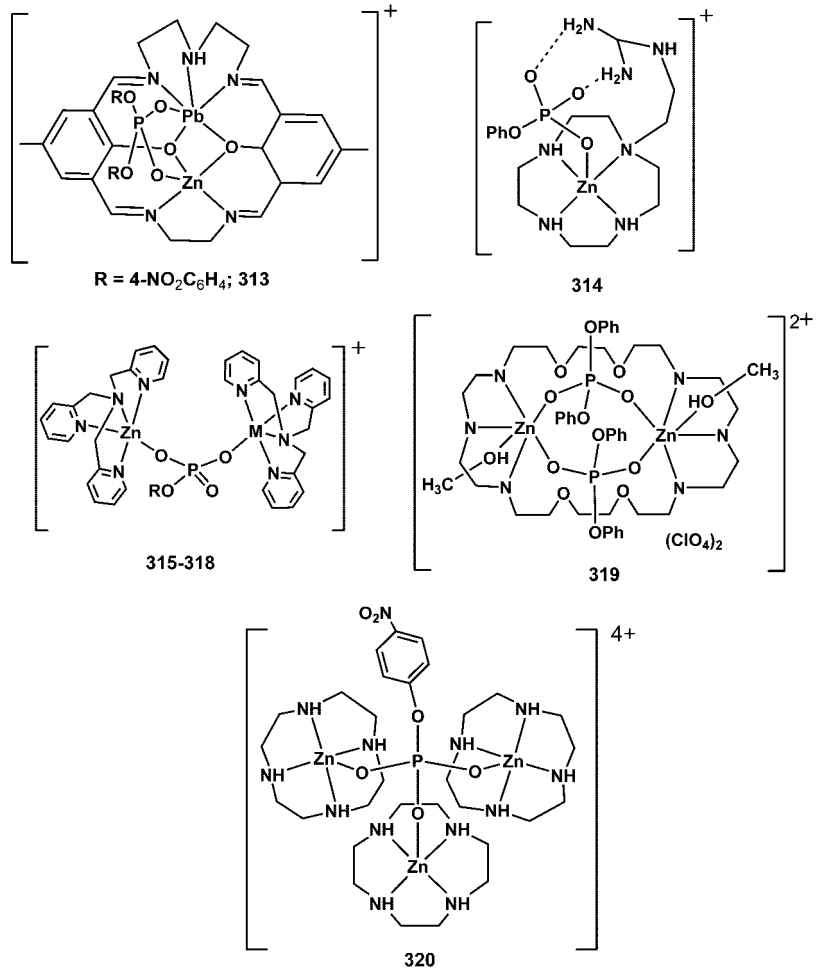

Figure 36. Zinc phosphates with macrocyclic and other polydentate ligands.

in the lattice. The zinc ion resides at the "salen" site, and the Pb resides at the "saldien" site. The two metal ions are bridged by two phenolic oxygens of the macrocycle $(L)^{2-}$ and the bnpp group through its two oxygen atoms. The geometry of the zinc is square-pyramidal with the "salen" site of the macrocycle on the basal plane and the oxygen atom of the $bnpp^-$ group at the axial site. The geometry about the lead ion is a pentagonal pyramid with the "saldien" site on the base and the oxygen atom of the $bnpp^-$ group at the axial position.[215,216]

A zinc−cyclen (1,4,7,10-tetrazacyclododecane) complex functionalized with a guanidinylethyl group with phenylphosphate anion leads to isolation of the monomeric zinc complex $[Zn(L^1H^+)((PhO)PO_3)]ClO_4$ (**314**) (Figure 36). While one of the P−O oxygens of the phenylphosphate ligand interacts with the metal ion, the other two P−O oxygen atoms form intramolecular hydrogen bonds to the guanidine N−H protons.[217]

The homodinuclear Zn(II) and heterodinuclear Zn(II)−Cu(II) complexes $[Zn_2L_2((RO)PO_3)][BPh_4]\cdot 2H_2O$ (**315**), $[Zn_2L_2((RO)PO_3)][ClO_4]\cdot 3H_2O$ (**316**), $[Zn_2L_2((HO)PO_3)][BPh_4]\cdot H_2O$ (**317**), and $[ZnCuL_2((RO)PO_3)][BPh_4]\cdot H_2O$ (**318**), derived from tris[(2-pyridyl)methyl]amine (L) were prepared and characterized (Figure 36). The crystal structure of heterodinuclear $[ZnCuL_2(npp)](BPh_4)_2\cdot H_2O$ shows that the metal atoms are separated by 5.86 Å and bridged by a phosphate monoester. The heterodinuclear CuZn complex is the first structurally characterized mixed CuZn complex bridged by a phosphate group, a fact of interest in the design of complexes as models for heteromultinuclear active sites in metalloproteins and enzymes.[218,219] A di-bridged dizinc diphosphate complex, $[Zn_2L(\mu\text{-dpp})_2(MeOH)_2](ClO_4)_2$ (**319**), was synthesized by Bazzicalupi et al. by the reaction of dpp-H with $Zn(L)(ClO_4)_2\cdot 2H_2O$ (L = [30]aneN6O4). Each zinc ion binds to three N-donors and one O-donor of the macrocyclic ring. Both the metal ions are further bridged by two dpp ligands above and below the macrocyclic ring (Figure 36).[220]

An interesting trinuclear zinc complex $[Zn(cyclen)_3(\mu_3\text{-npp})](ClO_4)_4$ (**320**) was assembled by Kimura et al. starting from *p*-nitrophenylphosphate disodium salt and $[Zn(cyclen)](ClO_4)_2$ in water (Figure 36). The three Zn−O bond distances are almost equal, and each of the Zn ions is in a distorted tetragonal-pyramidal environment constituted by four cyclen nitrogen atoms and the phosphate oxygen atom.[221]

The crystal and molecular structure of the ternary complex bis[(adenosine 5′-triphosphato)(2,2′-bipyridine)zinc(II)] tetrahydrate (**321**) has been established by Orioli et al. as early as 1981.[222] The structure consists of dimeric molecules in which two Zn atoms are held together by two −OPO− bridges from the γ-phosphate groups of two ATP molecules. Both Zn atoms show a distorted octahedral coordination formed by two O atoms from different γ-phosphate groups, one O atom from the β-phosphate group, and the two N atoms of the bipyridyl ligand. The sixth position is filled by an α-phosphate O atom, which is weakly bound. The structure is held together by strong intermolecular bipyridyl−purine and bipyridyl−bipyridyl stacking interactions. Weaker

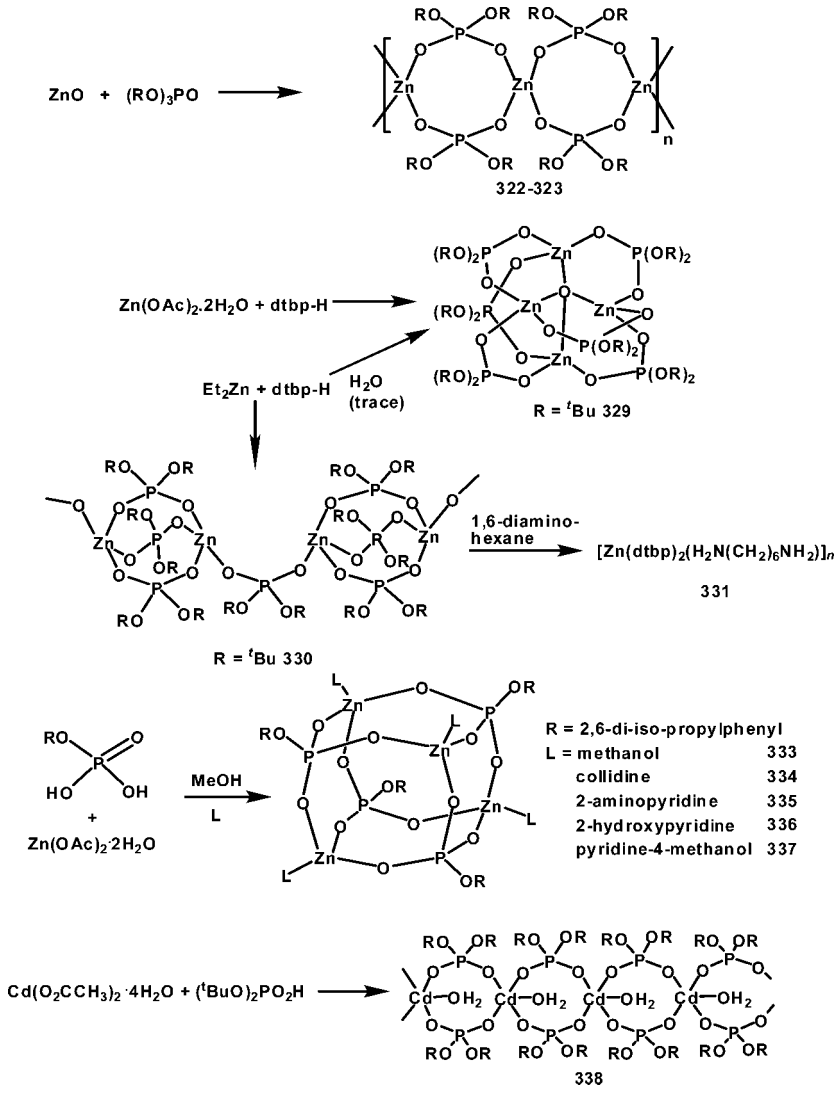

Figure 37. Zinc and cadmium polymeric and tetrameric complexes.

bipyridyl−purine intramolecular stacking is also observed. The molecule provides a possible model for ATP transport and phosphate group transfer mechanisms.

Zinc diethylphosphate, $[Zn(O_2P(OC_2H_5)_2)_2]_n$ (**322**) (Figure 37), has been reported in 1992 by Stucky et al. It has a chain-like polymeric structure, and these chains have a tetrahedral ZnO_4 core.[223] The physical data show a melting, followed by a decomposition reaction, eventually resulting in $Zn(PO_3)_2$. Compound **322** is soluble in several polar and nonpolar solvents, and the NMR data suggest that **322** maintains a polymeric state in solution.

A structurally similar 1D polymer, $Zn[O_2P(OMe)_2]_2$ (**323**), is hydrothermally prepared starting from $OP(OMe)_3$ and ZnO.[224,225] Polymer **323** consists of infinite one-dimensional chains of vertex-linked ZnO_4 and PO_4 tetrahedra forming eight-membered $P_2O_4Zn_2$ rings (4-rings) (Figure 37).

Even earlier than the synthesis of **322**, the synthesis and X-ray crystal structure of the zinc-2-aminoethylphosphate (**324**) had been reported by Bissinger et al.[33] The reaction between 2-aminoethylphosphate and ZnO in water gives the polymeric compound $[Zn(O_2P(OH)(OCH_2CH_2NH_2)_2].4H_2O$ (**325**) within a few minutes of mixing the slurries. The calcium complex of 2-aminoethylphosphate $[Ca(O_2P(OH)(OCH_2CH_2NH_2)_2(OH_2)_2]\cdot 2H_2O$ (**326**) is somewhat structurally different. The aminoethyl phosphate group exists as a zwitterionic $[^-O_3POCH_2CH_2NH_3^+]^-$ group in both the complexes. The calcium ions in **326** are octahedral by additional coordination of two water molecules.

Use of zinc acetate in place of ZnO and barium 2-aminoethylphosphate instead of free acid in the above reaction leads to the isolation of another polymeric compound of zinc 2-aminoethylphosphate with the composition $[Zn(O_3POCH_2CH_2NH_3)(OAc)]$ (**327**). Similarly, the polymeric compound $Zn(O_3POEt)\cdot H_2O$ (**328**) is prepared from $Zn(OAc)_2\cdot 2H_2O$ and ethyl phosphate.[226] Both compounds have layers formed by phosphate groups bridging the tetrahedral Zn atoms, which undulate perpendicular to the layer direction. The spacing between successive layers is determined by the pendant groups (the ethyl group in **328** and the acetate group in **327**). The amino groups in **327** fold back upon themselves to H-bond to the acetate groups. Hydrogen bonding produces sheet-like structures with only van der Waals forces holding adjacent sheets together.

Tilley et al.[227] and Murugavel et al.[130] have investigated in detail the reaction of zinc precursors with di-*tert*-butyl phosphate (dtbp-H). In contrast to the direct reaction between zinc(II) ions and dimethyl or diethyl phosphate yielding a one-dimensional polymer, the reaction between $Zn(OAc)_2$ and dtbp-H leads to the formation of a tetrameric phosphate $[Zn_4(\mu_4\text{-}O)(dtbp)_6]$ (**329**).[130] On the other hand, the reaction

of $ZnEt_2$ with dtbp-H gives the insoluble polymer $[Zn(dtbp)_2]_n$ (**330**) (Figure 37).[227] In the presence of slight amounts of H_2O, the same reaction however produces the oxo-centered tetranuclear cluster **329**. The molecular structure of **329** reveals a basic zinc acetate structure for this compound. Compound **329** is thermally labile and eliminates isobutene and H_2O over the temperature range 130−220 °C. The ceramic yield at 900 °C corresponds to the theoretical yield for a $Zn_4P_6O_{19}$ material, and the observed products at this temperature are α-$Zn_2P_2O_7$ and β-$Zn(PO_3)_2$. When heated in EtOH at 85 °C for 30 h, **329** converts to polymer **330** and ZnO. This transformation is facilitated by acids, which allow the conversion to occur at room temperature. Polymer **330**, characterized by X-ray crystallographic studies, adopts a zigzag structure with Zn atoms linked alternately by one and then three bridging phosphate groups. This structure is therefore different from that adopted by the other two organozincphosphate $\{Zn[O_2P(OR)_2]_2\}_n$ polymers **322** or **323**, which exist as linear chains with the Zn atoms bridged by two phosphate groups.

Polymer **330** undergoes a quantitative pyrolytic conversion to β-$Zn(PO_3)_2$. Exposure of **330** to 1,6-hexanediamine produces a coordination network $[Zn(dtbp)_2(H_2N(CH_2)_6NH_2)]_n$ (**331**) (Figure 37), with elimination of ZnO.[227] The polymeric strands of **331** are interconnected via H-bonds between the N−H and P═O groups. Addition of imidazole in the reaction between $Zn(OAc)_2$ and dtbp-H produces the monomeric complex $[Zn(dtbp)_2(imidazole)_4]$ (**332**).[130]

In a recent study, Murugavel et al. have synthesized zinc phosphate cubic complexes, $[Zn_4(ROPO_3)_4L_4]$ (R = 2,6-diisopropylphenyl, L = methanol (**333**), 2,4,6-trimethylpyridine (**334**), 2-aminopyridine (**335**), 2-hydroxypyridine (**336**), 4-(hydroxymethyl)pyridine (**337**)), with molecular structures that resemble the double-four-ring (D4R) secondary building unit of zeolites. Complexes **334**−**337** have been characterized by single-crystal X-ray diffraction studies revealing that when the appropriate ligands are chosen, the D4R cubanes could be assembled into one-, two- or three-dimensional supramolecular networks through noncovalent interactions arising out of the -NH_2, -NH, or -OH groups on the surface of the molecule.[228]

2.11.2. Cadmium

The reaction of diethyl phosphate and cadmium nitrate proceeds via the formation of KNO_3 to yield the polymeric compound $[Cd(O_2P(OEt)_2]_n$ (**338**).[229] The compound exists as a highly interlocked 1D polymer where each octahedral cadmium ion is linked to preceding and succeeding cadmium ions by one four-membered ring involving two bridging oxygen atoms and by one eight-membered ring involving two bridging phosphate groups. In other words, each adjacent pair of Cd ions is bridged by two phosphate anions on either side. Additionally, one of the oxygen atoms of each diethyl phosphate ligand bridges a third cadmium atom.

The structure of the cadmium polymeric complex formed by di-*tert*-butyl phosphate (dtbp-H) is much simpler. Reaction of $Cd(OAc)_2 \cdot xH_2O$ with dtbp-H in a 1:2 molar ratio in MeOH gave the polymeric metal phosphate $[Cd(dtbp)_2(H_2O)]_n$ (**339**) (Figure 37) in good yields.[90] The Cd ions in the structure of **339** are pentacoordinated. The polymer structure resembles very much the structure of $[Cu(dtbp)_2]$ (**179**) in the sense that adjacent cadmium ions are bridged by two dtbp ligands. A water molecule additionally coordinates each cadmium ion. Thermal analysis (TGA and DSC) indicates that **339** converts into crystalline metaphosphate $Cd(PO_3)_2$ at <500 °C.

2.12.2. Group 13 Metal Phosphates

2.12.1. Aluminum

Materials derived from group 13 metals or elements are useful as catalysts and catalyst supports. Making soluble aluminum phosphates and studying their properties is important in this context. Tilley et al.[230] have reported two aluminum phosphates, $[Me_2Al(O_2P(O^tBu)_2)]_2$ (**340**) and $[Al(O^iPr)_2(O_2P(O^tBu)_2)]_4$ (**341**), which were prepared from the reaction of di-*tert*-butylphosphate with Me_3Al and $(^iPrO)_3Al$, respectively (Figure 38).

Silicoaluminophosphates (SAPO's) are porous materials that find wide applications as catalysts and catalyst supports for reactions such as the conversion of methanol into hydrocarbons. Development of efficient molecular precursors for SAPO's containing "preformed" O−Si−O−Al−O−P−O linkages is of interest. In addition, such species might also serve as soluble models for SAPO materials. In this context, recently a soluble SAPO $[((^tBuO)_3SiO)_2Al(O_2P(O^tBu)_2)_2AlCH_3(OSi(O^tBu)_3)]$ (**342**) has been prepared by reacting excess of $(^tBuO)_3SiOH$ with **340** (Figure 38).[231] Complex **342** under thermolytic decomposition conditions yields mesoporous SAPO materials with large surface area (>500 m^2/g) and pore volume. These properties make them ideal candidates as catalysts and catalyst supports for organic reactions involving larger substrates.

Trialkyl phosphate−group 13 metal alkyl adducts $Me_3Al \cdot OP(OSiMe_3)_3$ (**343**), $Et_3Al \cdot OP(OSiMe_3)_3$ (**344**), and $Me_3Ga \cdot OP(OSiMe_3)_3$ (**345**) undergo a thermally induced dealkylsilylation with the formation of cyclic alumino- and gallophosphate dimers, $[R'_2M(\mu_2\text{-}O)_2P(OSiMe_3)_2]_2$ (R'_2M = Me_2Al (**346**), Et_2Al (**347**), and Me_2Ga (**348**)) (Figure 38). The molecular structures of these cyclic phosphates reveal the presence of a central $M_2O_4P_2$ ring on which organic groups are attached.[232]

Triesters $OP(OR)_3$ (R = Me, Et, Bu, $SiMe_3$) react with aluminum and gallium triamides $[M(NMe_2)_3]_2$ (M = Al, Ga) in nonaqueous aprotic solvents with the formation of amorphous alumino- and gallophosphates MPO_4 (M = Al, Ga). Aluminophosphate also results from the reaction of $AlCl_3$ with $OP(OSiMe_3)_3$.[233] The molecular structure of the first-step model compound $(Me_2N)_3Al \cdot OPPh_3$ (**349**) was established by single-crystal X-ray diffraction. Cyclotrialumazene [MeAlNDipp]$_3$ (Dipp = 2,6-diisopropylphenyl) forms a bis-adduct, [MeAlNDipp]$_3 \cdot 2OP(OMe)_3$ (**350**), with trimethyl phosphate.

Florjanczyk et al. have recently reported on the organically modified aluminophosphates by studying the reactions of diphenylphosphate with $AlMe_3$, $AlEt_3$, $Al(^tBu)_3$, and boehmite.[234] The reaction with $Al(^tBu)_3$ yields $[(^tBu)_2AlO_2P(OPh)_2]_2$ (**351**), which is structurally similar to **340**. Reactions with $AlMe_3$ or $AlEt_3$ lead to polymeric aluminum organophosphates ($\{Al[O_2P(OPh)_2]_3\}_n$) (**352**). These polymers were characterized by powder X-ray diffraction (PXRD), TGA, FTIR, scanning electron microscopy (SEM), and magic angle spinning (MAS) NMR techniques. The results of MAS NMR and FTIR studies showed that $Al(OP)_6$ units are the basic chain building blocks that produce condensed structures. The same type of Al environment was observed in aluminophosphate phase found in the products of the reaction with boehmite. This phase reveals a fibrous structure

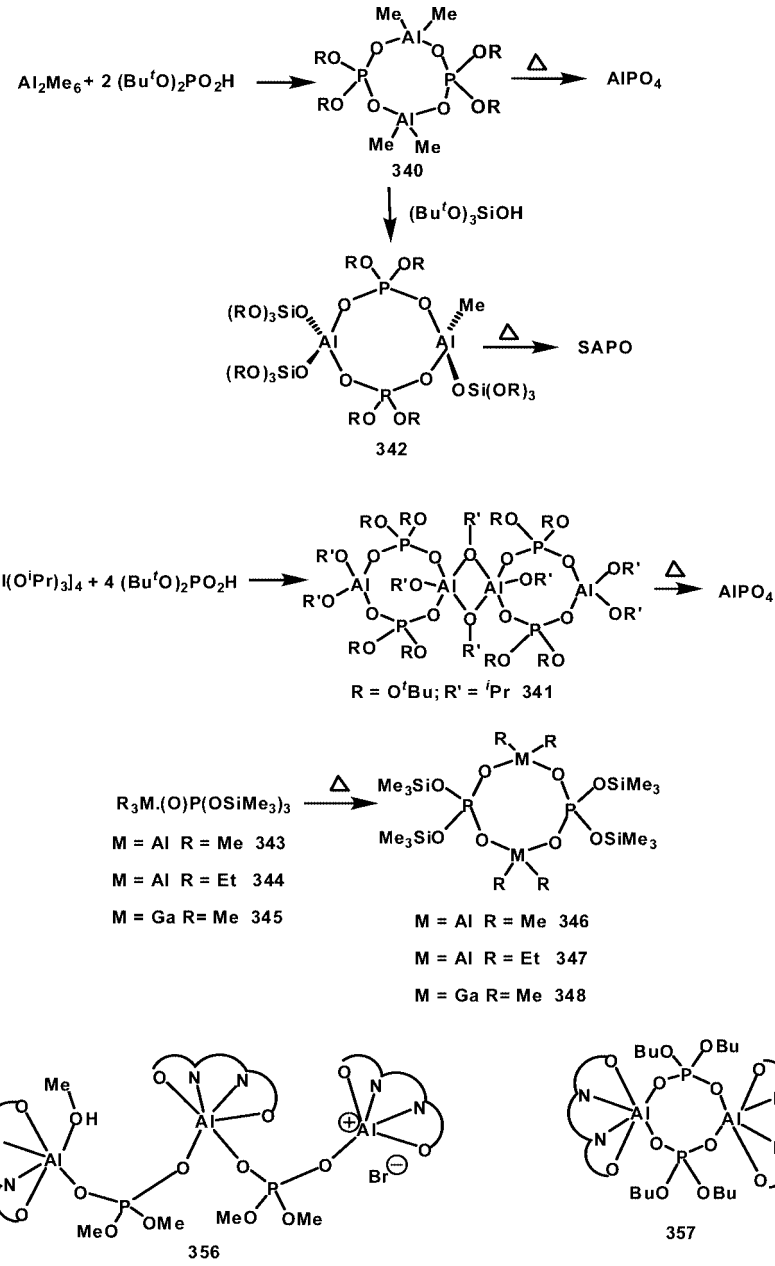

Figure 38. Synthesis of group 13 phosphates.

attributed to the close-packed hexagonal columnar structure consisting of polymeric chains of *catena*-Al(dpp)$_3$.[234]

The reaction of aluminum isopropoxide with (BuCH(Et)CH$_2$O)$_2$P(O)(OH) has been studied by Zheng et al. The product obtained in this reaction has been characterized as Al(O^{i}Pr)[O$_2$P(OR)$_2$]$_2$ (**353**) on the basis of IR and thermal studies.[235] Kumara Swamy and co-workers have reported on the X-ray structure determination of a hexacoordinated aluminum complex with a new type of seven-membered chelate ring involving a cyclic phosphate ester.[236]

Atwood and co-workers have recently examined the reaction of Al-sale type complexes with various phosphinic acids and phosphate esters.[237,238] The isolated and structurally characterized examples of aluminum phosphate complexes include trinuclear [(MeOH)Al(salen){O$_2$P(OMe)$_2$}-Al(salen){O$_2$P(OMe)$_2$}Al(salen)]Br (**354**) and dinuclear [(salpen)Al{O$_2$P(OBu)$_2$}]$_2$ (**355**) (Figure 38) complexes (salen = *N*,*N*′-ethylenebis(3,5-di-*tert*-butylsalicylideneimine), salpen = *N*,*N*′-propylenebis(3,5-di-*tert*-butylsalicylideneimine)).[237]

Murugavel and Kuppuswamy have recently reported on the reaction of a sterically hindered monoarylphosphate with aluminum isopropoxide.[239] Performing the reaction under slightly different conditions, octanuclear and decanuclear aluminophosphates [Al$_8$(μ_3-O$_3$P(OR))$_6$(μ_2-HO$_3$P(OR))$_2$(μ_3-O)$_2$(μ_2-OH)$_2$(THF)$_4$] (**356**) and [Al$_{10}$(μ_3-O$_3$P(OR))$_{12}$(μ_3-O)$_2$(O*i*Pr)$_2$(THF)$_4$] (**357**) (R = 2,6-di-isopropylphenyl) (Figure 39) were isolated and characterized by X-ray crystallography.[239] These compounds not only are among the largest molecular aluminophosphates synthesized thus far, but also are rare polyhedral cages that contain AlO$_4$, AlO$_5$, and AlO$_6$ coordination geometries. The cores of these aluminophosphates represent new structural building units (SBUs) in zeolite chemistry.

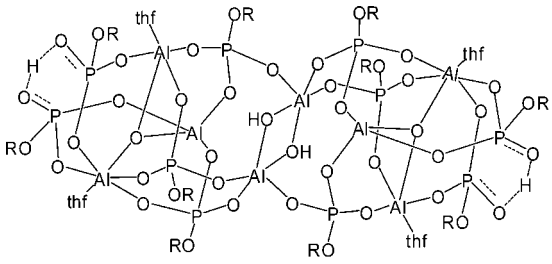

356

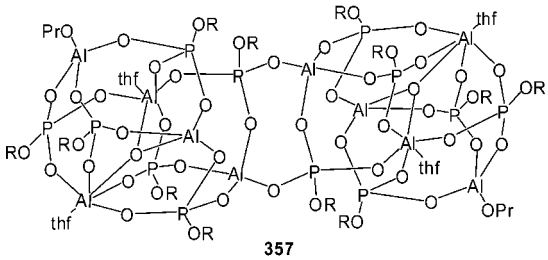

357

R = 2,6-diisopropylphenyl

Figure 39. Larger aluminum phosphates.

2.12.2. Boron, Gallium, Indium, and Thallium

The only available studies on the phosphate complexes of B, Ga, In, and Tl correspond to the preparation of trialkylphosphate adducts of these metals, which fall beyond the scope of this review.

2.13. Group 14 Metal Phosphates

Holmes et al. have prepared a number of organotin phosphate and phosphonate cage compounds from the reaction of stannoic acid with alkyl- and arylphosphorous and -phosphonic acids.[240] Hexameric *n*-butyloxotindiphenylphosphate, [^{n}BuSn(O)(dpp)]$_6$ (**358**) (Figure 40), has been prepared starting from *n*-butylstannoic acid with diphenylphosphate. An oxygen-capped cluster, [(^{n}BuSn(OH)(dpp)$_3$O][O$_2$P(PhO)$_2$] (**359**) (Figure 40), has been obtained by a small variation in the synthesis conditions.[241] Methyltin(tris(diphenylphosphate)), [MeSn(dpp)$_3$] (**360**) (Figure 40), has been obtained from the reaction between hexameric methyloxotin acetate and diphenylphosphate. Controlled hydrolysis of **360** leads to the isolation of the cage cluster [Me$_2$Sn$_2$(OH)(dpp)$_3$(O$_3$P(OPh))]$_2$ (**361**) (Figure 40).[242] Introduction of sulfur in place of oxygen in the organotin framework leads to additional types of cluster molecules.[243] The same authors have prepared a number of organotin sulfur clusters containing phosphate groups, for example, a sulfur-capped cluster, [(^{n}BuSn(S)(OP(OH)(O^{t}Bu)$_2$)$_3$S][O$_2$P(O^{t}Bu)$_2$]·2H$_2$S·H$_2$O (**362**) (prepared by passing H$_2$S at room temperature through a benzene solution of the triphosphate [^{n}BuSn(O$_2$P(O^{t}Bu)$_2$)$_3$] (**363**)) (Figure 40).[243]

A rare eight-coordinate lead compound with the formula [PbL$_4$][O$_2$P(OMe)$_2$]·2H$_2$O (**364**)[244] (L = 3-(2-pyridyl)pyrazole) has been obtained by slow crystallization of [Pb(L^1)$_2$]·H$_2$O (L^1 = 3-(2-pyridyl)pyrazol-1-yl]phosphinate) in MeOH.[245] The dimethylphosphate anion in this complex shows hydrogen bonds with the pyrazolyl protons.

Barring tin, there are no structurally characterized examples of phosphate complexes of group 14 elements (excluding carbon and silicon).

2.14. Group 15 Metal Phosphates

In 1998, Schmidt et al.[246] reported the synthesis of the binuclear antimony complexes [Cl$_3$Sb(O)(dpp)$_2$SbCl$_3$]$_2$ (**365**), [Cl$_3$Sb(O)(dpp)-(OCH$_3$)SbCl$_3$]$_2$ (**366**), [Cl$_3$Sb(O)(dpp)-(OH)SbCl$_3$] (**367**), and [Cl$_4$Sb(dpp)$_2$SbCl$_4$] (**368**) from the reaction of diphenylphosphate with SbCl$_5$, water, and methanol in varying molar ratios. In all cases, the diphenylphosphate groups bridge two antimony atoms resulting in a six-membered Sb$_2$O$_3$P central core (Figure 41).

2.15. Lanthanide and Actinide Phosphates

Although trialkyl phosphates have been used for solvent-extracting lanthanide ions, very few lanthanide phosphate complexes have been isolated and structurally characterized. Dimethyl and diethyl phosphate complexes of a few lanthanides have been prepared, and their X-ray structures have been established.

Dimethyl phosphates {Ln[O$_2$P(OMe)$_2$]$_3$}$_n$ (Ln = La (**369**);[247] Sm (**370**);[248] Eu (**371**);[249] Pr (**372**)[250]) are available from the reactions from the respective LnCl$_3$ and trimethylphosphate (Figure 42). Compounds **370** and **372** are isomorphous. Dimethyl phosphate anions coordinate with Sm or Eu atoms through double O−P−O bridges to form a special network of ring−linking−ring, each of which consists of 24 atoms. The coordination number of the metal is six, and the coordinate polyhedron is a slightly distorted octahedron. The La and Pr derivatives also have a very similar structure in the solid state with octahedral metal ions in a polymeric chain bridged by dimethyl phosphate ligands. The water and trimethyl phosphate adducts of **369**, {La[O$_2$P(OMe)$_2$]$_3$(OH$_2$)}$_n$ (**373**)[251] and {La[O$_2$P(OMe)$_2$]$_3$-(OP(OMe)$_3$}$_n$ (**374**),[252] have also been isolated, and their molecular structures have been established by diffraction studies. In **369**, each La is coordinated by seven O atoms (from six dimethyl phosphates and one water molecule), forming a distorted monocapped trigonal prism. Each dimethyl phosphate ligand is shared by two La atoms, building a two-dimensional network. The diethyl phosphate complexes {Ln[PO$_2$(OEt)$_2$]$_3$}$_n$ (Ln = Ce (**375**);[253] Pr (**376**);[254] Nd (**377**)[255]) have very similar structures to those of the dimethyl phosphate complexes.

Crystals of [(Tx)Dy(dpp)$_2$]·0.64(MeOH) (Tx = texaphyrin) (**378**) (Figure 42) were obtained by diffusion of diphenyl phosphate into methanolic Dy(Tx)(NO$_3$)$_2$.[256] The Dy(III) ion is seven-coordinate with five donor atoms being provided by the texaphyrin ligand and two by monodentate diphenyl phosphate ions. The Dy(III) ion is only 0.073 Å from the plane through the five N atoms of the macrocycle.

The syntheses of the uranyl phosphates, [U(O)$_2$(O$_2$P-(OR)$_2$)(OP(OR)$_3$)(NO$_3$)]$_2$ (R = Et (**379**); ^{n}Bu (**380**)), and [U(O)$_2$(O$_2$P(O^{n}Bu)$_2$)$_2$]$_n$ (**381**) have been accomplished by Stammler and Burns by the reaction of uranium nitrate with the respective phosphate triesters (Figure 42).[257,258] While two phosphate diester ligands bridge the two uranium centers in these complexes, each uranium center has one phosphate triester in the coordination sphere. Carrano et al. have subsequently reported a discrete-framework uranium phosphate, [U$_6$(OH)$_8$(dpp)$_{12}$] (**382**). The structure of complex **382** shows that the six uranium atoms are arranged in the form of an octahedron, and each face of this octahedron is capped by a μ_3-oxo(hydroxo) group. Each uranium atom is further coordinated by four diphenyl phosphate groups, which also form bridges with four neighboring uranium atoms.[259]

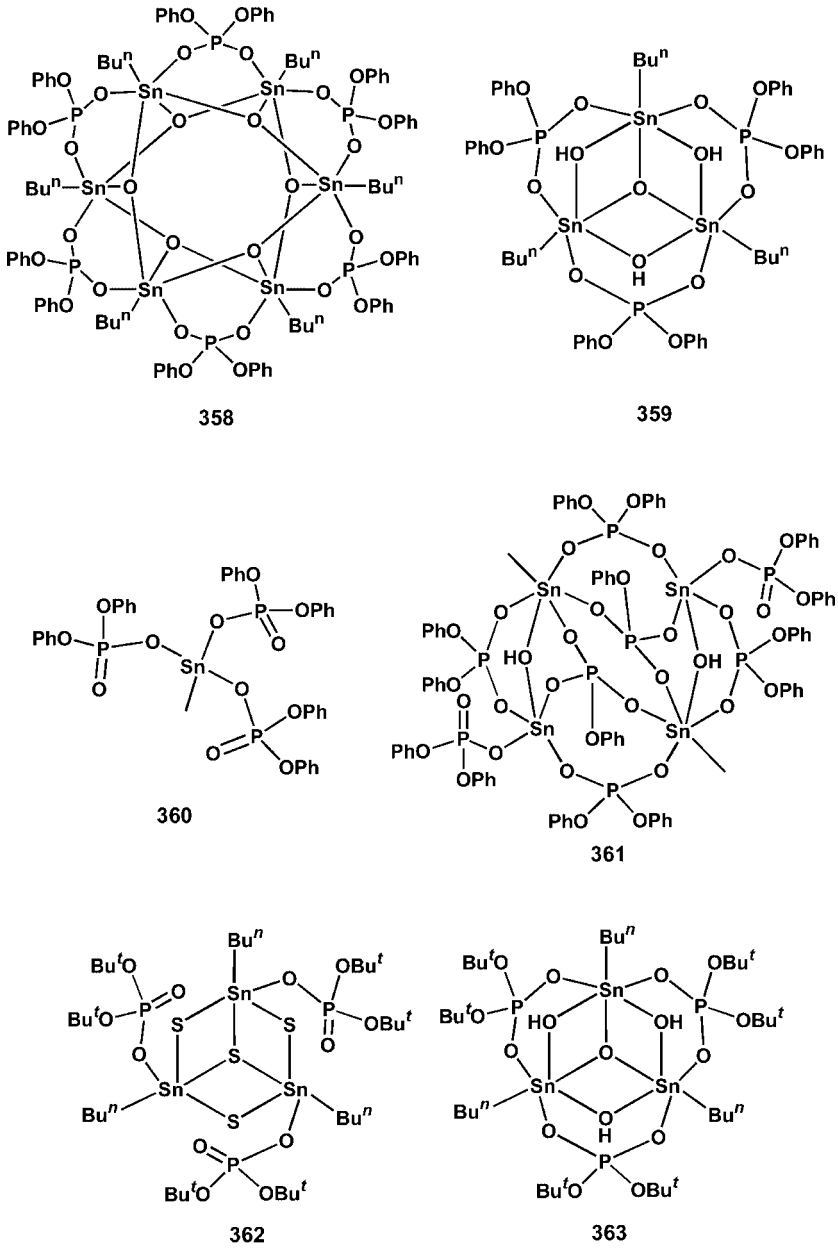

Figure 40. Alkyltin phosphates.

2.16. Summary

Unlike condensed inorganic phosphates, the area of discrete molecular phosphates, prepared from mono- and diesters of phosphoric acids as ligands, started to develop only in the 1980s. The material presented in the sections 2.2–2.15 clearly indicates that the developments in the area over last two decades were mainly triggered by synthesis of molecular models for larger phosphate framework materials, single-source precursors for ceramic materials, and the quest for smaller molecular models to understand the functions of phosphoesterases. While the developments in the area of transition metal phosphates have been impressive, the organophosphates of main group metals, B, Al, Ga, In, Sn, Bi etc., have not been studied in sufficient detail. Future work on these metals would be especially interesting in view of need for suitable precursors of these metal ions to prepare mixed metal phosphates (e.g., SAPO) through sol−gel or thermolysis routes.

Although recent work has shown that the *tert*-butoxy group substituted silanols and phosphorous acids could be used as starting materials for the preparation of metal complexes that decompose at low temperatures to yield metal silicates or metal phosphates, respectively, via a β-hydride elimination route, the use of di-*tert*-butylphosphate (dtbp-H) as a ligand in metal phosphate chemistry has been investigated only very recently and is limited to a very few metal ions (Al, Ti, Cu, Mn, Co, Zn, and Cd). The already demonstrated structural transformations among the dtbp complexes provide a new pathway to change the dimensionality of these metal−diorganophosphates. Hence, in view of the clean hydrolysis and thermolysis reactions exhibited by dtbp-H and its complexes and the demonstrated structural transformations, there is clearly a need to extend this chemistry to other elements in the periodic table as well.

Similarly, the use of mono-*tert*-butylphosphate (or similar thermally labile esters) as a ligand in metal−organophosphate chemistry would provide a very useful entry into the area of framework solids (second part of the review) in view of the discrete 3D cages one can build with the help of the three free oxygen atoms on the same phosphorus. Such cages, by

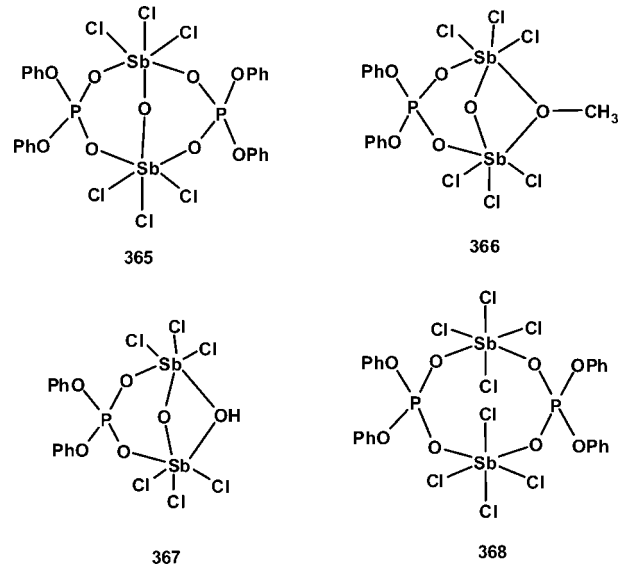

Figure 41. Structures of antimony phosphates.

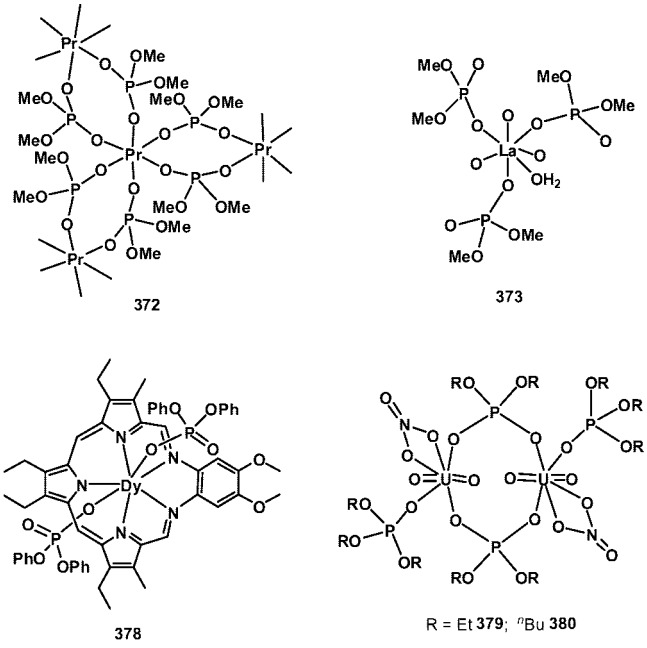

Figure 42. Phosphate complexes of f-block elements.

suitable synthetic strategies and through cleavage of the only P-OR linkage on phosphorus, could be transformed to designer framework solids in the future.

Finally, it should be stated that, parallel to the development of chemistry of metal phosphate complexes, there has been sustained activity in the area of metal complexes of phosphinic and phosphonic acids.[260] Since these developments fall outside the scope of this review, a separate review on molecular phosphinates and phosphonates is desirable.

3. Framework Phosphates

3.1. Framework Materials

The area of inorganic open-framework materials thrives on the rich variety of architectures that can be obtained through new chemical approaches. In the last two decades, there has been a great surge of activity in this area, in terms of discovering new frameworks based on oxides, chalcogenides, halides, and nitrides, as well as metal−organic frameworks based on carboxylates and polymeric coordination compounds. Among the chemically diverse open-framework materials, solids based on oxygen-containing polyhedra such as aluminosilicate zeolites and metal phosphates constitute the major part. Prior to the discovery of open-framework aluminium phosphates (AlPO's) in 1982 by Flanigen and co-workers,[261] the aluminosilicate zeolites with three-dimensional crystallographic structures dominated the field. The last two decades has, however, witnessed the rapid growth of open-framework materials based on metal phosphates, as indicated by the fact that as many as 20 chemical elements of the periodic table are able to form such frameworks. Phosphate-based framework solids are more diverse and complex, exhibiting a variety of properties and structures, many being different from the aluminosilicate zeolites. Aluminosilicate zeolites and early AlPO's were based on vertex-linked tetrahedra (AlO_4, SiO_4, PO_4, etc), but many of the new frameworks discovered in the phosphate family contain other polyhedra, involving octahedral [XO_6], pentacoordinated [XO_5], pyramidal [XO_4], or trigonal pyramidal [XO_3] units. The applications of open-framework materials continue to be dominated by the aluminosilicate zeolites because of their remarkable stability and properties that find utility in catalysis, separation processes, and ion exchange. The phosphate-based materials have also begun to show some applications in catalysis and hydrogen storage and promise to make an impact in the application front. Cheetham et al.[262] presented a major review of open-framework materials in 1999 covering a variety of compositions and structures. In 2001, Ferey[263] extended his concepts of secondary building units (SBUs) from purely inorganic networks to hybrid solids, and more recently, Harrison[264] has surveyed the recent developments in templated inorganic networks.

This part of the review is restricted to phosphate-based materials and covers not only three-dimensional open-framework phosphates but also the lower dimensional phosphates (of zero, one, and two dimensions), in an order to unravel the building process from lower to higher dimensional structures. The coverage includes the anionic inorganic phosphate networks wherein the charge is balanced by protonated organic amines or quaternary ammonium cations. In some cases, the framework charge is compensated by inorganic cations, while in other cases, the neutral metal phosphate frameworks occur with or without neutral amines. We have not made any distinction of the three-dimensional structures that are nanoporous remaining stable and crystalline after the removal of the contents of the channels and showing reversible absorption from those that collapse and lose crystallinity on removal of the contents of the channels.

We start with a brief description of aluminosilicate zeolites in order to introduce the terminology employed in the open-framework literature. This is followed by a discussion of the synthesis of open-framework materials and a chronological account of the various families of metal phosphates of different dimensionalities. Efforts have been made to archive many families of metal phosphates by tabulating the lattice parameters and citing references generously. We have also shown how the formation of three-dimensional materials could occur from molecular or lower dimensional materials. The inclusion of low-dimensional phosphates in this review is in fact inspired by the observation that they transform to higher dimensional structures under mild conditions and play

an important role in the building process.[265] The review ends with a short presentation of the properties and applications.

3.2. Aluminosilicate Zeolites: An Overview

Zeolite is a crystalline aluminosilicate with a framework based on an extensive three-dimensional network of vertex-sharing SiO_2 and AlO_2^- tetrahedra. The framework charge is determined by the presence of AlO_2^- tetrahedra and is balanced by extraframework cations. The empirical formula for a zeolite can be written as $M_{2/n}O \cdot Al_2O_3 \cdot xSiO_2 \cdot yH_2O$ where M represents the exchangeable cations and n represents the cation valence. These cations are present during the synthesis or introduced after the synthesis through ion exchange. The value of x is equal to or greater than 2 because Al^{3+} does not occupy adjacent tetrahedral sites (Loewenstein's rule). Loewenstein first rationalized the absence of Al−O−Al linkages in zeolites on the basis that clusters of negative charge are less stable than isolated negative charges.[266] The crystalline frameworks of zeolites contain voids and channels of discrete size. Depending on the structure, the pore or channel opening ranges from 3 to 8 Å. The water molecules present are located in these channels and cavities along with the cations that neutralize the negative charge created by the presence of the AlO_2^- tetrahedra in the structure. Typical cations include the alkali (Na^+, K^+, Rb^+, Cs^+) and alkaline earth (Mg^{2+}, Ca^{2+}) cations, NH_4^+, H_3O^+, TMA^+ (tetramethylammonium), and other nitrogen-containing organic cations, and the rare earth and noble metal ions. The first success in zeolite synthesis can be traced back to Saint Claire Deville in 1862,[267] and today the most widely used zeolites for sorbents, catalysis, and ion-exchange applications come from the synthetic varieties that are well-documented.[268,269]

All zeolites that are significant for catalytic and adsorbent applications can be classified by the number of T atoms, where T = Si or Al, that define the pore opening. There are only three pore openings in the aluminosilicate zeolite system that are of practical interest for catalytic applications. They are referred to as small (eight-membered ring), medium (10-membered ring), and large (12-membered ring) pore zeolites. Today more than 100 structures of zeolites are known, and these are listed in the atlas of zeolite framework types.[270] The International Zeolite Association (IZA) has assigned a three-letter code to each structure type[270] (e.g., zeolite gismondine is denoted as GIS). The framework density or openness is the number of T atoms (Al and Si) per 1000 $Å^3$. The smaller this number, the more space would be present, although all of them may not be accessible.

3.2.1. The Secondary Building Unit

In order to compare the structural properties of complex zeolite structures, there was a need to develop the concept of structural building units. The primary building unit of a zeolite structure is the individual tetrahedral TO_4 unit, where T is either Si or Al. Meier[271] proposed secondary building units (SBUs) based on selected geometric groupings of tetrahedra, which can be used to describe the known zeolite structures. Today, there are around 20 such building units consisting of four-, six- and eight-membered single rings, 4-4, 6-6, and 8-8 double rings, and 4-1, 5-1, 4-4-1, etc. branched rings.[270] The topologies of these units are shown in Figure 43. In the SBUs, Al or Si is present at each corner or termination, but the oxygens are not shown. They are

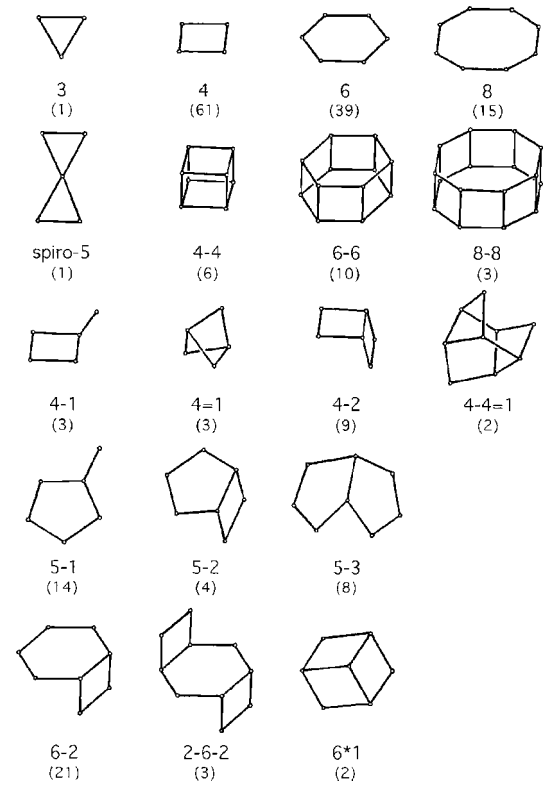

Figure 43. Various SBUs in zeolitic structure. Reproduced from ref 270 with permission from Elsevier.

located near the midpoints of the lines joining each pair of T atoms. These units are also used in efforts to understand the way the individual structures are formed from the reactant mixtures used in the synthesis.

3.2.2. Hydrothermal Synthesis of Zeolites

Zeolites have been synthesized hydrothermally using reactive alkali metal aluminosilicate gels at low temperatures (60−180 °C) and pressures (autogeneous pressure). This type of crystallization may involve structure-directing effects of hydrated alkali metal cations that organize the zeolite structural subunits and solution-mediated crystallization of the amorphous gel. Variation in the gel composition, temperature, charge compensating cations, time of reaction, and the pH value (typically greater than 12) enable the synthesis of a variety of low-silica zeolites. A good compilation of the synthesis of zeolites and related materials can be found in the *Handbook of Molecular Sieves* by Szostak.[272]

A major breakthrough in zeolite synthesis took place in 1961 by the use of organic bases as a replacement for inorganic bases by Barrer and Denny as well as by Kerr and Kokotailo (BDKK).[273] The use of hydroxides of quarternary ammonium ions or organic amines enabled the direct synthesis of high silica materials. The organic nitrogen compounds, which act as template molecules or structure-directing agents, are incorporated into the final product where they replace the charge-compensating cations. They play two important roles: (i) the size and shape of the quarternary amine or organoammonium cation can lead to the creation of new pore structures that cannot be made in other ways; (ii) the large size of these cations, when compared with traditional metal cations, makes room for only a limited number of big ions that can compensate for a relatively low framework charge (more sites, but less Al), thus leading to the formation of high-silica materials (ZSM-5 and ZSM-11).

The organic cation can normally be removed from the zeolite by calcination, leaving behind the acid form of the zeolite. The work of BDKK resulted in an extensive exploration of the use of organic bases in zeolite synthesis, with many interesting results. Davis and Lobo[274] have discussed zeolite synthesis, specially the role of amine in crystallization, nucleation, and other factors. A recent review deals with the chronological events in the hydrothermal synthesis of zeolites.[275]

3.2.3. Metastable Solids

Molecular sieves are metastable phases that are thermodynamically unstable with respect to the dense oxide phases. The calculated lattice energies of the structures show a direct correlation with the density. Both theoretical and calorimetric data show that in the case of high-silica zeolites, open frameworks are 8−20 kJ mol^{-1} less stable than quartz.[276] It therefore becomes clear that the formation of zeolitic materials cannot be rationalized on the basis of thermodynamics alone and that kinetics plays a large part in determining which particular phases are formed. Time is therefore an important factor in governing the products formed in molecular sieve synthesis. The synthesis of zeolitic materials follows Ostwald's law of successive reactions, which states that an initial metastable phase is successively converted into a thermodynamically more stable phase until the most stable phase is produced.

3.3. Synthesis of Open-Framework Phosphates

Similar to zeolites, open-framework phosphates are synthesized hydrothermally under autogenous pressure. Hydrothermal synthesis usually refers to reactions in aqueous media above 100 °C and 1 bar. Under these conditions, reactants otherwise difficult to dissolve go into solution, facilitated by the participation of water or mineralizers. A mineralizer is a highly soluble transport substance that increases the solubility of sparingly soluble compounds with high melting points.

Hydrothermal synthesis is not limited to open-framework materials but can be used to synthesize a wide range of materials from commercial quartz crystals to complex oxides, fluorides, and hybrid materials. The role of hydrothermal synthesis in preparative materials chemistry and crystal growth has been reviewed by Rabenau and Laudise.[277] Hydrothermal synthesis has an advantage over the conventional synthetic methods in forming the so-called low-temperature phases and metastable compounds. The various new materials synthesized under hydrothermal conditions have been reviewed by Feng and Xu.[278]

There are two striking differences between the synthesis of zeolites and open-framework metal phosphates. In the case of zeolites, synthesis is carried out in basic medium, while open-framework metal phosphates are obtained under highly acidic conditions. In zeolites, both inorganic cations and organic amines or ammonium ions are used, while for phosphates, mostly organic cations are used, though a few cases are known where inorganic cations or a mixture of the two are used.

To illustrate the procedure of metal phosphate synthesis, let us consider a typical example. In the first step, a metal salt is dissolved or dispersed in water under stirring. In the next step, the phosphate source (H_3PO_4 or P_2O_5) is added to the solution resulting in a highly acidic reaction mixture. The amine or ammonium salt is added to this mixture, which reduces the acidity of the medium. The entire reaction mixture is transferred to a Teflon beaker (fill factor ∼40−50%) and then sealed in a steel autoclave. The autoclave is heated to 125−180 °C for approximately 18−72 h. The typical pressure attained under these conditions is approximately 30−910 bar.[263] Upon completion of the reaction, the autoclave is removed from the oven, cooled to room temperature, and opened. The solid product obtained is filtered and washed thoroughly with water. A powder X-ray diffraction (PXRD) pattern recorded immediately reveals whether the compound is a known or an unknown phase. IR spectra are used to find out whether amines or ammonium ions are present in the material. Energy-dispersive X-ray analysis (EDAX) gives the metal/phosphorous ratio, while gravimetric analysis gives the total amount of amine, occluded water, etc. All this information helps to determine whether the material is an open-framework solid or a condensed phase material. If the material is a new phase, its structure can be solved by *ab initio* powder methods or by single-crystal powder diffraction methods.

In many preparations, a mixture of phases is obtained as the reaction product. In some of them, it is possible to obtain a pure phase of one component by varying parameters such as temperature, time, composition, and ratio of the reactants in the reaction mixture. Let us illustrate this point by looking at a typical reaction:

$$\text{metal source} + \text{phosphate source} + \text{amine} + \text{mineralizer} + H_2O \xrightarrow[18\text{–}72\ \text{h}]{120\text{–}180\ ^\circ\text{C}} \text{products}$$

Let us discuss each component in some detail.

3.3.1. Metal Source

The source of the metal can be a simple soluble salt, chloride, nitrate, or sulfate, or less-soluble fluoride, oxide, alkoxide, or coordination complex, or even the pure metal.

3.3.2. Phosphate Source

There is not much choice in the source of phosphate, and most of the time, it is H_3PO_4 or P_2O_5. Recently, organophosphate esters [$O{=}P(OR)_3$], such as tributylphosphate, have been used as a source of phosphorus by Cheetham and co-workers.[279] Rao et al.[280] used organoammonium phosphate (amine phosphate for simplicity), which supplies both the amine and phosphate in the medium, to prepare a range of materials. This procedure allows one to carry out reactions in a predominantly nonaqueous medium, which favors the formation of low-dimensional materials, specially those of cobalt. In a similar fashion, Neeraj and Cheetham[281] have used organophosphorous amides [$O{=}P(NR_2)_3$] (which on hydrolysis release the phosphoric acid and amine) to synthesize open-framework $ZnPO_4$.

Amines play an important role in the formation of open-framework metal phosphates, though their exact role is still unclear. This issue has been addressed by Davis and Lobo.[274] Apart from acting as charge balancing cations, the organic guest molecules can act in three distinct ways: (1) as space-filling species, (2) as structure-directing agents, and (3) as true templates. If the structure is flexible, the template acts only as a space-filling agent. On the other hand, when the shape of the template and the framework are related, the template is called a structure-directing agent (SDA). When

a template in its lowest energy conformation is held in a cage within the framework, with its symmetry matching with that of the cage, and the organic molecule is not able to rotate freely in the cage, the case is one of true templating.[274] However, examples of templating in the truest sense of the word are rare, and the term organically templated is used somewhat loosely to describe any case where a metal phosphate is present with an organic amine in the structure irrespective of their dimensionalities.

3.3.3. Amine

A large variety of organic amines and ammonium cations have been used as SDA or templates. These include aliphatic, linear monoamines, diamines, triamines, and tetramines, their amino-alkyl or alkyl derivatives, cyclic aliphatic monoamines and diamines, and their derivatives. Aromatic amines like pyridine and their substituents, amines with a backbone like 1,4-diazabicyclo-[2.2.2]-octane, quiniclidine, etc., and various quarternary ammonium cations have also been used. Examples of coordination complexes ($Co(en)_3^{2+/3+}$), aza-crown, etc., have also been found to serve the role of a template. More than 100 amines listed in Figure 44 have been used in various templated metal phosphate syntheses.

3.3.4. Solvent

Solvent plays an important role in the synthesis of open-framework phosphates. Hydrothermal synthesis, as the name indicates, has to be carried out with water. But it has been observed that nonaqueous solvents or a mixture of aqueous and nonaqueous solvents can be effective for the synthesis of known and new open-framework materials. This is because the transport of the chemicals and ions largely depends on their interaction with the solvent. Since organic solvents possess entirely different physical properties (viscosity, dielectric constants, etc) from those of water, the use of nonaqueous or mixed solvents leads to different mobilities of molecules and ions. Since kinetics play a major role in the formation of metastable open-framework solids, different mobilities of ions and molecules may lead to new open-framework materials. In the area of open-framework phosphates, Huo and Xu[282] initiated the use of nonaqueous solvents (alcohols such as butanol, tri(ethylene glycol)) to synthesize some known AlPO's (AlPO-5, AlPO-11 and AlPO-21, AlPO-*n* refers to a particular structure type). The most important discovery using nonaqueous solvents is the synthesis of JDF-20, an aluminophosphate with 20-ring elliptical apertures.[283] Nowadays, nonaqueous solvents are used quite frequently, and the subject has been reviewed by Morris and Weigel.[284] The most commonly used nonaqueous solvents are the alcohols (mono-ols like ethanol, butanol, etc. and polyols like ethylene glycol). THF, DMSO, and dialkyl formamides (like DMF, diethyl formamide (DEF)) have also been used. DMF and DEF often decompose to dimethylamine and diethylamine, which in turn act as templates.[285,286] Other solvents playing such a dual role are the amino alcohols (e.g. 2-hydroxy propylamine).[287]

3.3.5. Mineralizers

A mineralizer helps in solubilizing an insoluble or a sparingly soluble substance. In the area of open-framework phosphates, F^- ion has been extensively used as a mineralizer. Very often, the F^- ions gets incorporated in the framework backbone (joining two metals through M−F−M linkages or sometimes as terminal F) or gets occluded in the cage, thus giving rise to oxy-fluorinated frameworks with new architectures. The most notable discovery using F^- ions in the synthesis has been cloverite, a gallophosphate with a 20-membered pore opening.[288] The fluoride route for the synthesis of microporous solids was initiated by Guth et al[289] and extensively used by Ferey[290] leading to new series of oxy-fluorinated phosphates called ULM-*n*.[290] Another important feature of these families of solids (specially ULM-*n*, GaPO's and AlPO's) is the presence of secondary building units (SBUs) such as tetrameric and hexameric units. The SBUs, different from those found in zeolites, will be discussed later in the review. Interestingly, the fluoride route presented many large pore open-framework phosphates, and today it is not limited to only GaPO or AlPO but includes phosphates of V, Fe, Zr, Ti, Ni, In, and Sb. Other than the F^- ion, Cl^- ion has been used in the synthesis of many zinc phosphates, though it rarely gets incorporated in the framework. Nevertheless, there is evidence that the Cl^- ion gets into the framework as a terminal atom[291] or links two Zn atoms[292] in 2D and 3D zinc phosphates, respectively. Apart from F^- and Cl^- ions, tetraethylorthosilicate, $Si(OEt)_4$ (TEOS), has been used in the synthesis of gallophosphates[293,294] where it improves crystallinity and acts as a mineralizer.

3.3.6. pH, Temperature and Pressure

pH plays an important and complex role in the formation of open-framework phosphates.[263,290,295] It influences (i) the nature of the products formed, (ii) the hydration of the amine, and (iii) the nature and kind of connectivity of the metallic atom with the neighboring polyhedra. For example, aluminosilicate zeolites, which are always synthesized in basic media, consist of corner-shared tetrahedra, whereas metal phosphates, which are prepared under acidic conditions, seem to form bipyramids and octahedra in medium pH, and corner-shared and edge-shared metal octahedra at lower pH (in fluoride medium). It is also found that the size of the SBU increases with the lowering of pH.[263,290] Many of these observations are specific to Ga-phosphates and cannot be extended to Zn-phosphates, where the formation of a SBU based on oligomeric metal polyhedra is rare. Nevertheless, these observations suggest that the pH of the medium plays an important role.

Rao and co-workers[295,296] have studied the effect of the varying ratio of H_3PO_4 and amine in the cases of zinc phosphates. In this study, the ratio of H_3PO_4 and triethylene tetramine (TETA) concentrations was varied keeping the ratio of the other reactants and the reaction temperature fixed, as follows:

$$1ZnO/2HCl/xH_3PO_4/yTETA/100H_2O \xrightarrow[50\ h]{180\ ^\circ C} \text{products} \quad (2)$$

When $x/y = 6{:}2$ or $4{:}1$, (pH $\approx$ 2), one-dimensional and two-dimensional structures with terminal H_2PO_4/HPO_4 groups were obtained. When the x/y ratio was decreased to 2:1 (pH $\approx$ 4) or 1:1 (pH $\approx$ 6), three-dimensional structures were obtained with one or no terminal HPO_4 groups. When the x/y ratio was decreased further ($x/y \approx 1{:}1.5$, pH $\approx$ 6), the amine binds to Zn and forms a three-dimensional structure. However, such studies with other amines would be necessary to establish the generality of the above observations.

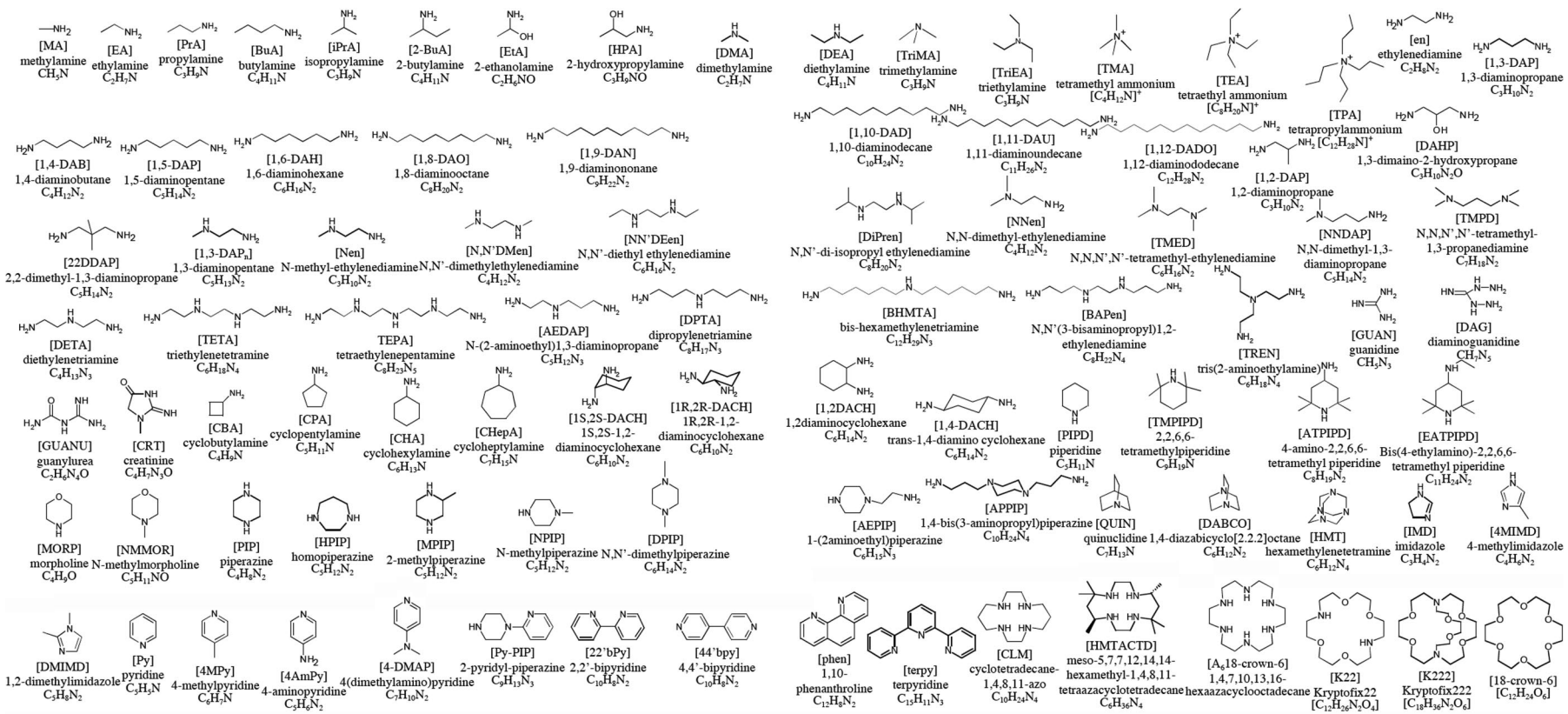

Figure 44. Various amines used as templates for the formation of open-framework metal phosphates along with the notations used in the tables and text given in brackets.

Most of the hydrothermal reactions are carried out for 18−72 h, and generally only the end-product is examined. There is always the possibility that the end-product is the result of transformation of several intermediates. It is, therefore, important to examine the evolution of phases with time in order to understand the mechanism of formation of such solids. But because hydrothermal reactions occur in closed vessels, special techniques are required for carrying out *in situ* studies. Some *in situ* studies have been carried out by a few workers.[297] We shall discuss these results later in the review.

At high pressures and temperatures, the physical properties of the solvent, such as the viscosity and the dielectric constant, change and can in turn influence the nature of the products. Though such data is well documented in the case of water (see Rabenau, ref 277), there is no study on the nature of the products as a function of pressure.

The formation of open-framework phosphates is not limited to hydrothermal synthesis. When a reaction mixture[298] or a gel formed by TEOS[299] is left at room temperature and ambient pressure over long periods (sometimes for several days) open-framework phosphates are formed. Sometimes, surfactants, reverse micelles, or microemulsions are used to grow open-framework phosphates under hydrothermal and non-hydrothermal conditions.[300] By this method, one can also modify or control the morphology of the open-framework material.[301] Combinatorial methods for the synthesis of phosphate-based materials allow one to explore many reaction conditions and the characterization of libraries of materials in one shot.[302] Though traditionally open-framework solids are synthesized hydrothermally or solvothermally in the presence of an organic amine, it is still a very mild or soft chemical process. But there are examples where stable open-framework phosphates such as $A_2Cu_3(P_2O_7)$ (A = K, Rb) and $Na_2Cs_2Cu_3(P_2O_7)Cl_2$ have been prepared by the molten salt method or in an alkali metal chloride flux at high temperatures (500−800 °C).[303] Incidentally, these are the first examples of open framework phosphates formed by copper, as well as by the P_2O_7 moiety. The only other example of an organically templated metal−P_2O_5 structure is the one-dimensional $Ni(HP_2O_7)F\cdot C_2N_2H_{10}$.[304]

3.4. Different Dimensionalities of the Open-Framework Structures

A crystal always refers to a three-dimensional periodic assembly of infinitely repetitive identical structural units. The structural units may be single atoms, ions, or groups of atoms connected together by covalent bonds, which may be a molecule, part of a molecule, or part of an extended structure. It is the last category that is relevant to our discussion. In open-framework phosphates, the asymmetric unit consists of covalently bound atoms forming the inorganic network (M, P, O, F/Cl) and the full or part of the organic amine (often protonated) as two separate entities. If within the crystalline structure, the covalent bonds do not extend in any direction infinitely, it is termed as a zero-dimensional structure. This could be a simple molecular cluster or a complex (e.g., a single four-membered ring formed by two metal and two phosphorous atoms connected by oxygens) or a more complex structure leading to a cluster of high nuclearity. When the covalent bonds extend in one and two particular directions, the structure is called one-dimensional and two-dimensional respectively. When the connectivity of the strong bonds extends in all three directions, it is called a three-dimensional structure. In relation to the templated metal phosphates, there is always an organo-ammonium cation that interacts with the anionic inorganic network through H-bonding or Coulombic and van der Waals forces to hold the three-dimensional crystalline assembly. For this reason, many authors prefer to add the adjective "predominant" while referring to lower dimensional structures (e.g., the structure is predominantly one-dimensional and so on). In the case of three-dimensional structures, there is no such ambiguity. When the framework density (FD) is low or close to the upper limit (FD = 21),[270] as in the case of cross-linked zeolites, it is called an open-framework structure. One can extend the same idea to open-framework phosphates to distinguish them from condensed 3D structures. The three-dimensional framework may be fully cross-linked (similar to zeolites) where all the oxygens of the PO_4 moiety are connected to the metal, or an interrupted framework with one of two terminal HPO_4 or H_2PO_4 groups. It can have intersecting or non-intersecting channels in one, two, or three directions. The framework in most of the cases is negatively charged (except in some of the early AlPO's[261] where it is neutral and the organic amine is also neutral, as in tetraalkylammoniumhydroxide), the organic amine (in protonated form) or the alkali cation residing in the channels and balancing the charge of the framework. The amine also interacts with the framework through H-bonding.

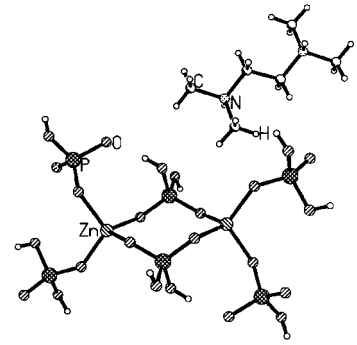

Figure 45. The negatively charged single four-ring (S4R) zinc phosphate, along with the charge balancing TMED.[305]

The zero-dimensional structure is often a four-membered ring formed by two metal and two phosphorous atoms connected through the oxygen atoms (Figure 45). In addition, there may be pendant HPO_4/H_2PO_4 groups to the metal center to fulfill the coordination of the metal as in the case of $[C_6H_{18}N_2][Zn(HPO_4)(H_2PO_4)_2]$;[305] the structure is built by the alternate sharing of H_2PO_4 and ZnO_4 tetrahedra to form the four ring, and also there are dangling HPO_4 and H_2PO_4 groups coordinated to the Zn center (Figure 45). The isolated four-membered rings are hydrogen bonded with the amine in the 3D crystalline assembly. The four-membered ring is a SBU, most frequently encountered in zeolites and open-framework phosphates, and is referred to as a single four-membered ring (S4R). When it was observed that this S4R transforms to higher dimensional structures, it was referred to as a monomer.[305]

One-dimensional structures in the templated metal phosphates show a large variety. It could be a single chain of alternate metal and phosphate polyhedra (wire-like) or a chain of metal polyhedra capped or bridged by the phosphate tetrahedra. There could be rings (e.g., the four-membered ring) joined together to form a chain or a mixture of all these leading to a complex structures. Many of the one-dimensional

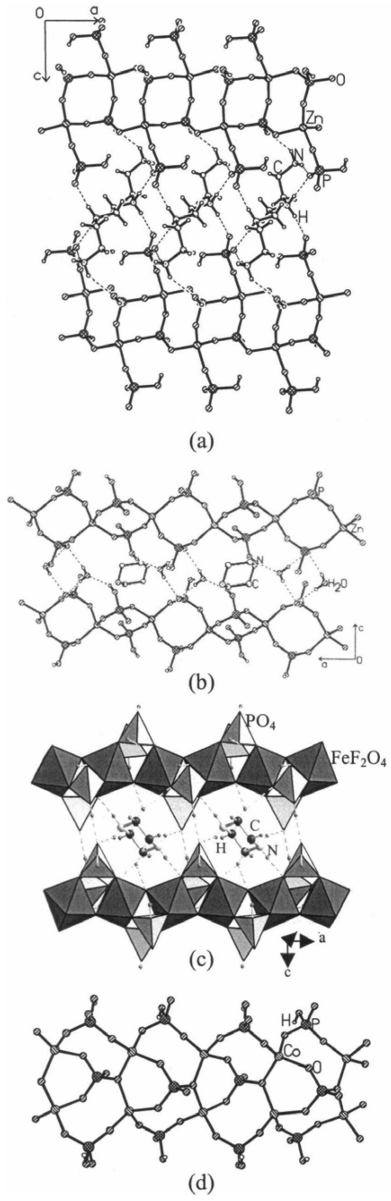

Figure 46. One-dimensional structures of organically templated phosphates: (a) edge-shared four-ring ladder zinc phosphate;[295] (b) corner-shared four-ring chain zinc phosphate;[280] (c) tancoite chain of iron phosphate;[306] (d) a strip-like 1D chain in cobalt phosphate.[280]

structures are isostructural to some minerals. One-dimensional infinite chains are described according to the connectivity between the polyhedra or rings and are also named after the minerals that they closely resemble.

Let us examine some of the one-dimensional structures encountered in the literature (Figure 46). For tetrahedral coordination of the metals, it is the corner- or the edge-sharing four-membered rings that form the chain, the latter being popularly known as the ladder,[295] while the former is referred to as a corner-shared chain (c.s. chain henceforth refers to corner-shared chain of four-membered rings).[280] On the other hand, for octahedral coordination of the metal, the most encountered structure is the corner-shared chain of octahedra doubly bridged by phosphate groups,[306] as in the mineral tancoite.[307] The structure of the ladder[295] in $[C_6N_4H_{22}]_{0.5}[Zn(HPO_4)_2]$ is constructed by alternate linkages involving ZnO_4 and $HP(2)O_4$ groups. The units are so connected to form four-membered rings, which are edge-shared to form ladder-like chains with the $HP(1)O_4$ tetrahedra grafted on to this chain. Thus, $HP(1)O_4$ acts as a pendant to the anionic one-dimensional chain (Figure 46a). A quadruply protonated TETA molecule present in the middle of this chain balances the charge and stabilizes the crystalline assembly through extensive H-bonding with the oxygens of the inorganic moiety. In contrast, four-membered rings formed by ZnO_4 and HPO_4 groups are corner-shared in $[C_4N_2H_{12}]$-$[Zn(HPO_4)_2]\cdot H_2O$[280] to form the one-dimensional chain (Figure 46b). It is to be noted that there is no pendant HPO_4 group from the Zn site because all the oxygens coordinated to Zn come from the bridging HPO_4 groups. In the case of $[C_4N_2H_{12}]_{0.5}[FeF(HPO_4)(H_2PO_4)]$,[306] where the metal is in octahedral coordination, the isolated infinite chains of $[FeF(HPO_4)(HPO_4)]^-_n$ run along the *a*-axis with the diprotonated piperazine molecules inserted between them as shown in Figure 46c. The macroanionic inorganic framework consists of vertex-sharing FeF_2O_4, $PO_3(OH)$, and $PO_2(OH)_2$ polyhedra. In the $[FeF(HPO_4)(HPO_4)]^-_n$ chain, the FeF_2O_4 units share their trans F apices, with the $PO_3(OH)$ and $PO_2(OH)_2$ tetrahedra grafted onto the chain in a symmetrical bridging manner. The trans F vertex sharing of the FeF_2O_4 octahedra creates the infinite linear {-Fe-μF-Fe-μF-Fe-} backbone. Such a topology of the inorganic framework is present in the mineral tancoite.[307] An interesting example of 1D structure is exhibited by a piperazine templated cobalt phosphate, $[C_4H_{12}N_2]_{1.5}[Co(HPO_4)(PO_4)]\cdot H_2O$,[280] where two corner-shared four-ring chains are fused together by a three-coordinated oxygen to form a *strip*-like structure (Figure 46d).

Two-dimensional layered templated metal phosphates are diverse both in terms of the stoichiometry as reflected by their varied M/P ratios and in terms of their rich structural variety. Even within the same stoichiometry, a diverse range of topologies is observed. A variety of 2D layered or sheet structures can be built by the corner-sharing of strictly alternating metal polyhedra and PO_4 tetrahedra leading to numerous apertures within the sheet. Sometimes, the layered structures are built by the condensation of some commonly occurring chains or SBUs. It is, therefore, difficult to find commonalities among the sheet structures. Furthermore, the frequency of occurrence of certain types of sheet structures varies from one family to the other. Two-dimensional sheets are mainly described in terms of the nets by the vertex symbols following the guidelines described by O'Keeffe and Hyde.[308] Let us look at three different layered structures encountered frequently in the literature (Figure 47). $[C_5H_{12}N][C_5H_{16}N_2][Al_3(PO_4)]$[309] has a layered structure with an Al/P ratio of 3:4 and is made up of 4.6.8 nets. The stoichiometry of $Al_3P_4O_{16}^{3-}$ is found in a number of 2D layered compounds with various topologies of which the present example is a common one. The structure is constructed from alternative linkages of AlO_4 and PO_4 tetrahedra in which all the vertices of AlO_4 but only three-quarters of the PO_4 are shared and the remaining vertex is a PO_4 group. Such connectivity of AlO_4 and PO_4 groups leads to a 4.6.8 net within the sheet (Figure 47a), which is stacked in an *AAAA* sequence. However, the stacking sequence could be different (e.g. *ABAB*) for the same stoichiometry and net with a different amine. The same layered topology can be described by the corner-sharing of a SBU, which is a capped six-membered ring (6MR) resembling a D4R with one corner missing (see inset of Figure 47a). Another common layered topology is exemplified by a cobalt phosphate,

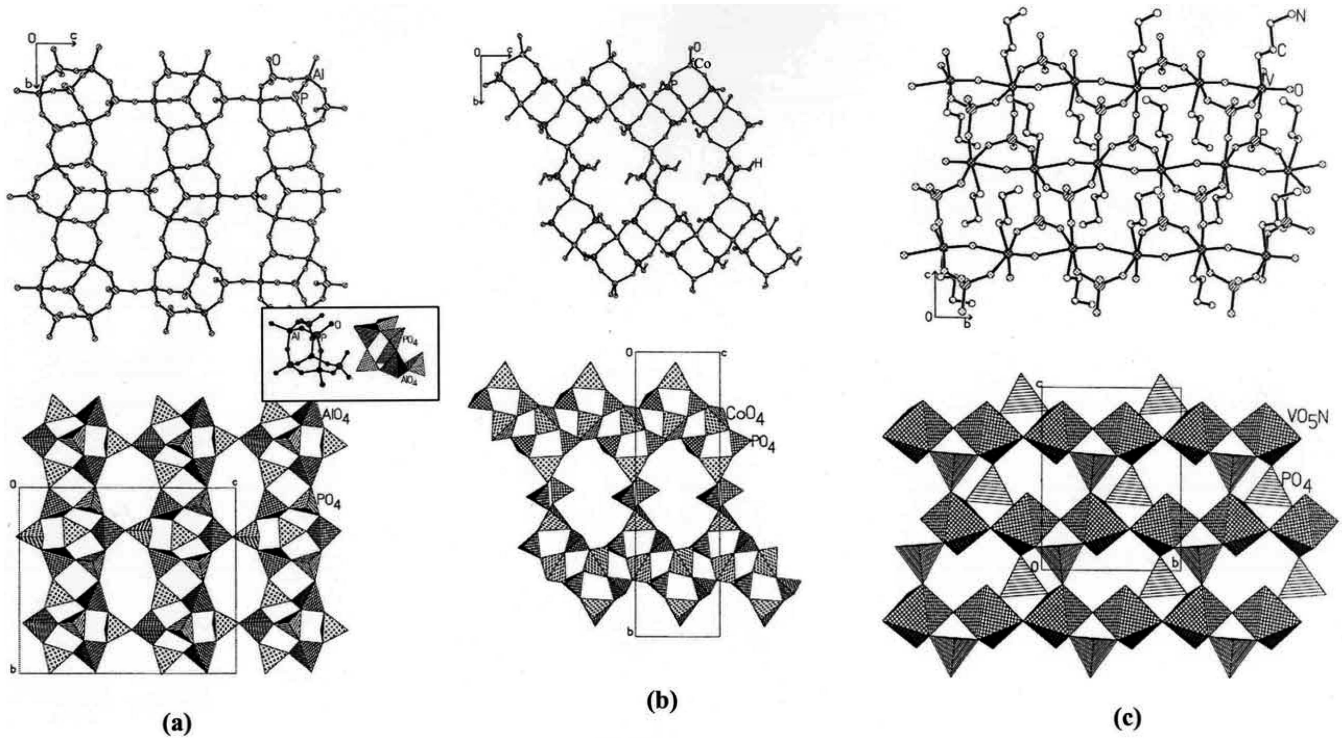

Figure 47. The polyhedral and ball-and-stick views of three common types of layers exemplified by (a) an aluminum phosphate,[309] (b) a cobalt phosphate,[280] and (c) a vanadium phosphate.[310]

$[C_4H_{12}N_2]_{1.5}[Co(HPO_4)(PO_4)]\cdot H_2O$,[280] found in other families of metal phosphates as well. The connectivity between the CoO_4 and HPO_4 tetrahedra gives rise to four-membered rings, which are connected edge-wise forming one-dimensional zigzag ladder-like chains. The chains are joined via a phosphate group as shown in Figure 47b, resulting in the formation of a bifurcated 12-membered aperture within the layer. On the other hand, the layered structure of $VOPO_4(C_2H_9N_2)$[310] is built up of isolated corner-shared trans chains of VO_5N octahedra. PO_4 tetrahedra cross-link such chains to form the layered structure (Figure 47c). Another interesting feature in this structure is that the N-atom of the ethylenediamine binds with vanadium to complete its octahedral coordination. This additional role of the amine to fulfill the coordination of the metal is observed in some of the metal phosphates.

A three-dimensional open-framework metal phosphate is sometimes fully cross-linked (similar to zeolite) where all the oxygen atoms of the PO_4 tetrahedra are connected to the metal or an interrupted framework with one or two terminal HPO_4 or H_2PO_4 groups. There are many metal phosphates where the coordination of the metal is more than 4, like a five-coordinated trigonal bipyramid or square pyramid or a six-coordinated octahedron where all the five or six coordination may not be satisfied by the oxygens from phosphate groups, and interruptions may occur due to the terminal -H_2O, -OH, or -F atom. Similarly, the PO_4 group may not be four-connected. For five- and six-coordinated systems, there is a frequent occurrence of M−X−M (X = O, −OH, F) linkages (finite or infinite), while in the case of four-coordinated tetrahedral systems such linkages are prohibited by Lowenstein's rule, which is strictly followed in the case of Al.[266] In the case of Zn phosphates, Zn−O−Zn linkages have been observed wherein the oxygen of the phosphate group becomes tricoordinated as in $[C_6H_{22}N_4]_{0.5}[Zn_3(HPO_4)(PO_4)_2]$.[295]

Open-framework structures can be described in terms of finite or infinite (chain or layer-like) components. Finite components in the case of zeolites are described in terms of the SBUs. Open-framework zeotypes can also be described in terms of 3D nets following Wells[311] and Smith[312] or the Schläfi symbols.[313] The open-framework phosphates are structurally complex with differing finite components or SBUs, wherein the metal polyhedra are condensed to form oligomeric species, which in combination with the PO_4 tetrahedra form various SBUs (Figure 48). Only a few of these are common with the zeolites. One can describe the structure in terms of the connectivity of the SBUs or find a one-to-one correspondence of nets by joining the center of these SBUs to a simple structure type like diamond or NbO (homeomorphism).[314,315] Férey has developed the concept of building units and scale chemistry, which can be used as an *a posteriori* tool to analyze the structure as well as to imagine new topologies.[316] Geometrical principles of this kind have been described by O'Keeffe and co-workers.[317] Even with all these techniques and concepts, structural descriptions often become hard. In such cases, a recognizable infinite component such as a chain or a layer is discerned and its polyhedral connectivity described in detail.

Let us take three prototype examples to understand the structural description (Figure 49). Let us take a relatively simple example of the structure description of a cobalt phosphate of the composition $[C_2N_2H_{10}]_2[Co_4(PO_4)_4]\cdot H_2O$,[318] with a Co/P ratio of 1/1. The connectivity of strictly alternating CoO_4 and PO_4 tetrahedra leads to the open-framework network as shown in Figure 49a. On inspection, it is found that the structure is built from double four rings (D4R) (see inset of Figure 49a) formed by the vertex linkage of the CoO_4 and PO_4 tetrahedra. The double four-rings are linked to each other via oxygens to eight other D4R units through Co−O−P or P−O−Co linkages, forming eight-membered channels along all the three crystallographic

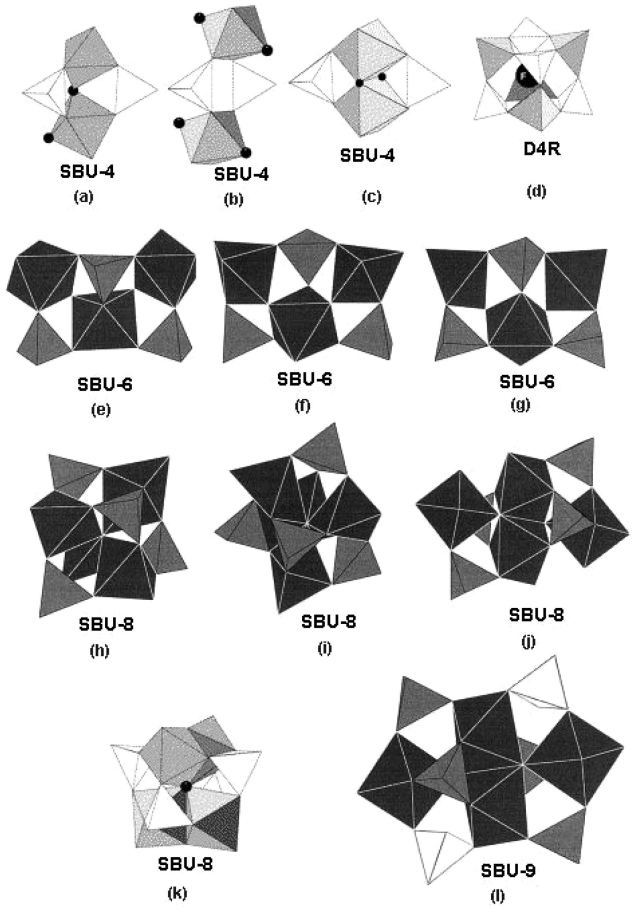

Figure 48. Various SBUs in Open-Framework Phosphates. Figure generated from refs **263** and **745** with permission. Copyright 2001, 1999 Elsevier.

directions. The water molecules and the protonated ethylenediamine molecules sit in the middle of these channels. This kind of framework topology built up exclusively from double four ring (D4R) units was theoretically predicted 40 years ago.[319] This framework type is called ACO, and to-date there is no aluminosilicate zeolite known to have the ACO framework type. On the other hand, MIL-31, $[C_{20}H_{52}N_4][Ga_9(PO_4)_9F_3(OH)_2(H_2O)]\cdot 2H_2O$,[320] is a perfect example of scale chemistry and homeomorphism to describe an otherwise complex structure (Figure 49b). The structure of MIL-31 is built from two different kinds of hexameric building units (SBU-6), where the gallium polyhedra exhibit three different coordinations: tetrahedral, trigonal bipyramidal (*tbp*), and octahedral. The connectivity between the SBU-6 units leads to the 3D structure with an 18-membered channel, the topology of which can be related to "hexagonal tungsten bronze" if one replaces the SBU-6 hexamer by a single octahedron (Figure 49b).[263]

Let us examine a complex case where there is no recognizable SBUs as exemplified by the FePO, $[C_4N_3H_{16}]_2[Fe_5F_4(H_2PO_4)(HPO_4)_2(PO_4)_4]\cdot 0.5H_2O$,[321] a 3D structure with an 18-membered channel. The complex network is built from FeO_4F_2, FeO_5F, FeO_6, PO_4, PO_3OH, and $PO_2(OH)_2$ polyhedra, having an infinite Fe−X−Fe (X = O, F) connectivity and the presence of an unusual edge-shared FeO_6 and PO_4 dimer. Without going into the intricacies of polyhedral connectivities, one can discern a layer from the 3D structure (inset of Figure 49c) by careful selection. Incidentally, the layer topology bears close resemblance to the one observed in $[Fe_5F_3(PO_4)_6(H_2O)_3](H_2O)_2\cdot[(H_3N(CH_2)_4NH_3)_3]$,[322] the only difference being that in the seven-membered aperture of the discerned layer, a pendant H_2PO_4 group protrudes, while in the former case it is just a terminal water connected to the iron site. The layers thus formed are cross-linked by the PO_4 tetrahedra along the *c*-axis in the *ABAB* fashion through the formation of a four-membered ring to form the 3D structure. Such cross-linking of layers forms an 18-membered elliptical channel along the *a*-axis (Figure 49b) and a 16-membered channel along the *b*-axis. The *ABAB* stacking of the layers parallel to the *ab*-plane renders the seven-membered aperture inaccessible. In this connection, it is to be noted that both MIL-31 and $[C_4N_3H_{16}]_2[Fe_5F_4(H_2PO_4)(HPO_4)_2(PO_4)_4]\cdot 0.5H_2O$ contain an 18-membered channel, which is quite large and should be denoted as an extra-large pore (greater than 12MR) molecular sieves.[323] Such extra-large pore frameworks are characteristic of the metal phosphate family, the first discovery being an 18-membered AlPO (VPI-5) by Davis et al.[324] Zeolites are primarily limited by 12MR channels[270] with the exception of UTD-1,[325] a high-silica zeolite with a 14MR channel. Thus, the quest for extra-large pore molecular sieves[323] has yielded many new extra-large frameworks in the metal phosphate family, which we will examine later in the review.

3.5. Main Group Metal Phosphates

3.5.1. Aluminium Phosphates

Playing with the iso-electronicity of $AlPO_4$ with SiO_2, Flanigen and co-workers discovered a new generation of microporous materials, aluminophosphate, $AlPO_4$-*n*, and subsequently promoted a tremendous growth in the area of open-framework metal phosphates.[261] The original $AlPO_4$-*n* family has an Al/P ratio of unity, and the framework is neutral. But it is no longer limited to neutral frameworks. Later discoveries reveal the presence of anionic 3D open-framework structures along with a range of lower-dimensional structures. The various low-dimensional structures (0, 1, 2), as well as 3D $AlPO_4$ structures, are listed in Table 1.[283,285–287,299,326–439] The rich structural diversity of aluminophosphate has been reviewed,[440,441] and we will briefly touch upon the various dimensionalities of AlPO's here.

Zero-Dimensional Structures. There is only one zero-dimensional AlPO reported with an Al/P ratio of 1:4, formed in the presence of an organic ammonium cation, $[C_2H_{10}N_2]_4[NH_4][Al(PO_4)_4]$,[343] where the central AlO_4 tetrahedron shares the four corners with four PO_4 tetrahedra but does not form a closed ring.

One-Dimensional Structures. The anionic 1D AlPO is mainly limited to the three most common types discussed earlier (Figure 46), namely, the corner-shared chain of four-membered rings, the ladder, and tancoite (Table 1). The Al/P ratio in these 1D materials is 1:2. The bridging phosphate in the corner-shared chain can have one or both HPO_4 groups instead of PO_4 groups, thus varying the charge of the macroanion from −1 to −3. Similarly, in the case of the ladder, the dangling phosphate group may be H_2PO_4 or HPO_4 except where it is a terminal F atom and the Al/P ratio turns out to be unity.[424] In the tancoite chain with $AlO_{6-x}(OH/F)_x$ ($x = 0-2$) octahedra, the corner-shared chain can have bridging PO_4, HPO_4, and H_2PO_4 groups. There are two rather uncommon 1D AlPO's reported in the literature (Figure 50). One of them reported by Ozin and co-workers[363,368] with an Al/P ratio of 3/5 (UT-2,7), can be described as three corner-shared four-membered rings connected to edge-shared

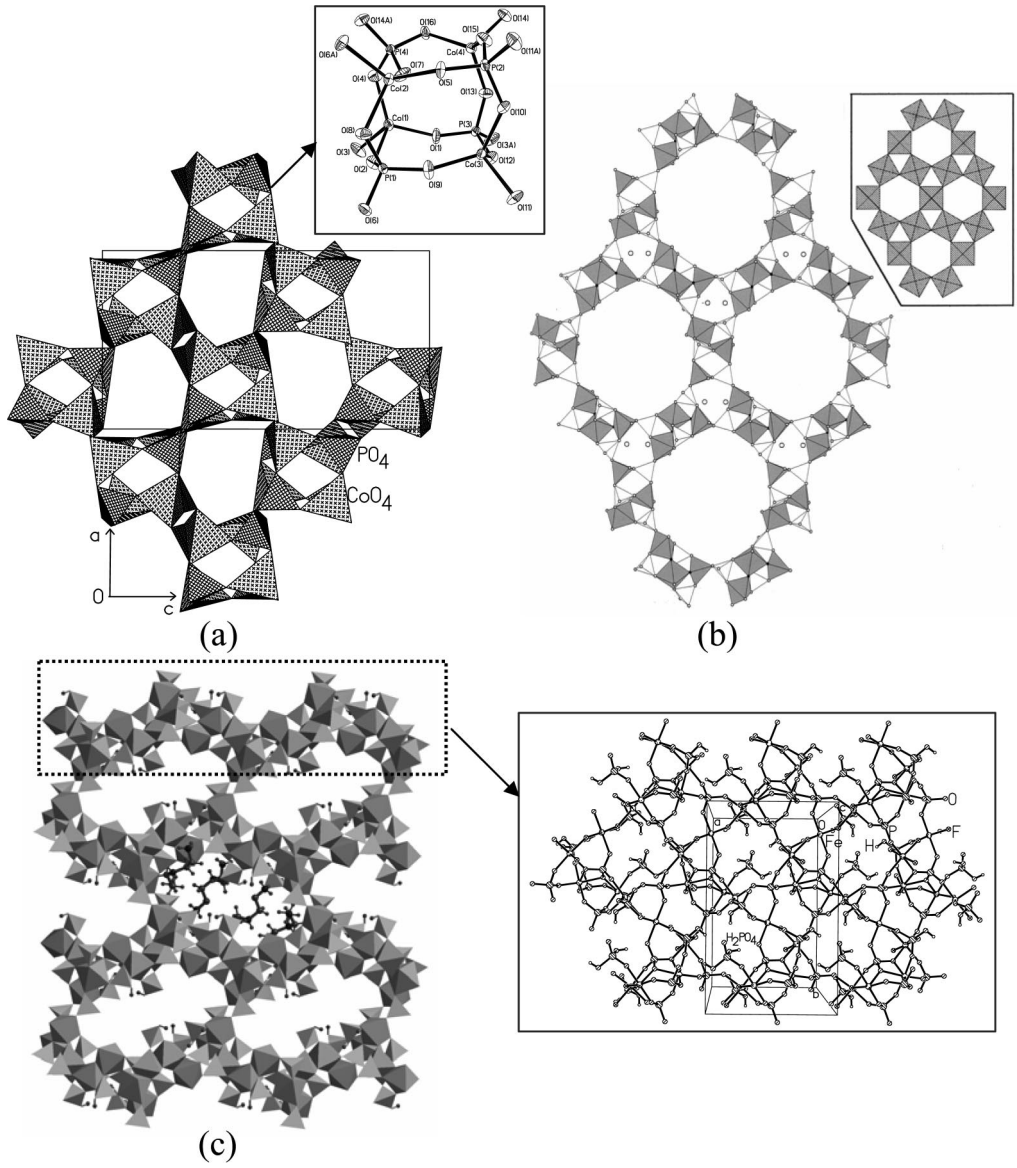

Figure 49. Structures of three open-framework phosphates: (a) a cobalt phosphate;[318] (b) a gallium phosphate[320] (Reprinted with permission from ref 263. Copyright 2001 American Chemical Society); (c) an iron phosphate.[321]

four-membered rings to form six-membered rings (Figure 50a). On the other hand, $[\Lambda,\Delta\text{-Ir(en)}_3][Al_3(PO_4)_4]\cdot xH_2O$ ($x \approx 3.45$)[402] with an Al/P ratio of 3/4 has a 1D structure that can be visualized as a ladder where the alternate dangling HPO_4/H_2PO_4 groups are absent and instead are bridged by another one (Figure 50b).

Two-Dimensional Structures. Two-dimensional layered AlPO's with a large variety in terms of the Al/P ratios and structures are known (Table 1). Among the sheet structures consisting of strictly alternating AlO_4 and PO_4 tetrahedra, the $Al_3(PO_4)_4^{3-}$ stoichiometry creates various layer topologies as identified by Yu and Xu (Figure 51).[441] The various types include 4·6·12,[287,341,370,436] 4·6·8(I)−,[309,339,349,368,373,383] 4·6·8(II),[400] 4·6(I)−,[361] 4·6(II)−,[354,356,365,372,402,414] 4·6(III)−,[395] 4·6(IV)−,[430] and 4·8 nets.[388,394] The next abundant stoichiometry in the sheet structures is $Al_2P_3O_{12}$ with an Al/P ratio of 2/3 and anionic charge of −1, $[Al_2(HPO_4)(PO_4)_2]^{1-}$, or −2, $[Al_2(HPO_4)_2(PO_4)]^{2-}$, where P and Al polyhedra occur alternately. There could be five different types of sheet structures as given in Figure 52.[384] Types 1 and 2 are found in $[C_6H_8N][Al_2(HPO_4)_2(PO_4)]$[384] and $[C_5H_6N][Al_2(HPO_4)_2(PO_4)]$.[342] Type 3 is found in UT-3[363] and UT-5,[367] while type 4 is found in UT-4.[367] Type 5 is found in $[C_4H_{12}N]_2[Al_2(HPO_4)(PO_4)_2]$.[342] In addition to the above, $[C_9H_{20}N][Al_2(HPO_4)_2(PO_4)]$[401] with the same stoichiometry bears close resemblance to type 2 where breaking the linkage between the five-coordinated Al and one of the four-coordinated P atoms generates the layer topology. The Al/P ratio of 1:2 is found in two sheet structures with strictly alternating AlO_4 and PO_4 tetrahedra connecting to form 4·20[369] and 4·12 nets,[410] respectively. There are single occurrences with Al/P ratios of 1:1[435] and 4:5[286] wherein the sheet structures are related to the AlPO-41 (AFO) type in the former case while the latter has a double sheet built from the D4R SBU.

Layered AlPO with Al in More than Four Coordination. Sheet structures involving Al in five or six coordination generally leads to Al−(OH)−Al linkages, which can be finite or infinite. However, there are examples where AlO_x ($x > 4$) polyhedra and PO_4 tetrahedra alternate, as in the $[Al(H_2O)_2(HPO_4)_2]^{-1}$ stoichiometry,[299,379,387] where AlO_4-$(H_2O)_2$ octahedra and PO_4 tetrahedra form eight-membered apertures. Similarly, alternating connectivity of AlO_5, AlO_4, and PO_4 polyhedra in $[C_3H_5N_2]_2[Al_3(HPO_4)(PO_4)_2]$[379,387]

Table 1. Lattice Parameters, Templates and Dimensionalities of the Various Templated Aluminium Phosphates Reported in the Literature

formula	SG[a]	lattice parameters	template	type	ref
$[C_2H_{10}N_2]_4[NH_4][Al(PO_4)_4]$	$I\bar{4}$	$a = b = 9.154$ Å, $c = 17.181$ Å; $\alpha = \beta = \gamma = 90°$	enH_2	0D	343
$[C_6H_{16}N]^+[Al(HPO_4)_2]$	$P2_1/n$	$a = 12.073$ Å, $b = 13.201$ Å, $c = 8.522$ Å; $\alpha = \gamma = 90°$, $\beta = 97.20°$	TriEAH	1D c.s. chain	337
$[C_2H_{10}N_2][Al(PO_4)_2]\cdot H_3O$	$Pbnb$	$a = 8.052$ Å, $b = 8.760$ Å, $c = 17.037$ Å; $\alpha = \beta = \gamma = 90°$	enH_2	1D c.s. chain	338
$Na_4[Al(OH)(PO_4)_2]$	$Pbcm$	$a = 15.279$ Å, $b = 14.660$ Å, $c = 6.947$ Å; $\alpha = \beta = \gamma = 90°$	Na^+	1D tancoite	353
$[C_5H_{12}N]_5[Al_3(HPO_4)(PO_4)_4]$ (UT-2)	$P\bar{1}$	$a = 10.063$ Å, $b = 15.447$ Å, $c = 15.736$ Å; $\alpha = 71.72°$, $\beta = 80.07°$, $\gamma = 79.57°$	CPAH	1D chain	363
$[C_2H_{10}N_2][NH_4][Al(PO_4)_2]$ (AlPO-enA)	$Pccn$	$a = 8.033$ Å, $b = 16.989$ Å, $c = 8.740$ Å; $\alpha = \beta = \gamma = 90°$	enH_2, NH_4	1D c.s. chain	366
$[C_7H_{16}N]_5[Al_3(HPO_4)(PO_4)_4]$ (UT-7)	$P\bar{1}$	$a = 10.118$ Å, $b = 15.691$ Å, $c = 18.117$ Å; $\alpha = 72.91°$, $\beta = 85.18°$, $\gamma = 79.42°$	ChepAH	1D chain	368
$[C_{10}H_9N_2][Al(H_2PO_4)_2(PO_4)]$	$P\bar{1}$	$a = 4.917$ Å, $b = 10.696$ Å, $c = 14.660$ Å; $\alpha = 107.84°$, $\beta = 95.68°$, $\gamma = 99.91°$	4,4′-bPyH	1D ladder	374
$[C_2H_{10}N_2][Al(HPO_4)(PO_4)]$	$P\bar{1}$	$a = 4.901$ Å, $b = 9.032$ Å, $c = 11.691$ Å; $\alpha = 81.38°$, $\beta = 82.27°$, $\gamma = 75.83°$	enH_2	1D ladder	375
$Na_3[Al(HPO_4)(OH)(PO_4)]$	$C2/m$	$a = 15.277$ Å, $b = 7.054$ Å, $c = 7.040$ Å; $\alpha = \gamma = 90°$, $\beta = 96.73°$	Na^+	1D tancoite	377
$[\Lambda,\Delta\text{-Co(en)}_3][Al(PO_4)_2]\cdot xH_2O$	$I\bar{4}2d$	$a = b = 22.600$ Å, $c = 8.567$ Å; $\alpha = \beta = \gamma = 90°$	$\Lambda,\Delta Co(en)_3$	1D c.s. chain	385
$[Ir(chxn)_3][Al_2(PO_4)_3]\cdot xH_2O$ ($x \approx 4$)	$P\bar{1}$	$a = 9.649$ Å, $b = 12.365$ Å, $c = 16.083$ Å; $\alpha = 100.02°$, $\beta = 101.64°$, $\gamma = 104.75°$	$Ir(chxn)_3^{3+b}$	1D chain	402
$[C_2H_{10}N_2][C_3H_{12}N_2]_2[Al_2(PO_4)_4]$	$P\bar{1}$	$a = 8.950$ Å, $b = 9.251$ Å, $c = 8.647$ Å; $\alpha = 115.76°$, $\beta = 99.70°$, $\gamma = 98.25°$	enH_2 1,3DAPH$_2$	1D c.s. chain	404
$[C_5H_{16}N_2][Al(HPO_4)(PO_4)_4]$	$P2_1/n$	$a = 7.878$ Å, $b = 10.469$ Å, $c = 16.068$ Å; $\alpha = \gamma = 90°$, $\beta = 95.15°$	1,5-DAPH$_2$	1D c.s. chain	422
$[C_8H_{22}N_2][Al_2F_2(PO_4)_2]$ (AlPO-CJ8)	$P\bar{1}$	$a = 5.031$ Å, $b = 9.363$ Å, $c = 10.613$ Å; $\alpha = 65.95°$, $\beta = 88.22°$, $\gamma = 77.19°$	DiPrenH$_2$	1D ladder	424
$[C_3H_{12}N_2][Al(HPO_4)(PO_4)]$	$P\bar{1}$	$a = 8.309$ Å, $b = 8.636$ Å, $c = 8.844$ Å; $\alpha = 111.9°$, $\beta = 107.6°$, $\gamma = 98.0°$	1,2-DAPH$_2$	1D c.s. chain	425
$[C_3H_{12}N_2][NH_4][Al(PO_4)_2]$	$Pccn$	$a = 16.832$ Å, $b = 8.289$ Å, $c = 8.694$ Å; $\alpha = \beta = \gamma = 90°$	1,2-DAPH$_2$	1D c.s. chain	425
$[C_3H_{12}N_2][H_6N_2O_2]_{0.5}[Al(PO_4)_2]$	$P\bar{1}$	$a = 8.669$ Å, $b = 8.943$ Å, $c = 9.266$ Å; $\alpha = 98.3°$, $\beta = 116.0°$, $\gamma = 99.7°$	1,3-DAPH$_2$, DHYDZ[c]	1D c.s. chain	425
$[C_6H_{13}N_2][Al(H_2PO_4)(HPO_4)F]$ (AlPO-CJ10)	$Pnma$	$a = 25.547$ Å, $b = 6.915$ Å, $c = 7.179$ Å; $\alpha = \beta = \gamma = 90°$	$HPIPH^+$	1D tancoite	427
$[C_5H_{18}N_3][Al(PO_4)_2]$	$Pbca$	$a = 16.850$ Å, $b = 8.832$ Å, $c = 17.688$ Å; $\alpha = \beta = \gamma = 90°$	AEDAPH$_3$	1D c.s. chain	437
$[C_2H_{10}N_2][C_2H_7O_2][Al(HPO_4)_2]$	$P2_12_12_1$	$a = 9.014$ Å, $b = 14.771$ Å, $c = 17.704$ Å; $\alpha = \beta = \gamma = 90°$	enH_2, EGH^{+d}	2D	339
$[C_4H_{14}N_2]_{1.5}[Al_3(PO_4)_4]$	$P3c1$	$a = b = 12.957$ Å, $c = 18.413$ Å; $\alpha = \beta = \gamma = 90°$	1,4-DABH$_2$	2D	341
$[C_4H_{12}N]_2[Al_2(HPO_4)(PO_4)_2]$	$P2_1/c$	$a = 9.261$ Å, $b = 8.365$ Å, $c = 27.119$ Å; $\alpha = \gamma = 90°$, $\beta = 91.50°$	2-BuAH	2D	342
$[C_5H_6N][Al_2(HPO_4)_2(PO_4)]$	$P\bar{1}$	$a = 8.574$ Å, $b = 8.631$ Å, $c = 10.371$ Å; $\alpha = 81.84°$, $\beta = 87.53°$, $\gamma = 69.07°$	PyH	2D	342
$AlF(HPO_4)(C_2H_8N_2)$	$P2_1/c$	$a = 9.285$ Å, $b = 7.083$ Å, $c = 9.649$ Å; $\alpha = \gamma = 90°$, $\beta = 101.544°$	bound en	2D	344
$[C_5H_{12}N][C_5H_{16}N_2][Al_3(PO_4)_4]$	$P2_1/c$	$a = 9.801$ Å, $b = 14.837$ Å, $c = 17.815$ Å; $\alpha = \gamma = 90°$, $\beta = 105.65°$	PIPDH, 1,5-DAPH$_2$	2D	349, 309
$[Co(en)_3][Al_3(PO_4)_4]\cdot 3H_2O$	$Pna2_1$	$a = 8.521$ Å, $b = 13.775$ Å, $c = 21.594$ Å; $\alpha = \beta = \gamma = 90°$	$Co(en)_3^{3+}$	2D	354
$[Co(tn)_3][Al_3(PO_4)_4]\cdot 2H_2O$	$P2_1$	$a = 8.862$ Å, $b = 14.706$ Å, $c = 11.402$ Å; $\alpha = \gamma = 90°$, $\beta = 108.87°$	$Co(tn)_3^{3+}$	2D	356
$[C_6H_{18}N_2]_{2.5}[Al_4(PO_4)_3(HPO_4)F_6]\cdot 3H_2O$	$Pnma$	$a = 9.501$ Å, $b = 14.14$ Å, $c = 27.057$ Å; $\alpha = \beta = \gamma = 90°$	1,6-DAHH$_2$	2D	357
$[C_3H_{12}N_2]_3[Al_6(PO_4)_8]\cdot H_2O$	Ia	$a = 14.736$ Å, $b = 16.236$ Å, $c = 18.119$ Å; $\alpha = \gamma = 90°$, $\beta = 91.35°$	1,2-DAPH$_2$	2D	361
$[C_5H_{12}N]_2[Al_2(HPO_4)(PO_4)_2]$ (UT-3)	$P2_1/c$	$a = 9.120$ Å, $b = 28.289$ Å, $c = 9.010$ Å; $\alpha = \gamma = 90°$, $\beta = 111.82°$	CPAH	2D	363
[*trans*-Co(dien)$_2$] $[Al_3(PO_4)_4]\cdot 3H_2O$	$P6_522$	$a = b = 8.457$ Å, $c = 63.27$ Å; $\alpha = \beta = 90°$, $\gamma = 120°$	*trans*-$Co(dien)_2^{3+}$	2D	365
$[C_6H_{14}N]_2[Al_2(HPO_4)(PO_4)_2]$ (UT-4)	$P2_1/c$	$a = 14.739$ Å, $b = 18.837$ Å, $c = 8.601$ Å; $\alpha = \gamma = 90°$, $\beta = 105.89°$	CHAH	2D	367

Table 1. Continued

formula	SG[a]	lattice parameters	template	type	ref
$[C_6H_{14}N]_2[Al_2(HPO_4)(PO_4)_2]$ (UT-5)	$P2_1/c$	a = 9.104 Å, b = 30.848 Å, c = 9.004 Å; α = γ = 90°, β = 111.17°	CHAH	2D	367
$[C_5H_{12}N]_2[C_4H_{10}N][Al_3(PO_4)_4]$ (UT-8)	$P2_1$	a = 8.993 Å, b = 14.884 Å, c = 9.799 Å; α = γ = 90°, β = 103.52°	PIPDH, CBAH	2D	368
$[NH_4]_3[Co(NH_3)_6]_3[Al_2(PO_4)_4]_2$	$Aba2$	a = 9.502 Å, b = 29.699 Å, c = 17.210 Å; α = β = γ = 90°	NH_4, $Co(NH_3)_3^{3+}$	2D	369
$[C_4H_{12}N]_3[Al_3(PO_4)_4]$	$P3$	a = b = 13.158 Å, c = 9.633 Å; α = β = 90°, γ = 120°	$BuAH^+$	2D	370
[d-$Co(en)_3$][$Al_3(PO_4)_4$]·$3H_2O$	$C222_1$	a = 8.502 Å, b = 14.620 Å, c = 20.890 Å; α = β = γ = 90°	d-$Co(en)_3$	2D, chiral	372
$[C_2H_8N]_2[Al_3(PO_4)_4]$	$P2_1/m$	a = 8.920 Å, b = 14.896 Å, c = 9.363 Å; α = γ = 90°, β = 106.07°	EAH	2D	373
$[C_3H_5N_2][Al(H_2O)_2(HPO_4)_2]$	$C2/c$	a = 21.854 Å, b = 7.188 Å, c = 6.990 Å; α = γ = 90°, β = 103.77°	IMDH	2D	299, 379, 387
$[C_3H_5N_2]_2[Al_3(HPO_4)(PO_4)_3]$	$P\bar{1}$	a = 8.940 Å, b = 9.360 Å, c = 11.721 Å; α = 97.10°, β = 95.10°, γ = 91.91°	IMDH	2D	379, 387
$[C_3H_{10}N]_3^+[Al_3(PO_4)_4]$	$P2_1/n$	a = 1 1.310 Å, b = 14.854 Å, c = 14.796 Å; α = γ = 90°, β = 93.64°	PrAH	2D	383
$[C_4H_{12}N]_2^+[Al_4(HPO_4)(PO_4)_4]$·1.25$H_2O$	$P\bar{1}$	a = 8.632 Å, b = 9.267 Å, c = 17.461 Å; α = 86.66°, β = 82.20°, γ = 89.28°	DEAH	2D	286
$[C_6H_8N][Al_2(HPO_4)_2(PO_4)]$	$P2_1/c$	a = 8.686 Å, b = 21.240 Å, c = 8.799 Å; α = γ = 90°, β = 113.23°	4MpyH	2D	384
$[CH_6N_3][Al(H_2O)_2(HPO_4)_2]$	$Pnma$	a = 6.965 Å, b = 20.624 Å, c = 7.268 Å; α = β = γ = 90°	GUANH	2D	386
$[CH_6N]_3[Al_3(PO_4)_4]$ (MU-7)	$P\bar{1}$	a = 8.368 Å, b = 11.274 Å, c = 11.462 Å; α = 72.40°, β = 89.45°, γ = 85.37°	MAH	2D, 4.8 net	388, 394
$[C_3H_{12}N_2][Al_2O(PO_4)_2]$	$P2_1/c$	a = 11.651 Å, b = 9.279 Å, c = 9.696 Å; α = γ = 90°, β = 103.14°	1,3-$DAPH_2$	2D	391
$Cs_2[Al_2O(PO_4)_2]$	$P\bar{1}$	a = 4.925A Å, b = 7.121A Å, c = 8.066 Å; α = 96.51°, β = 107.12°, γ = 108.68°	Cs^+	2D	392
$[H_4N][C_5H_9N_2]_2[Al_3(PO_4)_4]$	$P2_1/c$	a = 10.402 Å, b = 14.545 Å, c = 16.361A Å; α = γ = 90°, β = 96.40°	DMIMDH	2D	395
$[C_6H_{21}N_4][Al_2(HPO_4)_3F_2][H_2PO_4]$	$P2_1/c$	a = 13.154 Å, b = 9.518 Å, c = 17.889 Å; α = γ = 90°, β = 106.165°	$TRENH_3$	2D	396
$[C_2H_{10}N_2][Al_2(OH)_2(PO_4)_2(H_2O)]$·$H_2O$(UiO-15)	$P\bar{1}$	a = 10.375 Å, b = 6.607 Å, c = 9.909 Å; α = γ = 90.762°, β = 115.265°, γ = 90.162°	enH_2	2D	397, 415
$[C_2H_{10}N_2][Al_2(OH)_2(PO_4)_2]$ (UiO-15-125)	$P2_1/c$	a = 10.288 Å, b = 6.751 Å, c = 9.625 Å; α = γ = 90°, β = 116.124°	enH_2	2D	397
$[C_2H_{10}N_2][Al_2O(PO_4)_2]$ (UiO-15-225)	$P2_1/c$	a = 9.428 Å, b = 6.914 Å, c = 9.408 Å; α = γ = 90°, β = 113.002°	enH_2	2D	397
$[C_6H_{21}N_4][Al_3(PO_4)_4]$	$P2_1/c$	a = 9.550 Å, b = 24.064 Å, c = 9.601 Å; α = γ = 90°, β = 97.99°	$TETAH_3$	2D	400
$[C_9H_{20}N][Al_2(HPO_4)_2(PO_4]$	$P\bar{1}$	a = 8.541 Å, b = 9.298 Å, c = 12.660 Å; α = 73.26°, β = 89.58°, γ = 87.70°	TMPIPD	2D	401
[Λ,Δ-$Ir(en)_3$][$Al_3(PO_4)_4$]·xH_2O ($x \approx 3.45$)	$Pnna$	a = 8.548 Å, b = 21.983 Å, c = 13.970 Å; α = β = γ = 90°	$Ir(en)_3^{3+}$	2D	402
$[C_3H_{12}N_2][Al_2(PO_4)(OH_x,F_{5-x})]$ (x=2)	$P2_1/m$	a = 11.072 Å, b = 7.012 Å, c = 6.110 Å; α = γ = 90°, β = 100.98°	1,3-$DAPH_2$	2D	403
$[C_2H_{10}N_2][Al_2O(PO_4)_2]$	$Pbca$	a = 9.331 Å, b = 9.660 Å, c = 21.829 Å; α = β = γ = 90°	enH_2	2D	391
$[C_3H_{12}N_2][Al_2(OH)_2(PO_4)_2(H_4O)_2]$·$2H_2O$ (UiO-18)	$Pnma$	a = 6.918 Å, b =22.300 Å, c = 9.606 Å(UiO-18)	1,3-$DAPH_2$	2D	396
$[C_3H_{12}N_2][Al_2(OH)_2(PO_4)_2]$ (UiO-18-100)	$P2_1/n$	a = 21.551 Å, b = 6.964 Å, c = 8.163 Å; α = γ = 90°, β = 100.042°	1,3-$DAPH_2$	2D	406
$[C_6H_{21}N_4][C_2H_{10}N_2][Al_2(PO_4)_4]$	$P2_1$	a = 10.826 Å, b = 8.143 Å, c = 13.770 Å; α = γ = 90°, β = 95.104°	enH_2, $TETAH_4$	2D	410
$[C_6H_{21}N_4][Al_3(PO_4)_4]$·$H_2O$ (MIL-32)	$C2$	a = 19.142 Å, b = 8.527 Å, c = 14.545 Å; α = γ = 90°, β = 104.54°	$TRENH_3$	2D, chiral	414
$[C_3H_{10}NO]_3[Al_3(PO_4)_4]$	$R\bar{3}$	a = b = 13.107 Å, c = 26.935 Å; α = β = 90°, γ = 120°	HPAH	2D, 12MR	287
$[C_3H_{12}N_2][Al_2(OH)_2(PO_4)_2]$·$H_2O$	$Pca2_1$	a = 10.001 Å, b = 6.712 Å, c = 18.633 Å; α = β = γ = 90°	1,2-$DAPH_2$	2D	419, 420

Table 1. Continued

formula	SG[a]	lattice parameters	template	type	ref
$[C_3H_{12}N_2]_{0.5}[Al(OH)(PO_4)(H_2O)]\cdot H_2O$	*Pnma*	$a = 6.919$ Å, $b = 22.298$ Å, $c = 9.607$ Å; $\alpha = \beta = \gamma = 90°$	$1,3\text{-DAPH}_2$	2D	421
$[C_9H_{24}N_2]_7[Al_{13}(HPO_4)(PO_4)_{17}]\cdot 8H_2O$	$R\bar{3}$	$a = b = 16.593$ Å, $c = 51.617$ Å; $\alpha = \beta = 90°$, $\gamma = 120°$	$1,9\text{-DANH}_2$	2D	423
$[C_{10}H_{26}N_2]_7[Al_{13}(HPO_4)(PO_4)_{17}]\cdot 8H_2O$	$R\bar{3}$	$a = b = 16.538$ Å, $c = 55.622$ Å; $\alpha = \beta = 90°$, $\gamma = 120°$	$1,10\text{-DADH}_2$	2D	423
$[C_{11}H_{28}N_2]_7[Al_{13}(HPO_4)(PO_4)_{17}]\cdot 8H_2O$	$R\bar{3}$	$a = b = 16.574$ Å, $c = 58.493$ Å; $\alpha = \beta = 90°$, $\gamma = 120°$	$1,11\text{-DAUH}_2$	2D	423
$[C_{12}H_{30}N_2]_7[Al_{13}(HPO_4)(PO_4)_{17}]\cdot 8H_2O$	$R\bar{3}$	$a = b = 16.536$ Å, $c = 62.220$ Å; $\alpha = \beta = 90°$, $\gamma = 120°$	$1,12\text{-DADOH}_2$	2D	423
$[C_4H_{12}N_2]_{4.5}[Al_3(PO_4)_4]_3\cdot 5H_2O$	$P2_1/c$	$a = 22.039$ Å, $b = 19.113$ Å, $c = 16.479$ Å; $\alpha = \gamma = 90°$, $\beta = 99.91°$	$PIPH_2$	2D	430
$[C_8H_{22}N_2]_8[Al_{13}(PO_4)_{18}]\cdot 6H_2O$	$R\bar{3}$	$a = b = 16.508$ Å, $c = 48.715$ Å; $\alpha = \beta = 90°$, $\gamma = 120°$	$1,8\text{-DAOH}_2$	2D	431
$[C_4H_{12}N_2][Al_2(OH)_2(PO_4)_2]$ (AlPO-CJ9)	$P2_1/c$	$a = 8.883$ Å, $b = 6.874$ Å, $c = 9.553$ Å; $\alpha = \gamma = 90°$, $\beta = 93.82°$	$PIPH_2$	2D	433
$[C_{16}H_{38}N_4][Al_{10}F_2(PO_4)_{10}]$	$Pca2_1$	$a = 16.835$ Å, $b = 9.677$ Å, $c = 32.769$ Å; $\alpha = \beta = \gamma = 90°$	$HMTACTDH_2$	2D	435
$[C_5H_{14}N_2]_3[Al_6(H_2O)_2(PO_4)_8]$	$P\bar{3}$	$a = b = 13.240$ Å, $c = 9.672=$ Å; $\alpha = \beta = 90°$, $\gamma = 120°$	$MPIPH_2$	2D	436
$[C_5H_{14}N_2]_3][Al_6(PO_4)_8]$	$P\bar{3}$	$a = b = 13.220$ Å, $c = 9.533$ Å; $\alpha = \beta = \gamma = 90°$	$MPIPH_2$	2D	436
$[C_5H_{14}N_2]_{4.5}][Al_9(PO_4)_{12}]\cdot 2.5H_2O$	$P2_1/c$	$a = 22.125$ Å, $b = 19.087$ Å, $c = 16.541$ Å; $\alpha = \gamma = 90°$, $\beta = 99.96°$	$MPIPH_2$	2D	436
$[NH_4]_3[Al(PO_4)_2]$	$P2_1/n$	$a = 8.999$ Å, $b = 9.979$ Å, $c = 11.109$ Å; $\alpha = \gamma = 90°$, $\beta = 90.645°$	NH_4^+	2D	439
$[NH_4][Al_2(OH)(PO_4)_2(H_2O)]\cdot H_2O$ (AlPO-15)	$P2_1/n$	$a = 9.553$ Å, $b = 9.577$ Å, $c = 9.614$ Å; $\alpha = \gamma = 90°$, $\beta = 103.56°$	NH_4^+	3D	326, 328
$Al_3P_3O_{11}(OH)_2\cdot C_2H_8N_2$ (AlPO-12)	$P2_1/c$	$a = 14.542$ Å, $b = 9.430$ Å, $c = 9.630$ Å; $\alpha = \gamma = 90°$, $\beta = 98.21°$	en	3D	327
$Al_3P_3O_{12}(OH)\cdot 1.33C_7H_{21}N_2$ (AlPO-21)	$P2_1/a$	$a = 10.331$ Å, $b = 17.524$ Å, $c = 8.676$ Å; $\alpha = \gamma = 90°$, $\beta = 123.369$	TMPD	3D, 8MR	329
$Al_3(PO_4)_3\cdot C_2H_8N_2\cdot H_2O$ (AlPO-21-en)	$P2_1/n$	$a = 8.472$ Å, $b = 17.751$ Å, $c = 9.062$ Å; $\alpha = \gamma = 90°$, $\beta = 106.73°$	en	3D, 8MR	330
$Al_3(PO_4)_3\cdot C_4H_9N\cdot H_2O$ (AlPO-21-py)	$P2_1/n$	$a = 8.668$ Å, $b = 17.558$ Å, $c = 9.186$ Å; $\alpha = \gamma = 90°$, $\beta = 107.75°$	Py	3D, 8MR	330
$Al_3(PO_4)_3\cdot H_2O\cdot C_2H_8N_2$ [AlPO-12-(en)]	$P2_1/c$	$a = 14.542$ Å, $b = 9.430$ Å, $c = 9.630$ Å; $\alpha = \gamma = 90°$, $\beta = 98.21°$	en	3D	331
$Al_{18}P_{18}O_{72}\cdot 4(C_5H_{12}N\cdot OH)$ (AlPO-17)	$P6_3/m$	$a = b = 13.237$ Å, $c = 14.771$ Å; $\alpha = \beta = 90°$, $\gamma = 120°$	PIPDH	3D, ERI	332
$[C_3H_{10}N]_2^+[AlPO_4)_7(OH)_2]$ AlPO-14A	$C2/c$	$a = 24.085$ Å, $b = 14.393$ Å, $c = 8.712$ Å; $\alpha = \gamma = 90°$, $\beta = 94.26°$	$^iPrAH^+$	3D	334
$[Al_{18}(PO_4)_{18}]\cdot 42H_2O$ (VPI-5)	$P6_3$	$a = b = 18.975$ Å, $c = 8.104$ Å; $\alpha = \beta = \gamma = 90°$	nil	3D, 18MR	324
($AlPO_4$-CJ2)	$P2_12_12_1$	$a = 9.456$ Å, $b = 9.621$ Å, $c = 9.965$ Å; $\alpha = \beta = \gamma = 90°$	nil	3D	336
$[NH_4]_{0.88}(H_3O)_{0.12}AlPO_4(OH)_{0.33}F_{0.67}$	$P2_12_12_1$	$a = 9.416$ Å, $b = 9.563$ Å, $c = 9.933$ Å; $\alpha = \beta = \gamma = 90°$	NH_4, H_3O^+	3D, 8MR	346
$[C_6H_{16}N]_2[Al_5(HPO_4)(PO_4)_5]\cdot 2H_2O$	$C2/c$	$a = 32.035$ Å, $b = 14.308$ Å, $c = 8.852$ Å; $\alpha = \gamma = 90°$, $\beta = 104.65°$	TriEAH	3D, 20MR	283
$[C_4H_{10}NO]^+[Al_3(PO_4)_3F^-]$ ($AlPO_4$-CHA)	$P\bar{1}$	$a = 9.333$ Å, $b = 9.183$ Å, $c = 9.162$ Å; $\alpha = 88.45°$, $\beta = 102.57°$, $\gamma = 93.76°$	MORPH	3D, CHA	350
$[CH_6N]^+[Al_3(OH)(PO_4)_3]$ (JDF-2)	*Pcab*	$a = 10.281$ Å, $b = 13.844$ Å, $c = 17.064$ Å; $\alpha = \beta = \gamma = 90°$	MAH	3D, 8MR	351, 418, 417
$[C_2H_8N][Al_2(PO_4)_2F]$	$P2_1/c$	$a = 9.412$ Å, $b = 12.770$ Å, $c = 8.594$ Å; $\alpha = \gamma = 90°$, $\beta = 112.84°$	DMAH	3D, GIS-type	285
$[C_4H_{14}N_2]_2[Al_6F_6(PO_4)_6]$	$Pbc2_1$	$a = 10.023$ Å, $b = 18.180$ Å, $c = 15.841$ Å; $\alpha = \beta = \gamma = 90°$	$1,4\text{-DABH}_2$	3D, 10MR	362
$[C_3H_{11}N_2][Al_3(OH)O(PO_4)_3]\cdot H_2O$	*Pbca*	$a = 10.058$ Å, $b = 18.085$ Å, $c = 15.619$ Å; $\alpha = \beta = \gamma = 90°$	1,3-DAP	3D	364
$[C_5H_6N][Al_3F(PO_4)_3]$ ($AlPO_4$-CHA)	$P\bar{1}$	$a = 9.118$ Å, $b = 9.161$ Å, $c = 9.335$ Å; $\alpha = 85.98°$, $\beta = 77.45°$, $\gamma = 89.01°$	PyH	3D, CHA	371
$[K222^{2+}]_6[N(CH_3)_4^+]_6[Al_{72}P_{72}O_{288}][F^-]_{18}\cdot 12H_2O$	$R3c$	$a = b = 16.596$ Å, $c = 42.576$ Å; $\alpha = \beta = 90°$, $\gamma = 120°$	K222, TMA^+	3D, LTA-type	380
$Al_{32}P_{32}O_{128}(TMAF)_8$	*Pbca*	$a = 14.533$ Å, $b = 15.334$ Å, $c = 16.601$ Å; $\alpha = \beta = \gamma = 90°$	TMA^+	3D	360
$[C_3H_7NO][H_2O]_{1.25}[Al_3P_3O_{12}]$	*Cc*	$a = 12.948$ Å, $b = 12.482$ Å, $c = 8.638$ Å; $\alpha = \gamma = 90°$, $\beta = 95.757°$	DMAH	3D, SOD-type	381
$[C_6H_{18}N_2][Al_4(HPO_4)(PO_4)_4]$	*Cc*	$a = 17.682$ Å, $b = 5.108$ Å, $c = 25.488$ Å; $\alpha = \gamma = 90°$, $\beta = 103.07°$	$1,6\text{-DAHH}_2$	3D, 12,8MR	382
$[C_2H_8N][Al_3P_3O_{12}OH]$ (MU-10)	*Pbca*	$a = 13.678$ Å, $b = 10.318$ Å, $c = 17.357$ Å; $\alpha = \beta = \gamma = 90°$	DMAH	3D, 8MR	389

Table 1. Continued

formula	SG[a]	lattice parameters	template	type	ref
$[C_6H_{21}N_4]_4[Al_9(PO_4)_{12}]\cdot 17H_2O$	$I\bar{4}3m$	$a = b = c = 16.796$ Å; $\alpha = \beta = \gamma = 90°$	$TRENH_3$	3D, super Sodalite	390
$[C_4H_{16}N_3][Al_2(PO_4)_3]$ (AlPO-DETA)	$C2/c$	$a = 17.669$ Å, $b = 8.537$ Å, $c = 10.252$ Å; $\alpha = \gamma = 90°$, $\beta = 103.42°$	$DETAH_3$	3D, 12, 8MR	398
$[C_6H_{21}N_4][Al_6(PO_4)_6F_3]\cdot 2H_2O$	$C2/c$	$a = 14.260$ Å, $b = 11.599$ Å, $c = 18.325$ Å; $\alpha = \gamma = 90°$, $\beta = 90.324°$	$TRENH_3$	3D, 8MR	399
$[C_3H_{12}N_2][Al_4(H_2O)F_2(PO_4)_4]$	$P\bar{1}$	$a = 9.558$ Å, $b = 9.766$ Å, $c = 10.472$ Å; $\alpha = 68.370°$, $\beta = 80.509°$, $\gamma = 89.506°$	$1,3\text{-}DAPH_2$	3D, 8MR	405
$[Al_2(PO_4)_2](OCH_2CH_2NH_3)$ (AlPO-CJ3)	$Pbca$	$a = 9.993$ Å, $b = 8.583$ Å, $c = 19.705$ Å; $\alpha = \beta = \gamma = 90°$	bound ethanolamine	3D, 8MR	407
$[C_4H_{14}N_2][Al_4P_4O_{17}]$	$P2_1/c$	$a = 19.672$ Å, $b = 9.220$ Å, $c = 9.747$ Å; $\alpha = \gamma = 90°$, $\beta = 95.60°$	$1,4\text{-}DABH_2$	3D, 8MR	408
$[C_6H_{15}N_4][Al_{12}(PO_4)_{13}]$ (AlPO-CJB1)	$P42_1/c$	$a = b = 13.61$ Å, $c = 15.547$ Å; $\alpha = \beta = \gamma = 90°$	$HMTH_3$	3D, 8MR	409
$[H_3O][AlP_2O_6(OH)_2]$ (AlPO-CJ4)	$P\bar{1}$	$a = 7.118$ Å, $b = 8.673$ Å, $c = 9.220$ Å; $\alpha = 65.108°$, $\beta = 70.521°$, $\gamma = 68.504°$	H_3O^+	3D, 8MR	411
$[C_3H_{12}N_2][Al_4O(PO_4)_4(H_2O)]$ (UiO-26-as)	$P2_1/c$	$a = 19.191$ Å, $b = 9.347$ Å, $c = 9.638$ Å; $\alpha = \gamma = 90°$, $\beta = 92.71°$	$1,3\text{-}DAPH_2$	3D, 10MR	412
$[C_3H_{12}N_2][Al_4O(PO_4)_4]$ (UiO-26-250)	$P2_1/c$	$a = 19.249$ Å, $b = 9.275$ Å, $c = 9.702$ Å; $\alpha = \gamma = 90°$, $\beta = 93.79°$	$1,3\text{-}DAPH_2$	3D, 10MR	412
$[C_5H_{16}N_2][Al_4(HPO_4)(PO_4)_4]$	$P\bar{1}$	$a = 9.245$ Å, $b = 12.688$ Å, $c = 5.066$ Å; $\alpha = 96.02°$, $\beta = 105.89°$, $\gamma = 102.88°$	$1,5\text{-}DAPH_2$	3D, 12, 8MR	413
$Al_{24}P_{24}O_{96}$ (AlPO-53B, UiO-12-500)	$Pbca$	$a = 18.024$ Å, $b = 13.917$ Å, $c = 9.655$ Å; $\alpha = \beta = \gamma = 90°$	nil	3D	417, 418
$[C_2H_8N][Al_3(OH)(PO_4)_3]$ (AlPO-21)	$P2_1/n$	$a = 8.687$ Å, $b = 17.428$ Å, $c = 9.159$ Å; $\alpha = \gamma = 90°$, $\beta = 109.60°$	DMAH	3D	426
$6K22^{2+}[Al_{90}(PO_4)_{90}](OH)_{12}\cdot 11H_2O$ (MU-13)	$R\bar{3}c$	$a = b = 17.283$ Å, $c = 38.914$ Å; $\alpha = \beta = 90°$, $\gamma = 120°$	K22	3D	428
$[C_6H_{15}N_4][Al_{11}(PO_4)_{12}]\cdot H_2O$ (AlPO-CJB2)	$R\bar{3}c$	$a = b = 14.088$ Å, $c = 42.199$ Å; $\alpha = \beta = 90°$, $\gamma = 120°$	$HMTH_3$	3D	429
$[C_4H_{12}N_2][C_4H_{11}N_2][Al_{11}(PO_4)_{12}]$ (AlPO-CJ1 1)	$R3c$	$a = b = 14.045$ Å, $c = 42.091$ Å; $\alpha = \beta = 90°$, $\gamma = 120°$	$PIPH_2$, PIPH	3D	432
$[C_4H_{10}N][Al_4(OH)(PO_4)_4]$ (MIL-34)	$P\bar{1}$	$a = 8.701$ Å, $b = 9.210$ Å, $c = 12.385$ Å; $\alpha = 111.11°$, $\beta = 101.42°$, $\gamma = 102.08°$	CyBAH	3D	434
$(CH_3NH_2)_4(Ch_3NH_3^+)_4(OH^-)_4[Al_{12}P_{12}O_{48}]$ (IST-1)	$Pca2_1$	$a = 9.615$ Å, $b = 8.670$ Å, $c = 16.219$ Å; $\alpha = \beta = \gamma = 90°$	MAH	3D	438
$[NH_4]_{2\text{-}x}[H_3O]_x[Al_2(OH)_2(PO_4)_2]$	$P2_12_12_1$	$a = 9.422$ Å, $b = 9.570$ Å, $c = 9.931$ Å; $\alpha = \beta = \gamma = 90°$	NH_4, H_3O^+	3D	439
$[NH_4]_3[Al_2(PO_4)_3]$	$C2/c$	$a = 13.261$ Å, $b = 10.255$ Å, $c = 8.863$ Å; $\alpha = \gamma = 90°$, $\beta = 111.407°$	NH_4	3D	439

[a] SG = space group. [b] chxn = *trans*-1,2-diaminocyclohexane. [c] DHYDZ = dihydroxyhydrazine. [d] EG = ethylene glycol.

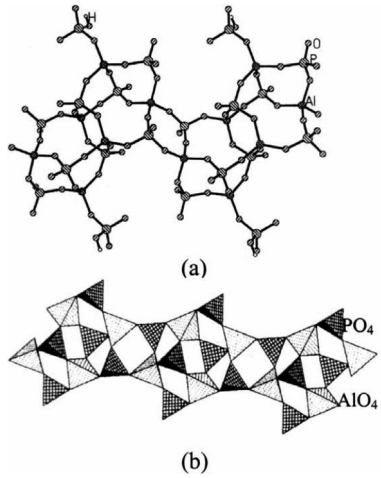

Figure 50. Two relatively complex and uncommon 1D structures found in the aluminium phosphate family.[363,402] Panel a adapted from refs 363 and 402. Copyright 1996 and 1999 American Chemical Society.

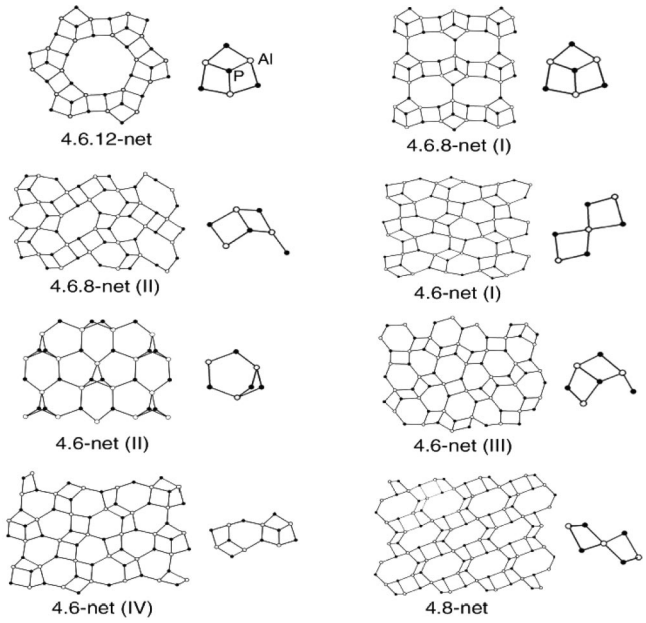

Figure 51. Two-dimensional sheet structures and their SBUs. Reprinted with permission from ref 441. Copyright 2003 American Chemical Society.

forms a double sheet built from D6R SBUs. Apart from the above examples,[299,342,379,384,387] all layered AlPO's (Al in more than four coordination) have Al−(OH)−Al linkages in some form.

A large number of layered AlPO's with an Al/P ratio of 1:1 with the general stoichiometry $Al_2X_2(PO_4)_2Y_2$ (X = OH, F, O and Y = H_2O, NH_2) where the Al coordination is more than four, have structures similar to $AlF(HPO_4)(C_2H_8N_2)$[344] closely related to the α-$VO(HPO_4)\cdot 2H_2O$ structure[442] (Figure 47c). In this structure, the corner-shared infinite metal polyhedra are cross-linked by PO_4 tetrahedra. The Al−(OH)−Al linkage can be generated by AlO_6 octahedra,[344,406,421] by alternate AlO_5 and AlO_6 polyhedra[397,415] or by AlO_5 distorted trigonal bipyramids.[419,420,430] The fifth and sixth coordination of Al polyhedra are satisfied by the N of the amine[344] or by the oxygen of water.[397,406,415,420,421,433] The bound water and bridging −OH groups can be removed by heating, thereby reducing the Al coordination. One can end up with a tetrahedral Al−O−Al linkage, breaking the so-called Lowenstein's rule. One such example is $[C_2H_{10}N_2][Al_2O(PO_4)]$[397] obtained by heating $[C_2H_{10}N_2][Al_2(OH)_2(PO_4)_2(H_2O)]\cdot H_2O$ at 225 °C. To our knowledge, the only other example where Lowenstein's rule is broken is $Cs_2[Al_2O(PO_4)_2]$.[392] There are structures with infinite Al−(OH)−Al linkages built from some common SBUs (SBU-4,[396] SBU-8[391]), from complex units,[357] or by joining tancoite-type chains (with infinite Al−X−Al linkages).[403]

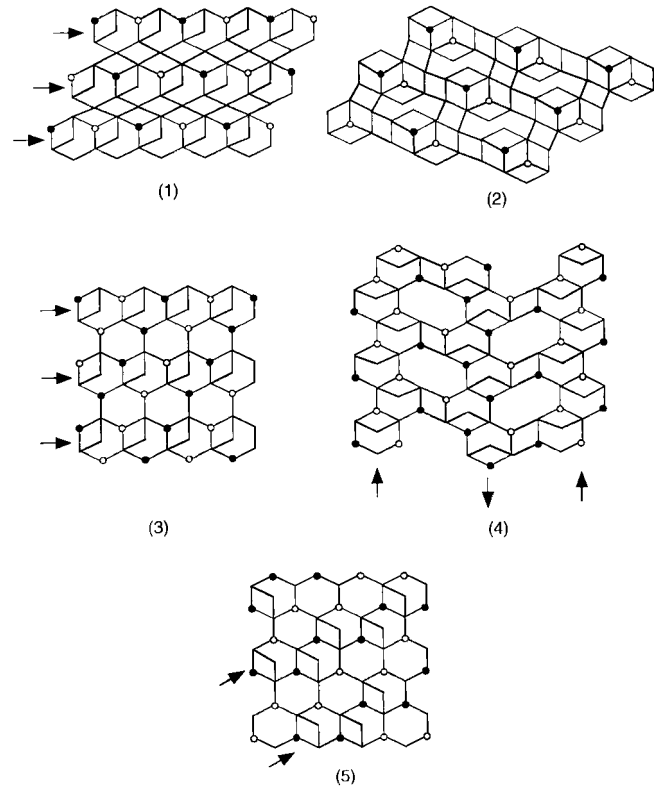

Figure 52. Schematic depiction of five different types of layer topologies found in $Al_2P_3O_{12}$ stoichiometry. Reprinted with permission from ref 384. Copyright 1998 American Chemical Society. The black and white circles indicate the up and down features of triply bridging phosphate groups. The arrows show the edge-sharing bridged-6MR.

Three-Dimensional Structures. The majority of AlPO-*n* possess a (4;2)-connected framework, which means that the Al and P atoms occupy four-connected vertices of a 3D net and O atoms occupy two-connected positions between the four-connected vertices. This immediately reveals the Al/P ratio to be unity, the framework to be neutral, and AlO_4 and PO_4 tetrahedra to be alternating. This rule also precludes the presence of rings formed by odd numbers of T atoms (P and Al) in the framework, and therefore MFI-type structures containing five-ring units are not found in the AlPO family. The most important feature of (4;2)-connected AlPO-*n* is that they are truly microporous because of their high stability (up to even 1000 °C) even after removal of the contents of the channel.[261] However, there are AlPO-*n* members that do not obey the (4;2) connection where the Al coordination is five or six with terminal −OH or H_2O groups, still maintaining the Al/P ratio of unity. In this class of materials, it is possible to remove the −OH bridges or the terminal waters by heating and making Al fully tetrahedral.

More than 25 AlPO framework types have been listed in the *Atlas of Zeolite Framework Types*.[270] Among them, some are analogues of aluminosilicate zeolites [e.g., AlPO-5 (AFI), AlPO-8 (AET), AlPO-16 (AST), AlPO-17 (ERI), AlPO-20

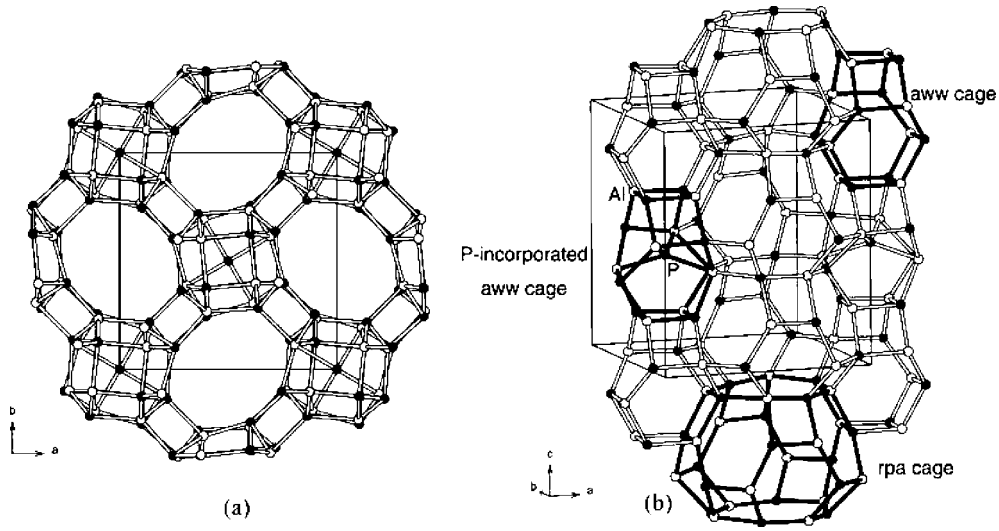

Figure 53. Framework of AlPO-CJB1 (a) viewed along *c* axis and (b) side view showing the connection of three types of cages. Reprinted with permission from ref.[441] Copyright 2003 American Chemical Society.

(SOD), AlPO-24 (ANA), AlPO-34 (CHA), AlPO-35 (LEV)], and the rest of them are novel [e.g., AlPO-11 (AEL), AlPO-12 (TAMU)/AlPO-33 (AIT), AlPO-14 (AFN), AlPO-18 (AEI), AlPO-21 (AWO), AlPO-22 (AWW), AlPO-25 (ATU), AlPO-31 (ATO), AlPO-40 (ARR), AlPO-41 (AFO), AlPO-52 (AFT), AlPO-53A/-53B/-EN_3/JDF-2, UiO-12-as, UiO-12.500 (AEN), AlPO-J4/VPI-5 (VFI), AlPO-H_2 (AHT), AlPO-H_3/AlPO-c (APC), AlPO-D (APD), UiO-6 (OSI), UiO-7 (ZON)].[270] Apart from these, 3D AlPO's related to some of the zeolite structures are the GIS-,[285] LTA-,[380] and SOD-types.[381] Synthesis of many of these AlPO's can be found in ref 272, and the structural details can be found in the Atlas.[270] We shall briefly touch upon a few important structural aspects.

Structures with strictly alternating AlO_4 and PO_4 tetrahedra as in zeolites are found in AlPO-5, AlPO-11, AlPO-12-TAMU, AlPO-16, AlPO-31, and AlPO-52. Structures with one or two −OH bridges leading to five coordination of Al on heating become fully tetrahedral as in AlPO-17,[332] AlPO-18, AlPO-21,[329,336,426] AlPO-40, AlPO-41, AlPO-EN_3, and MIL-34.[434] There are a few new members of this group, but detailed thermal studies leading to full tetrahedral frameworks are yet to be established (e.g., MU-10,[389] MU-13,[428] IST-1[438]). In some instances, the 3D structure is hydrated where the fifth and sixth coordinations of Al are satisfied by H_2O and the remaining four provided by phosphate oxygens (e.g., AlPO-H_2, AlPO-H_3, VPI-5).[324]

VPI-5 with 18-membered pore openings is the first extra-large pore molecular sieve. The structure of VPI-5 transforms to AlPO-8 with a 14-ring pore opening upon heating by changing the six coordination of Al. The structural transformation can be topotactic in the calcination process to remove the occluded template or bridging −OH groups (e.g., AlPO-21 to AlPO-25).[426] Complex Al−O(H)−Al linkages leading to edge-sharing between Al polyhedra are also common and many times form well-defined SBUs (e.g., AlPO-12,[327,331] AlPO-15,[326,328] AlPO-14, APDAB200,[408] UiO-26,[412] and others[364]). A large number of 3D AlPO's have been prepared in the presence of the F^- ion, which most of the time bridges the Al atoms through corner- or edge-sharing and increases the Al coordination to five or six forming various SBUs. In AlPO-CJ2[336,346] and ULM-3, an analogue of GaPO,[362] Al polyhedra are corner-shared to form SBU-4 and SBU-6 units, as well as in UiO-6 and -7,[359,360] with the Al polyhedra sharing corners through the F atoms. In MIL-27[399] and ULM-6,[405] complex structures containing F−F edge-shared Al polyhedra are seen.

There are a large number of AlPO's in which the Al/P ratio is less than unity and the framework is negative (see Table 1). JDF-20 (Al/P = 5/6)[283] with a 20-membered extra-large pore channel presents the first such example with an interrupted framework having a terminal P−O bond. A number of AlPO's with the Al/P ratio less than unity have since been prepared, and they include AlPO-HAD (Al/P = 4/5),[282] $[C_6H_{21}N_4]_4[Al_9(PO_4)_{12}]\cdot 17H_2O$ (Al/P = 3/4),[390] AlPO-DETA (Al/P = 2/3),[398] AlPO-CJB1 (Al/P = 12/13),[409] AlPO-CJ4 (Al/P = 1/2),[411] $[C_6H_{16}N_2][Al_4(HPO_4)(PO_4)]$,[413] AlPO-CJB2 (Al/P = 11/12),[429] AlPO-CJ11 (Al/P = 11/12),[433] and $(NH_4)_3[Al_2(PO_4)_3]$.[439] A good account of these structures has been given by Yu and Xu.[441] All these structures contain alternating PO_4 tetrahedra and Al-centered polyhedra where the Al coordination is sometimes five[382,409] or six.[411,429] The most important feature of these materials is that they are anionic, just as the aluminosilicate zeolites. So there is a possibility for these materials to show Bronsted acidity and ion-exchange capacity, if the occluded species is removed by calcination, with the protons remaining to balance the negative charge. Unfortunately, most anionic AlPO structures collapse during calcination. However, Ruren Xu and co-workers were able to show Bronsted acidity in AlPO-CJB1, $[(CH_2)_6N_4H_3][Al_{12}P_{13}O_{52}]$, which is stable upon removal of the template (Figure 53a). The structure of AlPO-CJB1 is also interesting with an 8MR channel and three different kinds of cages (Figure 53b).

3.5.2. Gallium Phosphates

After the tremendous success of AlPO molecular sieves, the next natural choice of the element to extend the idea was gallium. Parise[331] first described several GaPO frameworks related to the AlPO-*n* family. Several other groups have investigated the synthesis of GaPO frameworks in order to form large pore molecular sieves. The major breakthrough was the discovery of cloverite, a gallium phosphate framework with a 20-membered channel achieved by Kessler and co-workers[288] by employing the fluoride route. Ferey and co-workers[290] have contributed significantly to this family

through their systematic studies employing the fluoride route to produce a series of gallium fluorophosphates (ULM-*n* series). The ubiquitous presence of various SBUs in the fluoride-containing solids led them to propose a mechanism for their formation. Today, gallium phosphates constitute a large family of templated networks with a range of zero-, one-, two- and three-dimensional structures.[288,293,294,299,320,331,346,377,405,443–516] The formulae and unit cell parameters of the members of these families are listed in Table 2. Like in the AlPO family, the ratio of Ga and P varies from unity, but unlike AlPO, the Ga/P ratio is sometimes greater than unity. Like AlPO, GaPO also exhibits five and six coordination besides four, with a higher propensity for higher coordination.

Zero-Dimensional Structures. Two important types of 0D structures, namely, S4R and D4R, are found in the GaPO family. The molecular structure of the S4R $[C_6H_{21}N_4]$-$[Ga(HPO_4)(PO_4)(OH)]\cdot H_2O$[470] is similar to the ZnPO-S4R (Figure 45), the only difference being that the GaPO-S4R has one pendant HPO_4/H_2PO_4 group from a Ga site while the fourth coordination is satisfied by an −OH group. In ZnPO-S4R, there are two pendant HPO_4/H_2PO_4 groups. The other 0D structure is a D4R, which is obtained quite frequently.[465,496,502,506] The isolated D4R structures have occluded fluoride,[465] while others have occluded oxygen[496,506] (Figure 54). Considering the fact that the D4R units are present in several GaPO materials (cloverite,[288] ULM-5,[455] ULM-18,[480] etc.) and in many zeolites (LTA) and metal phosphate structures (Figure 49a), it is possible that this monomeric structures can be transformed to higher dimensional structures, similar to S4R-$ZnPO_4$.[305] This aspect will be discussed in a later section.

One-Dimensional Structures. Since the six coordination of Ga is more pronounced, the tancoite-type chain is commonly found in the GaPO system.[476,477,488,495,509] The corner-shared chains of four-membered rings[472,481] and ladders[512] also occur. Other than the three common 1D structures, two new types have been observed[477,492] (Figure 55). In one of them, the D4R units join by corner-sharing to give a chain structure (Figure 55a). The other (Figure 55b)[492] is also closely related to the corner-shared chain of four-membered rings (compare Figure 46a).

Two-Dimensional Structures. It is surprising that the number of 2D structures in the GaPO family is small compared with the 3D structures (see Table 2). Various types of sheet structures of GaPO are known with features such as alternating Ga and P polyhedra,[299,513,500] edge-shared Ga polyhedra cross-linked by phosphate,[449,499] linking of SBUs (SBU-6,[459,489] D4R,[480] side-opened D4R[498] or heptamer[503]), and zigzag ladders (Mu-23).[510] The last one is an example where the Ga/P ratio (5/4) is greater than unity.

Three-Dimensional Structures. Unlike the AlPO family, the number of zeotype frameworks in the GaPO system is less. However, few structures isotypic with the AlPO-*n* family (e.g., GaPO-14 (AFN), GaPO-34 (CHA), and GaPO-AEN, -ATU, -AWO, -LTA, and -ZON) have been observed. The 20-membered channel structure in cloverite (-CLO)[288] does not have an AlPO counterpart.[270] The smaller abundance of zeotype structures in GaPO is due to absence of the (4;2) connection. Instead, they show infinite Ga−X−Ga linkages in various SBUs and thereby new topologies[262,263,290] (ULM-*n*, MIL-*n*, MU-*n*, and others; see Table 2). This family of solids displays a variety of pore systems including a large number of extra-large pore channels bound by 14 (BIPYR-GaPO),[473] 16 (ULM-5,[455] ULM-16,[466,511] and others[292]), 18 (MIL-31, -46, -50),[320,511,514] 20,[288,483,493] and 24 polyhedra (Ga8P, NTHU-1).[504] The largest crystalline pore GaPO with a 24-membered channel $[Ga_2(DETA)(PO_4)_2]\cdot 2H_2O$ (NTHU-1; Figure 56) has a neutral framework with DETA coordinated to one of the Ga atoms and has one of the lowest framework densities (10.9 T-atom, Ga or P).

The 3D framework structures involving fluorinated GaPO's have been discussed by Ferey[290] with reference to their SBUs. We will discuss only the newer ones and their salient features. Two recently discovered GaPO structures, MIL-46[511] and MIL-50,[514] with 18-membered ring channels demonstrate the power of the SBU concept. The presence of the hexameric building unit Ga_3P_3 (SBU-6) is common in both the structures. This unit is also encountered in many layered (ULM-8,[459] MIL-30[489]) and 3D structures (ULM-3,[456,461,464,487] ULM-4,[458] ULM-5,[455] ULM-16,[466] TREN-GaPO,[471] and MIL-31[320]). The topological analysis of these 3D structures reveals the presence of a common layer formed by hexameric blocks of $Ga_3(PO_4)_3F_2$ connected by an additional building unit. Ferey and co-workers[511] have shown (Figure 57) that the size of the latter determines the space (and therefore the channel size) between the hexamer layers. For example, the direct condensation of such hexamer sheets leads to TREN-GaPO[471] with a 12MR channel. Connection by a four-ring unit (part of an infinite double crank-shaft chain) or by a cubane-shaped D4R unit creates a 16-ring channel as in ULM-16[466] and ULM-5,[455] respectively. Connecting the hexamer sheets by pentamer Ga_3P_2 induces an 18-ring channel as in MIL-46[511] (or similarly MIL-31 can also be explained). The important outcome of such a description is that one is able to employ the notion of scale chemistry[316] and predict a new structure. For example, if the hexamer sheets are connected by another hexameric SBU (SBU-6) $Ga_3(PO_4)_3F_2$, one should get a hexagonal bronze type structure as in tungstates.[517] Such a prediction has been realized in MIL-50.[514]

3.5.3. Indium Phosphates

The ability to form open-framework phosphates by Al and Ga with five and six coordination prompted researchers to explore indium phosphates, since In would be expected to adopt six coordination more readily. Dhingra and Haushalter[518] first reported organically templated open-framework InPO, $[C_2H_{10}N_2][In_2(HPO_4)_4]$, with an eight-membered channel where In had octahedral coordination. In Table 3, we list the layered and 3D InPO structures.[518–526] There are no reports of zero- and one-dimensional structures in this family.

Two-Dimensional Structures. The 2D sheet structure reported by Chippindale,[521] $[C_5H_5NH][In(HPO_4)(H_2PO_4)_2]$, is formed by the cross-linking of ladder-like ribbons by phosphate groups, while $InPO_4F(Hen)$[522] is similar to $AlF(HPO_4)en$[344] (Figure 47c). Alternate InO_6 and PO_4 groups form a 4−12 net,[525] isostructural with GaPO-CJ14.[513]

Three-Dimensional Structures. Among the 3D structures, a pillared-layered structure with a 16-membered channel[520] and others with 10MR,[522] 14MR,[523] 16MR,[524] and 8MR[526] channels made by the fluoride route with different amines are important (see Table 3). Most of these structures have been reviewed,[262] except two. $[C_4H_{16}N_3]_2[C_4H_{14}N_2]$-$[In_{6.8}F_8(H_2O)_2(PO_4)_4(HPO_4)]\cdot 2H_2O$[524] is formed in the presence of HF-pyridine and DETA. The 16-membered extra-large pore channel is formed when InO_4F_2 octahedra cross-link layers formed by the cross-linking of tancoite-type chains (Figure 58). $[C_6H_{14}N_2][In_4F_2(PO_4)_4]\cdot 4H_2O$,[526] on the other hand, has all the PO_4 groups connected by their

Table 2. Lattice Parameters, Templates. and Dimensionalities of the Various Templated Gallium Phosphates Reported in the Literature

formula	SG[a]	lattice parameters	template	type	ref
$[Cp_2Co]^+[Ga_4P_4O_{12}(OH)_8F]$ (Mu-1)	Tet[b]	$a = b = 13.220$ Å, $c = 7.448$ Å; $\alpha = \beta = \gamma = 90°$	Cp_2Co^+	0D, D4R	465
$[C_6H_{21}N_4][Ga(OH)(HPO_4)(PO_4)]\cdot H_2O$	$P2_1/c$	$a = 9.488$ Å, $b = 10.323$ Å, $c = 16.323$ Å; $\alpha = \gamma = 90°$, $\beta = 90.42°$	$TRENH_3$	0D, S4R	470
$[C_5H_7N_2]_2[Ga_4O(PO_4)_4(H_2O)_4]$	$Aba2$	$a = 18.879$ Å, $b = 18.481$ Å, $c = 7.469$ Å; $\alpha = \beta = \gamma = 90°$	$4AmPyH_2$	0D, D4R	506
$[C_5H_6N]_2[Ga_4(OH)_4(HPO_4)_2(PO_4)_2(H_2O)]$	$I42m$	$a = b = 13.016$ Å, $c = 17.356$ Å; $\alpha = \beta = \gamma = 90°$	PyH^+	0D	496, 502
$Na_3[Ga(OH)(HPO_4)(PO_4)]$	$C2/m$	$a = 15.432$ Å, $b = 7.164$ Å, $c = 7.056$ Å; $\alpha = \gamma = 90°$, $\beta = 96.637°$	Na^+	1D tancoite	377
$[C_3H_{12}N_2][Ga(HPO_4)(PO_4)]$	$P\bar{1}$	$a = 8.325$ Å, $b = 8.633$ Å, $c = 8.903$ Å; $\alpha = 111.73°$, $\beta = 107.56°$, $\gamma = 98.39°$	$1,3\text{-}DAPH_2$	1D c.s. chain	472
$[C_6H_{16}N_2][Ga(OH)(HPO_4)_2]\cdot H_2O$	$P2_1$	$a = 8.721$ Å, $b = 7.128$ Å, $c = 11.141$ Å; $\alpha = \gamma = 90°$, $\beta = 96.13°$	$(1R,2R)DACHH_2$	1D tancoite	476
$[C_6H_{16}N_2][Ga(OH)(HPO_4)_2]\cdot H_2O$	$Pbcm$	$a = 8.699$ Å, $b = 21.861$ Å, $c = 7.156$ Å; $\alpha = \beta = \gamma = 90°$	$(1,2)\text{-}DACHH_2$	1D tancoite	476
$[C_{11}H_{26}N_2]_2[Ga_4F_3(PO_4)_4][F^-]$ (Mu-3)	$P3$	$a = b = 20.075$ Å, $c = 8.584$ Å; $\alpha = \beta = 90°$, $\gamma = 120°$	$EATPIPDHH_2$	1D	477
$[C_4H_{14}N_2][Ga(HPO_4)(PO_4)]$	$Pnaa$	$a = 9.109$ Å, $b = 11.021$ Å, $c = 11.987$ Å; $\alpha = \beta = \gamma = 90°$	$1,4\text{-}DABH_2$	1D c.s. chain	481
$[C_3H_{12}N_2][Ga(HPO_4)_2F]\cdot 2H_2O$	$P\bar{1}$	$a = 7.703$ Å, $b = 8.506$ Å, $c = 11.620$ Å; $\alpha = 107.48°$, $\beta = 102.10°$, $\gamma = 90.28°$	$1,3\text{-}DAPH_2$	1D tancoite	488
$[Ga_4(C_{10}H_9N_2)_2(H_2PO_4)_2(HPO_4)_2(H_{0.5}PO_4)_2(PO_4)(H_2O)_2]\cdot H_2O$	$C2/c$	$a = 26.416$ Å, $b = 8.041$ Å, $c = 20.351$ Å; $\alpha = \gamma = 90°$, $\beta = 111.194°$	bound 4,4′-bPy	1D	492
$[C_3H_{12}N_2][GaF(HPO_4)_2]$	$Pbcm$	$a = 8.642$ Å, $b = 19.346$ Å, $c = 7.114$ Å; $\alpha = \beta = \gamma = 90°$	$1,3\text{-}DAPH_2$	1D tancoite	495
$[C_6H_{14}N_2][GaF(HPO_4)]$	$P2_12_12_1$	$a = 14.873$ Å, $b = 12.013$ Å, $c = 7.07$ Å; $\alpha = \beta = \gamma = 90°$	$DABCOH_2$	1D tancoite	509
$[C_4H_{14}N_2][Ga(HPO_4)(PO_4)]$	$P21/c$	$a = 4.892$ Å, $b = 18.364$ Å, $c = 13.746$ Å; $\alpha = \gamma = 90°$, $\beta = 94.581°$	$1,4\text{-}DABH_2$	1D ladder	512
$[C_5H_{16}N_2][Ga(HPO_4)(PO_4)]$	$P2_1/n$	$a = 4.924$ Å, $b = 13.284$ Å, $c = 19.534$ Å; $\alpha = \gamma = 90°$, $\beta = 96.858°$	$1,5\text{-}DAPH_2$	1D ladder	512
$[C_2H_{10}N_2]_{0.5}[Ga(OH)(PO_4)]$	$P2_1/c$	$a = 4.464$ Å, $b = 5.994$ Å, $c = 18.538$ Å; $\alpha = \gamma = 90°$, $\beta = 94.71°$	enH_2	2D	449
$[C_6H_{19}N_4][Ga_3F_2(HPO_4)\ (PO_4)_2(H_2O)]$ (ULM-8)	$Pbca$	$a = 10.163$ Å, $b = 21.989$ Å, $c = 17.279$ Å; $\alpha = \beta = \gamma = 90°$	TRENH	2D	459
$[C_4H_{12}N_2]_{0.5}[GaF(PO_4)]$ (ULM-9)	$P\bar{1}$	$a = 9.112$ Å, $b = 6.345$ Å, $c = 8.981$ Å; $\alpha = 77.04°$, $\beta = 79.62°$, $\gamma = 89.71°$	$PIPH_2$	2D	460
$[C_5H_6N][Ga(HPO_4)_2(H_2O)_2]$	$P\bar{1}$	$a = 7.056$ Å, $b = 7.315$ Å, $c = 12.165$ Å; $\alpha = 105.32°$, $\beta = 105.49°$, $\gamma = 90.25°$	PyH	2D	299
$[C_3H_5N_2][Ga(HPO_4)_2(H_2O)_2]$	$C2/c$	$a = 22.002$ Å, $b = 7.262$ Å, $c = 7.047$ Å; $\alpha = \gamma = 90°$, $\beta = 105.11°$	IMDH	2D	299
$[C_6H_{18}N_2]_{1.5}[Ga_4(PO_4)_5(HF)]\cdot H_2O$ (ULM-18)	$P\bar{1}$	$a = 8.528$ Å, $b = 9.251$ Å, $c = 17.870$ Å; $\alpha = 101.74°$, $\beta = 99.14°$, $\gamma = 87.02°$	$TMEDH_2$	2D	480
$[C_3H_{12}N_2][C_2H_8N][Ga_3F_3(PO_4)_3]$ (MIL-30)	$P2_12_12_1$	$a = 8.811$ Å, $b = 10.226$ Å, $c = 20.908$ Å; $\alpha = \beta = \gamma = 90°$	$1,3\text{-}DAPH_2$, DMAH	2D	489
$[C_7H_{11}N_2]_2[(GaPO_4)_4(OH)F]$	$P\bar{1}$	$a = 14.257$ Å, $b = 14.549$ Å, $c = 15.378$ Å; $\alpha = \beta = \gamma = 90°$	4-DMAPH	2D	498
$[C_{12}H_{30}N_2]_2[Ga_4F_4(PO_4)_4]$ (MIL-35)	$P\bar{1}$	$a = 5.393$ Å, $b = 9.813$ Å, $c = 19.285$ Å; $\alpha = 80.67°$, $\beta = 88.78°$, $\gamma = 89.86°$	$1,12\text{-}DADOH_2$	2D	499
$[C_6H_{16}N_2][Ga_2(1S,2S\text{-}DACH)(HPO_4)(PO_4)_2]$	$P2_1$	$a = 9.780$ Å, $b = 9.104$ Å, $c = 13.924$ Å; $\alpha = \gamma = 90°$, $\beta = 108.02°$	bound $1S,2S\text{-}DACHH_2$	2D, chiral	500
$[C_6H_{18}N_2]_2[Ga_3F_2(OH)_4(H_2PO_4)(HPO_4)_3]\cdot 3.5H_2O$	$P2_1/n$	$a = 10.201$ Å, $b = 14.417$ Å, $c = 23.195$ Å; $\alpha = \gamma = 90°$, $\beta = 95.91°$	$1,6\text{-}DAHH_2$	2D	503
$[C_6H_{15}N_2][C_6H_{16}N_2][Ga_5(H_2O)_2F_6(PO_4)_4]\cdot 4H_2O$ (MU-23)	$P\bar{1}$	$a = 8.735$ Å, $b = 8.864$ Å, $c = 12.636$ Å; $\alpha = 98.36°$, $\beta = 100.18°$, $\gamma = 115.84°$	$DPIPH/H_2$	2D	510
$[Co(en)_3][Ga_3(H_2PO_4)_6(HPO_4)_3]$ (GaPO-CJ-14)	$P2_1/m$	$a = 9.210$ Å, $b = 22.093$ Å, $c = 9.546$ Å; $\alpha = \gamma = 90°$, $\beta = 108.278°$	$Co(en)_3^{3+}$	2D	513
$[C_5H_{16}N_2][Ga_2F_2(2,2'\text{-bpy})(HPO_4)_2(H_2O)]$	$P\bar{1}$	$a = 7.582$ Å, $b = 9.994$ Å, $c = 11.174$ Å; $\alpha = 107.333°$, $\beta = 105.014°$, $\gamma = 99.261°$	bound 2,2′-bpy	2D	516
$[Co(en)_3][Ga_3(PO_4)_4]\cdot 5H_2O$	$Pnna$	$a = b = 8.662$ Å, $c = 63.278$ Å, $\alpha = \beta = 90°$, $\gamma = 120°$	$Co(en)_3^{3+}$	2D	[c]
$[Co(dien)_2][Ga_3(PO_4)_4]\cdot 3H_2O$	$P6522$	$a = 8.515$ Å, $b = 21.607$ Å, $c = 13.743$ Å; $\alpha = \beta = \gamma = 90°$	$Co(dien)_2^{3+}$	2D	[c]
$[C_3H_{10}N][Ga_4(OH)(PO_4)_4]\cdot H_2O$ (GaPO-14)	$P\bar{1}$	$a = 9.601$ Å, $b = 9.757$ Å, $c = 10.701$ Å; $\alpha = 74.20°$, $\beta = 75.01°$, $\gamma = 88.48°$	IPrAH	3D, 8MR	443, 445

Table 2. Continued

formula	SG[a]	lattice parameters	template	type	ref
$[Ga_3(PO_4)_3]\cdot H_2O\cdot$en (GaPO-12)	$P2_1/c$	$a = 14.656$ Å, $b = 9.625$ Å, $c = 9.672$ Å; $\alpha = \gamma = 90°$, $\beta = 97.9°$	en	3D, 8MR	331
$[C_3H_{10}N][Ga_3(OH)(PO_4)_3]$ (GaPO-21)	$P2_1/n$	$a = 8.70$ Å, $b = 18.146$ Å, $c = 9.087$ Å; $\alpha = \gamma = 90°$, $\beta = 107.28°$	IPrH	3D, 8MR	444
$[C_6H_{16}N][Ga_9(OH)(PO_4)_9]$	$P6_3$	$a = b = 12.266$ Å, $c = 16.746$ Å; $\alpha = \beta = 90°$, $\gamma = 120°$	TriEAH	3D, 10, 8MR	446
$[C_2H_7NO][Ga_3(H_2O)(PO_4)_3]$	$P2_1/n$	$a = 8.669$ Å, $b = 17.932$ Å, $c = 9.097$ Å; $\alpha = \gamma = 90°$, $\beta = 108.32°$	EtAH	3D, 8MR	447
$[NH_4][Ga_2(OH)(PO_4)_2(H_2O)]\cdot H_2O\cdot 0.16$PrOH ($GaPO_4$−C7)	$P2_1/n$	$a = 9.681$ Å, $b = 9.657$ Å, $c = 9.762$ Å; $\alpha = \gamma = 90°$, $\beta = 102.9°$	NH_4^+	3D, 8MR	448, 463
$[(C_7H_{14}N)_{24}]_8[Ga_{96}F_{24}(OH)_{12}(HPO_4)_{12}(PO_4)_{84}]_8$	$Fm3c$	$a = b = c = 51.712$ Å; $\alpha = \beta = \gamma = 90°$	QUINH	3D, 20MR	288
$[C_6H_{14}N_2][Ga_3(OH)F_3(HPO_4)_2(PO_4)]\cdot 0.5H_2O$	$C2_1/c$	$a = 17.983$ Å, $b = 9.859$ Å, $c = 19.840$ Å; $\alpha = \gamma = 90°$, $\beta = 106.24°$	$DABCOH_2$	3D, 8MR	450
$[C_6H_{14}N_2]_{0.5}[Ga_4(OH)_2(PO_4)_3(H_2O)_4]$	$I4_1/a$	$a = b = 13.455$ Å, $c = 18.902$ Å; $\alpha = \beta = \gamma = 90°$	$DABCOH_2$	3D	452
$[NH_4]_{0.93}[H_3O]_{0.07}[Ga(OH)_{0.5}F_{0.5}(PO_4)]$	$P2_12_12_1$	$a = 9.593$ Å, $b = 9.742$ Å, $c = 9.981$ Å; $\alpha = \beta = \gamma = 90°$	NH_4, H_3O^+	3D, 8MR	346
$[CH_6N][Ga_3(OH)(PO_4)_3]$ (GaPO-M2)	$Pbca$	$a = 10.257$ Å, $b = 16.941$ Å, $c = 14.130$ Å; $\alpha = \beta = \gamma = 90°$	MAH	3D	453, 293
$[C_2H_8N][Ga_3(OH)(PO_4)_3]$	$P2_1/n$	$a = 8.787$ Å, $b = 17.783$ Å, $c = 9.204$ Å; $\alpha = \gamma = 90°$, $\beta = 109.56°$	DMAH	3D, 8MR	454
$[C_6H_{18}N_2]_4[Ga_{16}(OH)_2F_7(HPO_4)_2(PO_4)_{14}]\cdot 6H_2O$ (ULM-5)	$P2_12_12_1$	$a = 10.252$ Å, $b = 18.409$ Å, $c = 24.639$ Å; $\alpha = \beta = \gamma = 90°$	1,6-$DAHH_2$	3D, 16MR	455
$[C_3H_{12}N_2][Ga_3F_2(PO_4)_3]\cdot H_2O$ (ULM-3)	$Pbca$	$a = 10.154$ Å, $b = 18.393$ Å, $c = 15.773$ Å; $\alpha = \beta = \gamma = 90°$	1,3-$DAPH_2$	3D, 10MR	456
$[NH_4][Ga_2(OH)(PO_4)_2(H_2O)]\cdot H_2O$	$P2_1/n$	$a = 9.689$ Å, $b = 9.703$ Å, $c = 9.788$ Å; $\alpha = \gamma = 90°$, $\beta = 102.78°$	NH_4	3D	457
$[CH_6N]_2[Ga_3F_2(PO_4)_3]\cdot H_2O$ (ULM-4)	$P2_1/n$	$a = 8.672$ Å, $b = 10.186$ Å, $c = 16.788$ Å; $\alpha = \gamma = 90°$, $\beta = 93.12°$	MAH	3D, 8, 10MR	458
$[C_4H_{14}N_2][Ga_3F_2(PO_4)_3]$	$Pbca$	$a = 16.023$ Å, $b = 10.062$ Å, $c = 18.486$ Å; $\alpha = \beta = \gamma = 90°$	1,4-$DABH_2$	3D, 10MR	461, 464
$Na_{1.5}[Ga_{2.5}O(OH)PO_4)_2]\cdot H_2O$	$P2_1/c$	$a = 9.716$ Å, $b = 13.485$ Å, $c = 6.391$ Å; $\alpha = \gamma = 90°$, $\beta = 99.82°$	Na^+	3D	462
$[C_6H_{18}N_2][Ga_4(HPO_4)(PO_4)_4]\cdot H_2O$	$P2_12_12_1$	$a = 9.574$ Å, $b = 14.00$ Å, $c = 17.435$ Å; $\alpha = \beta = \gamma = 90°$	$TMEDH_2$	3D, 16MR	294
$[C_5H_{16}N_2][Ga_4F_2(PO_4)_3]$	$Pbca$	$a = 10.156$ Å, $b = 18.672$ Å, $c = 16.367$ Å; $\alpha = \beta = \gamma = 90°$	1,5-$DAPH_2$	3D, 10MR	464
$[C_6H_{14}N]_{1.5}[H_3O]_6[Ga_4F_2(PO_4)_4]\cdot 0.5H_2O$ (ULM-16)	$Pbcn$	$a = 27.329$ Å, $b = 17.377$ Å, $c = 10.212$ Å; $\alpha = \beta = \gamma = 90°$	CHAH	3D, 16MR	466
$Rb_2[Ga_4(HPO_4)(PO_4)_4]\cdot 0.5H_2O$	$P2_1$	$a = 5.061$ Å, $b = 21.643$ Å, $c = 8.206$ Å; $\alpha = \gamma = 90°$, $\beta = 91.768°$	Rb	3D, 8MR	467
$[C_3H_{12}N_2]_{0.75}[H_3O]_{0.5}[Ga_3F_2(PO_4)_3]$ (ULM-4)	$P2_1/n$	$a = 8.674$ Å, $b = 10.190$ Å, $c = 16.826$ Å; $\alpha = \gamma = 90°$, $\beta = 94.21°$	1,3-$DAPH_2$	3D, 10MR	468
$[C_6H_{22}N_4][C_5H_5N][Ga_6F_4(PO_4)_6]$ (TREN-GaPO)	$Pnab$	$a = 10.406$ Å, $b = 17.023$ Å, $c = 17.992$ Å; $\alpha = \beta = \gamma = 90°$	$TRENH_4$, Py	3D, 12MR	471
$[C_{10}H_{10}N_2]_{0.87}[C_5H_6N]_{0.28}[Ga_7(OH)_2F_3(PO_4)_6]\cdot 2H_2O$ (DIPYR-GaPO)	$P\bar{1}$	$a = 12.00$ Å, $b = 13.895$ Å, $c = 10.280$ Å; =101.01°, $\beta = 100.91°$, $\gamma = 106.41°$	4,4′-$bpyH_2$, PyH	3D, 14MR	473
[d-Co(en)$_3$][$Ga_2(HPO_4)_3(PO_4)$]	I_2	$a = 9.580$ Å, $b = 12.679$ Å, $c = 9.963$ Å; $\alpha = \gamma = 90°$, $\beta = 97.85°$	d-$Co(en)_3^{3+}$	3D, chiral	474
$[C_{12}H_{27}N_6][Ga_5F_2(HPO_4)_2(PO_4)_4]$ (MIL-1)	C_2/n	$a = 8.655$ Å, $b = 16.452$ Å, $c = 11.939$ Å; $\alpha = \gamma = 90°$, $\beta = 102.993°$	$A_6$18crown-6	3D, 12MR	475
$[C_9H_{21}N_2]_6[Ga_{32}(OH)_{14}F_6(HPO_4)_2(PO_4)_{30}]\cdot 12H_2O$ (MU-2)	I	$a = b = c = 16.377$ Å; $\alpha = \beta = \gamma = 90°$	$ATPIPDH_2$	3D	478
$[C_{10}H_{24}N_4]_4[Ga_{20}P_{16}O_{64}F_8(OH)_4]$ (Mu-5)	$Pbcn$	$a = 13.373$ Å, $b = 10.447$ Å, $c = 18.538$ Å; $\alpha = \beta = \gamma = 90°$	CLM	3D, 10MR	479
$[C_4H_{14}N_2][Ga_4(HPO_4)(PO_4)_4]$	$P2_1$	$a = 5.040$ Å, $b = 22.738$ Å, $c = 9.297$ Å; $\alpha = \gamma = 90°$, $\beta = 103.80°$	1,4-$DABH_2$	3D, 8, 12MR	482
$[C_4H_{14}N_2]_2[Ga_4(OH)_3(HPO_4)_2(PO_4)_3]\cdot 5.4H_2O$	$I4_1/a$	$a = b = 15.261$ Å, $c = 28.894$ Å; $\alpha = \beta = \gamma = 90°$	1,4-$DABH_2$	3D, 20MR	483
$[C_3H_{12}N_2][Ga_4F_2(PO_4)_4(H_2O)]$ (ULM-6-Ga)	$P1$	$a = 9.683$ Å, $b = 9.868$ Å, $c = 10.622$ Å; $\alpha = 68.64°$, $\beta = 81.26°$, $\gamma = 89.82°$	1,3-$DAPH_2$	3D, 8MR	405
$[C_7H_{20}N_2][Ga_4F_3(HPO_4)(PO_4)_3]$	$P\bar{1}$	$a = 8.908$ Å, $b = 8.985$ Å, $c = 14.442$ Å; $\alpha = 91.84°$, $\beta = 90.86°$, $\gamma = 95.65°$	$TMPDH_2$	3D, 8MR	484
$[C_5H_6N]_2[Ga_6F_2(PO_4)_6]\cdot H_2O$	$P\bar{1}$	$a = 11.391$ Å, $b = 12.414$ Å, $c = 12.846$ Å; $\alpha = 71.04°$, $\beta = 68.39°$, $\gamma = 66.88°$	PyH	3D, 8MR	485, 502
$[C_6H_{18}N_2]_{0.5}[Ga_3(PO_4)_3F]$ (MIL-20)	$P2_1/n$	$a = 8.861$ Å, $b = 18.624$ Å, $c = 9.329$ Å; $\alpha = \gamma = 90°$, $\beta = 118.27°$	$TMEDH_2$	3D, 8MR	486
$[C_3H_{12}N_2][Ga_3(PO_4)_3(OH)_2]\cdot H_2O$	$Pcab$	$a = 10.043$ Å, $b = 15.989$ Å, $c = 18.308$ Å; $\alpha = \beta = \gamma = 90°$	1,3-$DAPH_2$	3D, 10MR	456, 487

Table 2. Continued

formula	SG[a]	lattice parameters	template	type	ref
$[Ga_3(PO_4)_3(H_2O)][NH_2(CH_2)_3NH_2]$	$Pbc2_1$	$a = 8.903$ Å, $b = 9.697$ Å, $c = 16.326$ Å; $\alpha = \beta = \gamma = 90°$	1,3-DAP	3D	487
$[NH_4][GaF(PO_4)]$	$Pna2_1$	$a = 12.921$ Å, $b = 6.44$ Å, $c = 10.415$ Å; $\alpha = \beta = \gamma = 90°$	NH_4	3D, KTP	490
$[NH_4]_2[Ga_2F_3(HPO_4)(PO_4)]$	$Pna2_1$	$a = 12.496$ Å, $b = 7.701$ Å, $c = 9.846$ Å; $\alpha = \beta = \gamma = 90°$	NH_4	3D	490
$[C_7H_{20}N_2]_4[Ga_{16}P_{16}O_{60}(OH)_2F_6O_4]$ (Mu-15)	$Pna2_1$	$a = 16.578$ Å, $b = 9.822$ Å, $c = 13.856$ Å; $\alpha = \beta = \gamma = 90°$	$TMPDH_2$	3D, 8,10MR	491
$[C_{10}H_{26}N_2]_2[H_3O][Ga_9(OH)_2F_3(PO_4)_9]\cdot 2H_2O$ (MIL-31)	$Pca2_1$	$a = 17.494$ Å, $b = 32.393$ Å, $c = 10.075$ Å; $\alpha = \beta = \gamma = 90°$	$1,10\text{-}DADH_2$	3D, 18MR	320
$[C_4H_{14}N_2]_2[Ga_4(OH)_2F(HPO_4)_2(PO_4)_3]\cdot 6H_2O$	$I4_1/a$	$a = b = 15.25$ Å, $c = 28.88$ Å; $\alpha = \beta = \gamma = 90°$	$1,4\text{-}DABH_2$	3D, 20MR	493
$[C_6H_{18}N_2]_2[Ga_{12}P_{12}O_{48}(OH)_4]\cdot 4H_2O$ (MU-8)	$P2_1/c$	$a = 9.513$ Å, $b = 9.048$ Å, $c = 17.490$ Å; $\alpha = \gamma = 90°$, $\beta = 114.7°$	$TMEDH_2$	3D, 8MR	494
$[C_5H_{16}N_3]_2[Ga_6F_2(OH)_2(HPO_4)(PO_4)_6]$ (MU-17)	$P\bar{1}$	$a = 10.283$ Å, $b = 12.096$ Å, $c = 16.911$ Å; $\alpha = 76.07°$, $\beta = 72.38°$, $\gamma = 65.20°$	$DETAH_2$	3D, 12MR	497
$[C_5H_{14}N_2][Ga_6(OH)_2(PO_4)_6]\cdot H_2O$	$Aba2$	$a = 18.035$ Å, $b = 10.513$ Å, $c = 14.293$ Å; $\alpha = \beta = \gamma = 90°$	$NPIPH_2$	3D, 8MR	501
$[C_5H_6N][(GaPO_4)_3F]\cdot 0.5H_2O$	$P\bar{1}$	$a = 9.265$ Å, $b = 9.397$ Å, $c = 9.238$ Å; $\alpha = 94.36°$, $\beta = 90.64°$, $\gamma = 103.67°$	PyH	3D	502
$[C_5H_6N]_2[(Ga_4(PO_4)_3(HPO_4)(OH)F_2]$	$P2_1/n$	$a = 12.157$ Å, $b = 14.202$ Å, $c = 13.065$ Å; $\alpha = \gamma = 90°$, $\beta = 91.85°$	PyH	3D, 8MR	502
$[Ga_2(DETA)(PO_4)_2]\cdot 2H_2O$ (NTHU-1)	$R\bar{3}$	$a = b = 23.781$ Å, $c = 13.466$ Å; $\alpha = \beta = 90°$, $\gamma = 120°$	DETA bound	3D, 24MR	504
$[C_7H_{11}N_2][Ga_4F(PO_4)_4]\cdot 0.5H_2O$	$C2/c$	$a = 22.093$ Å, $b = 13.904$ Å, $c = 14.230$ Å; $\alpha = \gamma = 90°$, $\beta = 98.43°$	4-DMAPH	3D, 12MR	505
$[C_4H_{12}N_2]_2[Ga_5F_4(PO_4)_5]$	$Pccn$	$a = 12.232$ Å, $b = 12.268$ Å, $c = 16.392$ Å; $\alpha = \beta = \gamma = 90°$	$PIPH_2$	3D, 8MR	507
$[C_2H_{10}N_2][Ga_3(OH)_2F_3(PO_4)_2]\cdot 2H_2O$	$P4_2/ncm$	$a = b = 10.043$ Å, $c = 13.828$ Å; $\alpha = \beta = \gamma = 90°$	enH_2	3D, 8MR	508
$[C_5H_{12}N]_{1.5}[H_3O]_{0.5}[Ga_4(PO_4)_4F_{1.33}(OH)_{0.67}]\cdot 0.5H_2O$ (ULM-16)	$Pbcn$	$a = 27.316$ Å, $b = 17.472$ Å, $c = 10.197$ Å; $\alpha = \beta = \gamma = 90°$	$CPAH^+$	3D, 16MR	511
$[C_5H_{12}N]_4[H_3O]_{0.5}[Ga_9(PO_4)_8F_{7.3}(OH)_{0.2}]\cdot 3.5H_2O$ (MIL-46)	$Pnnm$	$a = 10.273$ Å, $b = 18.596$ Å, $c = 29.628$ Å; $\alpha = \beta = \gamma = 90°$	$CPAH^+$	3D, 18MR	511
$[C_4H_{14}N_2][Ga_4(HPO_4)(PO_4)_4]$	$P\bar{1}$	$a = 9.362$ Å, $b = 10.115$ Å, $c = 12.645$ Å; $\alpha = 98.485°$, $\beta = 107.018°$, $\gamma = 105.42°$	$1,4\text{-}DABH_2$	3D, 12,8MR	512
$[C_5H_{16}N_2][Ga_4(HPO_4)(PO_4)_4]$	$P\bar{1}$	$a = 9.356$ Å, $b = 5.015$ Å, $c = 12.706$ Å; $\alpha = 96.612°$, $\beta = 102.747°$, $\gamma = 105.277°$	$1,5\text{-}DAPH_2$	3D, 8,12MR	512
$[C_6H_{18}N_2]_2[Rb]_2[Ga_9(HPO_4)(PO_4)_8(OH)F_6]\cdot 7H_2O$ (MIL-50)	$Cmc2_1$	$a = 32.151$ Å, $b = 17.229$ Å, $c = 10.212$ Å; $\alpha = \beta = \gamma = 90°$	$1,6\text{-}DAHH_2$, Rb	3D, 18MR	514
$K[(GaPO_4)\{F_{1/4}(GaPO_4)\}_4]$	$P42/n$	$a = b = 13.232$ Å, $c = 8.653$ Å; $\alpha = \beta = \gamma = 90°$	K	3D, 8MR	515

[a] SG = space group. [b] Tet = tetragonal. [c] Wang, Y.; Yu, J.; Du, Yu; Xu, R. J. Solid State Chem. 2004, 177, 2511.

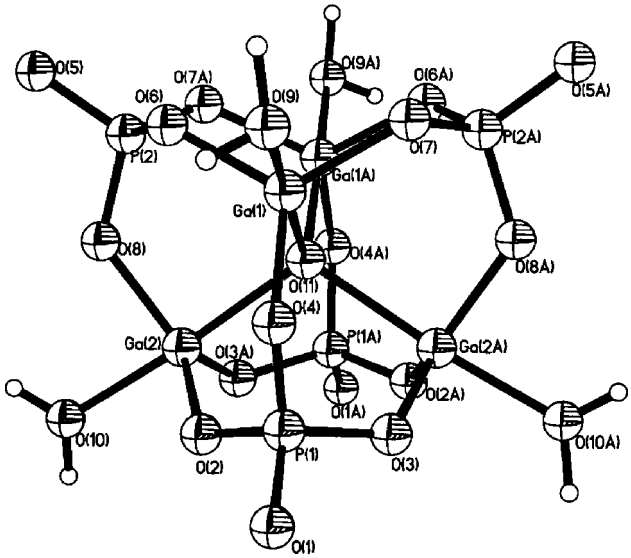

Figure 54. The molecular D4R unit found in a gallium phosphate.[506]

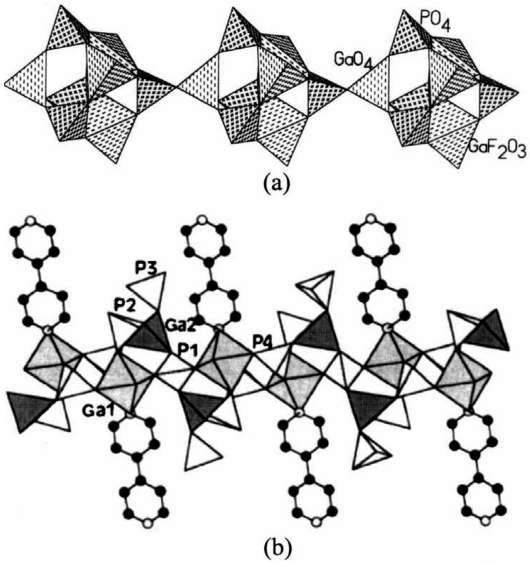

Figure 55. Complex 1D structures in the gallium phosphate family: (a) D4R units are corner-linked;[477] (b) closely related to a corner-shared chain of four-membered rings. Reference 492— Reproduced by permission of the Royal Society of Chemistry.

four corners to In polyhedra resulting in a fully connected framework with a 8MR channel.

3.5.4. Zinc Phosphates

Since the discovery of first microporous zinc phosphates with zeolite-like topologies by Stucky and co-workers,[298] a large number of zinc phosphates have been synthesized in the presence of organic, as well as inorganic templates.[279–281,291,292,295,298,305,527–625] The structural diversity among the zinc phosphates is remarkable and encompasses the entire hierarchy of open-framework structures including zero-, one-, two-, and three-dimensional structures (Table 4). Most of these structures are built from vertex-linked ZnO_4 and PO_4 tetrahedra, but examples of ZnO_6 and ZnO_5 subunits are also known.[305,550,574,581,585] Several zinc phosphates possessing zeolitic structures with strictly alternating Zn/P tetrahedra have also been reported (see Table 4). In most other structures, the frameworks are interrupted by the presence of terminal P−OH, P═O, or Zn−(OH_2) groups. In addition, connectivity between two or more ZnO_4 tetrahedra through Zn−O−Zn linkages[536,542] and coordination of the

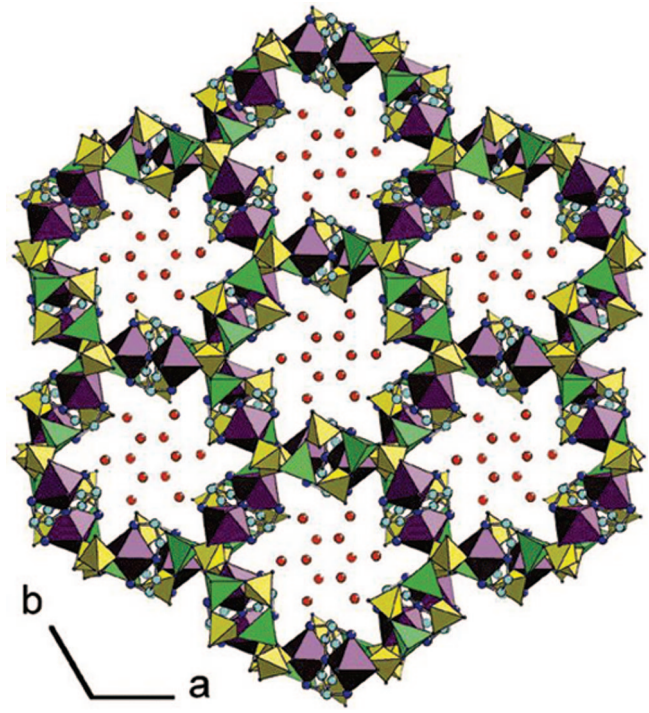

Figure 56. Three-dimensional GaPO with 24MR channel. Reprinted with permission from ref.[504] Copyright 2001 American Chemical Society.

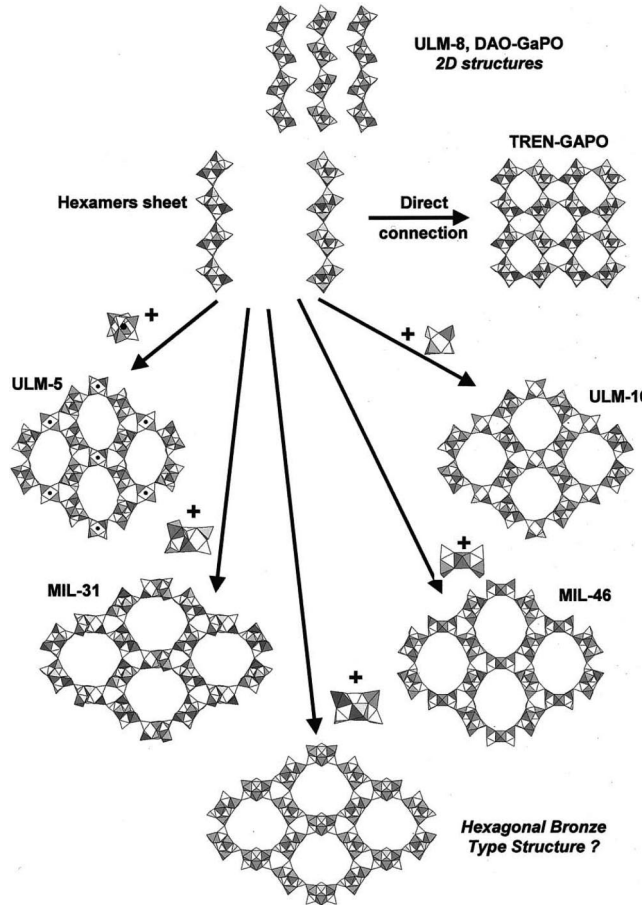

Figure 57. Occurrence of the hexameric building blocks $Ga_3(PO_4)_3F_2$ in fluorinated gallium phosphates. Reprinted with permission from ref 511. Copyright 2002 American Chemical Society.

Table 3. Lattice Parameters, Templates and Dimensionalities of the Various Templated Indium Phosphates Reported in the Literature

formula	SG[a]	lattice parameters	template	type	ref
$[C_5H_6N][In(HPO_4)(H_2PO_4)_2]$	$P\bar{1}$	$a = 6.615$ Å, $b = 9.629$ Å, $c = 11.553$ Å; $\alpha = 75.19°$, $\beta = 86.74°$, $\gamma = 73.90°$	PyH	2D	521
$In(PO_4)F[C_2H_9N_2]$	$P2_1/c$	$a = 9.214$ Å, $b = 7.781$ Å, $c = 10.049$ Å; $\alpha = \gamma = 90°$, $\beta = 101.68°$	bound enH	2D	522
$[Co(en)_3][In_3(H_2PO_4)_6(HPO_4)_3]\cdot H_2O$	$P2_1/n$	$a = 9.17$ Å, $b = 22.692$ Å, $c = 9.912$ Å; $\alpha = \gamma = 90°$, $\beta = 107.87°$	$Co(en)_3^{3+}$	2D	525
$[C_2H_{10}N_2][In_2(HPO_4)_4]$	$P2/n$	$a = 9.444$ Å, $b = 9.156$ Å, $c = 9.756$ Å; $\alpha = \gamma = 90°$, $\beta = 117.46°$	enH_2	3D, 8MR	518
$[C_6H_{15}N]_{0.1}[In(PO_4)(H_2O)_2]$	$Pbca$	$a = 8.842$ Å, $b = 10.187$ Å, $c = 10.327$ Å; $\alpha = \beta = \gamma = 90°$	TriEA	3D	519
$[C_3H_5N_2]_3[H_3O][In_8(H_2O)_6(HPO_4)_{14}]\cdot 5H_2O$	$P\bar{3}c1$	$a = b = 13.859$ Å, $c = 19.186$ Å; $\alpha = \beta = 90°$, $\gamma = 120°$	IMDH	3D, 16MR	520
$[In_5H_2O)_2(en)_3(PO_4)_4F_3]$	$Pbam$	$a = 10.562$ Å, $b = 13.406$ Å, $c = 9.827$ Å; $\alpha = \beta = \gamma = 90°$	bound en	3D, 10MR	522
$[C_3H_{12}N_2]_4[H_3O]_3[In_9(HPO_4)_2(PO_4)_6F_{16}]\cdot 3H_2O$	$P2_1/n$	$a = 13.616$ Å, $b = 9.372$ Å, $c = 23.293$ Å; $\alpha = \gamma = 90°$, $\beta = 99.44°$	1,3-$DAPH_2$, H_3O^+	3D, 14MR	523
$[C_4H_{16}N_3]_2[C_4H_{14}N_2][In_{6.8}F_8(H_2O)_2(PO_4)_4(HPO_4)_4]\cdot 2H_2O$	$C2/m$	$a = 19.569$ Å, $b = 9.7034$ Å, $c = 14.927$ Å; $\alpha = \gamma = 90°$, $\beta = 119.091°$	DETA	3D, 16MR	524
$[C_6H_{14}N_2][In_4F_2(PO_4)_4]\cdot 4H_2O$	$P2_1/n$	$a = 10.280$ Å, $b = 12.700$ Å, $c = 17.860$ Å; $\alpha = \gamma = 90°$, $\beta = 102.47°$	$DABCOH_2$	3D, 8MR	526

[a] SG = space group.

Figure 58. Three-dimensional indium phosphate with 16MR channel.[524] The arrow indicates the tancoite-type chain. Reprinted with permission from ref 524. Copyright 2003 Royal Society of Chemistry.

nitrogen of the amine to Zn can also occur.[530,560,568] The bridging oxygen atom is often trigonally coordinated, a situation not observed in aluminosilicate zeolites or AlPO's. Large pore materials bound by 16, 18, 20, and 24 T atoms (T = Zn or P) have been reported in the organically templated zinc phosphate family. It is difficult to control and predict the structural features of the zinc phosphates in the presence of a particular amine. Even a single amine can yield several structures of different dimensionalities (for example, as many as seven to eight structures are known with DABCO, 1,3-DAP, en, and PIP).

Zero-Dimensional Structures. Several 0D structures are found in the family of organically templated zinc phosphates.[280,305,547,585,613,618,621] The basic building unit for most of the structures[305,547,585,621] is the same S4R unit made with alternate Zn and P polyhedra where a H_2PO_4 or HPO_4 group bridges and remains dangling from the Zn centers as shown in Figure 45 in the case of $[C_6H_{18}N_2][Zn(H_2PO_4)_2(HPO_4)]$.[305] However, in $Zn(H_2O)(HPO_4)(C_4H_7N_3O)$,[613] there are no dangling H_2PO_4 or HPO_4 groups, but instead the N-atom of the amine and O-atom of H_2O bind to Zn to satisfy the coordination (Figure 59a). The structure of $[Zn(phen)]_2(H_{1.5}PO_4)_2(H_2PO_4)$[618] is somewhat complex wherein the S4R unit is capped by another bridging HPO_4 group and Zn adopts five coordination by binding to the 1,10-phenanthroline molecule (Figure 59b). This forms an important secondary building unit, namely 4=1, found in the zeolites, thomsonite, and edingtonite.[270] All these 0D structures are potential monomers[305] for the building of higher dimensional structures through transformation.

One-Dimensional Structures. A large number of 1D structures have been discovered in the family of templated zinc phosphates. Among the 1D structures, the corner-shared chain of four-membered rings and the ladder structures with a Zn/P ratio of 1:2 are most common (see Table 4). In the ladder compound $[(C_3H_4N_2)Zn(HPO_4)]$,[585] the Zn/P ratio is unity because of the absence of dangling HPO_4, which is replaced by an amine, imidazole. The absence of the tancoite-

Table 4. Lattice Parameters, Templates, and Dimensionalities of the Various Templated Zinc Phosphates Reported in the Literature

formula	SG[a]	lattice parameters	template	type	ref
$[C_4H_{12}N][Zn(H_2PO_4)_3]$	$P\bar{1}$	$a = 8.950$ Å, $b = 10.068$ Å, $c = 10.263$ Å; $\alpha = 61.65°$, $\beta = 76.04°$, $\gamma = 76.72°$	TMA	0D, S4R	547
$[C_6H_{18}N_2][Zn(H_2PO_4)_2(HPO_4)]$	$P\bar{1}$	$a = 8.627$ Å, $b = 8.894$ Å, $c = 12.674$ Å; $\alpha = 88.94°$, $\beta = 75.17°$, $\gamma = 63.06°$	$TMEDH_2$	0D, S4R	280, 305
$[C_6H_{21}N_4]_2[Zn(H_2PO_4)(HPO_4)_2]$	*Pbca*	$a = 12.325$ Å, $b = 14.837$ Å, $c = 19.327$ Å; $\alpha = \beta = \gamma = 90°$	$TRENH_3$	0D, S4R	585
$Zn(H_2O)(HPO_4)(C_4H_7N_3O)$	$P\bar{1}$	$a = 9.925$ Å, $b = 11.207$ Å, $c = 19.831$ Å; $\alpha = 80.314°$, $\beta = 78.829°$, $\gamma = 89.241°$	bound CRT	0D	613
$[Zn(phen)]_2(H_{1.5}PO_4)H_2PO_4)$	*Fdd*2	$a = 40.391$ Å, $b = 7.456$ Å, $c = 17.424$ Å; $\alpha = \beta = \gamma = 90°$	bound phen	0D	618
$[C_9H_{13}N_3][Zn(H_2PO_4)_2(HPO_4)]$	$P\bar{1}$	$a = 8.139$ Å, $b = 8.362$ Å, $c = 14.202$ Å; $\alpha = 73.36°$, $\beta = 87.56°$, $\gamma = 78.31°$	Py-$PIPH_2$	0D, S4R	621
$Na_2Zn(PO_4)(OH)\cdot 7H_2O$	$P2_1/a$	$a = 6.421$ Å, $b = 21.612$ Å, $c = 8.681$ Å; $\alpha = \gamma = 90°$, $\beta = 109.899°$	Na^+	1D	531
$[C_6H_{14}N_2][Zn(H_2PO_4)_2(HPO_4)]$	$P2_12_12_1$	$a = 9.777$ Å, $b = 10.640$ Å, $c = 15.384$ Å; $\alpha = \beta = \gamma = 90°$	$DABCOH_2$	1D	537
$[CH_6N_3]_6[Zn_2(OH)(PO_4)_3]$	$R\bar{3}$	$a = b = 20.016$ Å, $c = 13.955$ Å; $\alpha = \gamma = 90°$, $\beta = 120°$	$GUANH^+$	1D, chain	548
$Rb[Zn(H_2PO_4)(HPO_4)]\cdot H_2O$	$P\bar{1}$	$a = 7.712$ Å, $b = 7.982$ Å, $c = 8.042$ Å; $\alpha = 64.313°$, $\beta = 84.9°$, $\gamma = 72.364°$	Rb	1D c.s. chain	550
$[C_3H_{12}N_2][Zn(HPO_4)_2]$	$P2_12_12_1$	$a = 5.221$ Å, $b = 12.717$ Å, $c = 15.570$ Å; $\alpha = \beta = \gamma = 90°$	1,3-$DAPH_2$	1D ladder	553
$[C_2H_8N]_8[Zn_8(H_2PO_4)_8(HPO_4)_8]\cdot 4H_2O$	*Cc*	$a = 12.645$ Å, $b = 10.848$ Å, $c = 14.631$ Å; $\alpha = \gamma = 90°$, $\beta = 98.79°$	DMAH	1D c.s. chain	554
$[C_2H_{10}N_2][Zn(HPO_4)_2]$	$P2_1/c$	$a = 5.161$ Å, $b = 15.842$ Å, $c = 12.027$ Å; $\alpha = \gamma = 90°$, $\beta = 92.36°$	enH_2	1D ladder	562
$[C_6H_{14}N_2][Zn(HPO_4)_2]\cdot H_2O$	$P2_1/n$	$a = 9.864$ Å, $b = 8.679$ Å, $c = 15.78$ Å; $\alpha = \gamma = 90°$, $\beta = 106.86°$	$DABCOH_2$	1D c.s. chain	564
$[C_4H_{12}N_2][Zn(HPO_4)_2]\cdot H_2O$	$P2_1/n$	$a = 8.931$ Å, $b = 14.025$ Å, $c = 9.311$ Å; $\alpha = \gamma = 90°$, $\beta = 95.41°$	$PIPH_2$	1D c.s. chain	570, 280
$[C_6H_{22}N_4]_{0.5}[Zn(HPO_4)_2]$	$P2_1/c$	$a = 5.268$ Å, $b = 13.303$ Å, $c = 14.783$ Å; $\alpha = \gamma = 90°$, $\beta = 96.05°$	$TETAH_4$	1D ladder	295
$[C_3H_4N_2][Zn(HPO_4)]$	$P2_1/c$	$a = 5.197$ Å, $b = 7.697$ Å, $c = 17.336$ Å; $\alpha = \gamma = 90°$, $\beta = 90.61°$	bound IMD	1D ladder	585
$[C_5H_{14}N_2][Zn(HPO_4)_2]$	$P2_1/c$	$a = 8.603$ Å, $b = 13.529$ Å, $c = 10.880$ Å; $\alpha = \gamma = 90°$, $\beta = 94.9°$	$MPIPH_2$	1D c.s. chain	589
$[C_{10}H_{24}N_4]_{0.5}[Zn(HPO_4)_2]\cdot 2H_2O$	*Pbca*	$a = 8.393$ Å, $b = 15.286$ Å, $c = 22.659$ Å; $\alpha = \beta = \gamma = 90°$	$APPIPH_4$	1D c.s. chain	589
$Zn[C_4H_6N_2][HPO_4]$	$P2_1/c$	$a = 8.241$ Å, $b = 13.750$ Å, $c = 10.572$ Å; $\alpha = \gamma = 90°$, $\beta = 90.9°$	bound 4MIMD	1D wire	589
$[C_5H_{14}N_2][Zn(HPO_4)_2]\cdot H_2O$	*C*2/*c*	$a = 13.917$ Å, $b = 9.091$ Å, $c = 20.490$ Å; $\alpha = \gamma = 90°$, $\beta = 102.36°$	$NPIPH_2$	1D c.s. chain	600
$[C_5H_{14}N_2][Zn(HPO_4)_2]\cdot xH_2O$ ($x \approx 0.46$)	$P2_1/n$	$a = 8.605$ Å, $b = 13.713$ Å, $c = 10.818$ Å; $\alpha = \gamma = 90°$, $\beta = 97.95°$	$HPIPH_2$	1D c.s. chain	610
$[C_5H_{16}N_2][Zn(HPO_4)_2]\cdot H_2O$	$P2_1/c$	$a = 10.641$ Å, $b = 8.377$ Å, $c = 15.027$ Å; $\alpha = \gamma = 90°$, $\beta = 102.041°$	$N,NDAPH_2$	1D c.s. chain	611
$[C_2H_{10}N_2]_2[Zn(PO_4)_2]$	$P2_12_12_1$	$a = 8.480$ Å, $b = 17.201$ Å, $c = 8.752$ Å; $\alpha = \beta = \gamma = 90°$	enH_2	1D c.s. chain	614
$[Zn(phen)]_2(HPO_4)(H_2PO_4)_2\cdot xH_2O$	$P\bar{1}$	$a = 10.317$ Å, $b = 12.416$ Å, $c = 12.969$ Å; $\alpha = 65.057°$, $\beta = 74.625°$, $\gamma = 71.593°$	bound phen	1D	618
$[C_6H_{18}N_2][Zn(HPO_4)_2]$	*Pbca*	$a = 8.079$ Å, $b = 14.555$ Å, $c = 28.575$ Å; $\alpha = \beta = \gamma = 90°$	$NN'DEenH_2$	1D c.s. chain	622
$[C_6H_{16}N_2][Zn(HPO_4)_2]$	*C*2/*c*	$a = 14.097$ Å, $b = 13.685$ Å, $c = 7.912$ Å; $\alpha = \gamma = 90°$, $\beta = 96.362°$	$DPIPH_2$	1D c.s. chain	*b*
$[C_8H_{26}N_4][Zn_2(HPO_4)_4]$	$P2_1/c$	$a = 5.381$ Å, $b = 15.352$ Å, $c = 13.237$ Å; $\alpha = \gamma = 90°$, $\beta = 96.204°$	$BAPenH_4$	1D ladder	624
$NaH(ZnPO_4)_2$	$P\bar{1}$	$a = 8.641$ Å, $b = 8.817$ Å, $c = 5.127$ Å; $\alpha = 100.401°$, $\beta = 105.684°$, $\gamma = 96.924°$	Na^+	2D	532
$CsH(ZnPO_4)_2$	*Abma*	$a = 7.739$ Å, $b = 6.594$ Å, $c = 15.94$ Å; $\alpha = \beta = \gamma = 90°$	Cs	2D	532
$[Na_2Zn(HPO_4)_2]\cdot 4H_2O$	$P2_1/c$	$a = 8.947$ Å, $b = 13.254$ Å, $c = 10.098$ Å; $\alpha = \gamma = 90°$, $\beta = 116.358°$	Na^+	2D	533

Table 4. Continued

formula	SG[a]	lattice parameters	template	type	ref
$[C_6H_{18}N_2][Zn_3(H_2O)_4(HPO_4)_4]$	$P2_1/c$	$a = 8.932$ Å, $b = 9.693$ Å, $c = 13.503$ Å; $\alpha = \gamma = 90°$, $\beta = 96.01°$	$TMEDH_2$	2D	545
$Rb[Zn_2(H_2PO_4)(HPO_4)_2]\cdot 2H_2O$	$P2_12_12_1$	$a = 7.645$ Å, $b = 9.965$ Å, $c = 15.603$ Å; $\alpha = \beta = \gamma = 90°$	Rb^+	2D	550
$[C_4H_{14}N_2][Zn_2(H_2PO_4)(HPO_4)(PO_4)]$	$P\bar{1}$	$a = 8.4$ Å, $b = 8.669$ Å, $c = 10.352$ Å; $\alpha = 88.24°$, $\beta = 77.73°$, $\gamma = 86.41°$	1,4-$DABH_2$	2D	549
$[C_3H_{12}N_2][Zn_2(H_2PO_4)_2(HPO_4)_2]$	$P2_1/a$	$a = 15.056$ Å, $b = 7.845$ Å, $c = 16.344$ Å; $\alpha = \gamma = 90°$, $\beta = 115.47°$	1,3-$DAPH_2$	2D	553
$[C_6H_4N]_2[Zn_2(HPO_4)_2Cl_2]$	$P2_1/a$	$a = 8.830$ Å, $b = 9.278$ Å, $c = 26.950$ Å; $\alpha = \gamma = 90°$, $\beta = 90.74°$	$CHAH^+$	2D	557
$[C_6H_{18}N_2]_{0.5}[Zn_2(H_2O)(HPO_4)(PO_4)]\cdot H_2O$	$P\bar{1}$	$a = 8.822$ Å, $b = 9.236$ Å, $c = 8.451$ Å; $\alpha = 67.19°$, $\beta = 91.32°$, $\gamma = 111.10°$	$TMEDH_2$	2 D	558
$[C_2H_{10}N_2][LiZn(HPO_4)(PO_4)]\cdot H_2O$	$C2/c$	$a = 18.068$ Å, $b = 5.303$ Å, $c = 21.065$ Å; $\alpha = \gamma = 90°$, $\beta = 91.99°$	enH_2^+, Li^+	2D	561
$[C_2H_{10}N_2][Zn(H_2PO_4)(HPO_4)]_2$	$P2_1/c$	$a = 16.42$ Å, $b = 7.826$ Å, $c = 14.64$ Å; $\alpha = \gamma = 90°$, $\beta = 116.47°$	enH_2	2D	562
$[C_3H_{12}N_2O][Zn_2(HPO_4)_3]$	$P2_1/c$	$a = 8.615$ Å, $b = 9.648$ Å, $c = 17.209$ Å; $\alpha = \gamma = 90°$, $\beta = 93.02°$	$DAHPH_2$	2D	562, 570
$[C_6H_{18}N_2][Zn_3(HPO_4)_4]\cdot H_2O$	$C2/c$	$a = 16.815$ Å, $b = 8.970$ Å, $c = 15.080$ Å; $\alpha = \gamma = 90°$, $\beta = 97.25°$	1,6-$DAHH_2$	2D	562
$[C_4H_{15}N_3][Zn_4(HPO_4)_2(PO_4)_2]$	$C2/c$	$a = 25.075$ Å, $b = 5.127$ Å, $c = 17.726$ Å; $\alpha = \gamma = 90°$, $\beta = 125.40°$	$DETAH_2$	2D	563
$[C_3H_{12}N_2][Zn_2(HPO_4)_3]$	$P2_1/c$	$a = 8.593$ Å, $b = 9.602$ Å, $c = 17.001$ Å; $\alpha = \gamma = 90°$, $\beta = 93.57°$	1,3-$DAPH_2$	2D	564
$[CH_6N_3]_2[Zn_4(H_2PO_4)(HPO_4)_3(PO_4)]$	$I2/a$	$a = 23.770$ Å, $b = 5.104$ Å, $c = 18.100$ Å; $\alpha = \gamma = 90°$, $\beta = 94.49°$	$GUANH^+$	2D	567
$[C_3H_{12}N_2][Zn_4(HPO_4)_2(PO_4)_2]$	$C2/c$	$a = 17.279$ Å, $b = 5.193$ Å, $c = 20.115$ Å; $\alpha = \gamma = 90°$, $\beta = 92.60°$	1,3-$DAPH_2$	2D	569
$[C_6H_{14}N][Zn(HPO_4)Cl]$	$P2_1/c$	$a = 13.653$ Å, $b = 9.718$ Å, $c = 8.691$ Å; $\alpha = \gamma = 90°$, $\beta = 94.9°$	CHAH	2D	291
$[C_6H_{22}N_4]_{0.5}[Zn_2(HPO_4)_3]$	$P\bar{1}$	$a = 7.488$ Å, $b = 8.234$ Å, $c = 12.859$ Å; $\alpha = 98.72°$, $\beta = 101.26°$, $\gamma = 115.78°$	$TETAH_4$	2D	575, 295
$[C_6H_{17}N_3][Zn_3(HPO_4)(PO_4)_2]\cdot H_2O$	$P2_1/c$	$a = 12.671$ Å, $b = 8.243$ Å, $c = 18.484$ Å; $\alpha = \gamma = 90°$, $\beta = 109.13°$	$AEPIPH_2$	2D	579
$[C_6H_{17}N_3][Zn_3(HPO_4)(PO_4)_2]$	$P2_1/c$	$a = 12.290$ Å, $b = 8.400$ Å, $c = 18.499$ Å; $\alpha = \gamma = 90°$, $\beta = 114.25°$	$AEPIPH_2$	2D	579
$[C_3H_{12}N_2O][Zn_2(PO_4)_2]$	$Pbcn$	$a = 22.982$ Å, $b = 7.679$ Å, $c = 6.618$ Å; $\alpha = \beta = \gamma = 90°$	$DAHPH_2$	2D	603
$[C_5H_{18}N_3][Zn_2(HPO_4)_2(PO_4)]\cdot H_2O$	$P2_1/c$	$a = 14.398$ Å, $b = 13.766$ Å, $c = 8.924$ Å; $\alpha = \gamma = 90°$, $\beta = 100.84°$	$AEDAPH_3$	2D	604
$[C_2H_7N_4O][ZnPO_4]$	$P2_1/c$	$a = 13.645$ Å, $b = 5.071$ Å, $c = 10.601$ Å; $\alpha = \gamma = 90°$, $\beta = 95.918°$	GUANUH	2D	605
$[C_8H_{28}N_5][Zn_6(HPO_4)(PO_4)_5]\cdot 5H_2O$	$Pca2_1$	$a = 18.629$ Å, $b = 8.080$ Å, $c = 22.502$ Å; $\alpha = \beta = \gamma = 90°$	$TEPAH_5$	2D	606
$[C_{10}H_{28}N_4]_{0.5}[Zn_4(HPO_4)_2(PO_4)_2]\cdot 2H_2O$	$P2_1/c$	$a = 15.758$ Å, $b = 9.029$ Å, $c = 15.543$ Å; $\alpha = \gamma = 90°$, $\beta = 111.07°$	$CLMH_4$	2D	581
$[C_4H_{14}N_2]_2[Zn_4(H_2PO_4)_2(PO_4)_4]$	$P\bar{1}$	$a = 8.659$ Å, $b = 10.346$ Å, $c = 8.391$ Å; $\alpha = 102.180°$, $\beta = 93.676°$, $\gamma = 88.203°$	1,4-$DABH_2$	2D	583
$[C_6H_{22}N_4][Zn_6(HPO_4)_2(PO_4)_4]\cdot 2H_2O$	$Pna2_1$	$a = 18.785$ Å, $b = 8.278$ Å, $c = 18.747$ Å; $\alpha = \beta = \gamma = 90°$	$TRENH_4$	2D	585
$[C_6H_{22}N_4]_{0.5}[Zn_3(HPO_4)(PO_4)_2]$	$P2_1/c$	$a = 9.881$ Å, $b = 16.857$ Å, $c = 8.286$ Å; $\alpha = \gamma = 90°$, $\beta = 96.70°$	$TETAH_4$	2D	586
$[C_4H_{12}N_2][Zn_2(PO_4)_2]$	$P\bar{1}$	$a = 5.135$ Å, $b = 10.760$ Å, $c = 10.771$ Å; $\alpha = 66.54°$, $\beta = 89.03°$, $\gamma = 81.70°$	$PIPH_2$	2D	588
$[C_{12}H_{32}N_3]_2[Zn_3(HPO_4)_2(PO_4)_2][H_2PO_4]_2\cdot 10H_2O$	$P2_1/n$	$a = 8.782$ Å, $b = 15.356$ Å, $c = 43.080$ Å; $\alpha = \gamma = 90°$, $\beta = 90.02°$	$BHMTAH_3$	2D	592

Table 4. Continued

formula	SG[a]	lattice parameters	template	type	ref
$[C_{12}H_{32}N_3][Zn_2(H_2PO_4)(HPO_4)(PO_4)][H_2PO_4]$	$P\bar{1}$	$a = 8.515$ Å, $b = 8.571$ Å, $c = 19.694$ Å; $\alpha = 87.55°$, $\beta = 86.05°$, $\gamma = 73.18°$	$BHMTAH_3$	2D	592
$[C_{10}H_{28}N_4][Zn_6(HPO_4)_2(PO_4)_4]\cdot 2H_2O$	$P\bar{1}$	$a = 8.334$ Å, $b = 12.413$ Å, $c = 17.363$ Å; $\alpha = 75.27°$, $\beta = 78.87°$, $\gamma = 76.27°$	$APPIPH_4$	2D	594
$[C_5H_{12}N][Zn(HPO_4)Cl]$	$Pbca$	$a = 8.767$ Å, $b = 24.678$ Å, $c = 9.332$ Å; $\alpha = \beta = \gamma = 90°$	PIPDH	2D	595
$[Co^{II}(en)_3]_2[Zn_6(HPO_4)_8]$	$C2/c$	$a = 16.623$ Å, $b = 30.589$ Å, $c = 17.441$ Å; $\alpha = \gamma = 90°$, $\beta = 90.35°$	$Co^{II}(en)_3$	2D, 4.6 net	292
$[C_6H_{18}N_2][Zn_3(HPO_4)(PO_4)_2]\cdot H_3BO_3$	$P2_1/c$	$a = 12.955$ Å, $b = 8.295$ Å, $c = 18.805$ Å; $\alpha = \gamma = 90°$, $\beta = 91.34°$	$1,6\text{-}DAHH_2^{2+}$	2D	597
$[C_3H_4N_2]_3[Zn_4(HPO_4)(PO_4)_2]$	$P\bar{1}$	$a = 9.584$ Å, $b = 9.852$ Å, $c = 12.345$ Å; $\alpha = 77.48°$, $\beta = 77.958°$, $\gamma = 68.19°$	bound IMD	2D	598, 599
$[C_5H_{14}N_2][Zn_3(H_2O)(HPO_4)(PO_4)_2]$	$P2_1/c$	$a = 11.103$ Å, $b = 17.553$ Å, $c = 8.265$ Å; $\alpha = \gamma = 90°$, $\beta = 97.92°$	$HPIPH_2$	2D	610
$[C_9H_{15}N_3][C_4H_{10}N_2][Zn_2(H_2PO_4)(HPO_4)(PO_4)]\cdot 2H_2O$	$P\bar{1}$	$a = 8.683$ Å, $b = 9.997$ Å, $c = 12.094$ Å; $\alpha = 93.341°$, $\beta = 101.061°$, $\gamma = 98.583°$	$Py\text{-}PIPH_3$	2D	621
$[Co^{II}(en)_3][Zn_4(H_2PO_4)_3(HPO_4)_2(PO_4)(H_2O)_2]$	$Pbcn$	$a = 10.478$ Å, $b = 20.009$ Å, $c = 14.959$ Å; $\alpha = \gamma = \beta = 90°$	$Co^{II}(en)_3$	2D	*c*
$[C_8H_{26}N_4][Zn_6(HPO_4)_2(PO_4)_4]$	$P2_1/c$	$a = 10.214$ Å, $b = 17.108$ Å, $c = 8.431$ Å; $\alpha = \gamma = 90°$, $\beta = 95.309°$	$BAPenH_4$	2D	624
$[C_8H_{26}N_4][Zn_3Cl(HPO_4)_3(PO_4)]$	$Pca2_1$	$a = 9.841$ Å, $b = 15.091$ Å, $c = 16.122$ Å; $\alpha = \beta = \gamma = 90°$	BAPEN	2D	625
$Na_6[(ZnPO_4)_6]\cdot 8H_2O$	$P\bar{4}3n$	$a = b = c = 8.828$ Å; $\alpha = \beta = \gamma = 90°$	Na^+	3D, SOD	298, 527
$Li_4[Zn_4(PO_4)_4]\cdot 4H_2O$	$Pna2_1$	$a = 8.122$ Å, $b = 10.492$ Å, $c = 4.854$ Å; $\alpha = \beta = \gamma = 90°$	Li^+	3D, Li-ABW	527
$Na_{67}(TMA)_{12}[Zn_8(ZnPO_4)_{96}]\cdot 192H_2O$	$Fd3$	$a = b = c = 25.199$ Å; $\alpha = \beta = \gamma = 90°$	Na^+, TMA	3D, Zeo-X	527, 528
$[C_6H_{14}N_2][Zn_2(HPO_4)_3]$	$P\bar{1}$	$a = 9.933$ Å, $b = 9.966$ Å, $c = 9.518$ Å; $\alpha = 98.02°$, $\beta = 114.81°$, $\gamma = 107.70°$	$DABCOH_2$	3D, 8MR	529
$[C_6H_{14}N_2][Zn_4(HPO_4)_2(PO_4)_2]\cdot 3H_2O$	$P\bar{1}$	$a = 9.515$ Å, $b = 12.297$ Å, $c = 9.461$ Å; $\alpha = 91.03°$, $\beta = 98.66°$, $\gamma = 93.71°$	$DABCOH_2$	3D, 8MR	529
$[C_6H_{14}N_2]_2[Zn_5(HPO_4)_4(PO_4)_2(H_2O)]$	$P\bar{1}$	$a = 9.366$ Å, $b = 9.882$ Å, $c = 19.183$ Å; $\alpha = 85.41°$, $\beta = 85.03°$, $\gamma = 114.48°$	$DABCOH_2$	3D, 8MR	530
$Zn_3(HPO_4)_2(PO_4)\cdot HN_2C_6H_{12}$	$P2_12_12_1$	$a = 11.095$ Å, $b = 16.413$ Å, $c = 8.263$ Å; $\alpha = \beta = \gamma = 90°$	DABCOH bound	3D, 8MR	530
$[C_2H_{10}N_2][Zn_2(PO_4)_2]$ (DAF-3)	$P4_2bc$	$a = b = 14.701$ Å, $c = 8.942$ Å; $\alpha = \beta = \gamma = 90°$	enH_2	3D, 8MR	534
$[C_2H_{10}N_2][Zn_2(HPO_4)_3]$	$P\bar{1}$	$a = 8.215$ Å, $b = 8.557$ Å, $c = 9.760$ Å; $\alpha = 93.81°$, $\beta = 95.38°$, $\gamma = 109.75°$	enH_2	3D, 8,12MR	535
$[C_2H_8N][Zn_4(H_2O)(PO_4)_3]$	$P2_1/n$	$a = 5.252$ Å, $b = 15.197$ Å, $c = 17.570$ Å; $\alpha = \gamma = 90°$, $\beta = 91.46°$	EAH	3D, 8MR	536
$[C_4H_{11}N_2]^+[Zn_2(H_2PO_4)_2(PO_4)]$	$C2/c$	$a = 13.370$ Å, $b = 12.829$ Å, $c = 8.207$ Å; $\alpha = \gamma = 90°$, $\beta = 94.79°$	PIPH	3D, 8MR	538
$[C_4H_{14}N_2]^{2+}[Zn_2(H_2O)(HPO_4)(PO_4)]_2\cdot H_2O$	$C2/c$	$a = 12.093$ Å, $b = 14.897$ Å, $c = 11.849$ Å; $\alpha = \gamma = 90°$, $\beta = 97.821°$	$PIPH_2$	3D, 8MR	538
$LiZn(PO_4)\cdot H_2O$	$Pna2_1$	$a = 10.575$ Å, $b = 8.076$ Å, $c = 4.994$ Å; $\alpha = \beta = \gamma = 90°$	Li^+	3D, 8MR	539
$[C_6H_{14}N_2][Zn_2(HPO_4)_3]$	$Pna2_1$	$a = 10.540$ Å, $b = 10.05$ Å, $c = 14.370$ Å; $\alpha = \beta = \gamma = 90°$	$DABCOH_2$	3D, 8,12MR	540
$NaZn(PO_4)\cdot H_2O$	$P6_122$	$a = b = 10.479$ Å, $c = 15.089$ Å; $\alpha = \beta = \gamma = 90°$	Na^+	3D, 8MR, chiral	541
$NaZn(PO_4)\cdot H_2O$	$P6_522$	$a = b = 10.412$ Å, $c = 21.292$ Å; $\alpha = \beta = \gamma = 90°$	Na^+	3D, 8MR, chiral (CZP)	541
$Rb_3Zn_4O(PO_4)_3\cdot 3.5H_2O$	$F\bar{4}3c$	$a = b = c = 15.342$ Å; $\alpha = \beta = \gamma = 90°$	Rb^+	3D, 8MR	542
$Na_3Zn_4O(PO_4)_3\cdot 6H_2O$	$R3c$	$a = b = c = 10.749$ Å; $\alpha = \beta = \gamma = 90°$	Na^+	3D, 8MR	542
$[C_3H_{10}N][Zn_4(H_2O)(PO_4)_3]$	$P\bar{1}$	$a = 5.305$ Å, $b = 9.296$ Å, $c = 15.474$ Å; $\alpha = 86.46°$, $\beta = 86.42°$, $\gamma = 78.91°$	TriMAH	3D, 8MR	543
$H[Zn_4(PO_4)_3]\cdot H_2O$	$P\bar{1}$	$a = 5.055$ Å, $b = 9.624$ Å, $c = 13.158$ Å; $\alpha = 101.007°$, $\beta = 100.942°$, $\gamma = 103.606°$		3D, 8MR	543
$[CH_6N_3][Zn_7(H_2O)_4(PO_4)_6]\cdot(H_3O)$	$R3$	$a = b = 15.356$ Å, $c = 12.617$ Å; $\alpha = \beta = 90°$, $\gamma = 120°$	GUANH	3D, 18MR	544
$[NH_4][ZnPO_4]$	$P2_1$	$a = 8.804°$, $b = 5.448$ Å, $c = 8.981$ Å; $\alpha = \gamma = 90°$, $\beta = 90.092°$	NH_4	3D, ABW	551

Table 4. Continued

formula	SG[a]	lattice parameters	template	type	ref
$[NH_4][ZnPO_4]$	$P2_1$	$a = 8.796$ Å, $b = 5.456$ Å, $c = 8.965$ Å; $\alpha = \gamma = 90°$, $\beta = 90.323°$	NH_4	3D, ABW	551
$[C_4H_{12}N][Zn(H_2PO_4)(HPO_4)]$	$Fdd2$	$a = 15.972$ Å, $b = 9.863$ Å, $c = 15.156$ Å; $\alpha = \beta = \gamma = 90°$	TMA	3D, 12MR	546, 623
$[C_4H_{12}N][Zn(H_2PO_4)(HPO_4)]$	Pc	$a = 8.443$ Å, $b = 13.779$ Å, $c = 10.170$ Å; $\alpha = \gamma = 90°$, $\beta = 91.91°$	TMA	3D, 12MR	547, 623
$[CH_6N_3][Zn_2(H_2PO_4)(HPO_4)_2]$	$P2_1$	$a = 5.132$ Å, $b = 7.841$ Å, $c = 16.51$ Å; $\alpha = \gamma = 90°$, $\beta = 90.12°$	GUANH	3D, 12MR	548
$[CH_6N_3]_2[Zn(HPO_4)_2]$	$Pna2_1$	$a = 10.447$ Å, $b = 12.349$ Å, $c = 10.225$ Å; $\alpha = \beta = \gamma = 90°$	GUANH	3D, 12MR	548
$[C_2H_{10}N_2]_{0.5}[Zn_3(HPO_4)_{0.5}(PO_4)_2]$	$C2/c$	$a = 19.182$ Å, $b = 5.036$ Å, $c = 21.202$ Å; $\alpha = \gamma = 90°$, $\beta = 103.29$	enH_2	3D, 8MR	552, 555
β-$LiZnPO_4 \cdot H_2O$	$P2_1ab$	$a = 10.022$ Å, $b = 16.559$ Å, $c = 5.012$ Å; $\alpha = \beta = \gamma = 90°$	Li^+	3D	556
$[C_4H_{16}N_3][Zn_4(HPO_4)(PO_4)_3] \cdot H_2O$	$P2_1$	$a = 10.021$ Å, $b = 8.286$ Å, $c = 11.856$ Å; $\alpha = \gamma = 90°$, $\beta = 103.13°$	$DETAH_3$	3D, heli 8MR	559, 587
$[(C_4H_{15}N_3)^{2+}Zn_5(PO_4)_4]$	Cc	$a = 27.070$ Å, $b = 5.215$ Å, $c = 17.290$ Å; $\alpha = \gamma = 90°$, $\beta = 130.26°$	$DETAH_2$ bound	3D, 10MR	560
$[CH_7N_5][Zn_2(HPO_4)(PO_4)]$	$P2_1/n$	$a = 8.089$ Å, $b = 12.771$ Å, $c = 10.066$ Å; $\alpha = \gamma = 90°$, $\beta = 105.28°$	DAGH bound	3D, 8MR	560
$[C_6H_{14}N_2][Zn_3(HPO_4)_4]$	$P2_1/n$	$a = 9.535$ Å, $b = 23.246$ Å, $c = 9.587$ Å; $\alpha = \gamma = 90°$, $\beta = 117.74°$	$DABCOH_2$	3D, 12MR	564
$K[ZnPO_4] \cdot 0.8H_2O$ (ZP-4)	$Ccc2$	$a = 13.818$ Å, $b = 13.836$ Å, $c = 13.134$ Å; $\alpha = \beta = \gamma = 90°$	K^+	3D, EDI	565
$[C_6H_{16}N_2][Zn_3(HPO_4)(PO_4)_2] \cdot 2H_2O$	$R\bar{3}$	$a = b = 33.401$ Å, $c = 9.241$ Å; $\alpha = \beta = 90°$, $\gamma = 120°$	$1,2\text{-}DACHH_2$	3D, 24MR	566
$[C_3H_{12}N_2]_2[(NH_3(CH_2)_3NH_2)_2Zn_{12}(H_2O)(PO_4)_{10} \cdot H_2O$	Pn	$a = 13.092$ Å, $b = 14.272$ Å, $c = 14.220$ Å; $\alpha = \gamma = 90°$, $\beta = 90.31°$	$1,3\text{-}DAPH_2$ + bound DAP	3D, 8,10MR	568
$[CH_6N]_3[Zn_4O(PO_4)_3]$	$P2_1$	$a = 7.657$ Å, $b = 15.241$ Å, $c = 7.659$ Å; $\alpha = \gamma = 90°$, $\beta = 92.74°$	MAH	3D	571
$[C_4H_{12}N_2][Zn_7(H_2O)_2(PO_4)_6]$	$C2/c$	$a = 16.134$ Å, $b = 8.241$ Å, $c = 22.86$ Å; $\alpha = \gamma = 90°$, $\beta = 104.05°$	$PIPH_2$	3D, 8MR	572, 280
$[C_3H_5N_2][Zn_4(OH)(PO_4)_3]$	$P2_1/n$	$a = 5.235$ Å, $b = 15.437$ Å, $c = 17.975$ Å; $\alpha = \gamma = 90°$, $\beta = 91.79°$	IMDH	3D, 8MR	573
$[C_6H_{17}N_3]_2[Zn_7(PO_4)_6]$ (UiO-21)	$R\bar{3}$	$a = b = 13.725$ Å, $c = 15.332$ Å; $\alpha = \beta = 90°$, $\gamma = 120°$	$AEPIPH_2$	3D, CHA	574
$[C_6H_{17}N_3][Zn_4(OH)(PO_4)_3]$ (UiO-22)	$P\bar{1}$	$a = 5.270$ Å, $b = 12.14$ Å, $c = 13.916$ Å; $\alpha = 115.44°$, $\beta = 98.39°$, $\gamma = 91.16°$	$AEPIPH_2$	3D, 8, 12MR	574
$[C_6H_{22}N_4]_{0.5}[Zn_2(PO_4)_2]$	$P\bar{1}$	$a = 8.064$ Å, $b = 8.457$ Å, $c = 9.023$ Å; $\alpha = 111.94°$, $\beta = 107.96°$, $\gamma = 103.65°$	$TETAH_4$	3D, GIS	295
$[C_6H_{22}N_4]_{0.5}[Zn_3(HPO_4)(PO_4)_2]$	$P\bar{1}$	$a = 5.218$ Å, $b = 8.78$ Å, $c = 16.081$ Å; $\alpha = 89.34°$, $\beta = 83.54°$, $\gamma = 74.34°$	$TETAH_4$	3D, 16MR	295
$[C_6H_{20}N_4]_{0.5}[Zn_4(PO_4)_4]$	$P2_1/c$	$a = 9.219$ Å, $b = 15.239$ Å, $c = 10.227$ Å; $\alpha = \gamma = 90°$, $\beta = 105.2°$	$TETAH_2$ bound amine	3D, 8MR	295
$[C_3H_{12}N_2]_2[Zn_4(PO_4)_4]$	$P2_1$	$a = 10.200$ Å, $b = 9.998$ Å, $c = 10.447$ Å; $\alpha = \gamma = 90°$, $\beta = 92.24°$	$1,3\text{-}DAPH_2$	3D, GIS	577, 584
$[C_3H_{12}N_2]_2[Zn_5(H_2O)(HPO_4)(PO_4)_4]$	$P2_1$	$a = 9.299$ Å, $b = 9.751$ Å, $c = 14.335$ Å; $\alpha = \gamma = 90°$, $\beta = 90.97°$	$1,3\text{-}DAPH_2$	3D, THO	577
$[C_4H_{16}N_3][Zn_5(PO_4)_4]$	$P2_1/n$	$a = 15.935$ Å, $b = 7.404$ Å, $c = 16.209$ Å; $\alpha = \gamma = 90°$, $\beta = 111.89°$	$DETAH_2$	3D, 8MR	578
$[C_2H_8N]_2[Zn_2(HPO_4)_3]$	$C2/c$	$a = 17.351$ Å, $b = 9.507$ Å, $c = 9.806$ Å; $\alpha = \gamma = 90°$, $\beta = 102.68°$	EAH	3D, 12MR	580
$[C_6H_{18}N_2][Zn_4(HPO_4)_2(PO_4)_2] \cdot 3H_2O$	$P\bar{1}$	$a = 5.202$ Å, $b = 13.602$ Å, $c = 17.239$ Å; $\alpha = 97.87°$, $\beta = 93.30°$, $\gamma = 91.83°$	$1,6\text{-}DAHH_2$	3D, 20MR	582
$[C_6H_{21}N_4]_4[Zn_7(PO_4)_6]_3$	$R\bar{3}$	$a = b = 13.609$ Å, $c = 15.278$ Å; $\alpha = \beta = 90°$, $\gamma = 120°$	$TRENH_3$	3D, CHA	585
$[C_2H_{10}N_2]_{0.5}[ZnPO_4]$	$C2/c$	$a = 14.772$ Å, $b = 8.827$ Å, $c = 10.107$ Å; $\alpha = \gamma = 90°$, $\beta = 131.98°$	enH_2	3D, GIS	588
$[C_8H_{28}N_5][Zn_5(PO_4)_5] \cdot H_2O$	$C2/c$	$a = 14.018$ Å, $b = 13.479$ Å, $c = 14.278$ Å; $\alpha = \gamma = 90°$, $\beta = 90.466°$	$TEPAH_5$	3D, THO	590

Table 4. Continued

formula	SG[a]	lattice parameters	template	type	ref
$[C_3H_{12}N_2]_{0.5}[ZnPO_4]$	$P42_1/c$	$a = b = 9.902$ Å, $c = 13.420$ Å; $\alpha = \beta = \gamma = 90°$	1,3-$DAPH_2$	3D, EDI	591
$[C_5H_{12}NO][Zn(H_2PO_4)(HPO_4)]\cdot H_2O$ (MU-19)	$P2_12_12_1$	$a = 9.976$ Å, $b = 10.359$ Å, $c = 12.980$ Å; $\alpha = \beta = \gamma = 90°$	NMMORH	3D, 12MR	593
$[Co^{III}(en)_3][Zn_8(PO_4)_6Cl]\cdot 2H_2O$	$P\bar{3}c$	$a = b = 8.878$ Å, $c = 23.775$ Å; $\alpha = \beta = 90°$, $\gamma = 120°$	$Co^{III}(en)_3$	3D, 12MR	292
$[C_3H_{12}N_2]_{0.5}[ZnPO_4]$	$Pncn$	$a = 14.119$ Å, $b = 14.135$ Å, $c = 12.985$ Å; $\alpha = \beta = \gamma = 90°$	1,2-$DAPH_2$	3D, THO	596
$[C_5H_{18}N_3][Zn_3(HPO_4)_3(PO_4)]$	$P\bar{1}$	$a = 8.441$ Å, $b = 9.263$ Å, $c = 13.843$ Å; $\alpha = 81.12°$, $\beta = 83.64°$, $\gamma = 72.65°$	$AEDAPH_3$	3D, 16MR	279, 604
$[C_4H_{14}N_2][Zn_5(PO_4)_4]\cdot 1.25H_2O$	$P2_1/n$	$a = 5.16$ Å, $b = 25.075$ Å, $c = 14.986$ Å; $\alpha = \gamma = 90°$, $\beta = 92.61°$	1,4-$DABH_2$	3D, 12MR	279
$[C_6H_{22}N_4][ZnPO_4]_4$	$P\bar{1}$	$a = 9.784$ Å, $b = 10.074$ Å, $c = 8.057$ Å; $\alpha = 121.62°$, $\beta = 119.20°$, $\gamma = 98.37°$	$TETAH_4$	3D, GIS	601
$[C_4H_{12}N]_2[Zn_3(HPO_4)_4]$	$Fddd$	$a = 9.203$ Å, $b = 15.776$ Å, $c = 31.587$ Å; $\alpha = \beta = \gamma = 90°$	TMA	3D, GIS-related	602
$[C_4H_{12}N_2][Zn_2(HPO_4)_3]$	$P2_1/c$	$a = 12.829$ Å, $b = 26.611$ Å, $c = 8.275$ Å; $\alpha = \gamma = 90°$, $\beta = 96.82°$	$PIPH_2$	3D, SoD-related	607
$[C_4H_{12}N_2][Zn_2(H_{1.5}PO_4)_2(PO_4)]$	$C2/c$	$a = 13.416$ Å, $b = 12.860$ Å, $c = 8.226$ Å; $\alpha = \gamma = 90°$, $\beta = 94.71°$	$PIPH_2$	3D, SoD-related	607
$[C_6H_{16}N_2]_{0.5}[C_5H_{14}N_2][Zn_6(H_2O)(PO_4)_5]$	$P\bar{1}$	$a = 9.984$ Å, $b = 12.354$ Å, $c = 12.834$ Å; $\alpha = 88.32°$, $\beta = 74.57°$, $\gamma = 75.81°$	DPIPH $_2$, $NPIPH_2$	3D, 16,10,8MR	608
$[C_4H_{14}N_2][Zn_5(H_2O)(PO_4)_4]$	$Pna2_1$	$a = 20.794$ Å, $b = 5.227$ Å, $c = 17.963$ Å; $\alpha = \beta = \gamma = 90°$	$N,N'DMenH_2$	3D, 10MR	608, 622
$[C_2H_8N][H_3O][Zn_3(HPO_4)_3(PO_4)]\cdot H_2O$	$P2_1/c$	$a = 12.653$ Å, $b = 5.191$ Å, $c = 21.146$ Å; $\alpha = \gamma = 90°$, $\beta = 95.09$	DMAH	3D, 16MR	281
$[C_2H_8N][H_3O][Zn_4(H_2O)(PO_4)_3]\cdot H_2O$	$Pnn2$	$a = 15.284$ Å, $b = 17.726$ Å, $c = 5.188$ Å; $\alpha = \beta = \gamma = 90°$	DMAH	3D, 8MR	281
$[C_3H_{10}N][NH_4][Zn_3(HPO_4)(PO_4)_2]$	$P\bar{1}$	$a = 5.099$ Å, $b = 10.494$ Å, $c = 12.446$ Å; $\alpha = 87.61°$, $\beta = 87.26°$, $\gamma = 89.99°$	$PrAH^+$, NH_4	3D, 8, 16MR	609
$[C_6H_{20}N_3][Zn_3(H_2PO_4)(HPO_4)_2(PO_4)]\cdot H_2O$	$P\bar{1}$	$a = 8.482$ Å, $b = 9.133$ Å, $c = 14.796$ Å; $\alpha = 90.38°$, $\beta = 100.12°$, $\gamma = 107.04°$	DPTAH $_3$	3D, 10, 16MR	609
$[C_6H_{20}N_3][Zn_3(HPO_4)_3(PO_4)]$	Cc	$a = 15.109$ Å, $b = 8.840$ Å, $c = 17.263$ Å; $\alpha = \gamma = 90°$, $\beta = 114.54°$	$DPTAH_3$	3D, 8MR	609
$[C_5H_{14}N_2][Zn_2(HPO_4)_3]\cdot H_2O$	$P2_1$	$a = 8.031$ Å, $b = 10.248$ Å, $c = 10.570$ Å; $\alpha = \gamma = 90°$, $\beta = 109.65°$	$HPIPH_2$	3D, 8MR	610
$[C_5H_{16}N_2][Zn(PO_4)_2]\cdot 2H_2O$	$C2/c$	$a = 14.224$ Å, $b = 13.491$ Å, $c = 13.999$ Å; $\alpha = \gamma = 90°$, $\beta = 90.169°$	$N,NDAPH_2$	3D, THO	611
$Zn_{0.5}(H_2PO_4)\cdot 0.5H_2O$ (FJ-13)	$Fd2d$	$a = 9.881$ Å, $b = 15.189$ Å, $c = 16.004$ Å; $\alpha = \beta = \gamma = 90°$		3D, 12MR	612
$[C_5H_{12}NO]_4[Zn_4P_8O_{32}H_{12}]$ (MU-21)	$P2_12_12_1$	$a = 10.42$ Å, $b = 10.452$ Å, $c = 11.622$ Å; $\alpha = \beta = \gamma = 90°$	NMMORH	3D, 12MR	615
$[C_3H_{12}N_2][Zn_2(HPO_4)_3]$	$P2_1/c$	$a = 15.486$ Å, $b = 9.815$ Å, $c = 9.8365$ Å; $\alpha = \gamma = 90°$, $\beta = 105.99°$	1,2-$DAPH_2$	3D, 8,12MR	616
$[CH_6N][Zn_4(PO_4)_3]$	$Pbca$	$a = 14.680$ Å, $b = 10.12$ Å, $c = 16.602$ Å; $\alpha = \beta = \gamma = 90°$	MAH	3D, 8MR	617
$[CH_6N]_2[Zn_5(PO_4)]$	$P2_12_12_1$	$a = 7.265$ Å, $b = 13.432$ Å, $c = 18.078$ Å; $\alpha = \beta = \gamma = 90°$	MAH	3D, 8MR	617
$[C_6H_{18}N_3][Zn_3(HPO_4)_3(PO_4)]$ (FJ-11)	$P\bar{1}$	$a = 8.281$ Å, $b = 9.138$ Å, $c = 13.346$ Å; $\alpha = 83.77°$, $\beta = 84.446°$, $\gamma = 78.025°$	$AEPIPH_3$	3D, 16MR	619
$[Co(dien)_2][H_3O][Zn_2(HPO_4)_4]$	$Fdd2$	$a = 9.271$ Å, $b = 19.781$ Å, $c = 27.045$ Å; $\alpha = \beta = \gamma = 90°$	$Co(dien)_2^{3+}$	3D (helical)	620
$[C_6H_{16}N_2][Zn_2(HPO_4)_3]$	$P2_1/n$	$a = 8.693$ Å, $b = 14.439$ Å, $c = 12.649$ Å; $\alpha = \gamma = 90°$, $\beta = 96.418°$	$DPIPH_2$	3D, 8MR	*d*
$[NH_4][H_3O][Zn_4(PO_4)_3]_2\cdot H_2O$	$P\bar{1}$	$a = 5.040$ Å, $b = 9.584$ Å, $c = 13.117$ Å; $\alpha = 101.094°$, $\beta = 100.93°$, $\gamma = 103.598°$	NH_4, H_3O^+	3D, 8MR	622

[a] SG = space group. [b] Zhang, X.-M.; Bai, C.-J.; Zhang, Y.-L.; Wu, H.-S. Can. J. Chem. 2004, 82, 616. [c] Wang, Y.; Yu, J.; Li, Y.; Shi, Z.; Xu, R. Chem.—Eur. J. 2003, 9, 5048. [d] Song, Y.; Yu, J; Li, Y.; Zhang, M.; Xu, R. Eur. J. Inorg. Chem. 2004, 3718.

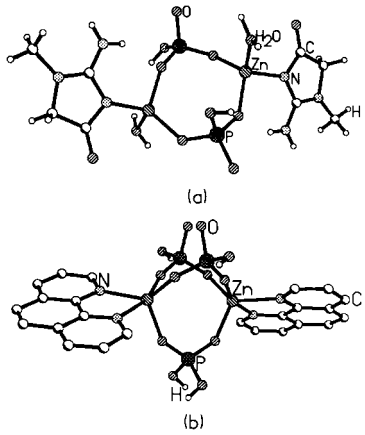

Figure 59. Monomeric zinc phosphate structures: (a) single S4R unit with bound amine;[613] (b) a molecular 4=1 unit.[618]

type chain indicates that Zn does not favor octahedral coordination in the templated phosphate family. Other than the corner-shared chain and ladder structures, there are a few other 1D structures shown in Figure 60. The structure $Na_2Zn(PO_4)(OH)\cdot 7H_2O$[531] consists of infinite corner-linked ZnO_4 tetrahedra, each bridged by a PO_4 group, thus forming a chain of corner-shared three-rings (Figure 60a). The structures of $[C_6H_{14}N_2][Zn(H_2PO_4)_2(HPO_4)]$[537] and $Zn(C_4H_6N_2)(HPO_4)$[589] are similar (Figure 60b,c) where Zn- and P-centered polyhedra are alternately corner-shared. In the former, there are two dangling H_2PO_4 groups from the Zn center, while for the latter, 4-methylimidazole binds to Zn. The structures of $[CH_6N_3]_6[Zn_2(OH)(PO_4)_3]$[548] and $[Zn(phen)_2](HPO_4)(H_2PO_4)$[618] are interesting. In the former, Zn centers of 4=1 SBUs are connected by a −OH bridge, while in the latter H_2PO_4 groups connect the S4R units to form the chain (Figure 60d,e).

Two-Dimensional Structures. The 2D sheet structures of the ZnPO family present rich variety, including strictly alternating ZnO_4 and PO_4 tetrahedra with various nets and Zn−O−Zn units linked by a tricoordinated oxygen from the phosphate. It is difficult to discuss all the 2D structure types (see Table 4), and we will limit ourselves to a few typical ones. Among the structures with strictly alternating ZnO_4 and PO_4 tetrahedra, the commonly found one is that with a Zn/P ratio of 2/3 where a 12-membered bifurcated aperture is formed when the HPO_4 groups cross-link zigzag ladders (Figure 47b).[295,562,564,570,575] Then, there are also structures with 4.8^2[291,557,558,604] and $4.6.8^2$[292] nets. Among the sheet structures with a tricoordinated oxygen, a stoichiometry of $Zn_6(HPO_4)_2(PO_4)_4$ with a Zn/P ratio of unity is the most common[579,585,586,594,597,624] (Figure 61). This structure is formed by the joining of strip-like quasi-1D structures (Figure 62) formed by corner-shared four-membered rings connected via a three-coordinated oxygen. The strip-like quasi-1D structure itself has been isolated in the cobalt phosphate family.[280] The sheet structure can be described in terms of columns formed by Zn_5P_4 cage-like units.[597] Some of the sheet structures contain the ladder unit, joined variously in the presence of a tricoordinated oxygen to give new topologies[563,569,588,605] (Figure 63).

Three-Dimensional Zinc Phosphates. The 3D open-framework structures of the ZnPO family are exotic and diverse (see Table 4). The Zn atom is tetrahedrally coordinated in these structures most of the time. But unlike the AlPO family, there is frequent occurrence of Zn−O−Zn linkages forbidden in the case of Al by the Lowenstein

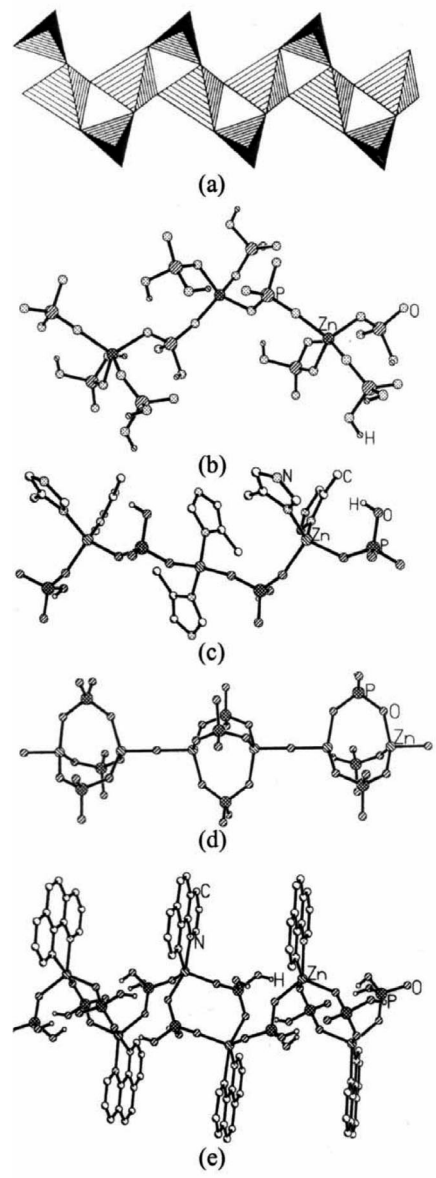

Figure 60. One-dimensional structures in the family of zinc phosphates: (a) chain of corner-shared three-rings;[531] (b, c) alternating Zn and P tetrahedra;[537,589] (d) chain of 4=1 SBUs;[548] (e) connected S4R units.[618] Partly reprinted with permission from ref 531. Copyright 2002 American Chemical Society.

rule.[266] In addition, the ratio of Zn/P is often less than one, because of the interruption caused by the terminal OH groups of the PO_4 moiety or terminal H_2O attached to the Zn atom. These are probably the reasons why Zn forms such a large variety of structures including zeotypes, interrupted frameworks, large pore structures, helical structures, and so on. Unfortunately, these frameworks are not stable once the template is removed, except in one or two cases,[542] where the structures have inorganic templates.

A large number of ZnPO structures analogous to zeolites, for example, SOD,[298,527] ABW,[527,551] ZEO-X,[527,528] EDI,[565,591] CHA,[574,585] GIS,[295,577,584,588,601] and THO[577,590,596,611] have been discovered with various templates. There are also 3D ZnPO structures related to gismondine[602] and sodalite.[607] The first chiral zeotype framework, $NaZnPO_4\cdot H_2O$,[541] called CZP-type, was discovered in the ZnPO family. Other than the zeotype chiral frameworks, there are structures with helical channels,[559,587,612,620] among which $[Co(dien)_2][H_3O][Zn_2(HPO_4)_4]$[620] is templated by a chiral coordination

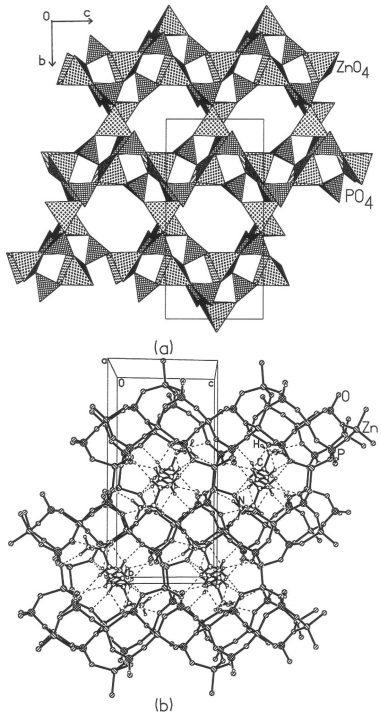

Figure 61. A common layer topology in the zinc phosphate family.[586]

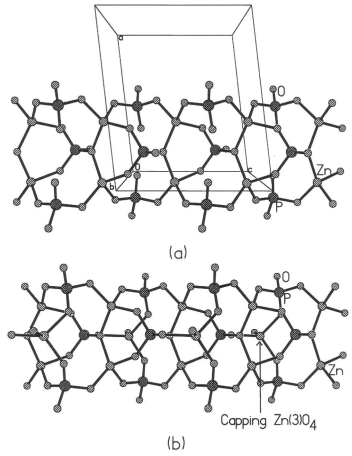

Figure 62. Strip-like features in the layered zinc phosphate shown in Figure 61.

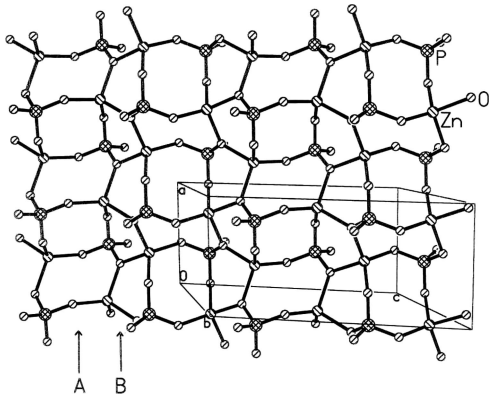

Figure 63. Zinc phosphate layer showing the presence of a four-ring ladder and a three-ring chain.[588]

complex (Figure 64) and has one of the lowest framework densities (FD = 9.7). The formation of extra-large pore

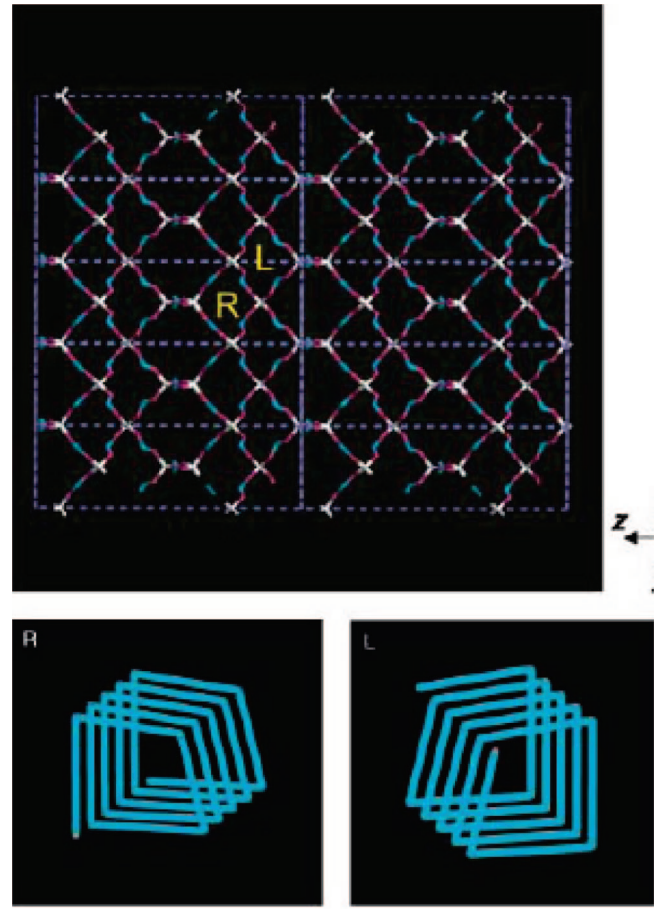

Figure 64. The ZnPO framework (top) viewed along the [110] direction showing the 12-membered ring channels and two types of helical channels and (bottom) the right-handed (R) and the left-handed (L) helical channels (color code: Zn white, P light blue, O pink). Reprinted with permission from ref.[620] Copyright 2003 Wiley-VCH.

channels bound by 16,[279,281,295,604,609,619] 18,[544] 20,[582] and 24[566] T-atoms (Zn and P) indicate that the ZnPO family has the potential to form many such structures with large channels. It is interesting that unlike the GaPO family, there is no commonality between the structures that can be described by the SBU concept. Most of these structures are described by infinite units such as a c.s. chain (Figure 65a) or a ladder (Figure 65b) connecting the layers to form the extra-large pore channels except in cases such as $[C_6H_{16}N_2]$-$[Zn_3(HPO_4)(PO_4)_2]\cdot 2H_2O$,[566] where an oligomeric building unit is present. It is interesting that several amines (TETA, en, and 1,3-DAP) form GIS-type or GIS-related structures. In en-GIS, the amine sits in the $[4^68^4]$ cage (Figure 66a), while in TETA-GIS, the amine extends from the cage to the channel (Figure 66b). It is unclear what role the amine plays in determining the formation of the GIS structure.

3.5.5. Beryllium Phosphates

An interesting feature associated with Be-containing open-framework structures is the tendency to form a three-ring unit as in lovdarite (LOV).[270] This is considered to be a necessary condition to form low framework density structures.[626] Due to the toxicity of Be, efforts to prepare these materials have been limited, and there are no reports of organically templated 0-, 1-, and 2D structures. After the

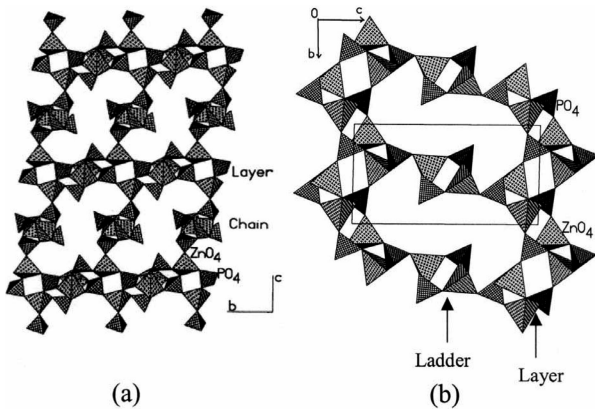

Figure 65. Three-dimensional zinc phosphates viewed along the *a*-axis where layers are connected by (a) c.s. chain[604] and (b) ladder[295] to form the 16-membered channel. Reference 604 — Reproduced by permission of the Royal Society of Chemistry.

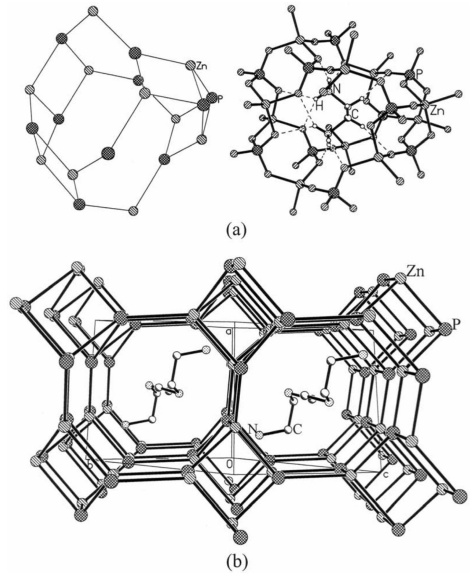

Figure 66. Location of the amine inside the GIS zinc phosphate with (a) en in the cage[588] and (b) TETA across the channel.

discovery of the zeotype open-framework structures of BePO by the groups of Meier[627] and Stucky,[527] a number of open-framework BePO structures have been reported.[528,551,628–633] Interestingly, the majority of these are templated by ammonium or inorganic cations, analogous to aluminosilicate zeolites that include ABW, ANA, EDI, FAU, GIS, LOS, MER, RHO, and SOD, as well as the new zeotype topology BPH[270] (many of these structures are listed in ref 631). The greater propensity to form a zeolitic structure in the BePO family probably lies in the fact that Be is always tetrahedrally coordinated in its oxygen environment and its size (0.27 Å) is close to Si^{4+} (0.24 Å) in the tetrahedral coordination. There are a few organically templated open-framework BePO's, dominated by zeolitic structures, (e.g., GME,[632] GIS,[632,633] and the novel structure described in ref 628).

3.5.6. Tin Phosphates

The first open-framework $SnPO_4$ was reported by Cheetham and co-workers.[634] Following this discovery, a number of organically templated SnPO's have been discovered, which include 0-, 1-, 2-, and 3D structures (Table 5).[280,570,634–647] Unlike other main block open-framework phosphates, the Sn(II) phosphates contain pyramidal SnO_3 building units, which share corners with three PO_4 units, and the lone pair of electrons presumably assumes the fourth vertex of the pseudotetrahedron. The presence of the square-pyramidal SnO_4 unit giving rise to Sn−O−Sn linkages is also encountered. To date, there is only one report of a Sn(IV) phosphate with an organic template, where Sn(IV) is octahedrally coordinated.[647]

Zero-Dimensional Structures. One of the first examples of a 0D monomeric structure was discovered in the organically templated SnPO family. The structure is made up of alternate Sn and P polyhedra, forming a S4R unit with dangling HPO_4 groups from the Sn centers,[640] similar to the ZnPO monomer shown in Figure 45. However, while the ZnPO monomer contains two dangling HPO_4 groups, the SnPO monomer has only one dangling HPO_4.

One-Dimensional Structures. There are two 1D structures in the organically templated SnPO family, of which one is related to the ladder structure[641] while the other one is complex.[647] The ladder is special in that it does not have any dangling HPO_4 or H_2PO_4 units from the metal sites. In the other 1D structure, a μ_3-O atom joins the Sn sites giving rise to an infinite chain of trimers of Sn(IV)−O octahedra (Figure 67).[647]

Two-Dimensional Structures. There are three 2D structures reported in the SnPO family. One of them has a complex structure formed by connecting the cage-like units (Figure 68a).[643] The other two structures having a Sn/P ratio of 1:1 and with the general formula of $[SnPO_4]^-$ form very simple nets including 6·6 and 4·8 rings[280,570,639,641,645] (Figure 68b,c).

Three-Dimensional Structures. The majority of open-framework 3D structures of the SnPO family have a Sn/P ratio of 4:3 with the general formula of $[Sn_4(PO_4)_3]^-$ and are invariably built from corner-sharing SnO_3 trigonal pyramidal and PO_4 tetrahedral units. There are a few oxy or hydroxy Sn(II) phosphates where the Sn/P ratio is 2:1[636] or 3:2,[638] which show the presence of Sn−O−Sn linkages with a square-pyramidal SnO_4 unit in addition to a SnO_3 unit. No extra-large pore channels are found in open-framework SnPO's, and they are mostly bound by 8-, 10- and 12-membered rings (see Table 5).

3.5.7. Other Main Group Open-Framework Phosphates

Magnesium. To our knowledge, there is a report of a 2D layered structure[648] where Mg is octahedrally coordinated and of one 3D open-framework zeotype structure of DFT topology.[649]

Antimony. Cheetham and co-workers[650] have reported the first open-framework Sb(III) phosphate. Like SnPO, the lone pair of electrons is associated with the Sb(III)-centered polyhedra. The framework of $[H_3N(CH_2)_2NH_3]_{1.5}$-$[(SbO)_2(SbF)_2(PO_4)]$ is based upon a network of SbO_5E, SbO_4FE (pseudo-octahedra, E = lone pair), SbO_4E and SbO_3FE (pseudo-*tbp*), and PO_4 tetrahedra with 8- and 12-membered channels.

Cadmium. Although Cd and Zn are in the same group, there is no report of an open-framework cadmium phosphate structure either by organic or by inorganic templating. However, there is one recent report of an 1D cadmium phosphate where 2,2′-Bpy chelates the metal.[651] Alkali metal intercalated layered cadmium phosphates have been reported by Rao and co-workers.[652]

Table 5. Lattice Parameters, Templates, and Dimensionalities of the Various Templated Tin Phosphates Reported in the Literature

formula	SG[a]	lattice parameters	template	type	ref
$[C_6H_{21}N_4][Sn(PO_4)(HPO_4)]\cdot 4H_2O$	$P\bar{1}$	$a = 9.579$ Å, $b = 10.507$ Å, $c = 10.976$ Å; $\alpha = 72.93°$, $\beta = 78.03°$, $\gamma = 69.82°$	$TRENH_3$	0D	640
$[C_6H_{18}N_2][Sn_2(PO_4)_2]$	$C2/m$	$a = 17.938$ Å, $b = 4.883$ Å, $c = 10.814$ Å; $\alpha = \gamma = 90°$, $\beta = 116.90°$	N,N′-$DEenH_2$	1D ladder	641
$[C_2H_8N_2]_{2.5}[Sn_3^{IV}O_2(H_2O)(HPO_4)_4]\cdot 2H_2O$ (MIL-76)	$P2_1/c$	$a = 11.152$ Å, $b = 22.193$ Å, $c = 9.532$ Å; $\alpha = \gamma = 90°$, $\beta = 95.57°$	en	1D	647
$[NH_4]_2[Sn_3O(PO_4)_2]\cdot H_2O$	$Cmc2_1$	$a = 7.240$ Å, $b = 19.552$ Å, $c = 8.438$ Å; $\alpha = \beta = \gamma = 90°$	NH_4	2D	643
$[C_2H_{10}N_2][Sn_2(PO_4)_2]\cdot H_2O$	$P2_1/c$	$a = 9.411$ Å, $b = 8.5990$ Å, $c = 15.992$ Å; $\alpha = \gamma = 90°$, $\beta = 100.00°$	enH_2	2D	639
$[C_6H_{14}N_2][Sn_2(PO_4)_2]\cdot H_2O$	$C2/c$	$a = 18.539$ Å, $b = 8.105$ Å, $c = 10.203$ Å; $\alpha = \gamma = 90°$, $\beta = 98.90°$	$DABCOH_2$	2D	641
$[C_3H_{12}N_2][Sn(PO_4)]_2$	$C2/c$	$a = 18.096$ Å, $b = 7.888$ Å, $c = 9.150$ Å; $\alpha = \gamma = 90°$, $\beta = 111.84°$	1,3-$DAPH_2$	2D	670, *b*
$[NH_4][Sn(PO_4)]$	$P2_1/c$	$a = 6.520$ Å, $b = 9.479$ Å, $c = 8.072$ Å; $\alpha = \gamma = 90°$, $\beta = 90.95°$	NH_4	2D	645
$[C_{14}H_{12}N_2][Sn_2(PO_4)_2]$	$P2_1/c$	$a = 9.064$ Å, $b = 7.811$ Å, $c = 10.067$ Å; $\alpha = \gamma = 90°$, $\beta = 115.26°$	$PIPH_2$	2D	280
$[C_2H_{10}N_2]_{0.5}[Sn_4(PO_4)_4]$	$Pnna$	$a = 9.787$ Å, $b = 15.068$ Å, $c = 20.852$ Å; $\alpha = \beta = \gamma = 90°$	enH_2	3D, 8MR	634
$[C_4H_{14}N_2]_{0.5}[Sn_4(PO_4)_3]$	$P2_1/c$	$a = 10.016$ Å, $b = 7.888$ Å, $c = 20.119$ Å; $\alpha = \gamma = 90°$, $\beta = 101.24°$	1,4-$DABH_2$	3D, 8,12MR	635
$[NH_4][(Sn_3O)_2(PO_4)_3]$	$Pbcn$	$a = 6.796$ Å, $b = 19.600$ Å, $c = 12.577$ Å; $\alpha = \beta = \gamma = 90°$	NH_4	3D, 10MR	636
$[C_5H_{16}N_2]_{0.5}[Sn_4(PO_4)_3]\cdot 2H_2O$	$P\bar{1}$	$a = 9.417$ Å, $b = 9.754$ Å, $c = 11.002$ Å; $\alpha = 80.51°$, $\beta = 71.64°$, $\gamma = 61.68°$	1,3-$DAPnH_2$	3D, 8MR	637
$[C_6H_{18}N_2]_{0.5}[Sn_3(OH)(PO_4)_2]$	$P2_1/n$	$a = 9.315$ Å, $b = 16.806$ Å, $c = 9.513$ Å; $\alpha = \gamma = 90°$, $\beta = 111.03°$	1,6-$DAHH_2$	3D, 8MR	638
$[C_8H_{22}N_2]_{0.5}[Sn_3(OH)(PO_4)_2]$	$Pbca$	$a = 10.390$ Å, $b = 16.087$ Å, $c = 18.717$ Å; $\alpha = \beta = \gamma = 90°$	1,8-$DAOH_2$	3D, 8MR	638
$[CH_6N_3][Sn_4(PO_4)_3]$	$P4_3$	$a = b = 8.888$ Å, $c = 20.603$ Å; $\alpha = \beta = \gamma = 90°$	GUANH	3D, 12MR	642
$[C_3H_{12}N_2]_{0.5}[Sn_4(PO_4)_3]\cdot H_2O$	$P2_1/c$	$a = 7.326$ Å, $b = 23.614$ Å, $c = 9.081$ Å; $\alpha = \gamma = 90°$, $\beta = 102.8°$	1,2-$DAPH_2$	3D, 8MR	644
$[NH_4][Sn_4(PO_4)_3]$	$P6_3$	$a = b = 9.697$ Å, $c = 8.0903$ Å; $\alpha = \beta = 90°$, $\gamma = 120°$	NH_4	3D, 12MR	645
$[C_4H_{12}N_2]_{0.5}[Sn_4(PO_4)_3]$	$P2_1/c$	$a = 7.088$ Å, $b = 23.336$ Å, $c = 9.043$ Å; $\alpha = \gamma = 90°$, $\beta = 103.34°$	$PIPH_2$	3D, 8MR	646

[a] SG = space group. [b] Vaidhyanathan, R.; Natarajan, S. J. Mater. Chem. 1999, 9, 1807.

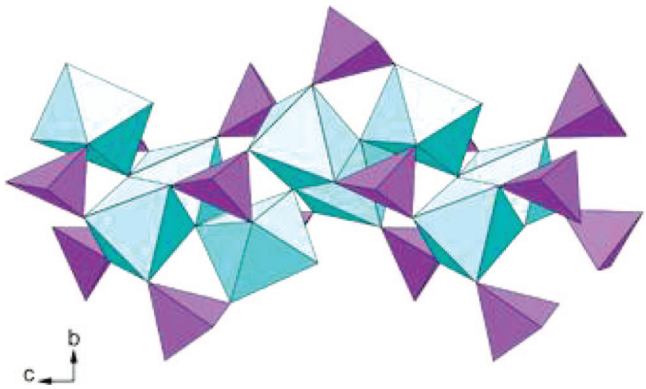

Figure 67. Complex 1D chain in a tin(IV) phosphate. Reference 647 — Reproduced by permission of the Royal Society of Chemistry.

3.6. Transition Metal Phosphates

Once it was realized that open-framework phosphates were not restricted to tetrahedral coordination of the metal and that transition metals can partly substitute Al in zeolitic AlPO frameworks,[653] efforts were initiated to form open-framework phosphates exclusively with transition metals. The discovery of an amazing iron phosphate mineral *cacoxenite*,[654] $[AlFe_{26}(OH)_{12}(PO_4)_{17}(H_2O)_{24}]\cdot 51H_2O$, a large pore open-framework structure with a free diameter of 14.2 Å, indicated that octahedral−tetrahedral open-framework structures can be formed with transition metals by hydrothermal reactions. There have been attempts to synthesize open-framework transition metal phosphates with properties related to redox-based catalysis, magnetism, and so on.

3.6.1. Molybdenum Phosphates

Molybdenum is well known to assume various oxidation states ranging from +6 to +3 forming MoO_6 octahedra in an oxo environment. Mo in the +6 state has a d^0 configuration and is not as interesting as Mo in the +5 state, which has unpaired d-electrons. Mo in +5 is characterized by short M═O bonds, leading to distorted MoO_6 octahedra, formation of dimers through Mo−Mo linkages, and a greater tendency of isopolymerization of Mo-centered polyhedra through Mo−O−Mo linkages. Several templated molybdenum phosphates have been synthesized hydrothermally, primarily by the groups of Haushalter.[655–665] The first organically templated open-framework molybdenum phosphate (MoPO) made under hydrothermal conditions by Haushalter et al.,[655] $(Me_4N)_{1.3}(H_3O)_{0.7}[Mo_4O_8(PO_4)_2]\cdot 2H_2O$, was also the first transition metal open-framework phosphate. It is to be noted here that the chemistry of reduced molybdenum phosphates has been studied by several groups, specially by Raveau and Haushalter, and their focus mainly pertained to solid-state high-temperature synthesis (>700°C). Many of the high-temperature materials incorporated inorganic cations into the framework, rendering them condensed most of the time. Reduced molybdenum phosphates have been reviewed by Haushalter[666] and Raveau[667] and briefly by Férey.[262] We shall briefly examine the hydrothermally synthesized Mo-PO's. In Table 6, we have listed the various molybdenum phosphates according to dimensionality.

Zero-Dimensional Structures. As mentioned earlier, Mo has a tendency to polymerize to Mo−O−Mo linkages; the 0D structures are based on multinuclear Mo−O clusters. Thus Keggin ions and related species are omnipresent, and these are well described by Pope and Müller.[668] There are a

Table 6. Lattice Parameters, Templates, and Dimensionalities of the Various Templated Molybdenum Phosphates Reported in the Literature

formula	SG[a]	lattice parameters	template	type	ref
$[PPh_4]_2[(H_3O)_2NaMo_6P_4O_{24}(OH)_7]\cdot 5H_2O$	$P\bar{1}$	a = 17.314 Å, b = 18.181 Å, c = 13.232 Å; α = 110.50°, β = 93.29°, γ = 63.42°	Na^+, PPh_4^+, H_3O^+	0D cluster	656
$[Et_4N]_6[Na_{14}Mo_{24}P_{17}O_{97}(OH)_{31}]\cdot xH_2O$	$Pn3$	a = b = c = 20.404 Å; α = β = γ = 90°	TEA	0D (cluster)	657
$(Et_4N)_2[Mo_4O_8(PO_4)(H_{1.5}PO_4)_2]\cdot 2H_2O$	$P2_12_12$	a = 12.235 Å, b = 19.141. Å, c = 7.497 Å; α = β = γ = 90°	TEA	1D	664
$[C_4H_{12}N_2][MoO_2(H_2PO_4)(PO_4)]\cdot H_2O$	$P\bar{1}$	a = 6.425 Å, b = 8.686 Å, c = 12.451 Å; α = 80.54°, β = 75.14°, γ = 70.16°	$PIPH_2$	1D ladder	665
$[N(C_3H_7)_4][NH_4][(MoO)_4O_4(PO_4)_2]$	$P\bar{4}2m$	a = b = 7.512 Å; α = β = γ = 90°	TPA, NH_4	2D	658
$Na_3[Mo_2O_4(HPO_4)(PO_4)]\cdot 2H_2O$	$P2_1/n$	a = 8.128 Å, b = 13.230 Å, c = 11.441 Å; α = γ = 90°, β = 108.84°	Na^+	2D	659
$(Me_4N)_{1.3}(H_3O)_{0.7}[Mo_4O_8(PO_4)_2]\cdot 2H_2O$	$I\bar{4}3m$	a = b = c = 15.048 Å; α = β = γ = 90°	TMA, H_3O^+	3D	655
$Mo_8O_{12}(PO_4)_4(HPO_4)_2\cdot 13H_2O$	$P\bar{1}$	a = 10.466 Å, b = 12.341 Å, c = 8.228 Å; α = 94.75°, β = 111.46°, γ = 89.48°		3D	660
$CH_3NH_3[Mo_2O_2(PO_4)_2(H_2PO_4)]$	$C2$	a = 9.126 Å, b = 9.108 Å, c = 8.654 Å; α = γ = 90°, β = 114.06°	MAH	3D	661
$[NH_4][Mo_2P_2O_{10}]\cdot H_2O$	$P2_1/n$	a = 9.78 Å, b = 9.681 Å, c = 9.884 Å; α = γ = 90°, β = 102.17°	NH_4	3D	662
$[NH_4]_3[Mo_4P_3O_{16}]$	$P\bar{4}3m$	a = b = c = 7.736; α = β-γ = 90°	NH_4	3D	663

[a] SG = space group.

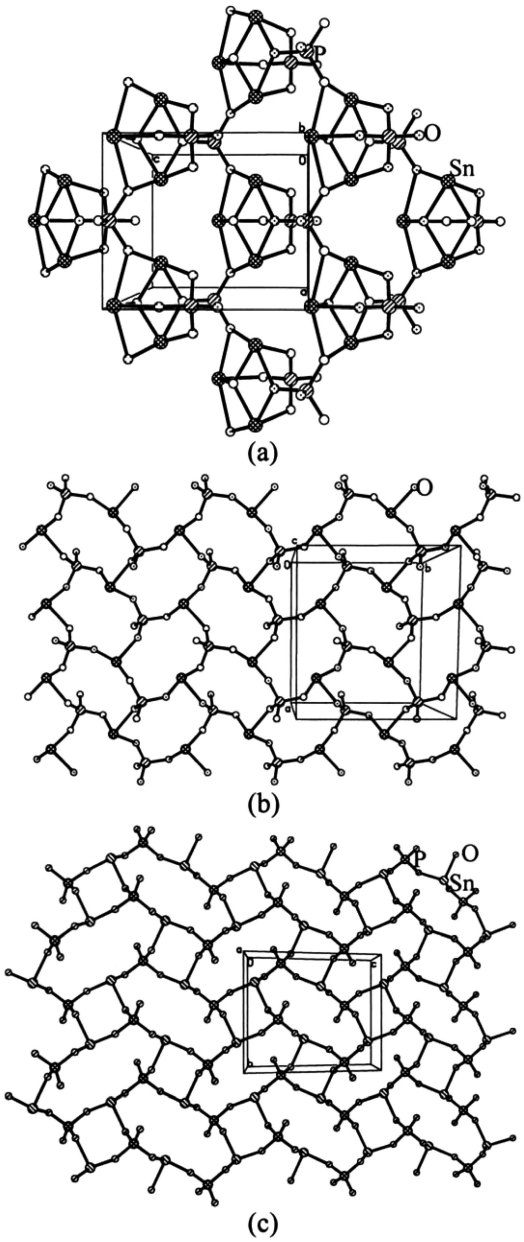

Figure 68. Layered structures in the tin(II) phosphate family: (a) cage-like units joined to form the layer;[643] (b) alternate Sn and P forming a 6·6 net;[639] (c) alternate Sn and P forming a 4·8 net.[280]

few 0D clusters (e.g., $Cs_2[Mo_2(HPO_4)_4(H_2O)_2]$[669]), containing the Mo−Mo triple bond. $(PPh_4)_2[(H_3O)_2NaMo_6P_4O_{24}(OH)_7]\cdot 5H_2O$[656] and $[Et_4N]_6[Na_{14}Mo_{24}P_{17}O_{97}(OH)_{31}]\cdot xH_2O$[657] contain the Mo_6P_4 unit (Figure 69). The cohesion between the cluster units is ensured by alkali cations.

One-Dimensional Structures. The 1D structures of molybdenum phosphates are mainly heterometallic where the Mo−O clusters (like the one in Figure 69) are joined by some other transition metal to form the chain. However, $[Et_4N]_2[Mo_4O_8(PO_4)(H_{1.5}PO_4)_2]\cdot 2H_2O$[664] is an example of a pure Mo−O cluster forming the 1D structure. The Mo_4O_8 cubes are connected by PO_4 tetrahedra to form the 1D chain, with two terminal $H_{1.5}PO_4$ groups (Figure 70a). There is a recent example of a 1D MoPO chain, where Mo- and P-centered polyhedra alternate to a form ladder-like 1D structure (Figure 70b).[665] In the ladder structure, $[C_4H_{12}N_2][MoO_2(H_2PO_4)(PO_4)]\cdot H_2O$, the coordination of Mo is six with two short terminal M═O bonds and a dangling

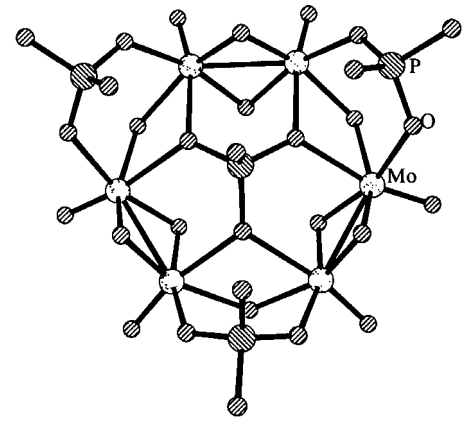

Figure 69. Molecular Mo_6P_4 unit in the MoPO family.[656]

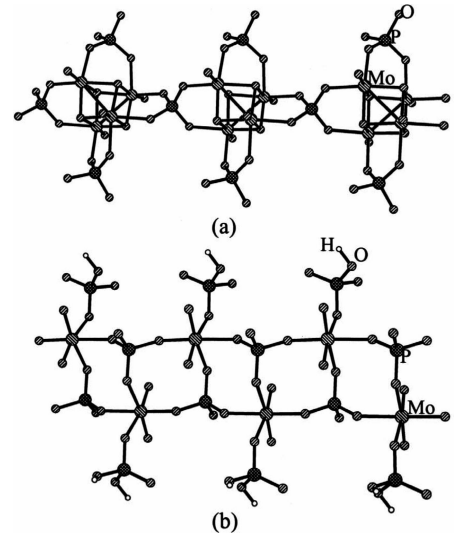

Figure 70. Two 1D structures in the MoPO family: (a) cubane-like units connected to form the chain;[664] (b) four-ring ladder.[665]

H_2PO_4 attached to Mo. This is a rare example of an octahedral−tetrahedral ladder structure (compare Figure 70b with Figure 46a).

Two-Dimensional Structures. There are several 2D MoPO's synthesized hydrothermally, with certain common building units. For example, $[N(C_3H_7)_4][NH_4][Mo_4O_8(PO_4)_2]$[658] is built from the cubic building block $[Mo_4O_8(PO_4)_2]^{2-}$, similar to the one observed in the 1D structure.[664] On the other hand, $Na_3[Mo_2O_4(HPO_4)(PO_4)]\cdot 2H_2O$[659] comprises an edge-shared dimeric Mo_2O_{10} building block with a Mo−Mo bond.

Three-Dimensional Structures. Several open-framework MoPO's have been synthesized hydrothermally as given in Table 6. The first MoPO,[655] built from the cubic building block displays interesting reversible water absorption isotherms. $Mo_8O_{12}(PO_4)_4(HPO_4)_2\cdot 13H_2O$[660] and $(NH_4)[Mo_2P_2O_{10}]\cdot H_2O$,[662] built from a Mo_4 unit, also exhibit reversible water absorption isotherms. In all these structures, Mo is in the +5 oxidation state.

3.6.2. Vanadium Phosphates

Vanadium phosphates have been extensively investigated, not only due to their catalytic activity[670] but also due to their rich structural chemistry. The diverse structural variety arises due to the ability of vanadium to exhibit variable oxidation states (+3, +4, and +5) and to adopt different coordination

geometries (tetrahedral, square-pyramidal, *tbp*, and octahedral).[671] Apart from the catalytic activity, layered compounds such as $VO(PO_4)\cdot 2H_2O$ are interesting due to their potential uses as solid sorbents and ion exchangers.[672] A large number of vanadium phosphates have been synthesized by solid-state methods, often incorporating inorganic cations. Like the molybdenum phosphates, condensed vanadium phosphates exhibit various vanadium subnetworks wherein the VO_x polyhedra are isolated, corner-shared, edge-shared into a V_xO_y oligomeric unit, or connected into infinite chains and are then linked to PO_4 tetrahdera.[673] Haushalter and co-workers,[674] successfully synthesized the open-framework VPO $[(CH_3)_2NH_2]K_4[V_{10}O_{10}(H_2O)_2(OH)_4(PO_4)_7]\cdot 4H_2O$ under hydrothermal conditions in the presence of an organic amine. Since then several VPO systems containing organic amines and possessing 0-, 1-, 2-, and 3D structures have been discovered (Table 7).[310,674–703]

Zero-Dimensional Structures. The 0D structures, as in the MoPO family, are hetero-polyanionic clusters as exemplified by $(H_3O)_2[V_4(HPO_4)(PO_4)_3O_6F]_2[NC_7H_{14}]_6$[689] and $[C_4H_{10}NO]_6[V^{IV}V^{V}O_{32}(OH)_6(PO_4)]\cdot 2H_2O$.[699] The former is an octameric anion built from the tetrahedral arrangement of $V^{V}O_5F$ octahedra sharing edges and vertices capped by phosphorous tetrahedra, while the latter is a bicapped Keggin cluster. There are several Keggin-type clusters as well, but we shall not be discussing them in this review.

One-Dimensional Structures. Three organically templated 1D VPO's are known in the literature, of which one has a complicated ribbon structure, constructed from $V^{IV}O_5N$ octahedra and PO_4 tetrahedra where monoprotonated en acts as a ligand.[684] Each VO_5N octahedron shares corners in a cis disposition with two adjacent VO_5N octahedra to produce a zigzag polyhedral chain capped by PO_4 tetrahedra (Figure 71a). The other two are relatively simple, one of them being tancoite-type[691] and the other being kronkite-type[695] (Figure 71b). In the tancoite-type, V is in +3 oxidation state and the $V^{III}O_6$ octahedra are trans-corner-shared by OH bridges,[691] while in the latter $VO_5(H_2O)$ octahedra are corner-linked by bridging H_2PO_4 and HPO_4 groups to form the 1D structure[695] similar to those in kronkite, $Na_2Cu(SO_4)_2\cdot 2H_2O$.[704]

Two-Dimensional Structures. There are several organically templated 2D VPO's with different sheet structures (Table 7). The oxidation states of V can be +3,[310,694,701] +4,[678,679,683,696,698,702] +5,[693] and sometimes mixed-valent (+4/+5).[696,697,702] The VO_x polyhedra adopt *tbp*,[678,679] square-pyramidal,[683,696] and octahedral arrangements[693,698] and sometimes combinations of two, such as *tbp* and octahedral[678,697] or square-pyramidal and octahedral.[702] The majority of the sheet structures are related to the layered $VO(PO_4)\cdot xH_2O$ structure type[705] (Figure 72), where the $VOPO_4$ layers have V(+4) in the *tbp* coordination,[678,679] in the square-pyramidal coordination,[696] in the octahedral coordination,[696,698] or in defective $VOPO_4$ layers,[678] with edge-sharing of VO_6 and PO_4 tetrahedra. Other than these, there are complex V_xO_y networks formed by edge-shared VO_5 square pyramids,[683] face-shared VO_6 octahedra,[683] or a trimer[697] of V−O−V−O−V involving trigonal bypyramidal and octahedral V polyhedra. Sometimes VO_x polyhedra form infinite chains through V−O−V linkages to form a tancoite-like chain, which is then linked by the VO_5 square-pyramidal unit to form the layer.[702] In $[C_4H_{12}N_2]_2[V_4O_6H(HPO_4)_2(PO_4)_2]$, the infinite trans-corner-shared V−O−V−O chain of VO_5 square pyramids are linked by a ladder-like unit[702] to form the layer (Figure 73a). An interesting example of VO_6 octahedra forming an infinite 2D sheet is found in $[CN_3H_6][(VO_2)_3(PO_4)(HPO_4)]$,[693] where it forms a hexagonal tungsten oxide[517] sheet, popularly known as the Kagome lattice (Figure 73b).

Three-Dimensional Structures. Open-framework VPO structures are numerous and versatile. Many important 3D structures have been already discussed in an earlier review,[262] (e.g., inorganic double helices,[674] giant voids,[687] and large elliptical channels[675]). Several vanado-fluoro phosphates have been reported by the groups of Férey[681] and Haushalter.[690] There are also structures containing V−O−V−O−V trimers made up of VO_6 octahedra and VO_5 square pyramids[677,703] or V−O−V infinite chains as in $(C_4H_{12}N_{12})[VO(H_2O)_3VO(H_2O)(VO)_2(HPO_4)(PO_4)_2]$[682,688] and $(NH_4)_2[VO(H_2O)_3]_2[VO(H_2O)][(VO)(PO_4)_2]_2\cdot 3H_2O$[696] (tancoite-type chain) (Figure 74a). A couple of mixed valent (+4/+5) VPO's have been reported with structures formed by connecting $VOPO_4$ layers (see Figure 72) with H_2PO_4 groups[686,697] (Figure 74b).

3.6.3. Iron Phosphates

Besides the ability of iron to exhibit different oxidation states and form various polyhedra, it also forms several phosphate minerals with dense structures,[706] as well as a large pore open-framework structure, cacoxenite,[654] as mentioned earlier. In these materials, iron assumes +2 and +3 or sometimes mixed valency and adopts octahedral, *sqp*, *tbp*, and tetrahedral geometries. Several iron phosphates incorporating inorganic cations have been synthesized.[707] Férey and co-workers, using the fluoride route, showed that open-framework iron phosphates could be formed incorporating organic cations. Another interest in exploring open-framework iron phosphates relates to their magnetic properties. The quest for magnetic molecular sieves led Férey and co-workers as well as others to discover a large number of oxy-fluorinated open-framework iron phosphates. Today, iron phosphates probably constitute the largest family of transition metal open-framework phosphates, encompassing 1-, 2-, and 3D structures.[306,321,322,708–743] Organically templated iron oxy-phosphates have been reviewed by Lii et al.,[744] and iron fluoro-phosphates have been reviewed by Férey et. al.[745] We have listed all the organically templated iron phosphates in Table 8 according to their dimensionality.

One-Dimensional Structures. One-dimensional FePO structures are dominated by the tancoite-type chains[306,716,730,736,738,743] with an Fe/P ratio of 1:2, with infinite trans-corner-shared F/OH-bridged FeF_xO_{6-x} ($x = 0-2$) octahedra (see Figure 46c). There are three 1D structures that are more complex, and one of them is formed by linking the SBU-9 unit (Figure. 75a).[729] In SBU-9, there is a tetranuclear Fe−O cluster, which consists of two central FeO_6 octahedra that share a common edge, with the two hydroxo oxygens involved in the shared edge serving as corners for two additional FeO_6 octahedra. This tetranuclear cluster is variously capped by PO_4 tetrahedra in different structures and their connectivity through the Fe−O−P linkage leads to different dimensionalities and different structure types in the same dimensionality. In another 1D structure, strip-like 1D ribbons contain Fe in the mixed-valent state, similar to that observed in the cobalt phosphate in Figure 46d. This is only the second example of such a strip-like structure and the only case of an organically templated FePO where Fe is solely in tetrahedral coordination.[740] The last case is a 1D ribbon-

Table 7. Lattice Parameters, Templates, and Dimensionalities of the Various Templated Vanadium Phosphates Reported in the Literature

formula	SG[a]	lattice parameters	template	type	ref
$[C_7H_{14}N]_6[H_3O]_2[V_4(HPO_4)(PO_4)_3O_6F]_2$	$P2_1/c$	$a = 21.475$ Å, $b = 17.722$ Å, $c = 20.162$ Å; $\alpha = \gamma = 90°$, $\beta = 94.33°$	QUIN H	0D cluster	689
$[C_4H_{10}NO]_6[V_3^{IV}V^{V}O_{32}(OH)_6(PO_4)]\cdot 2H_2O$	$C2/c$	$a = 19.354$ Å, $b = 14.166$ Å, $c = 21.229$ Å; $\alpha = \gamma = 90°$, $\beta = 92.03°$	MORPH	0D cluster	699
$[C_2H_9N_2][VO(PO_4)]$	$C2$	$a = 17.593$ Å, $b = 4.798$ Å, $c = 9.037$ Å; $\alpha = \gamma = 90°$, $\beta = 114.21°$	enH (bound)	1D zigzag	684
$[C_2H_{10}N_2][V(OH)(HPO_4)_2]\cdot H_2O$	$P\bar{1}$	$a = 8.538$ Å, $b = 9.853$ Å, $c = 7.225$ Å; $\alpha = 90.63°$, $\beta = 92.28°$, $\gamma = 65.43°$	enH_2	1D tancoite	691
$[CH_6N_3][VO(H_2O)(HPO_4)(H_2PO_4)]\cdot H_2O$	$C2/c$	$a = 13.956$ Å, $b = 11.717$ Å, $c = 13.961$ Å; $\alpha = \gamma = 90°$, $\beta = 94.47°$	GUANH	1D kronkite	695
$[C_4H_{12}N_2][(VO)_2(PO_4)_2]$	$P2_1/c$	$a = 8.786$ Å, $b = 8.257$ Å, $c = 8.566$ Å; $\alpha = \gamma = 90°$, $\beta = 111.07°$	$PIPH_2$	2D	678, 679
$[C_4H_{12}N_2]_2[(VO)_3(HPO_4)_2(PO_4)_2]\cdot H_2O$	$Pna2_1$	$a = 14.631$ Å, $b = 8.706$ Å, $c = 17.635$ Å; $\alpha = \beta = \gamma = 90°$	$PIPH_2$	2D	678
$[C_4H_{12}N_2][(VO)_4(OH)_4(PO_4)_2]$	$P2_1/c$	$a = 10.682$ Å, $b = 8.991$ Å, $c = 8.951$ Å; $\alpha = \gamma = 90°$, $\beta = 110.41°$	$PIPH_2$	2D	683
$[C_{10}H_{28}N_4][(VO)_5(OH)_2(PO_4)_4]\cdot 2H_2O$	$P\bar{1}$	$a = 9.433$ Å, $b = 17.799$ Å, $c = 9.356$ Å; $\alpha = 103.83°$, $\beta = 91.80°$, $\gamma = 95.90°$	$APPIPH_4$	2D	683
$[C_6H_{14}N_2][(VO)_8(HPO_4)_3(PO_4)_4(OH)_2]\cdot 2H_2O$	$P2/n$	$a = 9.559$ Å, $b = 8.840$ Å, $c = 24.309$ Å; $\alpha = \gamma = 90°$, $\beta = 100.07°$	$DABCOH_2$	2D	683
$[C_6H_{14}N_2][(VO)_3(OH)_2(PO_4)_2]$	$P2_1/n$	$a = 12.048$ Å, $b = 6.347$ Å, $c = 20.249$ Å; $\alpha = \gamma = 90°$, $\beta = 105.30°$	$DABCOH_2$	2D	683
$[CH_6N_3]_2[(VO_2)_3(PO_4)(HPO_4)]$	$C2/c$	$a = 12.446$ Å, $b = 7.287$ Å, $c = 17.819$ Å; $\alpha = \gamma = 90°$, $\beta = 97.23°$	GUANH	2D	593
$[C_2H_9N_2][V^{III}F(PO_4)]$ (ULM-11 type)	$P2_1/c$	$a = 9.227$ Å, $b = 7.353$ Å, $c = 9.849$ Å; $\alpha = \gamma = 90°$, $\beta = 101.31°$	enH (bound)	2D	310, 694, 701
$[NH_4]VOPO_4\cdot 1.5H_2O$	$I4/mmm$	$a = b = 6.316$ Å, $c = 13.540$ Å; $\alpha = \beta = \gamma = 90°$	NH_4	2D	696
$(NH_4)_{0.5}VOPO_4\cdot 1.5H_2O$	$P2_1/m$	$a = 6.966$ Å, $b = 17.663$ Å, $c = 8.930$ Å; $\alpha = \gamma = 90°$, $\beta = 105.347°$	NH_4	2D	696
$[C_4H_{12}N_2][(VO)(VO_2)_2(H_2O)(PO_4)_2]$	$P\bar{1}$	$a = 6.165$ Å, $b = 10.821$ Å, $c = 11.854$ Å; $\alpha = 66.60°$, $\beta = 76.01°$, $\gamma = 83.44°$	$PIPH_2$	2D	697
$[H_{0.6}(VO)_3(PO_4)_3(H_2O)_3]\cdot 4H_2O$	$P2_1/c$	$a = 7.371$ Å, $b = 26.373$ Å, $c = 8.827$ Å; $\alpha = \gamma = 90°$, $\beta = 106.777°$	H^+	2D	698
$[C_{15}H_{11}N_3O_2V][(VO_2)_2(PO_4)]$	$C2/c$	$a = 12.315$ Å, $b = 10.836$ Å, $c = 29.181$ Å; $\alpha = \gamma = 90°$, $\beta = 101.62°$	$[VO_2(terpy)]^+$	2D	700
$[C_2H_{10}N_2]_{1.5}[(VO)_2(HPO_4)_2(PO_4)]$	$C2/c$	$a = 18.605$ Å, $b = 7.119$ Å, $c = 23.459$ Å; $\alpha = \gamma = 90°$, $\beta = 96.558°$	EnH_2	2D	702
$[C_4H_{12}N_2]_2[V_4O_6H(HPO_4)_2(PO_4)_2]$	$Pna2_1$	$a = 13.181$ Å, $b = 15.292$ Å, $c = 6.282$ Å; $\alpha = \beta = \gamma = 90°$	$PIPH_2$	2D	702
$K_4[C_2H_8N][V_{10}O_{10}(H_2O)_2(OH)_4(PO_4)_7]\cdot 4H_2O$	$P43$	$a = b = 12.310$ Å, $c = 30.555$ Å; $\alpha = \beta = \gamma = 90°$	K^+, DMA	3D	674
$[C_2H_{10}N_2]_2[C_2H_9N_2][V^{III}(H_2O)_2(V^{IV}O)_8(OH)_4(HPO_4)_4(PO_4)_4(H_2O)_2]\cdot 2H_2O$	$P2_1/n$	$a = 14.313$ Å, $b = 10.151$ Å, $c = 18.374$ Å; $\alpha = \gamma = 90°$, $\beta = 90.39°$	enH_2, enH	3D	675
$K[C_3H_{12}N_2][(VO)_3(PO_4)_3]$	$P\bar{1}$	$a = 9.047$ Å, $b = 9.747$ Å; $c = 10.288$ Å, $\alpha = 109.68°$, $\beta = 101.78°$, $\gamma = 98.11°$	1,3-$DAPH_2$, K^+	3D, 8,12MR	676
$[C_3H_{12}N_2][(VO)_3(OH)_2(PO_4)_2\cdot 2H_2O$	$Pnma$	$a = 10.507$ Å, $b = 17.136$ Å, $c = 8.451$ Å; $\alpha = \beta = \gamma = 90°$	1,3-$DAPH_2$	3D, 8MR	677, 703
$[C_3H_{12}N_2][V_3P_2O_{13}(H_2O)_2]$	$Pnma$	$a = 10.567$ Å, $b = 16.970$ Å, $c = 8.413$ Å; $\alpha = \beta = \gamma = 90°$	1,3-$DAPH_2$	3D	680
$[C_2N_2H_{10}][V_2PO_8F]$	$P2_12_12_1$	$a = 8.294$ Å, $b = 9.226$. Å, $c = 12.502$ Å; $\alpha = \beta = \gamma = 90°$	enH_2	3D, 10MR	681
$[C_4H_{12}N_2][VO(H_2O)_3VO(H_2O)(VO)_2(HPO_4)(PO_4)_2]$	Cm	$a = 17.399$ Å, $b = 9.479$ Å, $c = 7.055$ Å; $\alpha = \beta = \gamma = 90°$	$PIPH_2$	3D, 8MR	682
$[C_2H_{10}N_2]_4[V^{III}(H_2O)_2(V^{IV}O)_6(OH)_2(HPO_4)_3(PO_4)_5]\cdot 3H_2O$	$C2/c$	$a = 20.674$ Å, $b = 9.956$ Å, $c = 23.694$; $\alpha = \gamma = 90°$, $\beta = 101.15°$	enH_2	3D, 16MR	685
$[C_2H_{10}N_2][(VO)_2(PO_4)_2(H_2PO_4)]$	$Pc2_1n$	$a = 8.891$ Å, $b = 15.971$ Å, $c = 18.037$ Å; $\alpha = \beta = \gamma = 90°$	enH_2	3D, 8MR	686
$[C_6H_{14}N_2]K_{1.35}[V_5O_9(PO_4)_2]\cdot xH_2O$	$I\bar{4}3m$	$a = b = c = 26.247$ Å, $\alpha = \beta = \gamma = 90°$	$DABCOH_2$, K^+	3D, 32,16MR	687
$Cs_3[V_5O_9(PO_4)_2]\cdot xH_2O$	$Fd\bar{3}m$	$a = b = c = 32.306$ Å, $\alpha = \beta = \gamma = 90°$	Cs^+	3D, 24MR	687
$[C_4H_{12}N_2][(VO)_4(H_2O)_4(HPO_4)_2(PO_4)_2]$	Im	$a = 7.025$ Å, $b = 9.470$ Å, $c = 16.570$ Å; $\alpha = \gamma = 90°$, $\beta = 96.03°$	$PIPH_2$	3D, 8MR	688

Table 7. Continued

formula	SG[a]	lattice parameters	template	type	ref
$[C_4H_{12}N_2]_{0.5}[(VO)_4V(HPO_4)_2(PO_4)_2F_2(H_2O)_4]\cdot 2H_2O$	$C2/m$	$a = 18.425$ Å, $b = 7.417$ Å, $c = 8.954$ Å; $\alpha = \gamma = 90°$, $\beta = 93.69°$	$PIPH_2$	3D	690
$K_2[(VO)_3(PO_4)_2F_2(H_2O)]\cdot H_2O$	$P\bar{1}$	$a = 7.298$ Å, $b = 8.929$ Å, $c = 10.090$ Å; $\alpha = 104.50°$, $\beta = 100.39°$, $\gamma = 92.13°$	K^+	3D	690
$[C_2H_{10}N_2][(VO)_3(H_2O)_2(HPO_4)(PO_4)_2]$	$P\bar{1}$	$a = 10.187$ Å, $b = 10.241$ Å, $c = 8.214$ Å; $\alpha = 90.40°$, $\beta = 95.93°$, $\gamma = 117.33°$	enH_2	3D	692
$[NH_4]_2[VO(H_2O)_3]_2[VO(H_2O)][(VO(PO_4)_2]_2\cdot 3H_2O$	$P\bar{1}$	$a = 10.252$ Å, $b = 12.263$ Å, $c = 12.362$ Å; $\alpha = 69.041°$, $\beta = 65.653°$, $\gamma = 87.789°$	NH_4	3D, 10MR	696
$[C_4H_{12}N_2][H_2O][(VOPO_4)_4(H_2O)H_2PO_4]\cdot 3H_2O$	$P2/n$	$a = 9.645$ Å, $b = 8.877$ Å, $c = 14.813$ Å; $\alpha = \gamma = 90°$, $\beta = 91.94°$	$PIPH_2$, H_3O^+	3D, 12MR	697

[a] SG = space group.

Figure 71. One-dimensional structures found in the VPO family: (a) en bound in a complex chain;[684] (b) kronkite-like chain.[695]

Figure 72. Layered structure of $VOPO_4\cdot xH_2O$.[705]

like structure built by the cross-linking of F−Fe−F−Fe−F−Fe−F corner-shared trimers of octahedra (Figure 75b).[741]

Two-Dimensional Structures. Two-dimensional structures of the FePO family are diverse in terms of the Fe polyhedra, the Fe oxidation states, and the connectivity between the Fe polyhedra and the PO_4 tetrahedra. For example, infinite chains of trans-corner-shared Fe octahedra are linked by PO_4 tetrahedra to form the layer[710] isostructural with AlPO,[344] InPO,[522] VPO,[310,694,701] and TiPO[694] (see Figure 47c) where en coordinates with the metal. In ULM-10,[709] corner-shared Fe octahedra are mixed-valent, and in MIL-4, the corner-shared chain of octahedra are in the cis orientation.[322] The chains are also formed by the edge-sharing of Fe octahedra, which are then connected by either PO_4 tetrahedra[711,712] or both PO_4 and Fe octahedra to form the layer.[737] Tetrameric clusters formed with all-FeO_5 *tbp* geometry can be connected by the PO_4 unit to form a layer.[720] In a similar way, a hexameric cluster, consisting of a dimer of edge-sharing octahedra, which again shares edges with four $Fe^{II}O_5$ *tbp* units to complete the hexamer, is connected to another by corner-sharing and through PO_4 groups to form the layer.[728] There are a few examples where dimeric FeF_xO_{6-x} octahedra in the form of SBU-4 are connected to form the layer[733] (Figure 76) or strictly alternating Fe and P polyhedra form the layer.[731,734]

Three-Dimensional Structures. This family of solids shows extra-large pore channels that include 16-,[717,718] 18-,[321] and 20-membered[719] channels. Like the GaPO family, a number of structures are built from the SBU-6 unit,[306,713,724,725,743] and some of them are isostructural with members of the

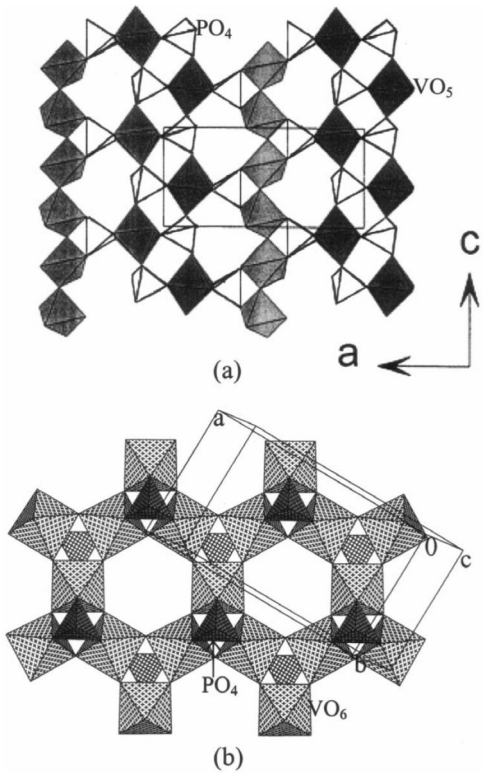

Figure 73. Structures of two layered vanadium phosphates: (a) with alternate ladder and V−O−V chain (Reprinted with permission from ref 702. Copyright 2003 Elsevier.); (b) a kagome lattice.[693]

GaPO[456,458,461,464] and AlPO[362] families (e.g., ULM-3 and -4). Other than the common SBU-6, complex SBUs such as the D4R formed by FeO_5 *tbp* structures with a tetrahedrally coordinated oxygen in the center get connected by Fe−O−P linkages to form a 3D structure.[723,726] A complex SBU-9 (see Figure 48i) can also get connected through Fe−O−P linkages to form an extra-large pore (20-membered ring) channel. The 3D structures are made with the linkages based on infinite chains of Fe polyhedra, (e.g., the 16MR channel in ULM-15 is built from tancoite-type trans chains,[717] the 18MR channel is formed from cis Fe−F−Fe corner-shared chains,[321] as in Figure 49c, or infinite edge-shared $Fe^{II}O_6$ octahedra further connected by $Fe^{III}O_6$ octahedra and HPO_4 form a layer, which is then pillared by HPO_4 groups to form the 3D structure).[728] Alternate edge- and corner-shared FeO_4F_2 octahedra get connected by SBU-4 to form a channel,[736] or a finite chain of Fe−F−Fe pentamers[735] or dimers[727] get interconnected by a PO_4 group or by both PO_4 and Fe polyhedra to form the 3D structure, the latter[727] also having edge-shared PO_4 tetrahedra and FeO_6 octahedra, a rare situation in the FePO family[321] and previously seen in VPO.[678] There are examples where FeO_6 octahedra and PO_4 tetrahedra are strictly alternating,[718,732] one of them with a pillared structure[718] and the other built from ladder-type units.[732] Interestingly, both these structures are analogous to InPO structures.[518,520]

3.6.4. Cobalt Phosphates

Cobalt(II) readily adopts tetrahedral coordination in addition to five and six coordination,[746] exhibits interesting magnetic properties, can be doped in AlPO[747] or GaPO frameworks,[748] and can give rise to catalytic activity.[749]

The first organically templated pure cobalt phosphate framework (CoPO) was reported by Thomas and co-workers.[750] There was not much progress in the CoPO system for some time,[751] probably due to the difficulty associated with stabilizing Co^{2+} in tetrahedral coordination in the presence of large organo-ammonium cations. Stucky and co-workers[752] reported a few interesting zeolitic CoPO's incorporating alkali or ammonium cations and organically templated cobalt phosphates stabilized by Al^{3+} doping in the framework.[747] Stucky also proposed the idea of template−framework charge matching whereby when the charge and volume of the organic cation is varied, Co^{2+} is incorporated into the framework extensively depending on the negative charge created by the Co^{2+}/M^{3+} (M = Al, Ga) ratio. However, Rao and co-workers have later shown that pure cobalt phosphate frameworks can be synthesized by employing organo-ammonium phosphates in a predominantly organic medium[280] or by using the $Co(en)_3^{3+}$ complex as the source of Co.[318] There are now several examples of organically templated CoPO's encompassing 1-, 2-, and 3D structures (Table 9).[279,280,318,573,576,622,750–761]

One-Dimensional Structures. There are several 1D organically templated CoPO's, and the more common types are those with corner-shared chains of four-membered rings[622,757,759,761] and ladders of edge-shared four-membered rings[753] with a Co/P ratio of 1:2 (Figure 46a,b). A rather unusual structure with a strip-like[280] 1D structure of fused corner-shared chains of four-membered rings having an infinite Co−O−Co linkage, due to the presence of a tricoordinated oxygen, was shown earlier in Figure 46d. The only other example of such a structure is that recently discovered in the FePO family.[740] There is a recent report of a complex 1D structure formed by a double chain of three rings where CoO_5 *tbp* units and distorted CoO_6 octahedra create a chain of Co−O−Co linkages through corner-sharing (Figure 77).[622]

Two-Dimensional Structures. There are several 2D sheet structures in the CoPO family, with Co in tetrahedral coordination, which show both Co−O−Co[279,751,758] and alternating Co−O−P[280,576,758] linkages. For example, there are three structures with a Co/P ratio of 1:1 having the same layer topology,[751,758] where an infinite chain of corner-shared CoO_4 tetrahedra are connected by PO_4 tetrahedra to form the layer structures (Figure 78a). A similar layer structure has been observed in the ZnPO family.[603] On the other hand, the sheet structure of $[C_4H_{12}N_2][Co_2(PO_4)_2]$,[279] with a Co/P ratio of 1:1 and containing infinite Co−O−Co linkages, can be considered to be formed by the fusion of alternate four-ring ladders and three-ring chains, similar to the structure of $[C_4H_{12}N_2][Zn_2(PO_4)_2]$[588] (Figure 63). There are a few structures formed by strictly alternating CoO_4 and PO_4 tetrahedra where zigzag ladders are joined by PO_4 tetrahedra to form a 12-membered bifurcated aperture within the layer (Figure 47b).[280,758] On the other hand, the structure of $[C_{10}H_{28}N_4]_{0.5}[Co(PO_4)Cl]$ contains strictly alternating CoO_3Cl tetrahedra and PO_4 tetrahedra and is better described in terms of corner-sharing SBU-4 units (Figure 78b).[576]

Three-Dimensional Structures. Several 3D open-framework structures have been discovered recently (see Table 9), and many of them are zeolitic or zeolite-related with strictly alternating CoO_4 and PO_4 tetrahedra (e.g., the first pure CoPO open-framework zeotype structure (called DFT-framework type),[750] NH_4- and Rb-templated ABW structures,[752] ethylenediammonium-templated ACO,[318] and GIS structures[754] and a couple of sodalite-related structures).[279,761] Specially interesting is the ACO framework type (Figure 49a)

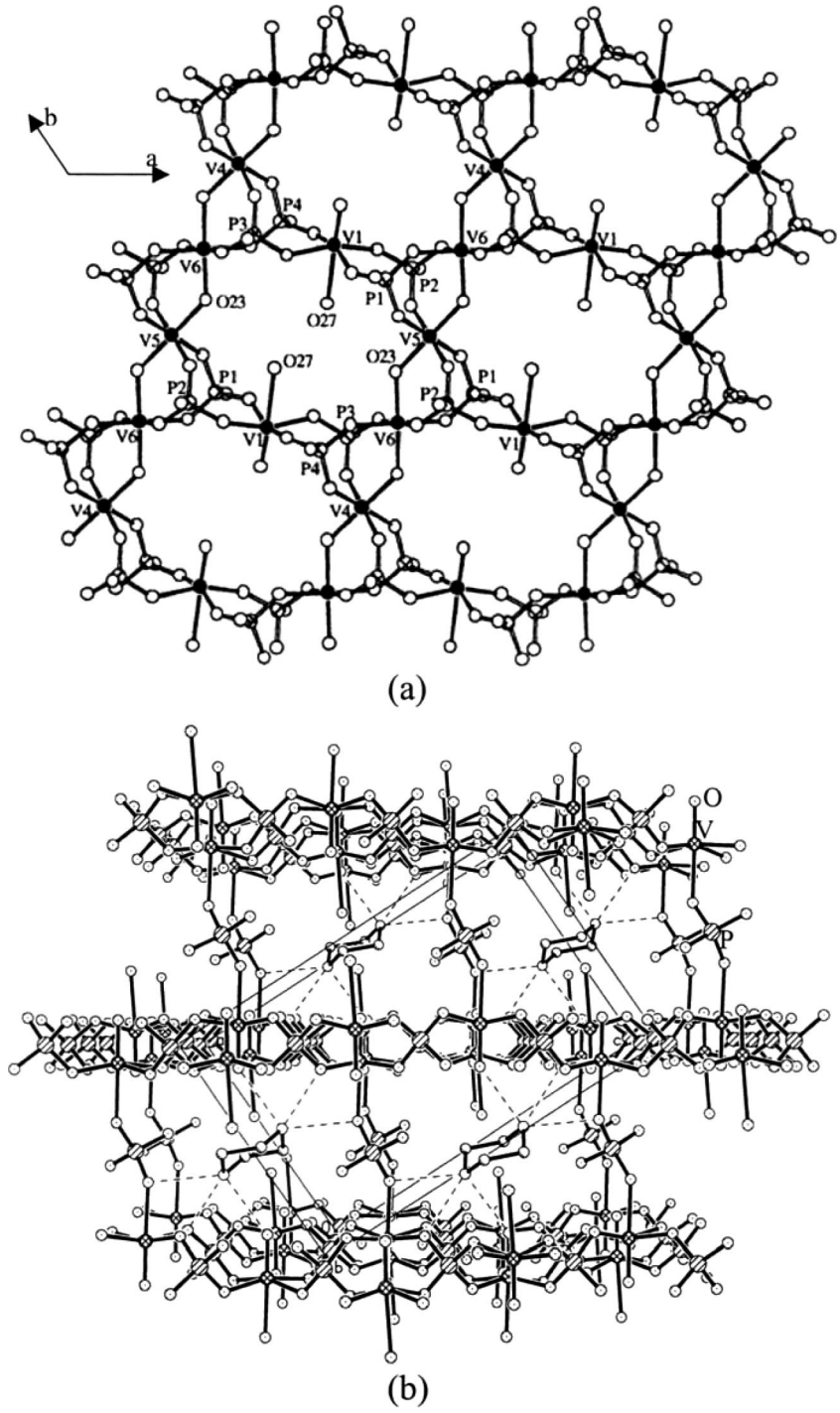

Figure 74. Three-dimensional vanadium phosphates showing the presence of (a) a tancoite-like chain (Reprinted with permission from ref 696. Copyright 2000 American Chemical Society.) and (b) pillaring of $VOPO_4$ layers by the PO_4 units.[697]

discovered in the pure CoPO family, although the same structure had been reported earlier but with small amount of Al^{3+} doping.[747] There are several chiral frameworks that can be considered to be hybrids of tridimite and ABW.[752] There are 3D structures with alternating CoO_4 and PO_4 tetrahedra forming eight-membered[573,576] and 16-membered channels, as in $[C_4H_{16}N_3]_3[Co_6(PO_4)_5(HPO_4)_3]\cdot H_2O$ templated by diethylenetriamine (Figure 79a).[318] There are examples within the 3D structures where infinite Co−O−Co linkages are present as in $[C_4H_{10}N_2]_2[Co_7(PO_4)_6]$ with a 12-membered channel[755,756] or in $Cs_2[Co_3(HPO_4)(PO_4)_2]\cdot H_2O$ with a 16-membered channel; Co exhibiting four, five, and six coordination in the former is noteworthy (Figure 79b).

3.6.5. Zirconium Phosphates

Zirconium phosphates are an important class of compounds because of their potential applications in proton ion conductivity, ion exchange, and catalysis.[762] The focus of zirconium chemistry research has been on the layered α- and γ-phases (α- and γ-ZrP) and their derivatives. By means of intercalation and ion-exchange under mild conditions, it has been possible to modify α- and γ-ZrP leading to inorganic−organic functional derivatives.[763] Zirconium adopts six-coordinated octahedral geometry with Zr in the +4 oxidation state. Clearfield and co-workers[764] reported a new layered zirconium phosphate-fluoride in DMSO, $[Zr(PO_4)F(OSMe_2)]$, and

Table 8. Lattice Parameters, Templates and Dimensionalities of the Various Templated Iron Phosphates Reported in the Literature

formula	SG[a]	lattice parameters	template	type	ref
$[C_3H_{12}N_2][FeF(HPO_4)_2]\cdot xH_2O$, $x \approx 0.20$ (ULM-14)	*Pmca*	$a = 7.221$ Å, $b = 8.655$ Å, $c = 19.329$ Å; $\alpha = \beta = \gamma = 90°$	$1,3\text{-DAPH}_2$	1D tancoite	716
$[C_4H_{12}N_2]_{1.5}[Fe_2(OH)(H_2PO_4)(HPO_4)_2(PO_4)]\cdot 0.5H_2O$	$P\bar{1}$	$a = 6.335$ Å, $b = 13.008$ Å, $c = 13.781$ Å; $\alpha = 62.83°$, $\beta = 81.40°$, $\gamma = 82.69°$	$PIPH_2$	1D	729
$[C_2H_{10}N_2][Fe(OH)(HPO_4)_2]\cdot H_2O$	$P\bar{1}$	$a = 8.526$ Å, $b = 9.796$ Å, $c = 7.232$ Å; $\alpha = 90.25°$, $\beta = 92.72°$, $\gamma = 65.20°$	enH_2	1D tancoite	730
$[C_6H_{14}N_2][Fe_2F_2(HPO_4)_2(H_2PO_4)_2]\cdot 2H_2O$	*C*2/*c*	$a = 7.232$ Å, $b = 20.52$ Å, $c = 13.933$ Å; $\alpha = \gamma = 90°$, $\beta = 97.68°$	$DABCOH_2$	1D tancoite	736
$[C_4H_{12}N_2]_{0.5}[FeF(HPO_4)(H_2PO_4)]$	*Pbca*	$a = 7.213$ Å, $b = 14.207$ Å, $c = 17.134$ Å; $\alpha = \beta = \gamma = 90°$	$PIPH_2$	1D tancoite	306
$[C_5H_{16}N_2][FeF(HPO_4)_2]$	$P2_1/m$	$a = 8.846$ Å, $b = 7.211$ Å, $c = 9.893$ Å; $\alpha = \gamma = 90°$, $\beta = 97.10°$	$1,3\text{-DAPnH}_2$	1D tancoite	738
$[C_4H_{11.6}N_2]_{1.5}[Fe^{II}Fe^{III}(PO_4)(H_{0.8}PO_4)_2]\cdot H_2O$	$P2_1/c$	$a = 8.370$ Å, $b = 8.562$ Å, $c = 23.865$ Å; $\alpha = \gamma = 90°$, $\beta = 93.95°$	$PIPH_{1.6}$	1D strip	740
$[C_8H_{26}N_4][Fe_3F_6(HPO_4)_2(PO_4)]\cdot 3H_2O$	$I2_12_12_1$	$a = 9.904$ Å, $b = 12.887$ Å, $c = 19.783$ Å; $\alpha = \beta = \gamma = 90°$	$BAPenH_4$	1D	741
$[C_5H_{14}N_2]_2[Fe_2F_2(HPO_4)_4]\cdot 2H_2O$	$P2_1/n$	$a = 7.226$ Å, $b = 16.5731$ Å, $c = 11.0847$ Å; $\alpha = \gamma = 90°$, $\beta = 97.265°$	$HPIPH_2$	1D tancoite	743
$[C_2H_9N_2][Fe^{2+}Fe^{3+}F_2(HPO_4)_2(H_2O)_2]$ (ULM-10)	$P\bar{1}$	$a = 5.172$ Å, $b = 7.518$ Å, $c = 8.773$ Å; $\alpha = 108.37°$, $\beta = 97.33°$, $\gamma = 109.86°$	enH	2D	709
$FeF(HPO_4)(C_2H_8N_2)$ (ULM-11)	$P2_1/c$	$a = 9.215$ Å, $b = 7.427$ Å, $c = 9.881$ Å; $\alpha = \gamma = 90°$, $\beta = 101.19°$	en bonded	2D	710
$[C_2H_{10}N_2]_{0.5}[Fe(PO_4)(OH)]$	$P2_1/c$	$a = 4.516$ Å, $b = 6.136$ Å, $c = 18.515$ Å; $\alpha = \gamma = 90°$, $\beta = 94.58°$	enH_2	2D	405, 711, 712
$[C_3H_{12}N_2][Fe_2O(PO_4)_2]$	$P2_1/c$	$a = 11.659$ Å, $b = 9.572$ Å, $c = 10.116$ Å; $\alpha = \gamma = 90°$, $\beta = 99.96°$	$1,3\text{-DAPH}_2$	2D	720
$[C_4H_{11}N_2]_{0.5}[Fe_3(HPO_4)_2(PO_4)(H_2O)]$	*C*2/*c*	$a = 30.892$ Å, $b = 6.373$ Å, $c = 12.555$ Å; $\alpha = \gamma = 90°$, $\beta = 101.95°$	PIPH	2D	728
$[C_4H_{14}N_2]_3[Fe_5F_3(PO_4)_6(H_2O)_3]\cdot 2H_2O$ (MIL-4)	$P2_12_12_1$	$a = 9.585$ Å, $b = 15.588$ $c = 29.256$; $\alpha = \beta = \gamma = 90°$	$1,4\text{-DABH}_2$	2D	322
$[NH_4][Fe_3(H_2PO_4)_6(HPO_4)_2]\cdot 4H_2O$	*C*2/*c*	$a = 16.845$ Å, $b = 9.611$ Å, $c = 17.647$ Å; $\alpha = \gamma = 90°$, $\beta = 90.91°$	NH_4	2D	731
$[C_6H_{21}N_4][Fe_2F_2(HPO_4)_3][H_2PO_4]\cdot 2H_2O$	$P2_1/c$	$a = 13.442$ Å, $b = 9.732$ Å, $c = 18.312$ Å; $\alpha = \gamma = 90°$, $\beta = 92.15°$	$TRENH_3$	2D	733
$[C_5H_6N][Fe(HPO_4)_2(H_2O)_2]$	$P\bar{1}$	$a = 7.117$ Å, $b = 7.371$ Å, $c = 12.181$ Å; $\alpha = 105.54°$, $\beta = 105.47°$, $\gamma = 90.27°$	PyH	2D	734
$[C_3H_5N_2][Fe(HPO_4)_2(H_2O)_2]$	*Pnam*	$a = 7.127$ Å, $b = 7.323$ Å; $c = 21.292$ Å, $\alpha = \beta = \gamma = 90°$	IMDH	2D	734
$[C_6H_{21}N_4][Fe_{3-x}^{III}Fe_x^{II}F_2(PO_4)(HPO_4)_2]_2$ ($x \approx 1.5$)	$P\bar{1}$	$a = 6.431$ Å, $b = 10.274$ Å, $c = 10.439$ Å; $\alpha = 80.56°$, $\beta = 89.53°$, $\gamma = 87.94°$	$TETAH_3$	2D	737
$[C_2H_{10}N_2][Fe_2O(PO_4)_2]$	$P2_1/c$	$a = 10.67$ Å, $b = 10.897$ Å, $c = 9.918$ Å; $\alpha = \gamma = 90°$, $\beta = 105.63°$	enH_2	2D	742
$Fe_2F_2(2,2'\text{-bpy})(HPO_4)_2(H_2O)$	$P\bar{1}$	$a = 7.659$ Å, $b = 10.101$ Å, $c = 11.260$ Å; $\alpha = 107.555°$, $\beta = 105.174°$, $\gamma = 98.975°$	bound 2,2′-bpy	2D	516
$[NH_4][Fe_2(PO_4)_2(OH)]\cdot 2H_2O$	$P2_1/n$	$a = 9.8232$ Å, $b = 9.7376$ Å, $c = 9.8716$ Å; $\alpha = \gamma = 90°$, $\beta = 102.803°$	NH_4	3D	708
$[C_6H_{14}N_2][Fe_4(PO_4)F_2(H_2O)_3]$ (ULM-12)	$P2_1/n$	$a = 9.987$ Å, $b = 12.275$ Å, $c = 17.462$ Å; $\alpha = \gamma = 90°$, $\beta = 102.8°$	$DABCOH_2$	3D, 8MR	713
$[C_4H_{14}N_2][Fe_3(PO_4)_3F_2]$ (ULM-3)	*Pbca*	$a = 10.203$ Å, $b = 18.670$ Å, $c = 16.268$ Å; $\alpha = \beta = \gamma = 90°$	$1,4\text{-DABH}_2$	3D, 10MR	715
$[C_3H_{12}N_2][Fe_4F_3(PO_4)(HPO_4)_4(H_2O)_4]$ (ULM-15)	*C*2/*c*	$a = 24.176$ Å, $b = 14.558$ Å, $c = 7.186$ Å; $\alpha = \gamma = 90°$, $\beta = 102.3°$	$1,3\text{-DAPH}_2$	3D, 16MR	717
$[C_4H_{14}N_2]_3[Fe_8(HPO_4)_{12}(PO_4)_2(H_2O)_6]$	$P\bar{3}c1$	$a = b = 13.527$ Å, $c = 19.26$ Å; $\alpha = \beta = 90°$, $\gamma = 120°$	$DABCOH_2$	3D, 16MR	718
$[C_3H_{12}N_2]_2[Fe_4(OH)_3(HPO_4)_2(PO_4)_3]\cdot xH_2O$	$I4_1/a$	$a = b = 15.402$ Å, $c = 28.94$ Å; $\alpha = \beta = \gamma = 90°$	$1,3\text{-DAPH}_2$	3D, 20MR	719
$[C_2H_{10}N_2][Fe^{(II/III)}{}_4O(PO_4)_4]\cdot H_2O$	$I4_2m$	$a = b = 10.138$ Å, $c = 9.628$ Å; $\alpha = \beta = \gamma = 90°$	enH_2	3D, 8MR	723, 726
$[CH_6N]_2[Fe_3(PO_4)_3F_2]\cdot H_2O$ (ULM-4)	$P2_1/n$	$a = 8.849$ Å, $b = 10.373$ Å, $c = 16.947$ Å; $\alpha = \gamma = 90°$, $\beta = 92.87°$	MAH	3D, 10MR	724
$[C_6H_{14}N_2][Fe_4(PO_4)_4F_3]$ (ULM-19)	$P2_1/n$	$a = 10.009$ Å, $b = 12.235$ Å, $c = 17.28$ Å; $\alpha = \gamma = 90°$, $\beta = 106.04°$	$DABCOH_2$	3D, 8MR	725

Table 8. Continued

formula	SG[a]	lattice parameters	template	type	ref
$[C_4H_{12}N_2]_2[Fe_6(HPO_4)_2(PO_4)_6(H_2O)_2]\cdot H_2O$	$P\bar{1}$	$a = 9.177$ Å, $b = 12.723$ Å, $c = 16.483$ Å; $\alpha = 68.53°$, $\beta = 83.28°$, $\gamma = 73.26°$	$PIPH_2$	3D, 8MR	727
$[C_4H_{12}N_2][Fe_4(OH)_2(HPO_4)_5]$	$C2/m$	$a = 25.706$ Å, $b = 6.449$ Å, $c = 6.379$ Å; $\alpha = \gamma = 90°$, $\beta = 102.6°$	$PIPH_2$	3D, 8MR	728
$[C_4H_{14}N_2]_3[Fe_8(HPO_4)_{12}(PO_4)_2(H_2O)_6]$	$P3$	$a = b = 13.495$ Å, $c = 9.396$ Å; $\alpha = \beta = \gamma = 90°$	$1,4DABH_2$	3D, 16MR	[b]
$[C_4H_{16}N_3][Fe_5F_4(H_2PO_4)(HPO_4)_2(PO_4)_4]\cdot 0.5H_2O$	$P2_1/n$	$a = 9.67$ Å, $b = 15.618$ Å, $c = 22.563$ Å; $\alpha = \gamma = 90°$, $\beta = 90.82°$	$DETAH_3$	3D, 18MR	321
$[C_2H_{10}N_2][Fe_2(HPO_4)_4]$	$P2/n$	$a = 9.341$ Å, $b = 8.892$ Å, $c = 9.48$ Å; $\alpha = \gamma = 90°$, $\beta = 117.6°$	enH_2	3D, 8MR	732
$[C_2H_{10}N_2][Fe_5F_4(PO_4)(HPO_4)_6]$	$P4_32_12$	$a = b = 9.864$ Å, $c = 30.353$ Å; $\alpha = \beta = \gamma = 90°$	enH_2	3D, 8MR	735
$[C_6H_{14}N_2]_2[Fe_3(OH)F_3(PO_4)(HPO_4)_2]_2\cdot H_2O$	$C2/c$	$a = 18.184$ Å, $b = 10.013$ Å, $c = 20.059$ Å; $\alpha = \gamma = 90°$, $\beta = 106.08°$	$DABCOH_2$	3D, 8MR	736
$[C_4H_{12}N_2][Fe_4F_2(H_2O)_4(PO_4)_4]\cdot 0.5H_2O$	$P2_1/n$	$a = 9.905$ Å, $b = 12.301$ Å, $c = 17.322$ Å; $\alpha = \gamma = 90°$, $\beta = 103.7°$	$PIPH_2$	3D, 8MR	306
$[C_4H_{12}N_2][Fe_3(PO_4)_3(HPO_4)(H_2O)]\cdot\sim 0.25H_2O$	$P\bar{1}$	$a = 6.355$ Å, $b = 9.166$ Å, $c = 15.311$ Å; $\alpha = 90.27°$, $\beta = 91.338°$, $\gamma = 106.594°$	$PIPH_2$	3D, 8MR	739
$[C_5H_{14}N_2][Fe_4(H_2O)_4F_2(PO_4)_4]$	$P2_1/n$	$a = 9.969$ Å, $b = 12.401$ Å, $c = 17.341$ Å; $\alpha = \gamma = 90°$, $\beta = 103.76°$	$HPIPH_2$	3D, 8MR	743

[a] SG = space group. [b] Korzenski, M. B.; Schimek, G. L.; Kolis, J. W. Eur. J. Solid State Chem. 1998, 35, 143.

Figure 75. Complex 1D structures found in the FePO family: (a) linking of the SBU-9 units;[729] (b) 1D ribbon-like structure with a trimer of the Fe octahedra. Reprinted with permission from ref.[741] Copyright 2003 Wiley-VCH.

Figure 76. Polyhedral view of a layered iron phosphate.[733]

subsequently Xu and co-workers[765] reported organically templated zirconium phosphate-fluoride with 1D double-stranded ladder structure. The first organically templated 3D open-framework zirconium phosphate-fluoride (ZrPO-1 or ZrPOF-1) was discovered by Kemnitz and co-workers.[766] The family of organically templated ZrPO has since expanded considerably with new structure types in 1-, 2-, and 3D networks (Table 10).[765–776]

One-Dimensional Structures. There are several interesting 1D structures in the ZrPO family (Figure 80), and many of them are not found in other organically templated metal phosphates. For example, a ladder-like 1D structure in the octahedral−tetrahedral system, $[C_4H_{10}N_2]_{1.5}[Zr(HPO_4)(PO_4)F_2]$,[765] has two terminal F atoms and a dangling HPO_4 group from the Zr atoms (Figure 80d). The only other octahedral−tetrahedral ladder-like structure is that in the MoPO family,[665] where there are terminal short Mo−O bonds (see Figure 70b). Especially interesting is the 1D structure, the first of its type in organically templated phosphates, in which each Zr is linked to neighboring Zr atoms in the chain by three bridging phosphate groups through Zr−O−P−O−Zr linkages[768] (Figure 80e). Such a chain structure is, however, found in an iron sulfate mineral.[777] Another interesting 1D structure is the kronkite type[704] chain where each Zr is linked to neighboring Zr atoms by two bridging phosphate groups using four equatorial

Table 9. Lattice Parameters, Templates, and Dimensionalities of the Various Templated Cobalt Phosphates Reported in the Literature

formula	SG[a]	lattice parameters	template	type	ref
$[C_3H_{12}N_2][Co(HPO_4)_2]$	$P2_12_12_1$	$a = 5.210$ Å, $b = 12.693$ Å, $c = 15.518$ Å; $\alpha = \beta = \gamma = 90°$	1,3-$DAPH_2$	1D ladder	753
$[C_4H_{12}N_2]_{1.5}[Co(HPO_4)(PO_4)]\cdot H_2O$	$P2_1/c$	$a = 8.388$ Å, $b = 8.576$ Å, $c = 23.899$ Å; $\alpha = \gamma = 90°$, $\beta = 93.98°$	$PIPH_2$	1D strip	280
$[C_5H_{14}N_2][Co(HPO_4)_2]$	$P2_1/n$	$a = 8.612$ Å, $b = 13.439$ Å; $c = 10.811$ Å, $\alpha = \gamma = 90°$, $\beta = 95.53°$	$MPIPH_2$	1D c.s. chain	622, 757, 759
$[C_6H_{16}N_2][Co(HPO_4)_2]$	$Pccn$	$a = 11.879$ Å, $b = 13.508$ Å, $c = 8.168$ Å; $\alpha = \beta = \gamma = 90°$	$DPIPH_2$	1D c.s. chain	759
$[C_4H_{12}N_2][Co(HPO_4)_2]$	$P2_1/n$	$a = 8.552$ Å, $b = 13.579$ Å, $c = 10.04$ Å; $\alpha = \gamma = 90°$, $\beta = 96.86°$	$PIPH_2$	1D c.s. chain	761
$[C_5H_{14}N_2][Co(HPO_4)_2]$	$C2/c$	$a = 11.939$ Å, $b = 13.803$ Å, $c = 7.947$ Å; $\alpha = \gamma = 90°$, $\beta = 91.514°$	$MPIPH_2$	1D c.s. chain	622
$[C_4H_{12}N_2]_3[Co_2(OH)(HPO_4)_3]_2$	$P2_1/n$	$a = 7.274$ Å, $b = 23.03$ Å, $c = 9.873$ Å; $\alpha = \gamma = 90°$, $\beta = 93.131°$	$PIPH_2$	1D complex chain	622
$[C_3H_{12}N_2]_{0.5}[Co(PO_4)]\cdot 0.5H_2O$	$Cmc2_1$	$a = 22.663$ Å, $b = 7.626$ Å, $c = 6.768$ Å; $\alpha = \beta = \gamma = 90°$	1,3-$DAPH_2$	2D	751
$[C_4H_{14}N_2]_{0.5}[Co(PO_4)]$	$P2_1/a$	$a = 7.508$ Å, $b = 23.655$ Å, $c = 6.775$ Å; $\alpha = \gamma = 90°$, $\beta = 90.55°$	1,4-$DABH_2$	2D	751
$[C_4H_{12}N_2]_{1.5}[Co(HPO_4)(PO_4)]\cdot H_2O$	$P2_1/c$	$a = 8.169$ Å, $b = 26.340$ Å, $c = 8.385$ Å; $\alpha = \gamma = 90°$, $\beta = 110.92°$	$PIPH_2$	2D	280
$[C_{10}H_{28}N_4]_{0.5}[Co(PO_4)C1]$	$P2_1/c$	$a = 11.484$ Å, $b = 8.723$ Å, $c = 11.01$ Å; $\alpha = \gamma = 90°$, $\beta = 111.37°$	$APPIPH_4$	2D	576
$[C_3H_{12}N_2O][Co_2(PO_4)_2]$	$Pbcn$	$a = 22.894$ Å, $b = 7.568$ Å, $c = 6.697$ Å; $\alpha = \beta = \gamma = 90°$	$DAHPH_2$	2D	758
$[C_3H_{12}N_2O][Co_2(HPO_4)_3]$	$P2_1/c$	$a = 8.608$ Å, $b = 9.64$ Å, $c = 17.258$ Å; $\alpha = \gamma = 90°$, $\beta = 92.20°$	$DAHPH_2$	2D	758
$[C_4H_{12}N_2][Co_2(PO_4)_2]$	$P\bar{1}$	$a = 5.153$ Å, $b = 10.758$ Å, $c = 10.833$ Å; $\alpha = 66.38$ $\beta = 89.06$ $\gamma = 81.67°$	$PIPH_2$	2D	279
$[C_2H_{10}N_2]_{0.5}CoPO_4$	$I2_1/b$	$a = 14.719$ Å, $b = 14.734$ Å, $c = 17.891$ Å; $\alpha = \gamma = 90°$, $\beta = 90.02°$	enH_2	3D, DFT	750
$NaCoPO_4$	$P6_1$	$a = b = 10.192$ Å, $c = 23.901$ Å; $\alpha = \gamma = 120°$, $\beta = 90°$	Na^+	3D, chiral	752
$KCoPO_4$	$P6_3$	$a = b = 18.23$ Å, $c = 8.521$ Å; $\alpha = \gamma = 120°$, $\beta = 90°$	K^+	3D, chiral	752
NH_4CoPo_4-hex	$P6_3$	$a = b = 10.719$ Å, $c = 8.71$ Å; $\alpha = \gamma = 120°$, $\beta = 90°$	NH_4	3D, chiral	752
NH_4CoPO_4-ABW	$P2_1$	$a = 8.797$ Å, $b = 5.462$ Å, $c = 9.011$ Å; $\alpha = \gamma = 120°$, $\beta = 89.95°$	NH_4	3D, ABW	752
$RbCoPO_4$	$P2_1$	$a = 8.838$ Å, $b = 5.415$ Å, $c = 8.972$ Å; $\alpha = \gamma = 90°$, $\beta = 93.95°$	Rb^+	3D, ABW	752
$[C_2H_{10}N_2]_2[Co_4(PO_4)_4]\cdot H_2O$	$P2_12_12_1$	$a = 10.277$ Å, $b = 10.302$ Å, $c = 18.836$ Å; $\alpha = \beta = \gamma = 90°$	enH_2	3D, 8MR, ACO	318
$[C_4H_{16}N_3]_3[Co_6(PO_4)_5(HPO_4)_3]\cdot H_2O$	$P2_1/c$	$a = 31.95$ Å, $b = 8.36$ Å, $c = 15.92$ Å; $\alpha = \gamma = 90°$, $\beta = 96.6°$	$DETAH_3$	3D, 16MR	318
$[C_2H_{10}N_2]_{0.5}[CoPO_4]$	$C2/c$	$a = 14.744$ Å, $b = 8.85$ Å, $c = 10.062$ Å; $\alpha = \gamma = 90°$, $\beta = 131.609°$	enH_2	3D, GIS	754
$[C_6H_{14}N_2][Co_2(HPO_4)_3]$	$P\bar{1}$	$a = 9.552$ Å, $b = 9.98$ Å, $c = 10.001$ Å; $\alpha = 107.67°$, $\beta = 97.93°$, $\gamma = 114.91°$	$DABCOH_2$	3D, 8MR	573, 576
$[C_2H_{10}N_2]_2[Co_7(PO_4)_6]$	$P2_1/n$	$a = 5.098$ Å, $b = 15.234$ Å, $c = 16.425$ Å; $\alpha = \gamma = 90°$, $\beta = 95.67°$	enH_2	3D, 12MR	755, 756
$Cs_2Co_3(HPO_4)(PO_4)_2\cdot H_2O$	$P2_1$	$a = 10.471$ Å, $b = 5.113$ Å, $c = 13.558$ Å; $\alpha = \gamma = 90°$, $\beta = 109.893°$	Cs^+	3D, 16MR	760
$[C_4H_{12}N_2][Co_2(PO_4)(H_2PO_4)_2]$	$C2/c$	$a = 13.444$ Å, $b = 12.874$ Å, $c = 8.224$ Å; $\alpha = \gamma = 90°$, $\beta = 94.64°$	$PIPH_2$	3D, 16MR, SOD-related	279, 761
$[C_4H_{12}N_2]_2[Co_4(HPO_4)_6]$	$P2_1/c$	$a = 12.878$ Å, $b = 26.671$ Å, $c = 8.259$ Å; $\alpha = \gamma = 90°$, $\beta = 96.93°$	$PIPH_2$	3D, 8MR, SOD-related	761

[a] SG = space group.

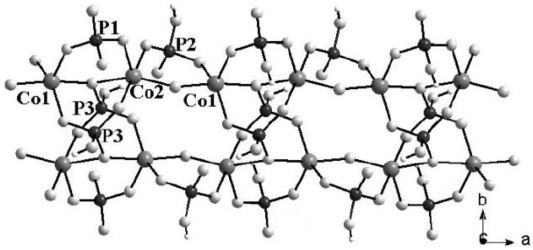

Figure 77. Complex 1D structure of a cobalt phosphate. Reference 622 — Reproduced by permission of the Royal Society of Chemistry.

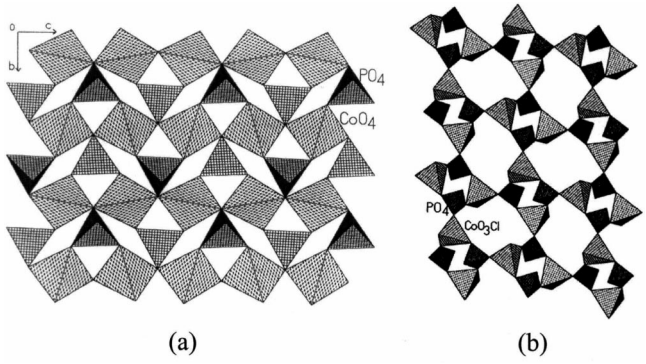

Figure 78. Structures of layered cobalt phosphates with (a) infinite Co−O−Co linkages[758] and (b) corner-sharing of SBU-4 units.[576]

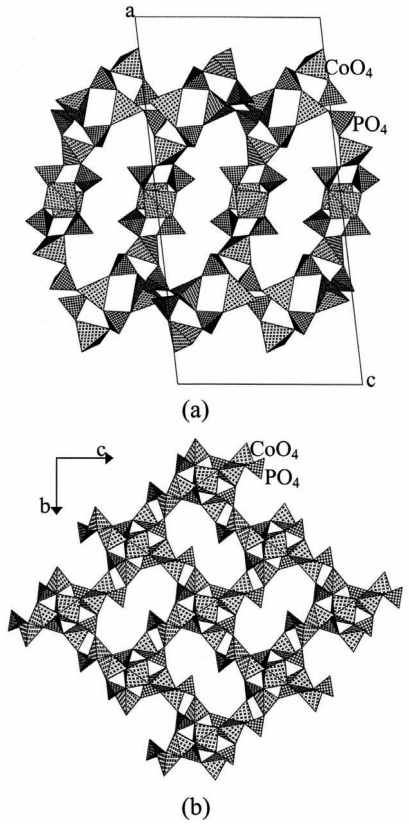

Figure 79. Three-dimensional cobalt phosphates (a) with a 16MR channel[318] and (b) with a 12MR channel.[755]

positions, while the two axial trans sites of Zr atoms have terminal -OH or F (Figure 80a,c).[774,776] The other example of a kronkite-type chain is that in the VPO family[695] (see Figure 71b). In $[NH_4]_3[Zr(PO_4)_2F]\cdot 0.5H_2O$,[776] two kronkite-type chains get fused together to form a ribbon-like 1D structure (Figure 80b), similar to that in the iron sulfate minerals ramsomite, krausite, and botryogen.[778]

Two-Dimensional Structures. The 2D structures of the ZrPO family are generally related to α- or γ-ZrP structures (Figure 81).[779,780] Thus, the structures of $[C_3H_5N_2][Zr(HPO_4)_2(H_2PO_4)]$[768] and $[C_2H_{10}N_2][Zr(PO_4)_2]$[772] are related to α-ZrP, where each Zr is connected to six PO_4 tetrahedra through Zr−O−P linkages, while the structures of $[C_6H_{18}N_2]_{0.5}[Zr_2(HPO_4)_2(PO_4)F_2]\cdot 0.5H_2O$,[767] $[C_2H_{10}N_2]_{0.5}[Zr(PO_4)(HPO_4)]$,[768] and $[C_6H_{16}N_2]_{0.5}[Zr_2(PO_4)(HPO_4)_2F_2]\cdot 0.5H_2O$[770] are related to γ-ZrP. In γ-ZrP, 1D ladder-like motifs[765] are connected into a 2D double layer sheet by bridging through PO_4 oxygens. Apart from these, there are sheet structures with four- and eight-membered ring apertures,[771,775] formed by alternating ZrO_6 octahedra and PO_4 tetrahedra via corner-sharing (Figure 82).

Three-Dimensional Structures. Though there are several 3D open-framework structures reported with different amines (Table 10), most of them[767,769] are identical to ZrPO-1,[767] made up of strictly alternating $ZrO_{6-x}F$ ($x = 0$ and 1) octahedra and PO_4 tetrahedra, with an eight-ring tunnel. The dehydrated forms of ZrPO-1 type structures are also reported.[773] There is one 3D ZrPO with a 10-membered channel made of ZrO_5, ZrO_5F, and ZrO_4F_2 octahedra and HPO_4 tetrahedra.[770]

3.6.6. Titanium Phosphates

Titanium phosphates are an attractive class of compounds with a range of potential applications. For example, the well-known layer structures, $\alpha\text{-}Ti(HPO_4)_2\cdot H_2O$[781] and $\gamma\text{-}Ti(H_2PO_4)(PO_4)\cdot 2H_2O$,[782] have been extensively studied for their ion-exchange properties.[783] The dense potassium titanylphosphate $KTiPO_4$ (KTP) has attracted much attention due to its nonlinear optical properties.[784] Microporous titanosilicates (ETS-4, -10) are used as oxidation catalysts,[785] while the mesoporous titanium phosphates show ion-exchange and catalytic properties.[786] Poojary et. al.[787] first reported 3D titanium phosphates with an open architecture, while Ekambaram and Sevov[788] characterized the first organically templated mixed-valent open-framework TiPO. Today the area of organically templated titanium phosphates has considerably expanded and includes 1-, 2-, and 3D structures as listed in Table 11.[694,772,787–800] Porous titanium phosphates have been briefly reviewed by Férey[801] with respect to their formation under hydrothermal conditions.

One-Dimensional Structures. There are only a couple of 1D structures in the family of organically templated TiPO's. Both the structures[795,796] are based on the corner-sharing of TiO_6 octahedra through −Ti−O−Ti− linkages but with interesting differences. One is analogous to the tancoite-type chain with all trans-corner-sharing while the other one is chiral with alternate cis- and trans-corner-sharing TiO_6 octahedra (Figure 83). Both the chains have similar PO_4 bridges (compare Figure 83 with Figure 46c).

Two-Dimensional Structures. Several 2D structures are known in the TiPO family. For example, the structures of MIL-6_n ($n = 2, 3$)[789] are made of alternate corner-sharing TiO_4F_2 octahedra and PO_4 tetrahedra, related to $VOPO_4\cdot 2H_2O$[705] (see Figure 72) but exhibiting different monoclinic distortions, while $[C_2H_9N_2][Ti(OH)(PO_4)]$[694,792,793] with bound ethylenediamine has the ULM-11 topology and is related to $VO(HPO_4)\cdot 2H_2O$[442] (Figure 47c). MIL-44[772,800] has a structure related to ethylenediamine-intercalated γ-TiP,[782] and MIL-28_n ($n = 2, 3$)[799] has a 10-membered

Table 10. Lattice Parameters, Templates, and Dimensionalities of the Various Templated Zirconium Phosphates Reported in the Literature.

formula	SG[a]	lattice parameters	template	type	ref
$[C_2H_{10}N_2]_{1.5}[Zr(HPO_4)(PO_4)F_2]$	$P2_1/n$	$a = 14.220$ Å, $b = 6.639$ Å, $c = 14.349$ Å; $\alpha = \gamma = 90°$, $\beta = 109.32$	enH_2	1D ladder	765
$[C_2H_{10}N_2][Zr(HPO_4)_3]$	$C2/c$	$a = 8.996$ Å, $b = 15.373$ Å, $c = 9.582$ Å; $\alpha = \gamma = 90°$, $\beta = 102.97°$	enH_2	1D	768
$[NH_4]_3[Zr(OH)_2(PO_4)(HPO_4)]$	$P\bar{1}$	$a = 8.143$ Å, $b = 12.718$ Å, $c = 5.246$ Å; $\alpha = 91.85°$, $\beta = 92.16°$, $\gamma = 74.25°$	NH_4^+	1D kronkite	774
$[NH_4]_4[Zr(PO_4)_2F_2]\cdot H_2O$	$P2_1/n$	$a = 10.889$ Å, $b = 10.52$ Å, $c = 12.412$ Å; $\alpha = \gamma = 90°$, $\beta = 115.7°$	NH_4^+	1D kronkite	776
$[NH_4]_3[Zr(PO_4)_2F]\cdot 0.5H_2O$	$P2_12_12_1$	$a = 5.351$ Å, $b = 9.246$ Å, $c = 22.644$ Å; $\alpha = \beta = \gamma = 90°$	NH_4^+	1D	776
$[C_6H_{18}N_2]_{0.5}[Zr_2(HPO_4)_2(PO_4)F_2]\cdot 0.5H_2O$	$C2/c$	$a = 21.647$ Å, $b = 6.648$ Å, $c = 21.282$ Å; $\alpha = \gamma = 90°$, $\beta = 103.03°$	$TMEDH_2$	2D	767
$[C_2H_{10}N_2]_{0.5}[Zr(PO_4)(HPO_4)]$	$Pnnn$	$a = 24.087$ Å, $b = 5.381$ Å, $c = 6.66$ Å; $\alpha = \beta = \gamma = 90°$	enH_2	2D	768
$[C_3H_5N_2][Zr(HPO_4)_2(H_2PO_4)]$	$C2/m$	$a = 21.45$ Å, $b = 5.428$ Å, $c = 9.134$ Å; $\alpha = \gamma = 90°$, $\beta = 97.22°$	IMDH	2D	768
$[C_6H_{16}N_2]_{0.5}[Zr_2(PO_4)(HPO_4)_2F_2]\cdot 0.5H_2O$	$C2/c$	$a = 16.754$ Å, $b = 6.621$ Å, $c = 27.094$ Å; $\alpha = \gamma = 90°$, $\beta = 90.57°$	$1,4\text{-}DACHH_2$	2D	770
$[C_6H_{16}N_2]_{1.5}[Zr_3(PO_4)_3F_6]\cdot 1.5H_2O$	$P\bar{1}$	$a = 10.622$ Å, $b = 10.668$ Å, $c = 13.643$ Å; $\alpha = 63.48°$, $\beta = 86.16°$, $\gamma = 68.104°$	$1,4\text{-}DCHH_2$	2D	770
$[C_2H_{10}N_2]_2[NH_4]_2[Zr_3(OH)_6(PO_4)_4]$	$P\bar{1}$	$a = 9.383$ Å, $b = 9.923$ Å, $c = 8.342$ Å; $\alpha = 97.85°$, $\beta = 111.75°$, $\gamma = 113.01°$	enH_2, NH_4^+	2D	771
$[C_2H_{10}N_2][Zr(PO_4)_2]$ (MIL-43)	$P2_1$	$a = 11.072$ Å, $b = 10.663$ Å, $c = 16.464$ Å; $\alpha = \gamma = 90°$, $\beta = 95.99°$	enH_2	2D	772
$[NH_4]_2[Zr(OH)_3(PO_4)]$	$P2_1/n$	$a = 7.661$ Å, $b = 9.699$ Å, $c = 10.473$ Å; $\alpha = \beta = \gamma = 90°$	NH_4^+	2D	775
$[C_2H_{10}N_2]_{0.5}[Zr_2(PO_4)_2(HPO_4)F]\cdot H_2O$	$C2/c$	$a = 17.277$ Å, $b = 6.620$ Å, $c = 23.104$ Å; $\alpha = 62.83°$, $\beta = 81.40°$, $\gamma = 82.69°$	enH_2	3D, 8MR	766, 767
$[C_3H_{12}N_2]_{0.5}[Zr_2(HPO_4)(PO_4)_2F]\cdot H_2O$	$C2_1/c$	$a = 17.224$ Å, $b = 6.630$ Å, $c = 23.181$ Å; $\alpha = \gamma = 90°$, $\beta = 94.53°$	$NenH_2$	3D, 8 MR	767
$[C_3H_{12}N_2]_{0.5}[Zr_2(HPO_4)(PO_4)_2F]\cdot H_2O$	$C2$	$a = 17.34$ Å, $b = 6.605$ Å, $c = 11.54$ Å; $\alpha = \gamma = 90°$, $\beta = 95.41°$	$1,3\text{-}DAPH_2$	3D, 8MR	767
$[C_4H_{16}N_3]_{0.33}[Zr_2(HPO_4)(PO_4)_2F]\cdot 94H_2O$	$C2/m$	$a = 17.233$ Å, $b = 6.626$ Å, $c = 11.523$ Å; $\alpha = \gamma = 90°$, $\beta = 94.82°$	$DETAH_2$	3D, 8MR	767
$[C_4H_{14}N_2]_{0.5}[Zr_2(HPO_4)(PO_4)_2F]\cdot 0.5H_2O$	$P\bar{1}$	$a = 6.611$ Å, $b = 9.109$ Å, $c = 11.56$ Å; $\alpha = 85.62°$, $\beta = 89.60°$, $\gamma = 70.57°$	$NNenH_2$	3D, 8MR	769
$[C_5H_{16}N_2]_{0.5}[Zr_2(HPO_4)(PO_4)_2F]$	$P\bar{1}$	$a = 6.616$ Å, $b = 9.045$ Å, $c = 11.565$ Å; $\alpha = 85.26°$, $\beta = 88.86°$, $\gamma = 71.46°$	$NNDAPH_2$	3D, 8MR	769
$[C_2H_{10}N_2]_{0.5}[Zr_2(HPO_4)(PO_4)_2F]$	$P\bar{1}$	$a = 6.605$ Å, $b = 8.787$ Å, $c = 11.499$ Å; $\alpha = 93.07°$, $\beta = 90.42°$, $\gamma = 104.66°$	enH_2	3D, 8MR	769
$[C_5H_{16}N_2]_{0.5}[Zr_3(PO_4)_3(HPO_4)F_2]\cdot 1.5H_2O$	$Pnnm$	$a = 15.168$ Å, $b = 18.972$ Å, $c = 6.628$ Å; $\alpha = \beta = \gamma = 90°$	$2,2\text{-}DDAPH_2$	3D, 10MR	770
$[C_3H_{12}N_2]_{0.5}[Zr_2(HPO_4)(PO_4)_2F]$	$P2_1/c$	$a = 11.539$ Å, $b = 6.637$ Å, $c = 17.092$ Å; $\alpha = \gamma = 90°$, $\beta = 94.95°$	$NenH_2$	3D, 8MR	773
$[C_3H_{12}N_2]_{0.5}[Zr_2(HPO_4)(PO_4)_2F]$	$P2_1/c$	$a = 11.506$ Å, $b = 6.638$ Å, $c = 17.148$ Å; $\alpha = \gamma = 90°$, $\beta = 96.05°$	$1,3\text{-}DAPH_2$	3D, 8MR	773
$[C_4H_{14}N_2]_{0.5}[Zr_2(HPO_4)(PO_4)_2F]$	$P\bar{1}$	$a = 6.654$ Å, $b = 8.939$ Å, $c = 11.505$ Å; $\alpha = 94.20°$, $\beta = 90.57°$, $\gamma = 107.12°$	$NNenH_2$	3D, 8MR	773

[a] SG = space group.

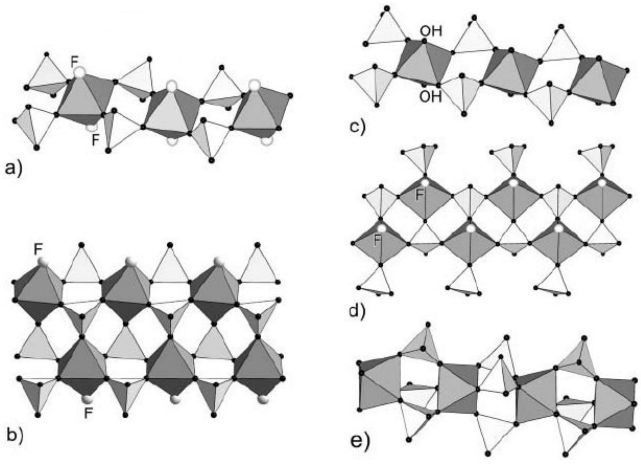

Figure 80. One-dimensional structures in the ZrPO family. Reference 776 — Reproduced by permission of the Royal Society of Chemistry.

aperture within the layer created by linking of the tancoite-type chains by $TiO_4(H_2O)_2$ octahedra (Figure 84).

Three-Dimensional Structures. The large family of open-framework TiPO's includes structures that are mixed-valent (+3/+4),[788,791,794] are oxy-fluorinated,[791,798] and have channels bound by eight polyhedra, except for a few cases with 12-membered channels.[788,790,800] Like in the ZrPO family, there is no report to date of an extra-large pore structure in the TiPO family. Titanium sometimes forms a subnetwork through Ti−X−Ti (X = F, −OH, −O) linkages but in most cases Ti and P polyhedra alternate in the framework. Thus $[Ti_2O(PO_4)_2(H_2O)_2]$ has a dimer of corner-shared TiO_6 octahedra,[787] $[NH_4]_2[Ti_3O_2(HPO_4)_2(PO_4)_2]$[787] has a trimer of TiO_6 corner-shared chains, and MIL-15[791] has Ti−F−Ti linkages with a 7MR channel. Frameworks built with alternating Ti and P polyhedra include $[Ti_3(PO_4)_4(H_2O)_2]\cdot NH_3$,[787] $[C_3H_{10}N_2]_{0.5}[Ti^{III}Ti^{IV}(PO_4)(HPO_4)_2(H_2O)_2]$ with mixed-valent Ti,[788] and another mixed-valent compound that becomes tetravalent on removal of the template.[794] Apart from these, there are several 3D structures with alternate Ti and P polyhedra reported by Pang and co-workers.[797,798,800]

3.6.7. Other Transition Metal Phosphates

Transition metals like Ni, Mn, Sc, Nb, and Cu form open-framework phosphates, and we list them in Table 12.[802–816]

Nickel. The only open-framework Ni phosphates known to date are those due to Férey, Cheetham, and co-workers. They have unusual magnetic properties and posses 24-membered ring large pores. The materials called VSB-1[802] and VSB-5,[803] (VSB = Versailles-Santa Barbara) are stable at relatively high temperatures, and some of their properties are discussed later in the review.

Manganese. Manganese is known to exhibit various oxidation states ranging from +2 to +7 and form layered and microporous oxide structures.[817] The family of organically templated MnPO's includes 1-, 2-, and 3D structures[804–812] but is dominated by 2D sheet structures.

Three common types of 1D structures occur in the MnPO family that include two tancoite-type chains,[807] one ladder-type,[812] and two simple chains of corner-shared alternate Mn and P polyhedra.[808] In all these structures, Mn is in the +3 oxidation state and has F ions coordinated to it. They exhibit pseudo-isomerism due to Jahn−Teller ordering of the Mn^{3+} ions.[807,808]

Several 2D MnPO's are reported. In these structures, Mn is in the +2 oxidation state, and most of them have the Mn subnetwork with extensive Mn−O−Mn linkages. Thus, two sheet structures are known with edge-shared MnO_6 octahedra, connected by MnO_5 *tbp* units and PO_4 tetrahedra[804,806] (Figure 85a). Both of them have ethylenediammonium cations in the interlamellar space, and one of them has the charge of the extra organo-ammonium cations compensated by an isolated $H_2PO_4^-$ anion sitting in the interlamellar space. The Mn−O network can also form a hexameric unit composed of two MnO_6, two $MnO_5(H_2O)$ octahedra, and two $MnO_4(H_2O)$ *tbp* units, all edge-shared, which are then further connected by Mn polyhedra and PO_4 tetrahedra to form the layer.[805] Similar structures with the same SBU have been observed in MgPO[648] and FePO[728] families. Even more extensive Mn−O−Mn linkages have been observed where square-planar chains of corner-sharing MnO_6 octahedra are capped by PO_4 tetrahedra, which share an edge with one MnO_6 and corners with three others[810] (Figure 85b). There is just one example where Mn and P polyhedra alternate to create a 4·6 net,[811] which is isostructural with an AlPO.[414] There is a recent report of a 3D structure with a small pore,[809] but a truly open-framework MnPO is yet to be made.

Scandium. The first pure scandium phosphate open-framework structure was reported by Riou et al[813] (Figure 86a); it has an eight-membered channel and is isostructural with an open-framework InPO[518] and FePO.[732] Open-framework ScPO's having 8-, 10-, 12-, and 14-membered channels are also known.[526,814] One of them is scandium phosphate-fluoride (Figure 86b), which has an InPO analogue.[526] In these structures, ScO_6 octahedra and PO_4 tetrahedra are alternately corner-shared and Sc has the +3 oxidation state.

Niobium and Copper. Both Nb and Cu have just made their appearance in the family of organically templated metal phosphates with a 2D and 1D structure, respectively.[815,816] The layered structure of the niobium phosphate[815] is analogous to that of $VOPO_4\cdot 2H_2O$ (see Figure 72) but with a negatively charged inorganic network, $[NbOF(PO_4)]^-$. An organically templated 1D CuPO chain[816] has just been discovered where CuO_4Cl_2 octahedra are edge-shared and the H_2PO_4 tetrahedra decorate the chain by both bridging and dangling modes (Figure 87); this is similar to the topology in fornacite and vauquilinite.[778]

3.6.8. Actinide and Lanthanide Phosphates

Both actinides and lanthanides are capable of showing variable oxidation states and high coordination numbers,[746] so it was quite natural to speculate that more structurally diverse framework types would be found in these families. Surprisingly, there are only a few organically templated actinide phosphates known, limited to uranium species. The first organically templated uranium phosphate was discovered by the group of O'Hare,[818] and now we have a few 1-, 2-, and 3D structures as shown in Table 13.[818–822] In all these structures, uranium is in the +6 oxidation state and generally assumes the pentagonal bipyramidal (pbp) geometry, thus leading to pbp−tetrahedral framework structures. In the 1D structure,[819] UO_7 pbp units and PO_4 tetrahedra alternate forming four-membered rings, which are corner-shared to form the neutral chain. The 2D structures[818] contain infinite chains of edge-sharing UO_7 pbp units cross-linked by bridging PO_4 tetrahedra to form 2D sheets (Figure 88). There are three 3D UPO open-framework structures known to

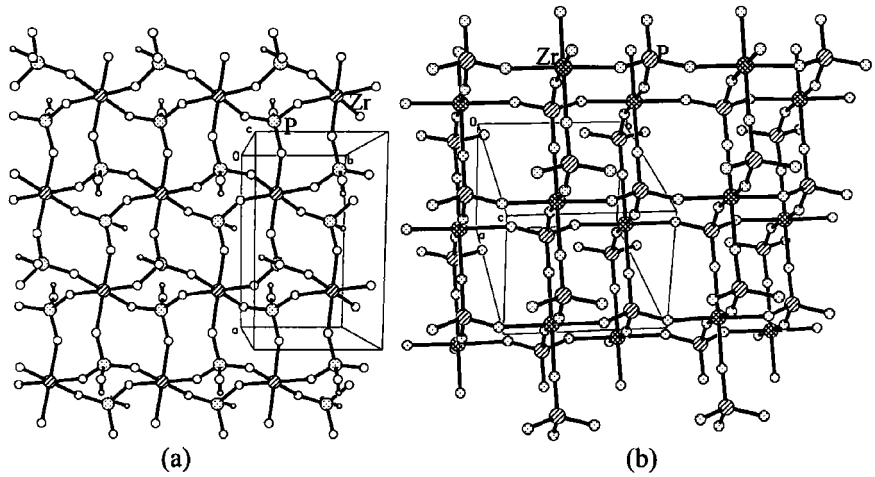

Figure 81. Layered topologies of (a) α-ZrP and (b) γ-ZrP.

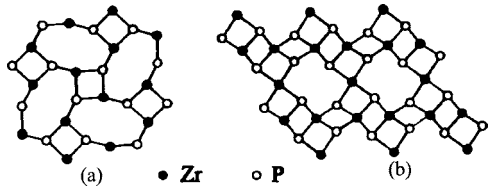

Figure 82. Layered structures in the ZrPO family. Reprinted with permission from ref.[775] Copyright 2002 Chemical Society of Japan.

date.[820–822] All are pillared layered structures (Figure 89). There are, however, interesting differences both in the topology of the layers and in the pillaring modes. For example, in $[(C_2H_5)_2NH_2]_2[(UO_2)_5(PO_4)_4]$[820] and $(N_2C_4H_{12})$-$(UO_2)[(UO_2)(PO_4)]_4 \cdot 2H_2O$,[822] the layers are the same as those in the anionic 2D sheets of $[(UO_2)_2(PO_4)(HPO_4)]^-$ (see Figure 88), and these layers are pillared by UO_6 octahedra and UO_7 pbp units, respectively, joining the PO_4 groups of the layer and thereby forming intersecting tunnels (Figure 89a). In $[N_2C_6H_{14}]_2[(UO_2)_6(H_2O)_2F_2(PO_4)_2(HPO_4)_4] \cdot 4H_2O$,[821] the layers are formed by infinite zigzag chains of alternate edge- and corner-shared UO_7 pbp units, cross-linked by PO_4 tetrahedra, and then pillared by $UO_5F(H_2O)$ pbp units to form the intersecting channels (Figure 89b).

Among the lanthanide phosphates, only a templated cerium phosphate fluoride is known. This has a layered structure built of CeO_3F_5 polyhedra and PO_4 tetrahedra.[823]

3.7. Substituted Metal Phosphates

After the discovery of AlPO frameworks in 1982, Union Carbide researchers realized immediately that in order to modify the chemical properties to make them catalytically active and ion-exchangeable, elements with different valences have to be doped in the tetrahedral site of the framework. There are two tetrahedral sites in the framework, namely, Al and P. The Union Carbide researchers discovered several exciting series of materials by substituting Si for P to form silico-aluminophosphates (SAPO-*n*),[824] by substituting other metals in the Al site to form metal aluminophosphates (MAPO-*n*),[653,825] and also by substituting metals in the SAPO-*n* framework to form metal-silico-aluminophosphates (MAPSO-*n*).[826] All these framework compositions can be written with the general formula $(Si_xM_wAl_yP_z)O_2$ where x varies from 0−0.20 and w from 0−0.25.[262] Substitution of Si preferentially takes place at the P site, while metal exclusively substitutes Al in the framework, making a negatively charged framework analogous to zeolites. These framework charges are balanced by H^+ after template removal by calcination. The materials thus exhibit acid catalytic activity that is altered as a function of framework type and the nature of the substituting element.[826] The various transition metal ions that have been substituted in the AlPO-*n* and SAPO-*n* frameworks and their catalytic activities have been documented in a review by Hartmann and Kevan.[827] Another interesting feature of these materials is that substitution by other elements not only modifies the parent AlPO-*n* framework but often creates unique framework types not known in the AlPO-*n* or aluminosilicate zeolites, for example, SAPO-40 (AFR),[270,824] MAPSO-46 (AFS), MAPO-39 (ATN), and MAPO-36 (ATS).[270] Today, substitution by other elements is no longer limited to the AlPO framework but has been extended to GaPO, ZnPO, and other metal phosphate frameworks, and sometimes the other metals take up independent crystallographic positions leading to a mixed metallic phosphate framework. Just as Si preferentially substitutes at the P site in AlPO to form the SAPO materials, pentavalent As also takes up P sites in AlPO framework to form AlAsPO-*n*[828] leading to doping in the anionic PO_4 moiety; more importantly, sometimes the anionic moiety can also have independent crystallographic positions making a mixed anionic framework. In the following section, we discuss these classes of materials briefly.

3.7.1. Doped and Bimetallic Open-Framework Phosphates

The discovery of MAPO-*n* and MAPSO-*n* prompted the incorporation of various metal ions in the AlPO framework, and as a result, a large number of doped AlPO frameworks, as well as new zeotype structures, have been discovered.[747,748,829–857] A large number of zeo-type structures are known with Mg containing aluminophosphates: MgAPO-50 (AFY),[270] DAF-1 (DFO),[829] STA-1 (SAO),[832] STA-2 (SAT,[833] CHA, and GIS[837]), STA-5 (BPH),[845] STA-6 (SAS),[847] Mg-STA-7,[848] and others.[852–854] Similarly, incorporation of Co has led to several zeo-type structures: ACP-1 (ACO),[747,843] ANA,[747] CHA,[747,850] EDI,[841] FAU,[747] Co-DAF-4 (LEV),[851] MER,[747] PHI,[747] RHO,[838] Co-STA-7,[848] SOD,[747] THO,[747] and others.[834–836,840,844,846,854] Stucky and co-workers[748] have reported a number of MAPO's (M = Co, Mn, Mg, and Zn) having large cage zeolitic structures with multidimensional channels (UCSB-6 and UCSB-10, now called SBS and SBT framework types, respectively). Other metals such as

Table 11. Lattice Parameters, Templates. and Dimensionalities of the Various Templated Titanium Phosphates Reported in the Literature

formula	SG[a]	lattice parameters	template	type	ref
$[C_2H_{10}N_2]_5[H_3O]_2[Ti_3O_3(PO_4)_6]$ (JTP-A)	$P2_12_12_1$	$a = 10.18$ Å, $b = 15.899$ Å, $c = 23.227$ Å; $\alpha = \beta = \gamma = 90°$	enH $_2$	1D	795
$[C_2H_{10}N_2]$ $[TiO(HPO_4)_2]$ (JTP-B)	$P2_1/n$	$a = 8.670$ Å, $b = 7.253$ Å, $c = 16.601$ Å; $\alpha = \gamma = 90°$, $\beta = 102.69°$	enH_2	1D tancoite	796
$[C_2H_{10}N_2][Ti_2(PO_4)_2F_4]$ (MIL-6_2)	$P2_1/c$	$a = 7.508$ Å, $b = 8.881$ Å, $c = 8.96$ Å; $\alpha = \gamma = 90°$, $\beta = 107.22°$	enH_2	2D	789
$[C_3H_{12}N_2][Ti_2(PO_4)_2F_4]\cdot H_2O$ (MIL-6_3)	$C2$	$a = 16.821$ Å, $b = 6.335$ Å, $c = 6.331$ Å; $\alpha = \gamma = 90°$, $\beta = 106.82°$	$1,3\text{-}DAPH_2$	2D	789
$[C_2H_9N_2][Ti(OH)(PO_4)]$ (ULM-11, Ti)	$P2_1/c$	$a = 9.265$ Å, $b = 7.329$ Å, $c = 9.911$ Å; $\alpha = \gamma = 90°$, $\beta = 100.89°$	bound en	2D	694, 792, 793
$[C_2H_{10}N_2]_3[Ti_3O_2F_2(PO_4)_4]\cdot 2H_2O$ (MIL-28_2)	$P\bar{1}$	$a = 10.071$ Å, $b = 18.92$ Å, $c = 7.107$ Å; $\alpha = 89.88°$, $\beta = 106.23°$, $\gamma = 100.45°$	enH_2	2D	799
$[C_3H_{12}N_2]_3[Ti_3O_2(OH)_2(HPO_4)_2(PO_4)_2]\cdot 2H_2O$ (MIL-28_3)	$Fm2m$	$a = 18.331$ Å, $b = 18.943$ Å, $c = 7.111$ Å; $\alpha = \beta = \gamma = 90°$	$1,3\text{-}DAPH_2$	2D	799
$[C_2H_{10}N_2][Ti_2(HPO_4)_2(PO_4)_2]$ (MIL-44)	$P\bar{1}$	$a = 6.307$ Å, $b = 10.181$ Å, $c = 12.644$ Å; $\alpha = 102.14°$, $\beta = 102.49°$, $\gamma = 90°$	enH_2	2D	772, 800
$[Ti_3(PO_4)_4(H_2O)_2]\cdot NH_3$	$P\bar{1}$	$a = 8.251$ Å, $b = 8.788$ Å, $c = 5.102$ Å; $\alpha = 90.703°$, $\beta = 91.083°$, $\gamma = 110.158°$	NH_3	3D, 8MR	787
$[Ti_2O(PO_4)_2(H_2O)_2]$	$P\bar{1}$	$a = 8.819$ Å, $b = 9.654$ Å, $c = 5.109$ Å; $\alpha = 93.818°$, $\beta = 93.665°$, $\gamma = 73.313°$	H_2O	3D, 8MR	787
$[NH_4]_2[Ti_3O_2(HPO_4)_2(PO_4)_2]$	$P2_1$	$a = 8.516$ Å, $b = 16.733$ Å, $c = 5.181$ Å; $\alpha = \gamma = 90°$, $\beta = 91.173°$	NH_4^+	3D	787
$[C_3H_{10}N_2]_{0.5}[Ti^{III}Ti^{IV}(PO_4)(HPO_4)_2(H_2O)_2]$	$Pnna$	$a = 12.702$ Å, $b = 9.365$ Å, $c = 11.253$ Å; $\alpha = \beta = \gamma = 90°$	$1,3\text{-}DAPH_2$	3D, 12MR	788
$[H_3O]_3[Ti_6O_3(H_2O)_3(PO_4)_7]\cdot H_2O$ (MIL-18)	$P6_3/m$	$a = b = 15.956$ Å, $c = 6.299$ Å; $\alpha = \beta = 90°$, $\gamma = 120°$	H_3O^+	3D, 12MR	790
$[Ti^{III}Ti^{IV}F(PO_4)_2]\cdot 2H_2O$ (MIL-15)	$P2_1/n$	$a = 10.935$ Å, $b = 14.447$ Å, $c = 5.105$ Å; $\alpha = \gamma = 90°$, $\beta = 90.5°$	H_2O	3D, 7MR	791
$[C_2H_9N_2][Ti^{III}Ti^{IV}$ $(HPO_4)_4]\cdot H_2O$	$I4_1$	$a = b = 6.371$ Å, $c = 16.571$ Å; $\alpha = \beta = \gamma = 90°$	enH	3D, 8MR	794
$Ti_2^{IV}(HPO_4)_4$	$I4_1/a$	$a = b = 6.335$ Å, $c = 16.389$ Å; $\alpha = \beta = \gamma = 90°$	Nil	3D, 8MR	794
$[C_4H_{12}N_2]_{0.5}[Ti_2(HPO_4)_3(PO_4)]$	$P2_1/n$	$a = 10.745$ Å, $b = 6.347$ Å, $c = 20.48$ Å; $\alpha = \gamma = 90°$, $\beta = 104.29°$	$PIPH_2$	3D, 8MR	797
$[C_6H_{14}N_2][Ti_7(HPO_4)_6(PO_4)_6]$	$R\bar{3}$	$a = b = 16.864$ Å, $c = 12.334$ Å; $\alpha = \beta = 90°$, $\gamma = 120°$	$DABCOH_2$	3D, 8MR	797
$[C_4H_{12}N_2][Ti_4(HPO_4)_2(PO_4)_4F_2]\cdot H_2O$	$C2/c$	$a = 16.655$ Å, $b = 6.338$ Å, $c = 22.208$ Å; $\alpha = \gamma = 90°$, $\beta = 94.862°$	$PIPH_2$	3D, 8MR	798
$[C_2H_{10}N_2][Ti_4(HPO_4)_2(PO_4)_4F_2]\cdot H_2O$	$C2/m$	$a = 16.632$ Å, $b = 6.322$ Å, $c = 11.073$ Å; $\alpha = \gamma = 90°$, $\beta = 94.362°$	enH_2	3D, 8MR	798
$[C_2H_{10}N_2][Ti_3(H_2PO_4)(HPO_4)_{3.5}(PO_4)_2]$	$P\bar{1}$	$a = 10.318$ Å, $b = 10.75$ Å, $c = 10.832$ Å; $\alpha = 73.44°$, $\beta = 79.65°$, $\gamma = 83.26°$	enH_2	3D, 8,12MR	800
$[C_3H_{12}N_2][Ti_7(HPO_4)_6(PO_4)_6]$	$R\bar{3}$	$a = b = 16.499$ Å, $c = 12.704$ Å; $\alpha = \beta = 90°$, $\gamma = 120°$	$1,3\text{-}DAPH_2$	3D, 8MR	800

[a] SG = space group.

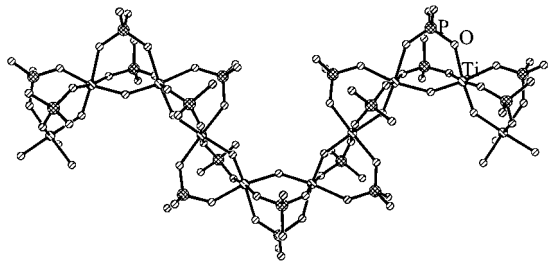

Figure 83. Chiral 1D chain of a titanium phosphate closely related to the tancoite chain.[795]

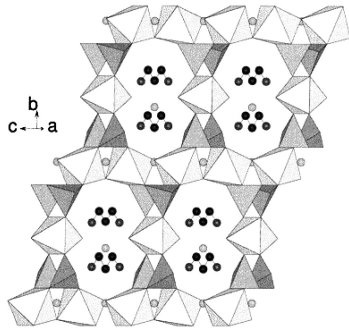

Figure 84. Layered titanium phosphate featuring the tancoite chain. Reprinted with permission from ref 799. Copyright 2002 American Chemical Society.

Zn,[839,843,848,854,855] Ni,[830,849] Fe,[852,856] Mn,[838,852,854,857] and V[831] have also been incorporated in the AlPO framework.

Various metals (including Ti, V, Mn, Fe, Co, Ni, Zn, and U)[747,748,858–874] have been incorporated in the GaPO framework in place of Ga. Several doped Ga phosphates, which have known zeotype structures (e.g., EDI,[841] GIS,[859,865] LAU,[858,862] SOD,[863] and THO[747]) and novel topologies (e.g., CGF[860,872] and CGS[866,869]) have also been reported. Apart from these, several MnGaPO are reported by Wang and co-worker,s[867,868,871] along with a chiral network. Structures with SBS and SBT topology have been reported in the MGaPO system doped with Co, Mg, and Zn.[748] Recently, V-doped GaPO,[870] layered Ni- and Ti-doped GaPO,[873] and uranium-containing gallium phosphates[874] with 3D structures have been reported.

Unlike AlPO and GaPO frameworks, transition metal incorporation in the ZnPO framework has not led to new structure types. Among the transition metals, mainly Co has been doped in the ZnPO structures.[875–884] There is one example where Fe^{2+} has been doped.[885] Co-ZnPO structures include 2D[877,879] and several 3D structures with CZP,[875,876,878] THO,[881] and DFT[884] topologies. There are a few 3D M-ZnPO's (M = Co/Fe) formed with piperazine or 2-methyl piperazine, which are ZnPO analogues.

Several bimetallic phosphates are known with Mo and other metals.[886–892] These include Mn- and Cd-containing 1D,[888,890] Zn-containing 2D,[886] and Fe-,[887] Co-,[889] Ni-,[891] and Cd-containing[890] 3D MoPO's, as well as Co- and Fe-containing WPO's.[892] A few bimetallic phosphates are also known with the combinations Fe and V,[893,894] Co and Be,[895] and Nb and V.[815] Al and Fe have been doped in the ZrPO-8 framework,[896] and V, Fe, Co, and Zn have been substituted in VSB-1.[897] To our knowledge, there are only a couple of trimetallic 3D phosphates.[898]

3.7.2. Metalloborophosphates

Boron forms both trigonal and tetrahedral coordination with its oxygen environment[746] and is known to form BPO_4 analogous to $AlPO_4$.[899] Surprisingly to date, there is no example of an open-framework structure of pure BPO_4, analogous to $AlPO_4$-*n*. However, B doping in the AlPO structure is known.[900] More importantly, B and P form complex anionic oxide networks built of BO_4, BO_3, and PO_4 units, which are stabilized by NH_4^+, alkali, alkaline earth, and other cations[901] or by a transition metal complex.[902] This area of research has been developed primarily by Kniep and co-workers, Jacobson, and others.[904–907] The first organically templated metal borophosphate with an open-framework structure reported by Sevov was $CoB_2P_3O_{12}(OH)\cdot enH_2$.[903] Since then, several inorganic−organically templated metalloborophosphates with 0-, 1-, 2-, and 3D structures have been reported.[901–929] Thus, 0D cluster anions of cyclic and noncyclic types are known with VBPO structural units stabilized by organo-ammonium cations or transition metal complexes.[906,907,909,911,913,914,924,925,927] A reduced MoBPO anion related to the Wells Dawson cluster has been reported.[922] A couple of chain metalloborophosphate structures are also known with V and Fe where NH_4^+ acts as the template.[918] A layered VBPO templated by imidazole is also reported.[912] A large number of templated metalloborophosphate 3D structures are known with metals such as Be, Mg, V, Mn, Fe, Co, Ni, Cu, and Zn.[903–905,908,910,915–917,919–921,923,926] Among the 3D structures, the most interesting ones are those with a zeotype topology related to CZP, made with various metals, $M^IM^{II}(H_2O)_2[BP_2O_8]\cdot yH_2O$ (M^I = Li, Na, K; M^{II} = Mn, Fe, Co, Ni, Zn; y = 0.5, 1).[904] One such compound, $NaZn(H_2O)_2[BP_2O_8]\cdot H_2O$, on dehydration transforms to the CZP topology.[919] Zeolitic MBPOs also include GIS (ZnBPO and $Zn_{1-x}Co_xBPO$),[908,915] ANA (M^IBeBPO, $M^I = K^+$, NH_4^+, Na^+),[893] and zeotype FeBPO.[916,920] There are isostructural borophosphates of $M(C_2H_{10}N_2)[B_2P_3O_{12}(OH)]$ (M = Mg, Mn, Fe, Ni, Cu, Zn)[910] and $M(C_4H_{12}N_2)$-$[B_2P_3O_{12}(OH)]$ (M = Co, Zn) families.[917] A hierarchical derivative of NbO has been found in a ZnBPO.[921] In a ZnBPOCl compound, DABCO binds to Zn as well as acting as a template[926] (Figure 90). A 3D structure of a fluorinated borophosphate related to the GIS topology has been isolated from a water-free flux of H_3BO_3 and $NH_4H_2PO_4$.[928] If we ignore the presence of F in the structure, it can be considered as the first open-framework pure borophosphate. There is also a fluorinated borophosphate, $(C_2H_{10}N_2)[BPO_4F_2]$, with a chain structure.[929]

3.7.3. Mixed Anionic Phosphate Framework

It is possible to substitute As^{5+} in the P site of AlPO-*n*.[828] A similar substitution gives rise to organically templated mixed anionic fluorinated iron(III) arsenate phosphates.[930,931] A scandium-containing open-framework sulfate-phosphate (cyclen-ScSPO) templated by the aza-macrocycle (cyclen) has been characterized (Figure 91).[932] The only other organically templated phosphate-sulfate known is a layered Ce-phosphatehydrogensulfate.[933] A few organically templated metal phosphate−phosphites are known with Zn[934,935] and Fe.[936,937] These possess 2D and 1D structures, respectively. One-dimensional structures containing both phosphate and diphosphate (P_2O_7) units have been reported with Ga and V in the presence of en[938] and 1,3-DAP.[939] Templated diphosphates of Ga,[940,941] Cu,[303] and Ni,[304] are reported. The

Table 12. Lattice Parameters, Templates, and Dimensionalities of the Various Templated Nickel, Manganese, Scandium, Niobium, and Copper Phosphates Reported in the Literature

formula	SG[a]	lattice parameters	template	type	ref
		$NiPO_4$			
$[H_3O^+,NH_4^+]_4[Ni_{18}(HPO_4)_{14}(OH)_3F_9]\cdot 12H_2O$	*P6mm*	$a = b = 19.652$ Å, $c = 5.018$ Å; $\alpha = \beta = 90°$, $\gamma = 120°$	H_3O^+, NH_4^+	3D, 24MR	802
$[Ni_{20}[(OH)_{12}(H_2O)_6][(HPO_4)_8(PO_4)_4]\cdot 12H_2O$	$P6_3/m$	$a = b = 18.209$ Å, $c = 6.389$ Å; $\alpha = \beta = 90°$, $\gamma = 120°$	nil	3D, 24MR	803
		$MnPO_4$			
$[C_5H_6N][MnF(H_2PO_4)(HPO_4)]\cdot 0.5H_2O$	$P2_1/n$	$a = 7.295$ Å, $b = 17.052$ Å, $c = 18.512$ Å; $\alpha = \gamma = 90°$, $\beta = 100.78°$	PyH	1D tancoite	807
$[C_5H_6N][MnF(H_2PO_4)(HPO_4)]\cdot H_2O$	$P\bar{1}$	$a = 7.374$ Å, $b = 8.628$ Å, $c = 10.329$ Å; $\alpha = 83.66°$, $\beta = 77.83°$, $\gamma = 68.54°$	PyH	1D tancoite	807
$[C_4H_{12}N_2][MnF_4(H_2PO_4)]$	$P2_1/c$	$a = 6.749$ Å, $b = 12.039$ Å, $c = 12.501$ Å; $\alpha = \gamma = 90°$, $\beta = 94.42°$	$PIPH_2$	1D	808
$[C_4H_{12}N_2][MnF_4(H_2PO_4)]$	$P2_1/c$	$a = 6.651$ Å, $b = 12.799$ Å, $c = 12.825$ Å; $\alpha = \gamma = 90°$, $\beta = 110.312°$	$PIPH_2$	1D	808
$[C_4H_{12}N_2][MnF_2(HPO_4)(H_2O)]\cdot H_2PO_4$	$P\bar{1}$	$a = 6.229$ Å, $b = 9.234$ Å, $c = 11.836$ Å; $\alpha = 98.343°$, $\beta = 100.747°$, $\gamma = 107.642°$	$PIPH_2$	1D, ladder	812
$[C_2H_{10}N_2][Mn_2(HPO_4)_3]\cdot H_2O$	$P2_1/n$	$a = 21.96$ Å, $b = 9.345$ Å, $c = 6.639$ Å; $\alpha = \gamma = 90°$, $\beta = 91.06°$	enH_2	2D	804
$[C_4H_{12}N_2][Mn_6(H_2O)_2(HPO_4)_4(PO_4)_2]\cdot H_2O$	$P\bar{1}$	$a = 12.819$ Å, $b = 15.874$ Å, $c = 6.479$ Å; $\alpha = 99.87°$, $\beta = 90.39°$, $\gamma = 103.43°$	$PIPH_2$	2D	805
$[C_2H_{10}N_2]_{1.5}[Mn_2(HPO_4)_3]\cdot H_2PO_4$	$P\bar{1}$	$a = 6.651$ Å, $b = 9.343$ Å, $c = 14.512$ Å; $\alpha = 87.69°$, $\beta = 84.1°$, $\gamma = 89.07°$	enH_2	2D	806
$[C_2H_{10}N_2][Mn_2(PO_4)_2]\cdot 2H_2O$	$P1$	$a = 4.910$ Å, $b = 5.762$ Å, $c = 9.832$ Å; $\alpha = 78.11°$, $\beta = 87.75°$, $\gamma = 85.63°$	enH_2	2D	810
$[C_6H_{21}N_4]_2[Mn_3(PO_4)_4]\cdot 6H_2O$	$P3c1$	$a = b = 8.871$ Å, $c = 26.158$ Å; $\alpha = \beta = \gamma = 90°$	$TRENH_3$	2D	811
$[NH_4][Mn_4(PO_4)]$	*Pnnm*	$a = 9.885$ Å, $b = 16.745$ Å, $c = 6.463$ Å; $\alpha = \beta = \gamma = 90°$	NH_4	3D	809
		$ScPO_4$			
$[C_2H_{10}N_2]_{0.5}[Sc(HPO_4)_2]$	$P2/n$	$a = 9.409$ Å, $b = 9.092$ Å, $c = 9.688$ Å; $\alpha = \gamma = 90°$, $\beta = 117.25°$	enH_2	3D, 8MR	813, 814
$[C_2H_{10}N_2]_8[Sc_8(ScO_2)_4(HPO_4)_{12}(PO_4)_4]\cdot 12H_2O$	$P2_1/n$	$a = 8.603$ Å, $b = 15.476$ Å, $c = 16.504$ Å; $\alpha = \gamma = 90°$, $\beta = 96.877°$	enH_2	3D, 14MR, 10MR	814
$[H_3O]_4[Sc_4(HPO_4)_8]$	$P2_1/c$	$a = 5.305$ Å, $b = 8.823$ Å, $c = 14.799$ Å; $\alpha = \gamma = 90°$, $\beta = 95.685°$	H_3O^+	3D, 12MR	814
$[Sc_4(PO_4)_4]\cdot 8H_2O$	$P2_1/n$	$a = 5.443$ Å, $b = 10.251$ Å, $c = 8.909$ Å; $\alpha = \gamma = 90°$, $\beta = 90.253°$	nil	3D, 8MR	814
$[C_6H_{14}N_2][Sc_4F_2(PO_4)_4]\cdot 4H_2O$	$P2_1/n$	$a = 10.283$ Å, $b = 12.698$ Å, $c = 17.864$ Å; $\alpha = \gamma = 90°$, $\beta = 102.761$	$DABCOH_2$	3D, 8MR	526
		$NbPO_4$			
$[C_5H_7N_2][NbOF(PO_4)]$	$P2_1/c$	$a = 11.442$ Å, $b = 9.198$ Å, $c = 9.169$ Å; $\alpha = \gamma = 90°$, $\beta = 109.94°$	4AmPyH	2D	815
		$CuPO_4$			
$[C_3H_5N_2][Cu(H_2PO_4)_2Cl]\cdot H_2O$	$P2_1/n$	$a = 8.999$ Å, $b = 7.019$ Å, $c = 18.986$ Å; $\alpha = \gamma = 90°$, $\beta = 102.964$	IMDH	1D	816

[a] SG = space group.

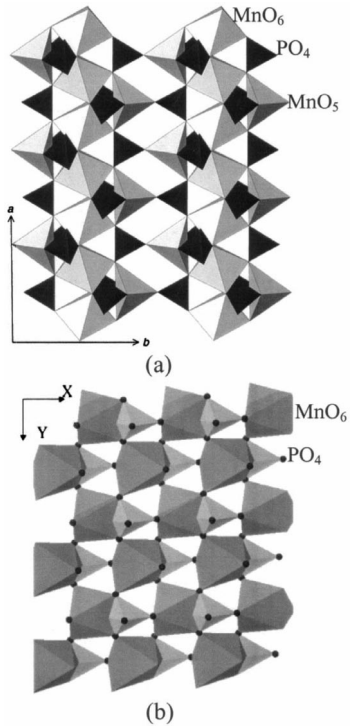

Figure 85. Polyhedral view of two layered manganese phosphates. Panel a: Reference 806 — Reproduced by permission of the Royal Society of Chemistry. Panel b reproduced from ref 810. Copyright 2003 American Chemical Society.

family of organically templated pure metal sulfates and phosphites is fast growing following the first reports by the groups of Rao[942] and Harrison,[943] respectively. On the other hand, reports on open-framework arsenates, though long-known,[262,270] are not as extensive due to the toxicity of As.[527,665,822,944]

3.8. Hybrid Structures Involving Phosphate Moieties

The use of phosphate alone in the design of open-framework materials imposes some limitations. The nature and size of the phosphate ion and more generally of tetrahedral polyanions are limiting factors because they have to share their oxygens with at least three cations to ensure a 3D structure. This difficulty can be overcome if the metallic center can be linked by a chelating agent. Thus, metal centers have been linked through multidentate organic ligands.[945] The structures of these coordination polymers have the potential for rational design through control of the shape, size, and functionality of the pores. The stability of these systems on removal of the space-filling species has been demonstrated.[946] The richness of the organic ligands and the thermal stability of the phosphate moiety can be combined to create new open-framework materials. This has led to the discovery of hybrid porous solids in which the framework is built from both organic and inorganic moieties. Open-framework metal phosphates can be fully or partially substituted by an appropriate choice of an organic chelating agent, which provides a greater flexibility and creates additional possibilities of making hybrid open-framework solids. Furthermore, since most inorganic open-framework structures are built of metallic centers or clusters linked by diamagnetic linkers (phosphates), strong long-range magnetic interactions are not favored. It becomes, therefore, desirable to have linkers that favor long-range superexchange coupling between magnetic centers. Several metallo-organic frameworks based on dicarboxylate linkers[947,948] and oxalate frameworks with organic templates have been reported.[948] We can classify these materials under three categories based on the incorporation of (i) anionic ligands such as carboxylates, (ii) neutral ligands, and (iii) transition metal complexes into the phosphate framework.

3.8.1. Anionic Ligand in Phosphate Frameworks

Carboxylates can act as flexible anionic linkers in forming open-framework structures. Among the carboxylates, the oxalate anion with four potential donor sites is attractive not only due to its ability to form framework structures[948] but because it can participate in strong magnetic superexchange.[949] The ability of the oxalate ion to partly substitute the phosphate in the framework was first reported in a Sn(II) oxalate-phosphate.[950] Several organically templated metal oxalate-phosphates have since been investigated.[665,696,951–969] Thus, oxalate phosphates of V,[696,961–963] Mn,[956,968] Fe,[952–957] Co,[967] Mo,[665] Zn,[969] Al,[958–960] Ga,[964–966] and In[951] having 1-, 2-, and 3D structures are known. There are three different types of oxalate coordinations in metal-oxalate-phosphate structures, namely, bis-bidentate, mono-bidentate and bis-mono and bis-bidentate.[958] Among them, the bis-bidentate mode is the most common, while the mono-bidentate is less common. In the 1D structures of V[961] and Mo,[665] the oxalate anion just caps the metal in a mono-bidentate coordination (Figure 92). On the other hand, there are several 2D oxalate-phosphates with Al,[958] Ga,[965,966] V,[696,962,963] Fe,[956] and Mn.[956] In most of these, 2D layers of metal polyhedra are linked by phosphates and oxalates with the oxalate anion acting as a bis-bidentate ligand within the plane (in-plane). One such compound is $(H_3TREN)[M_2(HPO_4)(C_2O_4)_{2.5}]\cdot 3H_2O$ ($M = Fe^{2+}$, Mn^{2+})[956] where a 2D honeycomb lattice is formed by the in-plane oxalate units along with $M^{II}O_6$ octahedra and HPO_4 units. The structure can also be described by partial replacement of the oxalate units in the 2D honeycomb structure of tris-oxalatometallate[948] by the phosphate group (Figure 93). The oxalate units acting only in the mono-bidentate manner are also known, for example, in a gallium oxalate-phosphate.[966] A new type of layer structure built by D6R units connected by phosphate and oxalate groups has been reported in V-Ox-PO_4 where both bis-bidentate and mono-bidentate oxalate units are present.[963] A column of D6R units has been previously observed in a 3D Al-Ox-PO_4.[959] On the other hand, most of the 3D framework structures are formed of metal-phosphate layers pillared by bis-bidentate oxalate bridges[953] where the oxalate units are out-of-plane with respect to the inorganic layer. The oxalate anion may be incorporated in the metal-phosphate layer and also act as a pillar to such hybrid layer, thus performing a dual role.[955] Among the 3D structures, specially noteworthy is the 3D Fe^{III} oxalate-phosphate with a large 1D channel of hexagonal symmetry (Figure 94).[954] An interesting mixed-valent $Fe^{3+/2+}$ oxalate-phosphate where the oxalate groups act as bis-bidentate and mono-bidentate ligands has been reported.[957] Metal phosphates incorporating other carboxylates such as acetate[970] and isonicotinate[971] have been reported.

3.8.2. Neutral Ligands in Phosphate Frameworks

Organic−inorganic hybrid compounds incorporating neutral ligands, 4,4′-bipyridine (4,4′-bpy), 2,2′-bipyridine (2,2′-bpy), 1,10-phenanthroline (1,10-phen), terpyridine (terpy),

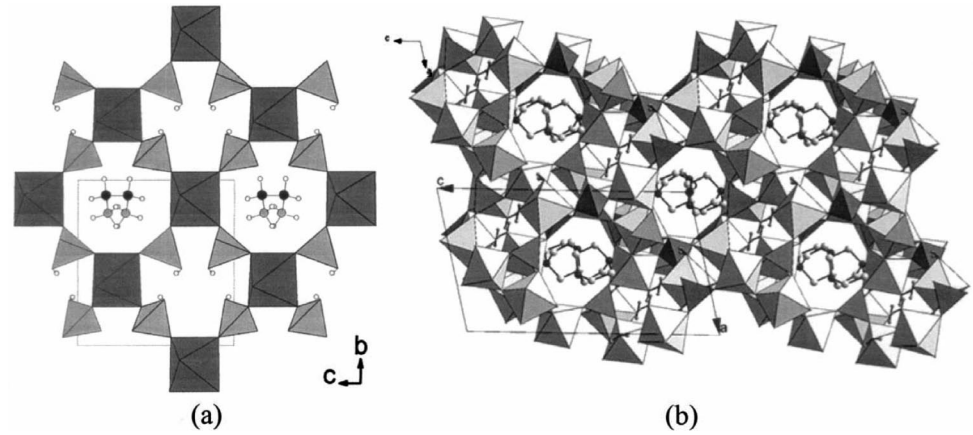

Figure 86. Three-dimensional scandium phosphates. Reprinted with permission from refs 813 and 526. Copyright 2002 and 2004 American Chemical Society.

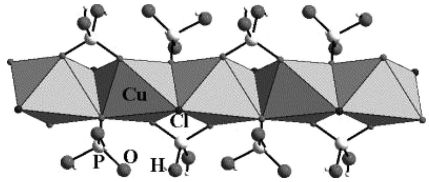

Figure 87. One-dimensional chain of a copper chlorophosphate. Reprinted with permission from ref 816. Copyright 2004 Elsevier.

pyrazine, etc., in combination with metal polyhedra and PO_4 tetrahedra have yielded many interesting structures. Today, a large number of structures are known[972–982] due to the systematic investigation mainly by the group of K. H. Lii. In many of these structures, the metal phosphate layers are covalently linked by 4,4′-bpy pillars. Such a structure was first reported by O'Hare,[972] where the $ZnPO_3F$ layers are pillared by 4,4′-bpy to form the 3D structure. This is a rare example of a fluorophosphate (PO_3F) framework. A few 1D structures are also known with Cu and Ag where the metal−bpy form the chains and the HPO_4 and H_2PO_4 units are dangling.[975] A two-dimensional network is known where V(III) or V(V) sites are linked through both 4,4′-bpy and phosphate ligands into a 2D layer structure.[976,978] Among the 3D structures, the pillared layer structure is the most common one with alternating organic and inorganic domains.[972–974,979–982] Two such interesting structures consist of neutral sheets of fluorinated cobalt phosphates, which are pillared through 4,4′-bpy and pyrazine (Figure 95), thus demonstrating the role of the pillaring organic linker in tuning the size of the pore as well as the magnetic coupling.[982] Many a time, the metal phosphate layer is bimetallic in nature.[974,980] Several complex structures are also described in the literature, for example, a $CdSO_4$ structure-type obtained in a Ni/4,4′-bpy/PO_4 system.[977] Organic linkers other than 4,4′-bpy that are used to construct hybrid networks are 2,2′-bpy,[983] 1,10-phen,[983,984] terpy,[983,985] bis-terpy,[986] and phenazine.[987]

3.8.3. Transition Metal Complexes in Phosphate Frameworks

A new class of hybrid materials is obtained when instead of having an organic template interacting weakly with an inorganic framework (as is normally the case), an inorganic complex is incorporated into the structure through covalent bonds. Quite a few such materials are reported by Morris and co-workers.[435,852,988–991] Generally aza-macrocyclic ligands are used for this purpose, although linear amines such as en have also been employed.[988] An interesting structure is obtained by CYCLAM, when D4R units are joined together by a six-coordinated Ga-CYCLAM complex (Figure 96).[989,991] This provides another extra parameter to modify the materials by incorporation of functional metals at the framework metal site as well as in the CYCLAM-complex, thereby leading to multifunctional materials.[991]

3.9. Mechanism of Formation of Open Framework Metal Phosphates

So far in this review, we have presented a large number of open-framework structures representing various geometries and pore sizes. The mechanism of formation of these structures under hydrothermal conditions is however not understood. The major challenge in the area of open-framework materials also relates to the rational design of new materials with desired properties. To achieve this goal, a full knowledge of reaction mechanism is most essential. Investigations of the reaction mechanism become difficult because of the reaction conditions (closed vessel, high temperature, several reactants, variables such as the concentration, pH, nature of amine, etc.). As a result, several different approaches have evolved to tackle this problem. The first approach is to propose a model based on the reaction products and a close inspection of the structural building units (SBU). Thus, Férey[263,290] proposed SBUs in the formation of open-framework structures, while Ozin and co-workers[992] proposed that the 3D structure may result from the transformation of the c.s. chain and layered structures. Another approach is to carry out real-time isolation of the reactive intermediates and transform them to the ultimate 3D solids, thus finding the condensation pathway. Thus, Rao and co-workers[265] proposed an Aufbau principle for complex open-framework structures of metal phosphates with different dimensionalities. A large number of transformation studies are now reported in the family of Zn,[305,585,588,603,604,621,993,994] Al,[995] and Ga phosphates,[488,495,502] wherein low-dimensional structures are transformed to higher dimensional ones including the 3D frameworks. It is important that *in situ* characterization methods are also employed to check the validity of the model through the identification of the intermediates.[996] The *in situ* studies require the investigation of both crystalline intermediates and soluble intermediates. Thus, an *in situ* study for the formation of transition metal doped aluminium phosphate has been reported based on angular

Table 13. Lattice Parameters, Templates, and Dimensionalities of the Various Templated Actinide and Lanthanide Phosphates Reported in the Literature

formula	SG[a]	lattice parameters	template	type	ref
		UPO_4			
$[(UO_2)(H_2PO_4)_2(H_2O)]_2[C_{12}H_{24}O_6]\cdot 5H_2O$	$P\bar{1}$	$a = 11.097$ Å, $b = 13$ Å, $c = 14.756$ Å; $\alpha = 107.82°$, $\beta = 102.77°$, $\gamma = 103.97°$	18-crown- 6	1D chain	819
$[(UO_2)(H_2PO_4)_2(H_2O)][C_{12}H_{24}O_6]\cdot 3H_2O$	$P2_12_12_1$	$a = 11.158$ Å, $b = 14.064$ Å, $c = 16.774$ Å; $\alpha = \beta = \gamma = 90°$	18-crown -6	1D chain	819
$[C_6H_{16}N][(UO_2)_2(HPO_4)(PO_4)]$	$P2_1/n$	$a = 9.336$ Å, $b = 18.325$ Å, $c = 9.864$ Å; $\alpha = \gamma = 90°$, $\beta = 93.08°$	TriEAH	2D	818
$[C_{12}H_{28}N][(UO_2)_3(HPO_4)_2(PO_4)]$	$P\bar{1}$	$a = 9.401$ Å, $b = 13.048$ Å, $c = 13.447$ Å; $\alpha = 108.02°$, $\beta = 103.16°$, $\gamma = 100.98°$	TPA	2D	818
$[C_4H_{12}N]_2[(UO_2)_5(PO_4)_4]$	$I2/m$	$a = 9.444$ Å, $b = 15.449$ Å, $c = 9.572$ Å; $\alpha = \gamma = 90°$, $\beta = 93.27°$	DEAH	3D	820
$[C_6H_{14}N_2]_2[(UO_2)_6(H_2O)_2F_2(PO_4)_2(HPO_4)_4]\cdot 4H_2O$	$P2_1/n$	$a = 13.448$ Å, $b = 17.921$ Å, $c = 19.902$ Å; $\alpha = \gamma = 90°$, $\beta = 90.98°$	$DABCOH_2$	3D	821
$[C_4H_{12}N_2][(UO_2)(PO_4)]_4\cdot 2H_2O$	Pn	$a = 9.3278$ Å, $b = 15.5529$ Å, $c = 9.6474$ Å; $\alpha = \gamma = 90°$, $\beta = 93.266°$	$PIPH_2$	3D	822
		$CePO_4$			
$[C_2H_{10}N_2]_{0.5}[CeF_3(HPO_4)]$	$P1$	$a = 6.248$ Å, $b = 7.079$ Å, $c = 8.794$ Å; $\alpha = 103.92°$, $\beta = 100.84°$, $\gamma = 110.28°$	enH_2	2D	823

[a] SG = space group.

Figure 88. The layered topology of a uranium phosphate.[818] Reprinted with permission from ref 822. Copyright 2004 Elsevier.

and energy dispersive X-ray diffraction (ADXRD and EDXRD) employing synchroton radiation.[997]

O'Hare, Férey, and co-workers employed time-resolved EDXRD to study the crystalline intermediates and elucidate the kinetics and mechanism of formation of organically templated Ga,[495,940,941,998,999] Zn,[1000,1001] and Al[1002] phosphates. *In situ* NMR spectroscopy has been used to investigate the soluble intermediates.[1003–1007] Theoretical and computational studies are also useful to design templates and microporous solids and to predict stabilities and conditions of formation.[1008–1010] Férey and co-workers[263,290] carried out a study of the chemistry and the structures of the ULM-*n* series in which they observed that all the structures could be described on the basis of a few types of SBUs (tetramers M_2P_2, hexamers M_3P_3, and octamers M_4P_4, see Figure 48) with a formal charge of −2, which form a neutral species with the organo-ammonium cations and allow the precipitation of the products.[263,290] Combined *ex situ* and *in situ* NMR measurements on the different nuclei have revealed the presence of a reactive species in the solution (called a prenucleation building unit, PNBU) with structures close to that of the SBU for $AlPO_4$-CJ2, ULM-3, and ULM-4.[1003–1005] The results suggest a crystallization mechanism by dissolution−nucleation−growth for $AlPO_4$-CJ2 and ULM-3 and crystallization via a solid−-solid reorganization from an amorphous phase for ULM-4. The existence of small oligomeric units seems to be a general phenomenon in metal phosphate chemistry and has been observed in both micro- and mesoporous Ti(IV) phosphates.[1007]

Ozin and co-workers[992] proposed a model for the formation of microporous aluminophosphates where a linear aluminophosphate c.s. chain would reassemble through hydrolysis−condensation reactions in solution to precipitate 2- and 3D networks, mediated only by the breaking and the creation of a few bonds. Rao and co-workers have carried out experimental studies on the transformation of various low-dimensional to higher dimensional zinc phosphates and also of the degradation of higher dimensional structures.[305,585,588,603,993,994] The studies indicate that the monomers (0D) transform to higher dimensional structures (1D c.s. chain or ladder, 2D layer, and 3D frameworks including sodalite-related networks) on mild heating in water in the presence of amine or zinc acetate. In most of the transformed structures, the presence of the S4R unit was evident.[305,585,994] The transformation of another S4R unit to a layered zinc phosphate on reaction with zinc acetate has been reported[621] (Figure 97). *In situ* ^{31}P MAS NMR investigations revealed the structural integrity of the S4Rs. The recent *in situ* EDXRD study[1001] on the transformation of the monomer $[C_6N_2H_{18}][Zn(HPO_4)(H_2PO_4)_2]$[305] has led to the conclusion that the transformations occurs via a

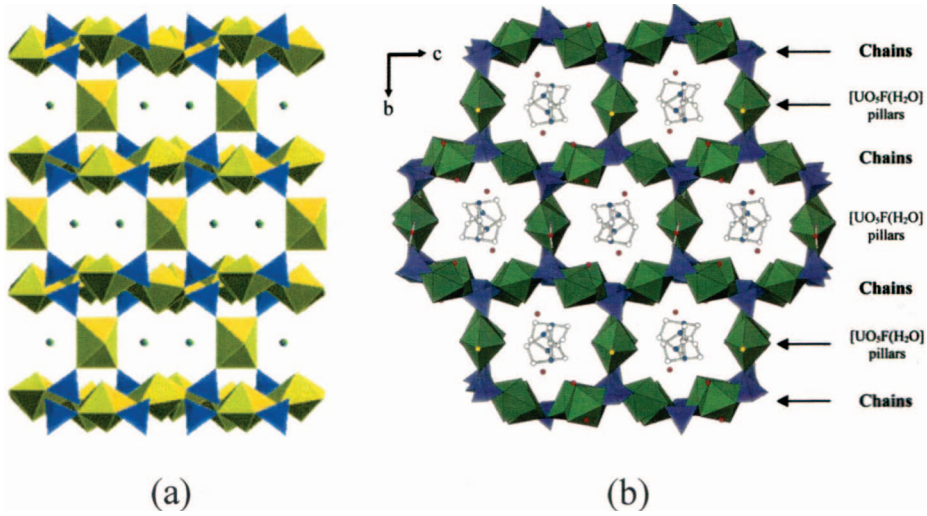

Figure 89. Three-dimensional uranium phosphates. Panel a: Reference 820 — Reproduced by permission of the Royal Society of Chemistry. Panel b reproduced from ref 821. Copyright 2004 American Chemical Society.

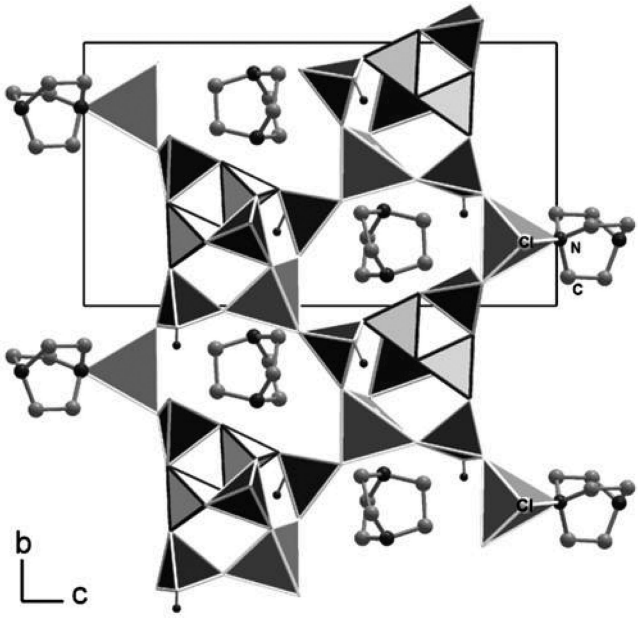

Figure 90. A 3D zinc borophosphate. Reprinted with permission from ref 926. Copyright 2003 American Chemical Society.

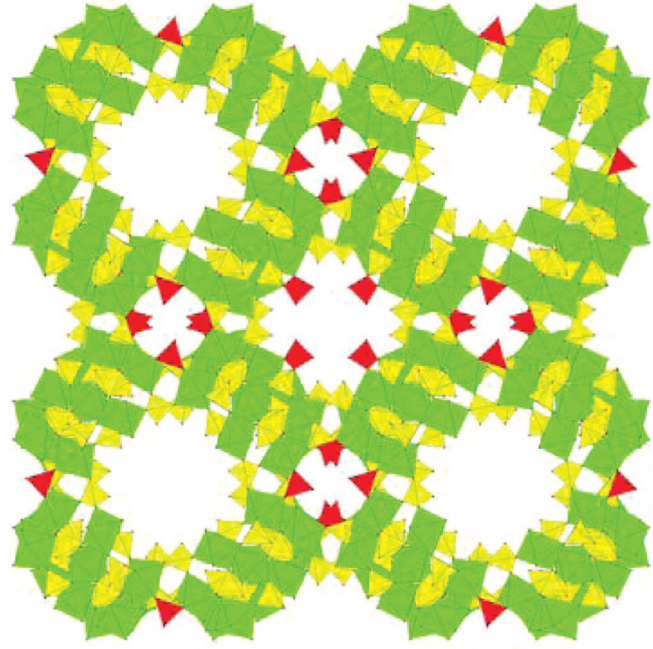

Figure 91. A 3D scandium sulfate-phosphate. Reference 932 — Reproduced by permission of the Royal Society of Chemistry.

dissolution−reprecipitation mechanism or in some cases by direct topochemical conversion of one organically templated solid to another.

A higher acid/amine ratio generally favors the formation of lower dimensional structures (with a high proportion of $H_2PO_4^-$ and HPO_4^{2-} groups), suggesting that the formation of the final structure is likely to be controlled by the degree of deprotonation of $H_2PO_4^-$ and HPO_4^{2-} moieties.[295,296] With a view to investigating the transformation of lower dimensional structures under appropriate conditions, transformations of one-dimensional zinc phosphate ladders (templated by TETA and DAP)[296,588] and three layered zinc phosphates (templated by TETA, DAP, and DAHP)[296,603] have been carried out. The ladder and the layer structures were subjected to (i) hydrothermal heating at 150 °C, (ii) hydrothermal treatment in the presence of zinc acetate, and (iii) hydrothermal treatment in the presence of varying concentrations of an added amine (mainly piperazine, PIP, or imidazole, IMD). The various products obtained by the transformation of the TETA ladder are shown in Figure 98.

In all the transformed structures, there are only a few or no HPO_4 and H_2PO_4 groups compared with the parent ladder. We also see the presence of the parent ladder motif in the structures as illustrated in Figure 98. For example, the ladder $[C_6H_{22}N_4]_{0.5}[Zn(HPO_4)_2]$ on treatment with excess PIP gives the gismondine structure constructed from crankshaft chains, which is nothing but four-membered rings connected through their edges (ladders).[588] A gallium phosphate with 1D tancoite chain structure has also been shown to transform to a 3D structure.[488,495]

The transformation of layered structures produced both 3D and 1D structures besides new 2D layered structures under simple reaction conditions.[603] Though the 2D layers give rise to 3D channel structures, the 2D to 3D transformation is not as straight forward as one may imagine.[992] Interestingly, heating the layered compound in water gives a ladder structure along with a 3D structure suggesting that the formation of the ladder structure may play an important role in the formation of the 3D structure. This led Rao and

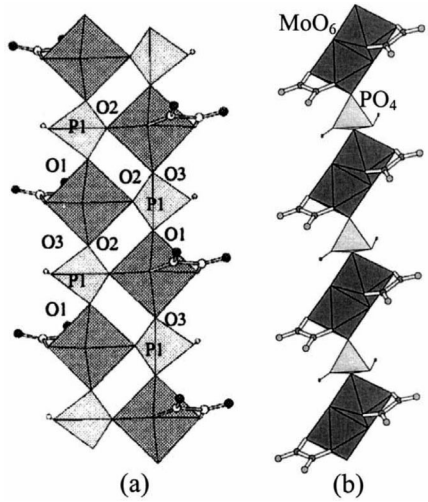

Figure 92. One-dimensional oxalate-phosphates. Reprinted with permission from refs 961 and 665. Copyright 1999 American Chemical Society.

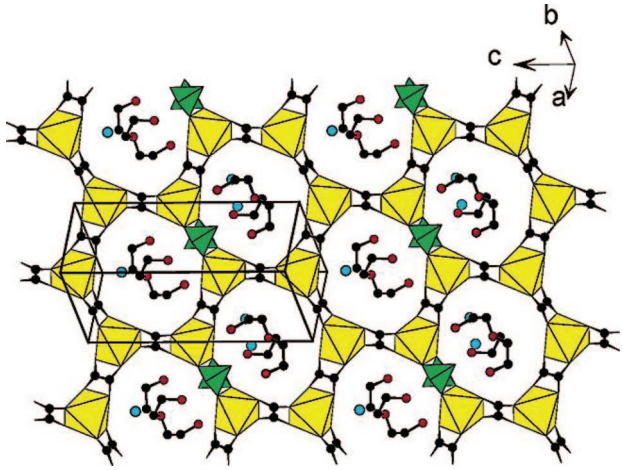

Figure 93. Honeycomb lattice topology in an iron oxalate-phosphate. Reprinted with permission from ref 956. Copyright 2003 American Chemical Society.

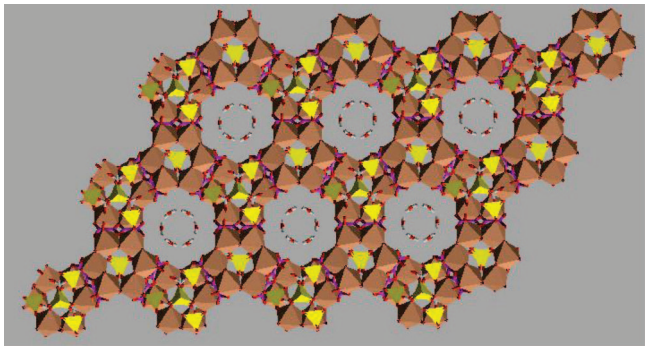

Figure 94. Iron oxalate-phosphate with a symmetrical 1D hexagonal channel.[954]

co-workers to propose that the one-dimensional ladder is the initial (primary) product of the transformation of the layer structures.[603] The ladder then transforms to the 3D structures as indeed described in the ladder transformation study.[588] When the layers were heated in presence of PIP, a c.s. chain was obtained, which can be derived from the ladder by a hydrolysis condensation reaction.[603] A recent *in situ* EDXRD study by Férey and co-workers[940,941] shows that the formation of 3D structures occurs after a one-dimensional structure is formed.[940,941] The study of zinc phosphates has also

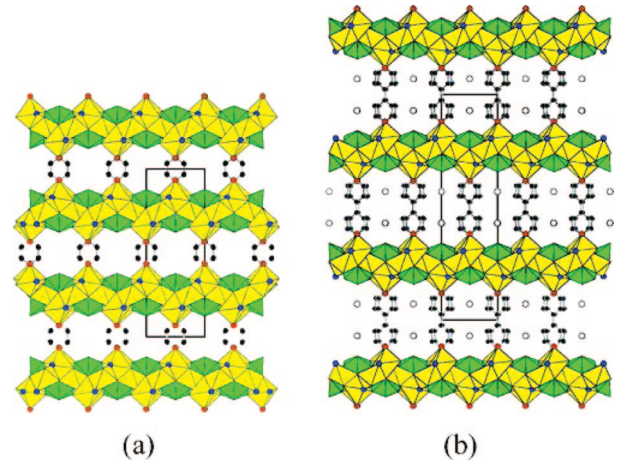

Figure 95. Organic−inorganic hybrid cobalt fluorophosphates with the amine molecules acting as pillars between the Co−F−PO_4 layers. Reprinted with permission from ref 982. Copyright 2004 American Chemical Society.

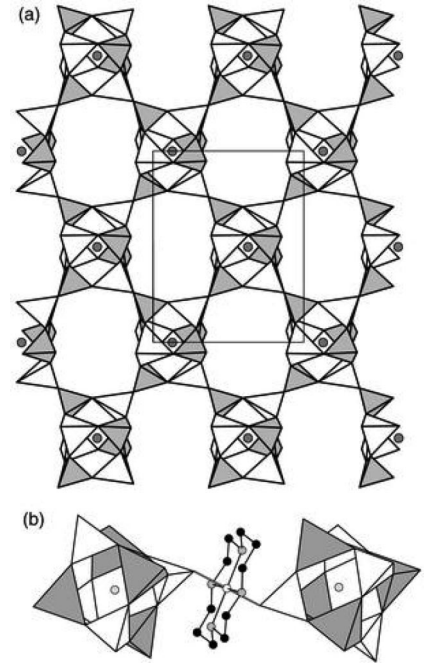

Figure 96. A 3D gallium phosphate where the Ga-CYCLAM complex joins the D4R units. Reference 991 — Reproduced by permission of the Royal Society of Chemistry.

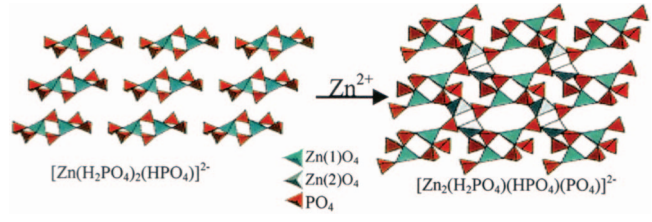

Figure 97. Scheme showing the transformation of a monomeric zinc phosphate to layered structures containing the features of the monomer.[621] Reprinted with permission from the table of contents of ref 621. Copyright 2003 American Chemical Society.

revealed a pathway of sequential crystallization involving the formation of a metastable low-dimensional chain phase before the growth of 3D complex structures.[1000] Férey and co-workers have found that a 1D c.s. chain species $([Al(PO_4)]^{3-})_n$ occurs during the hydrothermal synthesis of the supersodalite MIL-74.[1002]

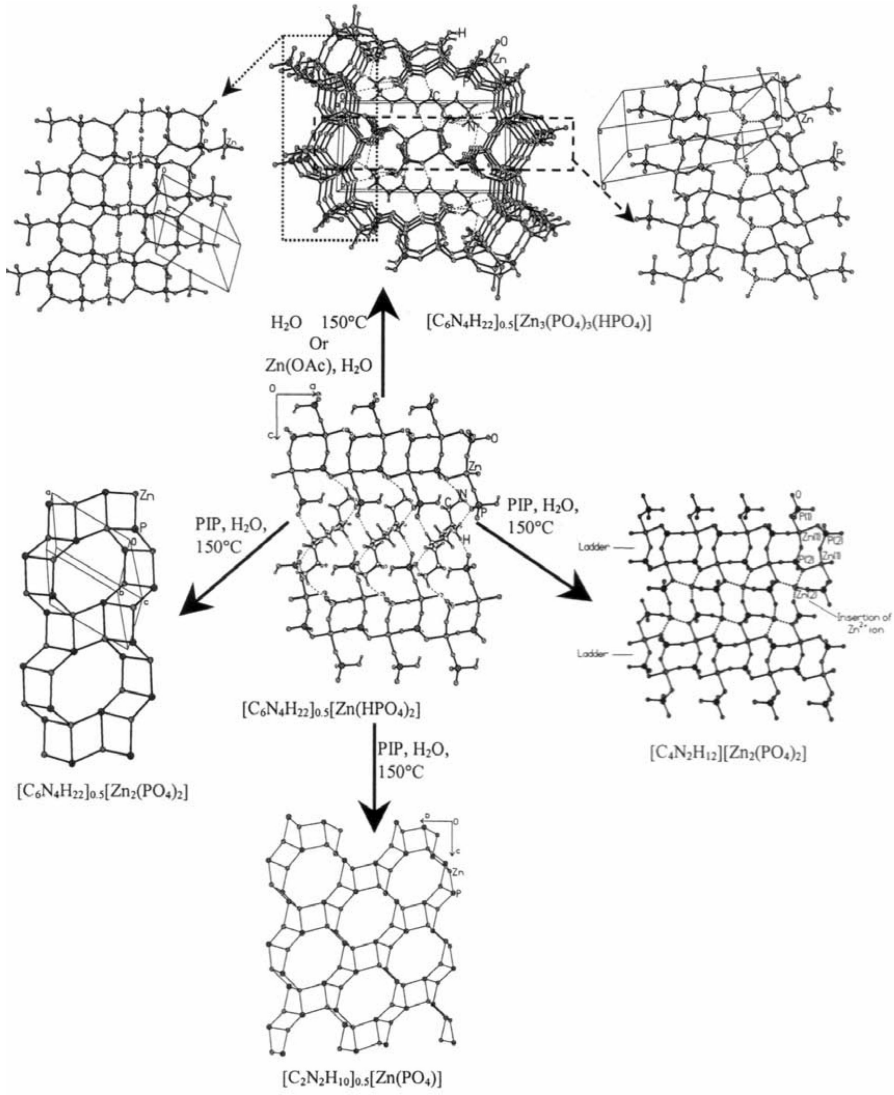

Figure 98. Schematic representation of the transformation of a ladder to various other structures under different reaction conditions. The features of the ladder are found in the transformed structures.

Since the deprotonation of the HPO_4 and H_2PO_4 groups drives the transformation reactions, it would be expected that in the presence of acid, the reverse should happen. That is, 3D or 2D structures should degrade to 1D or 0D structures. It has indeed been found that 3D structures undergo transformations under acidic conditions, while the layered structure remains almost unchanged under acidic conditions. The 3D zinc phosphate transforms sequentially to another 3D structure, the ladder, and the layer as the concentration of acid is increased[993] (Figure 99). The occurrence of the layer at higher acid concentrations suggests that the layer phase may possibly form via the intermediacy of the ladder. However, contrary to the general expectation, the absence of the ladder structure (more HPO_4 groups) in the most acidic regime is surprising. Clearly, the mechanism of formation of 3D open-framework phosphates is far more complex.

Xu and co-workers[849,995] have found that a 1D c.s. chain aluminium phosphate can be assembled into a 3D network through the insertion of transition metal cations, where the cations coordinate the terminal oxygen atoms of the chain and thereby retain the signature of the chain in the final 3D structure. These workers also report that the one 1D c.s. chain transforms to another chain as the ratio of H_3PO_4 and amine is varied. Férey and co-workers[488,495] have found that two

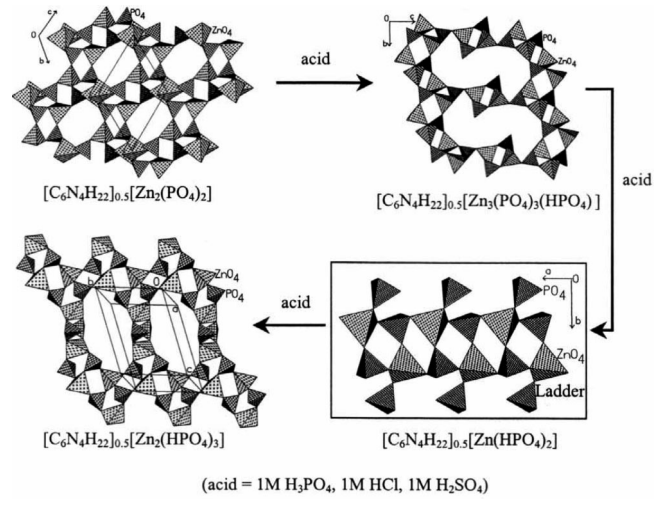

Figure 99. Schematic representation of the action of acid on a 3D zinc phosphate leading to structures of different dimensionalities.[993]

anionic chains similar to tancoite transform to 3D GaPO ULM-3. This process has been followed by *in situ*, time-resolved EDXRD, which reveals that the dissolution of the one-dimensional phase occurs before the rapid crystallization

of ULM-3. The role of chains in the formation of extended framework tin(II) phosphates and related materials has been pointed out.[1011]

It is instructive to examine the relative reactivities of the c.s. chain and the ladder structures. Which is more reactive? The ladder with dangling HPO_4 and H_2PO_4 groups from the Zn sites is expected to be more reactive. Transformation studies with PIP generally show the appearance of c.s. chain structures incorporating the PIP[585,603,994,1001] as the initial product, and the signature of this chain is maintained in the subsequently transformed 3D structures such as the interrupted sodalite (clover-like channel)[603] and expanded sodalite.[538,994] The supersodalite MIL-74 is also formed via a c.s. chain.[1002] Linear amines seem to stabilize ladder structure, and the transformed structures always have the ladder motif.[588] The nature of the amine could decide whether it stabilizes the c.s. chain or the ladder. It would be interesting to find an amine that stabilizes both the c.s. chain and the ladder and study the transformations of the two 1D structures.

Theoretical and computational studies have been employed to design microporus solids making use of designed templates as well as SBUs.[1008–1010] The correct experimental conditions to form these structures are, however, not known. Many discrete D4R units have been discovered recently in the GaPO system. Can one transform them to ACO or LTA topologies, which are exclusively built from D4R? In fact, such an attempt by Morris and co-workers[502] has led to layered structures, where the integrity of the D4R is hardly maintained.

3.10. Properties and Applications

The open-framework metal phosphates have been of great interest because of their potential applications in catalysis, gas separation, and ion exchange.[261,1012] The catalytic activities are mainly limited to AlPO and related materials (MAPO, SAPO, and MAPSO), because of their thermal stability. Catalytic activities of these materials have been reviewed by Corma,[1013] Hartman and Kevan,[827] Thomas,[1014] and others. Metal-containing aluminophosphate molecular sieves offer tremendous potential as heterogeneous catalysts for liquid-phase oxidation reactions in the production of fine chemicals.[827] The versatility of the CoAlPO-36 (and MnAlPO-36) molecular sieve catalyst in the aerobic oxidation of cyclohexane and in the aerobic (Baeyer−Villiger) lactonization of ketones (Mukiyama conditions) has been dicussed by Thomas.[1014] The recent success of Thomas and co-workers[1015] in preparing an AlPO-based catalyst for the oxidation of *n*-alkanes at the terminal C atoms with high selectivity using molecular oxygen in liquid-phase reaction has been considered to be a breakthrough. Recent developments in regio- and shape-selective oxyfunctionalization of alkanes in air have been reviewed by Thomas et al.[1016] Interestingly, other than AlPO-based materials, the applications of open-framework phosphates have been very limited. This is due to the poor thermal stability of the frameworks upon removal of the template by calcination. Some of the materials, such as the nickel phosphates (VSB-1 and VSB-5),[802,803] where there is no organic material inside the channel, are reasonably stable, have high BET surface areas, and exhibit ion-exchange properties, shape-selective catalysis, and hydrogen adsorption.[803,1017] Open-framework materials seem to be potential candidates for hydrogen storage.

Another interesting feature of the transition metal containing open-framework solids is the observation of interesting magnetic properties. This class of materials shows different types of magnetic ordering (from ferromagnetism to antiferromagnetism). Thus, oxalate-phosphate frameworks are classical antiferromagnets as observed in Fe,[953–957] Co,[967] and Mn[968] oxalate-phosphates. Some of the phosphate frameworks, on the other hand, show canted antiferromagnetic ordering (VSB-1),[802] ferromagnetic ordering around 15 K ($CoPO_4$),[755] and antiferromagnetic ordering as in several Fe(III) phosphates.[745] Hybrid framework solids containing transition metal ions also exhibit interesting magnetic exchange between the metal phosphate layers via the organic linkers, as seen in the cobalt fluorophosphate pillared by 4,4′-bpy and pyrazine.[982] It would be of great value if one were to discover a magnetic channel structure that can be used for separation of oxygen and nitrogen from air.

3.11. Future Prospects

The research in the area of open-framework phosphates will continue to be attractive not only because of the interest in the design and synthesis of new materials with tunable properties, but also because of the beautiful architectures and the complex mechanisms of formation. When we were finalizing this manuscript, an article appeared in *Nature* where ionic liquids and eutectic mixtures have been used for the first time both as solvent and as template to prepare zeotype AlPO.[1018] There is little doubt that many new interesting families of open-framework metal phosphates, some with valuable sorption, magnetic, or catalytic properties, will be discovered in the near future.

4. Note Added in Proof

The area of organically-templated metal phosphates is ever expanding with various groups across the world actively participating in the research. The main part of this review has covered the work in this area till 2004. There have been some interesting developments in 2005 and 2006, and we will briefly present some of these results in this note. A noticeable development is the emergence of ionic liquids in the synthesis of open-framework materials and has been reviewed recently by Parnham and Morris.[1019] Another significant discovery is the observation of tunable yellow-to-white luminescence in a zinc gallophosphate and tuning of luminescence through the insertion of heteroatoms in NTHU-1 by Wang and co-workers.[1020] A number of AlPO's have been reported with 1-,[1021,1022] 2-,[1023,1024] and 3-D structures.[1024–1026] A novel 1-D chain has been synthesized by an ionothermal method,[1022] and some of the 3-D structures adopt zeolytic topology.[1026] Recently Yu and Xu have discussed the various aspects of open-framework AlPO's in a tutorial review.[1027] Several templated GaPO's with 1-,[1028] 2-,[1029] and 3-D structures[1030] with various coordinations of Ga have been reported. Few templated InPO's[1031–1033] with 1-,[1031] 2-,[1032] and 3-D structures[1033] have been reported, including the first 1D tancoite-type chain in the InPO family, and its transformation to other structures is notable.[1031] A number of organically templated ZnPO's[1034–1040] with a range of structures encompassing 0-,[1034] 1-,[1035–1037] 2-,[1034,1035,1038,1039] and 3-D[1035,1036,1040] networks have been reported. The 0-D ZnPO, $[H_2(N_2C_9H_{20})]\cdot[Zn(H_2PO_4)_4]$, instead of forming a four-membered ring, has four dangling H_2PO_4 groups from

the Zn center,[1034] similar to a 0-D AlPO.[343] The authors have proposed that it is possible to form the four-membered ring through the condensation of two such 0-D monomers.[1034] Among the 2-D structures, a few chloro-derivatized ZnPO's with interesting layer topologies[1039] and the presence of exotic water hexamer's between the ZnPO lattices in NTHU-3 are worthy of mention (Liao et al.).[1038] In the 3-D ZnPO's, a reversible interconversion of two 3-D structures under hydrothermal conditions (Wiebcke et al.)[1040] and a report of an extra-large pore 20 MR channel are noteworthy (Zeng et al.).[1040] Low-dimensional structures of BePO's have been reported of which one is a 1-D double chain with a 10-ring aperture and another a 2-D layer with a 4.8 net.[1041] Amine-templated layered SnPO's with a Sn/P ratio of 1.0 have been reported.[1042]

There has been not much work in the area of organically templated transition metal phosphates, except for some layered vanadyl phosphates,[1043] 3-D zeotype CoPO's,[1044] and scandium phosphates with varying dimensionality (1-D, 2-D, and 3-D).[1045] Few substituted or bimetallic AlPO's (MAPO's),[1046–1048] GaPO's (MGaPO),[1020,1047,1049] and MZnPO's (M = Co, Ni)[1050] have been reported, among them zeolitic CoAlP's synthesized by ionothermal route is noteworthy.[1048] Metalloborophosphates have been reviewed by Kniep and co-workers.[1051] Mixed anionic phosphate-arsenate[1052] and metal-oxlate- phosphates involving main group and transitional metals have been reported.[1053,1054] Ionic liquids have been used for the synthesis of an iron-oxlate-phosphate.[1054] A large number of hybrid frameworks employing organic ligands and phosphate groups in combination with various metals have been reported.[1055] The ligands (for example, 2,2′-bipy, 4,4′-bipy, Phen, etc.) do not act as templates but connect or decorate the metallo- phosphate frameworks. Weckhuysen and co-workers have carried out detailed studies, which provide support for the crystallization of microporous CoAPO-5 from the intermediate low-dimensional structures.[1056] Catalytic application of porous metal phosphates is dominated by the transition metal in substituted AlPOs.[1057] However, a nanoporous nickel phosphate (VSB-5) exhibits some shape selectivity for epoxidation of cyclic olefins.[1058]

5. References

(1) Goldwhite, H. *Introduction to Phosphorus Chemistry*; Cambridge University Press: Cambridge, U.K., 1981.
(2) O'Hare, D. In *Inorganic Materials*; Bruce, D. W., O'Hare, D., Eds.; John Wiley & Sons: Chichester, New York, Brisbane, Toronto, Singapore, 1994; p 269.
(3) Shriver, D. F.; Atkins, P. W. *Inorganic Chemistry*, 3rd ed.; Oxford University Press: Oxford, U.K., 1999.
(4) Alvarez, C.; Llavona, R.; Garcia, J. R.; Suārez, M.; Rodriguez, J. *Inorg. Chem.* **1987**, *26*, 1045.
(5) Martin, S. W. *J. Am. Ceram. Soc.* **1991**, *74*, 1767.
(6) Monceaux, L.; Courtine, P. *Eur. J. Solid State Inorg. Chem.* **1991**, *28*, 233.
(7) *Luminescence of Inorganic Solids*; Bartolo, D., Ed.; Plenum: New York, 1978.
(8) Ungashe, S. B.; Wilson, W. L.; Katz, H. E.; Scheller, G. R.; Putvinski, T. M. *J. Am. Chem. Soc.* **1992**, *114*, 8717.
(9) Marion, J. E.; Weber, M. J. *Eur. J. Solid State Inorg. Chem.* **1991**, *28*, 271.
(10) Videau, J. J.; Dupuis, V. *Eur. J. Solid State Inorg. Chem.* **1991**, *28*, 303.
(11) Frankel, R. B.; Mann, S. In *Encyclopedia of Inorganic Chemistry*; King, R. B., Ed.; John Wiley & Sons: Chichester, New York, Brisbane, Toronto, Singapore, 1994, p 269.
(12) Griffin, E. R. *J. Vinyl Additive Technol.* **2000**, *6*, 187.
(13) Kim, J. S.; Choi, U. S.; Ko, Y. G.; Kim; S. H., *J. Ind. Eng. Chem.* **2002**, *8*, 218.
(14) Toy, D. F. *Phosphorus Chemistry in Everyday Living*; American Chemical Society: Washington, DC, 1976.
(15) Phosphorus in the Environment: Its Chemistry and Biochemistry, Ciba Foundation Symposium No. 57, Elsevier: Amsterdam, 1978.
(16) Corbridge, D. E. C. Phosphorus: An Outline of its Chemistry. *Biochemistry and Technology* 2nd ed.; Elsevier: Amsterdam−Oxford−New York, 1980.
(17) De Rosch, M. A.; Trogler, W. C. *Inorg. Chem.* **1990**, *29*, 2409.
(18) (a) Straeter, N.; Lipscomb, W. N.; Klabunde, T.; Krebs, B. *Angew. Chem., Int. Ed. Engl.* **1996**, *35*, 2024. (b) Williams, N. H.; Takasaki, B.; Wall, M.; Chin, J. *Acc. Chem. Res.* **1999**, *32*, 485. (c) Hegg, E. L.; Burstyn, J. N. *Coord. Chem. Rev.* **1998**, *173*, 133. (d) Parkin, G. *Chem. Rev.* **2004**, *104*, 699.
(19) Vioux, A.; Bideu, J. L.; Mutin, P. H.; Leclercq, D. *Top. Curr. Chem.* **2004**, *232*, 145.
(20) Murugavel, R.; Walawalkar, M. G.; Dan, M.; Roesky, H. W.; Rao, C. N. R. *Acc. Chem. Res.* **2004**, *37*, 763.
(21) Katzin, L. I.; Mason, G. W.; Peppard, D. F. *Spectrochim. Acta, Part A* **1978**, *34A*, 51.
(22) (a) Klooster, W. T.; Craven, B. M. *Acta Crystallogr.* **1992**, *C48*, 19. (b) Lugmair, C. G.; Tilley, T. D. *Inorg. Chem.* **1998**, *37*, 1821. (c) Kommana, P.; Swamy, K. C. K. *Ind. J. Chem.* **2003**, *A42*, 1061. (d) Kuczek, M.; Bryndal, I.; Lis, T. *CrystEngComm* **2006**, *8*, 150.
(23) (a) Paleos, C. M.; Kardassi, D.; Tsiourvas, D.; Skoulios, A. *Liq. Cryst.* **1998**, *25*, 267. (b) Brown, D. A.; Malkin, T.; Maliphant, G. K. *J. Chem. Soc.* **1955**, 1584.
(24) Onoda, A.; Yamada, Y.; Okamura, T.; Doi, M.; Yamamoto, H.; Ueyama, N. *J. Am. Chem. Soc.* **2002**, *124*, 1052.
(25) (a) Scanlon, J.; Collin, R. L. *Acta Crystallogr.* **1954**, *7*, 781. (b) Ezra, F. S.; Collin, R. L. *Acta Crystallogr.* **1973**, *B29*, 1398.
(26) (a) Ramirez, F.; Sarma, R.; Chaw, Y. F.; McCaffrey, T. M.; Marecek, J. F.; McKeever, B.; Nierman, D. *J. Am. Chem. Soc.* **1977**, *99*, 5285. (b) Narayanan, P.; Ramirez, F.; McCaffrey, T.; Chaw, Y. F.; Marecek, J. F. *J. Org. Chem.* **1978**, *43*, 24.
(27) Adams, H.; Rolfe, A.; Jones, S. *Acta Crystallogr.* **2005**, *E61*, m1251.
(28) Steitz, T. A.; Steitz, J. A. *Proc. Natl. Acad. Sci. U.S.A.* **1993**, *90*, 6498.
(29) York, J. D.; Ponder, J. W.; Chen, Z.-w.; Mathews, F. S.; Majerus, P. W *Biochemistry* **1994**, *33*, 13164.
(30) Pelletier, H.; Sawaya, M. R.; Kumar; A.; Wilson, S. H.; Kraut, J. *Science* **1994**, *264*, 1891.
(31) Yun, J. W.; Tanase, T.; Pence, L. E.; Lippard, S. J. *J. Am. Chem. Soc.* **1995**, *117*, 4407.
(32) Yun, J. W.; Tanase, T.; Lippard, S. J. *Inorg. Chem.* **1996**, *35*, 7590.
(33) Bissinger, P.; Kumberger, O.; Schier, A. *Chem. Ber.* **1991**, *124*, 509.
(34) Izumi, M.; Ichikawa, K.; Suzuki, M.; Tanaka, I.; Rudzinski, K. W. *Inorg. Chem.* **1995**, *34*, 5388.
(35) Lis, T. *Acta Crystallogr.* **1992**, *C48*, 424.
(36) Onoda, A.; Yamada, Y.; Okamura, T.; Yamamoto, H.; Ueyama, N. *Inorg. Chem.* **2002**, *41*, 6038.
(37) (a) Demadis, K. D.; Sallis, J. D.; Raptis, R. G.; Baran, P. *J. Am. Chem. Soc.* **2001**, *123*, 10129. (b) Demadis, K. D. *Inorg. Chem. Commun.* **2003**, *6*, 527.
(38) Lis, T.; Kuczek, M. *Acta Crystallogr.* **1991**, *C47*, 1598.
(39) Burns, J. H.; Kessler, R. M. *Inorg. Chem.* **1987**, *26*, 1370.
(40) Kyogoku, Y.; Iitaka, Y. *Acta Crystallogr.* **1966**, *21*, 49.
(41) Burns, J. H. *Inorg. Chim. Acta* **1985**, *102*, 15.
(42) Clearfield, A. *Inorganic Ion Exchange Materials*; CRC Press: Boca Roton, FL, 1982.
(43) Munowitz, M.; Jarman, R. H.; Harrison, J. F. *Chem. Mater.* **1992**, *4*, 1296.
(44) Wang, B.; Greenblatt, M.; Wang, S.; Hwu, S. J. *Chem. Mater.* **1993**, *5*, 23.
(45) Thorn, D. L.; Harlow, R. L. *Inorg. Chem.* **1992**, *31*, 3917.
(46) Guerrero, G.; Mehring, M.; Mutin, P. H.; Dahan, F.; Vioux, A. *J. Chem. Soc., Dalton Trans.* **1999**, 1537.
(47) Fortner, K. C.; Bigi, J. P.; Brown, S. N. *Inorg. Chem.* **2005**, *44*, 2803.
(48) Müller, J. F. K.; Kulicke, K. J.; Neuburger, M.; Spichty, M. *Angew. Chem., Int. Ed.* **2001**, *40*, 2890.
(49) Zhang, Q.-F.; Lam, T. C. H.; Chan, E. Y. Y.; Lo, S. M. F.; Williams, I. D.; Leung, W.-H. *Angew. Chem., Int. Ed.* **2004**, *43*, 1715.
(50) Kumara Swamy, K. C.; Veith, M.; Huch, V.; Mathur, S. *Inorg. Chem.* **2003**, *42*, 5837.
(51) Stulz, E.; Bürgi, H. B.; Leumann, C. *Chem.−Eur. J.* **2000**, *6*, 523.
(52) Johnston, D. C.; Johnson, J. W. *J. Chem. Soc., Chem. Commun.* **1985**, 1720.
(53) Toney, J. H.; Brock, C. P.; Marks, T. J. *J. Am. Chem. Soc.* **1986**, *108*, 7263.
(54) Bond, M. R.; Mokry, L. M.; Otieno, T.; Thompson, J.; Carrano, C. J. *Inorg. Chem.* **1995**, *34*, 1894.
(55) Bond, M. R.; Czernuszewicz, S.; Dave, B. C.; Yan, Q.; Mohan, M.; Verastegue, R.; Carrano, C. J. *Inorg. Chem.* **1995**, *34*, 5857.

(56) Dean, N. S.; Mokry, L. M.; Bond, M. R.; O'Connor, C. J.; Carrano, C. J. *Inorg. Chem.* **1996**, *35*, 2818.
(57) Dean, N. S.; Mokry, L. M.; Bond, M. R.; O'Connor, C. J.; Carrano, C. J. *Inorg. Chem.* **1996**, *35*, 3541.
(58) Otieno, T.; Mokry, L. M.; Bond, M. R.; Carrano, C. J.; Dean, N. S. *Inorg. Chem.* **1996**, *35*, 850. Murugavel, R.; Shanmugan, S. *Chem. Commun.* **2007**,in press.
(59) Mokry, L. M.; Thompson, J.; Bond, M. R.; Otieno, T.; Mohan, M.; Carrano, C. J. *Inorg. Chem.* **1994**, *33*, 2705.
(60) David, S. S.; Que, L. *J. Am. Chem. Soc* **1990**, *112*, 6455.
(61) Hansen, S.; Hansen, L. K.; Hough, E. *J. Mol. Biol.* **1992**, *225*, 543.
(62) Vallee, B. L.; Auld, D. S. *Biochemistry* **1993**, *32*, 6493.
(63) Hardman, K. D.; Agarwal, R. C.; Freiser, M. J. *J. Mol. Biol.* **1982**, *157*, 69.
(64) Dean, N. S.; Mokry, L. M.; Bond, M. R.; Mohan, M.; Otieno, T.; O'Connor, C. J.; Spartalian, K.; Carrano, C. J. *Inorg. Chem.* **1997**, *36*, 1424.
(65) (a) Thorn, D. L.; Harlow, R. L.; Herron, N. *Inorg. Chem.* **1996**, *35*, 547. (b) Herron, N.; Thorn, D. L.; Harlow, R. L.; Coulston, G. W. *J. Am. Chem. Soc.* **1997**, *119*, 7149.
(66) Lugmair, C.G.; Tilley, T. D. *Monatsh. Chem.* **2006**, *137*, 557.
(67) Langard, S. *Am. J. Ind. Med.* **1990**, *17*, 189.
(68) Lay, P. A.; Levina, A. *Inorg. Chem.* **1996**, *35*, 7709.
(69) Zhitkovich, A.; Voitkun, V.; Costa, M. *Carcinogenesis* **1995**, *16*, 907.
(70) Zhitkovich, A.; Voitkun, V.; Costa, M. *Biochemistry* **1996**, *35*, 7275.
(71) Ferreira, A. D. Q.; Bino, A.; Gibson, D. *Inorg. Chem.* **1998**, *37*, 6560.
(72) Dalley, N. K.; Kou, X.; O'Connor, C. J.; Holwerda, R. A. *Inorg. Chem.* **1996**, *35*, 2196.
(73) Partigianoni, C. M.; Chang, I.-J.; Nocera, D. G. *Coord. Chem. Rev.* **1990**, *97*, 105.
(74) Morrow, J. R.; Trogler, W. C. *Inorg. Chem.* **1989**, *28*, 615.
(75) Hsu, T-L. C.; Chang, I.-J.; Ward, D. L.; Nocera, D. G. *Inorg. Chem.* **1994**, *33*, 2932.
(76) Fujdala, K. L.; Tilley, T. D. *Chem. Mater.* **2004**, *16*, 1035.
(77) Sessoli, R.; Gatteschi, D.; Caneschi, A.; Novak, M. A. *Nature* **1993**, *365*, 141.
(78) Sessoli, R.; Tsai, H.-L.; Schake, A. R.; Wang, S.; Vincent, J. B.; Folting, K.; Gatteschi, D.; Christou, G.; Hendrickson, D. N. *J. Am. Chem. Soc.* **1993**, *115*, 1804.
(79) Wernsdorfer, W.; Aliaga-Alcalde, N.; Hendrickson, D. N.; Christou, G. *Nature* **2002**, *416*, 406.
(80) Coronado, E.; Palacio, F.; Veciana, J. *Angew. Chem., Int. Ed.* **2003**, *42*, 2570.
(81) Gatteschi, D.; Sessoli, R. *Angew. Chem., Int. Ed.* **2003**, *42*, 268.
(82) Mirebeau, I.; Hennion, M.; Casalta, H.; Andres, H.; Gudel, H. U.; Irodova, A. V.; Caneschi, A. *Phys. Rev. Lett.* **1999**, *83*, 628.
(83) Artus, P.; Boskovic, C.; Yoo, J.; Streib, W. E.; Brune, L. C.; Hendrickson, D. N.; Christou, G. *Inorg. Chem.* **2001**, *40*, 4199.
(84) Boskovic, C.; Pink, M.; Huffman, J. C.; Hendrickson, D. N.; Christou, G. *J. Am. Chem. Soc.* **2001**, *123*, 9914.
(85) Chakov, N. E.; Wernsdorfer, W.; Abboud, K. A.; Hendrickson, D. N.; Christou, G. *Dalton Trans.* **2003**, 2243.
(86) Kuroda-Sowa, T.; Handa, T.; Kotera, T.; Maekawa, M.; Munakata, M.; Miyasaka, H.; Yamashita, M. *Chem. Lett.* **2004**, *33*, 540.
(87) Kuroda-Sowa, T.; Fukuda, S.; Miyoshi, S.; Maekawa, M.; Munakata, M.; Miyasaka, H.; Yamashita, M. *Chem. Lett.* **2002**, 682.
(88) Bian, G. Q.; Kuroda-Sowa, T.; Konaka, H.; Hatano, M.; Maekawa, M.; Munakata, M.; Miyasaka, H.; Yamashita, M. *Inorg. Chem.* **2004**, *43*, 4790.
(89) Kuroda-Sowa, T.; Bian, G.-Q.; Hatano, M.; Konaka, H.; Fukuda, S.; Miyoshi, S.; Maekawa, M.; Munakata, M.; Miyasaka, H.; Yamashita, M. *Polyhedron* **2005**, *24*, 2680.
(90) Sathiyendiran, M.; Murugavel, R. *Inorg. Chem.* **2002**, *41*, 6404.
(91) Pothiraja, R.; Sathiyendiran, M.; Butcher, R. J.; Murugavel, R. *Inorg. Chem.* **2004**, *43*, 6314.
(92) Pothiraja, R.; Sathiyendiran, M.; Butcher, R. J.; Murugavel, R. *Inorg. Chem.* **2005**, *44*, 7585.
(93) Murugavel, R.; Sathiyendiran, M.; Pothiraja, R.; Butcher, R. J. *Chem. Commun.* **2003**, 2546.
(94) Yashiro, M.; Higuchi, M.; Komiyama, M.; Ishii, Y. *Bull. Chem. Soc. Jpn* **2003**, *76*, 1813.
(95) Shiraishi, H; Jikido, R.; Matsufuji, K.; Nakanishi, T.; Shiga, T.; Ohba, M.; Sakai, K.; Kitagawa, H.; Okawa, H. *Bull. Chem. Soc. Jpn.* **2005**, *78*, 1072.
(96) Belanger, S.; Beauchamp, A. L. *Inorg. Chem.* **1997**, *36*, 3640.
(97) Davis, J. C.; Lin, S. S.; Averill, B. A. *Biochemistry* **1981**, *20*, 4062.
(98) Sjoberg, B. M.; Graslund, A. *Adv. Inorg. Biochem.* **1983**, *5*, 87.
(99) Robitaille, P.-M. L.; Kurtz, D. M. *Biochemistry* **1988**, *27*, 4458.
(100) Theil, E. C. *Adv Inorg. Biochem.* **1983**, *5*, 1.
(101) Armstrong, W. H.; Lippard, S. J. *J. Am. Chem. Soc.* **1985**, *107*, 3730.
(102) Turowski, P. N.; Armstrong, W. H.; Roth, M. E.; Lippard, S. J. *J. Am. Chem. Soc.* **1990**, *112*, 681.
(103) Kuzelka, J.; Spingler, B.; Lippard, S. J. *Inorg. Chim. Acta* **2002**, *337*, 212.
(104) Drueke, S.; Wieghardt, K.; Nuber, B.; Weiss, J.; Fleischhauer, H.-P.; Gehring, S.; Haase, W. *J. Am. Chem. Soc.* **1989**, *111*, 8622.
(105) Turowski, P. N.; Armstrong, W. H.; Liu, S.; Brown, S. N.; Lippard, S. J. *Inorg. Chem.* **1994**, *33*, 636.
(106) Norman, R. E.; Yan, S.; Que, L.; Backes, G.; Ling, J.; Sanders-Loehr, J.; Zhang, J. H.; O'Connor, C. J. *J. Am. Chem. Soc.* **1990**, *112*, 1554.
(107) Yan, S.; Pan, X.; Taylor, L. F.; Zhang, J. H.; O'Connor, C. J.; Britton, D.; Anderson, O. P.; Que, L. *Inorg. Chim. Acta* **1996**, *243*, 1.
(108) Schepers, K.; Bremer, B.; Krebs, B.; Henkel, G.; Althaus, E.; Mosel, B.; Muller-Warmuth, W. *Angew. Chem., Int. Ed. Engl.* **1990**, *29*, 531.
(109) Albedyhl, S.; Averbuch-Pouchot, M. T.; Belle, C.; Krebs, B.; Pierre, J. L.; Saint-Aman, E.; Torelli, S. *Eur. J. Inorg. Chem.* **2001**, 1457.
(110) Belle, C.; Gautier-Luneau, I.; Karmazin, L.; Pierre, J.-L.; Albedyhl, S.; Krebs, B.; Bonin, M. *Eur. J. Inorg. Chem.* **2002**, *12*, 3087.
(111) Bremer, B.; Schepers, K.; Fleischhauer, P.; Haase, W.; Henkel, G.; Krebs, B. *J. Chem. Soc., Chem. Commun.* **1991**, 510.
(112) Jang, H. G.; Hendrich, M. P.; Que, L. *Inorg. Chem* **1993**, *32*, 911.
(113) Krebs, B.; Schepers, K.; Bremer, B.; Henkel, G.; Althaus, E.; Muller-Warmuth, W.; Griesar, K.; Haase, W. *Inorg. Chem.* **1994**, *33*, 1907.
(114) Lambert, E.; Chabut, B.; Chardon-Noblat, S.; Deronzier, A.; Chottard, G.; Bousseksou, A.; Tuchagues, J.-P.; Laugier, J.; Bardet, M.; Latour, J.-M. *J. Am. Chem. Soc.* **1997**, *119*, 9424.
(115) Yin, D.; Cheng, P.; Yao, X.; Wang, H. *J. Chem. Soc., Dalton Trans.* **1997**, 2109.
(116) Yin, L.-h.; Cheng, P.; Yan, S.-P.; Fu, X.-Q.; Li, J.; Liao, D.-Z.; Jiang, Z.-H. *J. Chem. Soc., Dalton Trans* **2001**, 1398.
(117) Rapta, M.; Kamaras, P.; Brewer, G. A.; Jameson, G. B. *J. Am. Chem. Soc.* **1995**, *117*, 12865.
(118) Mikuriya, M.; Kakuta, Y.; Nukada, R.; Kotera, T.; Tokii, T. *Bull. Chem. Soc. Jpn.* **2001**, *74*, 1425.
(119) (a) Yan, S.; Cheng, P.; Wang, Q.; Liao, D.; Jiang, Z.; Wang, G. *Sci. China, Ser. B: Chem.* **2000**, *43*, 405. (b) Yan, S.; Liu, B.; Cheng, P.; Liu, X.; Liao, D.; Jiang, Z.; Wang, G. *Sci. China, Ser. B: Chem.* **1998**, *41*, 168.
(120) Biswas, P.; Ghosh, M.; Dutta, S. K.; Floerke, U.; Nag, K. *Inorg. Chem.* **2006**, *45*, 4830.
(121) Lanzaster, M.; Neves, A.; Bortoluzzi, A. J.; Szpoganicz, B.; Schwingel, E. *Inorg. Chem.* **2002**, *41*, 5641.
(122) Karsten, P.; Neves, A.; Bortoluzzi, A.; Drago, V.; Lanznaster, M. *Inorg. Chem.* **2002**, *41*, 4624.
(123) Neves, A.; de Brito, M. A.; Drago, V.; Griesar, K.; Haase, W. *Inorg. Chim Acta* **1995**, *237*, 131.
(124) Karsten, P.; Neves, A.; Bortoluzzi, A. J.; Strähle, J.; Maichle-Mössmer, C. *Inorg. Chem. Commun.* **2002**, *5*, 434.
(125) Duboc-Toia, C.; Ménage, S.; Vincent, J. M.; Averbuch-Pouchot, M. T.; Fontecave, M. *Inorg. Chem.* **1997**, *36*, 6148.
(126) Kantacha, A.; Wongnawa, S. *Inorg. Chim. Acta* **1987**, *134*, 135.
(127) Huang, C.; Zhang, D.; Xu, G.; Zhang, S. *Sci. Sin., Ser. B (Engl. Ed.)* **1988**, *31*, 1153.
(128) Glowiak, T.; Szemik, A. W. *Acta Crystallogr.* **1988**, *C44*, 1725.
(129) Jones, D. R.; Lindoy, L. F.; Sargeson, A. M.; Snow, M. R. *Inorg. Chem.* **1982**, *21*, 4155.
(130) Murugavel, R.; Sathiyendiran, M.; Walawalkar, M. G. *Inorg. Chem.* **2001**, *40*, 427.
(131) Chin, J.; Chung, S.; Kim, D. H. *J. Am. Chem. Soc.* **2002**, *124*, 10948.
(132) Wahnon, D.; Lebuis, A. M.; Chin, J. *Angew. Chem., Int. Ed. Engl.* **1995**, *34*, 2412.
(133) Humphry, T.; Forconic, M.; Williams, N. H.; Hengge, A. C. *J. Am. Chem. Soc.* **2004**, *126*, 11864.
(134) Williams, N. H.; Lebuis, A.-M.; Chin, J. *J. Am. Chem. Soc.* **1999**, *121*, 3341.
(135) Seo, J.-S.; Sung, N.-D.; Hynes, R. C.; Chin, J. *Inorg. Chem.* **1996**, *35*, 7472.
(136) Jikido, R.; Shiraishi, H.; Matsufuji, K.; Ohba, M.; Furutachi, H.; Suzuki, M.; Okawa, H. *Bull. Chem. Soc. Jpn.* **2005**, *78*, 1795.
(137) Hodgson, D. M.; Selden, D. A.; Dossetter, A. G. *Tetrahedron: Asymmetry* **2003**, *14*, 3841.
(138) Hodgson, D.M.; Stupple, P.A.; Pierard, F.Y. T. M.; Labande, A.H.; Johnstone, C. *Chem.—Eur. J.* **2001**, *7*, 4465.
(139) Hodgson, D.M.; Stupple, P.A.; Johnstone, C. *Chem. Commun.* **1999**, 2185.
(140) Muller, P.; Maitrejean, E. *Coll. Czech. Chem. Commun.* **1999**, *64*, 1807.
(141) Mueller, P.; Fernandez, D. *Helv. Chim. Acta* **1995**, *78*, 947.

(142) Teleshev, A. T.; Popova, L. F.; Shishin, A. V.; Koroteev, M. P.; Shrileva, E. A.; Nifantyev, E. E.; Eismont, M. Yu.; Platonov, D. N.; Nefedov, O. M *Rhodium Express* **1994**, *5*, 14.
(143) Teleshev, A. T.; Shishin, A. V.; Popova, L. F.; Nifantyev, E. E.; Shapiro, E. A.; Kovalenko, L. I.; Nefedov, O. M. *Rhodium Express* **1993**, *1*, 22.
(144) McCarthy, N.; McKervey, M. A.; Ye, T.; McCann, M.; Murphy, E.; Doyle, M. P. *Tetrahedron Lett.* **1992**, *33*, 5983.
(145) Hendry, P.; Sargeson, A. M. *J. Am. Chem. Soc.* **1989**, *111*, 2521.
(146) Hendry, P.; Sargeson, A. M. *Inorg. Chem.* **1990**, *29*, 97.
(147) Ionkin, A.S.; Marshall, W. J.; Roe, D. C.; Wang, Y. *Dalton Trans.* **2006**, 2468.
(148) He, C.; Gomez, V.; Spingler, B.; Lippard, S. J. *Inorg. Chem.* **2000**, *39*, 4188.
(149) Yamaguchi, K.; Akagi, F.; Fujinami, S.; Suzuki, M.; Shionoya, M.; Suzuki, S. *Chem. Commun.* **2001**, 375.
(150) Ito, M.; Kawano, H.; Takeuchi, T.; Takita, Y. *Chem. Lett.* **2000**, 372.
(151) Santana, M. D.; Garcia, G.; Lozano, A. A.; Lopez, G.; Tudela, J.; Perez, J.; Garcia, L.; Lezama, L.; Rojo, T. *Chem.—Eur. J.* **2004**, *10*, 1738.
(152) Kemmitt, R. D. W.; Mason, S.; Fawcett, J.; Russell, D. R. *J. Chem. Soc., Dalton Trans.* **1992**, 851.
(153) Battle, A. R.; Platts, J. A.; Hambley, T. W.; Deacon, G. B. *J. Chem. Soc., Dalton Trans.* **2002**, 1898.
(154) Glowiak, T.; Podgorska, I.; Baranowski, J. *Inorg. Chim. Acta* **1986**, *115*, 1.
(155) Glowiak, T.; Podgorska, I. *Inorg. Chim. Acta* **1986**, *125*, 83.
(156) Glowiak, T.; Szemik, A. W.; Wnek, I. *J. Crystallogr. Spectrosc. Res.* **1986**, *16*, 41.
(157) Glowiak, T.; Wnek, I *Acta Crystallogr.* **1985**, *C41*, 507.
(158) Glowiak, T.; Wnek, I. *Acta Crystallogr.* **1985**, *C41*, 324.
(159) Murugavel, R.; Sathiyendiran, M. *Chem. Lett.* **2001**, 84.
(160) Murugavel, R.; Sathiyendiran, M.; Pothiraja, R.; Walawalkar, M. G.; Mallah, T.; Riviére, E. *Inorg. Chem.* **2004**, *43*, 945.
(161) Mahroof-Tahir, M.; Karlin, K. D.; Chen, Q.; Zubieta, J. *Inorg. Chim. Acta.* **1993**, *207*, 135.
(162) Zhu, L.; Santos, O.; Koo, C. W.; Rybstein, M.; Pape, L.; Canary, J. W. *Inorg. Chem.* **2003**, *42*, 7912.
(163) Barker, J. E.; Liu, Y.; Martin, N. D.; Ren, T. *J. Am. Chem. Soc.* **2003**, *125*, 13332.
(164) Fry, F. H.; Spiccia, L.; Jensen, P.; Moubaraki, B.; Murray, K. S.; Tiekink, E. R. T. *Inorg. Chem.* **2003**, *42*, 5594.
(165) He, C.; Lippard, S. J. *J. Am. Chem. Soc.* **2000**, *122*, 184.
(166) Koevari, E.; Kraemer, R. *J. Am. Chem. Soc.* **1996**, *118*, 12704.
(167) Wall, M.; Hynes, R. C.; Chin, J. *Angew. Chem., Int. Ed. Engl.* **1993**, *32*, 1633.
(168) Gajda, T.; Jancso, A.; Mikkola, S.; Lönnberg, H.; Sirges, H. *J. Chem. Soc., Dalton Trans.* **2002**, 1757.
(169) Deschamps, J. R.; Hartshorn, C. M.; Chang, E. L. *Acta Crystallogr.* **2002**, *E58*, m606.
(170) Jurek, P. E.; Martell, A. E. *Inorg. Chem.* **1999**, *38*, 6003.
(171) Young, M. J.; Wahnon, D.; Hynes, R. C.; Chin, J. *J. Am. Chem. Soc.* **1995**, *117*, 9441.
(172) Fry, F. H.; Jensen, P.; Kepert, C. M.; Spiccia, L. *Inorg. Chem.* **2003**, *42*, 5637.
(173) Butcher, R.J.; Gultneh, Y.; Allwar, *Acta Crystallogr.* **2005**, *E61*, m818.
(174) Rossi, L. M.; Neves, A.; Bortoluzzi, A. J.; Hoerner, R.; Szpoganicz, B.; Terenzi, H.; Mangrich, A. S.; Pereira-Maia, E.; Castellano, E. E.; Haase, W. *Inorg. Chim. Acta* **2005**, *358*, 1807.
(175) Itoh, T.; Hisada, H.; Usui, Y.; Fujii, Y. *Inorg. Chim. Acta* **1998**, *283*, 51.
(176) Itoh, M.; Nakazawa, J.; Maeda, K.; Kano, K.; Mizutani, T.; Kodera, M. *Inorg. Chem.* **2005**, *44*, 691.
(177) Barker, J. E.; Liu, Y.; Yee, G. T.; Chen, W.-Z.; Wang, G.; Rivera, V.M.; Ren, T. *Inorg. Chem.* **2006**, *45*, 7973.
(178) Selmeczi, K.; Giorgi, M.; Speier, G.; Farkas, E.; Reglier, M. *Eur. J. Inorg. Chem.* **2006**, 1022.
(179) Zeng, G.; Guo, X.; Wang, C.; Lin, Y.; Li, H. *Wuli Huaxue Xuebao* **1992**, *8*, 778.
(180) Rafizadeh, M.; Tayebee, R.; Amani, V.; Nasseh, M. *Bull. Korean Chem. Soc.* **2005**, *26*, 594.
(181) Jagoda, M.; Warzeska, S.; Pritzkow, H.; Wadepohl, H.; Imhof, P.; Smith, J. C.; Kraemer, R. *J. Am. Chem. Soc.* **2005**, *127*, 15061.
(182) Kato, M.; Tanase, T. *Inorg. Chem.* **2005**, *44*, 8.
(183) Kato, M.; Sah, A. K.; Tanase, T.; Mikuriya, M. *Inorg. Chem.* **2006**, *45*, 6646.
(184) Kato, M.; Tanase, T.; Mikuriya, M. *Inorg. Chem.* **2006**, *45*, 2925.
(185) Hazel, J, P.; Collin, R, L. *Acta Crystallogr.* **1972**, *B28*, 2951.
(186) Chatterji, D.; Nandi, U. S.; Podder, S. K. *Biopolymers* **1977**, *16*, 1863.
(187) Weis, K.; Rombach, M.; Ruf, M.; Vahrenkamp, H. *Eur. J. Inorg. Chem.* **1998**, 263.
(188) Weis, K.; Vahrenkamp, H. *Eur. J. Inorg. Chem.* **1998**, 271.
(189) Weis, K.; Rombach, M.; Vahrenkamp, H. *Inorg. Chem.* **1998**, *37*, 2470.
(190) Brombacher, H.; Vahrenkamp, H. *Inorg. Chem* **2004**, *43*, 6050.
(191) Maldonado Calvo, J. A.; Vahrenkamp, H. *Inorg. Chim. Acta* **2006**, *359*, 4079.
(192) Ibrahim, M. M.; Seebacher, J.; Steinfeld, G.; Vahrenkamp, H. *Inorg. Chem.* **2005**, *44*, 8531.
(193) Abufarag, A.; Vehrenkamp, H. *Inorg. Chem.* **1995**, *34*, 2207.
(194) Abufarag, A.; Vahrenkamp, H. *Inorg. Chem.* **1995**, *34*, 3279.
(195) Troesch, A.; Vahrenkamp, H. *Eur. J. Inorg. Chem.* **1998**, 827.
(196) Troesch, A.; Vahrenkamp, H. *Inorg. Chem.* **2001**, *40*, 2305.
(197) Troesch, A.; Vahrenkamp, H. *Z. Anorg. Allg. Chem.* **2004**, *630*, 2031.
(198) Gross, F.; Vahrenkamp, H. *Inorg. Chem.* **2005**, *44*, 3321.
(199) Ji, M.; Vahrenkamp, H. *Eur. J. Inorg. Chem.* **2005**, 1398.
(200) Muller-Hartmann, A.; Vahrenkamp, H. *Eur. J. Inorg. Chem.* **2000**, 2355.
(201) Gross, F.; Muller-Hartmann, A.; Vahrenkamp, H. *Eur. J. Inorg. Chem.* **2000**, 2363.
(202) Muller-Hartmann, A.; Vahrenkamp, H. *Eur. J. Inorg. Chem.* **2000**, 2371.
(203) Hikichi, S.; Tanaka, M.; Morooka, Y.; Kitajima, N. *J Chem Soc., Chem. Commun.* **1992**, 814.
(204) Tanase, T.; Yun, J. W.; Lippard, S. J. *Inorg. Chem.* **1996**, *35*, 3585.
(205) Tanase, T.; Yun, J. W.; Lippard, S. J. *Inorg. Chem.* **1995**, *34*, 4220.
(206) Bazzicalupi, C.; Bencini, A.; Berni, E.; Bianchi, A.; Fornasari, P.; Giorgi, C.; Valtancoli, B. *Inorg. Chem.* **2004**, *43*, 6255.
(207) Angeloff, A.; Daran, J. C.; Bernadou, J.; Meunier, B. *J. Organomet. Chem.* **2001**, *624*, 58.
(208) Ibrahim, M. M.; Shimomura, N.; Ichikawa, K.; Shiro, M. *Inorg. Chim. Acta* **2001**, *313*, 125.
(209) Ito, M.; Fujita, K.; Chitose, F.; Takeuchi, T.; Yoshida, K.; Takita, Y. *Chem. Lett.* **2002**, 594.
(210) Rivas, J. C. M.; Rosales, R. T. M.; Parsons, S. *J. Chem. Soc., Dalton Trans.* **2003**, 4385.
(211) Kinoshita, E.; Takahashi, M.; Takeda, H.; Shiro, M.; Koike, T. *Dalton Trans.* **2004**, 1189.
(212) Bauer-Siebenlist, B.; Meyer, F.; Farkas, E.; Vidovic, D.; Cuesta-Seijo, J. A.; Herbst-Irmer, R.; Pritzkow, H. *Inorg. Chem.* **2004**, *43*, 4189.
(213) Bauer-Siebenlist, B.; Meyer, F.; Farkas, E.; Vidovic, D.; Dechert, S. *Chem.—Eur. J.* **2005**, *11*, 4349.
(214) Hammes, B. S.; Carrano, C. J. *J. Chem. Soc., Dalton Trans.* **2000**, 3304.
(215) Yamami, M.; Furutachi, H.; Yokoyama, T.; Okawa, H. *Inorg. Chem.* **1998**, *37*, 6832.
(216) Yamami, M.; Furutachi, H.; Yokoyama, T.; Okawa, H. *Chem. Lett.* **1998**, 211.
(217) Aoki, S.; Iwaida, K.; Hanamoto, N.; Shiro, M.; Kimura, E. *J. Am. Chem. Soc.* **2002**, *124*, 5256.
(218) Adams, H.; Bailey, N. A.; Fenton, D. E.; He, Q.-Y. *J. Chem. Soc., Dalton Trans.* **1997**, 1533.
(219) Adams, H.; Bailey, N. A.; Fenton, D. E.; He, Q.-Y *J. Chem. Soc, Dalton Trans.* **1995**, 697.
(220) Bazzicalupi, C.; Bencini, A.; Bianchi, A.; Fusi, V.; Giorgi, C.; Paoletti, P.; Valtancoli, B.; Zanchi, D. *Inorg. Chem.* **1997**, *36*, 2784.
(221) Kimura, E.; Aoki, S.; Koike, T.; Shiro, M. *J. Am. Chem. Soc.* **1997**, *119*, 3068.
(222) Orioli, P.; Cini, R.; Donati, D.; Mangani, S. *J. Am. Chem. Soc.* **1981**, *103*, 4446.
(223) Harrison, W. T. A.; Nenoff, T. M.; Gier, T. E.; Stucky, G. D. *Inorg. Chem.* **1992**, *31*, 5395.
(224) William, T. A.; Nenoff, T. M.; Gier, T. E.; Stucky, G. D. *J. Mater. Chem.* **1994**, *4*, 1111.
(225) Zeng, G.; Guo, X.; Wang, C.; Lin, Y.; Li, H. *Yingyong Huaxue* **1992**, *9*, 39.
(226) Ortiz-Avila, Y.; Rudolf, P. R.; Clearfield, A. *Inorg. Chem.* **1989**, *28*, 2137.
(227) Lugmair, C. G.; Tilley, T. D.; Rheingold, A. L. *Chem. Mater.* **1997**, *9*, 339.
(228) Murugavel, R.; Kuppuswamy, S.; Boomishankar, R.; Steiner, A. *Angew. Chem., Int. Ed.* **2006**, *45*, 5536.
(229) Miner, V. W.; Prestegard, J. H.; Faller, J. W. *Inorg. Chem.* **1983**, *22*, 1862.
(230) Lugmair, C. G.; Tilley, T. D.; Rheingold, A. L. *Chem. Mater.* **1999**, *11*, 1615.
(231) Fujdala, K. L.; Tilley, T. D. *J. Am. Chem. Soc.* **2001**, *123*, 10133.
(232) Pinkas, J.; Chakraborty, D.; Yang, Y.; Murugavel, R.; Noltemeyer, M.; Roesky, H. W. *Organometallics* **1999**, *18*, 523.

(233) Pinkas, J.; Wessel, H.; Yang, Y.; Montero, M. L.; Noltemeyer, M.; Froeba, M.; Roesky, H.W. *Inorg. Chem.* **1998**, *37*, 2450.
(234) Florjanczyk, Z.; Lasota, A.; Wolak, A.; Zachara, J. *Chem. Mater* **2006**, *18*, 1995.
(235) Zheng, C.; Ou, Y.; Luo, Y.; Liao, K. *Zhongshan Daxue Xuebao, Ziran Kexueban* **1994**, *33*, 54.
(236) Kumar, N. S.; Vittal, J. J.; Swamy, K. C. K. *Acta Crystallogr.* **2004**, *E60*, m1321.
(237) Mitra, A.; Parkin, S.; Atwood, D. A. *Inorg. Chem.* **2006**, *45*, 3970.
(238) Mitra, A.; DePue, L. J.; Parkin, S.; Atwood, D. A. *J. Am. Chem. Soc.* **2006**, *128*, 1147.
(239) Murugavel, R.; Kuppuswamy, S. *Angew. Chem., Int. Ed.* **2006**, *45*, 7022.
(240) Holmes, R. R. *Acc. Chem. Res.* **1989**, *22*, 190.
(241) Day, R. O.; Chandrasekhar, V.; Kumara Swamy, K. C.; Holmes, J. M.; Burton, S. D.; Holmes, R. R. *Inorg. Chem.* **1988**, *27*, 2887.
(242) Kumara Swamy, K. C.; Schmid, C. G.; Day, R. O.; Holmes, R. R. *J. Am. Chem. Soc.* **1990**, *112*, 223.
(243) (a) Schmid, C. G.; Day, R. O.; Holmes, R. R. *Phosphorus, Sulfur, Silicon* **1989**, *41*, 69. (b) Nagabrahmanandachari, S.; Hemavathi, C.; Kumara Swamy, K. C.; Poojary, D. M.; Clearfield, A. *Main Group Met. Chem.* **1998**, *21*, 789.
(244) Psillakis, E.; Jeffery, J. C.; McCleverty, J. A.; Ward, M. D. *Chem. Commun.* **1997**, 1965.
(245) Psillakis, E.; Jeffery, J. C.; McCleverty, J. A.; Ward, M. D. *J. Chem. Soc., Dalton Trans.* **1997**, 1645.
(246) Burchardt, A.; Klinkhammer, K. W.; Schmidt, A. *Z. Anorg. Allg. Chem.* **1998**, *624*, 35.
(247) Zeng, G.; Guo, X.; Wang, C.; Lin, Y.; Li, H. *Jiegou Huaxue* **1994**, *3*, 24.
(248) Li, L.; Lin, Y.; Zeng, G.; Ma, A. *Yingyong Huaxue* **1989**, *6*, 53.
(249) Li, L.; Lin, Y.; Zeng, G.; Ma, A. *Jiegou Huaxue* **1991**, *10*, 155.
(250) Ma, A.; Li, L.; Lin, Y.; Zeng, G.; Li, H. *Zhongguo Xitu Xuebao* **1990**, *8*, 201.
(251) Liu, C.; Wu, G.; Tang, Z.; Han, Y.; Pan, Z.; Shi, N.; Liao, L. *Huaxue Xuebao* **1990**, *48*, 116.
(252) Ma, A.; Li, L.; Lin, Y.; Zeng, G.; Jin, S.; Li, H. *Yingyong Huaxue* **1989**, *6*, 99.
(253) Han, Y.; Pan, Z.; Shi, N.; Liao, L.; Liu, C.; Wu, G.; Tang, Z.; Xiao, Y. *Wuji Huaxue Xuebao* **1990**, *6*, 17.
(254) Huang, C.; Yi, T.; Lu, Y.; Xu, G.; Ling, H.; Ma, Z. *Chin. Chem. Lett.* **1992**, *3*, 947.
(255) Lebedev, V. G.; Palkina, K. K.; Maksimova, S. I.; Lebedeva, E. N.; Galaktionova, O. V. *Z. Neorg. Khim.* **1982**, *27*, 2980.
(256) Lisowski, J.; Sessler, J. L.; Lynch, V.; Mody, T. D. *J. Am. Chem. Soc.* **1995**, *117*, 2273.
(257) Kanellakopulos, B.; Dornberger, E.; Maier, R.; Nuber, B.; Stammler, H. G.; Ziegler, M. L. *Z. Anorg. Allg. Chem.* **1993**, *619*, 593.
(258) Burns, J. H. *Inorg. Chem.* **1983**, *22*, 1174.
(259) Mokry, L, M.; Dean, N, S.; Carrano, C, J. *Angew. Chem., Int. Ed. Engl* **1996**, *35*, 1497.
(260) (a) Clearfield, A. *Chem. Rev.* **1988**, *88*, 125. (b) Centi, G.; Trifirō, F.; Ebner, J. R.; Franchetti, V. M. *Chem. Rev.* **1988**, *88*, 55. (c) Alberti, G. *Comprehensive Supramolecular Chemistry*; Lehn, J. M., Ed.; Elsevier: New York, 1996; Vol. 7, pp 151−187. (d) Clearfield, A. Progress in Inorganic Chemistry; Karlin, K. D., Ed.; Wiley & Sons: Oxford, 1998; Vol. 47, p 371. (e) Walawalkar, M. G.; Roesky, H. W.; Murugavel, R. *Acc. Chem. Res.* **1999**, *32*, 117.
(261) Wilson, S. T.; Lok, B. M.; Messina, C. A.; Cannan, T. R.; Flanigen, E. M. *J. Am. Chem. Soc.* **1982**, *104*, 1146.
(262) Cheetham, A. K.; Férey, G.; Loiseau, T. *Angew. Chem., Int. Ed.* **1998**, *38*, 3268.
(263) Férey, G. *Chem. Mater.* **2001**, *13*, 3084.
(264) Harrison, W. T. A. *Curr. Opin. Solid State Mater. Sci.* **2002**, *6*, 407.
(265) Rao, C. N. R.; Natarajan, S.; Choudhury, A.; Neeraj, S.; Ayi, A. A. *Acc. Chem. Res.* **2001**, *34*, 80. Rao, C. N. R.; Natarajan, S.; Choudhury, A.; Neeraj, S.; Vaidhyanathan, R. *Acta Crystallogr.* **2001**, *B57*, 1.
(266) Loewenstein, W. *Am. Mineral.* **1954**, *39*, 92.
(267) Deville, H. de S. C. *C. R. Hebd. Seances Acad. Sci.* **1862**, *54*, 324.
(268) Breck, D. W. *Zeolite Molecular Sieves; Structure, Chemistry and Use*; J. Wiley & Sons: New York, 1974. Barrer, R. M. *Hydrothermal Chemistry of Zeolites*; Academic Press: New York, 1982. Szostak, R. *Molecular Sieves: Principles of synthesis and identification*; van Nostrand Reinhold: New York, 1989.
(269) Venuto, P. B. *Microporous Mater.* **1994**, *2*, 297.
(270) Baerlocher, Ch.; Meier, W. M.; Olson, D. H. *Atlas of Zeolite Framework Types*, 5th ed.; Elsevier: Amsterdam, 2001.
(271) Meier, W. M. *Molecular Sieves*, Society for Chemical Industry: London, 1968, p 10.
(272) Szostak, R. *Handbook of Molecular Sieves*; van Nostrand Reinhold: New York, 1992.
(273) Barrer, R. M.; Denny, P. J. *J. Chem. Soc.* **1961**, 971. Kerr, G. T.; Kokotailo, G. *J. Am Chem. Soc.* **1961**, *83*, 4675.
(274) Davis, M. E.; Lobo, R. F. *Chem. Mater.* **1992**, *4*, 757.
(275) Cundy, C. S.; Cox, P. A. *Chem. Rev.* **2003**, *103*, 663.
(276) Bennett, J. M.; Kirschmer, R. M. *Zeolites* **1992**, *12*, 338. Simmen, A.; McCusker, L. B.; Baerlocher, Ch.; Kirschmer, W. M. *Zeolites* **1999**, *11*, 654. Henson, N. J.; Cheetham., A. K.; Gale, J. D. *Chem. Mater.* **1994**, *6*, 1647. Petrovic, I.; Navrotsky, A.; Davis, M. E.; Zones, S. I. *Chem. Mater.* **1993**, *5*, 1805.
(277) Rabenau, R. *Angew. Chem., Int. Ed.* **1985**, *24*, 1026, and references therein. Landise, R. A. *Chem. Eng. News* **1987**, (Sept 28), 30, and references therein.
(278) Feng, S.; Xu, R. *Acc. Chem. Res.* **2001**, *34*, 239.
(279) Neeraj, S.; Forster, P. M.; Rao, C. N. R.; Cheetham, A. K. *Chem. Commun.* **2001**, 2716.
(280) Rao, C. N. R.; Natarajan, S.; Neeraj, S. *J. Am. Chem. Soc.* **2000**, *122*, 2810.
(281) Neeraj, S.; Cheetham, A. K. *Chem. Commun.* **2002**, 1738.
(282) Huo, Q.; Xu, R. *Chem. Commun.* **1990**, 783.
(283) Jones, R. H.; Thomas, J. M.; Chen., J.; Xu, R.; Huo, Q.; Li, S.; Ma, Z.; Chippindale, A. M. *J. Solid State Chem.* **1993**, *102*, 204.
(284) Morris, R. E.; Weigel, S. J. *Chem. Soc. Rev.* **1997**, *26*, 309.
(285) Paillaud, J.-L.; Marler, B.; Kessler, H. *Chem. Commun.* **1996**, 1293.
(286) Vidal, L.; Gramlich, V.; Patarin, J.; Gabelica, Z. *Eur. J. Solid State Inorg. Chem.* **1998**, *35*, 545.
(287) Yuan, H.-M.; Zhu, G.-S.; Chen, J.-S.; Chen, W.; Yang, G.-D.; Xu, R. *J. Solid State Chem.* **2000**, *151*, 145.
(288) Estermann, M.; McCusker, L. B.; Baerlocher, Ch.; Merrouche, A.; Kessler, H. *Nature* **1991**, *352*, 320.
(289) Guth, J. L.; Kessler, H.; Wey, R. *Stud. Surf. Sci. Catal.* **1986**, *28*, 121.
(290) Férey, G. *J. Fluorine Chem.* **1995**, *72*, 187. Férey, G. *C. R. Acad. Sci. Ser. II* **1998**, *1*, 1.
(291) Neeraj, S.; Natarajan, S. *J. Mater. Chem.* **2000**, *10*, 1171.
(292) Yu, J.; Wang, Y.; Shi, Z.; Xu, R. *Chem. Mater.* **2001**, *13*, 2972.
(293) Kan, Q.; Glasser, F. P.; Xu, R. *J. Mater. Chem.* **1993**, *3*, 983.
(294) Chippindale, A. M.; Walton, R. I.; Turner, C. *J. Chem. Soc., Chem. Commun.* **1995**, 1261.
(295) Choudhury, A.; Natarajan, S.; Rao, C. N. R. *Inorg. Chem.* **2000**, *39*, 4295.
(296) Choudhury, A. Ph.D. Thesis, Indian Institute of Science, Bangalore, India, 2002.
(297) Francis, R. J.; O'Hare, D. *J. Chem. Soc., Dalton Trans.* **1998**, 3133.
(298) Nenoff, T. M.; Harrison, W. T. A.; Gier, T. E.; Stucky, G. D. *J. Am. Chem. Soc.* **1991**, *113*, 378.
(299) Leech, M. A.; Cowley, A. R.; Prout, K.; Chippindale, A. M. *Chem. Mater.* **1998**, *10*, 451.
(300) Dutta, P. K.; Reddy, K. S. N.; Salvati, L.; Jakupca, M. *Nature* **1995**, *374*, 44. Castaghola, M. J.; Dutta, P. K. *Microporous Mesoporous Mater.* **1998**, *20*, 149. Singh, R.; Dutta, P. K. *Langmuir* **2000**, *16*, 4148.
(301) Yates, M. Z.; Ott, K. C.; Birnbaum, E. R.; McCleskey, T. M. *Angew. Chem., Int. Ed.* **2002**, *41*, 476. Lin, J.-C.; Dipre, J. T.; Yates, M. Z. *Chem. Mater.* **2003**, *15*, 2764.
(302) Choi, K.; Gardner, D.; Hilbrandt, H.; Bein, T. *Angew. Chem., Int. Ed.* **1998**, *38*, 2891.
(303) Huang, Q.; Ulutagay, M.; Michener, P. A.; Hwu, S.-J. *J. Am. Chem. Soc.* **1999**, *121*, 10323. Huang, Q.; Hwu, S.-J.; Mo; X., *Angew. Chem., Int. Ed.* **2001**, *40*, 1690.
(304) Liu, Y.; Zhang, L.; Shi, Z.; Yuan, H.; Pang, W. *J. Solid State Chem.* **2001**, *158*, 68.
(305) Neeraj, S.; Natarajan, S.; Rao, C. N. R. *J. Solid State Chem.* **2000**, *150*, 417.
(306) Choudhury, A.; Rao, C. N. R. *Zh. Strukt. Khim. (Russ.)* **2002**, *43*, 681; *J. Struct. Chem.* **2002**, *43*, 632.
(307) Ramik, R. A.; Sturman, B. D.; Dunn, P. J.; Poverennukh, A. S. *Can. Mineral.* **1980**, *18*, 185.
(308) O'Keeffe, M.; Hyde, B. G. *Philos. Trans. R. Soc. London* **1980**, *195*, 553.
(309) Chippindale, A. M.; Natarajan, S.; Thomas, J. M.; Jones, R. H. *J. Solid State Chem.* **1994**, *111*, 18.
(310) Zhang, D.; Shi, Z.; Feng, S.-H. *Chem. Res. Chin. Univ.* **2001**, *17*, 249.
(311) Wells, A. F. *Three-dimensional Nets and Polyhedra*; John-Wiley & Sons: New York, 1977.
(312) Smith, J. V. *Chem. Rev.* **1988**, *88*, 149.
(313) O'Keeffe, M.; Hyde, B. G. *Crystal Structures, I, Pattern and Symmetry*; Mineralogical Society of America: Washington, DC, 1996.
(314) Wells, A. F. *Further Studies of Three-dimensional Nets*; American Crystallographic Association: Pittsburg, PA, 1979.
(315) Schnider, M.; Hawthorne, F. C.; Baur, W. H. *Acta Crystallogr.* **1999**, *B55*, 811.

(316) Férey, G. *J. Solid State Chem.* **2000**, *152*, 37.
(317) O'Keeffe, M.; Eddaoudi, M.; Li, H.; Reineke, T.; Yaghi, O. M. *J. Solid State Chem.* **2000**, *152*, 3.
(318) Natarajan, S.; Neeraj, S.; Choudhury, A.; Rao, C. N. R. *Inorg. Chem.* **2000**, *39*, 1426.
(319) Smith, J. V.; Rinaldi, F. *Mineral. Mag.* **1962**, *33*, 202.
(320) Sassoye, C.; Loiseau, T.; Taulelle, F.; Férey, G. *Chem. Commun.* **2000**, 943.
(321) Choudhury, A.; Natarajan, S.; Rao, C. N. R. *Chem. Commun.* **1999**, 1305.
(322) Cavellec, M.; Grenèche, J. M.; Riou, D.; Férey, G. *Chem. Mater.* **1998**, *10*, 2434.
(323) Davis, M. E. *Chem.—Eur. J.* **1997**, *3*, 1745.
(324) Davis, M. E.; Saldarriaga, C.; Montes, C.; Garces, J.; Crowder, C. *Nature* **1988**, *331*, 698.
(325) Freyhardt, C. C.; Tsapatsis, M.; Lobo, R. F.; Balkus, K. J.; Davis, M. E. *Nature* **1992**, *381*, 295.
(326) Parise, J. B. *Acta Crystallogr.* **1984**, *C40*, 1641.
(327) Parise, J. B. *J. Chem. Soc., Chem. Commun.* **1984**, 1449.
(328) Pluth, J. J.; Smith, J. V. *Acta Crystallogr.* **1984**, *C40*, 1641.
(329) Bennett, J. M.; Cohen, J. M.; Artiolli, G.; Pluth, J. J.; Smith, J. V. *Inorg. Chem.* **1985**, *24*, 188.
(330) Parise, J. B.; Day, C. S. *Acta Crystallogr.* **1985**, *C41*, 515.
(331) Parise, J. B. *Inorg. Chem.* **1985**, *24*, 4312.
(332) Pluth, J. J.; Smith, J. V.; Bennett, J. M. *Acta Crystallogr.* **1986**, *C42*, 283.
(333) Bennett, J. M.; Dytrych, W. J.; Pluth, J. J.; Smith, J. V. *Zeolites* **1986**, *6*, 349.
(334) Pluth, J. J.; Smith, J. V. *Acta Crystallogr.* **1987**, *C43*, 866.
(335) Huo, Q.; Xu, R. *Chem. Commun.* **1990**, 783.
(336) Yu, L.; Pang, W.; Li, L. *J Solid State Chem.* **1990**, *87*, 241.
(337) Jones, R. H.; Thomas, J. M.; Xu, R.; Huo, Q.; Xu, Y.; Cheetham, A. K.; Beiber, D. *J. Chem. Soc., Chem. Commun.* **1990**, 1170.
(338) Wang, T.; Yu, L.; Pang, W. *J. Solid State Chem.* **1990**, *89*, 392.
(339) Jones, R. H.; Thomas, J. M.; Xu, R.; Huo, Q.; Cheetham, A. K.; Powell, A. V. *J. Chem. Soc., Chem. Commun.* **1991**, 266.
(340) Huo, Q.; Xu, R.; Li, S.; Ma, Z.; Thomas, J. M.; Jones, R. H.; Chippindale, A. M. *J. Chem. Soc., Chem. Commun.* **1992**, 875.
(341) Thomas, J. M.; Jones, R. H.; Xu, R.; Chen., J.; Chippindale, A. M.; Natarajan, S.; Cheetham., A. K. *Chem. Commun.* **1992**, 929.
(342) Chippindale, A. M.; Powell, A. V.; Bull, L. M.; Jones, R. H.; Cheetham, A. K.; Thomas, J. M.; Xu, R. *J. Solid State Chem.* **1992**, *96*, 199.
(343) Riou, D.; Loiseau, T.; Férey, G. *J. Solid State Chem.* **1992**, *99*, 414.
(344) Riou, D.; Loiseau, T.; Férey, G. *J. Solid State Chem.* **1993**, *102*, 4.
(345) Li, H.-X.; Davis, M. E. *J. Chem. Soc., Faraday Trans.* **1993**, *89*, 951; **1993**, *89*, 957.
(346) Férey, G.; Loiseau, T.; Lacorre, P.; Taulelle, F. *J. Solid State Chem.* **1993**, *105*, 179.
(347) Taulelle, F.; Loiseau, T.; Maquet, J.; Livage, J.; Férey, G. *J. Solid State Chem.* **1993**, *105*, 191.
(348) Czarnetzki, B. K.; Stork, W. H.-J.; Dogterom, R. J. *Inorg. Chem.* **1993**, *32*, 5029.
(349) Jones, R. H.; Chippindale, A. M.; Natarajan, S.; Thomas, J. M. *J. Chem. Soc., Chem. Commun.* **1994**, 565.
(350) Harding, M. M.; Kariuki, B. M. *Acta Crystallogr.* **1994**, *C50*, 852.
(351) Chippindale, A. M.; Powell, A. V.; Jones, R. H.; Thomas, J. M.; Cheetham, A. K.; Huo, Q.; Xu, R. *Acta Crystallogr.* **1994**, *C50*, 1537.
(352) Darie, C. S.; Patarin, J.; LeGoff, P. Y.; Kessler, H.; Benazzi, E. *Microporous Mesoporous Mater* **1994**, *3*, 123. Gao, Q.; Li, S.; Xu, R. *J. Chem. Soc., Chem. Commun* **1994**, 1465.
(353) Attfield, M. P.; Morris, R. E.; Burshtein, I.; Campana, C. P.; Cheetham, A. K. *J. Solid State Chem.* **1995**, *118*, 412.
(354) Morgan, K.; Gainsford, G.; Milestone, N. *J. Chem. Soc., Chem. Commun.* **1995**, 425.
(355) Barrett, P. A.; Jones, R. H. *J. Chem. Soc., Chem. Commun.* **1995**, 1979.
(356) Bruce, D. A.; Wilkinson, A. P.; White, M. G.; Bertrand, J. A. *J. Chem. Soc., Chem. Commun.* **1995**, 2059.
(357) Renandin, J.; Férey, G. *J. Solid State Chem.* **1995**, *120*, 197.
(358) Gao, Q.; Li, S.; Xu, R.; Yue, Y. *J. Mater. Chem.* **1996**, *6*, 1207.
(359) Niaki, M. H. Z.; Joshi, P. N.; Kaliaguine, S. *Chem. Commun.* **1996**, 1373. Akporiaye, D. E.; Fjellvag, H.; Halvorsen, E. N.; Haug, T.; Karlsson, A.; Lillerud, K. P *Chem. Commun.* **1996**, 1553.
(360) Akporiaye, D. E.; Fjellvag, H.; Halvorsen, E. N.; Hustveit, J.; Karlsson, A.; Lillerud, K. P. *J. Phys. Chem.* **1996**, *100*, 16641.
(361) Williams, I. D.; Gao, Q.; Chen, J.; Ngai, L.-Y.; Lin, Z; Xu, R. *Chem. Commun.* **1996**, 1781.
(362) Renandin, J.; Loiseau, T.; Taulelle, F.; Férey, G. *C. R. Acad. Sci., Ser. B (Phys.)* **1996**, *323*, 545.
(363) Oliver, S.; Kuperman, A.; Lough, A.; Ozin, G. A. *Chem. Mater.* **1996**, *8*, 2391.
(364) Natarajan, S.; Gabriel, J.-C. P.; Cheetham, A. K. *Chem. Commun.* **1996**, 1415.
(365) Bruce, D. A.; Wilkinson, A. P.; White, M. G.; Bertrand, J. A. *J. Solid State Chem.* **1996**, *125*, 228.
(366) Gao, Q.; Chen, J.; Li, S.; Xu, R. *J. Solid State Chem.* **1996**, *127*, 145.
(367) Oliver, S.; Kuperman, A.; Lough, A.; Ozin, G. A. *Chem. Commun.* **1996**, 1761.
(368) Oliver, S.; Kuperman, A.; Lough, A.; Ozin, G. A. *Inorg. Chem.* **1996**, *35*, 6373.
(369) Morgan, K. R.; Gainsford, G.-J.; Milestone, N. B. *Chem. Commun.* **1997**, 61.
(370) Chippindale, A. M.; Cowley, A. R.; Huo, Q.; Jones, R. H.; Law, A. D.; Thomas, J. M.; Xu, R. *J. Chem. Soc., Dalton Trans.* **1997**, 2639.
(371) Oliver, S.; Kuperman, A.; Lough, A.; Ozin, G. A. *J. Mater. Chem.* **1997**, *7*, 807.
(372) Gray, M. J.; Jasper, J. D.; Wilkinson, A. P. *Chem. Mater.* **1997**, *9*, 976.
(373) Gao, Q.; Li, B.; Chen, J.; Li, S.; Xu, R. *J. Solid State Chem.* **1997**, *129*, 37.
(374) Chipindale, A. M.; Turner, C. *J. Solid State Chem.* **1997**, *128*, 318.
(375) Williams, I. D.; Yu, J.; Gao, Q.; Che., J.; Xu, R. *Chem. Commun.* **1997**, 1273.
(376) Schreyeck, L.; Caullet, P.; Mougenel, J. C.; Patarin, J.; Pailland, J. L. *Microporous Mater.* **1997**, *11*, 161. Schreyeck, L.; D'Agosto, F.; Stumbe, J.; Caullet, P.; Mougenel, J. C. *Chem. Commun.* **1997**, 1241.
(377) Lii, K.-H.; Wang, S.-L. *J. Solid State Chem.* **1997**, *128*, 21.
(378) Gao, Q.; Chen, J.; Xu, R.; Yue, Y. *Chem. Mater.* **1997**, *9*, 457. Cheng, S.; Tzeng, J.-N.; Hsu, B.-Y. *Chem. Mater.* **1997**, *9*, 1788.
(379) Yu, J.; Williams, I. D. *J. Solid State Chem.* **1998**, *136*, 141.
(380) Schreyeck, L.; Stumbe, J.; Cavllet, P.; Mongenel, J.-C.; Marler, B. *Microporous Mesoporous Mater.* **1998**, *22*, 87.
(381) Vidal, L.; Pailland, J. L.; Gabelica, Z. *Microporous Mesoporous Mater.* **1998**, *24*, 189.
(382) Yu, J.; Sugiyama, K.; Zheng, S.; Qiu, S.; Chen, J.; Xu, R.; Sakamoto, Y.; Terasaki, O.; Hiraga, H.; Light, M.; Hursthouse, M. B.; Thomas, J. M. *Chem. Mater.* **1998**, *10*, 1208.
(383) Togashi, N.; Yu, J.; Zheng, S.; Sugiyama, K.; Hiraga, K.; Terasaki, O.; Yan, W.; Qiu, S.; Xu, R. *J. Mater. Chem.* **1998**, *8*, 2827.
(384) Yu, J.; Sugiyama, K.; Hiraga, K.; Togashi, N.; Teresaki, O.; Tanaka, Y.; Nakata, S.; Qiu, S.; Xu, R. *Chem. Mater.* **1998**, *10*, 3636.
(385) Jasper, J. D.; Wilkinson, A. P. *Chem. Mater.* **1998**, *10*, 1664.
(386) Bircsak, Z.; Harrison, W. T. A. *Chem. Mater.* **1998**, *10*, 3016.
(387) Yu, J.; Terasaki, O.; Williams, I. D.; Quiv, S.; Xu, R. *Supramol. Sci.* **1998**, *5*, 297.
(388) Vidal, L.; Gramlich, V.; Patarin, J.; Gabelica, Z. *Chem. Lett.* **1999**, *28*, 201.
(389) Soulard, M.; Patarin, J.; Marler, B. *Solid State Sci.* **1999**, *1*, 37.
(390) Xu, Y.-H.; Zhang, B.-G.; Chen, X.-F.; Liu, S.-H.; Duan, C.-Y.; You, X.-Z. *J. Solid State Chem.* **1999**, *145*, 220.
(391) Kongshaug, K. O.; Fjellvåg, H.; Lillerud, K. P. *Microporous Mesoporous Mater.* **1999**, *32*, 17.
(392) Huang, Q.; Hwu, S.-J. *Chem. Commun.* **1999**, 2343.
(393) Li, J.; Yu, J.; Yan, W.; Xu, Y.; Xu, W.; Qiu, S.; Xu, R. *Chem. Mater.* **1999**, *11*, 2600.
(394) Vidal, L.; Marichal, C.; Gramlich, V.; Patarin, J.; Gabelica, Z. *Chem. Mater.* **1999**, *11*, 2728.
(395) Yu, J.; Li, J.; Sugiyama, S.; Togashi, N.; Terasaki, O.; Hiraga, K.; Zhou, B.; Qiu, S.; Xu, R. *Chem. Mater.* **1999**, *11*, 1727.
(396) Simon, N.; Loiseau, T.; Férey, G. *J. Mater. Chem.* **1999**, *9*, 585.
(397) Kongshaug, K. O.; Fjellvåg, H.; Lillerud, K. P. *J. Mater. Chem.* **1999**, *9*, 1591.
(398) Wei, B.; Zhu, G.; Yu, J.; Qiu, S.; Xiao, F.-S.; Terasaki, O. *Chem. Mater.* **1999**, *11*, 3417.
(399) Simon, N.; Loiseau, T.; Férey, G. *Solid State Sci.* **1999**, *1*, 339.
(400) Yao, Y.-W.; Natarajan, S.; Chen, J.-S.; Pang, W.-Q. *J. Solid State Chem.* **1999**, *146*, 458.
(401) Chippindale, A. M.; Walton, R. I. *J. Solid State Chem.* **1999**, *145*, 731.
(402) Williams, D. J.; Kruger, J. S.; McLersy, A. F.; Wilkinson, A. P.; Hanson, J. C. *Chem. Mater.* **1999**, *11*, 2241.
(403) Simon, N.; Guillou, N.; Loiseau, T.; Taulelle, F.; Férey, G. *J. Solid State Chem.* **1999**, *147*, 92.
(404) Sugiyama, K.; Hiraga, K.; Yu, J.; Zhang, S.; Qiu, S.; Xu, R.; Terasaki, O. *Acta Crystallogr.* **1999**, *C55*, 1615.
(405) Simon, N.; Loiseau, T.; Férey, G. *J. Chem. Soc., Dalton Trans.* **1999**, 1147.
(406) Kongshang, K. O.; Fjellvåg, Lillerud, K. P. *Microporous Mesoporous Mater.* **2000**, *38*, 311.

(407) Wang, K.; Yu, J.; Zhu, G.; Zou, Y.; Xu, R. *Microporous Mesoporous Mater.* **2000**, *39*, 281.
(408) Maeda, K.; Tuel, A.; Caldarelli, S.; Baerlocher, Ch. *Microposous Mesoporous Mater.* **2000**, *39*, 465.
(409) Yan, W.; Yu, J.; Xu, R.; Zhu, G.; Xiao, F.; Han., Y.; Sugiyama, K. *Chem. Mater.* **2000**, *12*, 2517.
(410) Wei, B.; Yu, J.; Shi, Z.; Qiu, S.; Li, J. *J. Chem. Soc., Dalton Trans.* **2000**, 1979.
(411) Yan, W.; Yu, J.; Shi, Z.; Xu, R. *Chem. Commun.* **2000**, 1431.
(412) Kongshaug, K. O.; Fjellvåg, H.; Lillerud, K. P. *Microporous Mesoporous Mater.* **2000**, *40*, 313.
(413) Yu, J.; Li, J.; Wand, K.; Xu, R.; Sugiyama, K.; Terasaki, O. *Chem. Mater.* **2000**, *12*, 3783.
(414) Simon, N.; Loiseau, T.; Férey, G. *Solid State Sci.* **2000**, *2*, 389.
(415) Choudhury, A.; Natarajan, S.; Rao, C. N. R. *Int. J. Inorg. Chem.* **2000**, *2*, 87.
(416) Marichal, C.; Vidal, L.; Delmotte, L; Patarin, J. *Microporous Mesoporous Mater.* **2000**, *34*, 149.
(417) Kirchner, R. M.; Kuntsleve, R. W. G.; Pluth, J. J.; Wilson, S. T.; Broach, R. W.; Smith, J. V. *Microporous Mesoporous Mater.* **2000**, *39*, 319.
(418) Kongshaug, K. O.; Fjellvåg, H.; Klewe, B.; Lillerud, K. P. *Microporous Mesoporous Mater.* **2000**, *39*, 333.
(419) Yuan, H.-M.; Chen, J.-S.; Shi, Z.; Chen, W.; Wang, Y.; Zhang, P.; Yu, J.-H.; Xu, R. *J. Chem. Soc., Dalton Trans.* **2000**, 1981.
(420) Tuel, A.; Gramlich, V.; Baerlocher, Ch. *Microporous Mesoporous Mater.* **2000**, *41*, 217.
(421) Maeda, K.; Tuel, A.; Baerlocher, Ch. *J. Chem. Soc., Dalton Trans.* **2000**, 2457.
(422) Thanh, S. P.; Marrot, J.; Renaudin, J.; Maisonneuve, V. *Acta Crystallogr.* **2000**, *C56*, 1073.
(423) Feng, P.; Bu, X.; Stucky, G. D. *Inorg. Chem.* **2000**, *39*, 2.
(424) Yan, W.; Yu, J.; Shi, Z.; Xu, R. *Inorg. Chem.* **2001**, *40*, 379.
(425) Ayi, A. A.; Choudhury, A.; Natarajan, S. *J. Solid State Chem.* **2001**, *156*, 185.
(426) Li, J.; Yu, J.; Wang, K.; Zhu, G.; Xu, R. *Inorg. Chem.* **2001**, *40*, 5812.
(427) Yan, W.; Yu, J.; Shi, Z.; Wang, Y.; Zou, Y.; Xu, R. *J. Solid State Chem.* **2001**, *161*, 259.
(428) Paillaud, J.-L.; Caullet, P.; Schreyeck, L.; Marlen, B. *Microporous Mesoporous Mater.* **2001**, *42*, 177.
(429) Yan, W.; Yu, J.; Shi, Z.; Miao, P.; Wang, K.; Wang, Y.; Xu, R. *Microporous Mesoporous Mater.* **2001**, *50*, 151.
(430) Tuel, A.; Gramlich, V.; Baerlocher, Ch. *Microporous Mesoporous Mater.* **2001**, *46*, 57.
(431) Tuel, A.; Gramlich, V.; Baerlocher, Ch. *Microporous Mesoporous Mater.* **2001**, *47*, 217.
(432) Wang, K.; Yu, J.; Shi, Z.; Miao, P.; Yan, W.; Xu, R. *J. Chem. Soc., Dalton Trans.* **2001**, 1809.
(433) Wang, K.; Yu, J.; Miao, P.; Song, Y.; Li, J.; Shi, Z.; Xu, R. *J. Mater. Chem.* **2001**, *11*, 1898.
(434) Loiseau, T.; Draznieks, C. M.; Sassoye, C.; Girard, S.; Guillou, N.; Huguenard, C.; Taulelle, F.; Férey, G. *J. Am. Chem. Soc.* **2001**, *123*, 9642.
(435) Wheatley, P. S.; Love, C. J.; Morrison, J. J.; Shannon, I. J.; Morris, R. E. *J. Mater. Chem.* **2002**, *12*, 477.
(436) Tuel, A.; Gramlich, V.; Baerlocher, Ch. *Microporous Mesoporous Mater.* **2002**, *56*, 119.
(437) Natarajan, S.; Klein, W.; Nuss, J.; van Wüllen, L.; Jansen, M. *Z. Anorg. Allg. Chem.* **2003**, *629*, 339.
(438) Jordá, J. L.; McCusker, L. B.; Baerlocher, Ch.; Morais, C. M.; Rocha, J.; Fernandez, C.; Borges, C.; Lourenco, J. P.; Ribeiro, M. P.; Gabelica, Z. *Microporous Mesoporous Mater.* **2003**, *65*, 43.
(439) Medina, M. E.; Iglesias, M.; Puebla, E. G.; Monge, M. A. *J. Mater. Chem.* **2004**, *14*, 845.
(440) Yu, J.; Xu, R.; Li, J. *Solid State Sci.* **2000**, *2*, 181.
(441) Yu, J.; Xu, R. *Acc. Chem. Res.* **2003**, *36*, 481.
(442) LeBail, A.; Férey, G.; Amoros, P.; Porter, D. B. *Eur. J. Solid State Inorg. Chem.* **1989**, *26*, 419.
(443) Parise, J. B. *J. Chem. Soc., Chem. Commun.* **1985**, 606.
(444) Parise, J. B. *Acta Crystallogr.* **1986**, *C42*, 144.
(445) Parise, J. B. *Acta Crystallogr.* **1986**, *C42*, 670.
(446) Yang, G.; Feng, S.; Xu, R. *J. Chem. Soc., Chem. Commun.* **1987**, 1255.
(447) Yang, G.-D.; Feng, S.; Xu, R. *Chin. J. Struct. Chem.* **1988**, *7*, 235.
(448) Wang, T.; Yang, G.; Feng, S.; Shang, C.; Xu, R. *J. Chem. Soc., Chem. Commun.* **1989**, 948.
(449) Jones, R. H.; Thomas, J. M.; Huo, Q.; Xu, R.; Hursthouse, M. B.; Chen, J. *J. Chem. Soc., Chem. Commun.* **1991**, 1520.
(450) Loiseau, T.; Férey, G. *J. Chem. Soc., Chem. Commun.* **1992**, 1197.
(451) Huo, Q.; Xu, R. *J. Chem. Soc., Chem. Commun.* **1992**, 1391.
(452) Loiseau, T.; Férey, G. *Eur. J. Solid State Inorg. Chem.* **1993**, *30*, 381.
(453) Glasser, F.; Howie, R.; Kan, Q. *Acta Crystallogr.* **1994**, *C50*, 848.
(454) Loiseau, T.; Riou, D.; Licheron, M.; Férey, G. *J. Solid State Chem.* **1994**, *111*, 397.
(455) Loiseau, T.; Férey, G. *J. Solid State Chem.* **1994**, *111*, 403.
(456) Loiseau, T.; Retoux, R.; Lacorre, P.; Férey, G. *J. Solid State Chem.* **1994**, *111*, 427.
(457) Loiseau, T.; Férey, G. *Eur. J. Solid State Inorg. Chem.* **1994**, *31*, 575.
(458) Cavellec, M.; Riou, D.; Férey, G. *Eur. J. Solid State Inorg. Chem.* **1994**, *31*, 583.
(459) Serpaggi, F.; Loiseau, T.; Riou, D.; Férey, G. *Eur. J. Solid State Inorg. Chem.* **1994**, *31*, 595.
(460) Riou, D.; Férey, G. *Eur. J. Solid State Inorg. Chem.* **1994**, *31*, 605.
(461) Yin, X.; Nazar, L. F. *J. Chem. Soc., Chem. Commun.* **1994**, 2349.
(462) Attfield, M. P.; Morris, R. E.; Puebla, E. G.; Bravo, A. M.; Cheetham., A. K. *J. Chem. Soc., Chem. Commun.* **1995**, 843.
(463) Feng, S.; Xu, X.; Yang, G.; Xu, R.; Glasser, F. P. *J. Chem. Soc., Dalton Trans.* **1995**, 2147.
(464) Loiseau, T.; Taulelle, F.; Férey, G. *Microporous Mater.* **1996**, *5*, 365.
(465) Kallus, S.; Patarin, J.; Marler, B. *Microporous Mater.* **1996**, *7*, 89.
(466) Loiseau, T.; Férey, G. *J. Mater. Chem.* **1996**, *6*, 1073.
(467) Lii, K.-H. *Inorg. Chem.* **1996**, *35*, 7440.
(468) Loiseau, T.; Taulelle, F.; Férey, G. *Microporous Mater.* **1997**, *9*, 83.
(469) Reinert, P.; Darie, C.-S.; Patarin, J. *Microporous Mater.* **1997**, *9*, 107.
(470) Serpaggi, F.; Loiseau, T.; Férey, G. *Acta Crystallogr.* **1997**, *C53*, 1568.
(471) Weigel, S. J.; Weston, S. C.; Cheetham., A. K.; Stucky, G. D. *Chem. Mater.* **1997**, *9*, 1293.
(472) Loiseau, T.; Serpaggi, F.; Férey, G. *Chem. Commun.* **1997**, 1093.
(473) Weigel, S. J.; Morris, R. E.; Stucky, G. D.; Cheetham., A. K. *J. Mater. Chem.* **1998**, *8*, 1607.
(474) Stalder, S. M.; Wilkinson, A. P. *Chem. Mater.* **1997**, *9*, 2168.
(475) Serpaggi, F.; Loiseau, T.; Taulelle, F.; Férey, G. *Microporous Mesoporous Mater.* **1998**, *20*, 197.
(476) Lin, H.-M.; Lii, K.-H. *Inorg. Chem.* **1998**, *37*, 4220.
(477) Reinert, P.; Patarin, J.; Loiseau, T.; Férey, G.; Kessler, H. *Microporous Mesoporous Mater.* **1998**, *22*, 43.
(478) Reinert, P.; Marler, B.; Patarin, J. *Chem. Commun.* **1998**, 1769.
(479) Wessels, T.; McCusker, L. B.; Baerlocher, Ch.; Reinert, P.; Patarin, J. *Microporous Mesoporous Mater* **1998**, *23*, 67.
(480) Taulelle, F.; Samoson, A.; Loiseau, T.; Férey, G. *J. Phys. Chem. B* **1998**, *102*, 8587.
(481) Chippindale, A. M.; Bond, A. D.; Law, A. D.; Cowley, A. R. *J. Solid State Chem.* **1998**, *136*, 227.
(482) Chippindale, A. M.; Law, A. D. *J. Solid State Chem.* **1999**, *142*, 236.
(483) Chippindale, A. M.; Peacock, K. J.; Cowley, A. R. *J. Solid State Chem.* **1999**, *145*, 379.
(484) Munch, V.; Taulelle, F.; Loiseau, T.; Férey, G.; Cheetham, A. K.; Weigel, S.; Stucky, G. D. *Magn. Reson. Chem.* **1999**, *37*, 5100.
(485) Wragg, D. S.; Bull, I.; Hix, G. B.; Morris, R. E. *Chem. Commun.* **1999**, 2037.
(486) Loiseau, T.; Férey, G. *Microporous Mesoporous Mater.* **2000**, *35*−*36*, 609.
(487) Cabarrecq, C. B.; Mosset, A. *J. Mater. Chem.* **2000**, *10*, 445.
(488) Walton, R. I.; Millange, F.; LeBail, A.; Loiseau, T.; Serre, C.; O'Hare, D.; Férey, G. *Chem. Commun.* **2000**, 203.
(489) Paulet, C.; Loiseau, T.; Férey, G. *J. Mater. Chem.* **2000**, *10*, 1225.
(490) Loiseau, T.; Panlet, C.; Simon, N.; Munch, V.; Taulelle, F.; Férey, G. *Chem. Mater.* **2000**, *12*, 1393.
(491) Matijasic, A.; Paillaud, J.-L.; Patarin, J. *J. Mater. Chem.* **2000**, *10*, 1345.
(492) Chen, C.-Y.; Lo, F.-R.; Kao, H.-M.; Lii, K. H. *Chem. Commun.* **2000**, 1061.
(493) Walton, R. I.; Millange, F.; Loiseau, T.; O'Hare, D.; Férey, G. *Angew. Chem., Int. Ed.* **2000**, *39*, 4552.
(494) Reinert, P.; Marler, B.; Patarin, J. *Microporous Mesoporous Mater.* **2000**, *39*, 509.
(495) Walton, R. I.; Millange, F.; O'Hare, D. *Chem. Mater.* **2000**, *12*, 1977.
(496) Wragg, D. S.; Morris, R. E. *J. Am. Chem. Soc.* **2000**, *122*, 11246.
(497) Matijasic, A.; Gramlich, V.; Patarin, J. *Solid State Sci.* **2001**, *3*, 155.
(498) Wragg, D. S.; Morris, R. E. *J. Phys. Chem. Solids* **2001**, *62*, 1493.
(499) Sassoye, C.; Loiseau, T.; Férey, G. *J. Fluorine Chem.* **2001**, *107*, 187.
(500) Lin, C.-H.; Wang, S.-L. *Inorg. Chem.* **2001**, *40*, 2918.
(501) Josien, L.; Simon, A.; Gramlich, V.; Patarin., J. *Chem. Mater.* **2001**, *13*, 1305.

(502) Wragg, D. S.; Slawin, A. M. Z.; Morris, R. E. *J. Mater. Chem.* **2001**, *11*, 1850.
(503) Livage, C.; Millange, F.; Walton., R. I.; Loiseau, T.; Simon, N.; O'Hare, D.; Férey, G. *Chem. Commun.* **2001**, 994.
(504) Lin, C.-H.; Wang, S.-L.; Lii, K.-H. *J. Am. Chem. Soc.* **2001**, *123*, 4649.
(505) Bonhomme, F.; Thoma, S. G.; Rodriguez, M. A.; Nenoff, T. M. *Chem. Mater.* **2001**, *13*, 2112.
(506) Hsien, M.-C.; Kao, H.-M.; Lii, K.-H. *Chem. Mater.* **2001**, *13*, 2584.
(507) Bonhomme, F.; Thoma, S. G.; Rodriguez, M. A.; Nenoff, T. M. *Microporous Mesoporous Mater.* **2001**, *47*, 185.
(508) Matijasic, A.; Gramlich, V.; Patarin, J. *J. Mater. Chem.* **2001**, *11*, 2553.
(509) Bonhomme, F.; Thoma, S. G.; Nenoff, T. M. *J. Mater. Chem.* **2001**, *11*, 2559.
(510) Josien, L.; Masseron, A. S.; Gramlich, V.; Patarin, J. *Chem.—Eur. J.* **2002**, *8*, 1614.
(511) Sassoye, C.; Marrot, J.; Loiseau, T.; Férey, G. *Chem. Mater.* **2002**, *14*, 1340.
(512) Kissick, J. L.; Cowley, A. R.; Chippindale, A. M. *J. Solid State Chem.* **2002**, *167*, 17.
(513) Wang, Y.; Yu, J.; Shi, Z.; Xu, R. *J. Solid State Chem.* **2003**, *170*, 176.
(514) Beitone, L.; Marrot, J.; Loiseau, T.; Férey, G.; Henry, M.; Huguenard, C.; Gansmuller, A.; Taulelle, F. *J. Am. Chem. Soc.* **2003**, *125*, 1912.
(515) Sun, D.; Cao, R.; Sun, Y.; Bi, W.; Hong, M. *Eur. J. Inorg. Chem.* **2003**, 1303.
(516) Chang, W.-J.; Chen, C.-Y.; Lii, K.-H. *J. Solid State Chem.* **2003**, *172*, 6.
(517) Magneli, A. *Acta Chem. Scand.* **1953**, *7*, 315.
(518) Dhingra, S. S.; Haushalter, R. C. *J. Chem. Soc., Chem. Commun.* **1993**, 1665.
(519) Xu, Y.; Koh, L. L.; An, L. H.; Xu, R.; Qiu, S. L. *J. Solid State Chem.* **1995**, *117*, 373.
(520) Chippindale, A. M.; Brech, S. J.; Cowley, A. R.; Simpson, W. M. *Chem. Mater.* **1996**, *8*, 2259.
(521) Chippindale, A. M.; Brech, S. J. *Chem. Commun.* **1996**, 2781.
(522) Du, H.; Chen, J.; Pang, W.; Yu, J.; Williams, I. D. *Chem. Commun.* **1997**, 781.
(523) Williams, I. D.; Yu, J.; Du, H.; Chen., J.; Pang, W. *Chem. Mater.* **1998**, *10*, 773.
(524) Thirumurugan, A.; Natarajan, S. *Dalton Trans.* **2003**, 3387.
(525) Du, Y.; Yu, J.; Wang, Y.; Pan, Q.; Zou, Y.; Xu, R. *J. Solid State Chem.* **2004**, *177*, 3032.
(526) Park, H.; Bull, I.; Peng, L.; Young, V. G.; Grey, C.P.; Parise, J. B. *Chem. Mater.* **2004**, *16*, 5350.
(527) Gier, T. E.; Stucky, G. D. *Nature* **1991**, *349*, 508.
(528) Harrison, W. T. A.; Gier, T. E.; Moran, K. L.; Nicol, J. M.; Eckert, H.; Stucky, G. D. *Chem. Mater.* **1991**, *3*, 27.
(529) Harrison, W. T. A.; Martin, T. E.; Gier, T. E.; Stucky, G. D. *J. Mater. Chem.* **1992**, *2*, 175.
(530) Harrison, W. T. A.; Nenoff, T. M.; Eddy, M. M.; Martin, T. E.; Stucky, G. D. *J. Mater. Chem.* **1992**, *2*, 1127.
(531) Harrison, W. T. A.; Nenoff, T. M.; Gier, T. E.; Stucky, G. D. *Inorg. Chem.* **1993**, *32*, 2437.
(532) Nenoff, T. M.; Harrison, W. T. A.; Gier, T. E.; Calabrese, J. C.; Stucky, G. D. *J. Solid State Chem.* **1993**, *107*, 285.
(533) Harrison, W. T. A.; Nenoff, T. M.; Gier, T. E.; Stucky, G. D. *J. Solid State Chem.* **1994**, *113*, 168.
(534) Jones, R. H.; Chen., J.; Sankar, G.; Thomas, J. M. *Stud. Surf. Sci. Catal.* **1994**, *84*, 2229.
(535) Song, T.; Xu, J.; Zhaov, Y.; Yue, Y.; Xu, Y.; Xu., R.; Hu, N.; Wei, G.; Jia, H. *J. Chem. Soc., Chem. Commun.* **1994**, 1171.
(536) Song, T.; Hursthouse, M. B.; Chen., J.; Xu, J.; Abdul Malik, K. M.; Jones, R. H.; Xu, R.; Thomas, J. M. *Adv. Mater.* **1994**, *6*, 679.
(537) Patarin, J.; Marler, B.; Huve, L. *Eur. J. Solid State Inorg. Chem.* **1994**, *31*, 909.
(538) Feng, P.; Bu, X.; Stucky, G. D. *Angew. Chem., Int. Ed.* **1995**, *34*, 1745.
(539) Harrison, W. T. A.; Gier, T. E.; Nicol, J. M.; Stucky, G. D. *J. Solid State Chem.* **1995**, *114*, 249.
(540) Ahmadi, K.; Hardy, A.; Patarin, J.; Huve, L. *Eur. J. Solid State Inorg. Chem.* **1995**, *32*, 209.
(541) Harrison, W. T. A.; Gier, T. E.; Stucky, G. D.; Broach, R. W.; Bedard, R. A. *Chem. Mater.* **1996**, *8*, 145.
(542) Harrison, W. T. A.; Broach, R. W.; Bedard, R. A.; Gier, T. E.; Bu, X.; Stucky, G. D. *Chem. Mater.* **1996**, *8*, 691.
(543) Bu, X.; Feng, P.; Stucky, G. D. *J. Solid State Chem.* **1996**, *125*, 243.
(544) Harrison, W. T. A.; Phillips, M. L. F. *Chem. Commun.* **1996**, 2771.
(545) Reinert, P.; Khatyr, A.; Marler, B.; Patarin, J. *Eur. J. Solid State Inorg. Chem.* **1997**, *34*, 1211.
(546) Harrison, W. T. A.; Hannooman, L. *Angew. Chem., Int. Ed.* **1997**, *36*, 640.
(547) Harrison, W. T. A.; Hannooman, L. *J. Solid State Chem.* **1997**, *131*, 363.
(548) Harrison, W. T. A.; Phillips, M. L. F. *Chem. Mater.* **1997**, *9*, 1837.
(549) Natarajan, S.; Attfield, M. P.; Cheetham., A. K. *J. Solid State Chem.* **1997**, *132*, 229.
(550) Harrison, W. T. A.; Bircsak, Z.; Hannooman, L. *J. Solid State Chem.* **1997**, *134*, 148.
(551) Bu, X.; Feng, P.; Gier, T. E.; Stucky, G. D. *Zeolites* **1997**, *19*, 200.
(552) Chidambaram, D.; Natarajan, S. *Mater. Res. Bull.* **1998**, *33*, 1275.
(553) Harrison, W. T. A.; Bircsak, Z.; Hannooman, L.; Zhang, Z. *J. Solid State Chem.* **1998**, *136*, 93.
(554) Reinert, P.; Zabukovec Logar, N.; Patarin, J.; Kaučič, V. *Eur. J. Solid State Inorg. Chem.* **1998**, *35*, 373.
(555) Harmon, S. B.; Sevov, S. C. *Chem. Mater.* **1998**, *10*, 3020.
(556) Jensen, T. R. *J. Chem. Soc., Dalton Trans.* **1998**, 2261.
(557) Trojette, B.; Hajem, A. A.; Driss, A.; Jouini, T. *J. Chem. Crystallogr.* **1998**, *28*, 339.
(558) Hajem, A. A.; Trojette, B.; Driss, A.; Jouini, T. *J. Chem. Crystallogr.* **1999**, *29*, 217.
(559) Neeraj, S.; Natarajan, S.; Rao, C. N. R. *Chem. Commun.* **1999**, 165.
(560) Neeraj, S.; Natarajan, S.; Rao, C. N. R. *New J. Chem.* **1999**, 303.
(561) Jensen, T. R.; Hazell, R. G. *Chem. Commun.* **1999**, 371.
(562) Chidambaram, D.; Neeraj, S.; Natarajan, S.; Rao, C. N. R. *J. Solid State Chem.* **1999**, *147*, 154.
(563) Neeraj, S.; Natarajan, S.; Rao, C. N. R. *Chem. Mater.* **1999**, *11*, 1390.
(564) Chavez, A. V.; Nenoff, T. M.; Hannooman, L.; Harrison, W. T. A. *J. Solid State Chem.* **1999**, *147*, 584.
(565) Broach, R. W.; Bedard, R. L.; Song, S. G.; Pluth, J. J.; Bram, A.; Riekel, C.; Weber, H.-P. *Chem. Mater* **1999**, *11*, 2076.
(566) Yang, G.-Y.; Sevov, S. C. *J. Am. Chem. Soc.* **1999**, *121*, 8389.
(567) Harrison, W. T. A.; Phillips, M. L. F.; Clegg, W.; Teat, S. J. *J. Solid State Chem.* **1999**, *148*, 433.
(568) Vaidhyanathan, R.; Natarajan, S.; Rao, C. N. R. *J. Mater. Chem.* **1999**, *9*, 2789.
(569) Neeraj, S.; Natarajan, S. *Int. J. Inorg. Mater.* **1999**, *1*, 317.
(570) Neeraj, S.; Natarajan, S.; Rao, C. N. R. *Angew. Chem., Int. Ed.* **1999**, *38*, 3480.
(571) Harrison, W. T. A.; Phillips, M. L. F.; Chavez, A. V.; Nenoff, T. M. *J. Mater. Chem.* **1999**, *9*, 3087.
(572) Kongshaug, K. O.; Fjellvåg, H.; Lillerud, K. P. *J. Mater. Chem.* **1999**, *9*, 3119.
(573) Natarajan, S.; Neeraj, S.; Rao, C. N. R. *Solid State Sci.* **2000**, *2*, 87.
(574) Kongshaug, K. O.; Fjellvåg, H.; Lillerud, K. P. *Microporous Mesoporous Mater.* **2000**, *39*, 341.
(575) Liu, W.; Liu, Y.; Shi, Z.; Pang, W. *J. Mater. Chem.* **2000**, *10*, 1451.
(576) Rao, C. N. R.; Natarajan, S.; Neeraj, S. *J. Solid State Chem.* **2000**, *152*, 302.
(577) Neeraj, S.; Natarajan, S. *Chem. Mater.* **2000**, *12*, 2753.
(578) Neeraj, S.; Natarajan, S.; Rao, C. N. R. *J. Chem. Soc., Dalton Trans.* **2000**, 2499.
(579) Kongshaug, K. O.; Fjellvåg, H.; Lillerud, K. P. *Solid State Sci.* **2000**, *2*, 569.
(580) Ayi, A. A.; Choudhury, A.; Natarajan, S.; Rao, C. N. R. *J. Mater. Chem.* **2000**, *10*, 2606.
(581) Zhang, P.; Wang, Y.; Zhu, G.; Shi, Z.; Liu, Y.; Yuan, H.; Pang, W. *J. Solid State Chem.* **2000**, *154*, 368.
(582) Rodgers, J. A.; Harrison, W. T. A. *J. Mater. Chem.* **2000**, *10*, 2853.
(583) Echavarría, A.; Saldarriaga, C. *Microporous Mesoporous Mater.* **2001**, *42*, 59.
(584) Harrison, W. T. A. *Int. J. Inorg. Mater.* **2001**, *3*, 179.
(585) Ayi, A. A.; Choudhury, A.; Natarajan, S.; Neeraj, S.; Rao, C. N. R. *J. Mater. Chem.* **2001**, *11*, 1181.
(586) Choudhury, A.; Natarajan, S.; Rao, C. N. R. *J. Solid State Chem.* **2001**, *157*, 110.
(587) Zhao, Y.; Shi, Z.; Chen, X.; Mai, Z.; Feng, S. *Chem. Lett.* **2001**, 362.
(588) Choudhury, A.; Neeraj, S.; Natarajan, S.; Rao, C. N. R. *J. Mater. Chem.* **2001**, *11*, 1537.
(589) Ayi, A. A.; Choudhury, A.; Natarajan, S.; Rao, C. N. R. *J. Phys. Chem. Solids* **2001**, *62*, 1481.
(590) Neeraj, S.; Natarajan, S. *J. Phys. Chem. Solids* **2001**, *62*, 1499.
(591) Harrison, W. T. A. *Acta Crystallogr.* **2001**, *E57*, m248.
(592) Neeraj, S.; Natarajan, S. *Cryst. Growth Des.* **2001**, *6*, 491.
(593) Simon, A.; Josien, L.; Gramlich, V.; Patarin, J. *Microporous Mesoporous Mater.* **2001**, *47*, 135.
(594) Chiang, Y.-P.; Kao, H.-M.; Lii, K.-H J. *Solid State Chem.* **2001**, *162*, 168.
(595) Rayers, A.; Nasr, C. B.; Rzaigui, M. *Mater. Res. Bull.* **2001**, *36*, 2229.

(596) Ng, H. Y.; Harrison, W. T. A. *Microporous Mesoporous Mater.* **2001**, *50*, 187.
(597) Wiebcke, M. *J. Mater. Chem.* **2002**, *12*, 143.
(598) Cui, A.; Yao, Y. *Chem. Lett.* **2001**, 1148.
(599) Xing, Y.; Liu, Y.; Shi, Z.; Zhang, P.; Fu, Y.; Cheng, C.; Pang, W. *J. Solid State Chem.* **2002**, *163*, 364.
(600) Fleith, S.; Josien, L.; Masseron, A. S.; Gramlich, V.; Patarin, J. *Solid State Sci.* **2002**, *4*, 135.
(601) Zhao, Y.; Ju, J.; Chen, X.; Li, X.; Wang, R.; Mai, Z. *J. Solid State Chem.* **2002**, *165*, 182.
(602) Weibcke, M. *J. Mater. Chem.* **2002**, *12*, 421.
(603) Choudhury, A.; Neeraj, S.; Natarajan, S.; Rao, C. N. R. *J. Mater. Chem.* **2002**, *12*, 1044.
(604) Natarajan, S. *Chem. Commun.* **2002**, 780.
(605) Harrison, W. T. A.; Rodgers, J. A.; Phillips, M. L. F.; Nenoff, T. M. *Solid State Sci.* **2002**, *4*, 969.
(606) Liu, Y.; Liu, W.; Xing, Y.; Shi, Z.; Fu, Y.; Pang, W. *J. Solid State Chem.* **2002**, *166*, 265.
(607) Weibcke, M. *Microporous Mesoporous Mater.* **2002**, *54*, 331.
(608) Song, Y.; Yu, J.; Li, G.; Li, Y.; Wang, Y.; Xu, R. *Chem. Commun.* **2002**, 1720.
(609) Mandal, S.; Natarajan, S. *Cryst. Growth Des.* **2002**, *2*, 665.
(610) Natarajan, S. *Inorg. Chem.* **2002**, *41*, 5530.
(611) Natarajan, S. *Solid State Sci.* **2002**, *4*, 1331.
(612) Lin, Z. E.; Yao, Y.-W.; Zhang, J.; Yang, G.-Y. *J. Chem. Soc., Dalton Trans.* **2002**, 4527.
(613) McDonald, I.; Harrison, W. T. A. *Inorg. Chem.* **2002**, *41*, 6184.
(614) Yanxiong, K.; Jianmin, L.; Yugen, Z.; Gaofel, H.; Zheng, J.; Zhibin, L. *Cryst. Res. Technol.* **2002**, *37*, 169.
(615) Masseron, A. S.; Paillaud, J.-L.; Patarin, J. *Chem. Mater.* **2003**, *15*, 1000.
(616) Xing, Y.; Liu, Y.; Li, G.; Shi, Z.; Liu, L.; Meng, H.; Pang, W. *Chem. Lett.* **2003**, *32*, 802.
(617) Song, Y.; Zavalij, P. Y.; Whittingham, M. S. *J. Mater. Chem.* **2003**, *13*, 1936.
(618) Lin, Z.-E.; Yao, Y.-W.; Zhang, J.; Yang, G.-Y. *Dalton Trans.* **2003**, 3160.
(619) Lin, Z.-E.; Zeng, Q.-X.; Zhang, L.; Yang, G.-Y. *Microporous Mesoporous Mater.* **2003**, *64*, 119.
(620) Wang, Y.; Yu, J.; Guo, M.; Xu, R. *Angew. Chem., Int. Ed.* **2003**, *42*, 4089.
(621) Natarajan, S.; van Wullen, L.; Klein, W.; Jansen, M. *Inorg. Chem.* **2003**, *42*, 6265.
(622) Neeraj, S.; Rao, C. N. R.; Cheetham., A. K. *J. Mater. Chem.* **2004**, *14*, 814.
(623) Weibcke, M.; Marler, B. *Solid State Sci.* **2004**, *6*, 213.
(624) Mandal, S.; Natarajan, S. *Inorg. Chim. Acta* **2004**, *357*, 1437.
(625) Mandal, S.; Kavitha, G.; Narayana, C.; Natarajan, S. *J. Solid State Chem.* **2004**, *177*, 2198.
(626) Brunner, G. O.; Meier, W. M. *Nature* **1989**, *337*, 146.
(627) Harvey, G.; Meier, W. M. *Stud. Surf. Sci. Catal.* **1989**, *49A*, 411.
(628) Harrison, W. T. A.; Gier, T. E.; Stucky, G. D. *J. Mater. Chem.* **1991**, *1*, 153.
(629) Gier, T. E.; Harrison, W. T. A.; Stucky, G. D. *Angew. Chem., Int. Ed.* **1991**, *30*, 1169.
(630) Harrison, W. T. A. *Acta Crystallogr.* **1994**, *C50*, 471.
(631) Bu, X.; Gier, T. E.; Stucky, G. D. *Microporous Mesoporous Mater.* **1998**, *26*, 61.
(632) Zhang, H.; Chen. M.; Shi, Z.; Bu, X.; Zhou, Y.; Xu, X.; Zhao, D. *Chem. Mater.* **2001**, *13*, 2042.
(633) Harrsion, W. T. A. *Acta Crystallogr.* **2001**, *C57*, 891.
(634) Natarajan, S.; Attfield, M. P.; Cheetham, A. K. *Angew. Chem., Int. Ed.* **1997**, *36*, 978.
(635) Natarajan, S.; Cheetham, A. K. *Chem. Commun.* **1997**, 1089.
(636) Natarajan, S.; Cheetham, A. K. *J. Solid State Chem.* **1997**, *134*, 207.
(637) Natarajan, S.; Eswaramoorthy, M.; Cheetham., A. K.; Rao, C. N. R. *Chem. Commun.* **1998**, 1561.
(638) Natarajan, S.; Ayyappan, S.; Cheetham, A. K.; Rao, C. N. R. *Chem. Mater.* **1998**, *10*, 1627.
(639) Natarajan, S.; Cheetham, A. K. *J. Solid State Chem.* **1998**, *140*, 435.
(640) Ayyappan, S.; Cheetham, A. K.; Natarajan, S.; Rao, C. N. R. *J. Solid State Chem.* **1998**, *139*, 207.
(641) Ayyappan, S.; Bu, X.; Cheetham, A. K.; Natarajan, S.; Rao, C. N. R. *Chem. Commun.* **1998**, 2181.
(642) Ayyappan, S.; Bu, X.; Cheetham., A. K.; Rao, C. N. R. *Chem. Mater.* **1998**, *10*, 3308.
(643) Natarajan, S. *J. Mater. Chem.* **1998**, *8*, 2757.
(644) Natarajan, S. *J. Solid State Chem.* **1999**, *148*, 50.
(645) Ayyappan, S.; Chang, J.-S.; Stock, N.; Hatfield, R.; Rao, C. N. R.; Cheetham., A. K. *Int. J. Inorg. Mater.* **2000**, *2*, 21.
(646) Liu, Y.-L.; Zhu, G.-S.; Chen, J.-S.; Na, L.-Y.; Hua, J.; Pang, W.-Q.; Xu, R. *Inorg. Chem.* **2000**, *39*, 1820.
(647) Serre, C.; Férey, G. *Chem. Commun.* **2003**, 1818.
(648) Kongshaug, K.; Fjellvåg., H.; Lillerud, K. P. *Chem. Mater.* **1999**, *11*, 2872.
(649) Kongshaug, K.; Fjellvåg., H.; Lillerud, K. P. *Chem. Mater.* **2000**, *12*, 1095.
(650) Adair, B. A.; de Delgado, G. D.; Delgado, J. M.; Cheetham., A. K. *Angew. Chem., Int. Ed.* **2000**, *39*, 745.
(651) Lin, Z.-E.; Sun, Y.-Q.; Zhang, J.; Wei, Q.-H.; Yang, G.-Y. *J. Mater. Chem.* **2003**, *13*, 447.
(652) Jayaraman, K.; Vaidhyanathan, R.; Natarajan, S.; Rao, C. N. R. *J. Solid State Chem.* **2001**, *162*, 188. Jayaraman, K.; Choudhury, A.; Vaidhyanathan, R.; Rao, C. N. R. *New J. Chem.* **2001**, 1199.
(653) Flanigen, E. M.; Lok, B. M.; Patton, R. L.; Wilson, S. T. *Pure Appl. Chem.* **1986**, *58*, 1351.
(654) Moore, P. B.; Shen, J. *Nature* **1983**, *306*, 356.
(655) Haushaletr, R. C.; Strohmaier, K. G.; Lai, F. W. *Science* **1989**, *246*, 1289.
(656) Haushalter, R. C.; Lai, F. W. *Inorg. Chem.* **1989**, *28*, 2904.
(657) Haushalter, R. C.; Lai, F. W. *Angew. Chem., Int. Ed.* **1989**, *28*, 743.
(658) Corcoran, E. W. *Inorg. Chem.* **1990**, *29*, 157.
(659) Mundi, L. A.; Haushalter, R. C. *Inorg. Chem.* **1990**, *29*, 2879.
(660) Mundi, L. A.; Strohmaier, K. G.; Goshorn, D. P.; Haushalter, R. C. *J. Am. Chem. Soc.* **1990**, *112*, 8182.
(661) Mundi, L. A.; Strohmaier, K. G.; Haushalter, R. C. *Inorg. Chem.* **1991**, *30*, 153.
(662) King, H. E.; Mundi, L. A.; Strohmaier, K. G.; Haushalter, R. C. *J. Solid State Chem.* **1991**, *92*, 1.
(663) King, H. E.; Mundi, L. A.; Strohmaier, K. G.; Haushalter, R. C. *J. Solid State Chem.* **1991**, *92*, 154.
(664) Mundi, L. A.; Haushalter, R. C. *J. Am. Chem. Soc.* **1991**, *113*, 6340.
(665) Lee, M.-Y.; Wang, S.-L. *Chem. Mater.* **1999**, *11*, 3588.
(666) Haushalter, R. C.; Mundi, L. A. *Chem. Mater.* **1992**, *4*, 31.
(667) Costentin, G.; Leclaire, A.; Borel, M. M.; Grandin, A.; Raveau, B. *Rev. Inorg. Chem.* **1993**, *13*, 77.
(668) Pope, M. T.; Müller, A. *Angew. Chem., Int. Ed.* **1991**, *30*, 34.
(669) Bino, A.; Cotton., F. A. *Angew. Chem., Int. Ed.* **1971**, *18*, 462.
(670) Centi, G.; Trifiro, F.; Ebner, J. R.; Framchett, V. M. *Chem. Rev.* **1988**, *88*, 55.
(671) Lii, K. H. *J. Chin. Chem. Soc.* **1992**, *39*, 569.
(672) Johnson, J. W.; Jacobson, A. J.; Brody, J. F.; Rich, S. M. *Inorg. Chem.* **1982**, *21*, 3820. Johnson, J. W.; Jacobson, A. J. *Angew. Chem., Int. Ed.* **1985**, *22*, 412.
(673) Boudin, S.; Guesdon, A.; Leclaire, A.; Borel, M. M. *Int. J. Inorg. Mater.* **2000**, *2*, 561.
(674) Soghomonian, V.; Chen, Q.; Haushalter, R. C.; Zubieta, J.; O'Connor, C. J. *Science* **1993**, *259*, 1596.
(675) Soghomonian, V.; Chen., Q.; Haushalter, R. C.; Zubieta, J. *Angew. Chem., Int. Ed.* **1993**, *32*, 610.
(676) Soghomonian, V.; Chen, Q.; Haushalter, R. C.; Zubeita, J. *Chem. Mater.* **1993**, *5*, 1595.
(677) Soghomonian, V.; Chen, Q.; Haushalter, R. C.; Zubieta, J.; O'Connor, C. J.; Lee, Y.-S. *Chem. Mater.* **1993**, *5*, 1690.
(678) Soghomonian, V.; Haushalter, R. C.; Chen, Q.; Zubieta, J. *Inorg. Chem.* **1994**, *33*, 1700.
(679) Riou, D.; Férey, G. *Eur. J. Solid State Inorg. Chem.* **1994**, *31*, 25.
(680) Loiseau, T.; Ferey, G. *J. Solid State Chem.* **1994**, *111*, 416.
(681) Riou, D.; Férey, G. *J. Solid State Chem.* **1994**, *111*, 422.
(682) Bu, X.; Feng, P.; Stucky, G. D. *J. Chem. Soc., Chem. Commun.* **1995**, 1337.
(683) Soghomonian, V.; Chen, Q.; Zhang, Y.; Haushalter, R. C.; O'Connor, C. J.; Tao, C.; Zubieta, J. *Inorg. Chem.* **1995**, *34*, 3509.
(684) Khan, M. I.; Haushalter, R. C.; O'Connor, C. J.; Tao, C.; Zubieta, J. *Chem. Mater.* **1995**, *7*, 593.
(685) Zhang, Y.; Clearfield, A.; Haushalter, R. C. *Chem. Mater.* **1995**, *7*, 1221.
(686) Harrison, W. T. A.; Hsu, K.; Jacobson, A. J. *Chem. Mater.* **1995**, *7*, 2004.
(687) Khan, M. I.; Meyer, M. L.; Haushalter, R. C.; Schweitzer, A. L.; Zubieta, J.; Dye, J. L. *Chem. Mater.* **1996**, *8*, 43.
(688) Soghomonian, V.; Haushalter, R. C.; Zubieta, J.; O'Connor, C. J. *Inorg. Chem.* **1996**, *35*, 2826.
(689) Riou, D.; Taulelle, F.; Férey, G. *Inorg. Chem.* **1996**, *35*, 6392.
(690) Bonavia, G.; Haushalter, R. C.; Zubieta, J. *J. Solid State Chem.* **1996**, *126*, 292.
(691) Zhang, Y.; Warren, C. J.; Clearfield, A.; Haushalter, R. C. *Polyhedron* **1998**, *17*, 2575.
(692) Lu, Y.; Haushalter, R. C.; Zubieta, J. *Inorg. Chim. Acta* **1998**, *268*, 257.
(693) Bircsak, Z.; Harrison, W. T. A. *Inorg. Chem.* **1998**, *37*, 3204.

(694) Cavellec, M. R.; Serre, C.; Férey, G. *C. R. Acad. Sci. Paris, Ser. IIc. Chim.* **1999**, *2*, 147.
(695) Bircsak, Z.; Hall, A. K.; Harrison, W. T. A. *J. Solid State Chem.* **1999**, *142*, 168.
(696) Do, J.; Bontchev, R. P.; Jacobson, A. J. *Inorg. Chem.* **2000**, *39*, 3230.
(697) Do, J.; Bontchev, R. P.; Jacobson, A. J. *J. Solid State Chem.* **2000**, *154*, 514.
(698) Shpeizer, B. G.; Ouyang, X.; Heising, J. M.; Clearfield, A. *Chem. Mater.* **2001**, *13*, 2288.
(699) Sharma, S.; Ramanan, A.; Vittal, J. J. *Proc. Indian Acad. Sci. (Chem. Sci.)* **2001**, *113*, 621.
(700) Finn, R. C.; Zubieta, J. *Solid State Sci.* **2002**, *4*, 845.
(701) Alda, E.; Fernandez, S.; Mesa, J. L.; Pizzaro, J. L.; Jubera, V.; Rojo, T. *Mater. Res. Bull.* **2002**, *37*, 2355.
(702) Zima, V.; Lii, K.-H. *J. Solid State Chem.* **2003**, *172*, 424.
(703) Almeida Paz, F. A.; Shi, F.-N.; Trindad, T.; Rocha, J.; Klinowski, J. *Acta Crystallogr.* **2003**, *E59*, m179.
(704) Dahlman, B. *Arch. Mineral. Geol.* **1952**, *1*, 339. Fleck, M.; Kolitsch, U.; Hertweck, B. *Z. Krystallogr.* **2002**, *317*, 435. Fleck, M.; Kolitsch, U. *Z. Krystallogr.* **2003**, *218*, 553.
(705) Jordan, B.; Calvo, C. *Can J. Chem.* **1973**, *51*, 2621. Tietze, H. R. *Aust. J. Chem.* **1981**, *34*, 2035.
(706) Moore, P. B. *Am. Mineral.* **1970**, *55*, 135. Gleitzer, C. *Eur. J. Solid State Inorg. Chem.* **1991**, *28*, 77, and references therein.
(707) Lii, K. H. *J. Chem. Soc., Dalton Trans.* **1996**, 819, and references therein.
(708) Cavellec, M,; Riou, D.; Férey, G. *Acta Crystallogr.* **1994**, *C50*, 1379.
(709) Cavellec, M.; Riou, D.; Férey, G. *J. Solid State Chem.* **1994**, *112*, 441.
(710) Cavellec, M.; Riou, D.; Férey, G. *Eur. J. Solid State Inorg. Chem.* **1995**, *32*, 271.
(711) Cavellec, M.; Riou, D.; Férey, G. *Acta Crystallogr.* **1995**, *C51*, 2242.
(712) DeBord, J. R. D.; Reiff, W. M.; Haushalter, R. C.; Zubieta, J. *J. Solid State Chem.* **1996**, *125*, 186.
(713) Cavellec, M.; Riou, D.; Ninclaus, C.; Grenèche, J. M.; Férey, G. *Zeolites* **1996**, *17*, 250.
(714) Cavellec, M.; Riou, D.; Grenèche, J. M.; Férey, G. *Mater. Res. Soc. Symp. Proc.* **1996**, *57*, 431.
(715) Cavellec, M.; Riou, D.; Grenèche, J. M.; Férey, G. *J. Magn. Magn. Mater.* **1996**, *163*, 173.
(716) Cavellec, M.; Riou, D.; Grenèche, J. M.; Férey, G. *Inorg. Chem.* **1997**, *36*, 2187.
(717) Cavellec, M.; Grenèche, J. M.; Riou, D.; Férey, G. *Microporous Mater.* **1997**, *8*, 103.
(718) Lii, K.-H.; Huang, Y.-F. *J. Chem. Soc., Dalton Trans.* **1997**, 2221.
(719) Lii, K.-H.; Huang, Y.-F. *Chem. Commun.* **1997**, 839.
(720) Lii, K.-H.; Huang, Y.-F. *Chem. Commun.* **1997**, 1311.
(721) Cavellec, M.; Férey, G.; Grenèche, J. M. *J. Magn. Magn. Mater.* **1997**, *167*, 57.
(722) Cavellec, M.; Férey, G.; Grenèche, J. M. *J. Magn. Magn. Mater.* **1997**, *174*, 109.
(723) DeBord, J. R. D.; Reiff, W. M.; Warren, C. J.; Haushalter, R. C.; Zubieta, J. *Chem. Mater.* **1997**, *9*, 1994.
(724) Cavellec, M.; Egger, C.; Linaus, J.; Nogues, M.; Varret, F.; Férey, G. *J. Solid State Chem.* **1997**, *134*, 349.
(725) Cavellec, M.; Grenèche, J. M.; Férey, G. *Microporous Mesoporous Mater.* **1998**, *20*, 45.
(726) Huang, C.-Y.; Wang, S.-L.; Lii, K.-H. *J. Porous Mater.* **1998**, *5*, 147.
(727) Zima, V.; Lii, K.-H. *J. Solid State Chem.* **1998**, *139*, 326.
(728) Zima, V.; Lii, K.-H.; Nguyen, N.; Ducouret, A. *Chem. Mater.* **1998**, *10*, 1914.
(729) Zima, V.; Lii, K.-H. *J. Chem. Soc., Dalton Trans.* **1998**, 4109.
(730) Lethbridge, Z. A. D.; Lightfoot, P.; Morris, R. E.; Wragg, D. S.; Wright, P. A *J. Solid State Chem.* **1999**, *142*, 455.
(731) Mgaidi, A.; Boughzala, H.; Driss, A.; Clerac, R.; Coulon, C. *J. Solid State Chem.* **1999**, *144*, 163.
(732) Choudhury, A.; Natarajan, S. *Int. J. Inorg. Mater.* **2000**, *2*, 217.
(733) Choudhury, A. *Proc. Indian Acad. Sci. (Chem. Sci.)* **2002**, *114*, 93.
(734) Cowley, A. R.; Chippindale, A. M. *J. Chem. Soc., Dalton. Trans.* **2000**, 3425.
(735) Choudhury, A.; Natarajan, S. *J. Solid State Chem.* **2000**, *154*, 507.
(736) Mahesh, S.; Green, M. A.; Natarajan, S. *J. Solid State Chem.* **2002**, *165*, 334.
(737) Mandal, S.; Natarajan, S.; Grenèche, J. M.; Cavellec, M. R.; Férey, G. *Chem. Mater.* **2002**, *14*, 3751.
(738) Mandal, S.; Natarajan, S.; Klein, W.; Panthöfer, M.; Jansen, M. *J. Solid State Chem.* **2003**, *173*, 367.
(739) Shandi, K.-A.; Winkler, H.; Wu, B.; Janiak, C. *CrystEngComm.* **2003**, *5*, 180.
(740) Shandi, K.-A.; Winkler, H.; Gerdan, M.; Emmerling, F.; Wu, B.; Janiak, C. *Dalton. Trans.* **2003**, 2815.
(741) Mandal, S.; Pati, S. K.; Green, M. A.; Wang, S.-L.; Natarajan, S. *Z. Anorg. Allg. Chem.* **2003**, *629*, 2549.
(742) Song, Y.; Zavalij, P. Y.; Chernova, N. A.; Suzuki, M.; Whittingham, M. S. *J. Solid State Chem.* **2003**, *175*, 63.
(743) Mandal, S.; Green, M. A.; Natarajan, S. *J. Solid State Chem.* **2004**, *177*, 1117.
(744) Lii, K.-H.; Huang, Y.-F.; Zima, V.; Huang, C.-Y.; Lin, H.-M.; Jiang, Y.-C.; Liao, F.-L.; Wang, S.-L. *Chem. Mater.* **1998**, *10*, 2599.
(745) Cavellec, M. R.; Riou, D.; Férey, G. *Inorg. Chim. Acta* **1999**, *291*, 317.
(746) Cotton, F. A.; Wilkinson, G. *Advanced Inorganic Chemistry*; 3rd Ed.;Interscience Publishers, John Wiley and Sons, Inc.: New York, 1972.
(747) Feng, P.; Bu, X.; Stucky, G. D. *Nature* **1997**, *388*, 735.
(748) Bu, X.; Feng, P.; Stucky, G. D. *Science* **1997**, *378*, 2080.
(749) Sankar, G.; Raja, R.; Thomas, J. M. *Catal. Lett.* **1998**, *55*, 15.
(750) Chen, J.; Jones, R. H.; Natarajan, S.; Hursthouse, M. B.; Thomas, J. M. *Angew. Chem., Int. Ed.* **1994**, *33*, 639.
(751) DeBord, J. R. D.; Haushalter, R. C.; Zubieta, J. *J. Solid State Chem.* **1996**, *125*, 270.
(752) Feng, P.; Bu, X.; Tolbert, S. H.; Stucky, G. D. *J. Am. Chem. Soc.* **1997**, *119*, 2497.
(753) Cowley, A. R.; Chippindale, A. M. *J. Chem. Soc., Dalton Trans.* **1999**, 2147.
(754) Yuan, H.-M.; Chen, J.-S.; Zhu, G.-S.; Li, J.-Y.; Yu, J.-H.; Yang, G.-D.; Xu, R. *Inorg. Chem.* **2000**, *39*, 1476.
(755) Choudhury, A.; Neeraj, S.; Natarajan, S.; Rao, C. N. R. *Angew. Chem., Int. Ed.* **2000**, *39*, 3091.
(756) Chiang, R. K. *Inorg. Chem.* **2000**, *39*, 4985.
(757) Chiang, R. K. *J. Solid State Chem.* **2000**, *153*, 180.
(758) Choudhury, A.; Natarajan, S.; Rao, C. N. R. *J. Solid State Chem.* **2000**, *155*, 62.
(759) Choudhury, A.; Natarajan, S.; Rao, C. N. R. *J. Chem. Soc., Dalton Trans.* **2000**, 2595.
(760) Chiang, R. K.; Huang, C-C.; Lin, C.-R. *J. Solid State Chem.* **2001**, *156*, 242.
(761) Neeraj, S.; Noy, M. L.; Rao, C. N. R.; Cheetham, A. K. *J. Solid State Chem.* **2002**, *167*, 344.
(762) Clearfield, A. *Comments Inorg. Chem.* **1990**, *10*, 89. Alberty, G.; Casciola, M.; Costantino, U.; Vivani, R. *Adv. Mater.* **1996**, *8*, 291.
(763) Alberty, G. In *Comprehensive Supramolecular Chemistry*; Alberty, G., Bein, T., Eds.; Pergamon Press: Oxford, U.K., 1996; Vol. 7, Chapter 5. Clearfield, A.; Costantino, V. In *Comprehensive Supramolecular Chemistry*; Alberty, G., Bein, T., Eds.; Pergamon Press: Oxford, U.K., 1996; Vol. 7, Chapter 4. Clearfield, A. *Prog. Inorg. Chem.* **1998**, *47*, 374.
(764) Poojary, D. M.; Zhang, B.; Clearfield, A. *J. Chem. Soc., Dalton Trans.* **1994**, 2453.
(765) Xu, J.-N.; Zhao, Y.-E.; Chen, J.-S.; Song, T.-Y.; Xu, R. *Chem. Res. Chin. Univ.* **1996**, *12*, 108. Hursthouse, M. B.; Malik, K. M.; Thomas, J. M.; Chen, J.; Xu, J.; Song, T.; Xu; R., *Russ Chem. Bull.* **1994**, *43*, 1787.
(766) Kemnitz, E.; Wloka, M.; Trojanov, S. I.; Stiewe, A. *Angew. Chem., Int. Ed.* **1996**, *35*, 2677.
(767) Wloka, M.; Trojanov, S. I.; Kemnitz, E. *J. Solid State Chem.* **1998**, *135*, 293.
(768) Sung, H. H-Y.; Yu, J.; Williams, I. D. *J. Solid State Chem.* **1998**, *140*, 46.
(769) Wloka, M.; Trojanov, S. I.; Kemnitz, E. *Z. Anorg. Allg. Chem.* **1999**, *625*, 1028.
(770) Wloka, M.; Trojanov, S. I.; Kemnitz, E. *J. Solid State Chem.* **2000**, *149*, 21.
(771) Wang, D.; Yu, R.; Kumada, N.; Kinomura, N. *Chem. Mater.* **2000**, *12*, 956.
(772) Serre, C.; Taulelle, F.; Férey, G. *Solid State Sci.* **2001**, *3*, 623.
(773) Wloka, M.; Trojanov, S. I.; Kemnitz, E. *Solid State Sci.* **2002**, *4*, 1377.
(774) Wang, D.; Yu, R.; Takei, T.; Kumada, N.; Kinomura, N. *Chem. Lett.* **2002**, *31*, 398.
(775) Wang, D.; Yu, R.; Kumada, N.; Kinomura, N. *Chem. Lett.* **2002**, *31*, 804.
(776) Gatta, G. D.; Masci, S.; Vivani, R. *J. Mater. Chem.* **2003**, *13*, 1215.
(777) Hawthorne, F. C.; Krivovichev, S. V.; Burns, P. C. *Rev. Mineral. Geochem.* **2000**, *40*, 1.
(778) Hawthorne, F. C. *Acta Crystallogr.* **1994**, *B50*, 481.
(779) Troup, J. M.; Clearfield, A. *Inorg. Chem.* **1977**, *16*, 3311.
(780) Poojary, D. M.; Shpeizer, B.; Clearfield, A. *J. Chem. Soc., Dalton Trans.* **1995**, 111. Poojary, D. M.; Zhang, B.; Dong, Y.; Peng, G.; Clearfield, A *J. Phys. Chem.* **1994**, *98*, 13616.
(781) Clearfield, A.; Stynes, J. A. *J. Inorg. Nucl. Chem.* **1964**, *26*, 117.
(782) Allulli, S.; Ferragina, C.; LaGinestra, A.; Massucci, M. A.; Tomassini, N. *J. Inorg. Nucl. Chem.* **1977**, *39*, 1043. Christensen,

A. N.; Andersen, E. K.; Andersen, I. G. K.; Alberti, G.; Neilson, M.; Lehmann, M. S. *Acta Chem. Scand.* **1990**, *44*, 865.
(783) Clearfield, A. *Annu. Rev. Mater. Sci.* **1984**, *14*, 205.
(784) Stucky, G. D.; Phillips, M. L. F.; Gier, T. E. *Chem. Mater.* **1989**, *1*, 492.
(785) Reddy, J. S.; Kumar, R.; Ratnaswamy, P. *Appl. Catal.* **1990**, *58*, 1. Reddy, J. S.; Khire, U. R.; Ratnaswamy, P.; Mitra, R. B. *J. Chem. Soc., Chem. Commun.* **1992**, 1234.
(786) Bhaumik, A.; Inagaki, S. *J. Am. Chem. Soc.* **2001**, *123*, 691.
(787) Poojary, D. M.; Bortun, A. I.; Bortun, L. N.; Clearfield, A. *J. Solid State Chem.* **1997**, *132*, 213.
(788) Ekambaram, S.; Sevov, S. C. *Angew. Chem., Int. Ed.* **1999**, *38*, 372.
(789) Serre, C.; Férey, G. *J. Mater. Chem.* **1999**, *9*, 579.
(790) Serre, C.; Férey, G. *C. R. Acad. Sci. Paris, Ser. II* **1999**, *2*, 85.
(791) Serre, C.; Guillou, N.; Férey, G. *J. Mater. Chem.* **1999**, *9*, 1185.
(792) Zhao, Y.; Zhu, G.; Jiao, X.; Liu, W.; Pang, W. *J. Mater. Chem.* **2000**, *10*, 463.
(793) Kongshaug, K. O.; Fjellvåg, H.; Lillerud, K. P. *J. Chem. Soc., Dalton Trans.* **2000**, 551.
(794) Ekambaram, S.; Serre, C.; Férey, G.; Sevov, S. C. *Chem. Mater.* **2000**, *12*, 444.
(795) Guo, Y.; Shi, Z.; Yu, J.; Wang, J.; Liu, Y.; Bai, N.; Pang, W. *Chem. Mater.* **2001**, *13*, 203.
(796) Guo, Y. H.; Shi, Z.; Hong, D.; Wei, Y. B.; Pang, W. Q. *Chin. Chem. Lett.* **2001**, *12*, 373.
(797) Liu, Y.; Shi, Z.; Zhang, L.; Fu, Y.; Chen, J.; Li, B.; Hua, J.; Pang, W. *Chem. Mater.* **2001**, *13*, 2017.
(798) Fu, Y.; Liu, Y.; Shi, Z.; Zou, Y.; Pang, W. *J. Solid State Chem.* **2001**, *162*, 96.
(799) Serre, C.; Taulelle, F.; Férey, G. *Chem. Mater.* **2002**, *14*, 998.
(800) Liu, Y.; Shi, Z.; Fu, Y.; Chen, W.; Li, B.; Hua, J.; Liu, W.; Deng, F.; Pang, W. *Chem. Mater.* **2002**, *14*, 1555.
(801) Serre, C.; Taulelle, F.; Férey, G. *Chem. Commun.* **2003**, 2755.
(802) Guillou, N.; Gao, Q.; Nogues, M.; Morris, R. E.; Hervieu, M.; Férey, G.; Cheetham, A. K. *C. R. Acad. Sci Paris* **1999**, *2*, 387.
(803) Guillou, N.; Gao, Q.; Forster, P. M.; Chang, J.-S.; Nogues, M.; Park, S.-E.; Férey, G.; Cheetham, A. K. *Angew. Chem., Int. Ed.* **2001**, *40*, 2831.
(804) Escobal, J.; Pizaro, J. L.; Mesh, J. L.; Lezama, L.; Olazcuaga, R.; Arriortua, M. L.; Rojo, T. *Chem. Mater.* **2000**, *12*, 376.
(805) Kongshaug, K. O.; Fjellvåg, H.; Lillerud, K.P. *J. Solid State Chem.* **2001**, *156*, 32.
(806) Chippindale, A. M.; Gaslain, F. O. M.; Cowley, A. R.; Powell, A. V. *J. Mater. Chem.* **2001**, *11*, 3172.
(807) Stief, R.; Massa, W. *Z. Anorg. Allg. Chem.* **2002**, *628*, 1685.
(808) Stief, R.; Massa, W.; Pebler, J. *Z. Anorg. Allg. Chem.* **2002**, *628*, 2631.
(809) Neeraj, S.; Noy, M. L.; Cheetham, A. K. *Solid State Sci.* **2002**, *4*, 397.
(810) Song, Y.; Zavalij, P. Y.; Chernova, N. A.; Whittingham, M. S. *Chem. Mater.* **2003**, *15*, 4968.
(811) Thoma, S. G.; Bonhomme, F.; Cygan, R. T. *Chem. Mater.* **2004**, *16*, 2068.
(812) Steif, R.; Massa, W. *Z. Anorg. Allg. Chem.* **2004**, *630*, 1459.
(813) Riou, D.; Fayon, F.; Massiot, D. *Chem. Mater.* **2002**, *14*, 2416.
(814) Bull, I.; Young, V.; Teat, S. J.; Peng, L.; Grey, C. P.; Parise, J. B. *Chem. Mater.* **2003**, *15*, 3818.
(815) Wang, X.; Liu, L.; Jacobson, A. J. *J. Solid State Chem.* **2004**, *177*, 194.
(816) Neeraj, S.; Loiseau, T.; Rao, C. N. R.; Cheetham, A. K. *Solid State Sci.* **2004**, *6*, 1169.
(817) Suib, S. L. *Curr. Opin. Solid State Mater. Sci.* **1998**, *3*, 623.
(818) Francis, R. J.; Drewitt, M. J.; Halasyamani, P. S.; Ranganathachar, C.; O'Hare, D.; Clegg, W.; Teat, S. J. *Chem. Commun.* **1998**, 279.
(819) Danis, J. A.; Hawkins, H. T.; Scott, B. L.; Runde, W. H.; Schutz, B. E.; Eichhorn, B. W. *Polyhedron* **2000**, *19*, 1551.
(820) Danis, J. A.; Runde, W. H.; Scott, B.; Fattinger, J.; Eichhorn, B. *Chem. Commun.* **2001**, 2378.
(821) Doran, M. B.; Stuart, C. L.; Norquist, A. J.; O'Hare, D. *Chem. Mater.* **2004**, *16*, 565.
(822) Locock, A. J.; Burns, P. C. *J. Solid State Chem.* **2004**, *177*, 2675.
(823) Yu, R.; Wang, D.; Ishiwata, S.; Saito, T.; Azuma, M.; Takano, M.; Chen., Y.; Li, J. *Chem. Lett.* **2004**, *33*, 458.
(824) Lok, B. M.; Messina, C. A.; Patton, R. L.; Gajek, R. T.; Cannan, T. R.; Flanigen, E. M. *J. Am. Chem. Soc.* **1984**, *106*, 6092.
(825) Flanigen, E. M.; Lok, B. M.; Patton, R. L.; Wilson, S. T. In *New Developments in Zeolite Science and Technology, Proceedings of the 7th International Zeolite Conference, Tokyo, 1986*; Murakami, Y., Iijima, A., Ward, J. W., Eds.; Kodansha Ltd.: Tokyo; Elsevier science publishers: Amsterdam, 1986; p 103.
(826) Flanigen, E. M.; Patton, R. L.; Wilson, S. T. In *Innovation in Zeolite Materials Science*; Grobet, P. J., Mortier, W. J., Vansant, E. F., Schulz-Ekloff, G., Eds.; Studies in Surface Science and Catalysis; Elsevier: Amsterdam, 1988; Vol. 37, p 13.
(827) Hartmann, M.; Kevan, L. *Chem. Rev.* **1999**, *99*, 635.
(828) Bennett, J. M.; Cohen, J. P.; Flanigen, E. M.; Pluth, J. J.; Smith, J. V. *ACS Symp. Ser.* **1993**, *218*, 109.
(829) Wright, P. A.; Jones, R. H.; Natarajan, S.; Bell, R. G.; Chen, J.; Hursthouse, M. B.; Thomas, J. M. *J. Chem. Soc., Chem. Commun.* **1993**, 633.
(830) Meyer, L. M.; Haushalter, R. C. *Chem. Mater.* **1994**, *6*, 349.
(831) Meyer, L. M.; Haushalter, R. C.; Zubieta, J. *J. Solid State Chem.* **1996**, *125*, 200.
(832) Noble, G. W.; Wright, P. A.; Lightfoot, P.; Morris, R. E.; Hudson, K. J.; Kvick, Å; Graafsma, H. *Angew. Chem., Int. Ed.* **1997**, *36*, 81.
(833) Nobel, G. W.; Wright, P. A.; Kvick, Å *J. Chem. Soc., Dalton Trans.* **1997**, 4485.
(834) Bontchev, R. P.; Sevov, S. C. *Chem. Mater.* **1997**, *9*, 3155.
(835) Panz, C.; Polborn, K.; Behrens, P. *Inorg. Chim. Acta* **1998**, *269*, 173.
(836) Bu, X.; Feng, P.; Gier, T. E.; Stucky, G. D. *J. Solid State Chem.* **1998**, *136*, 210.
(837) Feng, P.; Bu, X.; Gier, T. E.; Stucky, G. D. *Microporous Mesoporous Mater.* **1998**, *23*, 221.
(838) Feng, P.; Bu, X.; Stucky, G. D. *Microporous Mesoporous Mater.* **1998**, *23*, 315.
(839) González, G.; Piña, C.; Jacas, A.; Hernández, M.; Leyva, A. *Microporous Mesoporous Mater.* **1998**, *25*, 103.
(840) Bu, X.; Feng, P.; Gier, T. E.; Stucky, G. D. *Microporous Mesoporous Mater.* **1998**, *25*, 109.
(841) Bu, X.; Gier, T. E.; Feng, P.; Stucky, G. D. *Chem. Mater.* **1998**, *10*, 2546.
(842) Muncaster, G.; Sankar, G.; Catlow, C. R. A.; Thomas, J. M.; Bell, R. G.; Wright, P. A.; Coles, S.; Teat, S. J.; Clegg, W.; Reeve, W *Chem. Mater.* **1999**, *11*, 158.
(843) Christensen, A. M.; Hazell, R. G. *Acta Chim. Scand.* **1999**, *53*, 403.
(844) Xu, Y.-H.; Yu, Z.; Chen, X.-F.; Liu, S.-H.; You, X.-Z. *J. Solid State Chem.* **1999**, *146*, 157.
(845) Patince, V.; Wright, P. A.; Aitken, R. A.; Lightfoot, P.; Purdie, S. D. J.; Cox, P. A.; Kvick, Å.; Vaugham, G. *Chem. Mater.* **1999**, *11*, 2456.
(846) Bontchev, R. P.; Sevov, S. C. *J. Mater. Chem.* **1999**, *9*, 2678.
(847) Patince, V.; Wright, P. A.; Lightfoot, P.; Aitken, R. A.; Cox, P. A. *J. Chem. Soc., Dalton Trans.* **1999**, 3909.
(848) Wright, P. A.; Maple, M. J.; Slawin, A. M. Z.; Patince, V.; Aitken, R. A.; Welsh, S.; Cox, P. A. *J. Chem. Soc., Dalton Trans.* **2000**, 1243.
(849) Wei, B.; Yu, J.; Shi, Z.; Qiu, S.; Yan, W.; Terasaki, O. *Chem. Mater.* **2000**, *12*, 2065.
(850) Fan, W.; Schoonheydt, R. A.; Weckhuysen, B. M. *Chem. Commun.* **2000**, 2249.
(851) Barrent, P. A.; Jones, R. H. *Phys. Chem. Chem. Phys.* **2000**, *2*, 407.
(852) Maple, M. J.; Philp, E. F.; Slawin, A. M. Z.; Lightfoot, P.; Cox, P. A.; Wright, P. W *J. Mater. Chem.* **2001**, *11*, 98.
(853) Kongshaug, K. O.; Fjellvåg, H.; Lillerud, K. P. *J. Mater. Chem.* **2001**, *11*, 1242.
(854) Garcia, R.; Philp, E. F.; Slawin, A. M. Z.; Wright, P. A.; Cox, P. A. *J. Mater. Chem.* **2001**, *11*, 1421.
(855) Beitone, L.; Huguenard, C.; Gansmüller, A.; Henry, M.; Taulelle, F.; Loiseau, T.; Férey, G. *J. Am. Chem. Soc.* **2003**, *125*, 9102.
(856) Beitone, L.; Loiseau, T.; Millange, F.; Huguenard, C.; Fink, G.; Taulelle, F.; Grenèche, J.-M.; Férey, G. *Chem. Mater.* **2003**, *15*, 4590.
(857) Shi, L.; Li, J.; Yu, J.; Li, Y.; Ding, H.; Xu, R. *Inorg. Chem.* **2004**, *43*, 2703.
(858) Chippindale, A. M.; Walton, R. I. *J. Chem. Soc., Chem. Commun.* **1994**, 2453.
(859) Cowley, A. R.; Chippindale, A. M. *Chem. Commun.* **1996**, 673.
(860) Chippindale, A. M.; Cowley, A. R. *Zeolites* **1997**, *18*, 176.
(861) Chippindale, A. M.; Bond, A. D.; Cowley, A. R.; Powell, A. V. *Chem. Mater.* **1997**, *9*, 2830.
(862) Bond, A. D.; Chippindale, A. M.; Cowley, A. R.; Readman, J. E.; Powell, A. V. *Zeolites* **1997**, *19*, 326.
(863) Bu, X.; Gier, T. E.; Feng, P.; Stucky, G. D. *Microporous Mesoporous Mater.* **1998**, *20*, 371.
(864) Chippindale, A. M.; Cowley, A. R. *Microporous Mesoporous Mater.* **1998**, *21*, 271.
(865) Chippindale, A. M.; Cowley, A. R.; Peacock, K. J. *Microporous Mesoporous Mater.* **1998**, *24*, 133.
(866) Cowley, A. R.; Chippindale, A. M. *Microporous Mesoporous Mater.* **1999**, *28*, 163.
(867) Hsu, K.-F.; Wang, S.-L. *Chem. Commun.* **2001**, 135.
(868) Hsu, K.-F.; Wang, S.-L. *Inorg. Chem.* **2000**, *39*, 1773.
(869) Lin, C.-H.; Wang, S.-L. *Chem. Mater.* **2000**, *12*, 3617.

(870) Chippindale, A. M.; Cowley, A. R. *J. Solid State Chem.* **2001**, *159*, 59.
(871) Lin, C.-H.; Wang, S.-L. *Chem. Mater.* **2002**, *14*, 96.
(872) Cowley, A. R.; Jones, R. H.; Teat, S. J.; Chippindale, A. M. *Microporous Mesoporous Mater.* **2002**, *51*, 51.
(873) Lin, C.-H.; Wang, S.-L. *Inorg. Chem.* **2005**, *44*, 251.
(874) Shvareva, T. Y.; Sullens, T. A.; Shehee, T. C.; Albrecht-Schmitt, T. E. *Inorg. Chem.* **2005**, *44*, 300.
(875) Logar, N. Z.; Rajić, N.; Kaučič, V.; Golič, L. *J. Chem. Soc., Chem. Commun.* **1995**, 1681.
(876) Rajić, N.; Logar, N. Z.; Kaučič, V. *Zeolites* **1995**, *15*, 672.
(877) Gao, Q.; Chippindale, A. M.; Cowley, A. R.; Chen, J.; Xu, R. *J. Phys. Chem. B* **1997**, *101*, 9940.
(878) Helliwell, M.; Helliwell, J. R.; Kaučič, V.; Logar, N. Z.; Barba, L.; Busetto, E.; Lausi, A. *Acta Crystallogr.* **1999**, *B55*, 327.
(879) Liu, Y.; Na, L.; Zhu, G.; Xiao, F.-S.; Pang, W.; Xu, R. *J. Solid State Chem.* **2000**, *149*, 107.
(880) Christensen, A. N.; Bareges, A.; Nielsen, R. B.; Hazell, R. G.; Norby, P.; Hanson, J. C. *J. Chem. Soc., Dalton Trans.* **2001**, 1611.
(881) Ke, Y.; He, G.; Li, J.; Zhang, Y.; Lu, S. *New J. Chem.* **2001**, *25*, 1627.
(882) Zhao, Y.; Ju, J.; Chen, X.; Li, X.; Wang, Y.; Wang, R.; Li, N.; Mai, Z. *J. Solid State Chem.* **2002**, *166*, 369.
(883) Chen, X.; Zhao, Y.; Wang, R.; Li, M.; Mai, Z. *J. Chem. Soc., Dalton Trans.* **2002**, 3092.
(884) Ke, Y.; He, G.; Li, J.; Zhang, Y.; Lu, S.; Lee, Z. *Cryst. Res. Technol.* **2002**, *37*, 803.
(885) Chen, W.; Zhao, Y.; Kwon, Y.-U. *Chem. Lett.* **2004**, *33*, 1616.
(886) Mundi, L. A.; Haushalter, R. C. *Inorg. Chem* **1992**, *31*, 3050.
(887) Mundi, L. A.; Haushalter, R. C. *Inorg. Chem* **1993**, *32*, 1579.
(888) Lightfoot, P.; Mason, D. *Mater. Res. Bull* **1995**, *30*, 1005.
(889) Lu, J. J.; Xu, Y.; Goh, N. K.; Chia, L. A. *Chem. Commun.* **1998**, 1709.
(890) Leclaire, A.; Guesdon, A.; Berrah, F.; Borel, M. M.; Raveau, B. *J. Solid State Chem.* **1999**, *145*, 291.
(891) Xu, L.; Sun, Y.; Wang, E.; Shen, E.; Liu, Z.; Hu, C. *J. Solid State Chem.* **1999**, *146*, 533.
(892) Yan, B.; Goh, N. K.; Chia, L. S.; Stucky, G. D. *J. Mater. Chem.* **2004**, *14*, 1567.
(893) Roca, M.; Marcos, M. D.; Amoòs, P.; Porter, A. B.; Edwards, A. J.; Porter, D. B. *Inorg. Chem.* **1996**, *35*, 5613.
(894) Cavellec, M. R.; Grenèche, J.-M.; Férey, G. *J. Solid State Chem.* **1999**, *148*, 150.
(895) Zhang, H.; Weng, L.; Zhou, Y.; Chen., Z.; Sun, J.; Zhao, B. *J. Mater. Chem.* **2002**, *12*, 658.
(896) Sun, Z.-G.; Liu, Z.-M.; Xu, L.; Wang, Y.; He, Y.-L. *Catal. Today* **2004**, *93*−*95*, 639.
(897) Zhung, S. H.; Chang, J.-S.; Yoon, J. W.; Grenèche, J.-M.; Férey, G.; Cheetham, A. K. *Chem. Mater.* **2004**, *16*, 5552.
(898) Wang, X.; Liu, L.; Chen, H.; Ross, K.; Jacobson, A. J. *J. Mater. Chem.* **2000**, *10*, 1203.
(899) Shafer, E. C.; Shafer, M. W.; Roy, R. *Z. Kristallogr.* **1956**, *107*, 263.
(900) Qiu, S.; Tian, W.; Pang, W.; Sun, T.; Jiang, D. *Zeolites* **1991**, *11*, 37.
(901) Kniep, R.; Engelhardt, H.; Hauf, C. *Chem. Mater.* **1998**, *10*, 2930.
(902) Yang, G.-Y.; Sevov, S. *Inorg. Chem.* **2001**, *40*, 2214.
(903) Sevov, S. C. *Angew. Chem., Int. Ed.* **1996**, *35*, 2630.
(904) Kniep, R.; Will, H. G.; Boy, I.; Röhr, C. *Angew. Chem., Int. Ed.* **1997**, *36*, 1013.
(905) Warren, C. J.; Haushalter, R. C.; Rose, D. J.; Zubieta, Z. *Chem. Mater.* **1997**, *9*, 2694.
(906) Bontchev, R. P.; Do, J.; Jacobson, A. J. *Inorg. Chem.* **1999**, *38*, 2231.
(907) Bontchev, R. P.; Do, J.; Jacobsonv, A. J. *Angew. Chem., Int. Ed.* **1999**, *38*, 1937.
(908) Kniep, R.; Schäfer, G.; Engelhardt, H.; Boy, I. *Angew. Chem., Int. Ed.* **1999**, *38*, 3642.
(909) Zhao, I.; Zhu, G.; Liu, W.; Zou, Y.; Pang, W. *Chem. Commun.* **1999**, 2219.
(910) Kniep, R.; Schäfer, G. *Z. Anorg. Allg. Chem.* **2000**, *626*, 141.
(911) Do, J.; Zheng, L.-M.; Bontchev, R. P.; Jacobson, A. J. *Solid State Sci.* **2000**, *2*, 343.
(912) Bontchev, R. P.; Do, J.; Jacobson, A. J. *Inorg. Chem.* **2000**, *39*, 3320.
(913) Bontchev, R. P.; Do, J.; Jacobson, A. J. *Inorg. Chem.* **2000**, *39*, 4179.
(914) Zhao, Y.; Shi, Z.; Ding, S.; Bai, N.; Liu, W.; Zou, Y.; Zhu, G.; Zhang, P.; Mai, Z.; Pang, W. *Chem. Mater.* **2000**, *12*, 2550.
(915) Schäfer, G.; Borrmann, H.; Kniep, R. *Microporous Mesoporous Mater.* **2000**, *41*, 161.
(916) Yilmaz, A.; Bu, X.; Kizilyalli, M.; Stucky, G. D. *Chem. Mater.* **2000**, *12*, 3243.
(917) Schäfer, G.; Borrmann, H.; Kniep, R. *Z. Anorg. Allg. Chem.* **2001**, *627*, 61. Bontchev, R. P.; Jacobson, A. J. *Mater. Res. Bull.* **2002**, *37*, 1997.
(918) Kritikos, M.; Wikstad, E.; Walldén, K. *Solid State Sci.* **2001**, *3*, 649.
(919) Boy, I.; Stowasser, F.; Schäfer, G.; Kniep, R *Chem.*—*Eur. J.* **2001**, *7*, 834.
(920) Huang, Y.-X.; Schäfer, G.; Cabrera, W. C.; Cardoso, R.; Schnelle, W.; Zhao, J.-T.; Kniep, R. *Chem. Mater.* **2001**, *13*, 4348.
(921) Schäfer, G.; Cabrera, W. C.; Leoni, S.; Borrmann, H.; Kniep, R. *Z. Anorg. Allg. Chem.* **2002**, *628*, 67.
(922) Dumas, E.; Chouvy, C. D.; Sevov, S. C. *J. Am. Chem. Soc.* **2002**, *124*, 908.
(923) Zhang, H.; Chen, Z.; Weng, L.; Zhou, Y.; Zhao, D. *Microporous Mesoporous Mater.* **2003**, *57*, 309.
(924) Wikstad, E.; Kritikos, N. *Acta Crystallogr.* **2003**, *C59*, M87.
(925) Asnani, M.; Ramanan, A.; Vittal, J. J. *Inorg. Chem. Commun.* **2003**, *6*, 589.
(926) Huang, Y.-X.; Schäfer, G.; Cabrera, W. C.; Borrmann, H.; Gil, R. C.; Kniep, R. *Chem. Mater.* **2003**, *15*, 4930.
(927) Wang, Y.; Yu, J.; Pan, Q.; Do, Y.; Zou, Y.; Xu, R. *Inorg. Chem.* **2004**, *43*, 559.
(928) Li, M.-R.; Liu, W.; Ge, M.-H.; Chen, H.-H.; Yang, X.-X.; Zhao, J.-T. *Chem. Commun.* **2004**, 1272.
(929) Huang, Y.-X.; Schäfer, G.; Borrmann, H.; Zhao, J.-T.; Kniep, R. *Z. Anorg. Allg. Chem.* **2003**, *629*, 3.
(930) Bazán, B.; Mesa, J. L.; Pizarro, J. L.; Lezama, L.; Garitaonandia, J. S.; Arriortua, M. I.; Rojo, T. *Solid State Sci.* **2003**, *5*, 1291.
(931) Bazán, B.; Mesa, J. L.; Pizarro, J. L.; Arriortua, M. I.; Rozzo, *Mater. Res. Bull.* **2003**, *38*, 1193.
(932) Bull, I.; Wheatley, P. S.; Lightfoot, P.; Morris, R. E.; Sastre, E.; Wright, P. A. *Chem. Commun.* **2002**, 1180.
(933) Wang, B.; Yu, R.; Xu, Y.; Feng, S.; Xu, R.; Kumada, N.; Kinomura, N.; Matsumura, Y.; Takano, M. *Chem. Lett.* **2002**, *31*, 1120.
(934) Wang, Y.; Yu, J.; Du, Y.; Shi, Z.; Zou, Y.; Xu, R. *J. Chem. Soc., Dalton Trans.* **2002**, 4060.
(935) Chen, X.; Wang, Y.; Yu, J.; Zou, Y.; Xu, R. *J. Solid State Chem.* **2004**, *177*, 2518.
(936) Armas, S. F.; Mesa, J. L.; Pizarro, J. L.; Garitaonandia, J. S.; Arriortua, M. I.; Rojo, T. *Angew. Chem., Int. Ed.* **2004**, *43*, 977.
(937) Mandal, S.; Pati, S.; Green, M. A.; Natarajan, S. *Chem. Mater.* **2005**, *17*, 638.
(938) Chippindale, A. M. *Chem. Mater.* **2000**, *12*, 818.
(939) Kissick, J. L.; Chippindale, A. M. *Acta Crystallogr.* **2002**, *E58*, M80.
(940) Millange, F.; Walton, R. I.; Guillou, N.; Loiseau, T.; O'Hare, D.; Férey, G. *Chem. Commun.* **2002**, 826.
(941) Millange, F.; Walton, R. I.; Guillou, N.; Loiseau, T.; O'Hare, D.; Férey, G. *Chem. Mater.* **2002**, *14*, 4448.
(942) Choudhury, A.; Krishnamoorthy, J.; Rao, C. N. R. *Chem. Commun.* **2001**, 261. Paul, G.; Choudhury, A.; Rao, C. N. R. *J. Chem. Soc., Dalton Trans.* **2002**, 3859. Louer, D.; Bataille, P. *J. Mater. Chem.* **2002**, *12*, 3487. Doran, M. B.; Cockbain, B. E.; Norquist, A. J.; O'Hare, D. *Dalton Trans.* **2004**, 3810, and references therein.
(943) Harrison, W. T. A.; Phillips, M. L. F.; Stanchfield; J.; Nenoff, T. M. *Inorg. Chem.* **2001**, *40*, 895. Harrison, W. T. A.; Phillips, M. L. F.; Nenoff, T. M. *Int. J. Inorg. Mater.* **2001**, *3*, 1033. Fernandez, S.; Mesa, J. L.; Pizarro, J. L.; Lesama, L.; Arriortua, M. I.; Rojo, T. *Angew. Chem., Int. Ed.* **2002**, *41*, 3683.
(944) Gier, T. E.; Bu, X.; Feng, P.; Stucky, G. D. *Nature* **1998**, *395*, 154. Feng, P.; Zhang, T.; Bu, X. *J. Am. Chem. Soc.* **2001**, *123*, 8608.
(945) Abrahams, B. F.; Hoskins, B. F.; Michail, D. M.; Robson, R. *Nature (London)* **1994**, *369*, 727. Gardner, G. B.; Vankataraman, D.; Moore, J. S.; Lee, S. *Nature (London)* **1995**, *374*, 792.
(946) Yaghi, O. M.; Li, G. M.; Li, H. L. *Nature (London)* **1995**, *378*, 703.
(947) Chui, S. S.-Y.; Lo, S. M.-F.; Charmant, J. P. H.; Orpen, A. G.; Williams, I. D. *Science* **1999**, *283*, 1148. Li, H.; Eddaoudi, M.; O'Keeffe, M.; Yaghi, O. M. *Nature* **1999**, *402*, 276. Eddaoudi, M.; Moler, D. M.; Li, H.; Chen, B.; Reineke, T. M.; O'Keeffe, M.; Yaghi, O. M. *Acc. Chem. Res* **2001**, *34*, 319, and references therein.
(948) Rao, C. N. R.; Natarajan, S.; Vaidhyanathan, R. *Angew. Chem., Int. Ed.* **2004**, *43*, 1466, and references therein.
(949) Tamaki, H.; Zhong, Z.; Matsumoto, N.; Kida, S.; Koykawa, M.; Aihiwa, N.; Hashimoto, Y.; Okawa, H. *J. Am. Chem. Soc.* **1992**, *114*, 6974. Watts, I. D.; Carling; S. G.; Day, P. *J. Chem. Soc., Dalton Trans.* **2002**, 1429, and references therein.
(950) Natarajan, S. *J. Solid State Chem.* **1998**, *139*, 200.
(951) Huang, Y.-F.; Lii, K.-H. *J. Chem Soc., Dalton Trans.* **1998**, 4085.
(952) Lin, H.-M.; Lii, K-H.; Jiang, Y. C.; Wang, S.-L. *Chem. Mater.* **1999**, *11*, 519. Lethbridge, Z.; Lightfoot, P. *J. Solid State Chem.* **1999**, *143*, 58. Choudhury, A.; Natarajan, S.; Rao, C. N. R. *J. Solid State Chem.* **1999**, *146*, 538. Chang, W.-J.; Lin, H.-M.; Lii, K.-H. *J. Solid*

State Chem. **2001**, *157*, 233. Meng, H.; Li, G.-H.; Xing, Y.; Yang, Y.-L.; Cui, Y.-J.; Liu, L.; Ding, H.; Pang, W.-Q. *Polyhedron* **2004**, *23*, 2357.
(953) Choudhury, A.; Natarajan, S. *J. Mater. Chem.* **1999**, *9*, 3113.
(954) Choudhury, A.; Natarajan, S.; Rao, C. N. R. *Chem. Mater.* **1999**, *11*, 2316.
(955) Choudhury, A.; Natarajan, S.; Rao, C. N. R. *Chem.—Eur. J.* **2000**, *6*, 1168.
(956) Jiang, Y.-C.; Wang, S.-L.; Lee, S.-F.; Lii, K.-H. *Inorg. Chem.* **2003**, *42*, 6154.
(957) Jiang, Y.-C.; Wang, S.-L.; Lii, K.-H. *Chem. Mater.* **2003**, *15*, 1633.
(958) Lightfoot, P.; Lethbridge, Z.; Morris, R. E.; Wragg, D. S.; Wright, P. A. *J. Solid State Chem.* **1999**, *143*, 74.
(959) Kedarnath, K.; Choudhury, A.; Natarajan, S. *J. Solid State Chem.* **2000**, *150*, 324.
(960) Rajic, N.; Logar, N. Z.; Mali, G.; Kaučič, V *Chem. Mater.* **2003**, *15*, 1734.
(961) Tsai, Y.-M.; Wang, S.-L.; Huang, C.-H.; Lii, K.-H. *Inorg. Chem.* **1999**, *38*, 4183.
(962) Do, J.; Bontchev, R. P.; Jacobson, A. J. *Chem. Mater.* **2001**, *13*, 2601.
(963) Tang, M.-F.; Lii, K.-H. *J. Solid State Chem.* **2004**, *177*, 1912.
(964) Chen, C.-Y.; Chu, P. P.; Lii, K.-H. *Chem. Commun.* **1999**, 1473. Hung, L.-C.; Kao, H.-M.; Lii, K.-H. *Chem. Mater.* **2000**, *12*, 2411. Choi, C. T. S.; Anokhina, E. V.; Day, C. S.; Zhao, Y.; Taulelle, F.; Huguenard, C.; Gan, Z.; Lachgar, A. *Chem. Mater.* **2002**, *14*, 4096. Loiseau, T.; Férey, G.; Haouas, M.; Taulelle, F. *Chem. Mater.* **2004**, *16*, 5318.
(965) Lii, K.-H.; Chen, C.-Y. *Inorg. Chem.* **2000**, *39*, 3374.
(966) Mark, M.; Kolitsch, U.; Lengauer, C.; Kaučič, V.; Tillmanns, E. *Inorg. Chem.* **2003**, *42*, 598.
(967) Choudhury, A.; Natarajan, S. *Solid State Sci.* **2000**, *2*, 365.
(968) Lethbridge, Z. A. D.; Hillier, A. D.; Cywinski, R.; Lightfoot, P. *J. Chem. Soc., Dalton Trans.* **2000**, 1595. Lethbridge, Z. A. D.; Tiwary, S. K.; Harrison, A.; Lightfoot, P. *J. Chem. Soc., Dalton Trans.* **2001**, 1904. Lethbridge, Z. A. D.; Smith, M. J.; Tiwary, S. K.; Harrison, A.; Lightfoot, P. *Inorg. Chem.* **2004**, *43*, 11.
(969) Neeraj, S.; Natarajan, S.; Rao, C. N. R. *J. Chem. Soc., Dalton Trans.* **2001**, 289.
(970) Ayi, A. A.; Choudhury, A.; Natarajan, S.; Rao, C. N. R. *New J. Chem.* **2001**, *25*, 213. Natarajan, S. *J. Chem. Soc., Dalton Trans.* **2002**, 2088.
(971) Wang, C.-M.; Chuang, S.-T.; Chuang, Y.-L.; Kao, H.-M.; Lii, K.-H. *J. Solid State Chem.* **2004**, *177*, 1252. Wang, C.-M.; Chuang, Y.-L.; Chuang, S.-T.; Lii, K.-H. *J. Solid State Chem.* **2004**, *177*, 2305.
(972) Halasyamani, P. S.; Drewitt, M. J.; O'Hare, D. *Chem. Commun.* **1997**, 867.
(973) Lii, K.-H.; Huang, Y.-F. *Inorg. Chem.* **1999**, *38*, 1348.
(974) Shi, Z.; Feng, S.; Gao, S.; Zhang, L.; Yang, G.; Hua, J. *Angew. Chem., Int. Ed.* **2000**, *39*, 2325.
(975) Tong, M.-L.; Chen, X.-M.; Ng, S. W. *Inorg. Chem. Commun.* **2000**, *3*, 436. Abu-Shandi, K.; Janiak, C.; Kersting, B. *Acta Crystallogr.* **2001**, *B57*, 1261. Liang, Y.-C.; Hong, M.-C.; Cao, R.; Su, W.-P.; Zhao, Y.-J.; Weng, J.-B. *Polyhedron* **2001**, *20*, 2477.
(976) Huang, C.-H.; Huang, L.-H.; Lii, K.-H. *Inorg. Chem.* **2001**, *40*, 2625.
(977) Jiang, Y.-C.; Lai, Y.-C.; Wang, S.-L.; Lii, K.-H. *Inorg. Chem.* **2001**, *40*, 5320.
(978) Huang, L.-H.; Kao, H.-M.; Lii, K.-H. *Inorg. Chem.* **2002**, *41*, 2936.
(979) Hung, L.-I.; Wang, S.-L.; Kao, H.-M.; Lii, K.-H. *Inorg. Chem.* **2002**, *41*, 3929.
(980) Wang, C.-M.; Lii, K.-H. *J. Solid State Chem.* **2003**, *172*, 194.
(981) Chen, C.-Y.; Lii, K.-H.; Jacobson, A. J. *J. Solid State Chem.* **2003**, *172*, 252.
(982) Chang, W.-K.; Chiang, R.-K.; Jiang, Y.-C.; Wang, S.-L.; Lee, S.-F.; Lii, K.-H. *Inorg. Chem.* **2004**, *43*, 2564. Lee, S. F.; Chang, C. R.; Yang, J. S.; Lii, K. H.; Lee, M. D.; Yao, Y. D. *J. Appl. Phys.* **2004**, *95*, 7073.
(983) Finn, R. C.; Zubieta, J. *J. Chem. Soc., Dalton Trans.* **2002**, 856.
(984) Shi, Z.; Feng, S; Zhang, L.; Yang, G.; Huav, J. *Chem. Mater.* **2000**, *12*, 2930. Zhang, X.-M.; Tong, M.-L.v.; Feng, S.-H.; Chen, X.-M. *J. Chem. Soc., Dalton Trans.* **2001**, 2069. Finn, R. C.; Zubieta, J. *J. Phys. Chem. Solids* **2001**, *62*, 1513. Yuan, N.; Li, Y.; Wang, E.; Lu, Y.; Hu, C.; Hu, N.; Jia, H. *J. Chem. Soc., Dalton Trans.* **2002**, 2916.
(985) Burkholder, E.; Golub, V.; O'Connor, C. J.; Zubeita, J. *Inorg. Chem. Commun.* **2004**, *7*, 363.
(986) Koo, B.-K.; Quellette, W.; Burkholder, E. M.; Golub, V.; O'Connor, C. J.; Zubeita, J. *Solid State Sci.* **2004**, *6*, 461.
(987) Kuroda-Sowa, T.; Munakata, M.; Matsuda, H.; Akiyama, S.; Maekawa, M. *J. Chem. Soc., Dalton Trans.* **1995**, 2201.
(988) Helliwell, M.; Gallois, B.; Kariuki, B. M.; Kaučič, V.; Helliwell, J. R. *Acta Crystallogr.* **1993**, *B49*, 420. Meden, A.; McCusker, L. B.; Baerlocher, Ch.; Rajić, N.; Kaučič, V. *Microporous Mesoporous Mater.* **2001**, *47*, 269.
(989) Wragg, D. S.; Hix, G. B.; Morris, R. E. *J. Am Chem. Soc.* **1998**, *120*, 6822.
(990) Reinart, P.; Patarin, J.; Marler, B. *Eur. J. Solid State Inorg. Chem.* **1998**, *38*, 389.
(991) Wragg, D. S.; Morris, R. E. *J. Mater. Chem.* **2001**, *11*, 513.
(992) Oliver, S.; Kupermann, S.; Ozin, G. A. *Angew. Chem., Int. Ed.* **1998**, *37*, 46.
(993) Choudhury, A.; Rao, C. N. R. *Chem. Commun.* **2003**, 366.
(994) Dan, M.; Udaykumar, D.; Rao, C. N. R. *Chem. Commun.* **2003**, 2212.
(995) Wang, K.; Yu, J.; Song, Y.; Xu, R. *Dalton Trans.* **2003**, 99. Wang, K.; Yu, J.; Li, C.; Xu, R *Inorg. Chem.* **2003**, *42*, 4597.
(996) Cheetham, A. K.; Mellot, C. F *Chem. Mater.* **1997**, *9*, 2269. Francis, R. J. v.; O'Hare, D. *J. Chem. Soc., Dalton Trans.* **1998**, 3133.
(997) Rey, F.; Sankar, G.; Thomas, J. M.; Barret, P. A.; Lewis, D. W.; Catlow, R. A. *Chem. Mater.* **1995**, *7*, 1435. Christensen, A. N.; Jensen, T. R.; Norby, P.; Hanson, J. C. *Chem. Mater.* **1998**, *10*, 1688. Norby, P; Christensen, A. N; Hanson, J. C. *Inorg. Chem.* **1999**, *38*, 1216.
(998) Francis, R. J.; Price, S. J.; O'Brien, S.; Fogg, A. M.; O'Hare, D.; Loiseau, T.; Férey, G. *Chem. Commun.* **1997**, 521. Francis, R. J.; O'Brien, S.; Fogg, A. M.; Halasyamani, P. S.; O'Hare, D.; Loiseau, T.; Férey, G *J. Am. Chem. Soc.* **1999**, *121*, 1002.
(999) Walton, R. I.; Loiseau, T.; O'Hare, D.; Férey, G. *Chem. Mater.* **1999**, *11*, 3201.
(1000) Walton, R. I.; Norquist, A. J.; Neeraj, S.; Natarajan, S.; Rao, C. N. R.; O'Hare, D. *Chem. Commun.* **2001**, 1990.
(1001) Norquist, A. J.; O'Hare, D. *J. Am. Chem. Soc.* **2004**, *126*, 6673.
(1002) Loiseau, T.; Beitone, L.; Millange, F.; Taulelle, F.; O'Hare, D.; Férey, G. *J. Phys. Chem. B* **2004**, *108*, 20011.
(1003) Haouas, M.; Géradin, C.; Taulelle, F.; Estournes, C.; Loiseau, T.; Férey, G. *J. Chim. Phys.* **1998**, *95*, 302.
(1004) Taulelle, F.; Haouas, M.; Géradin, C.; Estournes, C.; Loiseau, T.; Férey, G. *Colloids Surf. A* **1999**, *158*, 299.
(1005) Taulelle, F. *Curr. Opin. Solid State Mater. Sci.* **2001**, *5*, 397, and references therein.
(1006) Vistad, Ø. B.; Akporiaye, D. E.; Taulelle, F.; Lillerud, K. P. *Chem. Mater.* **2003**, *15*, 1639.
(1007) Serre, C.; Loretz, C.; Taulelle, F.; Férey, G. *Chem. Mater.* **2003**, *15*, 2328.
(1008) Lewis, D. W.; Willock, D. J.; Catlow, C. R. A.; Thomas, J. M.; Hutchings, G. J. *Nature* **1996**, *382*, 604. Lewis, D. W.; Sankar, G.; Wyles, J. K.; Thomasv, J. M.; Catlow, C. R. A.; Willock, D. J. *Angew. Chem., Int. Ed.* **1997**, *36*, 2675.
(1009) Mellot-Draznieks, C.; Newsam, J. M.; Gormann, A.M.; Freeman, C. M.; Férey, G. *Angew. Chem., Int. Ed.* **2000**, *39*, 2271. Mellot-Draznieks, C.; Girard, S.; Férey, G. *J. Am. Chem. Soc.* **2002**, *124*, 15326.
(1010) Zhou, B.; Yu, J.; Li, J.; Xu, Y.; Xu, W.; Qiu, S.; Xu, R. *Chem. Mater.* **1999**, *11*, 1094. Li, J.; Yu, J.; Yan, W.; Xu, Y.; Xu, W.; Qiuv, S.; Xu, R. *Chem. Mater.* **1999**, *11*, 2600. Yu, J.; Li, J; Xu, R. *Microporous Mesoporous Mater.* **2001**, *48*, 47. Li, Y.; Yu, J.; Liu, D.; Yan, W.; Xu, R.; Xu, Y. *Chem. Mater.* **2003**, *15*, 2780.
(1011) Adair, B. A.; Neeraj, S.; Cheetham, A. K. *Chem. Mater.* **2003**, *15*, 1518.
(1012) Davis, M. E. *Nature* **2002**, *417*, 813, and references therein.
(1013) Corma, A. *Chem. Rev.* **1995**, *95*, 559, and references therein.
(1014) Thomas, J. M. *Angew. Chem., Int. Ed.* **1999**, *38*, 3588, and references therein.
(1015) Thomas, J. M.; Raja, R.; Sankar, G.; Bell, R. G. *Nature* **1999**, *398*, 227. Raja, R.; Thomas, J. M. *Chem. Commun.* **1998**, 1841.
(1016) Thomas, J. M.; Raja, R.; Sankar, G.; Bell, R. G. *Acc. Chem. Res.* **2001**, *34*, 191.
(1017) Chang, J.-S.; Park, S.-E.; Gao, Q.; Férey, G.; Cheetham, A. K. *Chem. Commun.* **2001**, 859. Chang, J.-S.; Hwang, J.-S.; Jhung, S. H.; Park, S.-E.; Férey, G.; Cheetham, A. K. *Angew. Chem., Int. Ed.* **2004**, *43*, 2819. Forster, P. M.; Eckert, J.; Chang, J.-S.; Park, S.-E.; Férey, G.; Cheetham, A. K. *J. Am. Chem. Soc.* **2003**, *125*, 1309.
(1018) Cooper, E. R.; Andrews, C. D.; Wheatley, P. S.; Webb, P. B.; Wormald, P; Morris, R. E. *Nature* **2004**, *430*, 1012.
(1019) Parnham, E. R.; Morris, R. E. *Acc. Chem. Res.* **2007**, *40*, 1005.
(1020) Liao, Y.-C.; Lin, C.-H.; Wang, S.-L. *J. Am. Chem. Soc.* **2005**, *127*, 9986. Lin, C.- H.; Yang, Y.-C.; Chen, C.-Y.; Wang, S.-L *Chem. Mater.* **2006**, *18*, 2095.
(1021) Chen, P.; Li, J.; Yu, J.; Wang, Y.; Pan, Q.; Xu, R. *J. Solid State Chem.* **2005**, *178*, 1929.
(1022) Parnham, E. R.; Morris, R. E. *J. Mater. Chem.* **2006**, *16*, 3682.
(1023) (a) Peng, L.; Yu, J.; Li, J.; Li, Y.; Xu, R. *Chem. Mater.* **2005**, *17*, 2101. (b) Tuel, A.; Lorentz, Ch.; Gramlich, V.; Baerlocher, Ch. *J. Solid State Chem.* **2005**, *178*, 2322. (c) Parnham, E. R.; Wheatley, P. S.; Morris, R. E. Chem. Commun. 2006, *380*. (d) Marichal, C.;

Chézeau, M. J.; Roux, M.; Patarin, J.; Jordá, J. L.; McCusker, L. B.; Baerlocher, Ch.; Pattison, P. *Microporous Mesoporous Mater.* **2006**, *90*, 5. (e) Wang, M.; Li, J.; Pan, Q.; Yu, J.; Song, X.; Xu, R. *Solid State Sci.* **2006**, *8*, 1079.

(1024) Tuel, A.; Jordá, J.-L.; Gramlich, V.; Baerlocher, Ch. *J. Solid State Chem.* **2005**, *178*, 782.

(1025) (a) Zhou, D.; Chen, L.; Yu, J.; Li, Y.; Yan, W.; Deng, F.; Xu, R. *Inorg. Chem.* **2005**, *44*, 4391. (b) Shi, L.; Li, J.; Yu, J.; Li, Y.; Xu, R. *Microporous Mesoporous Mater.* **2006**, *93*, 325. (c) Simon, L.; Marrot, J.; Loiseau, T.; Férey, G. *Solid State Sci.* **2006**, *8*, 1361.

(1026) (a) Tuel, A.; Lorentz, C.; Gramlich, V.; Baerlocher, Ch. *C. R. Chimie* **2005**, *8*, 531. (b) Fernandes, A.; Ribeiro, M. F.; Borges, C.; Lourenco, J. P.; Rocha, J.; Gabelica, Z. *Microporous Mesoporous Mater.* **2006**, *90*, 112. (c) Wheatley, P. S.; Morris, R. E. *J. Mater. Chem.* **2006**, *16*, 1035. (d) Parnham, E. R.; Morris, R. E. *Chem. Mater.* **2006**, *18*, 4882.

(1027) Yu, J.; Xu, R. *Chem. Soc. Rev.* **2006**, *35*, 593.

(1028) Lin, C.-H.; Wang, S.-L. *Acta Crystallogr.* **2006**, *E62*, m3289.

(1029) (a) Lakiss, L.; Simon-Masseron, A.; Gramlich, V.; Patarin, J. *Solid State Sci.* **2005**, *7*, 141. (b) Loiseau, T.; Férey, G. *Solid State Sci.* **2005**, *7*, 1556. (c) Loiseau, T.; Férey, G. *Acta Crystalbgr.* **2005**, *C61*, m315. (d) Hasnaoui, M. A.; Simon-Masseron, A.; Gramlich, V.; Patarin, J.; Bengueddach, A. *Eur. J. Inorg. Chem.* **2005**, 536. (e) Lakiss, L.; Simon-Masseron, A.; Porcher, F.; Patarin, J. *Eur. J. Inorg. Chem.* **2006**, 237.

(1030) (a) Yang, Y.; Mu, Z.; Xu, Y.; Liu, Y.; Chen, C.; Wang, W.; Yi, Z.; Ye, L.; Pang, W. *Solid State Sci.* **2005**, *7*, 103. (b) Yang, L.; Li, G.; Shi, Z.; Feng, S. *J. Solid State Chem.* **2005**, *178*, 1197. (c) Lakiss, L.; Simon-Masseron, A.; Patarin., J. *Microporous Mesoporous Mater.* **2005**, *84*, 50.

(1031) Chen, C.; Yi, Z.; Bi, M.; Liu, Y.; Wang, C.; Liu, L.; Zhao, Z.; Pang, W. *J. Solid State Chem.* **2006**, *179*, 1478.

(1032) Li, J.; Li, L.; Yu, J.; Xu, R. *Inorg. Chem. Commun.* **2006**, *9*, 624.

(1033) (a) Chen, C.; Yi, Z.; Ding, H.; Li, G.; Bi, M.; Yang, Y.; Li, S.; Li, W.; Pang, W. *Microporous Mesoporous Mater.* **2005**, *83*, 301. (b) Chen, C.; Liu, Y.; Fang, Q.; Liu, L.; Eubank, J. F.; Zhang, N.; Gong, S.; Pang, W. *Microporous Mesoporous Mater.* **2006**, *97*, 132.

(1034) Dakhlaoui, A.; Maisonneuve, V.; Leblanc, M.; Smiri, L. S. *J. Solid State Chem.* **2005**, *178*, 1880.

(1035) Jensen, T. R.; Gérentes, N.; Jepsen, J.; Hazell, R. G.; Jakobsen, H. J. *Inorg. Chem.* **2005**, *44*, 658.

(1036) Yilmaz, V. T.; Demir, S.; Kazak, C.; Harrison, W. T. A. *Solid State Sci.* **2005**, *7*, 1247.

(1037) Rayes, A.; Nasr, C. B.; Rzaigui, M. *Phosphorus, Sulfur, Silicon* **2005**, *181*, 41.

(1038) (a) Rajić, N.; Logar, N. Z.; Stojaković, D.; Sajić, S.; Golobić, A.; Kaućić, V. *J. Serb. Chem. Soc.* **2005**, *70*, 625. (b) Logar, N. Z.; Rajić, N.; Stojaković, D.; Golobić, A.; Kaućić, V. *Pure Appl. Chem.* **2005**, *77*, 1707. (c) Logar, N. Z.; Rajić, N.; Stojaković, D.; Sajić, S.; Golobić, A.; Kaućić, V. *Acta Crystallogr.* **2005**, *E61*, m1354. (d) Wang, Y.; Chen, P.; Li, J.; Yu, J.; Xu, J.; Pan, Q.; Xu, R. *Inorg. Chem.* **2006**, *45*, 4764. (e) Kefi, R; Nasr, C. B.; Lefebvre, F.; Rzaigui, M. *Poyhedron* **2006**, *25*, 2953. (f) Liao, Y.-C.; Jiang, Y.-C.; Wang, S.-L. *J. Am. Chem. Soc.* **2005**, *127*, 12749.

(1039) (a) Natarajan, S.; Ewald, B.; Prots, Y.; Kniep, R. *Z. Anorg. Allg. Chem.* **2005**, *631*, 1622. (b) Harrison, W. T. A. *Solid State Sci.* **2006**, *8*, 371. (c) Kefi, R.; Nasr, C. B.; Lefebvre, F.; Rzaigui, M. *Phosphorus, Sulfur, Silicon* **2006**, *181*, 2231.

(1040) (a) Gaslain, F. O. M.; Chippindale, A. M. C. R. *Chimie* **2005**, *8*, 521. (b) Weibcke, M.; Kühn, C.; Wildermuth, G. *J. Solid State Chem.* **2005**, *178*, 694. (c) Zeng, Q.-X.; Xiang, Y.; Zhang, L.-W.; Chen, W.-H.; Chen, J.-Z. *Microporous Mesoporous Mater.* **2006**, *93*, 270.

(1041) Guo, M.; Yu, J.; Li, J.; Li, Y.; Xu, R. *Inorg. Chem.* **2006**, *45*, 3281.

(1042) Ramaswamy, P.; Natarajan, R. *Eur. J. Inorg. Chem.* **2006**, 3463.

(1043) (a) Yang, Y.-C.; Hung, L.-I.; Wang, S.-L. *Chem. Mater.* **2005**, *17*, 2833. (b) Cui, Y.; Sun, J.; Meng, H.; Li, G.; Chen, C.; Liu, L.; Yuan, X.; Pang, W. *Inorg. Chem. Commun.* **2005**, *8*, 759.

(1044) Chang, W.-K.; Wur, C.-S.; Wang, S.-L.; Chiang, R.-K. *Inorg. Chem.* **2006**, *45*, 6622.

(1045) Miller, S. R.; Slawin, A. M. Z.; Wormald, P.; Wright, P. A. *J. Solid State Chem.* **2005**, *178*, 1738.

(1046) (a) Shi, L.; Li, J.; Duan, F.; Yu, J.; Li, Y.; Xu, R. *Microporous Mesoporous Mater.* **2005**, *85*, 252. (b) Wang, M.; Li, J.; Yu, J.; Li, G.; Pan, Q.; Xu, R. *Inorg. Chem. Commun.* **2005**, *8*, 866. (c) Li, Y.-X.; Zhang, H.-T.; Li, Y.-Z.; Xu, Y.-H.; You, X.-Z. *Microporous Mesoporous Mater.* **2006**, *97*, 1.

(1047) Loiseau, T.; Beitone, L.; Taulelle, F.; Férey, G. *Solid State Sci.* **2006**, *8*, 346.

(1048) Parnham, E. R.; Morris, R. E. *J. Am. Chem. Soc.* **2006**, *128*, 2204.

(1049) Chippindale, A. M.; Grimshaw, M. R.; Powell, A. V.; Cowley, A. R. *Inorg. Chem.* **2005**, *44*, 4121.

(1050) (a) Sorensen, M. B.; Hazell, R. G.; Chevallier, J.; Pind, N.; Jensen, T. R. *Microporous Mesoporous Mater.* **2005**, *84*, 144. (b) Lin, Z.-E.; Fan, W.; Chino, N.; Gao, F.; Yokoi, T.; Okubo, T. *Z. Anorg. Allg. Chem.* **2006**, *632*, 465.

(1051) Ewald, B.; Huang, Y.-X.; Kniep, R. *Z. Anorg. Allg. Chem.* **2007**, *633*, 1517.

(1052) Bázan, B.; Mesa, J. L.; Pizarro, J. L.; Lezama, L.; Pena, A.; Arriortua, M. I.; Rojo, T. *J. Solid State Chem.* **2006**, *179*, 1459.

(1053) (a) Yu, R.; Xing, X.; Saito, T.; Azuma, M.; Takano, M.; Wang, D.; Chen, Y.; Kumada, N.; Kinomura, N. *Solid State Sci.* **2005**, *7*, 221. (b) Chang, W.-M.; Wang, S.-L. *Chem. Mater.* **2005**, *17*, 74. (c) Peng, L.; Li, J.; Yu, J.; Li, G.; Fang, Q.; Xu, R. *J. Solid State Chem.* **2005**, *178*, 2686. (d) Chen, Z.; Tan, S.; Weng, L.; Zhou, Y.; Gao, X.; Zhao, D. *J. Solid State Chem.* **2006**, *179*, 1931.

(1054) Sheu, C.-Y.; Lee, S.-F.; Lii, K.-H *Inorg. Chem.* **2006**, *45*, 1891.

(1055) (a) Lin, Z.-E.; Zhang, Z.; Zheng, S.-T.; Yang, G.-Y. *Z. Anorg. Allg. Chem.* **2005**, *631*, 155. (b) Fan, J.; Slebodnick, C.; Angel, R.; Hanson, B. E. *Inorg Chem.* **2005**, *44*, 552. (c) Fan, J.; Hanson, B. E. *Inorg. Chem.* **2005**, *44*, 6998. (d) Chippindale, A. M. *Acta Crystallogr.* **2006**, *C62*, m372. (e) Chen, C.; Liu, Y.; Wang, S.; Li, G.; Bi, M.; Yi, Z.; Pang, W. *Chem. Mater.* **2006**, *18*, 2950. (f) Wang, L.; Yang, M.; Li, G.; Shi, Z.; Feng, S. *J. Solid State Chem.* **2006**, *179*, 156. (g) Chang, W.-J.; Jiang, Y.-C.; Wang, S.-L.; Lii, K.-H. *Inorg. Chem.* **2006**, *45*, 6586.

(1056) Grandjean, D.; Beale, A. M.; Petukhov, A. V.; Weckhuysen, B. M. *J. Am. Chem. Soc.* **2005**, *127*, 14454.

(1057) (a) Thomas, J. M.; Raja, R *Proc. Natl. Acad. Sci. U.S.A.* **2005**, *102*, 13732. (b) Raja, R.; Thomas, J. M.; Xu, M.; Harris, K. D. M.; Greenhill-Hooper, M.; Quill, K. *Chem. Commun.* **2006**, 448. (c) Raja, R.; Thomas, J. M. *Solid State Sci.* **2006**, *8*, 326.

(1058) Jhung, S. H.; Lee, J.-H.; Cheetham, A. K.; Férey, G.; Chang, J.-S. *J. Catal.* **2006**, *239*, 97.

CR000119Q